Controls on aeolian bed-set architecture and implications for reservoir heterogeneity

Hollie Gemma Romain

Submitted in accordance with the requirements for the degree of
Doctor of Philosophy

The University of Leeds
School of Earth and Environment
September 2014

The candidate confirms that the work submitted is her own, except where work which has formed part of jointly-authored publications has been included. The contribution of the candidate and the other authors to this work has been explicitly indicated below. The candidate confirms that appropriate credit has been given within the thesis where reference has been made to the work of others.

A version of Chapter 2 is published in American Association of Petroleum Geologists Bulletin (2014, v. 8, p. 1-22) under the title "Reconstruction of three-dimensional eolian dune architecture from one-dimensional core data through adoption of analog data from outcrop", with the following list of authors (in order): Romain, H.G. and Mountney, N.P. The candidate set the scientific scope of the work, devised and developed the methodology, collected data during two field seasons in SE Utah, performed all data analysis, drew the illustrations and graphs, and wrote the text. The co-author proposed the broader general concepts that underlie the employed methodology, and provided guidance during the design of the method and feedback on the manuscript.

A version of Chapter 4 has been submitted for publication in Sedimentary Geology under the title "Interpretation of aeolian dune type from subsurface data: a case study from the Permian Auk Formation, Central North Sea, UK", with the following list of authors (in order): Romain, H.G., Mountney, N.P. and Besley, B. The candidate set the scope of the work within the framework of the broader research programme, made detailed process and palaeoenvironmental interpretations from a set of subsurface core descriptions and associated subsurface data, related the subsurface data to aspects of analogous ancient outcropping and modern aeolian systems, and wrote the text. The co-authors proposed the broader general concepts that underlie the research, devised the general methodology, logged the subsurface core intervals as part of an earlier project and provided guidance and feedback on provisional drafts of the manuscript text.

A version of Chapter 5 has been submitted for publication in Marine and Petroleum Geology under the title "Modelling three-dimensional lithofacies distributions in subsurface aeolian successions: Permian Auk Formation, Central North Sea, UK.", with the following list of authors (in order): Romain, H.G., Mountney, N.P. and Besley, B. The candidate set the scientific scope of the work, performed the detailed data analysis, drew the illustrations and graphs, and wrote the text. The co-authors proposed the broader general concepts that underlie the employed methodology, and provided guidance and feedback on provisional drafts of the manuscript text.

Acknowledgements

First and foremost, I would like to thank Nigel Mountney for his consistent and unwavering support – for leaving me to get on with it, but also being available almost 24/7 if I needed help. I wish I could duplicate him for every PhD student. Special thanks must also go to Bill McCaffrey, and to all of the companies who sponsor the Fluvial and Eolian Research Group at the University of Leeds – thank you for giving me the opportunity to work in one of the most amazing places I have ever visited; I have memories from my fieldwork in Utah that I will cherish for a lifetime.

Sarah Southern – any attempt to eloquently convey how much your friendship has meant to me over the past 4 years has been harder than writing this whole thesis. I'm not even going to try. Here's to many more adventures and geolidays!

To my fellow residents of Level 7, past and present (especially the legendary Room 7.131) – Alan Wood, Jessica Ross, Jo Venus, Luke Faggetter, Robbie Jones, Steve Banham, James Witts and Tom Fletcher – you have made everything about the last 4 years so much easier, thank you for the endless in-jokes and restocking the biscuit tin.

Thank you to every person who has put a roof over my head – Rachael Spraggs, Sarah Cobain, Jane Templeton, Rachael Cooper, Katie Farrell, and Laura Gregory.

Special thanks also to the following people: Andrew McCann, for painstakingly proof-reading my data chapters in record-breaking time; Naomi Leeds, for moving me up and down the country every five minutes; Shaun Kendrick, for always being just a phone call away (I treasure your friendship); Rebecca Vincent, who at times seemed to be the only person who understood the gravity of what I was trying to achieve; Nathan Clark and the Brudenell Social Club, where I have the happiest memories of my time in Leeds; Martin Declan Kelly, for numerous trips to the seaside which kept me relatively sane, and for igniting my unadulterated love for Yorkshire; John Wagner, Nathaniel Ball and Scott Douglas – thank you for rescuing me from camping in the snow at the top of White Canyon (I've never been happier to see a bed and a hot shower); Jim English, for the endless cat videos; Mila, for leaving muddy paw prints all over my paper drafts; Lyndsey Fox; Richard Rigby (you deserve a knighthood); the SoEE Geobabes, Andy Bray, Lagertown (gone but never forgotten), Bruce Springsteen, Yorkshire Tea, the Chelmlords, my ATP family, the Barmy Army, and all of my friends from all corners of the globe who continually reminded me that it is possible to have a life whilst completing a PhD!

Thank you to my Mum and Dad for the seemingly infinite emotional (and financial!) support, but most importantly for teaching me that there is no substitute for hard work. Thanks also to my sisters – Emily, Maddison and especially to Rachel, who has been a consistent source of intellectual inspiration for the past 30 years.

"The answer my friend, is blowin' in the wind,
The answer is blowin' in the wind"
Bob Dylan

Abstract

This research has developed novel techniques to reconstruct a variety of aeolian dune architectures using subsurface datasets, supplemented by outcrop studies and data from analogous modern aeolian systems. These methods demonstrate the ability to reconstruct larger-scale aeolian architectural elements in the subsurface, aeolian bedform geometries, regional reservoir stratigraphic heterogeneity, and original bedform morphology and style of migration. Once the original bedform morphology and style of migration has been determined, three-dimensional forward stratigraphic models have been developed which enable the reconstruction of the three-dimensional spatial arrangements of sets, internal facies arrangements, quantitative estimates of three-dimensional sand-body geometries, and likely geometry and degree of interconnectivity of net reservoir facies. This research has additionally investigated predictable responses in well log data (e.g. dipmeter data) for a variety of aeolian bedform types to determine original bedform morphology. The effect that original bedform morphology has on the overall reservoir quality of a volume through the interpretation of facies distributions, net reservoir calculations and connectivity has also been explored.

Table of Contents

List of Figures

Coyote Buttes North, Paria Canyon-Vermilion Cliffs Wilderness, AZ, USA. 29th May 2013.

Chapter 1 – Introduction

This chapter sets out the rationale for this research, explains the significance of the work and provides an overview of the thesis structure.

1.1 – Thesis rationale

Since the late 1970s, a considerable body of research relating to aeolian sedimentology has been focused toward gaining an improved understanding of the large-scale stratigraphic relationships and the development of sequence stratigraphic models with which to account for the origin of the aeolian rock record in terms of both intrinsic (autogenic) and external (allogenic) controls on sedimentation (e.g. Brookfield, 1977; Kocurek, 1988; Kocurek and Havholm, 1993; George and Berry, 1997; Howell and Mountney, 1997; Mountney, 2012). As a result of this emphasis, a wide variety of data have been published relating to large-scale stratigraphic architectures preserved in a number of ancient aeolian successions, many of which have been driven by the need to characterise subsurface aeolian reservoir architectures through adoption of outcrop analogues (e.g. Glennie and Provan, 1990; Herries, 1993; Mountney and Thompson, 2002; Mountney and Jagger, 2004; Taggart et al., 2010). However, there remain relatively few studies that have investigated the sedimentary style of small-scale dune elements and the arrangement of facies present within individual preserved aeolian dune-sets, originating from the migration of different types of aeolian bedforms (e.g. Ellwood et al., 1975; Hunter, 1977a; 1977b; Kocurek and Dott, 1981; Fryberger and Schenk, 1988).

From an applied perspective, although some explanation has been offered to account for how such types of small-scale stratification impact on reservoir quality (Lindquist, 1988; Chandler et al., 1989; Prosser and Maskall, 1993; Cox et al., 1994; Howell and Mountney, 2001; Stanistreet and Stollhofen, 2002; Garden et al., 2005; Bloomfield et al., 2006), a sophisticated and predictive method to relate deposits seen in one-dimensional core and ancient outcropping successions to larger-scale architectural elements, which have three-dimensional form, has yet to be fully developed for aeolian dune and interdune successions. Specifically, current aeolian facies models are not sufficiently refined to account for the inherent variability and complexities present in dunes of different morphologies and migratory behaviours. Therefore, they cannot consistently explicate the nature of the preserved deposits (Rodríguez-López et al., 2014), or be used as reliable predictive tools. A comprehensive technique to successfully interpret the preserved sedimentary architecture of ancient aeolian deposits, in particular with reference to their formative processes, has yet to be fully developed. This research aims to bridge a gap between process sedimentology and reservoir modelling which has long been recognised, but rarely considered in detail. The ability to successfully reconstruct aspects of aeolian bedform architecture, the resultant facies distributions and subsequent influences on overall reservoir quality is a key benefit when attempting to understand aeolian successions which are often known only from the subsurface.

1.2 – Research aims and objectives

The aim of this study is to develop a set of novel and innovative techniques that can be applied to demonstrate how key attributes of aeolian dune architecture directly measurable from one-dimensional core and outcrop datasets can be related back to the original morphology of the bedforms that migrated and accumulated to preserve such deposits. This research outlines methods for reconstructing the original morphology and style of migratory behaviour of aeolian bedforms from subsurface datasets and outcropping successions, and develops forward stratigraphic models which allow for the determination of the geometry, scale and degree of interconnectivity of net reservoir units in subsurface aeolian successions. In particular, this study demonstrates how the measurement of predictable sedimentological features present in aeolian successions can be used for the gross-scale reconstruction of three-dimensional aeolian bedform architecture, and how informed predictions can be made relating to resultant reservoir quality. Specifically, this project seeks to address these research issues through fulfilment of the following objectives:

1) to investigate whether there are any predictable sedimentological features present in core and ancient outcropping aeolian successions that can be used to reliably reconstruct aspects of the original aeolian form, including bedform and interdune morphology, scale (height, wavelength, spacing) orientation and style of migratory behaviour;

2) to determine expected facies distributions and their resultant architectures for a variety of common aeolian bedform morphologies;

3) to reconstruct the original bedform morphology and style of migratory behaviour of an aeolian reservoir interval known only from the subsurface, and to demonstrate how the geological complexities and lithological heterogeneities present in the interval can be modelled to provide insight into likely stratigraphic complexity that induces heterogeneity at a variety of scales;

4) to investigate any predictable responses in well log data (e.g. dipmeter data) for a variety of aeolian bedform types that could be used to determine original bedform morphology;

5) to investigate the effect that original bedform morphology and style of migratory behaviour has on the overall reservoir quality of the volume (facies distributions, net reservoir calculations and connectivity).

1.3 – Thesis significance

1.3.1 – 1D to 3D extrapolation

The wide range of data available to exploration and asset appraisal teams working in hydrocarbon companies are almost exclusively one-dimensional in form at the sub-seismic scale, meaning that determination of sedimentary system type and elucidation of the three-dimensional geometry of the various architectural elements present in a reservoir volume, and their reciprocal relationships to one another, are usually highly subjective. This can result in potentially ambiguous interpretations with their use as a basis for exploration, and the postulation of equivocal depositional models which fail to effectively account for observed reservoir performance (Kocurek, 1988; Schenk, 1990; North and Prosser, 1993; North and Boering, 1999). In particular, quantitative estimates of architectural element geometries and their internal facies compositions are important; these are required to estimate volumetric sand content in subsurface reservoir successions, and the subsequent porosity and permeability values of these successions. Therefore, a generally applicable technique or set of techniques is required that enables the reconstruction of three-dimensional architecture from one-dimensional datasets, such as core data. The use of outcrop analogues for the interpretation of subsurface data is a useful technique, as three-dimensional facies distributions known from outcrop can be used to populate a reservoir volume and thereby inform detailed characterisations and minimise risk. Key to the successful application of this technique is the ability to fit the sedimentary architecture of the chosen outcrop analogue to available core and well log data from the subsurface reservoir. The major limitation of this technique is that the chosen analogues are not necessarily appropriate, and for many subsurface successions appropriate outcrop analogues are not known, or simply do not exist. The issues outlined above are especially problematic in the analysis and characterisation of aeolian successions because such successions have few reliable markers, are hard to date, and can generate a wide range of architectural styles from a range of markedly different controls.

Previous workers have identified key parameters of aeolian dune architecture which can be directly related to one another. A positive relationship has long been recognised whereby increased climb angles tend to preserve thicker sets (e.g. Mountney and Howell, 2000), but such increased angles-of-climb do not necessarily arise from the accumulation of larger bedforms with longer wavelengths. Larger bedforms with longer wavelengths tend to climb at shallower angles, primarily because larger bedforms are likely to respond only slowly to changes in sand availability (Lancaster, 1988b) and will therefore tend to climb at shallow angles, though they can preserve relatively thick sets by virtue of their long wavelength.

A positive correlation has been demonstrated between dune slipface height and thickness of preserved grainflow packages that are generated as a consequence of lee-slope avalanching down such slipfaces in modern, small-to-medium-sized dunes (Kocurek and Dott, 1981).

Grainflow thickness is also known to vary as a function of slipface length, with thicker grainflows developing on longer slipfaces associated with larger bedforms (Kocurek and Dott, 1981). However, Howell and Mountney (2001) noted that there was no apparent significant relationship between preserved set thickness and grainflow thickness for the Cretaceous Etjo Formation of Namibia, and suggested that in this case, original bedform height was unlikely to have been the only primary control on long-term preservation of sets of aeolian bedforms. Kocurek and Dott (1981) also suggest that original bedform size can be estimated based on proportions of grainfall strata to grainflow strata in preserved dune sets. For many modern bedform types, dune height exhibits a positive correlation with bedform wavelength and spacing (e.g. Wilson, 1973; Lancaster, 1988a; Al-Masrahy and Mountney, 2013). Bedform type (simple, compound or complex bedforms of transverse, linear and star morphologies) can also potentially be deduced from a thick succession of core by ascribing different genetic significance to bounding surfaces of various types (e.g. interdune migration surfaces, superimposition surfaces, reactivation surfaces; see Brookfield, 1977; Rubin, 1987a; and Rubin and Carter, 2006, for a summary of the technique). The recognition of key features present in aeolian core and outcropping successions that could be related to larger-scale architectural elements and potentially used to reconstruct original bedform type and style of migratory behaviour is therefore imperative in making informed forward interpretations from limited datasets.

1.3.2 – Theoretical models of aeolian bedforms

Prediction of facies variability in three dimensions is a key requirement for quantitative reservoir characterisation (e.g. Sweet et al., 1996; Fischer et al., 2007) because it enables reliable predictions to be made of the characteristics of subsurface aeolian reservoir bodies such as the extent, type and pattern of distribution of stratigraphic heterogeneities at a bed-set-scale away from the points of data control provided by subsurface wells (Pryor, 1973). The migration of aeolian dunes with different morphologies has been shown to leave deposits characterised by distinct distributions of facies, and therefore also distinct heterogeneities and arrangements of net reservoir packages; quantitative estimates of architectural-element geometries and their internal facies compositions are therefore needed to better predict the heterogeneities inherent in aeolian reservoirs, and a technique to reconstruct three-dimensional architecture from one-dimensional datasets, such as core data, is also required. There is also a growing need to develop more detailed and accurate three-dimensional models of aeolian bedform architecture to account for stratigraphic heterogeneity in aeolian reservoirs if recovery of hydrocarbons is to be maximised (Rodríguez-López et al., 2014), especially in systems where stored hydrocarbon fluids have a high viscosity that renders fluid flow especially sensitive to lithofacies arrangements, such as the Permian Auk Field of the Central North Sea, where the oil has a viscosity of 0.9 centipoises (cP); heavy oil has viscosity values from 10 to 100 cP (Trewin et al., 2003).

The development of purely qualitative depositional (facies) models of aeolian systems commenced in earnest in the 1970s, and these models depicted packages of aeolian dune and interdune facies as elements delineated by bounding surfaces (e.g. Brookfield, 1977). These ‘static’ aeolian models – whereby the various parameters that control the construction, accumulation, and preservation of the aeolian system remain constant through both time and space (Mountney, 2006a) – typically accounted for stratigraphic complexities in two spatial dimensions, but changes in both the spatial and temporal aspects of aeolian bedform architecture need to be addressed to successfully account for inherent complexities which arise as a result of differences in dune morphology, scale and style of migration and accumulation (Rodríguez-López et al., 2014) and changes in such parameters over both time and space – classed as ‘dynamic’ models (*sensu* Mountney, 2012). Quantitative forward stratigraphic modelling provides a method to demonstrate the link between these spatial and temporal changes, and the observed preserved sedimentary architectures from outcropping or subsurface datasets. The ability to model the effect of modest changes in original bedform architecture in three dimensions conveniently allows for a better informed link between original bedform morphology and migratory style, and expected preserved stratigraphic architectures (e.g. Rubin, 1987a; Rubin and Carter, 2006).

Although the ability to interrogate these models to reconstruct bedform type and expected architectural geometries is an advantage, more sophisticated methods are needed for informed prediction of facies distributions within these bedform models for specific morphologies and styles of migration, especially for the prediction of the distribution and connectivity of net-reservoir units in the subsurface and the projection of fluid-flow pathways (Lindquist, 1988; Garden et al., 2005). Establishment of the most likely three-dimensional sedimentary architecture from one-dimensional core and well log data is typically equivocal (Lindquist, 1988; Luthi and Banavar, 1988; North and Boering, 1999). Several parameters govern the morphology and geometry of aeolian bedforms and their preserved bedsets can be measured directly from subsurface core. These data provide a means to directly relate the subsurface architecture present in reservoir successions to outcrop successions with analogous characteristics for which larger-scale three-dimensional architectural configurations can be determined.

1.3.3 – Bedform variability

The deposits of aeolian bedforms are highly variable over short lateral distances. They show lithological heterogeneity at a number of scales arising from various autogenic and allogenic controls, therefore unequivocal elucidation of three-dimensional architecture and original formative processes is problematic. The informed reconstruction of aeolian bedform type from subsurface data is important, as many ancient aeolian successions are only known in the subsurface. Although variability in dune morphology is known to occur across many large dune fields (e.g. Namib Desert – Lancaster, 1983; Rub' Al-Khali – Al-Masrahy and Mountney, 2013), there are few documented examples from ancient successions (e.g. Porter, 1986; Langford and Chan, 1993). The majority of palaeoenvironmental reconstructions of aeolian systems envisage transverse (and related barchanoid) dune types, whereas successions representing linear, star and other bedform types remain apparently under-recognised, meaning quantitative and qualitative data for accumulated deposits of these bedforms is limited.

The preserved deposits of several aeolian dune fields revealed by both subsurface and outcrop data have previously been interpreted as having arisen from the migration and accumulation of transverse bedforms, yet re-evaluation of primary data from such successions can lead to alternative interpretations whereby the formative dune bedforms were not necessarily transverse in form or migratory behaviour. Specific examples include the Permian Auk Formation of the Central North Sea (cf. Heward, 1991), now interpreted to have arisen from the accumulation of linear bedforms (Chapter 4), and the Permian Bridgnorth Sandstone of the Stafford Basin, UK, now understood to represent a complex combination of transverse and barchanoid draas with superimposed oblique crescentic and linear dunes (cf. Steele, 1981; Karpeta, 1990). Dunes represented by the Triassic Helsby Sandstone Formation of the Cheshire Basin, UK, were likely oblique forms, and the reconstruction by Mountney and Thompson (2002) argues that they were likely oriented 30° oblique from transverse. The Cedar Mesa Sandstone in SE Utah was also initially interpreted as arising from the migration and accumulation of transverse bedforms (Stanesco and Campbell, 1989), but which is now understood to have been deposited by oblique bedforms (Mountney and Jagger, 2004; Mountney, 2006b).

Given that there is no reason to suspect that linear and star bedforms were less abundant in the geological past, this suggests that current models and methods for the recognition and reconstruction of primary bedform type from preserved sedimentary architectures are not sufficiently refined to reliably distinguish between bedform types. There are several potential reasons why the majority of ancient aeolian deposits were interpreted as transverse bedforms. In particular, linear bedforms are now known to accumulate sets of cross-strata that are very difficult to distinguish from the deposits of transverse bedforms (Rubin and Hunter, 1985; Bristow et al., 2000). Additionally, many linear and star dune forms in modern sand seas tend to be isolated by extensive interdune flats which suggests that the bedforms were not necessarily undergoing active accumulation, even during times of active construction (Kocurek, 1999; Rodríguez-López et al., 2014). This reduction in accumulation implies that the preservation potential of such bedforms may be rare in the geological record. Recent studies outline new methods to recognise and interpret the deposits of a more varied range of bedform types, but it remains the case that most interpretations envisage transverse bedform types. The factors that control the preservation potential of different types of aeolian bedforms are yet to be fully understood. A fundamental research question remains: are there any diagnostic characteristics in deposits of different bedform types that can be used for effective and reliable reconstruction of original bedform morphology?

1.3.3.1 – Foreset dip-azimuth data

Although dip-azimuth data have been used in previous studies to reconstruct palaeodune migration directions, and in some cases original dune morphology (Nurmi, 1985), the assumptions implicit in the interpretation of such data must be made with care. Specifically, it has long been recognised that dune foreset dip-azimuths are not necessarily an indicator of palaeowind direction. Of note, Rubin and Hunter (1983) and Rubin (1987a; 1987b) document numerous examples where mean foreset azimuths differ markedly from the migration direction of parent and/or superimposed bedforms, usually from the migration of superimposed bedforms or scour pits either obliquely, or along-crest of the parent bedforms. It is now recognised that in all but the very simplest of straight-crested, transverse bedforms, foreset dip-azimuths are an unreliable method of reconstructing palaeodune migration direction (Mountney, 2006a).

1.3.3.2 – Linear dunes

There are few published accounts of ancient linear dune successions, yet linear dunes represent over fifty percent of the dune types present in modern dune fields (Rubin and Hunter, 1985; Rodríguez-López et al., 2014). As such, there are very few published descriptions relating to the internal facies and bounding-surface distributions of ancient linear dune successions. Qualitative and quantitative data relating to the stratigraphy of successions generated by the accumulation of linear bedforms are also rare. Given that linear aeolian dune systems can potentially accumulate via bedform climbing or other mechanisms, such system types must be significantly under recognised in the ancient rock record. Whilst it is unlikely that such types were less represented back through geologic time than at present, the reduction in accumulation associated with linear and star dunes implies that the preservation potential of such bedforms may be low in the geological record (Rodríguez-López et al., 2014). A literature survey undertaken by Rubin and Hunter (1985) showed that out of 28 published interpretations of aeolian sandstones; only 3 (Tanner, 1965; Glennie, 1972; and Steele, 1982) were attributed, even partially, to linear dunes – although there have been more recognised since (e.g. Quebrada Monardes Formation, Chile – Bell, 1991; Troncoso Member of the Huitrfn Formation, Argentina - Strömbäck et al., 2005). Of these, it was only the study by Glennie (1972) that based the interpretation of linear deposits on the classic bimodal distribution of cross bed azimuths envisaged to demonstrate deposition on opposing flanks of linear dunes by Bagnold (1941). Such an approach would likely only work for exceptional preservation of intact bedform morphologies (e.g. Glennie and Buller, 1983; Story, 1998; Mountney et al., 1999; Benan and Kocurek, 2000), which would generate the classic bimodal dip-azimuth distribution. However, the minor component of transverse motion envisaged for the migration of most linear dunes (Rubin and Hunter, 1985; Bristow et al., 2000), enabling linear dunes to deposit layers of cross-strata with unimodal dip directions, would preserve a succession of unimodal foreset dip-azimuths for such bedforms.

Linear bedform processes

Linear dunes are formed under conditions of systematically varying wind direction (Fryberger, 1979a; Livingstone, 1989b). Most large linear dunes develop in response to the convergence of two oblique wind directions which, in many cases, are dominant at separate times, with alternations of wind direction typically occurring on a seasonal basis (e.g. Lancaster, 1983; McKee, 1982). The trend of the bedform crestline will not usually be parallel to either of these wind directions and neither will the mean azimuth of the preserved foresets (Rubin and Hunter, 1987). Linear dunes commonly display a crestline sinuosity of up to 15° around the direction of elongation (Hunter et al., 1983). There have been several models presented to account for the structure, mode of migration, and likely preserved architecture of linear dune deposits. Bagnold (1941) proposed that linear dunes migrate as a consequence of two equal and opposing winds, thereby preserving simple ‘tent-like’ structures in outcrop and subsurface deposits, with preserved strata dipping in opposite directions on either side of the dune arising from the vertical aggradation of such forms. Although this model was not suggested to be the universal mechanism for the formation of all types of linear dunes at the time, it gave rise to the view that linear dunes were the product of bidirectional wind regimes of equal magnitude, and that linear dunes extended in the resultant direction of sand movement (Lancaster, 1982).

The model proposed by Bagnold (1941) was supported by McKee and Tibbits (1964), who dug a series of trenches through a modern linear dune in Libya, and proposed that the existence of large scale cross-strata either side of the dune crest were the product of a bidirectional wind regime (Figure 1.1). Another bidirectional wind model of linear dune migration was proposed by Tsoar (1978), whose study of linear dunes in the Negev Desert did much to establish dynamic and structural evidence of linear dune development by winds from two directions (McKee, 1982). Concluding this work, Tsoar (1978) indicated that linear dunes are secondary forms developed from other types of aeolian dunes, such as barchans, and the additional sand made available to linear dune types causes elongation, whereas with transverse dunes it would increase their height; most deposition on linear

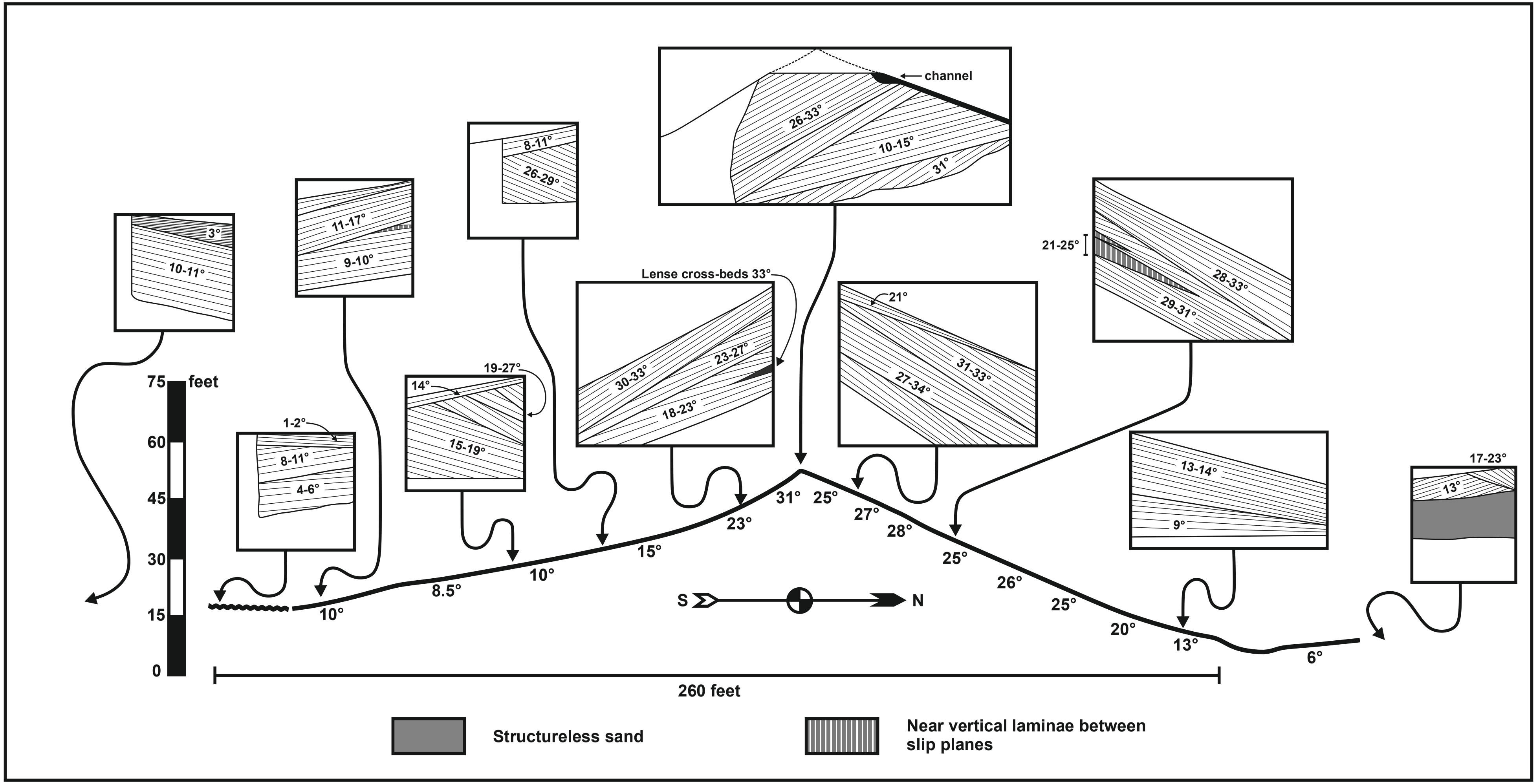

Figure 1.1. Structure observed by McKee and Tibbitts (1964) in shallow pits on a linear dune in Libya, commonly cited in published literature pre-1985 as verification of the model of linear dune structure initially proposed by Bagnold (1941).

dunes was therefore interpreted to not be formed by avalanching of sand grains, but by lee-side accretion.

Preservation of linear bedforms

The Bagnold (1941) model is partly appropriate for modern dunes, but will not usually lead to this style of preservation in ancient deposits where the dune forms have accumulated via bedform climbing. However, there are instances in the geological record that preserve this style of morphology, usually in cases of exceptional preservation following rapid inundation by water or lava flows (e.g. Glennie and Buller, 1983; Mountney et al., 1999; Benan and Kocurek, 2000), but these examples are rare. Seismic mapping of the Jurassic (Oxfordian) Norphlet Sandstone aeolian deposits at Mobile Bay in the subsurface of the Gulf of Mexico (Figure 1.2) shows linear dune morphologies preserved within the subsurface. A rapid, low-energy marine transgression during the Oxfordian, represented by the Smackover Formation (Mancini et al., 1985; Story, 1998; Ajdukiewicz et al., 2010) facilitated this rare preservation of linear dunes in the stratigraphy.

A study by Rubin and Hunter (1985) aimed to determine why the deposits of linear dunes were under recognised in the rock record. They initially proposed three possible reasons: (i) that linear dunes were rare in the past – which is untestable with existing data; (ii) that linear dunes rarely leave deposits, arguing that linear dunes were either erosional bedforms or that they were non-depositional and restricted to areas of scarce sediment supply; or (iii) that linear dunes deposit structures that are significantly different to the structures predicted by the model proposed by Bagnold (1941). It is not necessarily the case that linear dunes are *constructed* in a different manner to the model envisaged by Bagnold (1941), but rather it is that they *accumulate* to preserve a succession in a previously unrealised way (Figure 1.3). Rubin and Hunter (1985) were critical of Bagnold’s model, and asserted that winds are not always equal in strength in natural systems, in addition to the crestlines of linear dunes not being perfectly parallel to the long term sand transport direction. This pivotal study was the first to propose, using a convincing argument, that linear dunes must therefore undertake a component of transverse motion in addition to their primary along-crest migration direction. It is this minor component of lateral migration that is key in enabling linear dunes to deposit layers of cross-strata with unimodal dip directions, therefore closely resembling deposits arising from the migration and accumulation of transverse dunes in ancient preserved aeolian successions, and plays an important part in controlling the preserved architectural style of the accumulation (Figure 1.3).

The study of Rubin and Hunter (1985) provided the foundation for many more published studies which also recognise that it is usual for linear aeolian dunes to undertake a minor component of transverse motion in addition to their primary along-crest component of motion (e.g. Hesp et al., 1989; Rubin, 1990). In particular, the work of Bristow et al. (2000) demonstrated unequivocally that linear dunes slowly creep laterally (relative to the primary

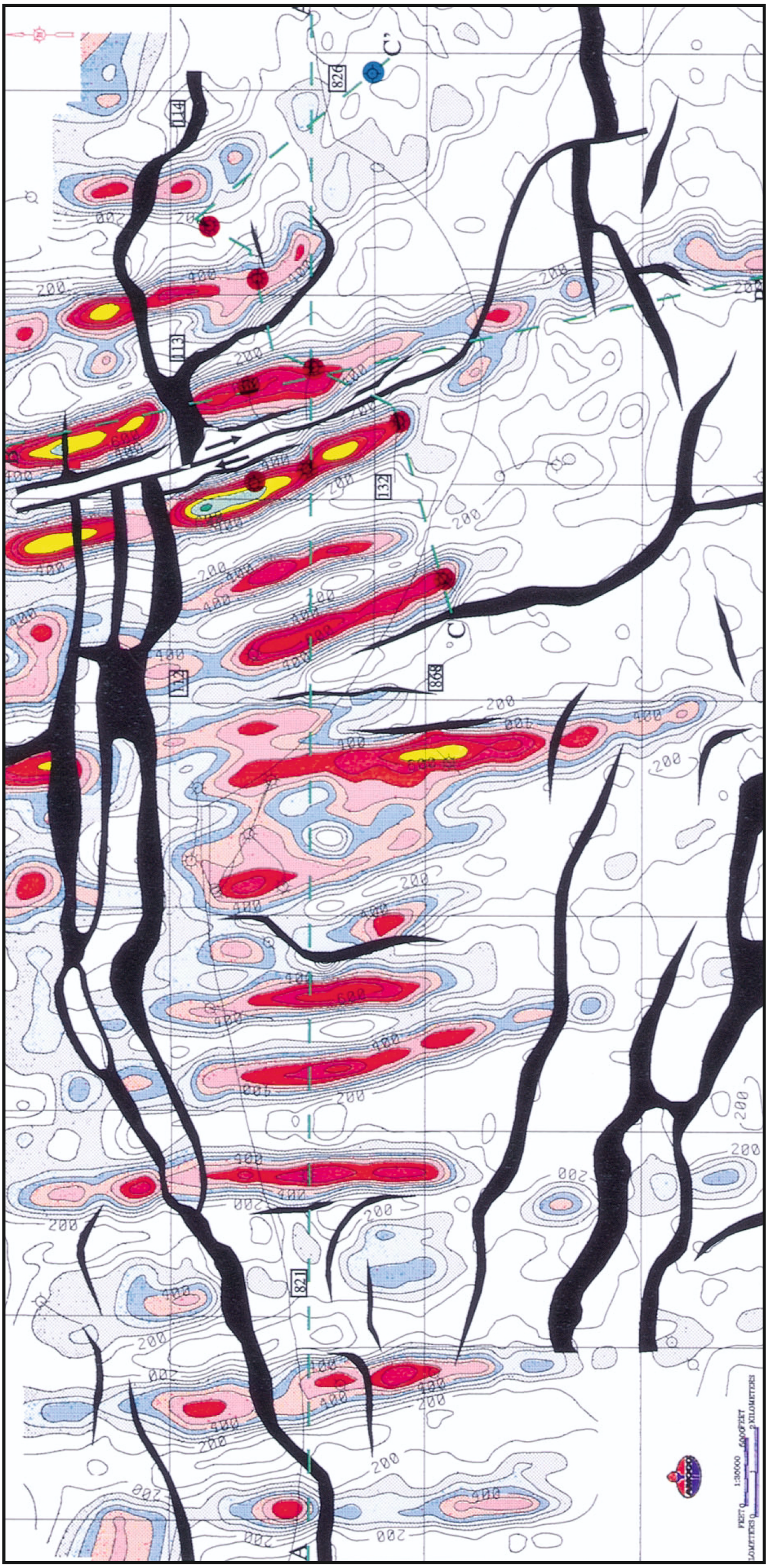

Figure 1.2. Jurassic (Oxfordian) Norphlet Sandstone aeolian deposits at Mobile Bay in the subsurface of the Gulf of Mexico, showing linear dune morphologies preserved within the subsurface. A rapid, low-energy marine transgression during the Oxfordian, represented by the Smackover Formation (Mancini et al., 1985; Story, 1998; Ajdukiewicz et al., 2010) facilitated this rare preservation of linear dunes in the stratigraphy. Image from Story (1998), based on FWL's (free water levels) on the seismic sections at well-ties. Contour lines in feet. Cross-section lines refer to those displayed in Story (1998).

sand migration direction) over long episodes. Images produced by ground penetrating radar (GPR) in this study show clear evidence for lateral migration of a linear dune in the Namib Desert (Figure 1.4), as suggested by Rubin and Hunter (1985).

Along-crest migrating sinuosities, spurs and re-entrants. Most linear dunes possess sinuosities which migrate along the bedform crest in a downwind direction (Tsoar, 1983), and the presence of these sinuosities adds an additional complexity to the sections of the linear dune profile which undergo accumulation and preservation (Figure 1.5a). The main transport of sand in linear dunes occurs parallel to the length of the dune, but a subordinate lateral migration occurs in response to the weaker of the two principal wind directions. The resulting lateral growth of the dune allows accumulation of dune deposits on the lee-side sections of the sinuous dune crest that are nearly normal to the resulting wind direction, however the other orientations of the sinuous dune crest are sites of bypass or erosion (Figure 1.5a; Figure 1.5b). The along-crest migration of a sinuous plan form crestline along the dune produces divergent sets of cross-strata, which can become stacked as the dune increases in height (Bristow et al., 2000). With a sinuous crestline, sand is deposited on the convex side rather than the concave side, and this can result in bimodal dips where sinuous curves propagate along the crest of the dune. These bimodal dips will not necessarily be 180° opposite to one another due to the wavelength of the crestline sinuosity not being exactly equal in natural systems (Figure 1.4, profiles 4 and 5).

Superimposed bedforms. It has been demonstrated that large linear dunes can also support superimposed dunes at multiple scales, whereby superimposed bedforms migrate with different trajectories and at different rates to parent bedforms, responding to different scales of airflow variability and reflecting spatial and temporal variations in secondary flow patterns developed on the dune (Lancaster, 1988b) (Figure 1.5c; Figure 1.5d). These superimposed bedforms appear with increasing dune height, width and sinuosity, because sand transport rates are then sufficient to support migrating dunes on the dune slopes (Lancaster, 1995). The addition of these superimposed bedforms can change the style of deposition considerably, preserving stacked sets of trough cross-bedding within larger cosets of cross-stratification (Figure 1.6 – Stage 4) all bounded by a hierarchy of bounding surface types of different orders (*sensu* Rubin, 1987a). The superimposition surfaces dip at lower angles than the strata in the dune set that they bound, and always dip down in a direction within the hemisphere of the resultant migration direction. These superimposition surfaces are themselves bounded by higher-order interdune migration surfaces that climb in the aforementioned resultant migration direction (Kocurek, 1988; 1996). Three-dimensional GPR images from the Namib Desert of superimposed transverse dunes migrating along linear dune flanks are documented in Bristow et al. (2007) (Figure 1.7). These studies have been fundamental in providing clear structural signatures to facilitate the informed recognition of linear dunes.

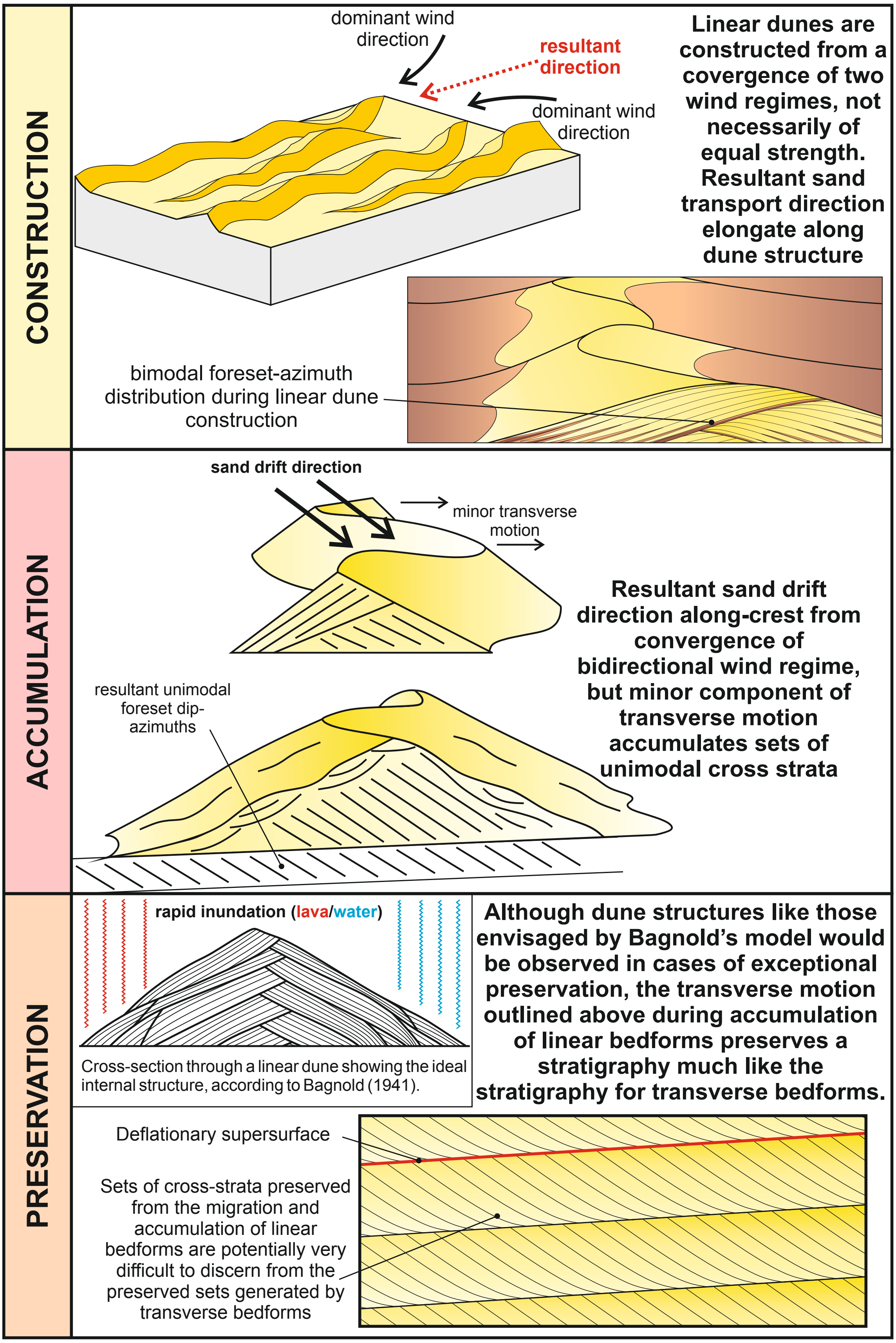

Linear dunes are constructed from a covergence of two wind regimes, not necessarily of equal strength. Resultant sand transport direction elongate along dune structure

Resultant sand drift direction along-crest from convergence of bidirectional wind regime, but minor component of transverse motion accumulates sets of unimodal cross strata

Cross-section through a linear dune showing the ideal internal structure, according to Bagnold (1941).

Although dune structures like those envisaged by Bagnold's model would be observed in cases of exceptional preservation, the transverse motion outlined above during accumulation of linear bedforms preserves a stratigraphy much like the stratigraphy for transverse bedforms.

Sets of cross-strata preserved from the migration and accumulation of linear bedforms are potentially very difficult to discern from the preserved sets generated by transverse bedforms

Figure 1.3. Schematic illustration to display modes of construction, accumulation and preservation of linear bedforms (*sensu* Kocurek, 1999). It is not necessarily the case that linear dunes are constructed in a different manner to the model envisaged by Bagnold (1941), but rather it is that they accumulate to preserve a succession in a previously unrealised way, except in cases of exceptional preservation following rapid inundation by water or lava flows (e.g. Glennie and Buller, 1983; Story, 1998; Mountney et al., 1999; Benan and Kocurek, 2000).

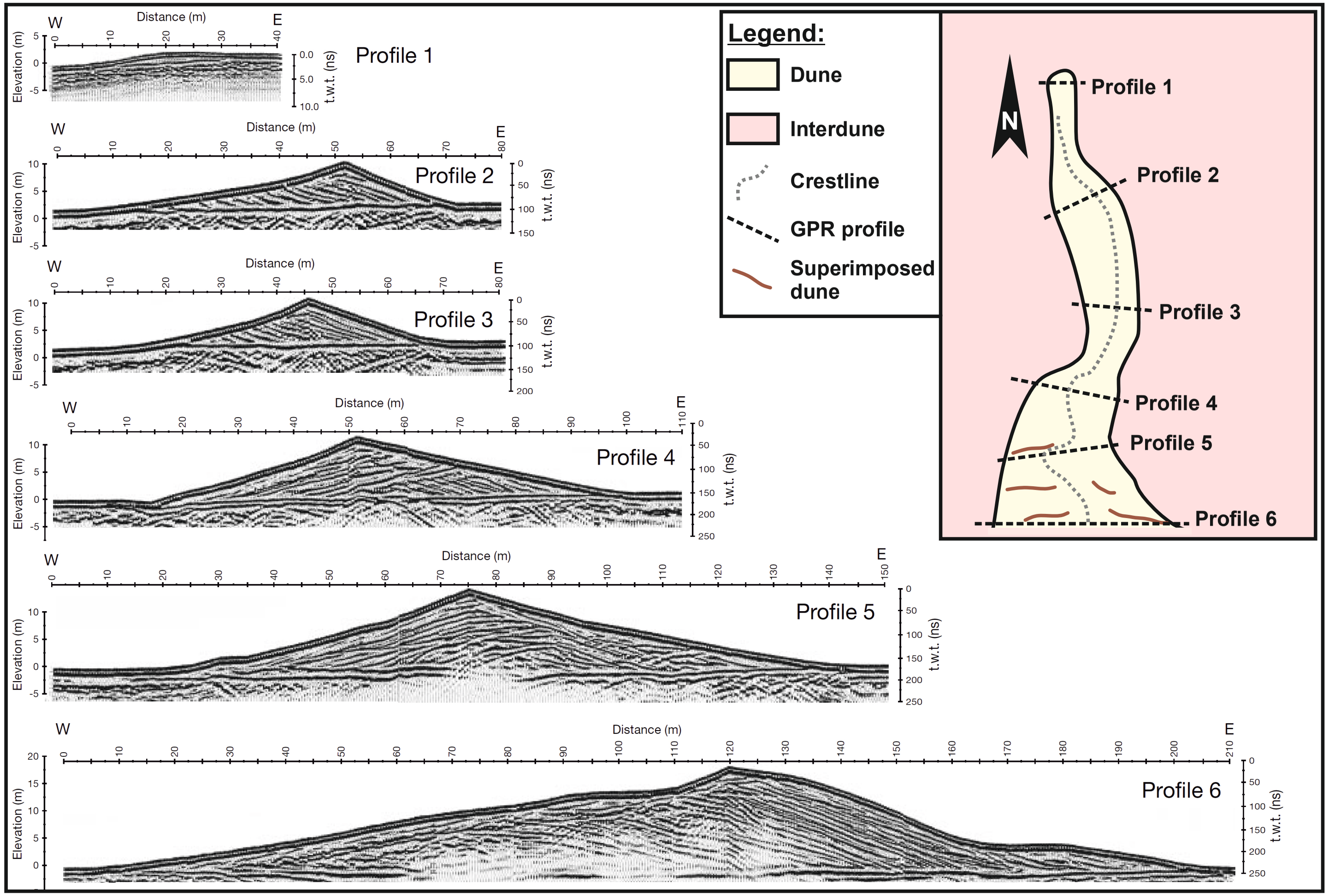

Figure 1.4. GPR profiles across a sinuous linear dune in the Namib Sand sea, from Bristow et al. (2000). Profile 1 crosses the distal end of the dune and contains wind-ripple sand that is not resolved by the radar. Profiles 2 and 3 image strata dipping from left to right indicating lateral migration of the dune toward the east. Profile 4 shows a set of strata dipping from left to right, truncated and overlain by strata that dip from right to left on the outside of the bend. Profile 5 shows increased complexity with strata dipping to left and right as a second bend propagates along the dune. Profile 6 shows sets of strata dipping from left to right, consistent with the lateral migration shown in profiles 2 and 3 but truncated and overlain by a superimposed dune on the left side.

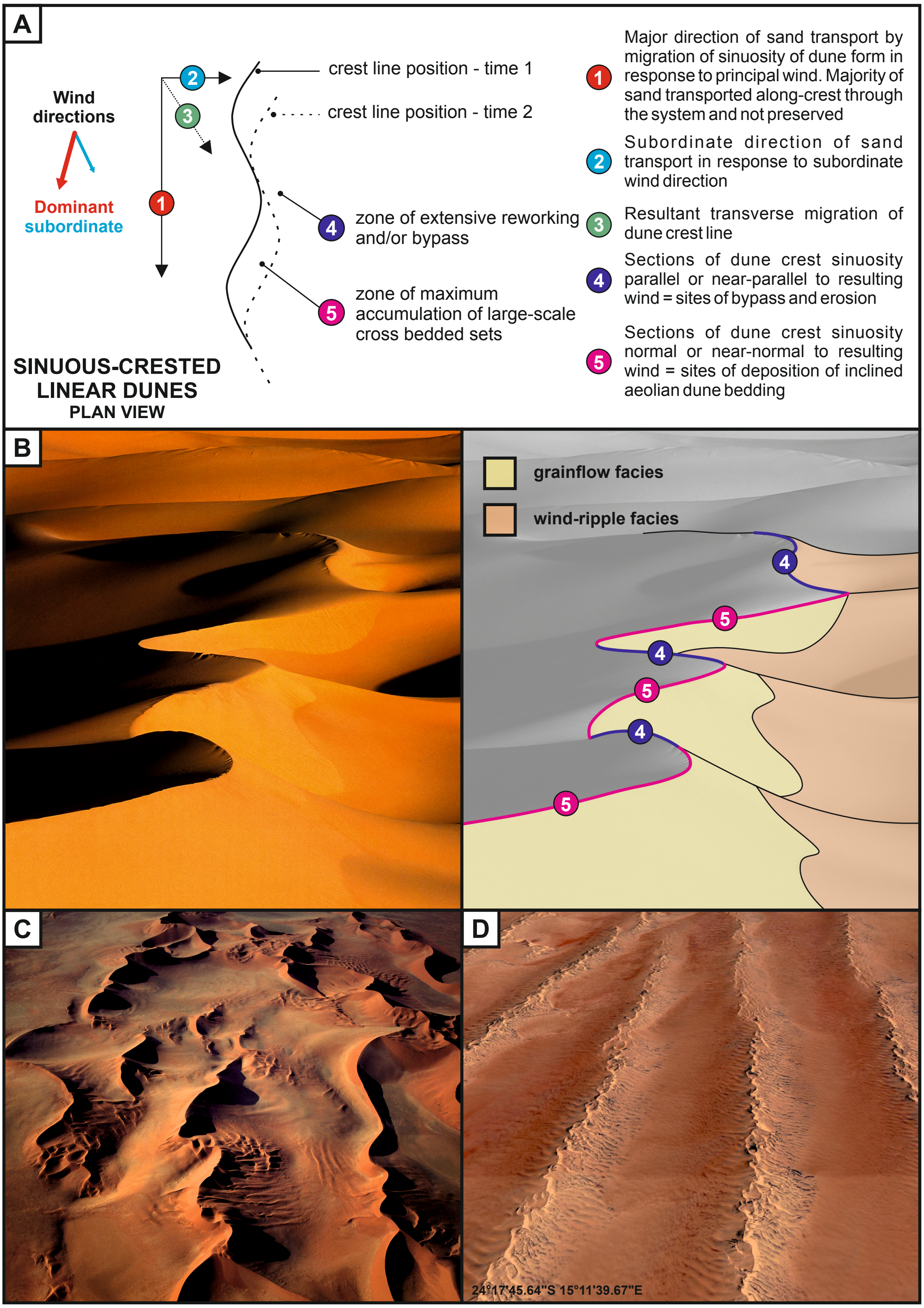

Figure 1.5. Modern examples of inherent complexities in linear dune forms: a) Basic geometry of sand transport and deposition in linear dunes. Plan view of pattern of sand transport in relation to wind directions, indicating zones of accumulations and bypass/erosion; b) Photograph along-axis of sand transport of a simple linear dune from the Namib desert, showing relationship of dune flank slopes and slipfaces to gross dune morphology; c) Sinuous-crested star and linear draa from the Namib Desert, with barchanoid dune fields superimposed on the lower flank of a linear draa. Bedforms up to 180m high. Image courtesy Bernhard Edmaier; d) Oblique aerial view image of large scale complex linear draa in the central Namib Desert. Regularly spaced elongate linear ridges have a complex morphology, with smaller transverse dunes migrating along the axes of the interdraa corridors. Net sand transport direction is to the north via seasonally variable SW and SE winds. Oblique aerial view image courtesy of Google Earth.

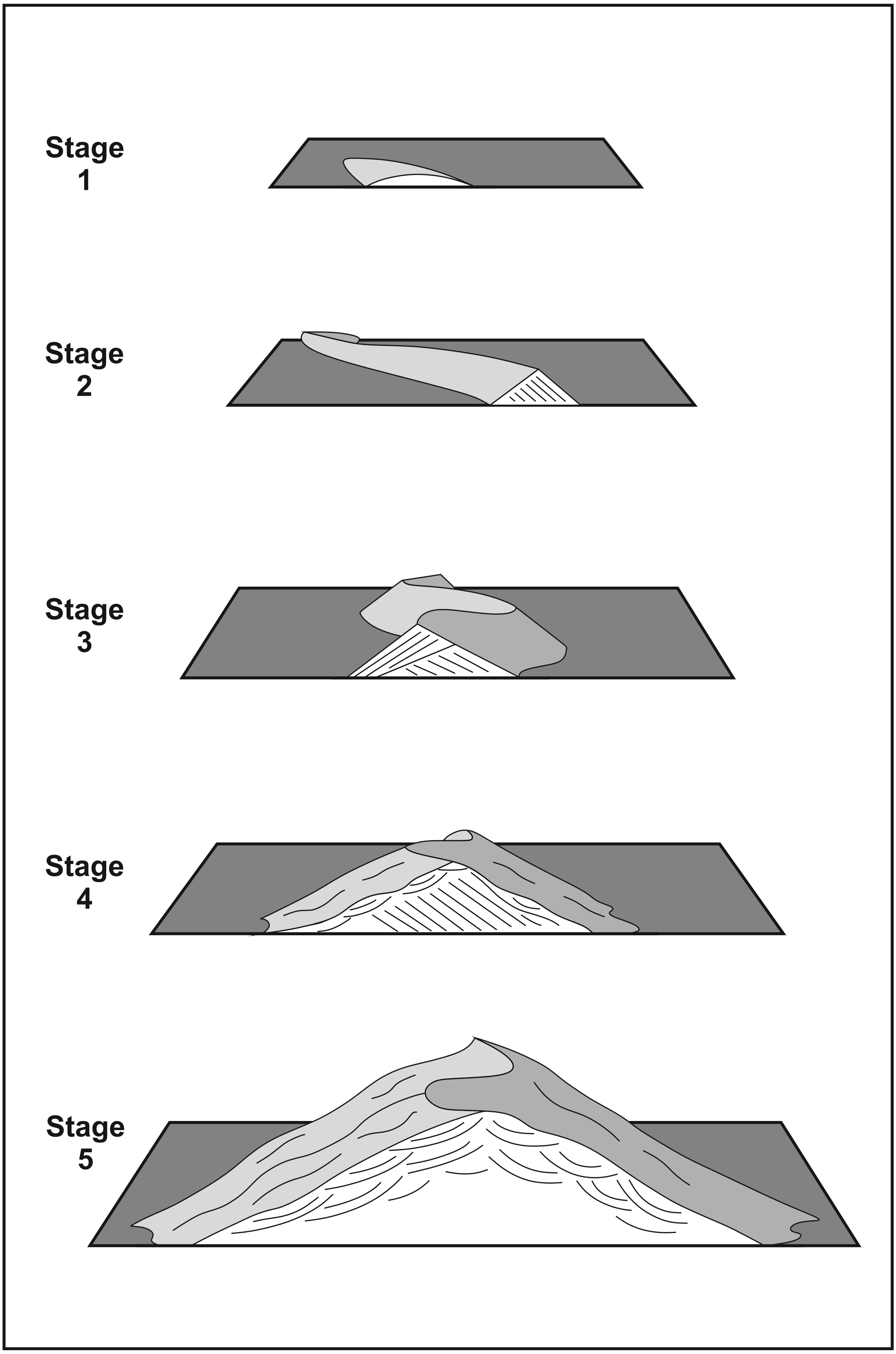

Figure 1.6. Five-stage model of linear dune evolution (from Bristow et al., 2000). Stage 1: initial plume of wind-rippled sand; Stage 2: slip-face development and migration towards the resultant drift direction produces simple sets of cross-stratification resembling a transverse dune; Stage 3: lateral displacement of the sinuous crest-line creates bidirectional dips; Stage 4: flow deflection along dune flanks leads to the development of superimposed dunes; Stage 5: complex linear megadunes are dominated by sets of trough cross-stratification from superimposed dunes.

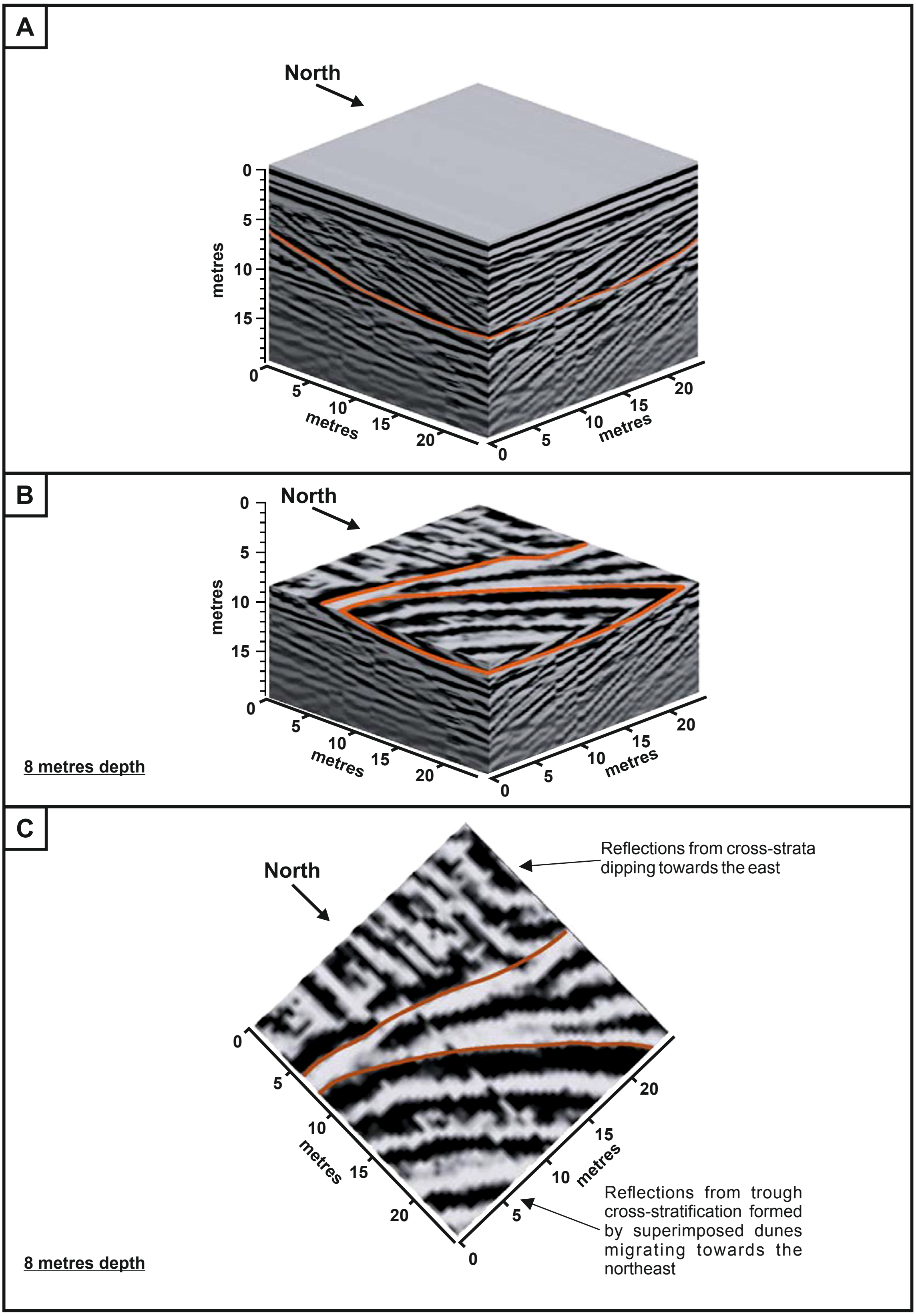

8 metres depth

8 metres depth

Reflections from cross-strata dipping towards the east

Reflections from trough cross-stratification formed by superimposed dunes migrating towards the northeast

Figure 1.7. Three-dimensional ground-penetrating radar (GPR) showing reflections from sets of trough cross-stratification and bounding surfaces produced by superimposed transverse dunes migrating along the western flank of a linear dune from the Namib Sand Sea (modified from Bristow et al., 2007): a) Sets of cross-stratification produced by superimposed transverse dunes migrating north along the dune flank. The orientation of the superimposed dunes can be confirmed using a time slice at a depth equivalent to 8 m (b) into the dune, which shows the strike of foresets produced by the north-northeastward migration of the superimposed dunes, which truncate earlier east-dipping sets of cross-stratification (c).

1.4 – Aeolian facies types

Aeolian dunes of different morphological type exhibit varying yet predictable configurations of primary depositional facies (principally packages of grainflow, wind-ripple and grainfall strata) and associations of such facies (Hunter, 1977a; 1977b; 1981; Kocurek and Dott, 1981). Recognising these aeolian facies types is fundamental in understanding and reconstructing the form and behaviour of aeolian dunes and interdunes from ancient preserved aeolian successions, and for making informed predictions on proportions and distributions of net reservoir units in subsurface successions. Detailed observations on the occurrence and distribution of these facies types in outcrop and core data may provide insight on original dune size and morphology, and the orientation of the original dune form to palaeowind direction. The three basic facies types described below commonly occur in various proportions bundled together as packages of interlaminated strata; prediction of the occurrence of such packages and the proportion of the basic facies types contained therein has implications for small-scale heterogeneity and directional permeability, discussed further in Section 1.6. The applied significance of facies distributions on different bedform types is discussed further in Section 1.4.4. Descriptions of the most common aeolian facies types and their mode of deposition are outlined below. An explanation of the terminology used to describe aeolian bedforms herein is illustrated in Figure 1.8.

1.4.1 – Wind-rippled facies

Wind-rippled sands are formed by migration of grains by creep and saltation, with a mixture of very fine sand, silt and clay material by fall-out from suspension. Wind-ripple sediment transport processes are well documented in recent aeolian systems (e.g. Kocurek, 1991; Mountney, 2006a) and have been simulated in experimental wind tunnels (Fryberger and Schenk, 1981). The deposits of wind-ripples typically take the form of thin laminations that are each a few millimetres thick (Figure 1.9). Individual laminations tend to be inversely graded due to grain segregation, with the coarsest grains found on the upper parts of lee slopes of ripples and the silt and very fine sand material being concentrated in the troughs of advancing wind-ripple translatent strata (Hunter, 1977b). This finer material is sheltered from bombardment from saltating sand grains or airflow along the top of the ripple (Fryberger and Schenk, 1988). This inverse grading is often referred to as ‘pin-stripe’ lamination and bimodally sorted grain size distribution (Fryberger and Schenk, 1988; Figure 1.9a), and is commonly seen in ancient aeolian deposits as a cemented, resistant layer due to early cementation of the finer layers of the stratigraphy.

1.4.2 – Grainflow facies

Grainflow facies are deposited by the avalanche flow of sand grains down steeply dipping dune slipfaces inclined at or close to the angle of repose for dry and non-consolidated sand (Hunter, 1977a; Kocurek, 1991; 1996). Sand is fed to the slipfaces by saltation on the upwind-facing slope of the dune, resulting in the build-up of loose sand at the dune brink. The finer-grained component of the sand tends to be removed by winnowing and transport in suspension to source grainfall deposits (Hunter, 1977a; 1981). The elevated position of the brink may militate against the presence of the coarser parts of the overall sand grain size population (Lancaster, 1995), such coarser grain fractions being restricted to interdune and lower dune-plinth regions. A significant outcome of the operation of these discriminatory sorting processes is that grainflow deposits tend to be very well sorted and have a unimodal grain size distribution, which is characterised by a limited grain size range with a strong peakedness (cf. Lancaster, 1981). The grainflow (avalanche) depositional process slows as the energy of grain-to-grain interactions in the flow is dissipated: this results in a grain fabric that is much more loosely packed than the wind-rippled facies that are dominated by tractional reworking (Hunter, 1977a; Lindquist, 1988). Grainflow movement usually ceases within the middle section of the steep lee-side face of the dune due to energy dissipation, especially on dune forms where the lee-slope angle reduces down slope, although more energetic flows may run out beyond the usual area of grainflow activity to form thin intercalations within lower parts of the dune slopes that are otherwise dominated by wind-rippled strata (Figure 1.10). Slipfaces formed largely by grainflows are subject to tractional reworking during the times between grainflow events, and grainflow facies therefore commonly occur in close association with and intercalated with wind-rippled facies (Hunter, 1977a; 1981).

1.4.3 – Grainfall facies

Grainfall deposits are typically indistinctly laminated and show an intermediate packing (Anderson, 1988). They are formed by fine-grained sands being entrained by the wind into suspension at the brink of the dune (Figure 1.11a), and falling onto other facies on the dune slipface, plinth and interdune areas (Hunter, 1977a). Grainfall deposits of very-fine sand form thin veneers that drape grainflow facies in dune slipface regions (Hunter, 1977a; 1977b; 1981). Grainfall deposits are extensively preserved in close association with wind-rippled facies that have not been subject to reworking, especially where such deposits form on slopes of low depositional dips or in interdune areas (Figure 1.11b). However, grainfall deposits are commonly hard to discern (Hunter, 1981). In interdune depositional settings, at some distance in front of active dunes, grainfall deposits are dominated by silt- and clay-sized material (Clemmensen and Abrahamsen, 1983). This falls from suspension further from the dune than the very fine sand-sized material that forms the grainfall deposits associated with slipfaces, and has a very high preservation potential owing to its ability to infiltrate the pore system of the sands it lands on. The cohesive nature of fine-grained sediment acts to protect such deposits from later reworking (Fryberger and Schenk, 1988). The preservation potential of grainfall deposits is especially high if deposition occurs within a low-lying dry interdune setting, where such deposits accumulate interbedded with other interdune deposits; by contrast, deposits formed *exclusively* of grainfall material are usually only found on the upper parts of active dunes, but these tend to have very low preservation potential in ancient dune deposits because they are unlikely to accumulate as part of a succession arising from the climb of migratory bedforms over one another since they are truncated and reworked as the following dune in the train of bedforms migrates over them.

1.4.4 – Facies distributions on bedforms

The distribution of associations of the fundamental aeolian facies types described above tends to vary predictably over the surface of individual modern aeolian bedforms as a function of the various aeolian processes that operate on the flank, lee-slope, stoss-slope and brink areas of bedforms (Hunter, 1977a). Detailed observations on the occurrence and distribution of these facies types in outcrop and core data may provide insight on original dune size and morphology, and the orientation of the original dune form to palaeowind direction. For example, in successions interpreted to have arisen in response to the migration and aggradation of large linear dune bedforms, a vertical stacking of thick packages of relatively low-angle-inclined, wind-ripple-dominated packages of strata is common, with only the uppermost parts of sets having foresets that steepen-upward sufficiently to preserve grainflow strata (Krystinik, 1990). From observations on modern aeolian dunes, it is evident that larger dunes (>10 m in height) deposit thicker avalanching grainflow deposits, and these grainflow events have greater lateral extent in larger dune deposits (Hunter, 1981; Kocurek and Dott, 1981). Determining the proportions of wind-ripple and grainflow strata and the distribution of their occurrence within preserved sets is key to understanding the three-dimensional configuration of packages of facies, and this is most readily achieved through comparison to analogous outcrop examples.

Even though the stratification types described above record instantaneous flow configurations, general associations have been made between styles of stratification and the orientation of the original dune to the long-term palaeowind direction. In the case of large linear aeolian bedforms, slipfaces on which grainflows occur tend to be preferentially located on the middle and upper parts of the lee slopes (e.g. Sneh and Weissbrod, 1983) because such dune types tend to have large low-angle-inclined plinths at their bases where wind-ripple strata preferentially accumulate (McKee and Tibbitts, 1964). If the preserved sets are dominated by facies known to accumulate in the lower parts of the dune slope, such as wind-rippled facies, the implication is that the original dune either had low-angle-inclined plinths, commonly associated with larger bedforms; or that the dune was truncated and preserved at a very low level, implying that the original dunes were climbing at very low angles, which is another indication that the original bedform was large; larger bedforms are likely to respond only slowly to changes in sand availability (Lancaster, 1988b) and will therefore tend to climb at only shallow angles.

By contrast, other types of large dunes (e.g. transverse and barchanoid forms) tend to have slipfaces that extend directly to the base of the lee slope, and therefore to the bottom of the preserved set. In such dune types, grainflow facies will tend to be present close to the base of preserved sets (Kocurek and Dott, 1981). Although this is a general trend that has been observed, there are exceptions abound. In the Namib Desert, more than 250 m-high star forms have slipfaces which extend to the bases of the bedforms (Figure 1.12), and therefore using the criteria considered previously to reconstruct dune height or dune morphology would be problematic. Star dunes can also show arms that have simultaneously active transverse, oblique, and linear elements (Nielson and Kocurek, 1987), further complicating the issue. More robust criteria for identifying original dune morphology from subsurface datasets need to be made. From an applied perspective, disparity in identification of original aeolian bedform type can lead to misleading calculations of net reservoir in the subsurface. Identifying key features in outcrop or core data is essential to well-informed interpretations of aeolian dune type from subsurface data alone.

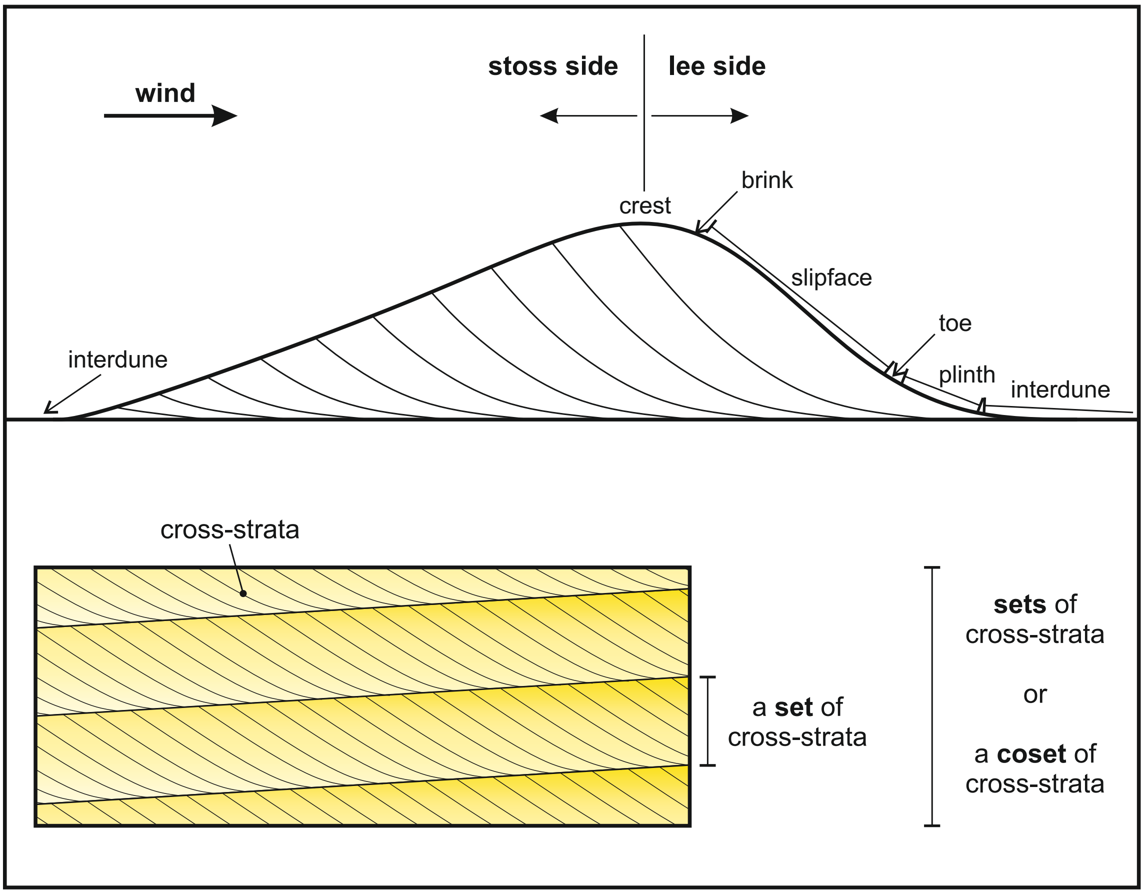

Figure 1.8. Summary of aeolian bedform terminology used in this research.

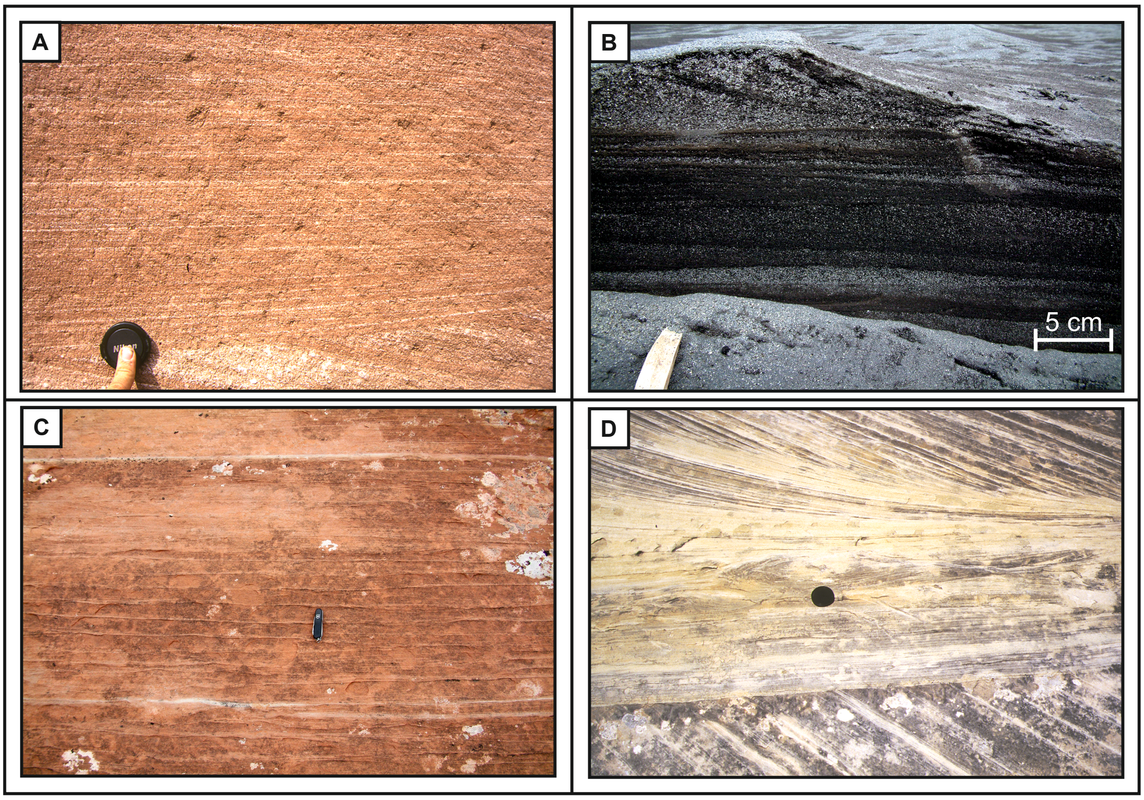

Figure 1.9. Examples of aeolian wind-rippled facies: a) Pinstripe lamination (*sensu* Fryberger and Schenk, 1988), Etjo Formation, Cretaceous, Namibia; b) Inversely graded translatent strata, Askja, Iceland; c) Sharply defined wind-ripple laminae interbedded with thin grainfall laminae. Lower Cutler Beds, Pennsylvanian–Permian, Utah, U.S.A; d) Wind-ripple strata on a dune plinth. Cedar Mesa Sandstone, Permian, Utah, U.S.A. (modified from Mountney, 2006a).

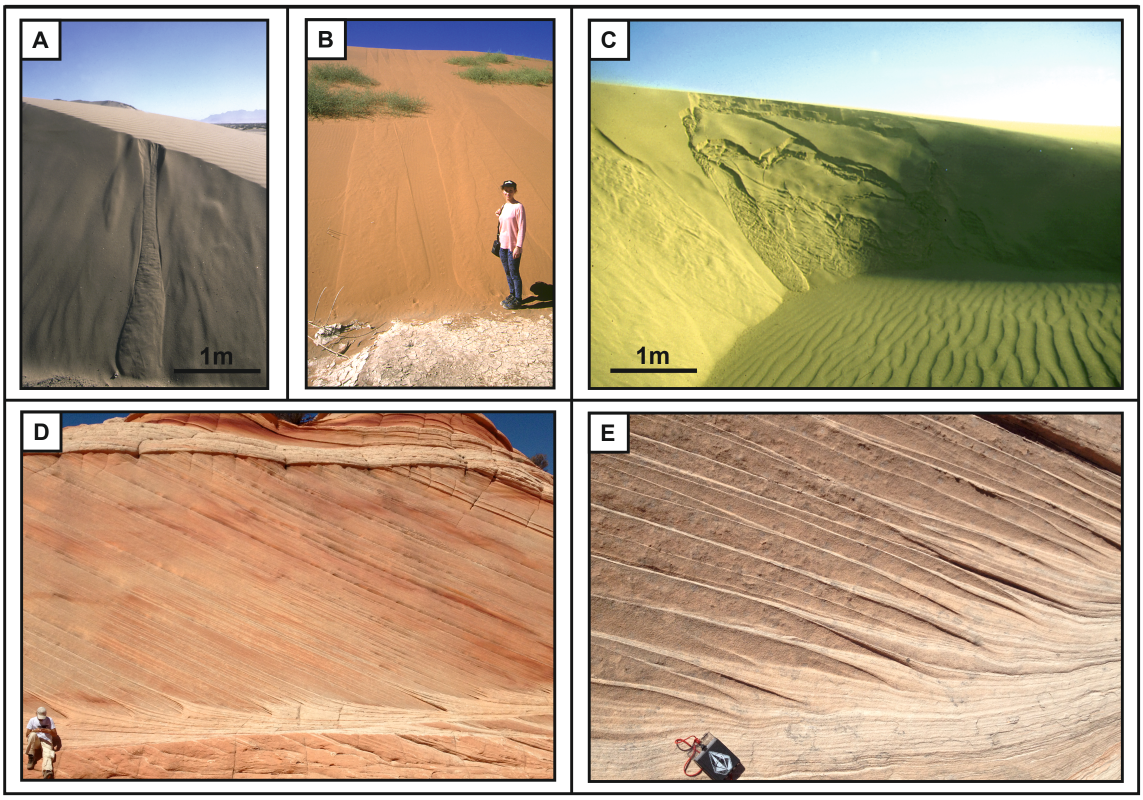

Figure 1.10. Examples of aeolian grainflows and the characteristic strata that they produce: a) Scarp recession grainflow, Namibia; b) Slump degradation grainflows, Namibia; c) Slab slide failure degenerates downslope into a slump degradation grainflow, Namibia; d) and e) Grainflow tongues pinching out into wind ripple strata. Navajo Sandstone, Jurassic, Utah (modified from Mountney, 2006a).

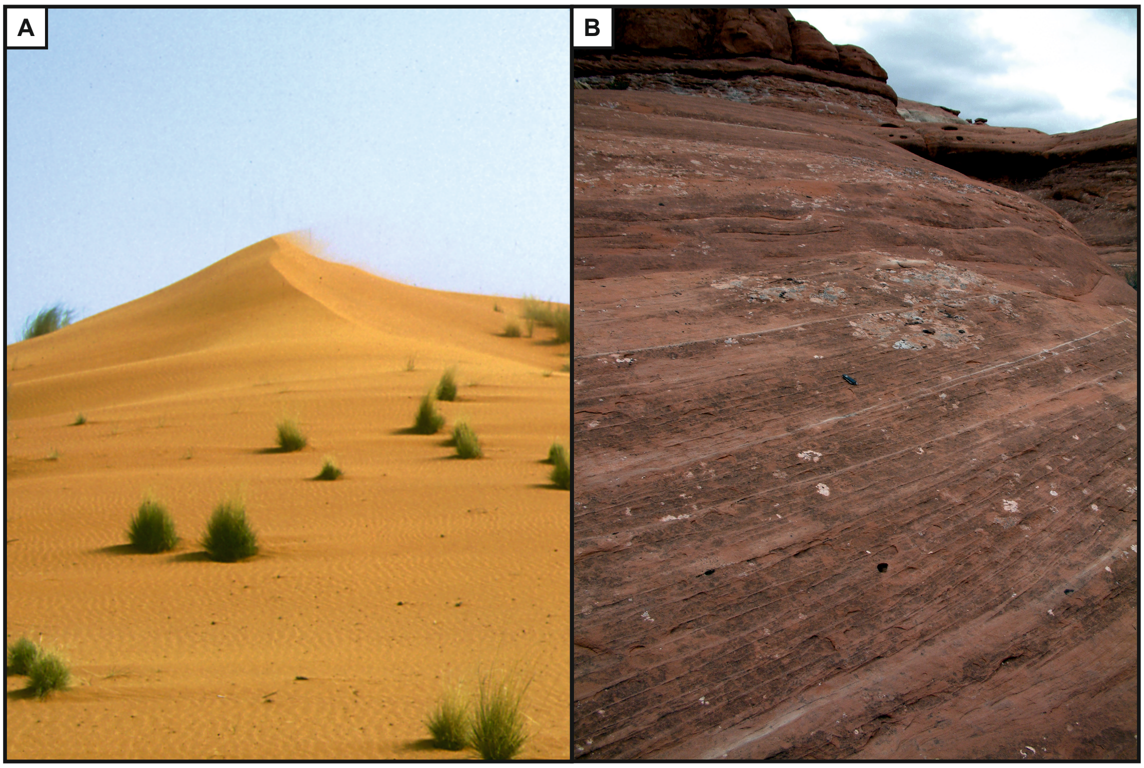

Figure 1.11. Examples of aeolian grainfall and the characteristic strata that it produces: a) Saltation of sand-sized particles over the brink of a dune to form a suspension cloud. Expansion of the airflow in the lee side depression results in a loss of carrying capacity and the grains fall onto the upper part of the lee slope as grainfall deposits. Kalahari Desert; b) Grainfall facies interbedded with wind-ripple strata. Individual grainfall units rarely exceed 5mm in thickness but tend to be laterally continuous along the strike of the cross bedding for several metres to tens of metres. Interbedded units of wind-ripple strata are thicker (1-2cm). Cedar Mesa Sandstone, Permian, Utah. Penknife for scale. (Modified from Mountney, 2006a)

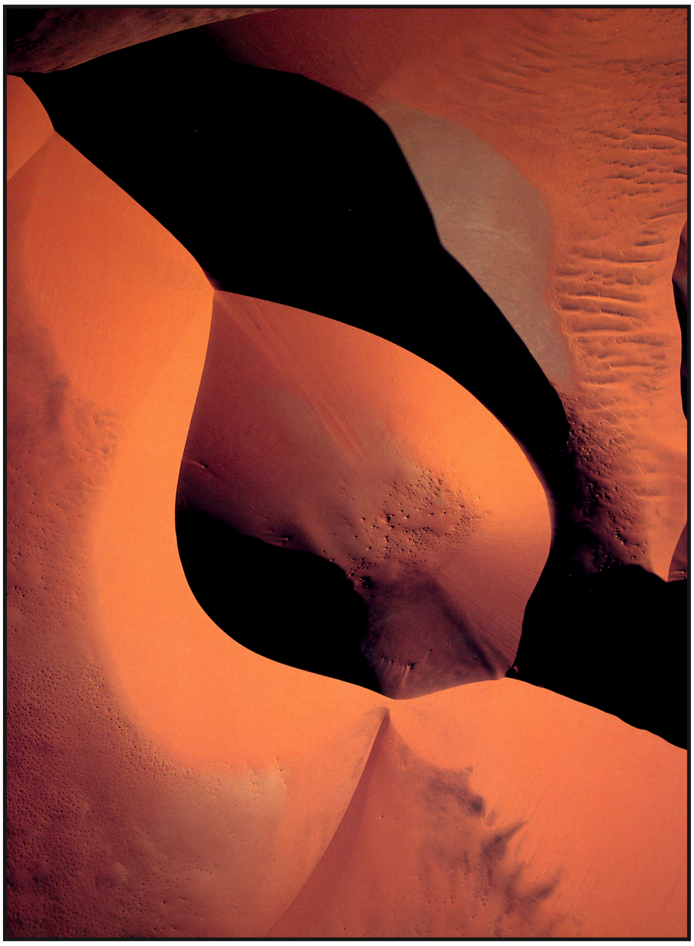

Figure 1.12. Amalgamated star draa with closely spaced pyramidal peaks. Note the widespread development of very large active slipfaces which extend from the draa crest lines across most of the bedform slope, and highly varied orientation of the draa slipfaces. The colour differences in the sediment reflect changes in composition, grain size and sorting between the draa slipface, draa lower flank and interdraa elements. Bedforms of varying height up to 250 m. Image reproduced with permission from Bernhard Edmaier.

1.5 – Architectural elements

The individual aeolian facies types described in Section 1.4 typically form predictable associations of facies, and these associations of facies are used as the building blocks of architectural elements (e.g. dune elements – Figure 1.13; interdune elements – Figure 1.14, Figure 1.15 and Figure 1.16; and non-aeolian elements – Figure 1.16). Successive grainflow avalanche events commonly occur in close association, and intercalated, with wind-rippled facies due to the tractional reworking on the slipface during the times between grainflow events (Hunter, 1977a; 1981; Figure 1.17). Grainfall deposits often form thin veneers that drape grainflow facies in dune slipface regions (Hunter, 1977a; 1977b; 1981), and are extensively preserved in close association with wind-rippled facies that have not been subject to reworking (Figure 1.11b), especially where such deposits form on slopes of low depositional dips or in interdune areas (Figure 1.9c). The relative proportions and distributions of facies associations are determined by the type of bedforms on which the processes responsible for their generation operated.

Architectural elements (i.e. three-dimensional sediment bodies with specific internal facies characteristics) are defined in accordance with their relationship between dune and interdune lithofacies (and their style of bundling into packages that comprise associations of basic facies types in various proportions), scale and degree of amalgamation of cross-bedded units, characteristics of cross-stratified foresets, orientation of these structures and characteristics of bounding surfaces of varied hierarchy (Spalletti et al., 2010).

1.5.1 – Aeolian dune architectural elements

Aeolian dune architectural elements represent the deposits that accumulated on the lee slope of a migrating dune. The preserved form of these elements does not typically reflect the morphology of the formative dune due to the processes inherent in the preservation of such elements. Dune elements are composed of sets of cross-stratified sandstone of predominantly grainflow facies, with intercalations of wind-rippled facies and often thin veneers of grainfall facies (Figure 1.13). The grainflow facies typically thin and pinch-out down slope, and are intercalated with the wind-ripple facies which dominate the deposition at the base of slope (Figure 1.13; Figure 1.17), and in interdune areas. Grainfall facies occupy the upper areas of the dune crest, and are also found intercalated with wind-rippled facies on the stoss-slope on the dune. The relative distributions and proportions of these facies associations within individual dune elements is largely controlled by the morphology and style of migratory behaviour of the original dune form which migrated and accumulated to preserve the sets of cross-strata.

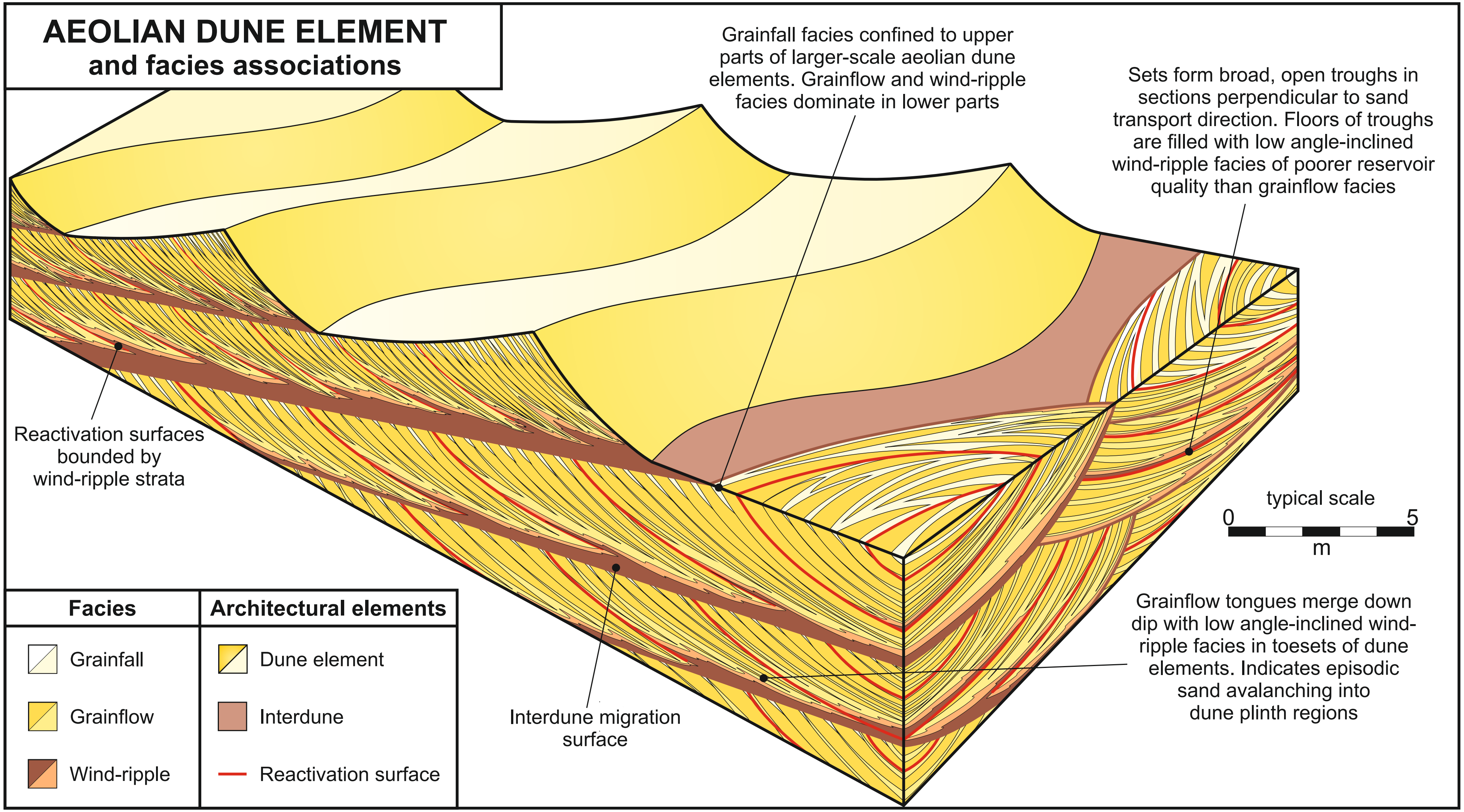

Figure 1.13. Schematic diagram depicting aeolian dune elements and their common internal compositions, formed from a variety of associations of fundamental aeolian lithofacies types. Modified from Mountney (2006b).

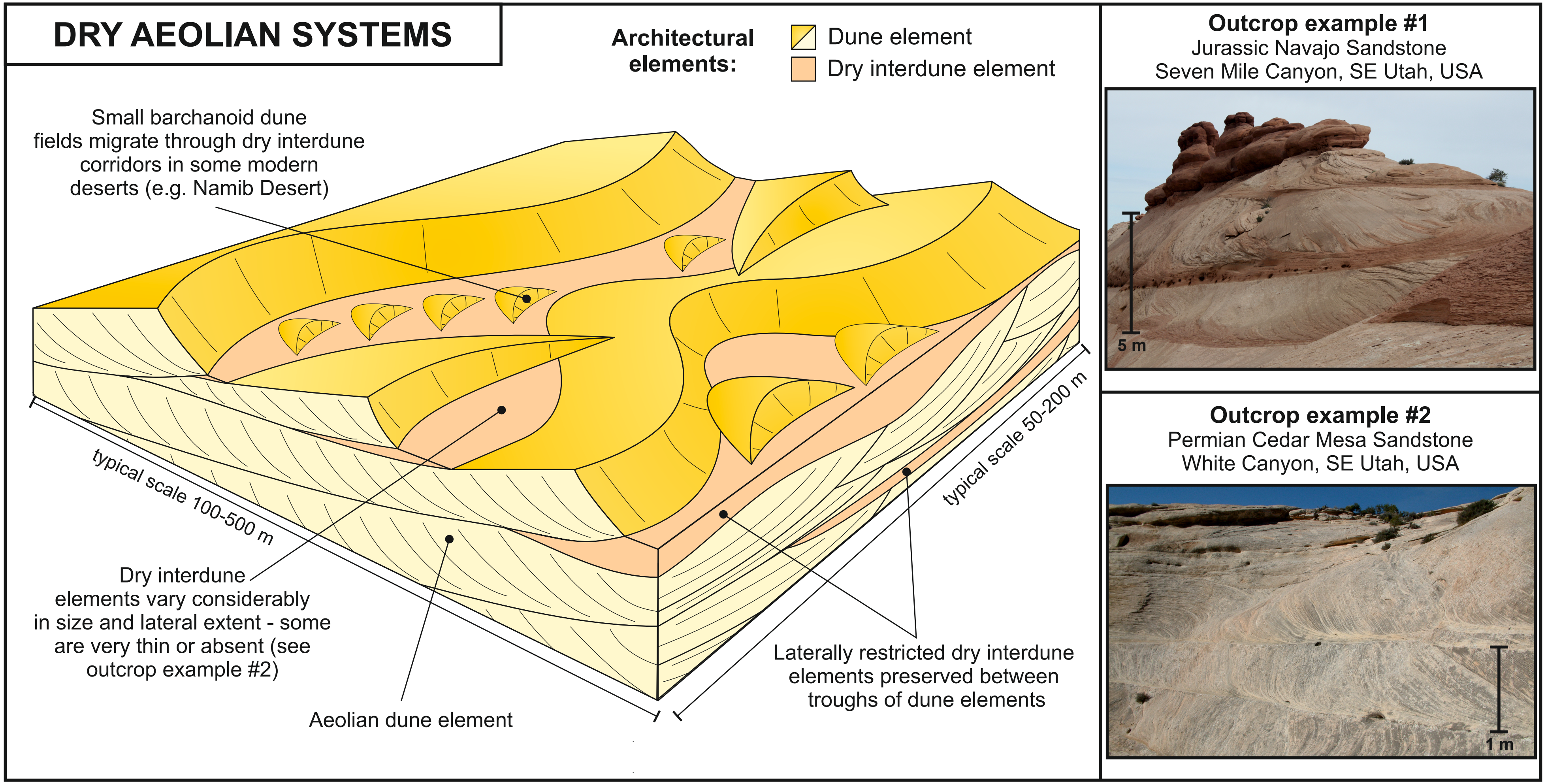

Figure 1.14. Schematic diagram depicting dry aeolian systems, with smaller barchanoid dunes migrating through the interdune corridors of the main bedforms. In dry aeolian systems, dune construction occurs whereby bedforms grow until interdune flats are reduced to isolated depressions between bedforms; the dry interdune is dominated by wind-rippled facies. Accumulation of such systems leads to stacked cross-bedded sets separated by so-called interdune migration bounding surfaces. Outcrop examples of dry aeolian systems: 1) Jurassic Navajo Sandstone, Seven Mile Canyon, SE Utah, USA; 2) Permian Cedar Mesa Sandstone, White Canyon, SE Utah, USA. Modified from Bristow and Mountney (2013); in part courtesy of Oliver Wakefield.

1.5.2 – Interdune architectural elements

The geometry of interdune architectural elements is controlled by the spacing and morphology of the aeolian dunes, and ranges from spatially isolated hollows, to narrow interdune corridors, to extensive interdune flats. As the dunes increase in size from an erg margin to an erg centre, so the length, width and connectivity of the interdunes tends to decrease (Al-Masrahy and Mountney, 2013). The original bedform morphology of the dune elements also exerts a fundamental control on the geometry of the interdune regions; straight-crested bedforms give rise to straight, open interdune corridors, whereas dunes with highly-sinuous crestlines will generate interdune flats which are divided into isolated closed areas. The phase of crestline sinuosities through successive bedforms also exerts a control on the geometry of the interdune flats (Figure 1.14; Figure 1.15; Figure 1.16; Figure 37 in Mountney, 2006a).

Interdune flats between the aeolian dune elements are defined as dry, damp or wet (Kocurek, 1981). Dry interdunes show no evidence for sedimentation controlled or influenced by water and are dominated by wind-rippled facies (Figure 1.14); damp interdunes have a depositional surface which is in contact with the capillary fringe of the water table, and is characterised by adhesion structures, plants, roots and burrows (Figure 1.15); the depositional surface of wet interdunes is periodically or episodically inundated with water, as a consequence of the water table rising above or to the depositional surface (Mountney, 2006a). These wet interdune areas are commonly associated with non-aeolian elements, such as fluvial deposits and carbonate ponds (Figure 1.16).

1.5.3 – Non-aeolian architectural elements

Non-aeolian architectural elements are found in aeolian sedimentary systems which are intimately associated with a range of other depositional environments (Figure 1.16), and include ephemeral fluvial systems, alluvial fans, permanent lake bodies, and shoreline and shallow marine systems (Chan and Kocurek, 1988; Kocurek et al., 2001; Jordan and Mountney, 2010; 2012; Wakefield and Mountney, 2013). The boundaries between the various aeolian and non-aeolian architectural elements may be either sharp or gradational, and non-aeolian architectural elements may sporadically occur within otherwise exclusively aeolian systems (e.g. ephemeral fluvial systems in the Namib Sand Sea).

The architectural elements described above have specific geometries and styles of juxtaposition which arise as a consequence of the migration of hierarchies of aeolian bedforms of differing sizes and shapes, moving at varying rates and in varying directions relative to one another. They form the building blocks of aeolian reservoir successions and, in most examples, both the elements themselves and the lithofacies of which they are composed internally exhibit a strong preferred directional heterogeneity due to the inherent preferred orientation of layering of laminations and beds of facies, often in a complex nested manner (Weber, 1987; Chandler et al., 1989; Krystinik, 1990).

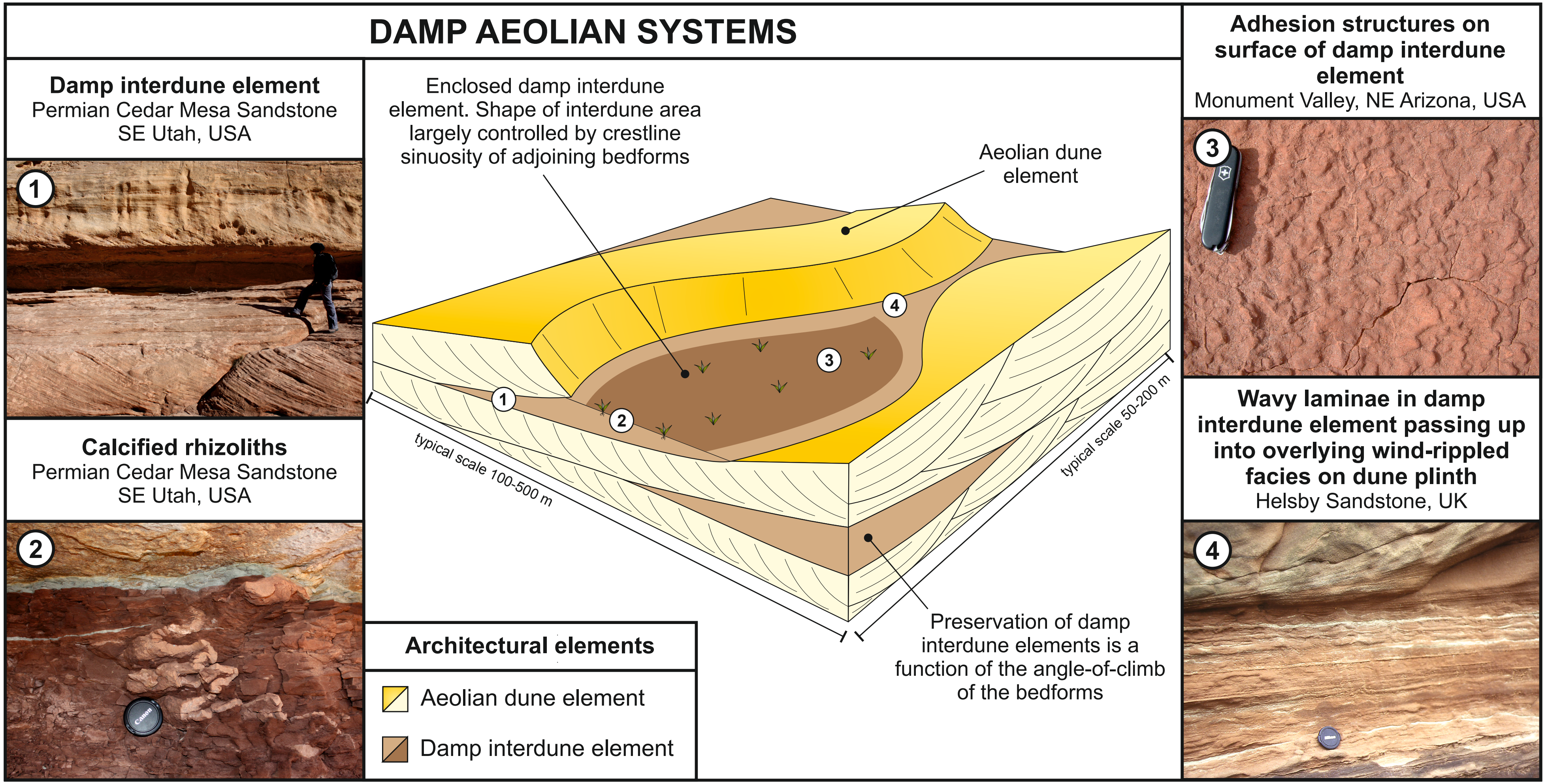

Figure 1.15. Schematic diagram depicting damp aeolian systems. Damp interdune elements indicate deposition in close association with the water table. Deposition of damp interdune elements in low-relief areas of migrating dunes, therefore closely associated with cross-bedded dune sets of aeolian dune architectural elements. Often found in close proximity of palaeosols.

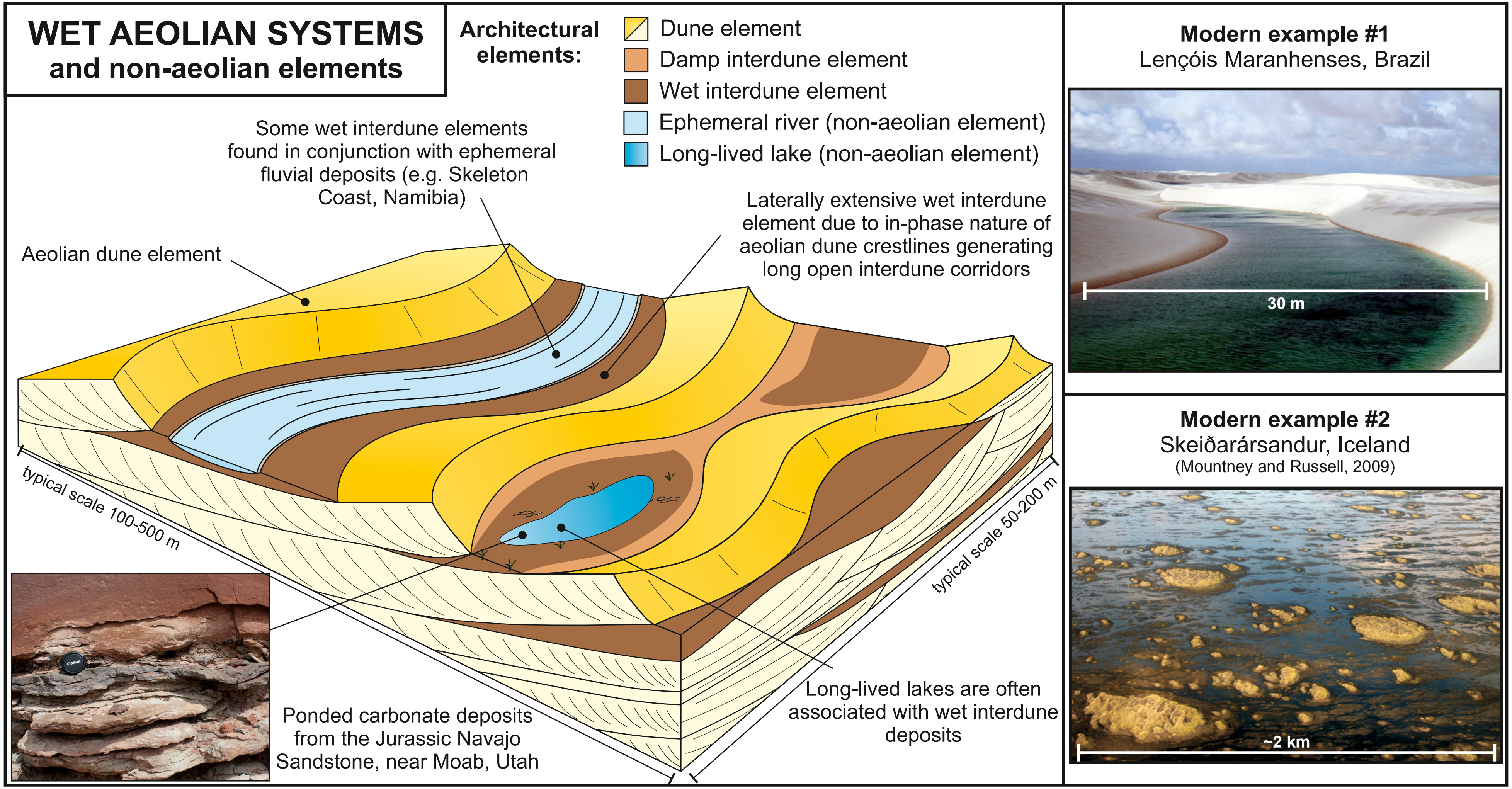

Figure 1.16. Schematic diagram depicting wet aeolian systems, with a contemporaneous fluvial system and long-lived lake (non-aeolian elements). This is the result of the depositional surface being periodically or episodically inundated with water, as a consequence of the water table rising above or to the depositional surface. Modern examples of wet aeolian systems: 1) Lençóis Maranhenses, Brazil (Image licensed under the Creative Commons Attribution 2.0 Generic license); 2) Skeiðarársandur, Iceland (Mountney and Russell, 2009).

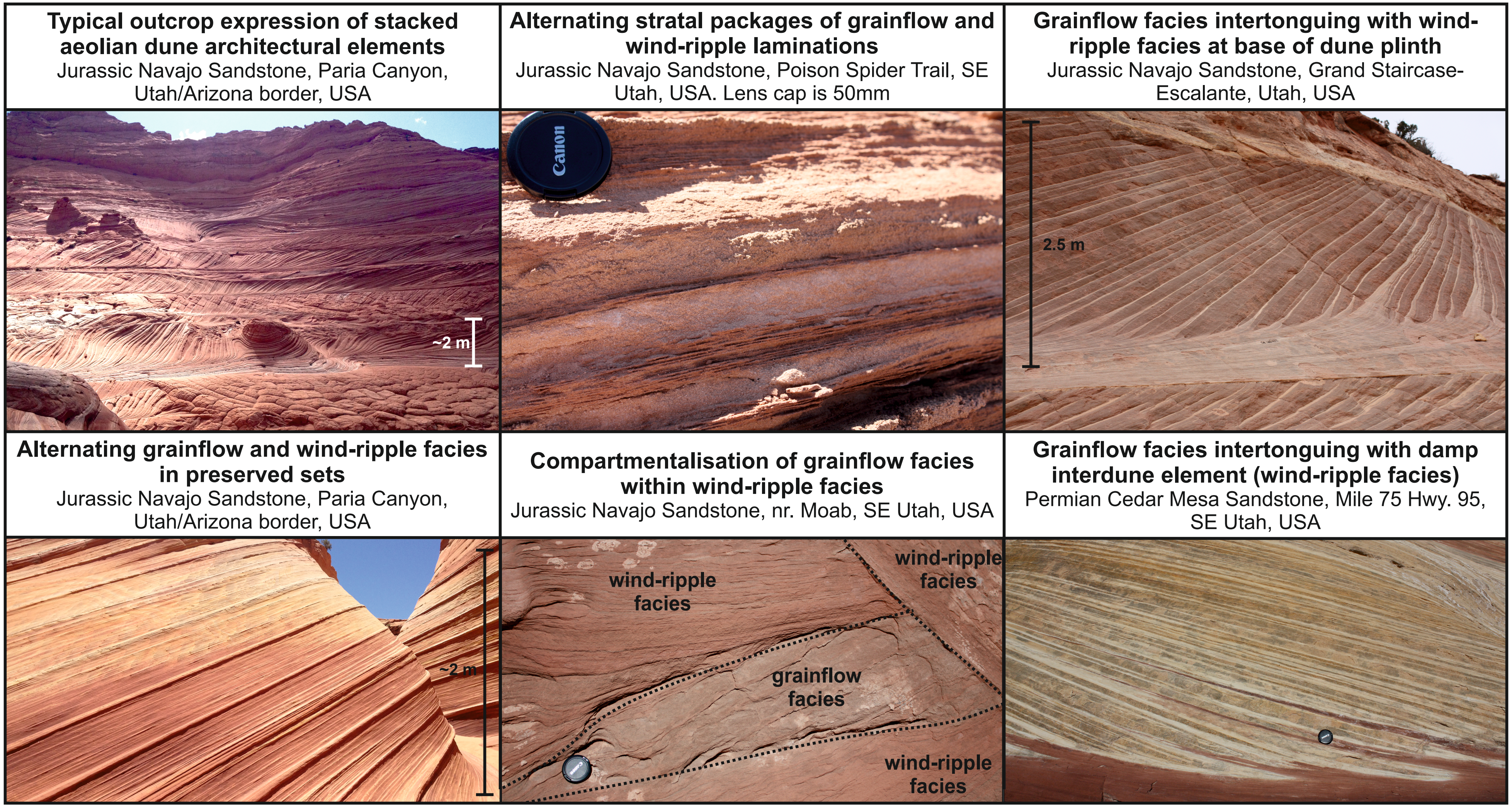

Typical outcrop expression of stacked aeolian dune architectural elements
Jurassic Navajo Sandstone, Paria Canyon, Utah/Arizona border, USA

Alternating stratal packages of grainflow and wind-ripple laminations
Jurassic Navajo Sandstone, Poison Spider Trail, SE Utah, USA. Lens cap is 50mm

Grainflow facies intertonguing with wind-ripple facies at base of dune plinth
Jurassic Navajo Sandstone, Grand Staircase-Escalante, Utah, USA

Alternating grainflow and wind-ripple facies in preserved sets
Jurassic Navajo Sandstone, Paria Canyon, Utah/Arizona border, USA

Compartmentalisation of grainflow facies within wind-ripple facies
Jurassic Navajo Sandstone, nr. Moab, SE Utah, USA

Grainflow facies intertonguing with damp interdune element (wind-ripple facies)
Permian Cedar Mesa Sandstone, Mile 75 Hwy. 95, SE Utah, USA

Figure 1.17. Examples of aeolian dune architectures with typical facies associations and features observed in aeolian dune architectural elements from outcrop studies. Packages of wind-ripple facies commonly entirely encase packages of grainflow facies with higher porosity and permeability values.

1.6 – Facies control on reservoir properties

Different types of bedforms can yield markedly different distributions of facies arrangements within preserved accumulations, and each of these will in turn have their own distinct set of reservoir properties. Given that a clear relationship between stratification type and reservoir quality has already been noted (Figure 1.18; Figure 1.19), the ability to recognise and predict the arrangement of packages of various stratal types is important for reservoir prediction. For the majority of aeolian reservoirs, production behaviour and characteristics are primarily influenced and controlled by original sediment fabric (grain size distribution), though secondary alteration of sediment fabric by diagenesis is also important (e.g. Mou and Brenner, 1982).

Each individual lithofacies type described in Section 1.4 has specific thickness, continuity, grain size and sorting characteristics. Typically, the lower in the dune the sample originates, the poorer it's reservoir quality (Krystinik, 1990) although there are exceptions. There are instances where facies normally associated with the upper part of the slipface (e.g. grainflow avalanches) extend much lower down the lee slope than expected, such as in cases where the original dune had a steep plinth and facilitated the grainflow avalanches terminating near the base of the lee slope. In terms of hydrocarbon production, it is usually preferential to target regions of the subsurface stratigraphy that are dominated by a high proportion of grainflow and grainflow-dominated aeolian dune strata. This is because grainflow strata tend to form packages of well-sorted, loosely-packed sandstone with permeabilities that are typically one to three (or more) orders of magnitude greater than those composed predominantly of packages of grainfall and wind-ripple strata and which dominate in some aeolian elements (Figure 1.18; Figure 1.19; Chandler et al., 1989; Prosser and Maskall, 1993; Howell and Mountney, 2001; Romain and Mountney, 2014).

Porosity values for wind-rippled sands from the Jurassic Nugget Sandstone in the Utah-Wyoming thrust belt, USA, range between 3% - 12% (average 7-8%), and horizontal permeabilities are commonly < 1mD, ranging from hundredths to tens of mD's (Lindquist, 1998). By contrast, in the same succession, grainflow strata show porosity ranges from approximately 5 to 25% (average 12-13%), and horizontal permeabilities from several mD's to hundreds of mD's (Lindquist, 1998). Similar relationships are observed for porosity and permeability values from aeolian facies in the Auk Formation, Central North Sea (Figure 1.19; Follows, 1997; Prosser and Maskall, 1993), and this is explored in more detail in Chapter 4 (Section 4.4). Although the recorded porosity and permeability values for wind-rippled facies are by no means substandard when compared to more extensive and significant baffles or barriers to flow, such as wet interdune facies; in reservoirs where the hydrocarbon fluids have a relatively high viscosity (e.g. Auk Formation, Central North Sea, UK), fluid flow is especially sensitive to lithofacies arrangements (Chandler et al., 1989; Howell and Mountney, 2001).

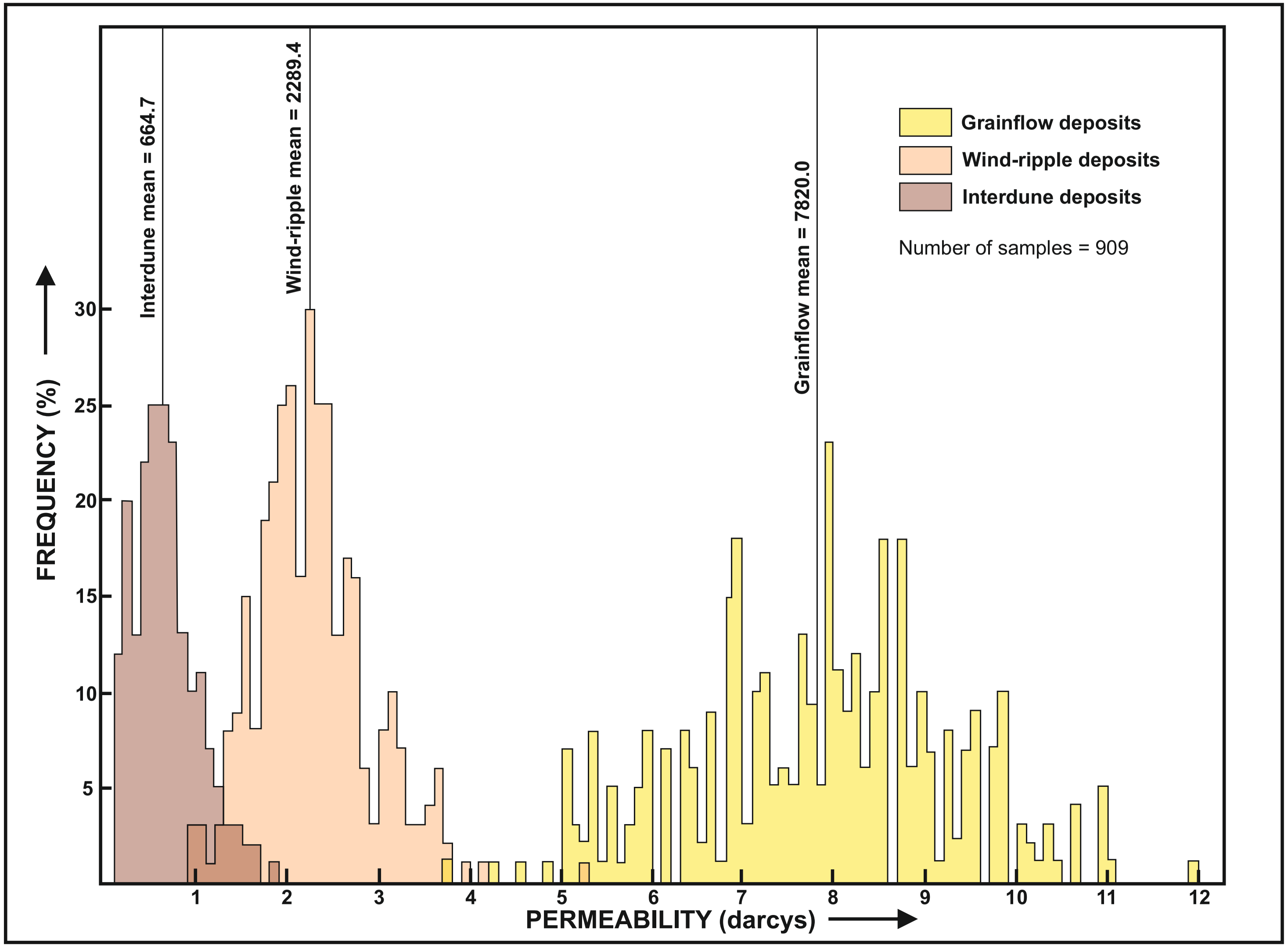

Figure 1.18. Histogram showing Page Sandstone permeameter data for various aeolian facies types. Modified from Chandler et al. (1989)

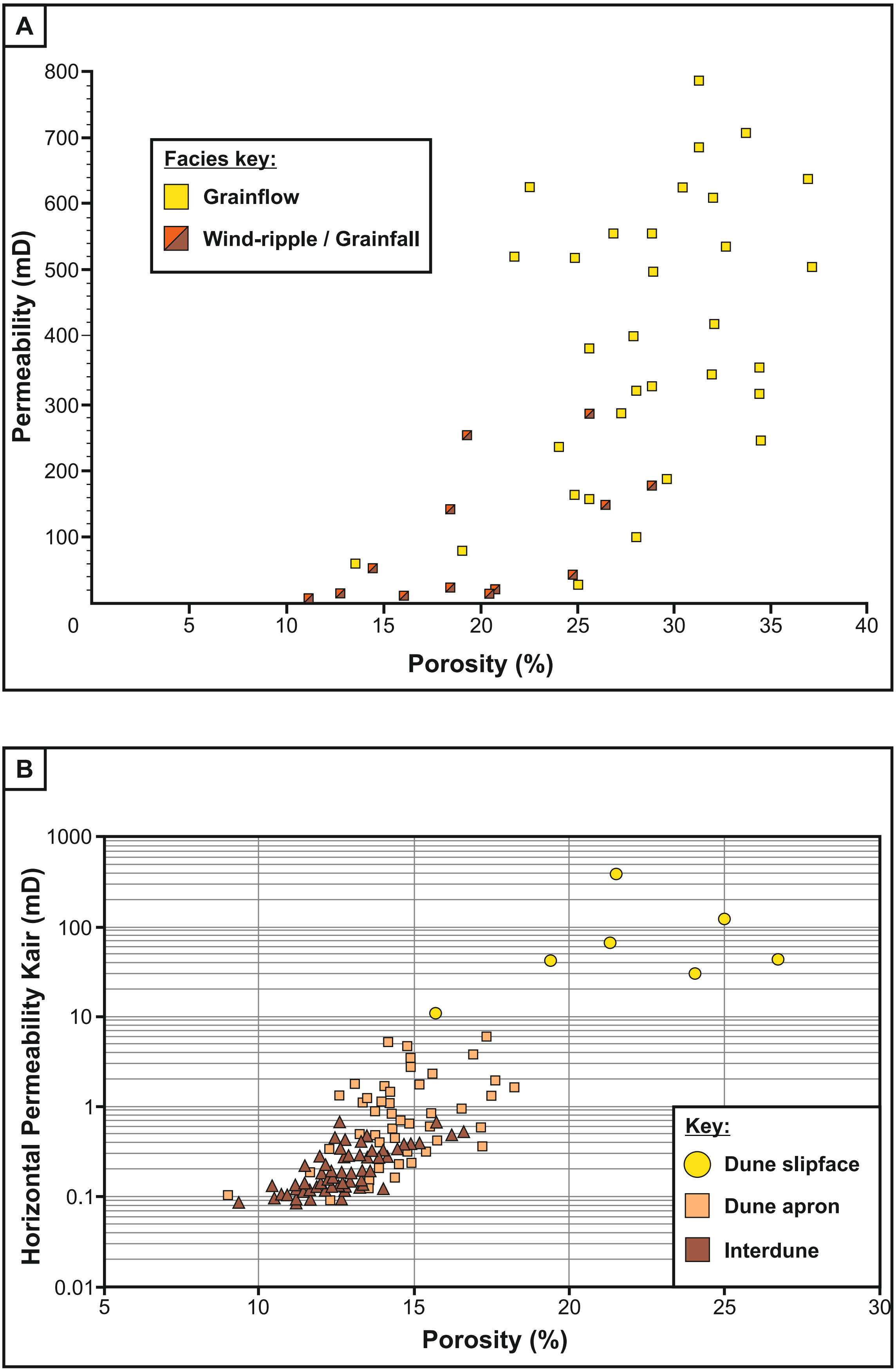

Figure 1.19. Porosity/permeability data for sedimentary facies in the Permian Auk Formation, Rotliegend Group, Central North Sea. It is evident that there is a strong sedimentological control on observed porosity and permeability, with the presence of grainfall or wind-rippled facies shown in a) resulting in significantly lower recorded porosities and permeabilities: a) Modified from Prosser and Maskall (1993); b) Modified from Follows (1997).

Given this inherent disparity in reservoir quality for different aeolian facies types, a method to enable the prediction of the spatial occurrence of the original depositional processes that occurred on dunes and in interdunes, and the resultant distribution of lithofacies in preserved aeolian architectural elements is therefore essential (Lewis and Couples, 1993).

1.6.1 – Directional permeability

Understanding the detailed arrangement of the style of heterogeneity present in architectural elements is crucial for reservoir prediction as this exerts a primary control on porosity and permeability structure within aeolian reservoirs and therefore dictates production flow rates and patterns within complex aeolian reservoir bodies (Nagtegaal, 1979; Heward, 1991; Ellis, 1993; Stanistreet and Stollhofen, 2002; Garden et al., 2005; Bloomfield et al., 2006). Observations from the literature indicate that permeabilities along the axis of aeolian dunes average 4 to 25 times greater than those parallel with transport direction (Krystinik, 1990); aeolian dune type, and therefore dune morphology, also affects directional permeability calculations (Figure 1.20).

For a predominantly unidirectional wind system, straight-crested transverse or oblique dune lee faces should have less azimuth variability than more sinuous-crested varieties (Figure 1.20; Lindquist, 1988). The dipmeter responses from Lindquist (1988) are associated with the dune lee slipface, and therefore absolute permeability directions can be determined. The components of preferred permeability have not only a value, but also a length attribute, which becomes crucial if the value of permeability for each lithofacies type is considered equal across the reservoir volume. The shortest permeability component is oriented up the lee slope, and the longest permeability component is along the strike of the dune, which is restricted by the lateral extent and morphology of the dune (Lindquist, 1988). The linear dune system represented by the Jurassic (Oxfordian) Norphlet Sandstone at Mobile Bay has permeability values that are higher in a direction parallel to the linear dune crests (Story, 1998).

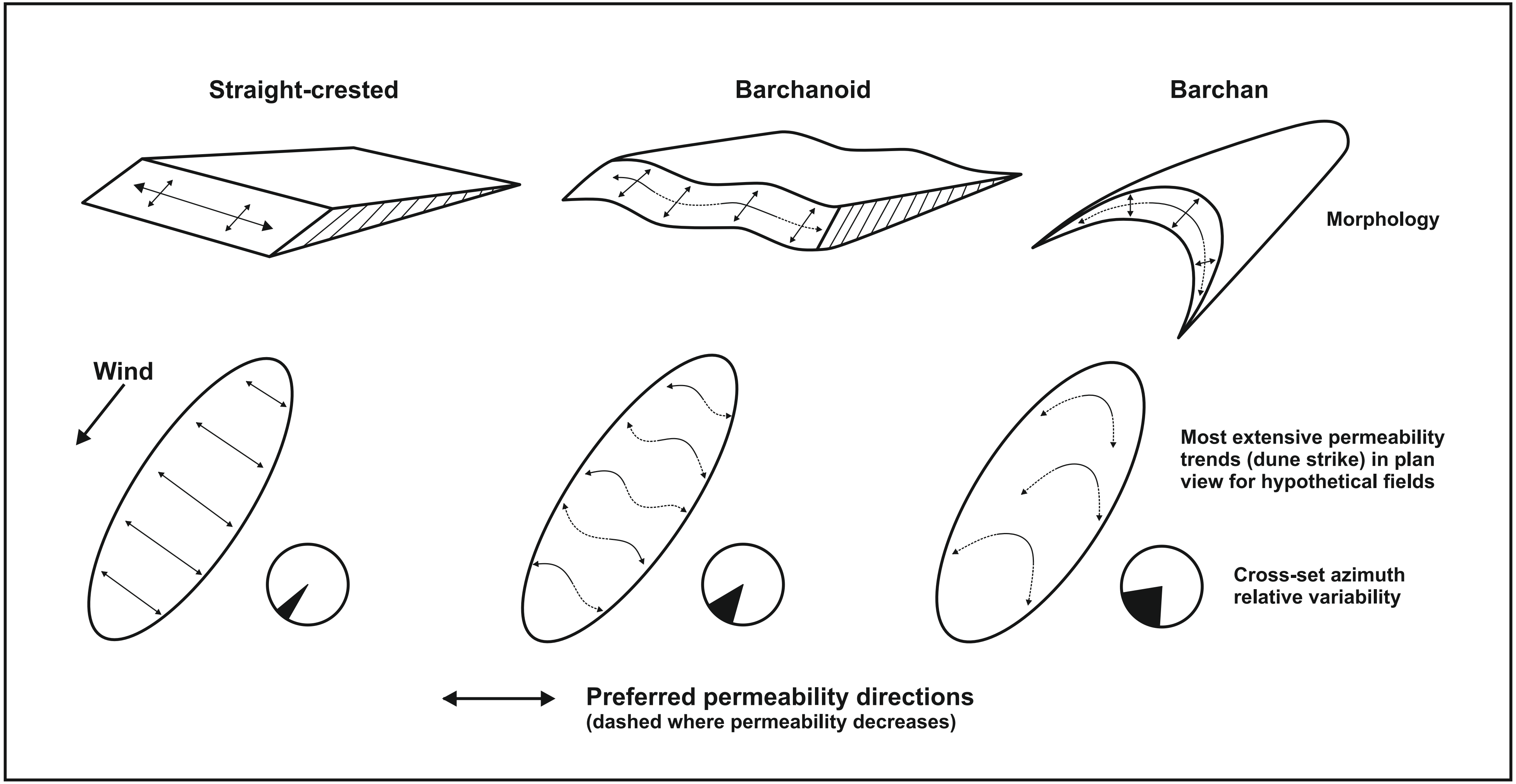

Figure 1.20. Trend and continuity of preferred permeability directions for three common dune morphologies. Relative differences in azimuth variability for lee face cross-sets are also shown. Note the perpendicular relationship between bedding-plane dip-azimuth and the trend of the most extensive permeability line. After Lindquist (1988).

1.7 – Thesis structure

This thesis represents an analysis and discussion based around three papers prepared for publication in internationally recognised academic journals. The structure of this thesis reflects this; some chapters reiterate key background information regarding the previous state of research in the literature.

Chapter 2 – Reconstruction of three-dimensional aeolian-dune architecture from one-dimensional core data through adoption of analogue data from outcrop

The majority of information relating to subsurface aeolian deposits at sub-seismic scale is one-dimensional in nature, and the ability to reliably reconstruct the larger-scale architectural elements which make up the deposit is problematic. Estimating volumetric sand content and therefore porosity-permeability estimates for subsurface datasets is difficult, as the geometries of dune, interdune and extradune deposits are poorly constrained. These elements have distinct reservoir properties based on the composition and distribution of facies which all have individual porosity-permeability characteristics. A reliable method to reconstruct the shape, style of juxtaposition and internal facies arrangements of aeolian elements in three-dimensions is required. This chapter outlines a method for this reconstruction based on detailed characterisation of individual aeolian dune sets and relationships between neighbouring dune and interdune elements. This is achieved through outcrop studies of the Permian Cedar Mesa Sandstone and the Jurassic Navajo Sandstone in southern Utah.

Empirical relationships have been devised from these outcrop studies, regarding the relationship between preserved set thickness, individual grainflow thickness, original bedform dimensional properties (e.g. wavelength and height), the likely proportion of the original bedform that is preserved to form a set, the angle-of-climb of the system, and the likely along-crest variability of facies distributions in sets generated by the migration of sinuous-crested bedforms. Therefore parameters that can be measured from analogous one-dimensional core data can be related to larger scale aeolian elements in the subsurface. These empirical relationships underpin a methodology to reconstruct aeolian geometry from one-dimensional subsurface datasets alone. This methodology allows for the reconstruction of larger scale sedimentary architecture and therefore regional reservoir stratigraphic heterogeneity.

Chapter 3 – Modelling facies distributions and heterogeneity in aeolian reservoir successions

If only one-dimensional core or seismic data is available, the determination of expected facies distributions and their resultant architectures in the subsurface is challenging, and often equivocal. There is potential for ambiguous interpretations used as a basis for exploration, with reservoir models failing to effectively account for observed reservoir performance.

This chapter outlines a method to reliably reconstruct expected facies distributions using three-dimensional quantitative forward modelling software (Rubin, 1987a) for a range of end-member aeolian bedform types and styles of migratory behaviour, which allow for autogenic and allogenic controls and the resultant change in aeolian bedform architecture to be modelled. This provides quantitative estimates of three-dimensional sand body geometries for a range of aeolian bedform types with individual migration and accumulation styles. It is apparent that modest changes in bedform architecture can have a marked difference in net reservoir distribution and connectivity. Furthermore, bedforms with very different morphologies can generate net reservoir distributions that are very similar and hard to distinguish from one another. The likely geometry and degree of interconnectivity of net reservoir facies in three-dimensional space has also been determined for a range of bedform styles. This demonstrates how facies distributions on different bedform types can enhance or deplete overall reservoir quality.

Chapter 4 – Reconstruction of linear dunes from ancient aeolian successions using subsurface data: a case study from the Permian Auk Formation, Central North Sea, UK

Deposits of aeolian bedforms are highly variable over very short lateral distances; they show lithological heterogeneity at a number of scales caused by various autogenic and allogenic controls, and therefore elucidation of three-dimensional architecture and original formative processes is problematic. The Permian Auk Formation is an aeolian reservoir interval which is known only from the subsurface. This chapter describes a method to reconstruct original bedform morphology and style of migratory behaviour using only subsurface data and information from analogous modern dune fields.

The Auk Formation was previously interpreted as arising from the migration and accumulation of transverse bedforms (e.g. Glennie et al., 1978; 1998a; Heward, 1991), including barchanoid forms, with linear bedforms interpreted from some parts of the succession (e.g. Steele, 1983). Although variability in dune morphology is known across large dune fields (e.g. Namib Desert; Lancaster, 1983), there are few documented examples from ancient successions. Linear dunes are underrepresented in the rock record; therefore analogues are few, as are quantitative and qualitative data for the accumulation of linear bedforms. Reconstruction of aeolian bedform type from subsurface data is important as most aeolian bedforms are only known in the subsurface. From an applied perspective, different dune types have distinct distributions of facies, therefore also distinct heterogeneity and arrangement of net reservoir packages (as described in Chapter 3).

Chapter 4 outlines a method whereby a detailed core and well log analysis, analogous outcropping successions and modern dunes was utilised to reconstruct original bedform type, size, and style of migratory behaviour for a succession of linear draa in a large dry aeolian system. This research is therefore a valuable case study of linear bedforms which are under recognised in literature.

Chapter 5 – Modelling three-dimensional lithofacies distributions in subsurface aeolian successions: Permian Auk Formation, Central North Sea, UK

As the Auk Formation is only known from the subsurface (one-dimensional core and well logs), modelling the geological complexities and lithological heterogeneities present in the succession is highly subjective. Quantitative estimates of architectural element geometries and their internal facies compositions are needed, and therefore also a technique to reconstruct three-dimensional aeolian architecture from one-dimensional core data. There is a growing need for more detailed forward models to account for stratigraphic heterogeneity in reservoirs if recovery of reserves is to be maximised, especially in systems like Auk where the high viscosity of hydrocarbons makes fluid flow especially sensitive to arrangements of lithofacies.

The type of bedforms responsible for the accumulation of the Auk Formation and their style of migratory behaviour was determined in Chapter 4. To characterise the three-dimensional architecture of the bedforms and their preserved architectural elements, the three-dimensional bedform modelling software of Rubin (1987a) and Rubin and Carter (2006), initially introduced in Chapter 3, was used to reconstruct the three-dimensional spatial arrangement of sets and their internal facies arrangements. Six models are presented which account for the variations observed in Chapter 4 in different parts of the Auk succession. It is apparent that subtle variations in original bedform architecture can have significant effects on distribution and connectivity of net reservoir facies. The method outlined here is a valuable technique which can be applied to other reservoir successions where core data do not necessarily provide insight on sand body geometry, orientation and style of interconnectivity.

Chapter 6 – Synthesis and key advances

Chapter 6 is a synthesis of the interpretations made in Chapters 2, 3, 4 and 5, and provides a further interrogation of the bedform models which are initially introduced in Chapters 3 and 5. This is the key chapter that brings together all the specific findings from the earlier chapters and convolves the findings into a series of generic results, ideas and models that can then be applied as a unifying concept to the modelling of aeolian stratigraphic complexity. Several fundamental concepts are discussed, such as the ability to relate ancient preserved sets of aeolian strata to the morphology and migratory behaviour of the original bedforms, and to the conditions that enabled accumulation and preservation. The effect that original bedform morphology and migratory behaviour has on the resultant reservoir quality is also investigated. By interrogating the bedform models initially introduced in Chapters 3 and 5, overall expected net reservoir calculations for a number of different bedforms has been calculated, supplemented by the expected facies distributions on these different bedforms as well as an indication on their individual preferred permeability directions at a bed- and architectural element-scale.

Chapter 7 – Conclusions and future work

Chapter 7 provides a concise overview of the information presented in this thesis, in view to consolidate the research aims and objectives outlined in Section 1.2. It makes suggestions on future work, postulating additional research questions which have arisen as a result of this research, and suggesting where future research efforts in this field should be focussed.

Chapter 2 – Reconstruction of three-dimensional aeolian dune architecture from one-dimensional core data through adoption of analogue data from outcrop

---

A version of this chapter has been published:

Romain, H.G. and Mountney, N.P. (2014) Reconstruction of three-dimensional eolian dune architecture from one-dimensional core data through adoption of analog data from outcrop. American Association of Petroleum Geologists Bulletin, 98, 1-22.

2.1 – Introduction

Exploration and asset appraisal teams working in hydrocarbon companies typically have access to a varied set of data derived from core and well log investigations relating to the sedimentology of deposits that make up potential subsurface reservoir intervals. However, at the sub-seismic scale, such datasets are almost exclusively one-dimensional in form, meaning that determination of sedimentary system type and elucidation of the three-dimensional geometry of the various architectural elements present in a reservoir volume, and their reciprocal relationships to one another, are usually highly subjective, resulting in potentially ambiguous interpretations and the postulation of equivocal depositional models (Kocurek 1988; Schenk, 1990; North and Boering, 1999; North and Prosser, 1993). This is especially true for aeolian reservoir intervals where the ability to reliably correlate between neighbouring wells – even those spaced only a few hundred metres apart, such as deviated sidetracks – is severely hindered by the absence of beds or bounding surfaces that can demonstrably be shown to serve as reliable markers for correlation purposes (Mountney, 2006a). In many cases, the inability to even establish the presence of features regarded to be reliable indicators of palaeo-horizontal in preserved aeolian reservoir successions is highly problematic (Kocurek, 1988; 1991). This presents difficulties when estimating volumetric sand content and regional porosity-permeability distributions for aeolian reservoirs, where the geometries of the various dune, interdune and extradune elements present within the overall three-dimensional rock volume are poorly constrained in the subsurface (e.g. Nagtegaal, 1979; Heward, 1991).

The aim of this study is to demonstrate how a suite of predictable sedimentological features present in aeolian successions can be used to relate detailed sedimentary architectural relationships observable in core and well log data to the larger-scale sedimentological elements of aeolian dune and interdune successions, to enable the gross-scale reconstruction of aeolian architecture, including estimates of bedform and interdune type, and bedform height, wavelength and spacing. Specific objectives of this study are as follows: (i) to describe the small-scale stratigraphic relationships expected for various different types of aeolian bedform morphologies and their resultant preserved deposits arising as a product of aeolian bedform migration and accumulation; (ii) to show how the sedimentological attributes of modern aeolian systems and ancient outcrop successions can be used to quantify predictable trends in small-scale aeolian architecture, and to demonstrate the style of occurrence of these features within larger scale elements (Figure 2.1); and (iii) to develop and demonstrate a workflow to enable first-order reconstruction of original dune and interdune morphology and preserved three-dimensional architecture from measurements made directly from the limited data provided by one-dimensional cores and well logs through employment of a series of empirical relationships.

Aeolian dunes of different morphological type exhibit varying yet predictable configurations of primary depositional facies (principally packages of grainflow, wind-ripple and grainfall strata) and associations of such facies (Hunter, 1977a; 1977b; 1981; Kocurek and Dott, 1981). The distribution of associations of these facies tends to vary predictably over the surface of individual modern aeolian bedforms as a function of the various aeolian processes that operate on the flank, lee-slope, stoss-slope and brink areas of bedforms (Hunter, 1977a), meaning that primary lithological characteristics such as grain size distribution, grain packing, and styles of small-scale lamination are also predictable (Livingstone, 1987).

In most systems, the mechanics by which aeolian bedforms and their constituent stratal packages of associated facies undergo accumulation is dictated by the style by which bedforms undertake migration synchronously with a rise in the accumulation surface (Kocurek, 1988; Kocurek and Havholm, 1993), leading to bedform climbing (Rubin and Hunter, 1982) and the accumulation of sets of cross-strata. Although several alternative mechanisms for the accumulation and preservation of sets of aeolian strata have been proposed – including the infilling of localised accommodation space (e.g. Langford et al., 2008; Luzón et al., 2012), accumulation around relic aeolian topography (Fryberger, 1986), and exceptional bedform preservation following rapid inundation by water or lava flows (e.g. Glennie and Buller, 1983; Mountney et al., 1999; Benan and Kocurek, 2000) – the “bedform climbing” mechanism remains a convincing explanation for the origin of the majority of ancient preserved aeolian dune successions (Mountney, 2012).

Importantly, accumulation of sets of aeolian strata via the climbing of bedforms over one another means that typically only the lowermost flanks of migrating bedforms undergo accumulation and preservation into the long-term rock record, whereas the upper parts of bedforms (in most cases the upper 90% or more of a bedform) are truncated by the advance of the following bedform in the train (Rubin and Carter, 2006), with the majority of the original dune sediment being reworked (Figure 2.2). Thus, the proportion and distribution of primary lithofacies preserved in successions in the ancient record does not necessarily reflect the proportion and distribution of primary lithofacies present in modern bedforms. Care must therefore be exercised when using modern bedforms as analogues with which to make predictions about likely facies distributions in reservoir successions. Methods for the accurate prediction and characterisation of zones of good reservoir quality in subsurface aeolian successions require a clear understanding of the geometry of the various preserved architectural elements and the distribution of packages of facies associated within these elements.

Architectural elements (i.e. three-dimensional sediment bodies with specific internal facies characteristics) form the building blocks of aeolian reservoir successions and, in most examples, both the elements themselves and the lithofacies of which they are composed internally exhibit a strong preferred directional heterogeneity due to the inherent preferred orientation of layering of laminations and beds of facies, often in a complex nested manner (Weber, 1987; Chandler et al., 1989; Krystinik, 1990). Understanding the detailed arrangement of the style of heterogeneity present in these elements is crucial for reservoir prediction as this exerts a primary control on porosity and permeability structure within aeolian reservoirs and therefore dictates production flow rates and patterns within complex aeolian reservoir bodies (Nagtegaal, 1979; Heward, 1991; Ellis, 1993; Stanistreet and Stollhofen, 2002; Garden et al., 2005; Bloomfield et al., 2006). In most aeolian hydrocarbon plays, it is particularly important to target those intervals within a reservoir that contain a high proportion of grainflow laminae – the deposits of avalanches down dune lee slopes – as these tend to form packages of well-sorted, loosely-packed sandstone with permeabilities that are typically one or more orders of magnitude greater than those in packages of grainfall and wind-ripple strata that dominate in other aeolian elements (Chandler et al., 1989; Prosser and Maskall, 1993; Howell and Mountney, 2001).

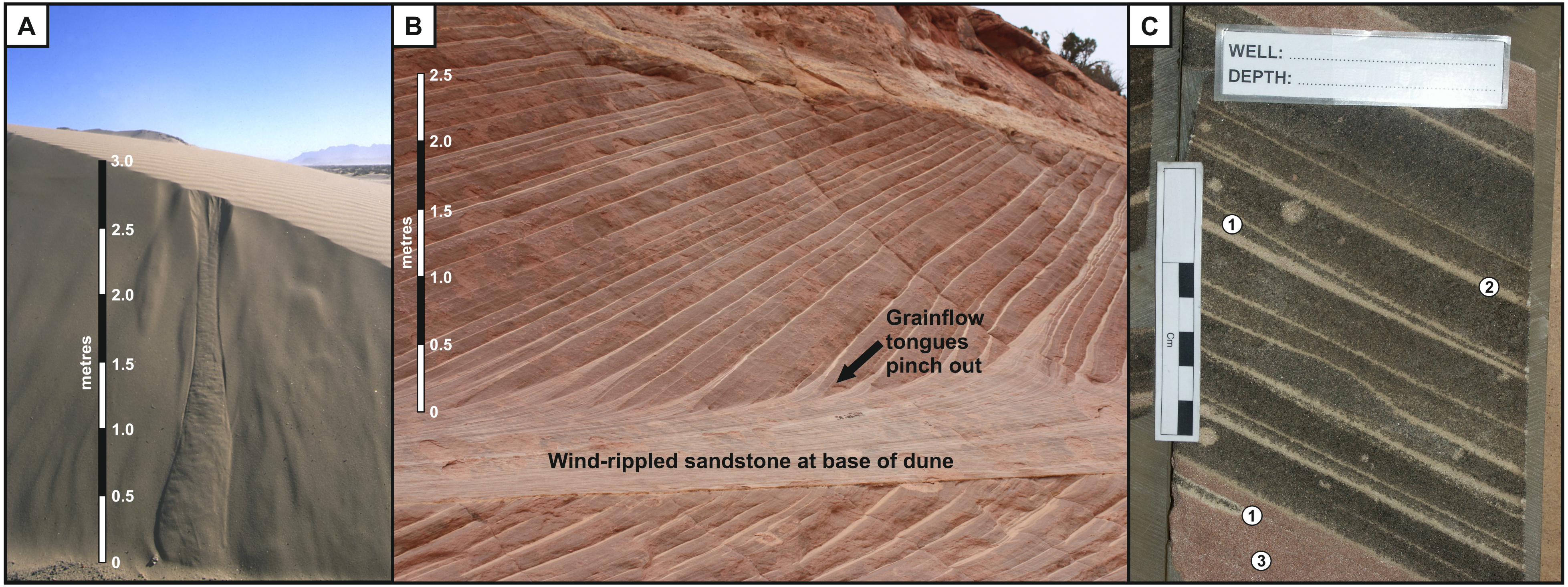

Figure 2.1. Examples of aeolian strata in modern, outcrop and core datasets: (a) Scarp-recession grainflow (*sensu* Hunter, 1977a), on a barchan dune of the Skeleton Coast, Namibia; (b) Grainflow tongues pinching out into wind-ripple strata, Navajo Sandstone, Jurassic, Utah, USA (photo courtesy of Nathaniel Ball); (c) Grainflow-laminated aeolian sandstone seen in core from the Permian Auk Formation (Rotliegend Group) of the Central North Sea. Note how grainflow laminae pinch-out locally (1). The black colouration is oil staining. Grainfall laminae are also evident (2); Wind-rippled sandstone at base of photo (3). Limited sedimentological data can be measured directly from core, and these are primarily restricted to grainflow thickness, preserved set thickness, ratio of grainflow to wind-rippled strata, rate of upward-steepening of strata in the set, dip-azimuth data, and style of bundling of packages of grainflow-dominated and wind-ripple-dominated strata.

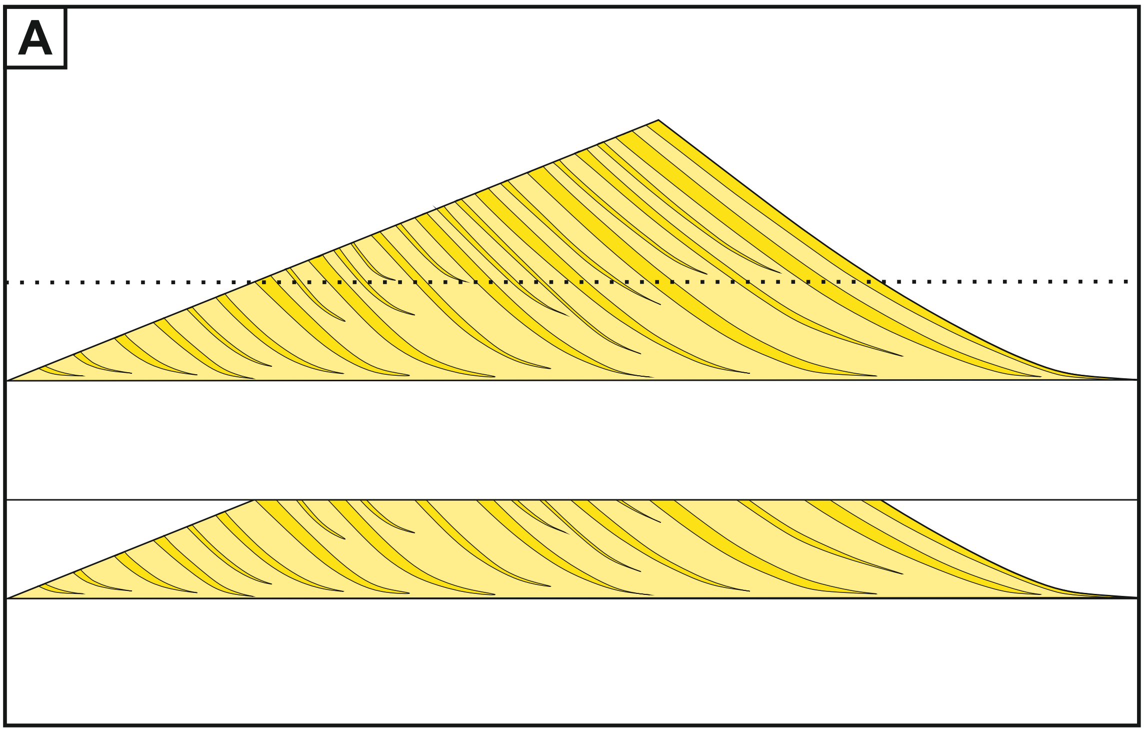

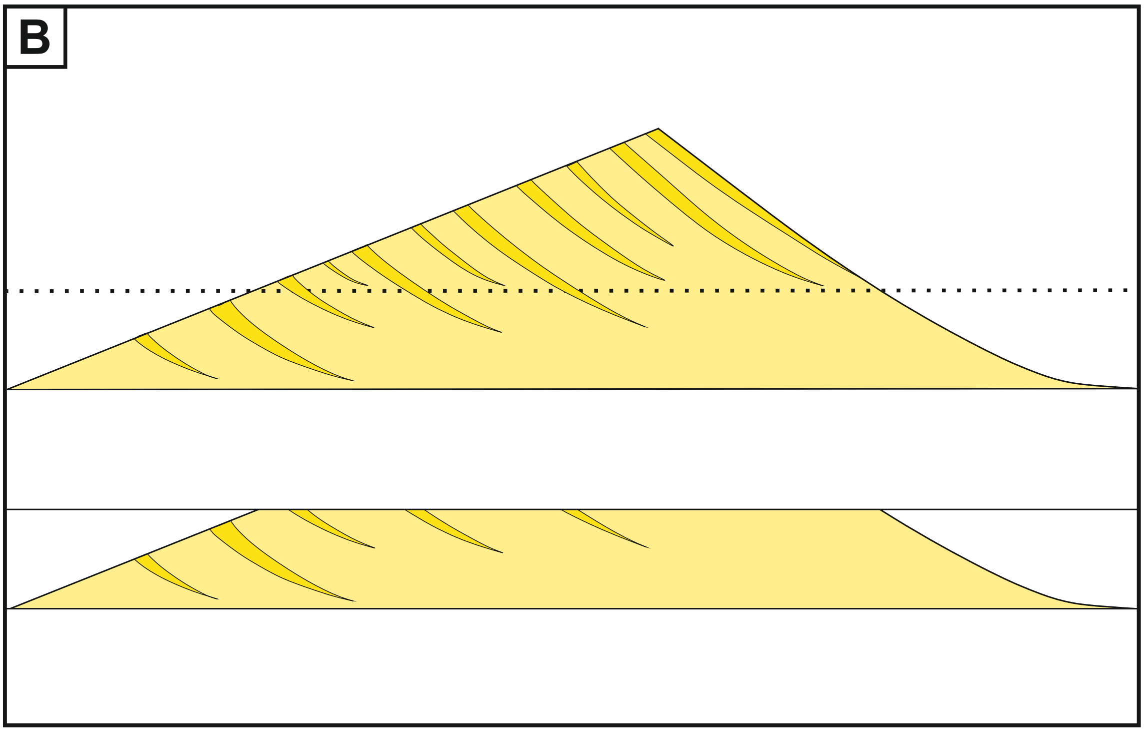

Figure 2.2. For aeolian successions that accumulate via climbing bedform migration, it is only the lowermost flanks of migrating aeolian bedforms that typically undergo accumulation and preservation into the rock record (see Rubin and Carter (2006) for examples). The upper parts of the bedforms are usually truncated by the advance of the following bedform in a migrating train, and the sediment reworked. Schematic examples shown here for (a) migrating aeolian sets where the majority of grainflows reach the base of slope, and (b) migrating aeolian sets where grainflows rarely reach the base of slope. Dotted line depicts level at which original dune bedforms might typically be truncated to preserve sets.

2.2 – Background

Since the late 1970s, considerable aeolian sedimentological research has focused on large-scale stratigraphic relationships and the development of sequence stratigraphic models with which to account for the origin of the aeolian record in terms of external controls on sedimentation (e.g. Brookfield, 1977; Kocurek, 1988; Kocurek and Havholm, 1993; Mountney, 2012). As a result of this emphasis, a wide variety of data has been published relating to large-scale stratigraphic architectures preserved in a number of ancient aeolian successions (e.g. Glennie and Provan, 1990; Herries, 1993; Mountney and Thompson, 2002; Mountney and Jagger, 2004; Taggart et al., 2010). However, there remain relatively few studies that have investigated the sedimentary style of small-scale dune elements and the arrangement of facies present within preserved aeolian sets originating from the migration of different types of aeolian bedforms (Ellwood et al., 1975; Hunter, 1977a; 1977b; Kocurek and Dott, 1981; Fryberger and Schenk, 1988). Although some explanation has been offered to account for how such types of small-scale stratification impact on reservoir quality (Lindquist, 1988; Chandler et al., 1989; Prosser and Maskall, 1993; Cox et al., 1994; Howell and Mountney, 2001; Stanistreet and Stollhofen, 2002; Garden et al., 2005; Bloomfield et al., 2006), an effective method to relate deposits seen in one-dimensional core to larger-scale architectural elements has yet to be fully developed.

Prediction of facies variability in three dimensions is a key requirement for quantitative reservoir characterisation (e.g. Sweet et al., 1996; Fischer et al., 2007) because it enables reliable predictions to be made of the characteristics of a subsurface aeolian reservoir body such as the extent, type and pattern of distribution of heterogeneities away from the points of data control provided by wells (Pryor, 1973). For the majority of aeolian reservoirs, production behaviour and characteristics are primarily influenced and controlled by original sediment fabric (Lindquist, 1988; Chandler et al., 1989; Prosser and Maskall, 1993; Howell and Mountney, 2001), though secondary alteration of sediment fabric by diagenesis is also important (e.g. Mou and Brenner, 1982). A method to enable the prediction of the spatial occurrence of the original depositional processes that occurred on dunes and in interdunes, and the resultant distribution of lithofacies in preserved aeolian architectural elements is therefore essential (Lewis and Couples, 1993).

Given that most aeolian reservoirs are penetrated by a relatively small number of wells and that the typical spacing of these wells is many hundreds of metres to several kilometres, traditional subsurface lithostratigraphic correlation techniques involving the tracing of key stratal surfaces and depositional units are not typically possible. Instead, a commonly adopted method with which to adequately account for facies architecture and with which to predict the scale over which variations in architecture occur is to employ one or more outcrop analogues to provide proxy data (e.g. Weber, 1987; Lewis and Rosvoll, 1991, Howell and Mountney, 2001). Such outcrop-analogue studies are important because they provide a method by which regional three-dimensional facies distributions known from outcrop can be used to populate a reservoir volume and thereby inform detailed characterisations and minimise risk. Key to the successful application of this technique is the ability to fit the sedimentary architecture of the chosen outcrop analogue to available core and well log data from the subsurface reservoir.

An inherent problem with reservoir modelling from core and well log data alone is that such data types are essentially one-dimensional in form and establishing the most likely three-dimensional sedimentary architecture from such data is typically equivocal (Lindquist, 1988; Luthi and Banavar, 1988; North and Boering, 1999). However, several parameters that effectively define the morphology and geometry of aeolian bedforms and their preserved bedsets can be measured directly from subsurface core and these provide a method to directly relate the subsurface architecture present in reservoir successions to outcrop successions for which first order estimates of larger-scale three-dimensional architectural configurations can be determined.

Parameters that can be measured directly from core include: (i) preserved set thickness, which for bedsets that originated via bedform climbing is a function of both original bedform wavelength and the angle at which the bedforms climbed over one another as accumulation proceeded (Mountney and Howell, 2000); (ii) the thickness of grainflow units arising from individual sandflow avalanches, which is primarily a function of the length of the lee slope of the original bedform down which avalanching grains of sand cascaded to generate the deposit (Kocurek and Dott, 1981; Howell and Mountney, 2001); (iii) the shape of dune toesets and their style of interaction with deposits of underlying interdune elements, which is an indicator of the style of advance of the original bedform over a neighbouring interdune area (e.g. Pulvertaft, 1985; Mountney and Thompson, 2002); (iv) the rate of upward-steepening of foresets within a set, which is an indicator of the profile of the lower flanks of the original bedform (Rubin, 1987a); (v) the distribution of primary lithofacies (grainflow, wind-ripple and grainfall) within sets, which is a function of processes that operated on the lee slope of the original bedform (Hunter 1977a; 1977b; Kocurek and Dott, 1981); and (vi) the distribution of the occurrence of reactivation surfaces within cosets, which is an indicator of the periodicity with which the original bedforms undertook changes in lee-slope steepness, asymmetry, or migration direction (Rubin, 1987a; Fryberger, 1993).

Within the remit of this study, detailed examination of the relationships arising between preserved set thicknesses and the thickness of preserved grainflow units has been undertaken. By relating quantitative measurements of these attributes from subsurface core intervals to equivalent sedimentary features observed in exposed outcrop successions, a workflow has been established for the quantification of larger-scale three-dimensional subsurface aeolian architecture from limited one-dimensional core data through a suite of empirical relationships. Although the empirical relationships derived from this study serve as useful tools for generalised prediction of sedimentary architecture, application of such relationships should be undertaken with caution: relationships between many measured parameters record significant variability meaning that R^2 values determined for best-fit trend lines are low and not statistically significant in many instances, chiefly as a result of the variability inherent in natural depositional systems such as those studied in this work.

Despite these shortcomings, the data show a series of relationships that are useful as a basis for a generalised technique to reconstruct the three-dimensional architecture from primary depositional facies in aeolian successions. Specifically, the empirical relationships presented herein are useful for the determination of trends between features observable in core and several aspects of wider three-dimensional sedimentary architecture that cannot be determined by direct observation from subsurface datasets. Thus, such trends are useful for making first-order predictions of the likely internal three-dimensional sedimentary architectures of subsurface reservoir successions and can be used to assist in the construction of reservoir models for the prediction of porosity-permeability distributions and likely flow properties.

For example, in successions interpreted to have arisen in response to the migration and aggradation of large linear dune bedforms, a vertical stacking of thick packages of relatively low-angle-inclined, wind-ripple-dominated packages of strata is common, with only the uppermost parts of sets having foresets that steepen-upward sufficiently to preserve grainflow strata (Krystinik, 1990). The ability to determine the proportions of wind-ripple and grainflow strata and the distribution of their occurrence within preserved sets is key to understanding the three-dimensional configuration of packages of facies, and this is most readily achieved through comparison to analogous outcrop examples.

2.3 – Data and methods

To establish a suite of empirical relationships between aeolian sedimentary parameters that can be measured directly from both one-dimensional core and from the larger-scale aeolian architectural elements observable from outcrop successions, data have been collected from the Permian Cedar Mesa Sandstone and Jurassic Navajo Sandstone, two aeolian successions that are well exposed in the South East Utah area, U.S.A. Four localities were studied in the so-called erg centre region of the Permian Cedar Mesa Sandstone succession (Mountney, 2006b) in the White Canyon and Hite areas and an additional three localities were studied in the so-called erg margin region at Squaw Butte, Salt Creek Butte and Mosquito Butte (Figure 2.3a). Four localities were also studied in the Jurassic Navajo Sandstone in the area around the town of Moab, Utah (Figure 2.3b), which represents an erg centre setting within the palaeo-erg system (Blakey and Ranney, 2008).

Primary measurements of aeolian bed-set architectures were made at each study locality to determine three-dimensional relationships present in the successions of aeolian dune sets. Aspects of aeolian architecture measured included: (i) maximum preserved set thicknesses for 42 individual trough cross-bedded sets exposed in orientations both parallel and perpendicular to aeolian transport direction (itself determined through analysis of dip-azimuth data relating to grainflow deposits representative of accumulation on the slipface of the original bedforms) – care was taken to account for set thickness variations arising from the curved nature of trough cross-bedded sets; (ii) geometries of packages of grainflow strata representative of individual lee-slope sand avalanches, including thickness (932 readings in total), width (30 readings in total) and length (517 readings in total); (iii) measurements of bedform wavelength (42 readings in total) determined in directions parallel to aeolian palaeo-transport by the measurement of the spacing between the points at which successive interdune migration surfaces climb off basal supersurfaces that are themselves inferred to represent palaeo-horizontal surfaces (see Mountney and Howell, 2000 and Mountney, 2006b for details of the methodology); (iv) measurements of angles of set climb (42 readings in total), determined trigonometrically in directions parallel to aeolian palaeo-transport (again determined through analysis of dip-azimuth data relating to grainflow deposits representative of accumulation on the slipface of the original bedforms) by evaluating the rate of rise of interdune migration surfaces relative to underlying supersurfaces (see Mountney, 2006b for methodology); (v) measurements of the rate of upward-steepening of aeolian dune toeset deposits with increasing height above the base of sets (36 readings in total).

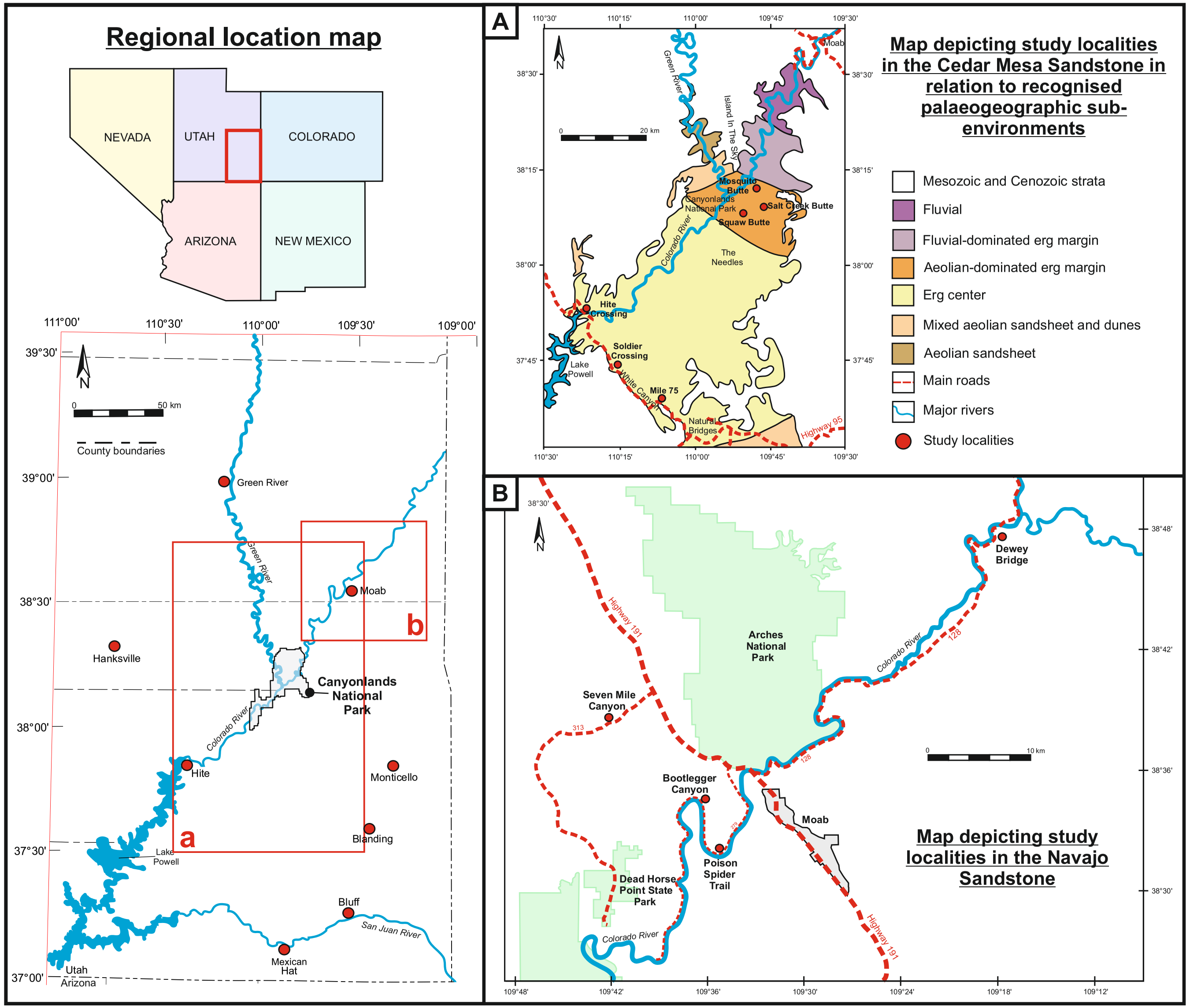

Figure 2.3. Study locations and regional location map: (a) Geological map to show the limit of outcrop of the Cedar Mesa Sandstone in SE Utah, USA. This formation is predominantly aeolian, but contemporaneous fluvial deposits of Wolfcampian age (Undifferentiated Cutler Group) are also shown here. Data presented from the Cedar Mesa Sandstone have been collected from localities in the erg centre around White Canyon (Hite Crossing, Soldier Crossing and Mile 75). Map modified from Mountney (2006b); (b) Map of the area around Moab, SE Utah, USA. Data from the Navajo Sandstone have been collected from the key localities shown: Seven Mile Canyon, Bootlegger Canyon, Poison Spider Trail and Dewey Bridge.

2.4 – Results

2.4.1 – Grainflow geometry

The mean lengths and widths of single units of grainflow strata in the Navajo Sandstone are 4.22 m (standard deviation = 2.43; n = 517) (Figure 2.4a), and 4.63 m (standard deviation = 1.58; n = 30) (Figure 2.4b), respectively. The widths of individual grainflow units were not measured in examples from the Cedar Mesa Sandstone. The mean thicknesses of single units of grainflow strata (i.e. deposits representative of a single sandflow avalanche event) in the Navajo Sandstone and Cedar Mesa Sandstone are 23.77 mm (standard deviation = 7.32; n = 517), and 54.68 mm (standard deviation = 23.11; n = 415), respectively (Figure 2.4c). Individual grainflow units have been identified by their subtle inverse grading, which gives rise to a sharp grain size contrast across unit boundaries that typically takes the form of a change from lower to upper fine-grained sand. Additionally, these units are in many instances identified by their style of interfingering and intercalation with thin accumulations of wind-ripple strata, especially in the lower parts of preserved sets, and with thin accumulations of grainfall strata, most notably in the upper parts of preserved sets.

2.4.2 – Preserved set thickness

Preserved set thicknesses have been measured from the central axes of troughs (i.e. at the location of the thickest development of the set). The mean thicknesses of simple preserved sets (*sensu* McKee, 1979a) of strata bounded by interdune migration bounding surfaces in the Navajo Sandstone and Cedar Mesa Sandstone are 3.10 m (standard deviation = 1.60; n = 25), and 4.71 m (standard deviation = 2.72; n = 17), respectively (Figure 2.4d). For the Cedar Mesa Sandstone, measured set thicknesses are representative of the succession overall, though considerable variability exists in some locations. For the Navajo Sandstone, which is exposed over large areas of Utah, Arizona and Colorado, preserved set thicknesses vary considerably and the sets measured as part of this study from parts of the succession exposed around the town of Moab, Utah, are not necessarily representative of the formation overall. Indeed, significantly thicker compound sets are known from other parts of this formation (see, for example, Herries, 1993 and Rubin, 1987a), though these have not been examined for this study.

2.4.3 – Bedform wavelength reconstruction

Original dune wavelengths were mostly determined via direct measurement. In directions parallel to aeolian palaeo-transport, the spacing between the points at which successive interdune migration surfaces climb off basal supersurfaces that are themselves inferred to represent palaeo-horizontal surfaces is a measure of bedform spacing, where bedform spacing is defined as the bedform wavelength plus the additional component of width of any adjoining interdune flat. Additional calculations of original dune wavelengths were derived trigonometrically from estimates of set thicknesses and angles of climb: see Mountney and Howell (2000) for details of the method. The mean reconstructed dune bedform wavelengths in directions parallel to inferred aeolian bedform migration direction for studied parts of the Navajo Sandstone and Cedar Mesa Sandstone are 138.26 m (standard deviation = 70.75; n = 25), and 202.42 m (standard deviation = 159.19; n = 15), respectively (Figure 2.4e).

Based on relationships observed from outcrops of the Navajo Sandstone, where sets are seen to rise (climb) off supersurfaces, reconstructed dune bedforms are estimated to have had original wavelengths ranging from 80 to 340 m. The erg centre region of the Cedar Mesa Sandstone exhibits a wider range of reconstructed dune wavelength values (65 to 668 m). Overall, these data fall within the ranges determined previously for aeolian dunes of the Cedar Mesa Sandstone in the White Canyon region of SE Utah (Mountney, 2006b). However, one exception is Set 1 from Mile 101 of Highway 95 (a 12.8 m-thick set climbing at an angle of 1.1°), which is estimated to represent the preserved deposit of a bedform that had an anomalously large wavelength of 668 m, considerably greater than values determined for other bedforms in the succession.

2.4.4 – Angle-of-climb

The Navajo Sandstone exhibits a narrow range of observed angles of climb, with the majority of sets climbing up through the stratigraphy in a downwind direction at angles between 1 to 1.5°. The mean angle-of-climb of studied sets in the Navajo Sandstone is 1.29° (standard deviation = 0.30; n = 25). Sets in the erg centre region of the Cedar Mesa Sandstone reveal a wider range of climb angles, which were derived by Mountney (2006b – his Figure 12) trigonometrically from measurements of preserved set thicknesses and reconstructed original dune bedform wavelengths (the latter determined from the spacing between points where sets rise off supersurfaces which themselves define a palaeo-horizontal surface). The mean angle-of-climb of studied sets in the Cedar Mesa Sandstone is 1.54° (standard deviation = 0.75; n = 17 (Figure 2.4f).

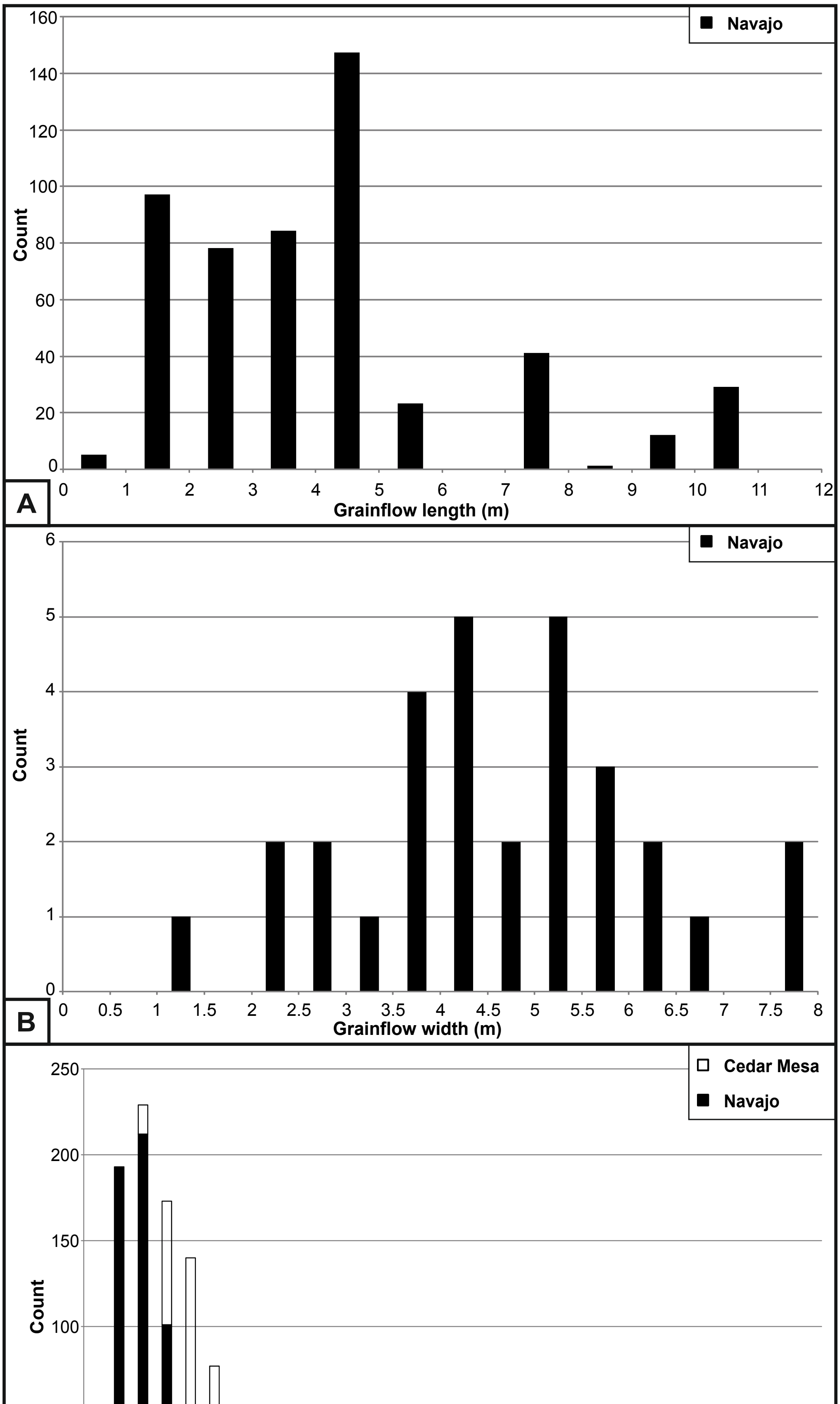

Figure 2.4. (continued overleaf). Frequency distributions of key parameters relating to aeolian facies and architecture measured from the Navajo Sandstone and Cedar Mesa Sandstone: (a) Grainflow length; (b) Grainflow width; (c) Grainflow thickness; (d) Preserved set thickness; (e) Dune wavelength; (f) Angle-of-climb.

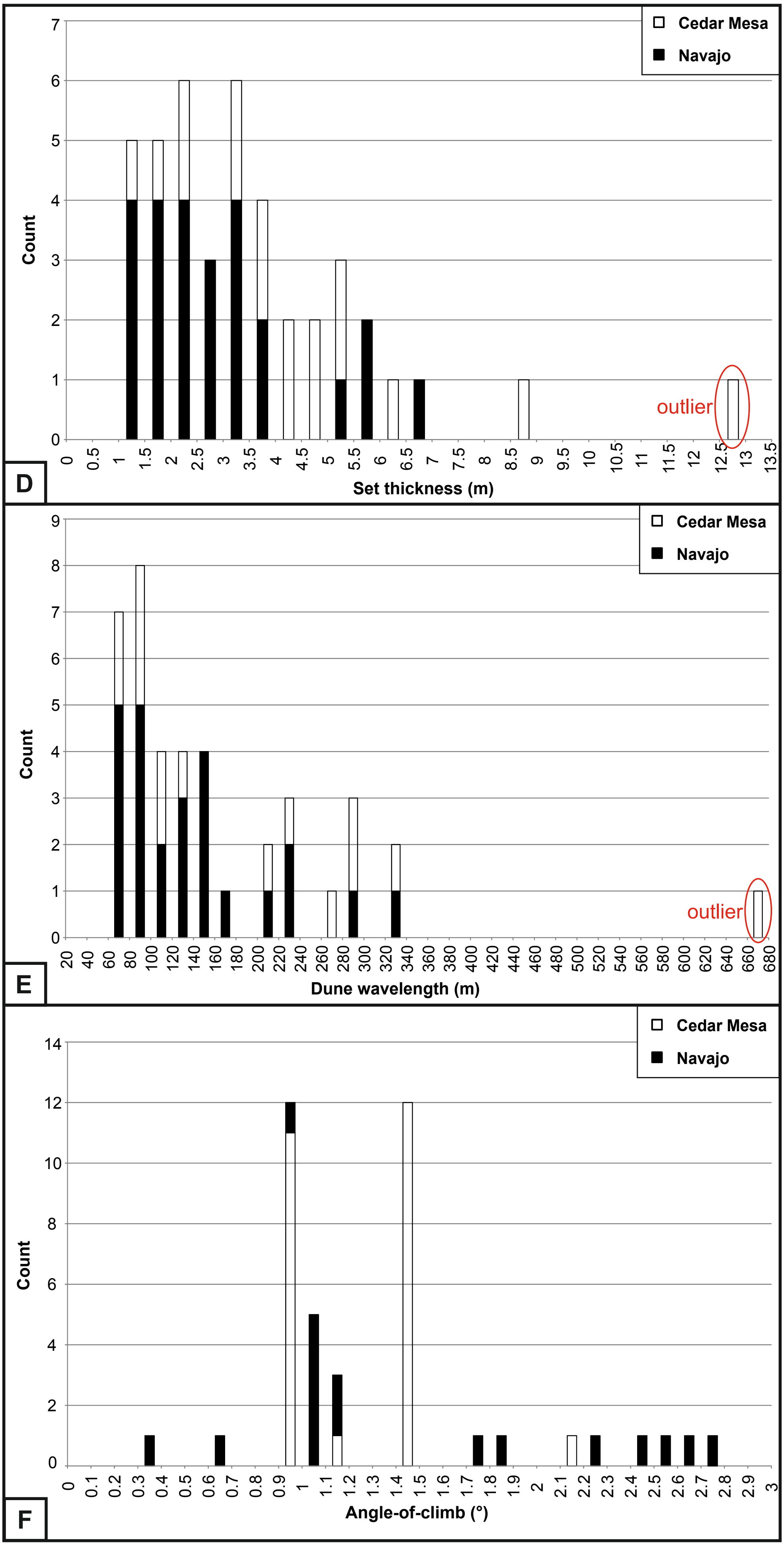
D
Cedar Mesa
Navajo
Count
0
1
2
3
4
5
6
7
outlier
0 0.5 1 1.5 2 2.5 3 3.5 4 4.5 5 5.5 6 6.5 7 7.5 8 8.5 9 9.5 10 10.5 11 11.5 12 12.5 13 13.5
Set thickness (m)
E
Cedar Mesa
Navajo
Count
0
1
2
3
4
5
6
7
8
9
outlier
20 40 60 80 100 120 140 160 180 200 220 240 260 280 300 320 340 360 380 400 420 440 460 480 500 520 540 560 580 600 620 640 660 680
Dune wavelength (m)
F
Cedar Mesa
Navajo
Count
0
2
4
6
8
10
12
14
0 0.1 0.2 0.3 0.4 0.5 0.6 0.7 0.8 0.9 1 1.1 1.2 1.3 1.4 1.5 1.6 1.7 1.8 1.9 2 2.1 2.2 2.3 2.4 2.5 2.6 2.7 2.8 2.9 3
Angle-of-climb (°)

2.5 – Discussion

Several important empirical relationships describing relationships between the spatial arrangement of observed lithofacies and the geometry and style of distribution of larger-scale aeolian architectural elements are identified from analysis of the field-derived data.

2.5.1 – Relationship between preserved grainflow thickness, length and width

Where the pattern of outcrop has allowed, for every grainflow unit measured in the Navajo Sandstone (n = 517), the preserved thickness has been related to a corresponding grainflow length and width (Figures 2.5 and 2.6). In the Navajo Sandstone, measured grainflow widths exhibit a strong positive correlation with corresponding grainflow thickness (Figure 2.5; $y = 0.0041x + 0.0035$; $R^2 = 0.86$). The overall relationship between measured grainflow length and preserved grainflow thickness for sets in the Navajo Sandstone shows a positive correlation but with substantial scatter (Figure 2.6; $y = 0.0019x + 0.0156$; $R^2 = 0.41$). However, preserved grainflow thickness and length relationships from 25 *individual* sets are also depicted in Figure 2.6 and strong positive correlations between preserved thickness and length exist in almost every case. Significantly, data from different sets plot in distinct and, in many cases, non-overlapping fields on the graph. Together, these observations suggest that, although a simple overall general relationship between grainflow thickness and grainflow length exists, data from individual sets each preserve grainflows with their own geometry and this likely reflects the shape of the slipface that developed on the lee of the dune at the time of sedimentation.

Empirical relationships identified from outcrop data between grainflow thickness, length and width are important because they potentially allow the three-dimensional reconstruction of the expected geometry of grainflow sediment packages solely from a measurement of their thicknesses preserved in core. This is important for modelling lamina- and bed-scale heterogeneity and directional permeability in aeolian reservoirs (Weber, 1982; 1986; 1987; Chandler et al., 1989; Krystinik, 1990).

2.5.2 – Relationship between preserved set thickness, dune wavelength and angle-of-climb

In both the Cedar Mesa Sandstone and the Navajo Sandstone, sets generated by the migration and climb of larger bedforms (as determined by reconstructed estimates of longer wavelengths) preserve thicker grainflow units, though considerable spread exists between the data (Figure 2.7a; Cedar Mesa Sandstone; $y = 0.00001x + 0.0532$; $R^2 = 0.02$; Navajo Sandstone; $y = 0.00006x + 0.0148$; $R^2 = 0.38$). Although the studied dune-sets from the Navajo Sandstone are indicative of original bedforms characterised by generally smaller wavelengths than those of the Cedar Mesa Sandstone, considerable overlap in original

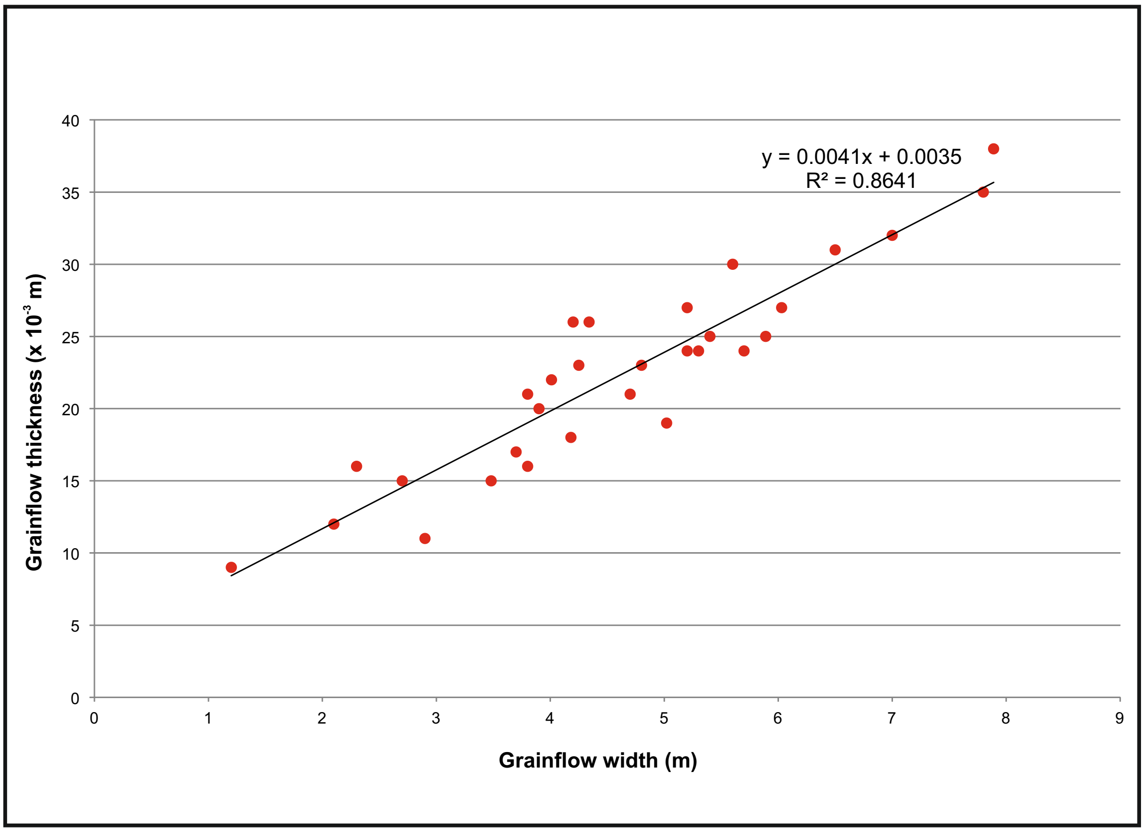

Figure 2.5. (above) Grainflow thickness versus grainflow width for selected preserved sets in the Navajo Sandstone.

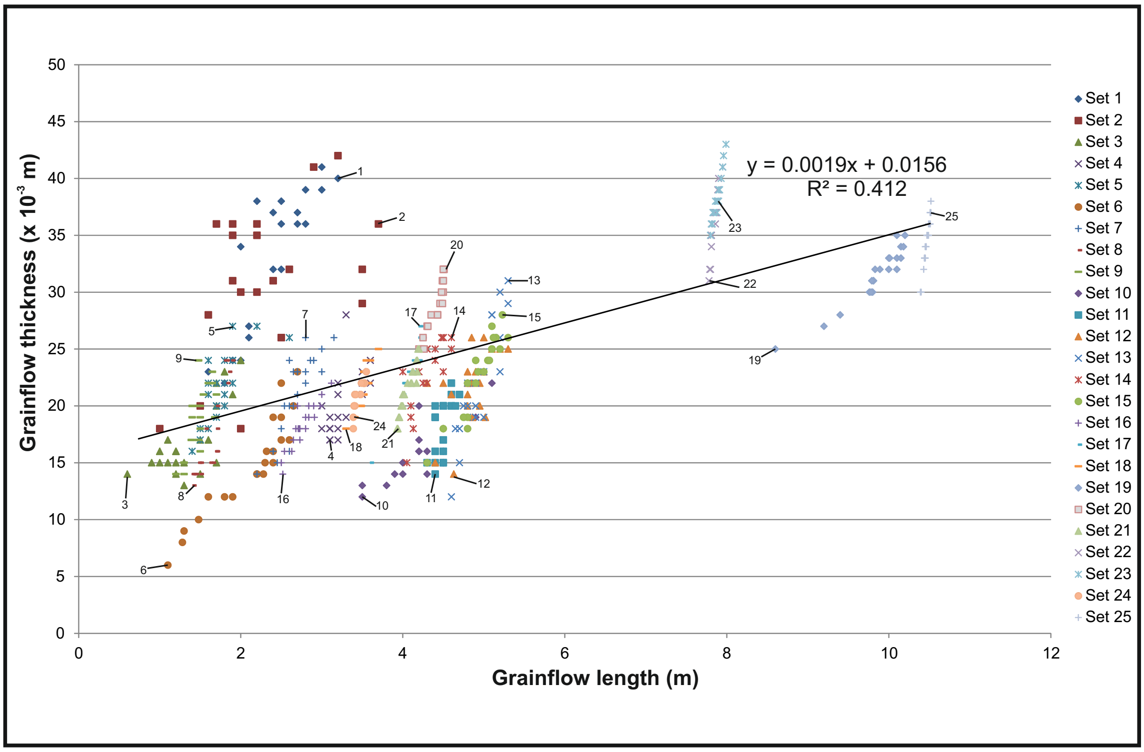

Figure 2.6. (above) Grainflow thickness versus grainflow length for a number of measured sets in the Navajo Sandstone. See text for explanation.

bedform wavelength exists. Of the preserved dune-sets for which estimates of reconstructed original bedform wavelengths are similar, examples from the Navajo Sandstone are characterised by distinctly thinner grainflow units than those from the Cedar Mesa Sandstone (Figure 2.7a). This could have arisen due to a number of reasons: different dune types, different slipface configurations, variations in dune-plinth shape, variations in dune height (a likely influence on slipface length) despite bedforms having similar wavelengths, and different grain size distributions or grain-shape properties giving rise to different types of avalanches down the dune lee slopes. The overall correlation between preserved grainflow thickness and original bedform wavelength represents a possible method for making a first-order estimate of original bedform size from subsurface data since the former can be measured directly from core. However, the spread of the data and the different trends in the data for the Navajo and Cedar Mesa sandstones demonstrate that it is essential to pick an appropriate analogue when making extrapolations regarding larger-scale architecture from core data.

For climbing aeolian systems that accumulate a succession through a progressive climb of bedforms over one another, preserved set thickness is a function of both bedform size (wavelength) and angle-of-climb (Figure 2.8; Rubin, 1987a; Rubin and Carter, 2006). Despite preserved set thickness being only partly dependent on original dune wavelength, for the studied successions there exists a clear positive relationship between preserved set thickness and dune wavelength (Figure 2.7b – Cedar Mesa Sandstone - $R^2 = 0.61$; Navajo Sandstone - $R^2 = 0.78$). However, note that ignoring the outlier representing the anomalously large bedform studied in the Cedar Mesa Sandstone reduces the R^2 value for the best-fit line for these data from 0.61 to 0.20.

The nature of the relationship between preserved set thickness and dune wavelength is similar for both the Cedar Mesa and Navajo sandstones, principally because sets from both systems in the areas studied are climbing at similar angles (the majority in the range 1 to 1.5°), which means that the effects of angle-of-climb are largely normalised. However, although sets in some other systems are known to climb at similar angles (e.g. Triassic Helsby Sandstone – 1 to 1.5°, Mountney and Thompson, 2002), other successions climb at lower angles (e.g. the transition zone between the Undifferentiated Cutler Group and the Cedar Mesa Sandstone at Indian Creek, SE Utah – 0.35°, Mountney and Jagger, 2004) or steeper angles (e.g. parts of the Etjo Sandstone, Namibia – up to 4°, Mountney and Howell, 2000, as well as examples from some very dry dune systems characterised by small dunes, which have not been addressed in this study). Thus, it is important to consider angle-of-climb when using preserved set thickness to reconstruct likely original bedform size.

Although a positive relationship has long been recognised whereby increased climb angles tend to preserve thicker sets (e.g. Mountney and Howell, 2000), such increased angles-of-climb do not necessarily arise from the accumulation of larger bedforms with longer

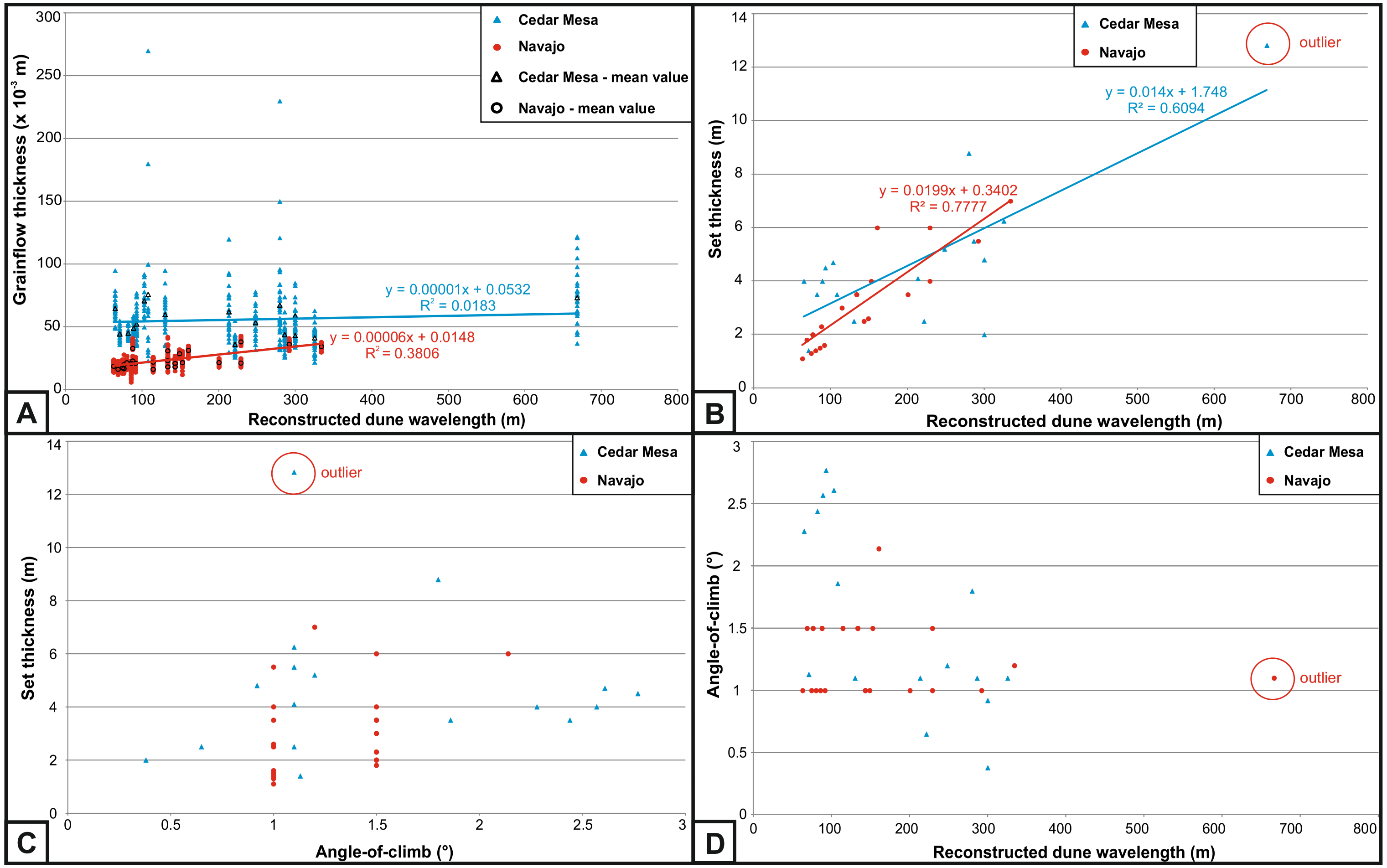

Figure 2.7. Relationships between parameters measured from the Navajo Sandstone and the Cedar Mesa Sandstone: (a) Grainflow thickness versus reconstructed dune wavelength. Outliers arise due to amalgamation of two or more grainflow units such that apparently homogenous grainflow deposits actually represent multiple events. Best-fit lines computed from mean values from each set in the individual formations; (b) Set thickness versus reconstructed dune wavelength; (c) Set thickness versus angle-of-climb of the dune sets; (d) Angle-of-climb versus reconstructed dune wavelength. Outlier in b, c and d represents a solitary large compound draa.

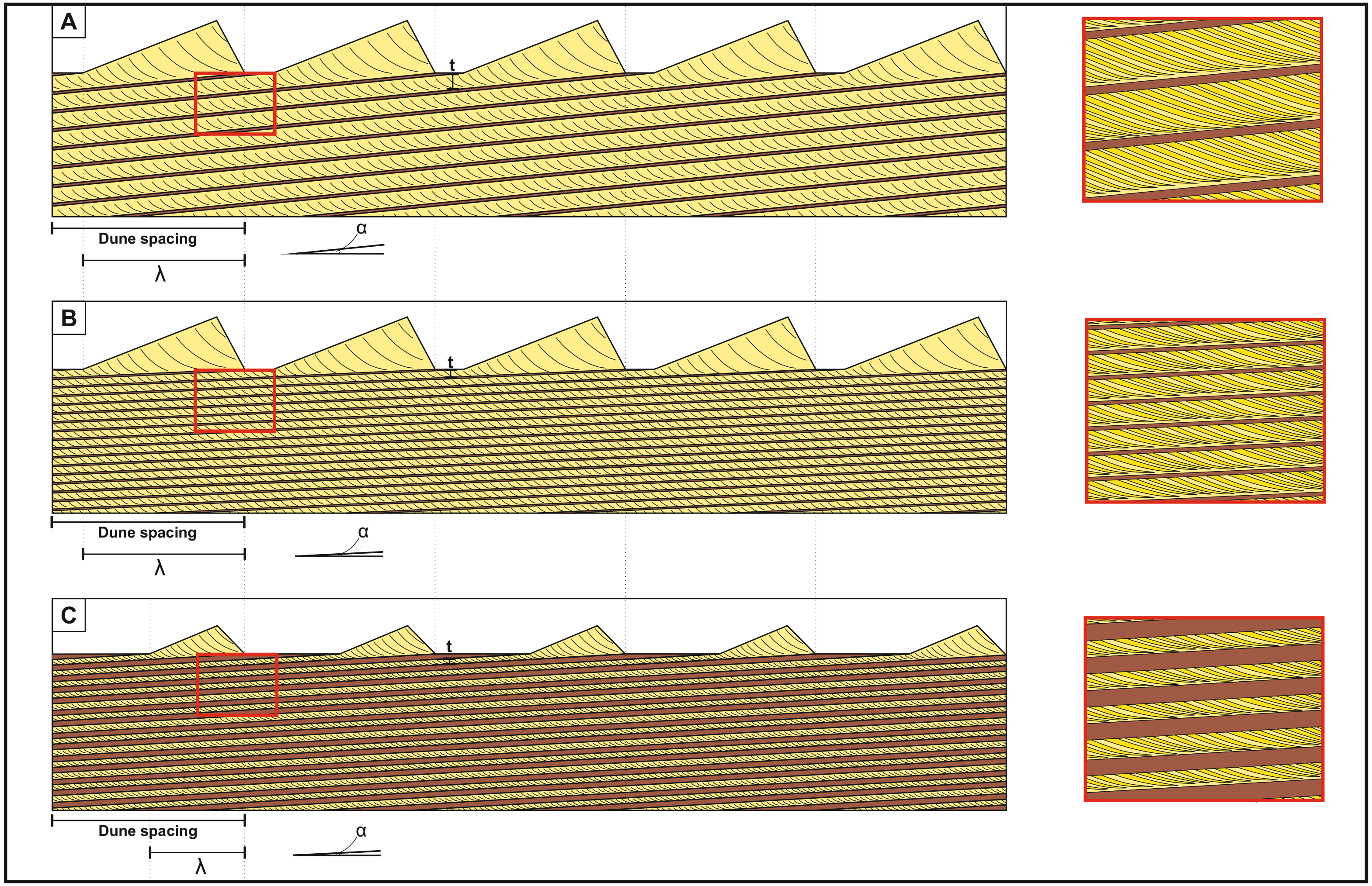

Figure 2.8. Schematic illustration to show how angle-of-climb and bedform wavelength jointly affect preserved dune set thickness. In all three cases the bedform spacing (dune wavelength plus interdune wavelength) is constant: (a) Sets climb more steeply than in case b); (b) Sets climb less steeply than in case a), and therefore preserve thinner sets. In a) and b) the wavelength of the dunes is equal; (c) Dunes with smaller wavelengths but climbing at the same angle as those in case b) preserve relatively thicker interdune elements but thinner dune sets.

wavelengths. Indeed, larger bedforms with longer wavelengths tend to undertake accumulation through climb at shallower angles, primarily because larger bedforms are likely to respond only slowly to changes in sand availability (Lancaster, 1988b) and will therefore tend to climb at only shallow angles, though they can preserve relatively thick sets by virtue of their long wavelength. Thus, preserved set thickness alone is not necessarily a reliable indicator of original bedform size.

2.5.3 – Relationship between preserved set thickness and grainflow thickness

In this study, for each set where preserved thickness has been measured, 15 to 25 grainflow thicknesses have also been measured; the relationship between preserved set thickness and grainflow thickness shows significant scatter (Figure 2.9; Cedar Mesa Sandstone, $y = 102.09x - 0.9557$, $R^2 = 0.2137$; Navajo Sandstone, $y = 182.79x - 1.2566$, $R^2 = 0.5797$). However, overall results demonstrate a weak positive correlation for data from both studied outcrop successions. Comparable ranges of preserved grainflow thicknesses measured from sets of known thickness were also demonstrated by Howell and Mountney (2001), whose results concluded that there was no apparent significant relationship between preserved set thickness and grainflow thickness for the Cretaceous Etjo Formation of Namibia.

Plotting preserved set thicknesses against grainflow thicknesses does not necessarily reveal an obvious correlation for several reasons (Figure 2.10): (i) set thickness is a function of not only bedform size (wavelength), but also angle-of-climb and set-thickness data collected from multiple aeolian successions or from different geographic locations or stratigraphic levels within the same succession will be partly dictated by bedforms that locally climbed at different angles (Figure 2.10a); (ii) values of set thicknesses determined from two-dimensional outcrops or from one-dimensional core do not necessarily represent the maximum thickness of a set since they might be clipping the edges of troughs that are significantly thicker in their central parts (Figure 2.10b); (iii) because preserved grainflow units thin and pinch-out laterally, two-dimensional outcrops and one-dimensional core might be clipping the ‘thin’ edges of grainflow units, thereby not recording their true maximum thickness (Figure 2.10c); (iv) sets might only preserve the basal-most toes of grainflow units, which typically thin and pinch-out in the lower parts of dune lee slopes as the angle of inclination of the slope decreases (Figure 2.10d) where packages of wind-ripple strata become dominant. Such situations most commonly arise when seasonally-reversing wind regimes encourage the development of a gently inclined dune plinth at the base of the lee slope (e.g. Rubin, 1987a). For these reasons, when analysing grainflow units in core data for the purpose of reconstructing likely bedform architecture, it is preferable to record data from the thickest sets that are likely most representative of a penetration through the centres of troughs. Within these, the thickest-preserved grainflow units will most closely reflect the maximum developed grainflow thickness, which might provide an indicator of lee

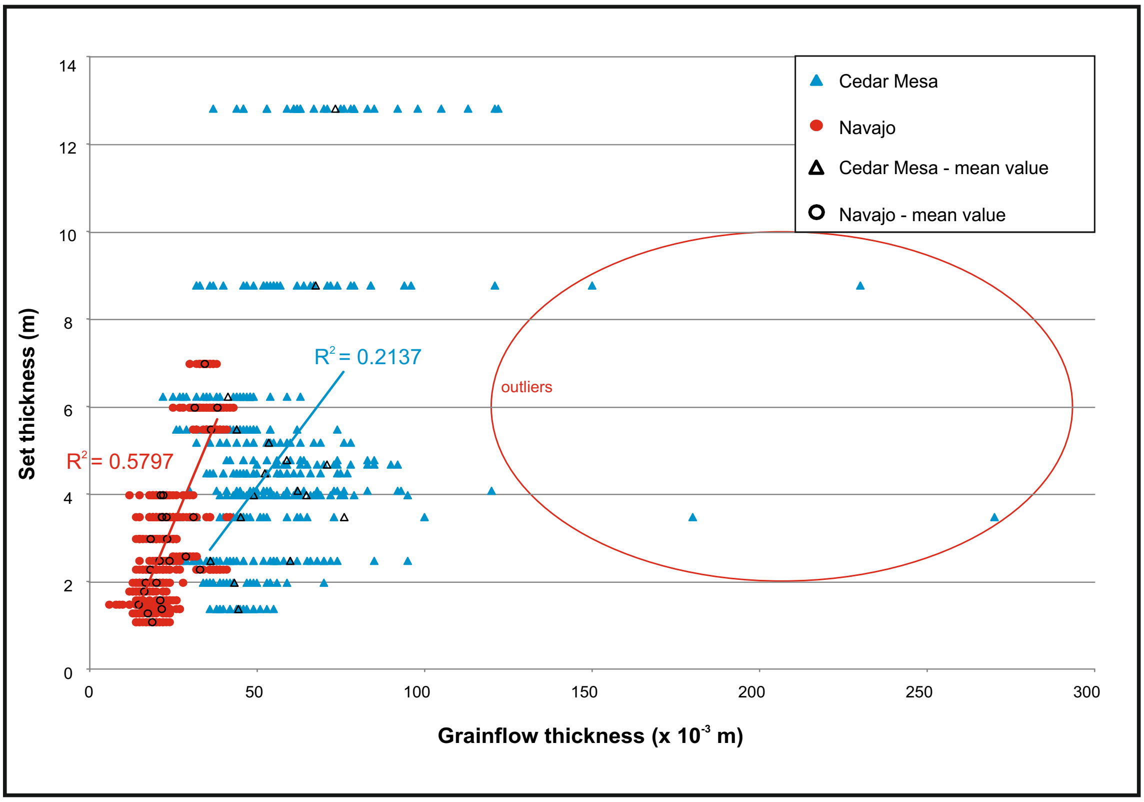

Figure 2.9. Preserved set thickness plotted against grainflow thickness. Outliers due to amalgamation of two or more grainflow units representing multiple events. Best-fit lines computed from mean values from each set in the individual formations.

Figure 2.10. (next page) Stratigraphic explanations with which to account for the apparent lack of a significant relationship between preserved set thicknesses and grainflow thickness. (a) Set thickness is a function of not only bedform size, but also angle-of-climb. Set thickness data collected from multiple aeolian successions will be partly dictated by bedforms that climbed at different angles. (b) Set thicknesses seen in 2D outcrops or 1D core might be clipping the edges of troughs and the actual maximum preserved set thickness may be considerably more. (c) Grainflow thicknesses pinch and thin laterally and 2D outcrop or 1D core might be clipping the edges of grainflow units such that the maximum grainflow thicknesses might be significantly greater. Also shown are cylindrical core expressions of strata, and 'unrolled' cylinders yielding standard depiction of dipping surfaces, as is routinely used for the portrayal of formation micro-imaging (FMI) and similar tools. (d) Sets may only preserve the basal toes of grainflow units, which typically thin and pinch-out in the basal part of dune lee flanks. The thicknesses of these grainflow toes are not necessarily representative of thicker grainflows that would have been present higher up the lee slope of the original dune.

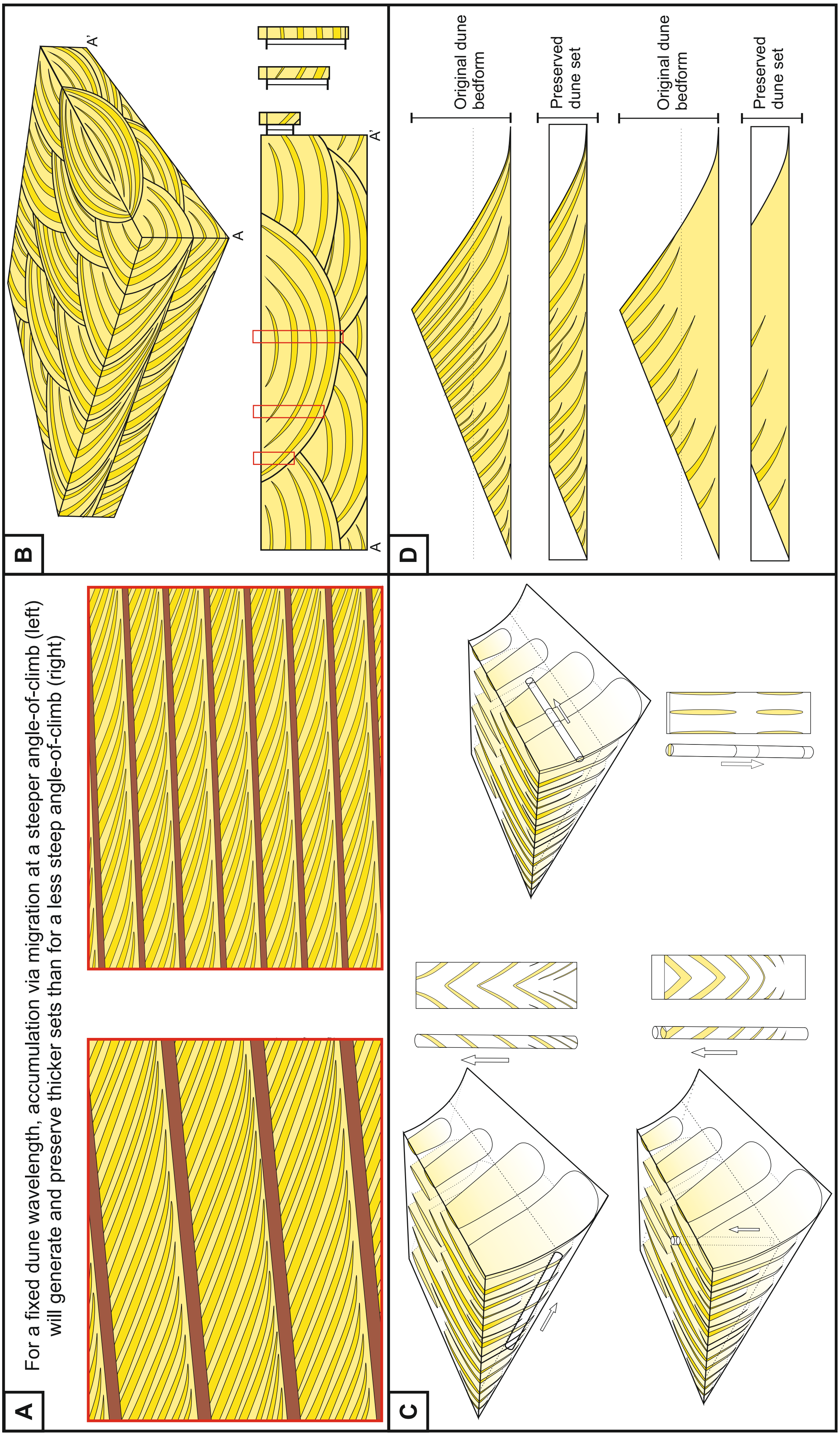
A
For a fixed dune wavelength, accumulation via migration at a steeper angle-of-climb (left) will generate and preserve thicker sets than for a less steep angle-of-climb (right)
B
A
A'
A
A'
C
D
Original dune bedform
Preserved dune set
Original dune bedform
Preserved dune set

slope length and therefore bedform height and overall size; thinner grainflow units will likely record examples where the well bore has intersected grainflows at points close to either their lateral or downslope margins.

The Cedar Mesa Sandstone offers the opportunity to examine this problem in more detail because the overall succession in both the erg centre setting (e.g. Mile 75 of White Canyon) and in the erg margin setting (e.g. Squaw Butte) is divided into a number of separate aeolian erg sequences each bounded both above and below by regionally extensive deflationary supersurfaces (Loope, 1985; Mountney and Jagger, 2004; Mountney 2006b). This partitioning into a series of stacked supersurface-bounded aeolian sequences means that reliable estimates can be made of both the angle-of-climb of sets and of original dune wavelength. This provides the basis for a method with which to demonstrate how preserved set thickness is related to grainflow thickness.

Preserved set thicknesses plotted against grainflow thicknesses for a number of dune sequences in the erg centre and lateral erg margin areas of the Cedar Mesa Sandstone are shown in Figure 2.11 ($y = 0.2614e^{99.347x}$, $R^2 = 0.6238$). The scatter in the data is less than that shown for the plot in Figure 2.9 for several reasons: (i) set thicknesses were determined from the centres of troughs (i.e. at their point of maximum thickness), which could be reliably and consistently picked because of the exceptionally high-quality nature of the outcrop; (ii) for each set examined, 10 grainflows units were measured at their point of *maximum* thickness and the mean of these 10 values was recorded so as to negate the effects of thinning and pinching of grainflow units at their lateral and downslope margins.

Results from the eight individual aeolian sequences examined and plotted on Figure 2.11 demonstrate that each sequence exhibits a strong positive correlation between preserved set thickness and grainflow thickness but considerable scatter exists *between* each separate aeolian sequence if the dataset is considered in its entirety. The origin of the scatter in these data arises partly because preserved set thickness is a function of both angle-of-climb and original bedform wavelength, which varied between each studied aeolian sequence. Additionally, grainflow thickness is also known to vary as a function of slipface length, with thicker grainflows developing on longer slipfaces associated with larger bedforms (Kocurek and Dott, 1981). Thus, the strong positive correlation between preserved set thickness and grainflow thickness *within* each sequence indicates a direct relationship between grainflow thickness and bedform size (height), a relationship that is discussed in more detail in Section 2.5.4.

Little overlap exists between the population of data describing reconstructed dune wavelength versus grainflow thickness from the Cedar Mesa and Navajo sandstones (Figure 2.7a). This demonstrates the importance of identifying and applying the most appropriate outcrop analogue when applying these types of data as a predictive tool with which to reconstruct likely bedform size from subsurface grainflow and set-thickness data

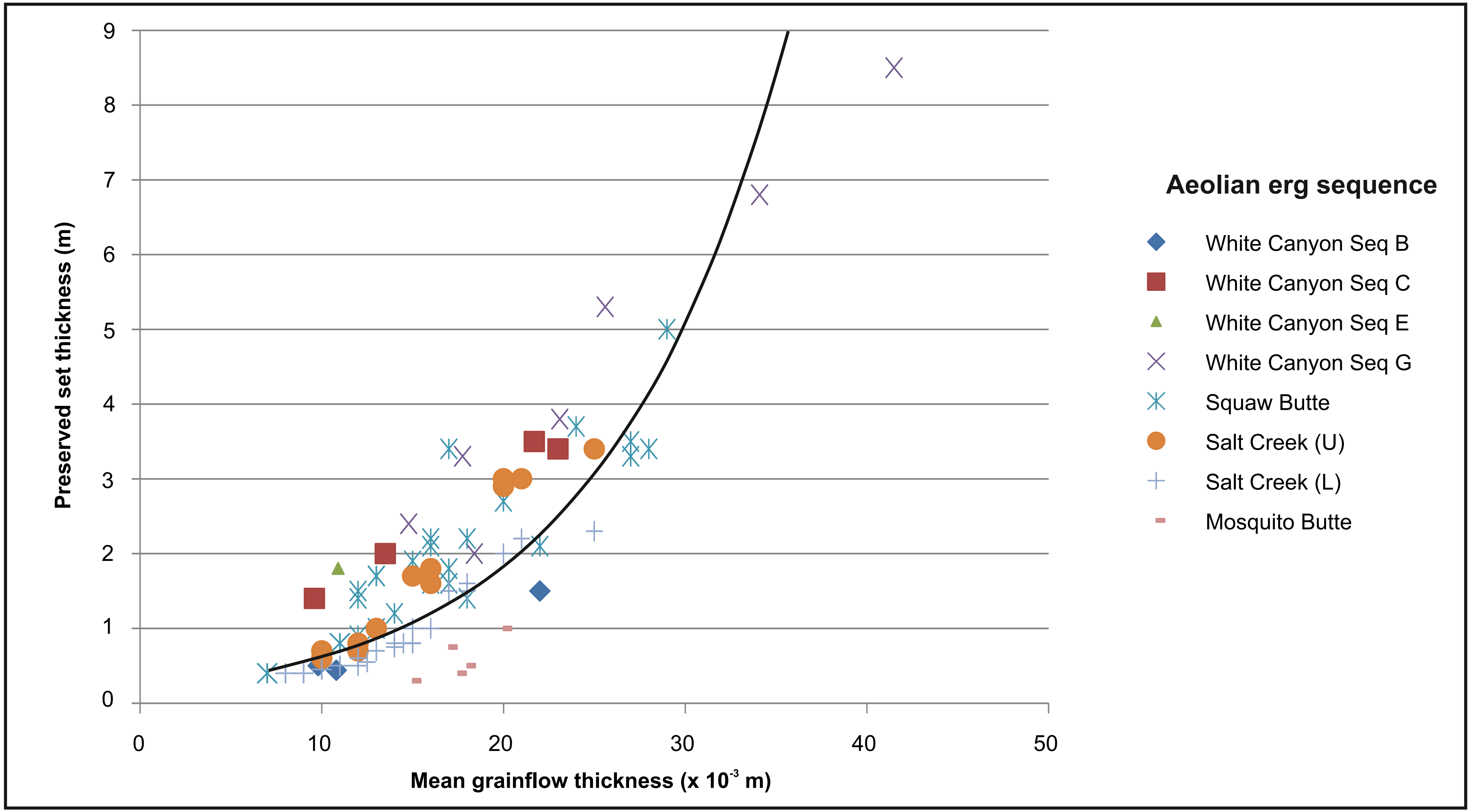

Figure 2.11. Preserved set thickness plotted against the average thickness of the ten thickest grainflow units within each set for a number of aeolian sequences in the erg centre and lateral erg margin areas of the Cedar Mesa Sandstone as identified by Mountney and Jagger (2004) and Mountney (2006b). See text for explanation.

recorded in core. Selection of an appropriate analogue should be based on the following: comparable preserved set thicknesses, comparable grainflow thickness distribution, proportion of facies which are comparable (grainflow, wind-ripple and grainfall), the arrangement of such facies, and the variability of foreset azimuth data. Overall, for sets thought to have been generated by dunes with similar wavelengths, the Navajo system has preserved significantly thinner grainflows than the Cedar Mesa system (Figure 2.7a). A possible reason for this disparity is that the dunes of the two systems may have had markedly different morphologies with different slipface configurations – the dunes which migrated to accumulate the Navajo Sandstone potentially had slipfaces that were shorter than the examples for the Cedar Mesa Sandstone, and which merged into lower-angle inclined plinth deposits higher on the dune flanks.

2.5.4 – Relationship between preserved grainflow thickness and original bedform size (dune height and wavelength)

A positive correlation has been demonstrated previously between dune slipface height and the thickness of grainflow units that are generated as a consequence of lee-slope avalanching down such slipfaces in modern, small-to-medium-sized dunes (Kocurek and Dott, 1981) and a similar relationship is noted for data collected as part of this study (Figure 2.12; Navajo Sandstone, $y = 1532.7x^{1.6006}$, $R^2 = 0.5965$; Kocurek and Dott (1981) dataset, $y = 988.78x^{1.4796}$, $R^2 = 0.5555$). In their initial stages of development, sandflow avalanches thicken as an increasing volume of sand becomes entrained in the flow. For small and medium-sized dunes, grainflow deposits therefore become thicker with increasing slope length and, by implication, bedform height (Kocurek and Dott, 1981). Once fully developed, sandflow avalanches tend to attain an equilibrium thickness and individual preserved grainflow deposits rarely exceed 60 to 80 mm in thickness.

Departures from the trend can arise for a number of reasons: (i) successive avalanches may be erosional at their base, such that previously emplaced avalanche deposits are partly reworked by later deposits, thereby reducing preserved grainflow thickness; (ii) deposits of individual grainflows tend to thin to a point of pinch-out at their downslope limit where they interfinger with packages of wind-ripple strata (e.g. Figure 2.1b), and it is these thinner grainflow deposits that have greater preservation potential in cases where bedform climbing at low angles allows for preservation of only the basal most parts of the original dune lee slope, or where grainflows do not extend to the base of the set (Figure 2.2b); (iii) the generally well sorted texture of aeolian lee-slope deposits means that multiple, separate grainflow units might appear as a single apparently homogenous package of sand lacking any internal stratification and such deposits could be misinterpreted as a single anomalously thick avalanche deposit (e.g. “outliers” in Figure 2.7a and 2.9). Additionally, the effects of sediment compaction will influence comparisons between modern grainflow deposits and ancient preserved grainflow strata.

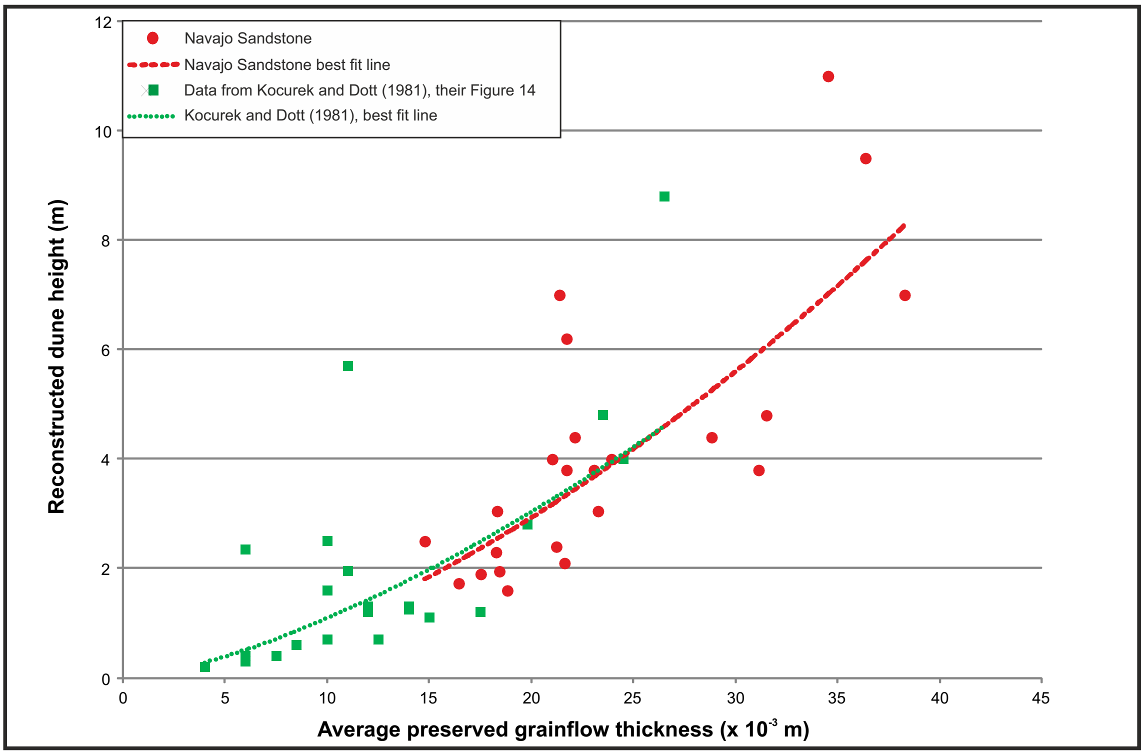

Figure 2.12. (above) Average preserved grainflow thickness plotted against reconstructed dune height for data from the Navajo Sandstone (this study) and data from modern dunes of the Little Sahara dune field (Kocurek and Dott, 1981, their Figure 14). Dune heights for sets of the Navajo Sandstone have been calculated from reconstructed bedform wavelength readings taken in the field and derived using the general relationship between bedform wavelength and dune height of Kocurek and Dott (1981) shown in this figure. The effects of sediment compaction have not been considered.

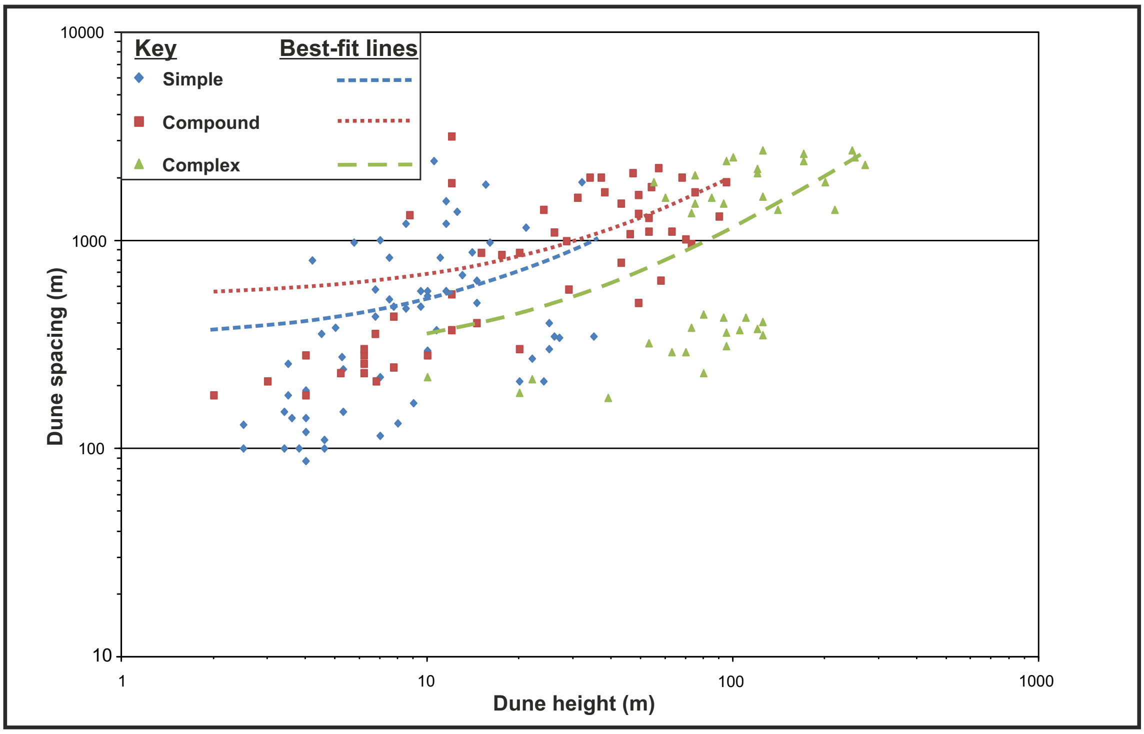

Figure 2.13. (above) Dune height versus dune spacing for a variety of different aeolian dune types from present-day dune fields. Data from Lancaster (1988a). Dune spacing as defined by Lancaster (1988a) is the same as dune wavelength used in this paper. Dunes in the Cedar Mesa and Navajo Sandstone are unlikely to have exceeded 40m in height, based on reconstructions discussed herein.

For many modern bedform types, dune height exhibits a positive correlation with bedform wavelength and spacing (e.g. Wilson, 1973; Lancaster, 1988a; Figure 2.13; simple dunes, $y = 18.944x + 333.56$, $R^2 = 0.0885$; compound dunes, $y = 14.959x + 538.74$, $R^2 = 0.2854$; complex dunes, $y = 8.8474x + 268.74$, $R^2 = 0.3502$). It is therefore possible to demonstrate an indirect relationship between grainflow thicknesses preserved in ancient successions and original bedform height via this relationship between bedform wavelength and height (Figures 2.7a and 2.12). Importantly, this means that if grainflow thickness is known solely from subsurface core data, then a first-order estimate of both original bedform height and wavelength can tentatively be suggested. Furthermore, if both bedform wavelength and preserved set thickness are known, then a generalised estimate of the angle-of-climb of the succession can be made through a simple trigonometric relationship based on the approach outlined by Mountney and Thompson (2002). For this approach to be applied reasonably, care must be taken to determine which type of aeolian bedform has been encountered in core, since mis-interpretation can result in errors of up to two orders of magnitude in reconstructed estimates of likely bedform spacing (Figure 2.13). Bedform type (simple, compound or complex) can potentially be deduced from a thick succession of core by ascribing different genetic significance to bounding surfaces of various types (e.g. interdune migration surfaces, superimposition surfaces, reactivation surfaces; see Brookfield, 1977; Rubin, 1987a; and Rubin and Carter, 2006, for a summary of the technique).

The likely presence of an anomalously large bedform in the Cedar Mesa Sandstone at Mile 101 on Highway 95 (White Canyon) is supported by the relationships of Kocurek and Dott (1981), who suggest that original bedform size can be estimated based on proportions of grainfall strata to grainflow strata in preserved dune sets. Dune sets at Mile 101 preserve no grainfall strata and are composed almost entirely of grainflow strata (95%), with only minor intercalations of wind ripple strata (5%). The average grainflow thickness for this set at Mile 101 is 73 mm, 9mm greater than the average for other sets at this locality, again supporting the interpretation of a large bedform with an unusually high and long slipface.

2.5.5 – Applied workflow for reconstruction of aeolian architecture from core data

The series of empirical relationships identified as part of this study enable aspects of small-scale aeolian stratigraphy observable in core to be related to larger-scale architectural elements; this potentially allows for the first-order reconstruction of the probable geometry and scale of aeolian bedforms responsible for giving rise to preserved aeolian accumulations directly from core data. Sedimentological attributes that can be measured directly from core (and in some cases wireline log) data include preserved set thickness, grainflow thickness, shape of dune toesets, rate of upward-steepening of foresets within a set, and the distribution of primary lithofacies (grainflow, wind-ripple, and grainfall) within sets. Of these, this study has focused on the establishment of a series of empirical relationships based on measurements of preserved set thickness and grainflow thicknesses within the core sections.

For climbing aeolian systems that have accumulated and preserved a succession through a progressive climb of bedforms over one another, preserved set thickness is a function of both bedform size (wavelength) and the angle of system climb. Although preserved set thickness is only partly dependent on original bedform wavelength, there exists a positive linear relationship between preserved set thickness and reconstructed original bedform wavelength. Fundamental relationships exist between slipface height and thickness of grainflow packages preserved for small to medium dunes and the relationships established from this study of two ancient aeolian successions compare closely to a similar relationship established previously for modern dunes (Kocurek and Dott, 1981). Preserved grainflow thicknesses observed in core can be used as a proxy (albeit with some reservations) to predict original bedform height, and therefore size (Figure 2.12), given that bedform height can be related to bedform wavelength for various types of dunes (Figure 2.13). If grainflow thickness is known, then an estimate of bedform wavelength can be made. If both original bedform wavelength and preserved set thickness are known, then the angle-of-climb of the succession can be determined using a simple trigonometric method in the absence of high-resolution seismic data. Although steeper angles of system climb preserve thicker sets for the accumulation of bedforms of a given wavelength, steeper angles of climb do not necessarily result from the migration and accumulation of larger dunes with longer wavelengths.

2.6 – Conclusions

A suite of empirical relationships has been developed based on analysis of aeolian outcrop data from parts of the Permian Cedar Mesa Sandstone and the Jurassic Navajo Sandstone in SE Utah. These relationships enable parameters measured directly from one-dimensional core to be related to larger scale aeolian architectural elements observable in outcrop successions and underpin a simple method for reconstructing aeolian geometry from one-dimensional subsurface datasets alone. However, care must be exercised in the application of this technique: as with most statistical data derived from natural datasets, the spread of the data is, in many cases, considerable and significant; resulting in data distributions that yield best-fit trends with low R^2 values that are statistically weak. However, despite these shortcomings, relationships between measurements of small- and larger-scale aspects of sedimentary architecture form the basis for the development of a predictive tool that can potentially be applied with care to subsurface datasets for elucidation of larger-scale sedimentary architecture and therefore for prediction of regional reservoir stratigraphic heterogeneity.

Chapter 3 – Modelling facies distributions and heterogeneity in aeolian reservoir successions

3.1 – Introduction

A series of semi-quantitative sedimentological models have been developed for use as a predictive tool with which to account for the three-dimensional distribution of facies and architectural elements present in a variety of aeolian successions. These models are based on the reconstructed morphology, scale and style of migratory behaviour of bedforms from a variety of aeolian outcrop successions, coupled with an understanding of the processes that control the distribution of primary lithofacies in aeolian environments.

The models used in this study, generated by the software developed by David Rubin (Rubin, 1987a; Rubin and Carter, 2006), account for the likely mode of evolution of the dune and interdune systems and the mechanisms that dictate their style of preservation. In the forward development of these models, whereby individual aeolian lithofacies have been mapped onto the modelled outputs, emphasis has been placed on field and subsurface techniques for modelling the expected three-dimensional distribution of aeolian facies types (especially net reservoir facies) and the architectural elements within the succession. This further development of the existing models from Rubin (1987a) has been supplemented with selected ancient case examples. This approach is then applied to the Permian Auk Formation in Chapter 5.

Key parameters derived from interpretations of a variety of aeolian successions have been used as an input to numerical modelling software programs (Rubin, 1987a; Rubin and Carter, 2006) that model the expected two-dimensional and three-dimensional pattern of dune and interdune elements, plus their bounding surfaces, generated by the migration and climb of a series of bedform types. The style of migration, accumulation and preservation of dunes and interdunes is simulated by mapping the migration of bedforms over a series of time steps, and by applying rules to determine how older strata are truncated by younger strata. Most common types of aeolian bedforms can be simulated, and the effect of changes in bedform morphology, migration speed, migration direction and rate of accumulation can be assessed. The results from a range of models are presented, each of which assesses the significance of modest changes in bedform morphology and/or style of migratory behaviour with regard to preserved stratigraphic architecture and lithofacies distribution.

3.2 – Background

Difficulty arises when attempting to determine expected facies distributions and resultant architecture in aeolian reservoir successions, where only one-dimensional core data and/or seismic data are available. This can lead to potentially ambiguous interpretations which are then used as a basis for exploration, thereby leading to the development of reservoir models that fail to account effectively for observed reservoir performance. One way to overcome this problem is to use three-dimensional modelling software packages to predict the likely pattern of facies and architectural elements in the subsurface. The models presented in this chapter describe the style of stratigraphic architectures typically present in a range of aeolian successions, and provide quantitative estimates of likely three-dimensional sand-body geometries. These are sufficient to define the shape of architectural elements that can be used, for example, for the development of reservoir models.

The models used in this study have utilised the software developed by David Rubin (Rubin, 1987a; Rubin and Carter, 2006), and analysis is based upon established methods for constructing aeolian facies and architecture models, as explained in Rubin (1987a) and Section 3.3 herein. The original source code (in Matlab and Fortran), modelling software, user guide, plus multiple examples of model-run outputs are available from http://walrus.wr.usgs.gov/seds/bedforms/index.html.

The aims of this study are twofold: (i) to demonstrate how the construction, migration and style of accumulation of aeolian bedforms, of varying morphological type and migratory behaviour, act to control resultant preserved facies distribution and the arrangement of such facies into a series of architectural elements that reflect the preserved expression of a range of types of aeolian depositional systems; (ii) to demonstrate how the distribution of these facies within a suite of architectural elements can either enhance the quality of the resulting reservoir, or be detrimental to overall reservoir quality. Specific objectives are as follows: (i) to develop a suite of end-member aeolian bedforms models for a variety of bedform morphologies by utilising the software developed by David Rubin (Rubin, 1987a); (ii) to map specific aeolian facies on to these base models using an understanding of dune types from modern and outcrop studies; (iii) to further develop these facies models by exploring how the net-reservoir units preserved by each bedform type are arranged, and make comments on the potential quality of this reservoir by interrogating the initial bedform facies models.

3.3 – Data and methods

The generation of the sedimentological models has been achieved through a two-step process: (i) the simulation of the gross-scale architecture of the succession using a specialised piece of numerical modelling software (Rubin, 1987a; Rubin and Carter, 2006); (ii) the population of this architectural “framework” with specific facies, based on commonly recognised arrangements of facies that are known from studies of ancient outcropping aeolian successions, as well as dunes and interdunes present in modern sand seas. The 8 models presented in this study represent end-member models of aeolian bedform types as theoretical examples.

The software package (Rubin, 1987a; Rubin and Carter, 2006) predicts the three-dimensional pattern of cross-bedding and erosive bounding surfaces that are generated by the migration and climb of a series of bedforms. This is achieved by simulating the morphology of the bedforms through an approximation of their shape that involves the modification and convolution of a series of sine waves that are tracked over both space and time in the model. The style of migration, accumulation and preservation of dunes and interdunes within aeolian systems is simulated by mapping (tracking) the migration of bedforms over a series of time steps and by applying a set of rules to determine how older strata are truncated by younger strata. All the major types of aeolian bedforms can be simulated and the effects of changes in bedform steepness, asymmetry, migration speed, migration direction and rate of deposition can all be assessed.

The resultant architecture from each model run is compared to the sedimentary style observed in the case-study data (e.g. preserved set and coset thickness measured from outcropping successions). Input parameters are then adjusted and the model re-run until an appropriate match is achieved. Once the architectural framework of the succession has been modelled, specific aeolian facies are mapped onto the preserved set architectures, based on distributions predicted from quantitative assessments made from a variety of outcrop successions and from distributions known to occur on modern aeolian bedforms. This procedure is based on an understanding of how aeolian facies types are distributed in similar modern dunes and in ancient aeolian successions exposed in outcrop. The geometry and degree of inter-connectedness of the various architectural elements and the facies that they contain can then be assessed and used as input for reservoir models. Both spatial and temporal units within the models produced by the software are dimensionless. Angular directions are expressed in degrees (0-360°). This allows for the resultant model output to be appropriately scaled to the phenomenon being modelled *a posteriori*.

For each of the models, expected aeolian lithofacies have been mapped onto the modelled outputs using CorelDraw, based on a series of rules to determine the positions on the modelled dunes where the different facies packages accumulate. This serves as a mechanism to dictate the arrangement of the various facies packages. The implemented rules are based on the following criteria: (i) the position on modern dunes where the various lithofacies packages are known to occur; (ii) the inclination of the dune slope at the time of accumulation; and (iii) the distance downwind of the brink. The facies deposits incorporated into the models developed for this study have been mapped onto the dune forms in a manner consistent with observations from ancient outcrop and modern dune settings; discussed further in Section 3.4.3.

For each example shown herein, an example of how to further process the modelled output for subsequent input into reservoir modelling software is provided (Figure 3.1), which serves as a reference diagram and is useful by way of explanation for figures that follow later in this discussion. Part (i) of Figure 3.1 refers to Figures 3.7, 3.10, 3.13, 3.17, 3.20, 3.23, 3.26, and 3.29. Sections marked as a) are sections parallel to the trend of the main bedforms. Sections marked as b) are sections perpendicular to the trend of the main bedforms. Sections c) are the top section of these bedform models. Part (ii) refers to Figures 3.8, 3.11, 3.14, 3.15, 3.18, 3.21, 3.24, 3.27, and 3.30. The units shown in a) show a portion of the top section (previously displayed in part (i) c). A – A' in section b) is the same vertical slice as through A – A' in a). B – B' in b) is inclined at an angle that matches the angle-of-climb of the aeolian system and is for a position directly beneath an interdune migration bounding surface that truncates the top of a set; such sections tend to reveal the maximum extent of development of grainflow packages. Part c), shows the maximum extent of grainflow development for the same level as that in b), but in plan-view rather than section-view. Packages of facies associations that are deemed to represent both effective net reservoir and non-net reservoir intervals are simplified in d) to geometric shapes (e.g. ellipses) for forward reservoir modelling purposes. Figures depicting information like that presented in Figure 3.1, but for various alternative modelled scenarios, form the basis for the novel technique developed as part of this research for constraining geo-body shapes in reservoir models.

3.3.1 – Input variables

Each model described here is based on a number of input variables that serve to define the bedform behaviour simulated by the algorithms in the Rubin modelling software package (Rubin, 1987a; Rubin and Carter 2006). Each variable can be modified to enable the depositional situation to be adjusted until an appropriate match to a natural dataset (e.g. outcrop pattern) is achieved. The number of variables that can be manipulated is large (86 variables in total), and can be related to either the first, second or third set of bedforms (or a combination thereof) that migrate as a train (series of genetically related bedforms moving through the model space). The rules to define how these multiple bedforms are superimposed on one another can also be adjusted. Additionally, some variables (parameters) are applied to the entire depositional situation that is being modelled. An explanation of all these features is outlined in Figure 3.2 (modified from Rubin, 1987a); input variables used for the models in the study are shown in Figure 3.3.

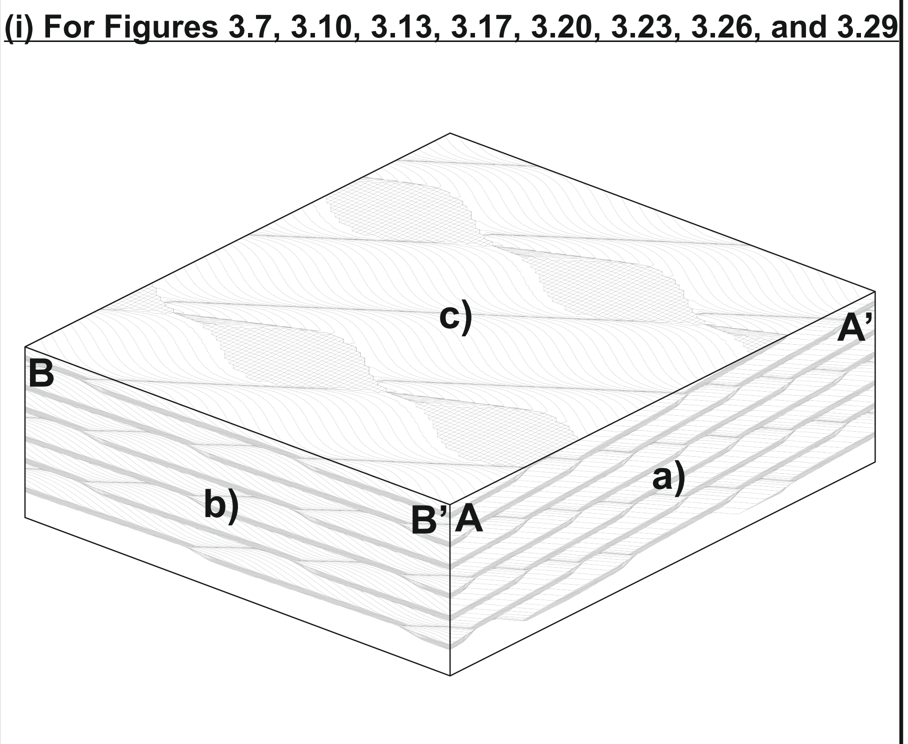
(i) For Figures 3.7, 3.10, 3.13, 3.17, 3.20, 3.23, 3.26, and 3.29

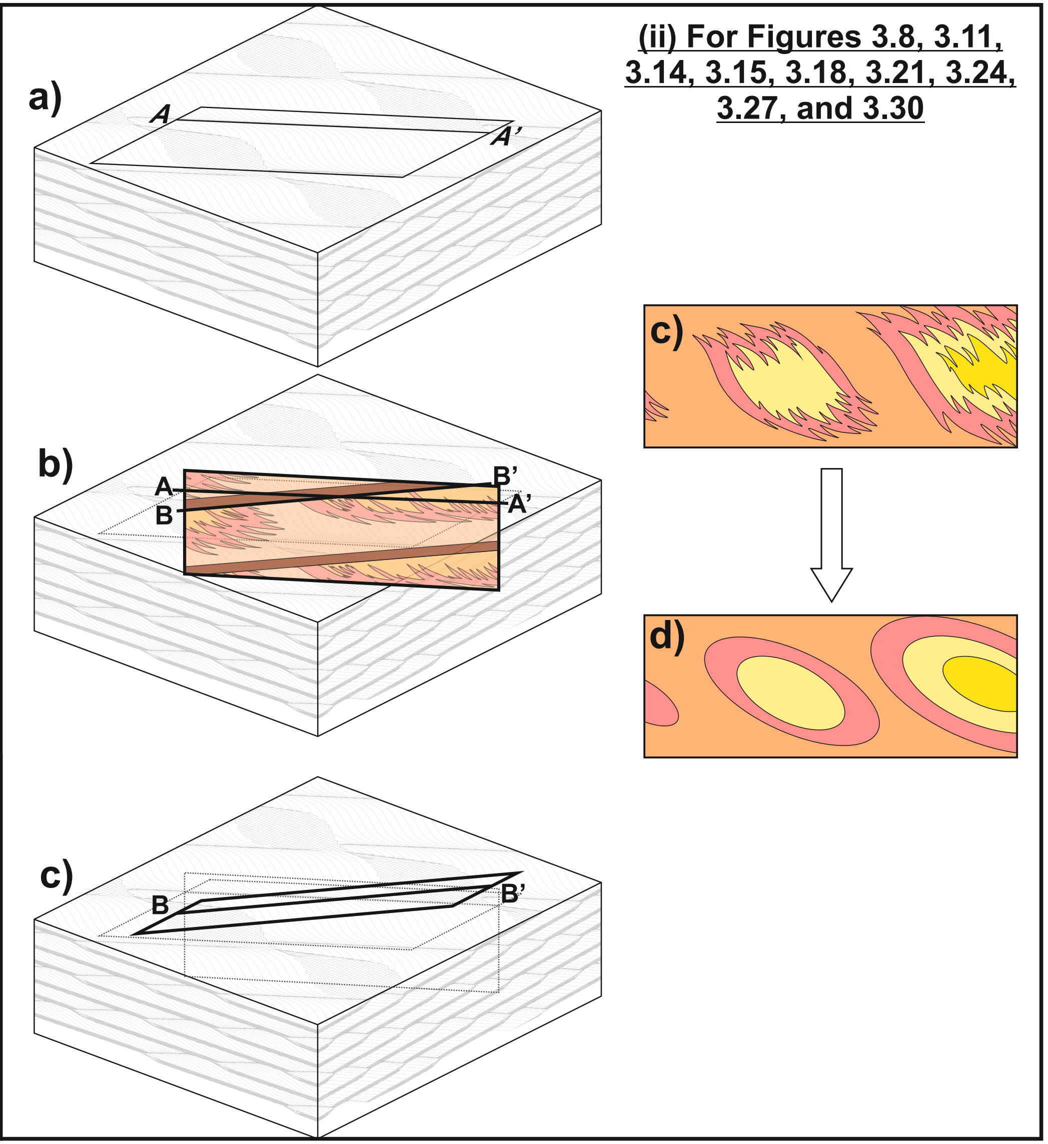
(ii) For Figures 3.8, 3.11, 3.14, 3.15, 3.18, 3.21, 3.24, 3.27, and 3.30

Figure 3.1. Explanation of how reservoir models have been derived. Part (i) refers to Figures 3.7, 3.10, 3.13, 3.17, 3.20, 3.23, 3.26, and 3.29. Sections marked as a) are sections parallel to the trend of the main bedforms. Sections marked as b) are sections perpendicular to the trend of the main bedforms. Sections c) are the top section of these bedform models. Part (ii) refers to Figures 3.8, 3.11, 3.14, 3.15, 3.18, 3.21, 3.24, 3.27, and 3.30. The units shown in a) show a portion of the top section. A – A' in section b) is the same vertical slice as through A – A' in a). B – B' in b) is inclined parallel to climbing upper bounding surface to allow the maximum expression of net reservoir facies to be demonstrated in c), which is shown in plan-view. These packages of net reservoir facies are simplified in d) to geometric shapes for forward reservoir modelling purposes.

Input variable	Description
Wavelength of bedforms	The sides of the block diagrams have lengths of 100.0 units. A bedform wavelength input of 100.0 will generate a single bedform with its peak in the centre of the block diagram; whereas an input of 50.0 will generate a series of parallel-crested bedforms
Bedform phase (°)	This parameter controls the placement at time = zero of the bedform within the block diagram. When the bedform wavelength has been set to 100.0, this variable will have no effect on the structure produced; it will simply control where the structure is placed within the block model. However, if the bedform wavelength is set to more than 100.0, the bedform phase will determine which part of the structure is depicted within the block model
Mean asymmetry	Relates to bedform symmetry or asymmetry as an arbitrary and dimensionless variable. Values of 0.0 here will produce bedforms which are symmetrical, with values between 0.1 and 1.0 producing bedforms with a varying amount of asymmetry (1.0 having the greatest asymmetry). If the value here is positive, then the steeper flank will face in the direction of positive bedform migration as defined by the user; conversely a negative asymmetry value input will generate bedforms whose steepest flank faces in the opposite direction to bedform migration. A mean value of asymmetry is used here in circumstances where asymmetry varies through time.
Amplitude of asymmetry cycle	A complete cycle varies between mean asymmetry *plus* amplitude of asymmetry, and mean asymmetry *minus* amplitude of asymmetry. If bedforms do not vary over time, a value of 0.0 should be used which produces bedforms with no change in their asymmetry. Units are dimensionless, as above.
Period of asymmetry cycle	This variable can be based on any arbitrary time unit as specified by the user. All variables that specify periods or velocities can be based on these units, as long as they are consistent throughout the input file.
Phase of asymmetry cycle	Measured in degrees. Variable relates to phase in the asymmetry cycle at time = zero; this is at a maximum when specified at 90.0 (equals the mean asymmetry plus the amplitude of asymmetry cycle)
Mean bedform steepness	This defines the mean bedform steepness; if height varies through time, then height will also be a function of the amplitude, phase and period of bedform steepness. A value of 1.0 here causes bedform height to be equal to 1/15 of the bedform wavelength, if the effects of bedform superpositioning are neglected. When other variables remain constant, bedform height is proportional to the value chosen.
Amplitude of steepness cycle	During a complete height-fluctuation cycle, bedform height will vary between mean bedform steepness *plus* amplitude of bedform-steepness cycle, and mean bedform steepness *minus* amplitude of bedform-steepness cycle. Units used here are the same as those used for mean bedform steepness. This variable should be set at zero to generate bedforms which do not vary in height.
Period of steepness cycle	The period of time in which bedform steepness changes
Phase of steepness cycle	Phase at time = zero in the steepness-fluctuation cycle. A value of 0.00 produces bedforms with a steepness that is a minumum in the cycle. All values in degrees.
Wavelength of plan-form sinuosities	It is possible to have up to two sets of plan-form sinuosities for each set of bedforms. When specifiying the appropriate values for the wavelength and amplitude of these sinuosities, it is possible to create sinuous, linguoid or lunate plan forms. If the value is set at 0.0 for the wavelength of the first set of sinuosities, no sinuosities will be created. To create sine-shaped plan-form sinuosities, the value for the wavelength of the second set of sinuosities should be 0.0; for lunate or linguoid bedforms, this value should be half of that specified for the first set of bedforms.
Amplitude of sinuosities	Specifies the amplitude, measured in plan-form, of the bedform sinuosities. To create realistic linguoid or lunate bedforms, the value for the amplitude of the second set of plan-form sinuosities should be set to a quarter of the value specified for the wavelength of the second set of sinuosities.

Input variable	Description
Phase of first set of sinuosities	Along-crest placement of the bedform sinuosities.To create in-phase bedforms, the value for the first set of sinuosities should be the same value for the second set of sinuosities. To create out-of-phase bedforms, the two should differ by 180.0.
Migration speed of sinuosities	Units are in length/time. For the most natural looking results, this value should be approximately 3.0 - 4.0. Positive values cause the sinuosities to migrate towards 90° clockwise of the specified migration direction of the bedform; negative values cause the sinuosities to migrate towards 90° anticlockwise of the specified migration direction of the bedform.
Wavelength of second set of plan-form sinuosities	For sine-shaped planform sinuosities, this variable should have value of 0.0. For lunate or linguoid bedforms, this value should be set to half of that specified for the wavelength of the sinuosities.
Amplitude of second set of sinuosities	The plan form amplitude of the second set of sinuosities. To create linguiod or lunate bedforms with a realistic curvature, this value should be set to 1/4 of the value set for the wavelength of the second set of sinuosities.
Phase of second set of sinuosities	The along-crest placement of the plan form sinuosities. For lunate bedforms, this value should be equal to the phase of the first set of sinuosities, plus 270.0. For linguoid bedforms, this value should be equal to the phase of the first set of sinuosities, plus 90.0.
Migration speed of second set of sinuosities	The along-crest migration speed of the second set of sinuosities. If this value differs from the phase of the second set of sinuosities, then the bedform plan-form shape will vary through time.
Migration direction of bedform	Migration direction of the first set of bedforms, normal to the bedform crestlines. Specifying the migration direction therefore also sets the value for the bedform orientation.
Mean migration speed of bedform	Mean migration speed of the first set of bedforms. For the most realistic results, this value should be less than ~ 3.0 or 4.0.
Amplitude of speed cycle	The same velocity units as used for the mean migration speed of the first set of bedforms. If a constant migration speed is needed, then a value of 0.0 should be used here.
Period of speed cycle	Period of migration-speed cycle.
Phase of speed cycle	Phase in the migration speed cycle at time = 0. A value of 0.0 inputted here will generate bedforms that at time = 0 have a minimum speed.
Type of superpositioning	A variable to determine the rules used to superimpose the second and third sets of bedforms on the first set. If this variable is 1, then the superimposed bedforms are added to the main bedforms by simple addition. If this variable is set to 2, the local height of the superimposed bedforms is proportional to the local elevation of the main bedforms. Steepnesses of the superimposed bedforms therefore vary from zero in the troughs of the main bedforms, to a maximum at the crests. The mean steepness of the superimposed bedforms is therefore half of their steepness specified for the second and third set of bedforms. If the value here is 3, the elevations of all the bedforms are calculated separately, and the elevation at any point on the surface is chosen to be that of whichever bedform is locally highest. This is the value to use to produce out-of-phase sinuous, lunate, or linguoid bedforms. Mean steepness of the resulting bedforms varies with the steepness, spacing and phase relationships of the various sets of bedforms. If the value here is 4, the height of the superimposed bedforms is inversely proportional to the local elevation of the main bedform. Steepnesses of superimposed bedforms vary from those specified for the second and third set of bedforms in the troughs of the main bedforms, to zero at the crests. The mean steepness of the superimposed bedforms is thus half of the specified value. If the value here is 5, two sets of superimposed bedforms are created, following the rules if the variable was set to 3; that assemblage is then added to the main bedforms as if the variable was 1. If the value here is 6, the first set of superimposed bedforms is summed as if the variable were 2, and the second set is added as if the variable were 1.

Input variable	Description
Rotation option	Variable that can be used to rotate all bedforms and migration directions such that trough axes are normal or parallel to the sides of the block diagrams. If equal to 0, no rotation is performed. Values of 1, 2, 3, or 4 can be selected to cause scour pits to migrate out of any of the four vertical sides of the block (1 for the back right, 2 for the front right, 3 for the front left, and 4 for the back left).
Elevation of interdune flats	A value of less than -1.0 will generally produce no interdune flats. A value of 0.0 will cause approximately half of the surface area to be occupied by interdune flats.
Rate of deposition	Mean rate of deposition; same units of length/time as migration rates.
Amplitude of cycle in rate of deposition	Amplitude of cycle in the rate of deposition; same units of length/time as migration rates.
Period of cycle in rate of deposition	Period of cycle in the rate of deposition; same units as all other time periods.
Phase of cycle in rate of deposition	Phase of cycle in the rate of deposition (in degrees). If equal to 0.0°, the rate of deposition is at a minimum at time = zero.
Time from t=0 to beginning of depositional episode	Integer number of steps backward through time to the beginning of the depositional event that is being simulated.
Interval between drawing of crossbeds	Interval between the plotting of the foresets. This is normally equal to 1, but can be increased. Larger numbers require less computing time but produce less detailed images.
Time from t=0 to end of depositional episode	Integer that specifies the time of the end of the depositional episode (i.e. the time when the surface is illustrated). Changing this number causes a change in the location of the bedforms within the block diagram.
Precision or speed?	Integer variable that chooses between long computation times (with high precision of plots) and shorter computation times (accompanied by lower precision); the value of this variable must equal 1, 2, 4, 5, or 10. Small values create more natural-looking images (smoother curves, particularly in horizontal sections) but take longer to run and require more disk space for each image. In general, values of 2, 4, and 5 are good starting points for this variable.
Elevation of horizontal surface	Elevation of the horizontal section, expressed in non-dimensional units (relative to 0.0 at the lowest point on the bedform surface and 1.0 at the highest point). A value of 1.0 will cause the horizontal section to be equal to the highest point on the bedform surface; the entire bedform surface will be shown in a mesh diagram. A value of 0.0 will cause the elevation of the horizontal section to coincide with the lowest elevation of the bedform surface; the top of the block diagram will consist entirely of a horizontal section

Figure 3.2. (previous pages) Descriptions of the input variables to the Rubin software package (Rubin, 1987a) for the Sedimentological Models.

Model # Input variable	1	2	3	4	5	6	7	8
Wavelength of bedforms in first set	50.0	100.0	75.0	100.0	50.0	100.0	80.0	50.0
Bedform phase (°)	0.0	0.0	0.0	0.0	0.0	0.0	0.0	0.0
Mean asymmetry	1.0	1.0	1.0	1.0	0.0	1.0	1.0	0.0
Amplitude of asymmetry cycle	0.0	0.0	0.0	0.0	0.0	0.0	0.0	1.0
Period of asymmetry cycle	1.0	1.0	1.0	1.0	1.0	1.0	1.0	13.0
Phase of asymmetry cycle	0.0	0.0	0.0	0.0	0.0	0.0	0.0	0.0
Mean bedform steepness	1.0	0.7	0.8	1.0	1.0	1.0	1.0	1.0
Amplitude of steepness cycle	0.0	0.4	0.0	0.0	0.0	0.0	0.0	0.0
Period of steepness cycle	1.0	14.0	1.0	1.0	1.0	1.0	1.0	1.0
Phase of steepness cycle	0.0	180.0	0.0	0.0	0.0	0.0	0.0	0.0
Wavelength of first set of plan-form sinuosities	0.0	0.0	75.0	0.0	50.0	0.0	0.0	50.0
Amplitude of first set of sinuosities	0.0	0.0	9.0	0.0	6.0	0.0	0.0	6.0
Phase of first set of sinuosities	0.0	0.0	0.0	0.0	0.0	0.0	0.0	0.0
Migration speed of first set of sinuosities	0.0	0.0	0.0	0.0	-1.0	0.0	0.0	-1.0
Wavelength of second set of plan-form sinuosities	0.0	0.0	25.0	0.0	0.0	0.0	0.0	0.0
Amplitude of second set of sinuosities	0.0	0.0	0.0	0.0	3.0	0.0	0.0	3.0
Phase of second set of sinuosities	0.0	0.0	270.0	0.0	270.0	0.0	0.0	270.0
Migration speed of second set of sinuosities	0.0	0.0	0.0	0.0	0.0	0.0	0.0	0.0
Migration direction of bedform	90.0	90.0	0.0	90.0	90.0	90.0	90.0	90.0
Mean migration speed of bedform	1.0	1.0	1.0	1.0	0.0	0.5	1.0	0.0
Amplitude of speed cycle	0.0	0.0	0.0	0.0	0.0	0.0	0.0	0.0
Period of speed cycle	1.0	1.0	1.0	1.0	1.0	1.0	1.0	1.0
Phase of speed cycle	0.0	0.0	0.0	0.0	0.0	0.0	0.0	0.0

Figure 3.3. (continued overleaf) Input variables to the Rubin software package (Rubin, 1987a) for the Sedimentological Models. Parameters have been split into those which relate to the first, second or third set of bedforms that have been modelled, or those parameters which relate to the entire depositional situation that is being modelled. Length: all length dimensions are defined relative to the lengths of the sides of the block, which are 100 units long. Phase: all phases are given in degrees and describe the situation at t=zero. Symmetry: dimensionless. Time: arbitrary units that describe all parameters of time (periods of cyclicity, migration speeds, and deposition rate). Direction: in degrees (from Rubin and Carter, 2006).

This page - input variables to describe the first set of bedforms.

Model # Input variable	1	2	3	4	5	6	7	8
Wavelength of bedforms in second set	0.0	0.0	75.0	30.0	0.0	50.0	60.0	0.0
Bedform phase (°)	0.0	0.0	180.0	0.0	180.0	60.0	0.0	180.0
Mean asymmetry	0.0	0.0	1.0	1.0	1.0	0.0	0.0	1.0
Amplitude of asymmetry cycle	0.0	0.0	0.0	0.0	0.0	0.5	1.0	0.0
Period of asymmetry cycle	1.0	1.0	1.0	1.0	1.0	9.0	18.0	1.0
Phase of asymmetry cycle	0.0	0.0	0.0	0.0	0.0	0.0	180.0	0.0
Mean bedform steepness	0.0	0.0	0.8	1.0	0.8	1.0	1.0	0.8
Amplitude of steepness cycle	0.0	0.0	0.0	0.0	0.0	0.0	0.0	0.0
Period of steepness cycle	1.0	1.0	1.0	1.0	1.0	1.0	1.0	1.0
Phase of steepness cycle	0.0	0.0	0.0	0.0	0.0	0.0	0.0	0.0
Wavelength of first set of plan-form sinuosities	0.0	0.0	75.0	0.0	50.0	0.0	0.0	50.0
Amplitude of first set of sinuosities	0.0	0.0	9.0	0.0	6.0	0.0	0.0	6.0
Phase of first set of sinuosities	0.0	0.0	180.0	0.0	0.0	0.0	0.0	0.0
Migration speed of first set of sinuosities	0.0	0.0	0.0	0.0	0.0	0.0	0.0	0.0
Wavelength of second set of plan-form sinuosities	0.0	0.0	0.0	0.0	0.0	0.0	0.0	0.0
Amplitude of second set of sinuosities	0.0	0.0	0.0	0.0	3.0	0.0	0.0	3.0
Phase of second set of sinuosities	0.0	0.0	270.0	0.0	270.0	0.0	0.0	270.0
Migration speed of second set of sinuosities	0.0	0.0	0.0	0.0	0.0	0.0	0.0	0.0
Migration direction of bedform	0.0	0.0	0.0	0.0	0.0	0.0	0.0	0.0
Mean migration speed of bedform	0.0	0.0	1.0	1.0	1.0	0.0	1.8	1.0
Amplitude of speed cycle	1.0	1.0	0.0	0.0	0.0	2.5	2.8	0.0
Period of speed cycle	1.0	1.0	1.0	1.0	1.0	9.0	18.0	1.0
Phase of speed cycle	0.0	0.0	0.0	0.0	0.0	0.0	90.0	0.0

This page - input variables to describe the second set of bedforms.
All terms analogous to the corresponding terms for the first set of bedforms on the previous tables

Model # Input variable	1	2	3	4	5	6	7	8
Wavelength of bedforms in third set	0.0	0.0	0.0	0.0	0.0	0.0	0.0	0.0
Bedform phase (°)	0.0	0.0	0.0	0.0	0.0	0.0	0.0	0.0
Mean asymmetry	0.0	0.0	0.0	0.0	0.0	0.0	0.0	0.0
Amplitude of asymmetry cycle	0.0	0.0	0.0	0.0	0.0	0.0	0.0	0.0
Period of asymmetry cycle	1.0	1.0	1.0	1.0	1.0	1.0	1.0	1.0
Phase of asymmetry cycle	0.0	0.0	0.0	0.0	0.0	0.0	0.0	0.0
Mean bedform steepness	0.0	0.0	0.0	0.0	0.0	0.0	0.0	0.0
Amplitude of steepness cycle	0.0	0.0	0.0	0.0	0.0	0.0	0.0	0.0
Period of steepness cycle	1.0	1.0	1.0	1.0	1.0	1.0	1.0	1.0
Phase of steepness cycle	0.0	0.0	0.0	0.0	0.0	0.0	0.0	0.0
Wavelength of first set of plan-form sinuosities	0.0	0.0	50.0	0.0	50.0	50.0	0.0	50.0
Amplitude of first set of sinuosities	0.0	0.0	7.0	0.0	7.0	7.0	0.0	7.0
Phase of first set of sinuosities	0.0	0.0	0.0	0.0	0.0	0.0	0.0	0.0
Migration speed of first set of sinuosities	0.0	0.0	0.0	0.0	0.0	0.0	0.0	0.0
Wavelength of second set of plan-form sinuosities	0.0	0.0	50.0	0.0	50.0	50.0	0.0	50.0
Amplitude of second set of sinuosities	0.0	0.0	7.0	0.0	7.0	7.0	0.0	7.0
Phase of second set of sinuosities	0.0	0.0	0.0	0.0	0.0	0.0	0.0	0.0
Migration speed of second set of sinuosities	0.0	0.0	0.0	0.0	0.0	0.0	0.0	0.0
Migration direction of bedform	0.0	0.0	0.0	0.0	0.0	0.0	0.0	0.0
Mean migration speed of bedform	0.0	0.0	0.0	0.0	0.0	0.0	0.0	0.0
Amplitude of speed cycle	0.0	0.0	0.0	0.0	0.0	0.0	0.0	0.0
Period of speed cycle	1.0	1.0	1.0	1.0	1.0	1.0	1.0	1.0
Phase of speed cycle	0.0	0.0	0.0	0.0	0.0	0.0	0.0	0.0

This page - input variables to describe the third set of bedforms.
All terms analogous to the corresponding terms for the first and second sets of bedforms on the previous tables

Model # Input variable	1	2	3	4	5	6	7	8
Type of superpositioning	2	2	3	2	3	2	2	3
Rotation option	0	0	0	0	0	0	0	0
Elevation of interdune flats	-1.0	-1.0	-1.0	-1.0	-1.0	-1.0	-1.0	-1.0
Rate of deposition	0.08	0.08	0.08	0.08	0.08	0.04	0.08	0.08
Amplitude of cycle in rate of deposition	0.0	0.0	0.0	0.0	0.0	0.0	0.0	0.0
Period of cycle in rate of deposition	1.0	1.0	1.0	1.0	1.0	1.0	1.0	1.0
Phase of cycle in rate of deposition	0.0	0.0	0.0	0.0	0.0	0.0	0.0	0.0
Time from t=0 to beginning of depositional episode	150	150	250	150	150	300	350	150
Interval between drawing of crossbeds	2	1	2	1	4	2	1	2
Time from t=0 to end of depositional episode	1	1	1	20	1	0	43	1
Precision or speed?	1	1	1	1	1	1	1	1
Elevation of horizontal surface	1.0	1.0	1.0	1.0	1.0	1.0	1.0	1.0

This page - input variables that apply to the entire depositional situation which is being modelled. All terms analogous to the corresponding terms for the bedforms on the previous tables.

3.3.2 – Terminology

Terminology descriptions used in this study are described below, to explain the form and migratory behaviour of the types of bedforms that have been modelled; these have been modified from Rubin (1987a). See Figure 3.4 for descriptions relating to the bedform variables used in this modelling process.

Two-dimensional bedforms. Bedforms with straight crestlines, constant crest and trough elevations relative to the generalised depositional surface, and identical across-crest profiles at all locations along the crestline. Two-dimensional bedforms deposit two-dimensional cross-bedding — cross-bedding in which all foresets and bounding surfaces have identical strikes. In nature no bedforms are perfectly two-dimensional because their crestlines cannot have infinite extent. Nevertheless, the term two-dimensional is useful for describing bedforms with relatively simple morphology and behaviour.

Three-dimensional bedforms. Bedforms that possess one or more of the following characteristics: sinuous crestlines or sinuous troughs (either in plan form or in elevation), or across-crest profiles that vary along the crestline. All of these variations produce three-dimensional cross-bedding — cross-bedding in which cross-bed strike varies within a set of cross-strata. Classic trough cross-bedding is one common expression of the migration and accumulation of three-dimensional bedforms.

Invariable. Bedforms that do not change in morphology or path of climb through time or space. Invariable bedforms deposit sets of invariable cross-strata — sets in which all foresets, when considered in three dimensions, are geometrically identical. No bedforms are perfectly invariable, because they cannot exist indefinitely without changing. Nevertheless, the term invariable is useful for describing bedforms with relatively simple morphology and behaviour.

Variable. Bedforms which undergo a change in morphology or path of climb through time or space. Individual foresets in the sets of variable cross-beds are not geometrically identical.

Transverse, oblique and linear bedforms. Bedforms can be classified based on the orientation of their crestlines relative to the long-term resultant sediment-transport direction (Rubin, 1987a). Perfectly transverse bedforms have crestlines that trend exactly perpendicular to the transport direction; in nature, many such types have crestlines that trend close to perpendicular, up to 15° from exactly perpendicular to the transport direction (Hunter et al., 1983). Perfectly linear bedforms have crestlines that trend exactly parallel to the transport direction; in nature, many such types have crestlines that trend close to parallel to the transport direction, up to 15° from exactly parallel (Hunter et al., 1983). Oblique bedforms have intermediate trends: previous studies have arbitrarily selected 15° as the maximum permissible divergence from perfectly transverse or perfectly linear before bedforms are considered to be oblique (Hunter et al., 1983).

TWO-DIMENSIONAL Two-dimensional bedforms are straight and parallel in plan form ; the flanks of the bedforms have the same strike in all locations. Two-dimensional bedforms produce two-dimensional cross-bedding: cross-bedding in which all foresets and bounding surfaces have the same strike. In plots showing the direction and inclination of dips and cross-beds and bounding surfaces, dips of all planes plot along a single straight line through the centre of the plot.	**INVARIABLE** Invariable bedforms are those that do not change in morphology or path of climb. Cross-bedding deposited by invariable two-dimensional bedforms has bounding surfaces that are parallel planes; their poles plot as a single point.	**TRANSVERSE, OBLIQUE & LINEAR** Transverse, oblique and linear cross-bedding are not distinguishable unless bedforms are at least slightly three-dimensional. *Example - Sedimentological Model 1 (Figure 3.6)*
	VARIABLE Variable bedforms are those that change in morphology or path of climb. Variability causes dispersion in the inclinations of bounding surfaces. Cross-bedding deposited by variable two-dimensional bedforms has bounding surfaces with a constant strike but with varying inclination; their poles plot as a straight line that parallels the line of cross-bed dips.	**TRANSVERSE, OBLIQUE & LINEAR** Transverse, oblique and linear cross-bedding are not distinguishable unless bedforms are at least slightly three-dimensional *Example - Sedimentological Model 2 (Figure 3.9)*
THREE-DIMENSIONAL Three-dimensional bedforms are curved in plan form or have plan-form complexities such as scour pits or superimposed bedforms with a different trend from the main bedform; the strike of the flanks varies with location. Three-dimensional bedforms produce three-dimensional cross-bedding: cross-bedding in which foreset and bounding-surface strikes vary with location; dips of foresets do not plot along a single straight line through the centre of polar plots.	**INVARIABLE** Cross-bedding deposited by invariable three-dimensional bedforms has bounding surfaces that are trough-shaped; bounding surface dips in a single trough (or in identical troughs) plot as a nearly straight line.	**PERFECTLY TRANSVERSE** Plots of cross-bed and bounding-surface dips have bilateral symmetry; the axis of symmetry is the same for both plots; dip directions are distributed unimodally. *Example - Sedimentological Model 3 (Figure 3.12)*
		OBLIQUE, IMPERFECTLY TRANSVERSE OR IMPERFECTLY LINEAR Plots of cross-bed and bounding-surface dips do not have bilateral symmetry; cross-bed dips are asymmetrically distributed relative to bounding surface dips. *Example - Sedimentological Model 4 (Figure 3.16)*
		PERFECTLY LINEAR Plots of cross-bed and bounding-surface dips have bilateral symmetry; dip directions may be distributed bimodally (as in Figure 3.19) or may be unimodal as a result of migration on the nose of the main bedforms. The perfectly linear attribute is evidenced by vertical accretion of bedforms; cross-beds dip in opposing directions on opposite flanks *Example - Sedimentological Model 5 (Figure 3.19)*
	VARIABLE Bounding surfaces have complex shapes produced by such processes as zig-zagging of scour-pits; dips of bounding surfaces plot as scatter diagrams.	**PERFECTLY TRANSVERSE** Same as perfectly transverse, invariable, three-dimensional cross-bedding. *Example - Sedimentological Model 6 (Figure 3.22)*
		OBLIQUE, IMPERFECTLY TRANSVERSE OR IMPERFECTLY LINEAR Same as oblique or imperfectly aligned, invariable, three-dimensional cross-bedding. *Example - Sedimentological Model 7 (Figure 3.25)*
		PERFECTLY LINEAR Same as perfectly linear, invariable, three-dimensional cross-bedding. *Example - Sedimentological Model 8 (Figure 3.28)*

Figure 3.4. Bedform classification scheme; modified from Rubin (1987a).

3.4 – Facies and reservoir properties

Descriptions of the aeolian facies types used in this study and their associated reservoir properties were described in Chapter 1 (Section 1.4; Section 1.6); rules determined for predicted facies distributions on the bedform models are discussed here. A routinely applied facies colour-code scheme is introduced herein and this is summarised in Figure 3.5.

3.4.1 – Composite facies

Architectural units used in the modelling process for this study are not based solely on the discrete and individual facies types described in Section 1.4; instead they may incorporate combinations of two or more basic facies types in varying proportions. These are packages of strata that are composed internally of associations of the aforementioned basic facies types, occurring in varying configurations and proportions. The sedimentological models described herein have adopted a scheme whereby wind-ripple-dominated facies is a separate facies type from wind-ripple strata. This wind-ripple-dominated facies is predominately characterised by wind-ripple deposits; units are composed of >50% wind-rippled facies but additionally incorporate a minor component of grainflow strata. Similarly, grainflow-dominated facies in this study is a separate facies type from grainflow strata. This grainflow-dominated facies is predominately characterised by grainflow deposits; units are composed of >50% grainflow facies but additionally incorporate a minor component of wind-ripple strata.

3.4.2 – Reservoir properties

In hydrocarbon plays, it is preferential to target regions of the subsurface stratigraphy that are dominated by a high proportion of grainflow and grainflow-dominated aeolian dune strata. This is because grainflow strata tend to form packages of well-sorted, loosely-packed sandstone with permeabilities that are typically one to three (or more) orders of magnitude greater than those composed predominantly of packages of grainfall and wind-ripple strata and which dominate in some aeolian elements (Chandler et al., 1989; Prosser and Maskall, 1993; Howell and Mountney, 2001; Romain and Mountney, 2014). Porosity and permeability values for specific aeolian facies types are described in Section 1.6, Figure 1.18 and Figure 1.19.

3.4.3 – Rules for determining facies distributions on bedforms

Further to the discussion in Section 3.3, a series of rules have been implemented to determine the positions on the modelled bedforms where the different facies packages accumulate. This serves as a mechanism to dictate the expected arrangement and distribution of facies packages on both the bedform surfaces and as their accumulated deposits. Implementation of these rules is based on the following criteria determined from an awareness of sedimentary processes on modern bedforms: (i) an understanding of the timing and spatial occurrence of processes that are known to operate on modern dune surfaces that lead to the accumulation of lithofacies packages; (ii) an awareness of how the inclination of the dune slope at the time of accumulation governs the process of deposition of various lithofacies types; and (iii) an understanding of how the distance downwind of the brink point, for a given size of bedform, is known to govern how airflow separation cells detach and reattach, and thereby govern where grainfall deposits likely accumulate (Anderson, 1988). The facies deposits incorporated into the models developed for this study have been mapped onto the dune forms in a manner consistent with observations from ancient outcrop and modern dune settings, as explained below.

3.4.3.1. Wind-rippled facies

Modern setting. Wind-rippled sands occur most commonly on the stoss-side of aeolian dune bedforms (Section 1.4.1; Figure 1.8), on low-angle-inclined dune plinths (0-15°) representing the lower parts of lee slopes (Figure 1.8; Figure 1.9d), and in associated interdune areas (Figure 1.8).

Modelled position on bedform models. Wind-rippled facies in the models developed as part of this study have been modelled on stoss slopes of bedforms, in dune plinth regions that have a depositional dip between 0 - 10°, and all interdune areas. They have additionally been modelled on the flanks of elevated areas (e.g. spurs, superimposed bedforms) and as a thin veneer at the base of reactivated surfaces, in a style that is consistent with the distributions noted by Hunter (1977a).

3.4.3.2. Wind-ripple-dominated facies

Modern setting. Wind-ripple-dominated facies in this study are classified as a lithofacies type that comprises >=50% wind-ripple facies and <50% grainflow facies. In nature, wind-ripple-dominated facies accumulate on the upper parts of dune plinths (typically 5 - 15°; very rarely up to a maximum of ~ 30°) on the dune lee-slope where wind-ripple facies grade into the grainflow facies around the intersection with the lower dune lee-slope slipface (Figure 1.8). This is the point on the majority of aeolian bedforms where this transition occurs (Figure 1.9; Figure 1.10).

Modelled position on bedform models. Wind-ripple-dominated facies have been modelled on slopes inclined at angles from 10-15°, thereby reflecting their distribution in natural systems.

3.4.3.3. Grainflow facies

Modern setting. Grainflow deposits are developed on the active slipfaces of dunes (Kocurek and Dott, 1981), and movement usually ceases within the middle section of a steeply-dipping dune lee-slope, although more energetic flows may reach to the base of this slope. Inclination of the slope is therefore the primary factor in determining the proportion of grainflow deposits which will be preserved in ancient successions. The distance down the lee slope that grainflow deposits extend is especially important in bedforms that accumulate at low angles-of-climb because such a style of accumulation preserves only the bottommost portions of the bedforms: for grainflow deposits to become preserved in such systems, they must extend down to the lowermost part of the dune lee slope. This is a fundamental control on likely reservoir quality. Many transverse bedform types have a high proportion of grainflow deposits present on the lowermost parts of their lee slopes (Kocurek and Dott, 1981); modern examples include coastal aeolianites in Israel (Yaalon and Laronne, 1971) and Baja California (Inman et al., 1966). By contrast, many linear bedform types tend to have thick, but relatively low-angle-inclined, plinths that prevent grainflows from reaching the lowermost parts of the dune slope; modern examples include large linear draa of the Rub' Al-Khali Desert (Al-Masrahy and Mountney, 2013); an ancient example is the Permian Auk Formation of the Central North Sea (Chapters 4 and 5).

Modelled position on bedform models. In this study, grainflow deposits have been modelled on the upper slipfaces of aeolian bedforms (Figure 1.8), at angles between 20-34°, reflecting the angle-of-repose for loose sand.

3.4.3.4. Grainflow-dominated facies

Modern setting. Grainflow-dominated facies in this study are classified as a lithofacies type that comprises >=50% grainflow facies and <50% wind-ripple facies. Grainflow-dominated facies are deposited at the lower dune lee-slope slipface where grainflow facies grade into the wind-ripple facies around the intersection with the upper plinth of the dune lee-slope. This is because grainflow deposits avalanche down-slope under momentum over slightly lower-angle-inclined surfaces that are otherwise subject to wind-ripple development.

Modelled position on bedform models. Grainflow-dominated facies have been modelled herein on the dune plinths and slipfaces of both the primary and any superimposed bedforms, on slopes inclined at angles from 5-20°, thereby reflecting their distribution in natural systems.

3.4.3.5. Grainfall facies

Modern setting. Grainfall deposits are initiated at zones of flow separation at the brink of the dune slipface, where grains in saltation lose momentum and fall onto the lee slope (Kocurek and Dott, 1981). These deposits tend to accumulate on the slipface, plinth and interdune areas of aeolian dunes (Hunter, 1977a). Grainfall deposits are most commonly preserved in interdune areas associated with wind-ripple deposits (Figure 1.11b), although differentiation of these two facies types in this setting is commonly problematic (Hunter, 1981).

Modelled position on bedform models. Although grainfall facies are known to accumulate on the slipface, plinth and interdune areas of some aeolian dunes (Hunter, 1977a), the preservation potential of such deposits is low because they are typically reworked by ensuing ripple development or avalanching. As such, these deposits are typically reworked to form wind-ripple and grainflow strata in accumulated deposits. For the purpose of this modelling exercise the distribution of grainfall deposits that are likely to become accumulated as part of a preserved succession have been restricted to those occurring on the upper brink position on the dune slipface, though it should be noted that their preservation potential in this region is low where bedforms accumulate via climbing at low angles (Mountney, 2006b).

3.5 – An approach to modelling stratigraphic complexity in aeolian successions

The forward stratigraphic models (Figures 3.6 – 3.30) were run based on the end-member reference cases from the classification scheme introduced and described by Rubin (1987a; see also Figure 3.4 herein). This classification scheme directly relates bedform morphology to the bedform behaviour. These eight end-member models demonstrate how distinct and measurable changes in dimensionality (two-dimensional or three-dimensional), variability of bedform morphology or migratory behaviour over time (invariable or variable), and orientation of bedform crestlines relative to net migration direction, influence the final bedform morphology and resultant accumulated stratigraphy. In addition to the initial model runs, which have been replicated here from those first depicted by Rubin (1987a), facies distributions have been mapped onto the resultant modelled output architectures to demonstrate how variations in bedform morphology and facies distributions thereon exert a fundamental control on the distribution of reservoir zones, each of which have varying amounts of effective net reservoir and therefore affect fluid flow properties of the reservoir. Where appropriate, a modern or ancient outcrop example is given which displays the style of morphology and migratory behaviour of the bedform which has been modelled (Figure 3.31).

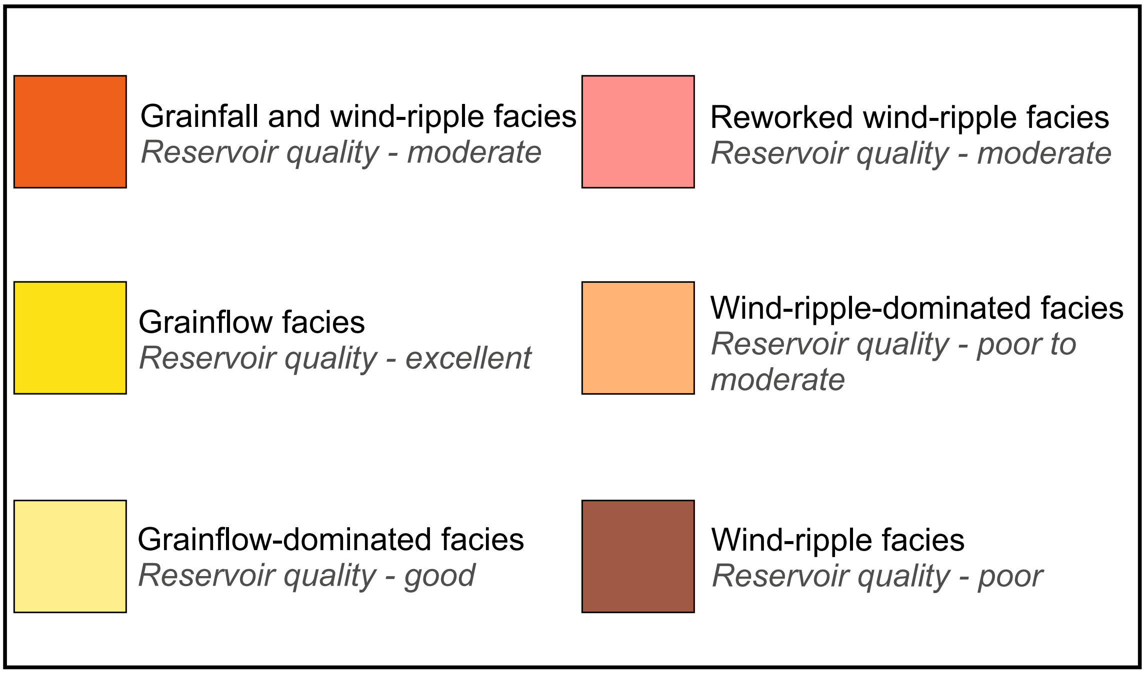

Figure 3.5. A key to the facies colouration used in the modelling process. Grainflow and grainflow-dominated facies have the most favourable reservoir quality, whereas wind-ripple and wind-ripple-dominated facies tend to have less favourable reservoir properties (see Figure 1.19).

3.6 – Sedimentological Model 1: Two-dimensional, invariable, transverse bedforms

See Figure 3.3 for detailed input parameters used in the Rubin modelling software package to generate this model.

3.6.1 – Facies distributions on bedforms

Figure 3.6 depicts the depositional architecture arising from the migration of two-dimensional bedforms climbing at a stoss-erosional, lee-depositional, net-positive angle-of-climb (Figure 5 in Rubin, 1987a). The preservation potential of grainflow-dominated units is dependent on three primary factors: (i) the distance down the lee-slope that the original grainflow facies extended; (ii) the wavelength of the original bedforms, where the bedforms accumulate via a bedform climbing mechanism; and (iii) the angle at which the bedforms climbed over one another to generate the accumulated sets. The first parameter is governed by the shape of the dune lee slope: where a thick, low-angle-inclined plinth is present, grainflows will tend to terminate higher up the dune slope. The latter two parameters jointly determine the level at which dunes are truncated to preserve sets of cross-strata of a given thickness.

In this example, low to medium angles-of-climb preferentially preserve wind-ripple-dominated units at the toe of bedforms, and there is little opportunity for pure grainflow units to be preserved. Preserved set thickness of these bedforms is a function of original bedform wavelength, and the angle-of-climb (Mountney and Howell, 2000; Romain and Mountney, 2014). More energetic grainflow deposits might occasionally run out down-slope into the otherwise wind-ripple-dominated upper dune plinth region; such grainflows would have a greater chance of preservation (see Section 3.10.1 for an example of this).

The facies belts preserved here are parallel to the strike of the original bedforms. They are parallel to original bedform trend; however in nature these would eventually terminate to preserve highly elongate units. In this simplistic model, the facies packages produce a layer-cake stratigraphy. The inclination of these packages is dictated by the angle-of-climb. In ‘dry’ aeolian systems (*sensu* Kocurek and Havholm, 1993) units are characterised by dry interdune depressions dominated by wind-ripple strata with no extensive interdune flats present, as is the case depicted in this example.

3.6.2 – Geometry of stratigraphic architecture

Figure 3.7 depicts the internal stratigraphic architecture relating to Sedimentological Model 1. The example shown in Figure 3.7a depicts the geometry of the stratigraphic architecture of the facies generated in a section parallel to the trend of the main bedforms. Here, the facies units are deposited in a flat-lying, layer-cake stratigraphy with no fluctuations in height. The geometry depicted here would be unlikely in natural systems, at least over distances in excess of a few tens of metres, without any change in the dune form architecture. The example shown in Figure 3.7b depicts the facies geometries generated by Sedimentological Model 1 in a section perpendicular to the trend of the main bedforms. The bed sets climb at an identical angle to one another, and therefore generate a layer-cake stratigraphic architecture with the facies belts running parallel to one another. The horizontal section in Figure 3.7c underplays the degree to which the grainflow and grainflow-dominated units are interconnected, as the flat upper-surface of these sand bodies will be inclined at the angle-of-climb, and are therefore projecting out of the horizontal section at a slight angle.

3.6.3 – Geometry and orientation of net reservoir units

Figure 3.8 depicts the geometry and orientation of net reservoir units in Sedimentological Model 1. As described in Section 3.6.2, the geometry of the sand bodies seen in the horizontal section of Sedimentological Model 1 (Figure 3.7d) underplays the likely degree of connectivity of the grainflow-dominated units (packages of strata) arising from the accumulation of the bedforms via a climbing mechanism. The vertical section depicted in Figure 3.8b attempts to rectify this by illustrating the maximum likely grainflow connectivity in a zone parallel to the climbing upper bounding surface, defining the top of a preserved dune set. Figure 3.8c depicts the plan-view geometry at a level directly beneath the interdune migrating bounding surface that caps the set and which is inclined at the angle-of-climb; this allows for the maximum predicted grainflow connectivity to be depicted. This geometry is then simplified in Figure 3.8d to provide a summary model output in a form that is appropriate for input into reservoir modelling software. In this simple model (Figure 3.8d), the grainflow facies occupy the entire modelled area for a surface just beneath the upper interdune migration bounding surface that truncates the set which would not be typical in natural systems. This is a two-dimensional bedform model and by definition the facies belts extend infinitely along strike which, as mentioned previously, is unlikely in nature.

3.6.4 – Outcrop examples

This is the most common structure formed by migrating bedforms (stoss-erosional, lee-depositional). These types of structures are found in a variety of depositional settings, such as wind-ripple strata in aeolian sandstones and rippled deposits in fluvial and shallow-marine sandstones. An example of such bedforms is shown in Figure 3.31a, depicting two-dimensional transverse bedforms from the Navajo Sandstone at Paria Canyon-Vermilion Cliffs Wilderness, South Utah, USA.

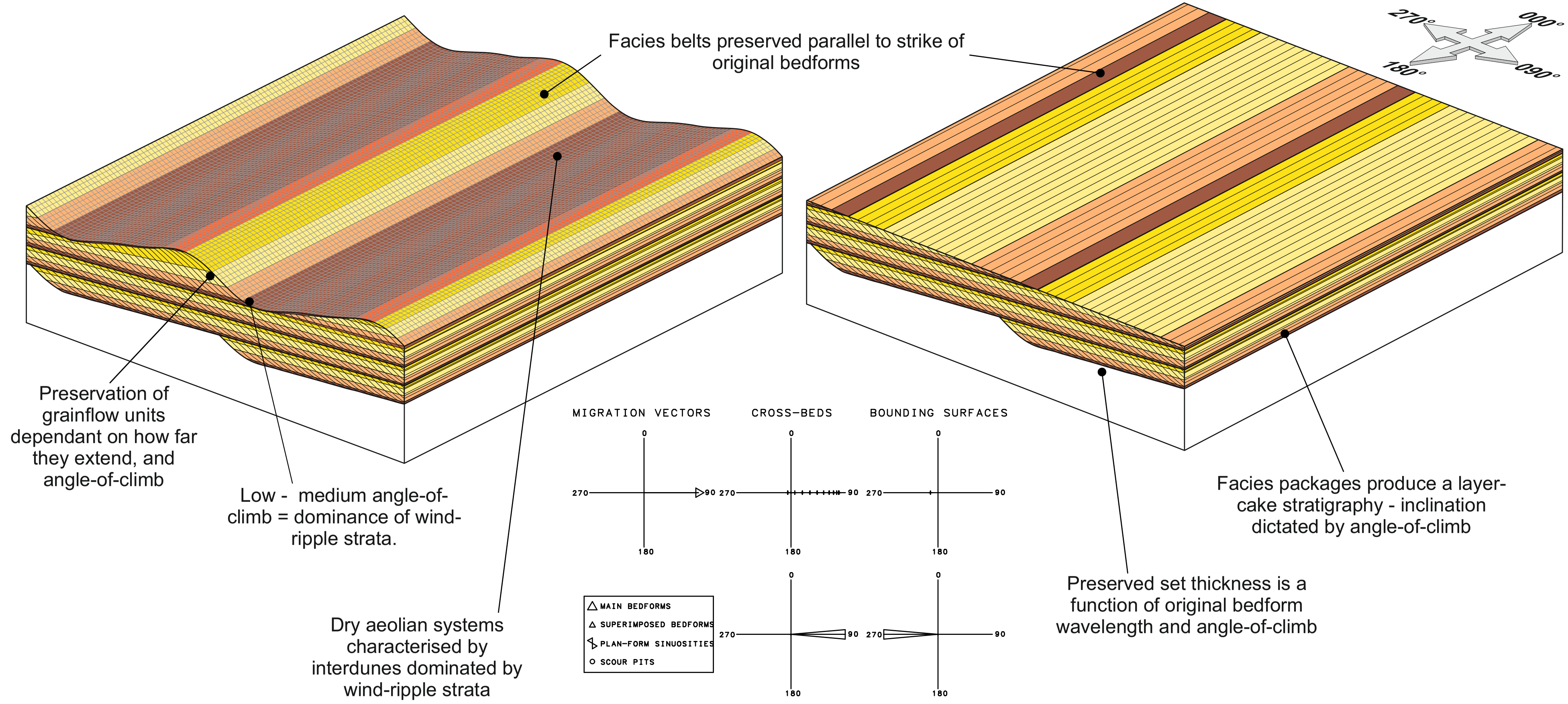

Figure 3.6. Sedimentological Model 1 (see Figure 3.3 for the input parameters used to generate this model). This model is generated by two-dimensional bedforms climbing at a stoss-erosional, lee-depositional, net-positive angle-of-climb. No scale implied.

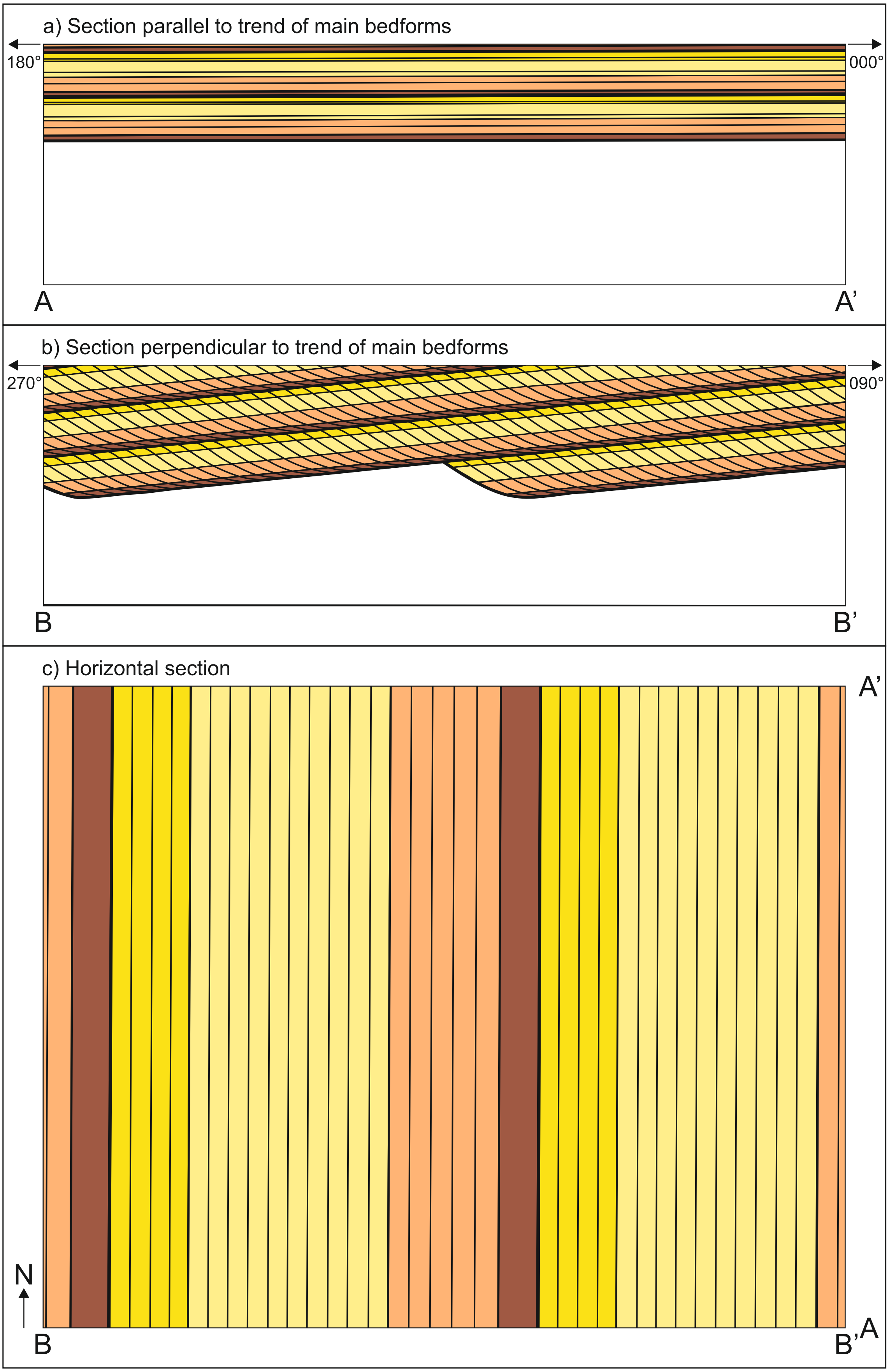

Figure 3.7. Stratigraphic architecture produced by Sedimentological Model 1. Estimated geometry of grainflow strata; note that the view in the horizontal section (c) under-plays the degree to which grainflow tongues are interconnected because the flat upper surface of these sand bodies will be inclined at the angle-of-climb and are therefore projecting out of the horizontal section at a slight angle.

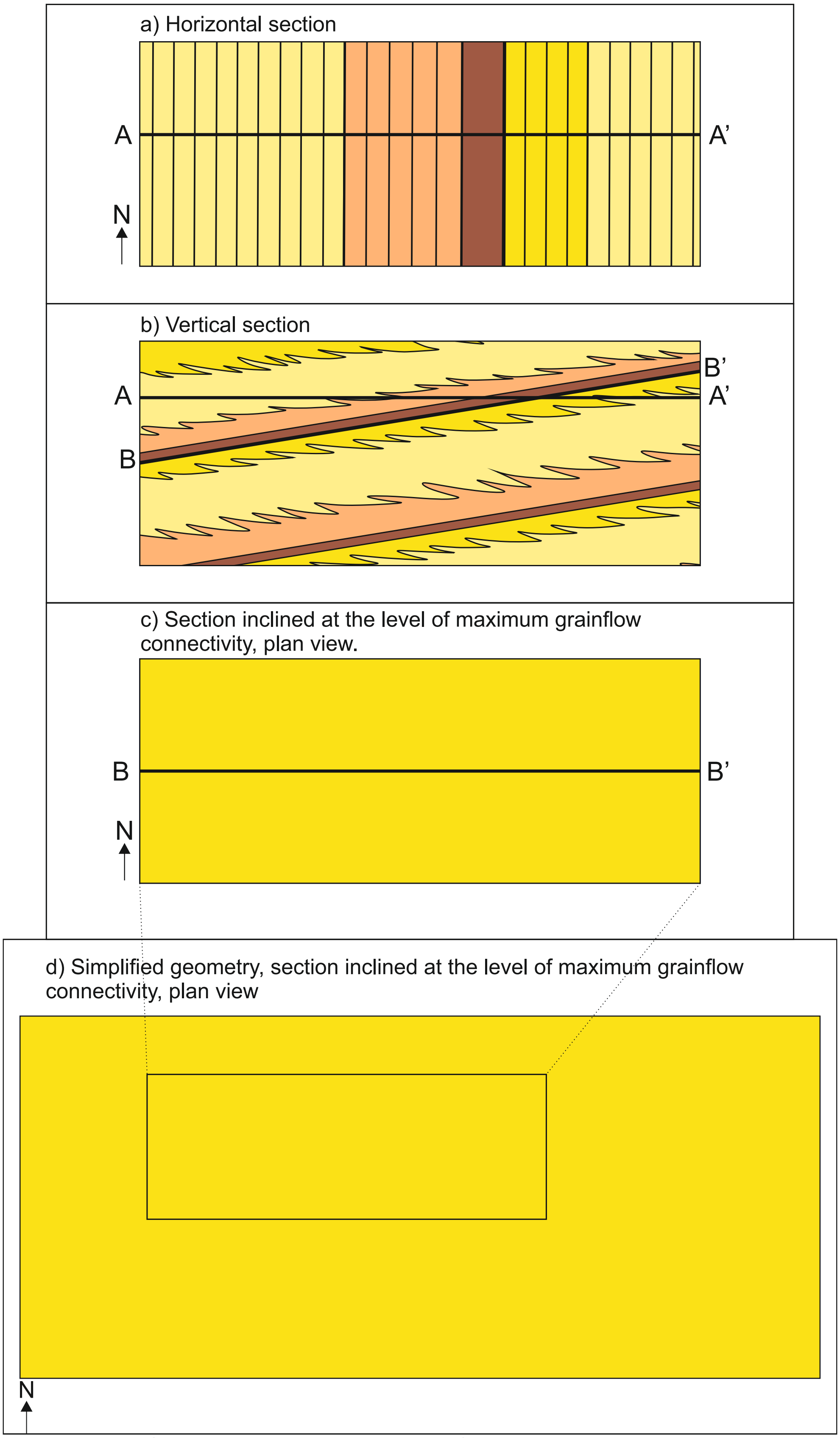

a) Horizontal section

b) Vertical section

c) Section inclined at the level of maximum grainflow connectivity, plan view.

d) Simplified geometry, section inclined at the level of maximum grainflow connectivity, plan view

Figure 3.8. Geometry and orientation of net reservoir units predicted by Sedimentological Model 1: a) geometry seen in horizontal section under-plays the likely degree of connectivity of the grainflow units; b) vertical cross section illustrating maximum grainflow development in zone parallel to climbing upper bounding surface, and pinch-out of grainflow units in the middle part of the climbing cosets; c) plan view geometry seen in a section taken immediately beneath a surface at the level of likely maximum degree of connectivity of the grainflow units; d) resulting facies geometry simplified to geometric shapes for reservoir modelling purposes.

3.7 – Sedimentological Model 2: Two-dimensional, variable, transverse bedforms

See Figure 3.3 for detailed input parameters used in the Rubin modelling software package to generate this model.

3.7.1 – Facies distributions on bedforms

Figure 3.9 depicts the depositional architecture arising from the migration of bedforms which undertake large and rapid fluctuations in height (Figure 17 in Rubin, 1987a). Unless the rate of deposition is high enough to provide enough sediment to make the bedforms larger, then the increase in height must be achieved by transferring sediment from the troughs of the bedforms to their crests (Terwindt, 1981). This is the most common way to achieve a fluctuation in the bedform height, as any increase in the rate of deposition is not normally sufficient (Terwindt, 1981).

The structure generated as an outcome of this process is a type of scalloped cross-bedding (Rubin and Hunter, 1983; Rubin, 1987b), which is formed by either: (i) cyclical fluctuations in bedform height (seen here in Sedimentological Model 2); (ii) cyclical reversals in bedform asymmetry and migration direction; or (iii) migration of superimposed bedforms over the lee slope of larger bedforms, seen in Sedimentological Model 4 (Figure 3.16) and Sedimentological Model 7 (Figure 3.25). An example of the migration of superimposed bedforms on the lee slope of larger bedforms is explored in Section 5.11 (Auk Model 6).

The two-dimensional nature of these bedforms means that facies are oriented parallel to the bedform crest. Regular fluctuations in height in this model give rise to regularly repeating reactivation surfaces, and this repeated reactivation means that pure grainflow packages developed on the upper flanks of the original bedforms are only rarely preserved and the strata immediately overlying scoured reactivation surfaces are dominated by wind-ripple facies, commonly seen in ancient preserved successions of this type. Grainflow-dominated stratal packages are entirely encapsulated by surrounding wind-ripple packages in each of the reactivated sets. The facies type exposed on the top-surface depends on the level at which the horizontal surface slices through the reactivated sets.

3.7.2 – Geometry of stratigraphic architecture

Figure 3.10 depicts the geometry of the stratigraphic architecture generated by Sedimentological Model 2. The only difference between this model and that of Sedimentological Model 1 (Figure 3.6) is that the bedforms generated here undergo fluctuations in their height, which classifies these forms as variable bedforms as opposed to the invariable bedforms generated by Sedimentological Model 1.

Figure 3.10a depicts the stratigraphic architecture generated in a section parallel to the trend of the main bedforms of Sedimentological Model 2. This generates a stratigraphy which is very similar to that of Sedimentological Model 1 (Figure 3.7a), but in this case substantially thicker packages of grainflow and grainflow-dominated facies units are preserved. This would have favourable implications for the reservoir quality of this model, as grainflow and grainflow-dominated facies tend to possess higher porosity and permeability values compared to wind-ripple and wind-ripple-dominated facies (see Section 3.4). The fluctuations in bedform height mean that when the elevation of the horizontal top surface of these bedforms is defined in the modelling process, the vertical position at which the bedforms are sliced varies. In one area, there will be a greater proportion of grainflow strata preserved (when the bedforms are cut-off near their tops), and in other areas a larger proportion of wind-ripple and wind-ripple dominated strata preserved (when the bedforms are cut-off closer to their bases). This will occur all on one horizontal surface at one single time slice.

Figure 3.10b shows the stratigraphic architecture of facies distributions generated by Sedimentological Model 2 in a section perpendicular to the trend of the main bedforms. The bedforms here show a consistent angle-of-climb and the fluctuations in height gives rise to variability in the amount of net reservoir facies (here, grainflow and grainflow-dominated facies). Sets that are generated at a time when the bedforms had a greater height allow for more of the upper lee slope of the dune to be preserved, thereby creating a scenario for the preferential preservation of thicker units with generally favourable reservoir quality. By contrast, sets that are generated at a time when the bedforms had a lesser height have a pattern of preservation whereby deposits from the dune-plinth region, namely wind-ripple and wind-ripple-dominated facies, represent a greater proportion of the preserved succession. This results in a reduced overall reservoir quality. The horizontal section shown in Figure 3.10c depicts facies belts which run parallel to the transverse component of linear dune migration. Although this model preserves a greater proportion of grainflow and grainflow-dominated strata compared to Sedimentological Model 1, parts of the accumulated stratigraphy remain dominated by wind-ripple and wind-ripple-dominated stratal packages, the occurrence of which is related to the preservation of sets of cross-strata generated when the bedform height was at a minimum. However, the horizontal section (Figure 3.10c) once again underplays the connectivity of the net reservoir facies, as these sand bodies are inclined at the angle-of-climb and therefore project out of this horizontal section at a slight angle. Further consideration to this issue is discussed in Section 3.7.3.

3.7.3 – Geometry and orientation of net reservoir units

Figure 3.11 depicts the geometry and orientation of net reservoir units predicted by Sedimentological Model 2. The horizontal section shown in Figure 3.11a significantly underplays the connectivity of the grainflow and grainflow-dominated facies. Figures 3.11b, c and d attempt to rectify this issue: Figure 3.11b is a vertical cross-section which illustrates the maximum grainflow development in a zone parallel to the upper climbing bounding surface; the grainflow units pinch-out in the middle parts of the climbing cosets. The plan-view geometry of this section is portrayed in Figure 3.11c, which depicts a section directly beneath the upper bounding surface of a preserved set that is inclined at the angle-of-climb and therefore portrays the likely maximum degree of connectivity of the grainflow and grainflow-dominated units of Sedimentological Model 2. Figure 3.11d depicts the same example as Figure 3.11c, but the facies geometries here have been simplified for reservoir modelling purposes. As with Sedimentological Model 1, the two-dimensional nature of these bedforms means that by definition, the facies belts continue indefinitely along strike. This predicts a geometry that would be highly unlikely in natural systems as most bedforms undergo changes in the dune form architecture, at least over distances in excess of a few tens of metres.

3.7.4 – Outcrop examples

Scalloped cross-bedding is a common and distinctive structure in aeolian, fluvial, tidal and near shore marine sands (Rubin, 1987b). The type of scalloped cross-bedding depicted here, where the bedforms undergo fluctuations in height, can be distinguished by the three-dimensional geometry of the structure. Bedforms increase in height when sediment is transferred to the crests from the troughs of the bedforms, and the bounding surfaces fall; bedforms decrease in height when sediment is transferred from the crests to the troughs of the bedforms, and the bounding surfaces rise. This process causes cyclic scouring into the underlying foresets and generates the type of scalloped cross-bedding seen in Sedimentological Model 2 (Rubin, 1987b; Boersma and Terwindt, 1981; Terwindt, 1981). An ancient outcrop example of scalloped cross-bedding is shown in Figure 3.31b, from an outcrop of Navajo Sandstone at Zion National Park, SW Utah.

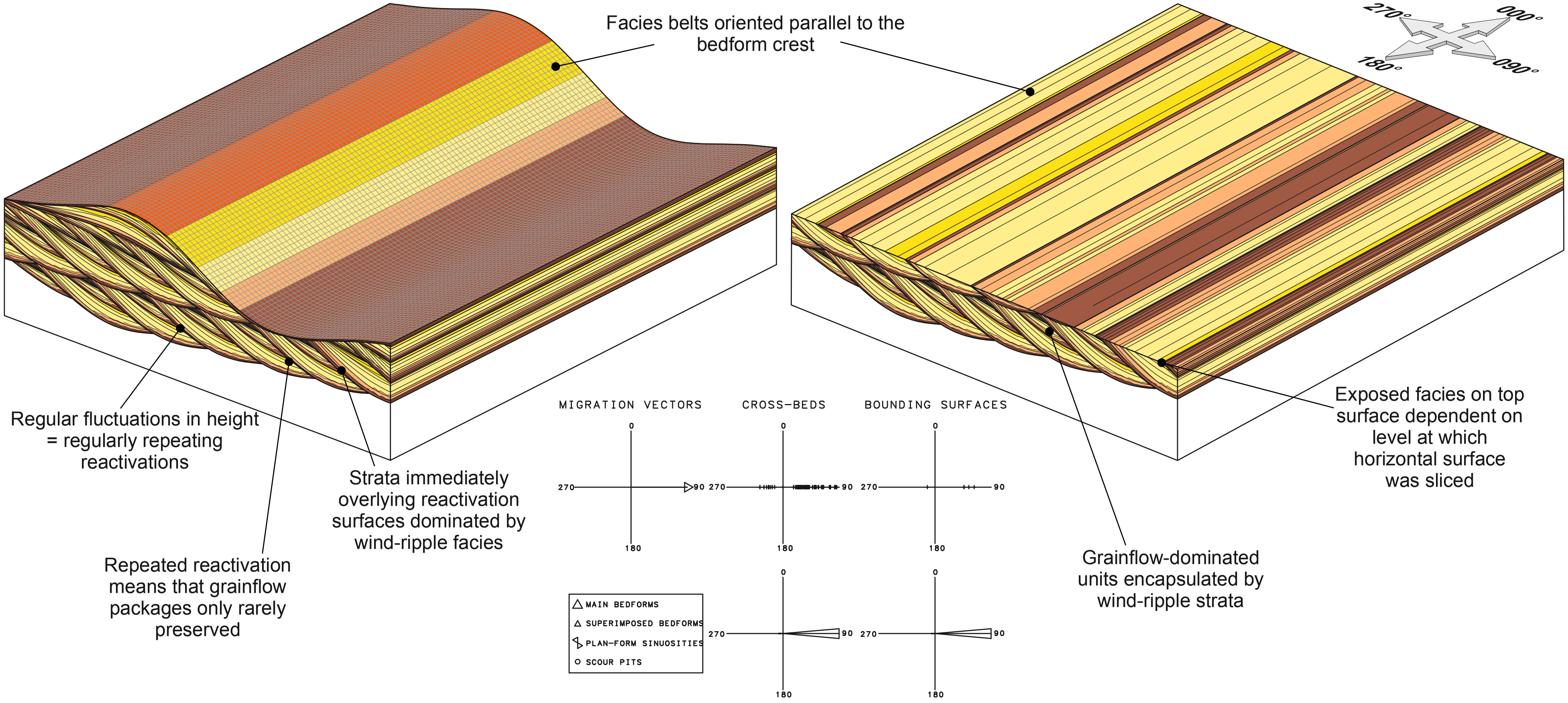

Figure 3.9. Sedimentological Model 2 (see Figure 3.3 for the input parameters used to generate this model). This model is generated by bedforms which are undergoing large and rapid fluctuations in height. No scale implied.

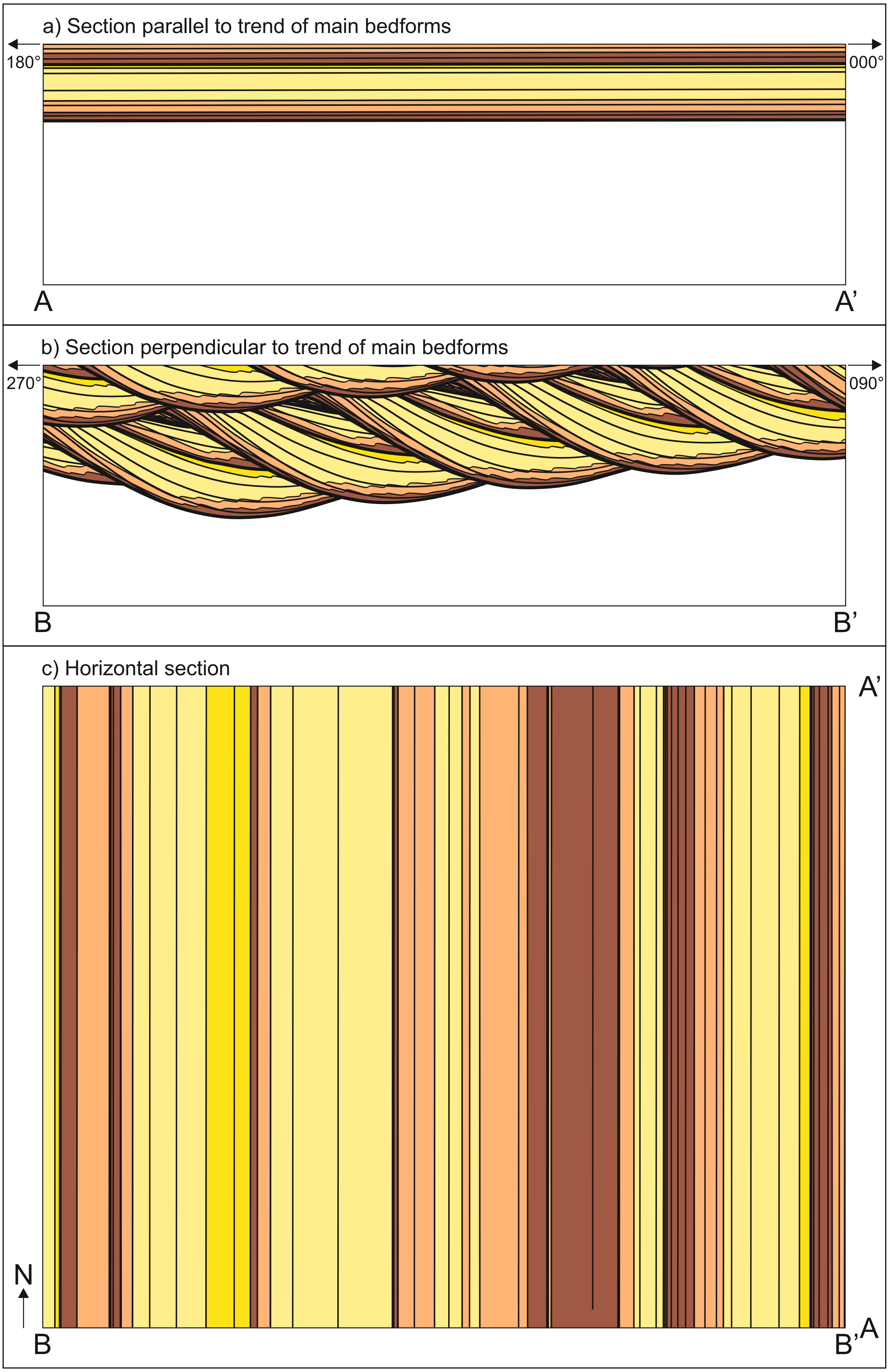

Figure 3.10. Stratigraphic architecture produced by Sedimentological Model 2. Estimated geometry of grainflow strata; note that the view in the horizontal section (c) under-plays the degree to which grainflow tongues are interconnected because the flat upper surface of these sand bodies will be inclined at the angle-of-climb and are therefore projecting out of the horizontal section at a slight angle.

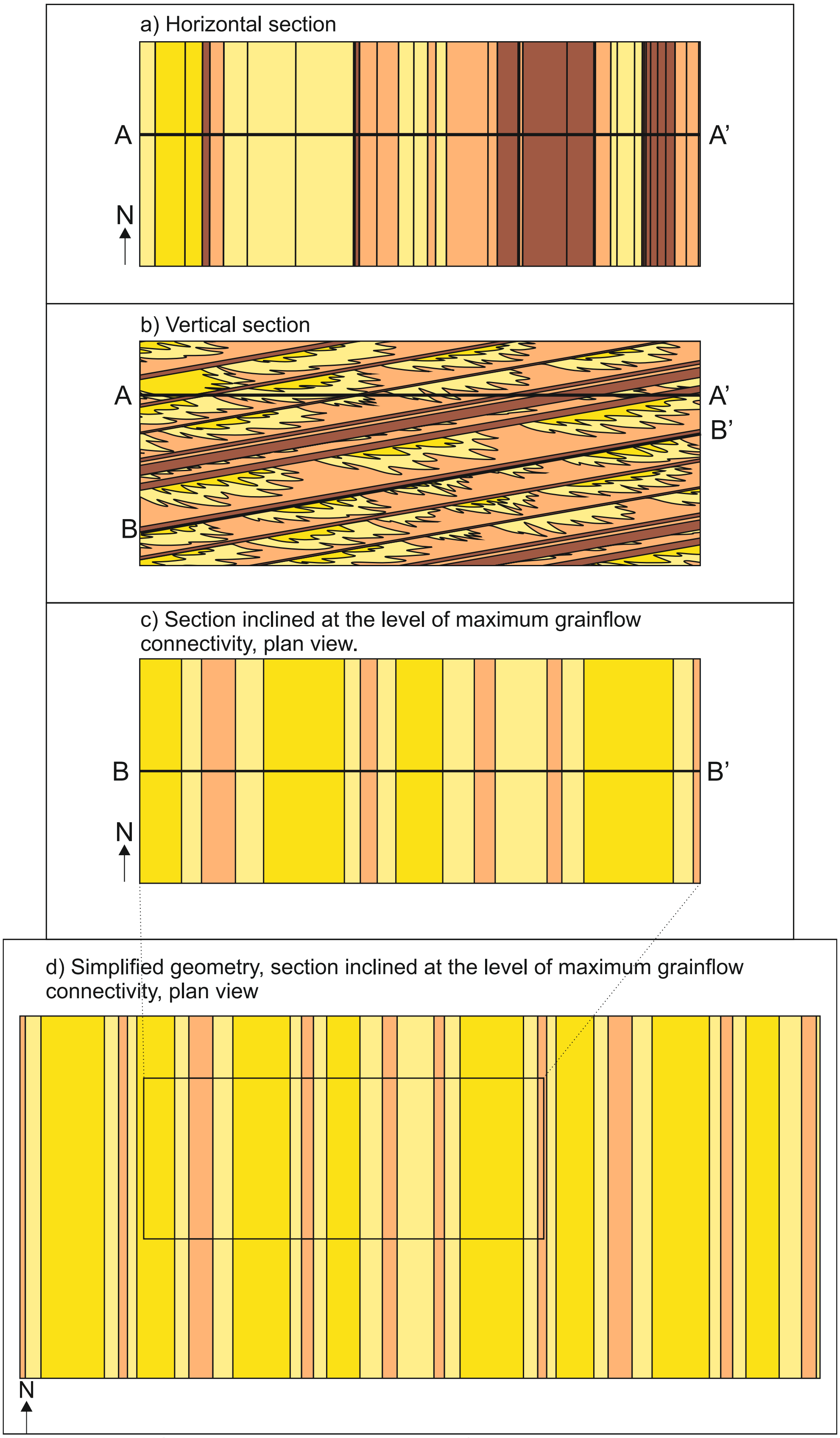

Figure 3.11. Geometry and orientation of net reservoir units predicted by Sedimentological Model 2: a) geometry seen in horizontal section under-plays the likely degree of connectivity of the grainflow units; b) vertical cross section illustrating maximum grainflow development in zone parallel to climbing upper bounding surface, and pinch-out of grainflow units in the middle part of the climbing cosets; c) plan view geometry seen in a section taken immediately beneath a surface at the level of likely maximum degree of connectivity of the grainflow units; d) resulting facies geometry simplified to geometric shapes for reservoir modelling purposes.

3.8 – Sedimentological Model 3: Three-dimensional, invariable, perfectly transverse bedforms

See Figure 3.3 for detailed input parameters used in the Rubin modelling software package to generate this model.

3.8.1 – Facies distributions on bedforms

Figure 3.12 shows deposition by transverse bedforms with sinuous, out-of-phase crestlines (Figure 34a in Rubin, 1987a). The accumulation of these three-dimensional invariable bedforms with out-of-phase crestlines generates ‘classic’ trough cross-bedding, as displayed in Figure 3.12. Elongate trough axes are aligned parallel to the direction of bedform migration, with the trough widths being dictated by the wavelength of crestline sinuosity. Facies belts are arranged within each trough, with facies generated on higher parts of the original bedform preferentially preserved in the axis of the trough but above the trough base. This tends to generate lozenge-shaped dune elements within which wind-ripple-dominated strata at the edges of the element encapsulate grainflow strata within the centre of the element.

With regards to the cross-bed azimuths, the migration of perfectly transverse sinuous-crested bedforms yields azimuths that are bimodally distributed in this example. However, transverse bedforms do not necessarily display a bimodal cross-bed azimuth distribution – the distribution of the cross-bed azimuths depends on the shape of the trough in plan-view. If there is a gentle rate of curvature, then there would be a broad spread of cross-bed dip-azimuths over a wide range, the range itself being dictated by the amount of curvature in the trough. If the troughs depict a ‘diamond-shape’, with a tight trough apex, then the cross-bed azimuths would be more obviously bimodal.

3.8.2 – Geometry of stratigraphic architecture

In Figure 3.13a, the expression of classic trough cross-bedding is seen in a section parallel to the trend of the main bedforms. These lozenge-shaped architectural elements encapsulate the grainflow and grainflow-dominated facies packages in the centre, and are each surrounded by a zone of lower porosity and lower permeability wind-ripple and wind-ripple-dominated stratal packages that can potentially act as a baffle to fluid flow within a reservoir. This has significant implications for the reservoir quality of bedforms which adopt this shape – most notably the ability for hydrocarbons to punctuate through baffles formed of wind-ripple facies. This could have repercussions for the ability of hydrocarbons to flow freely through the reservoir volume, especially in the case of more viscous fluids such as heavy oils that might potentially be prevented from reaching the grainflow and grainflow-dominated facies and being stored at all (i.e. a non-charged reservoir). An alternative and likely scenario is that the reservoir may be charged, but would not produce at a commercially viable rate as individual pockets would only drain very slowly.

Figure 3.13b depicts the stratigraphic architecture generated in a section perpendicular to the trend of the main bedforms. In this case, the facies belts are aligned parallel to one another and uniformly at the angle-of-climb. The geometry of wind-ripple strata encapsulating grainflow strata is also seen in the horizontal section (Figure 3.13c). However, as discussed for other cases, this view does not allow for the greatest extent of grainflow and grainflow-dominated packages to be displayed, as the sand packages are inclined at the angle-of-climb of the bedforms, and therefore will project out of this horizontal section at a slight angle.

3.8.3 – Geometry and orientation of net reservoir units

As described in Section 3.8.2, the degree of connectivity of the grainflow and grainflow-dominated units is underestimated in the horizontal sections of Sedimentological Model 3 (Figures 3.13c and 3.14a). In Figure 3.14b, a vertical cross-section is presented in which the maximum grainflow development is shown for a level that captures the likely maximum grainflow development. Figure 3.14c illustrates this geometry in plan-view, and this section is taken directly beneath a surface which shows the maximum net-reservoir development of the trough cross-bedded sets. This geometry is simplified to geometric shapes in Figure 3.14d for the purpose of summarising the overall gross-scale geometry and orientation of the facies packages, and their relationship to surrounding packages. This simplified summary configuration is useful for reservoir modelling purposes.

Each package of grainflow, grainflow-dominated and wind-ripple-dominated facies is arranged individually within the reservoir volume in this example, with no connectivity between the net-reservoir units. This raises issues relating to the ability of hydrocarbon fluids to pass freely throughout the reservoir volume. If this method was adopted by rotating the horizontal section 90°, shown in Figure 3.15a, then the following figures would portray the reservoir volume from a section parallel to the crestline of the bedforms, as in Figure 3.13b. This indicates that significantly different *apparent* reservoir geometries can be demonstrated depending on how the reservoir volume is sliced through, and that bedforms which have distinctly different morphologies can generate preserved facies relationships that are potentially very difficult to distinguish from one another.

3.8.4 – Outcrop examples

The migration of a train of bedforms with out-of-phase crestline sinuosities generates trough cross-bedding, one of the most common architectural features in aeolian outcrop successions. Large-scale troughs are evident in sections perpendicular to sand transport and the morphology and spacing of the sinuous crestlines determines the lateral continuity of aeolian facies. An example of ancient preserved trough cross-bedding is displayed in Figure 3.31c, from an outcrop of the Navajo Sandstone on the Poison Spider Trail, near Moab, SE Utah; Figure 3.31d and Figure 3.31e, from two outcrops of the Navajo Sandstone at the top of 7 Mile Canyon, near Moab, SE Utah.

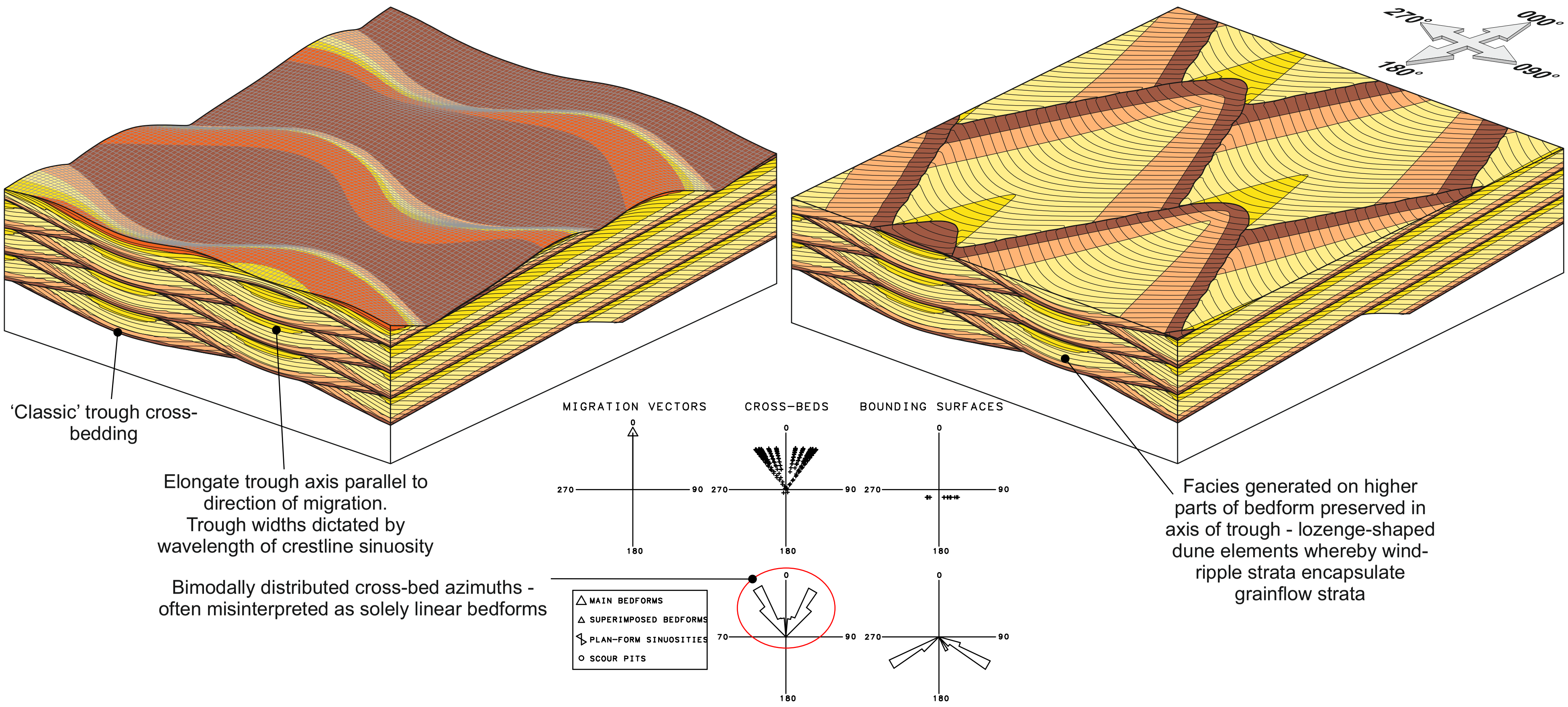

Figure 3.12. Sedimentological Model 3 (see Figure 3.3 for the input parameters used to generate this model). This model is generated by transverse bedforms with sinuous, out-of-phase crestlines. No scale implied.

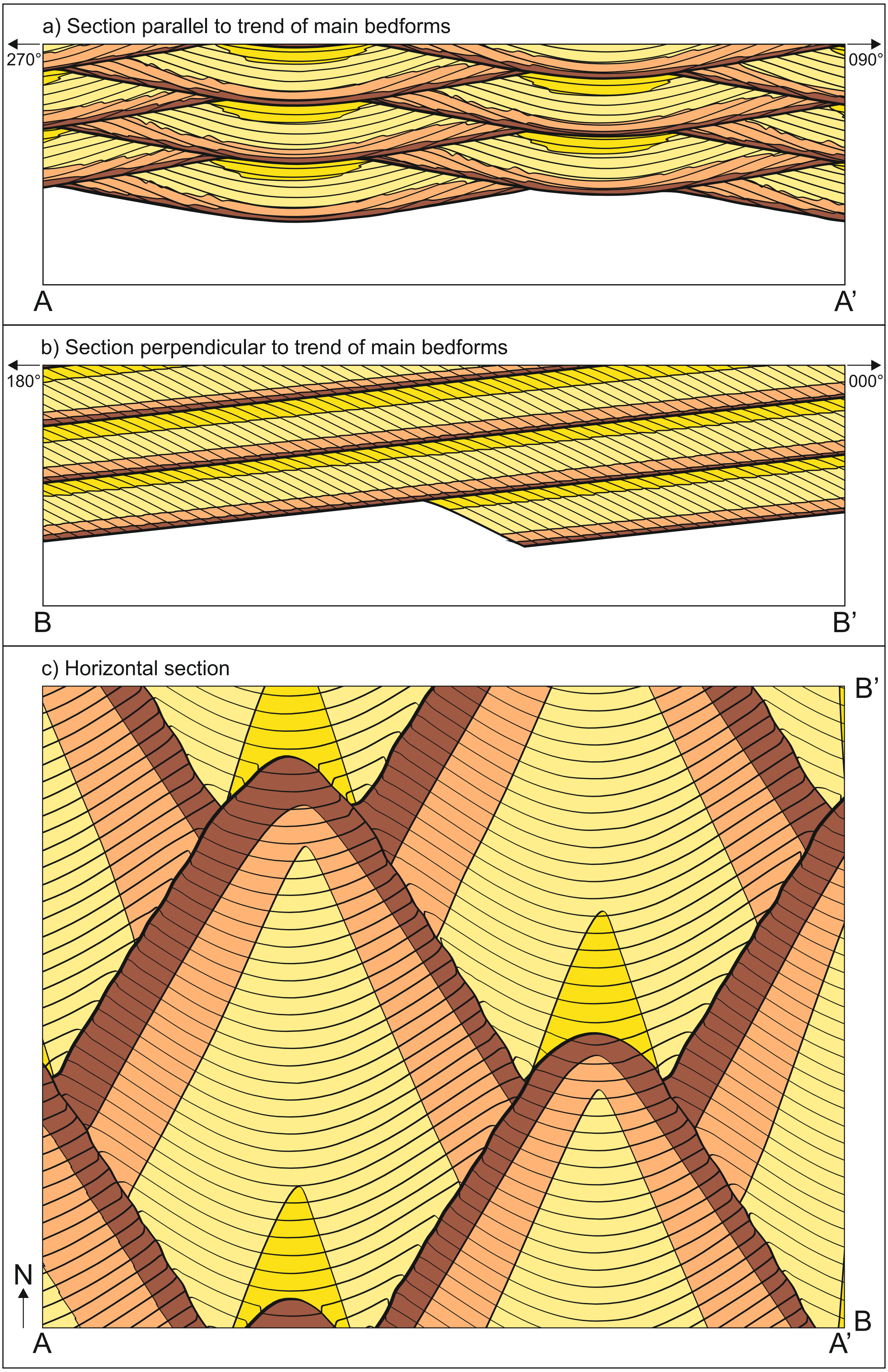

Figure 3.13. Stratigraphic architecture produced by Sedimentological Model 3. Estimated geometry of grainflow strata; note that the view in the horizontal section (c) under-plays the degree to which grainflow tongues are interconnected because the flat upper surface of these sand bodies will be inclined at the angle-of-climb and are therefore projecting out of the horizontal section at a slight angle.

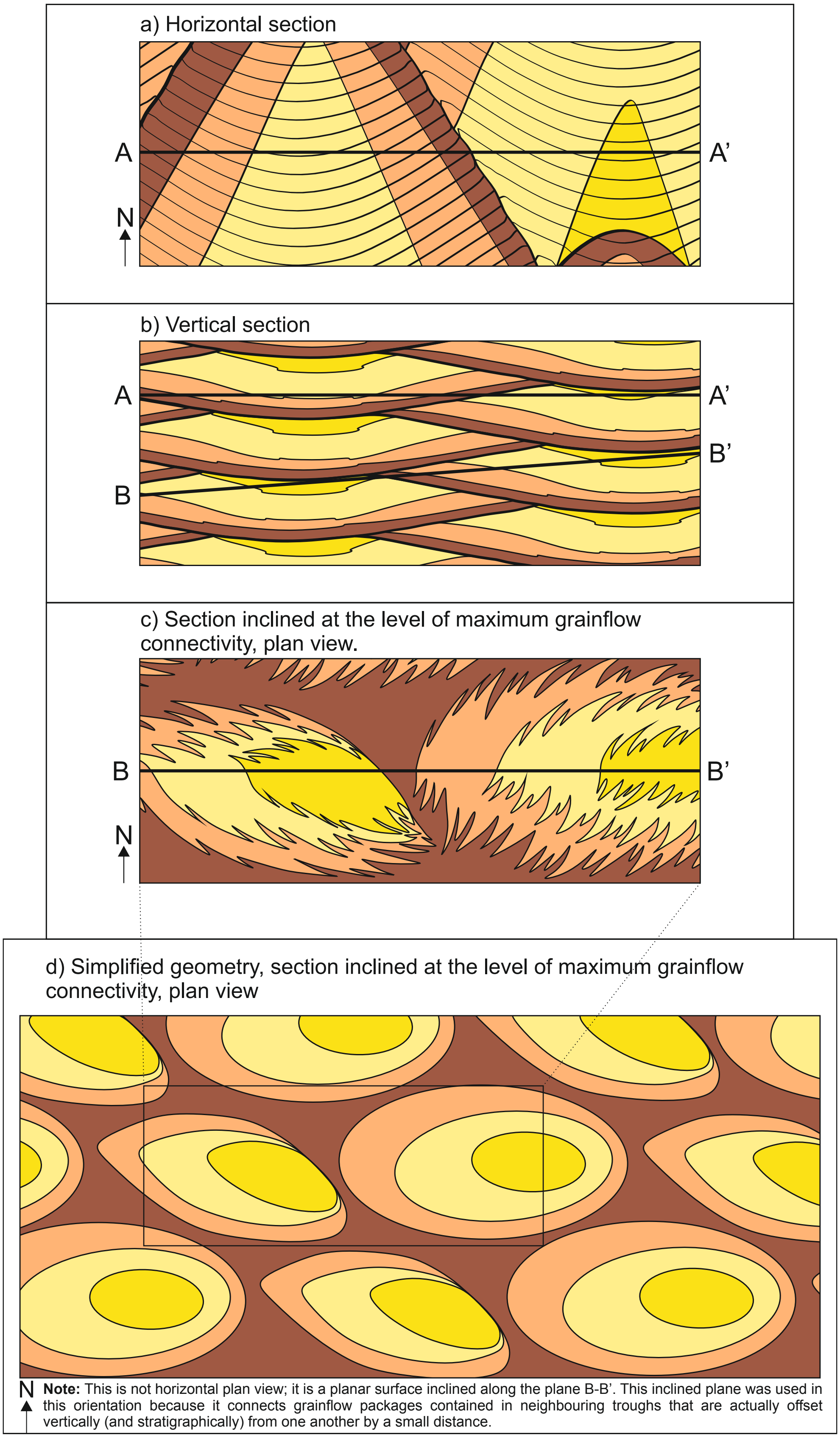

Note: This is not horizontal plan view; it is a planar surface inclined along the plane B-B'. This inclined plane was used in this orientation because it connects grainflow packages contained in neighbouring troughs that are actually offset vertically (and stratigraphically) from one another by a small distance.

Figure 3.14. Geometry and orientation of net reservoir units predicted by Sedimentological Model 3: a) geometry seen in horizontal section under-plays the likely degree of connectivity of the grainflow units; b) vertical cross section illustrating maximum grainflow development in zone parallel to climbing upper bounding surface; c) plan view geometry seen in a section taken immediately beneath a surface at the level of likely maximum degree of connectivity of the grainflow units; d) resulting facies geometry simplified to geometric shapes for reservoir modelling purposes.

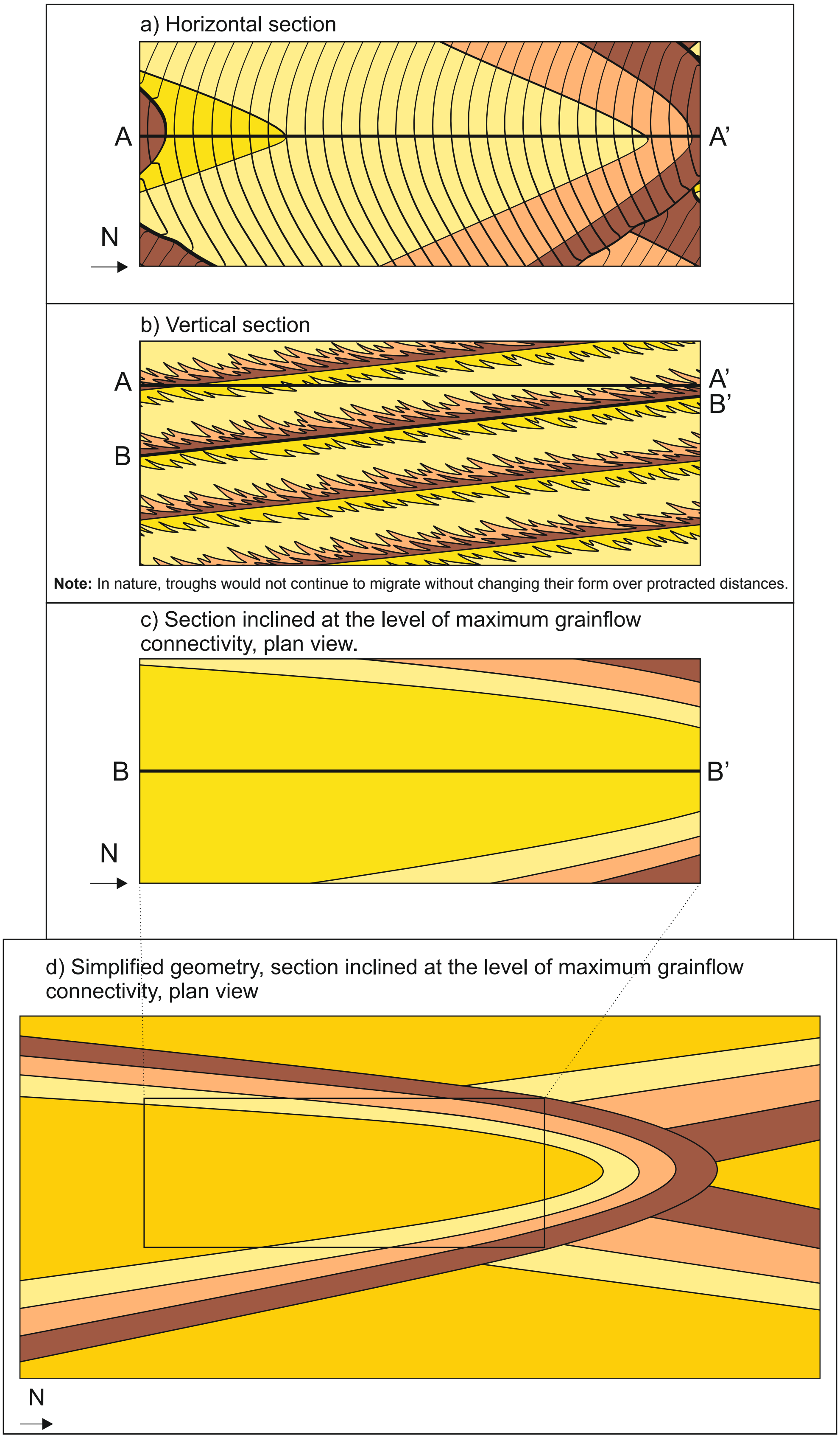
a) Horizontal section

b) Vertical section

Note: In nature, troughs would not continue to migrate without changing their form over protracted distances.

c) Section inclined at the level of maximum grainflow connectivity, plan view.

d) Simplified geometry, section inclined at the level of maximum grainflow connectivity, plan view

Figure 3.15. Geometry and orientation of net reservoir units predicted by Sedimentological Model 3; horizontal section rotated 90° to that shown in Figure 3.13c: a) geometry seen in horizontal section under-plays the likely degree of connectivity of the grainflow units; b) vertical cross section illustrating maximum grainflow development in zone parallel to climbing upper bounding surface, and pinch-out of grainflow units in the middle part of the climbing cosets; c) plan view geometry seen in a section taken immediately beneath a surface at the level of likely maximum degree of connectivity of the grainflow units; d) resulting facies geometry simplified to geometric shapes for reservoir modelling purposes.

3.9 – Sedimentological Model 4: Three-dimensional, invariable, oblique bedforms

See Figure 3.3 for detailed input parameters used in the Rubin modelling software package to generate this model.

3.9.1 – Facies distributions on bedforms

Figure 3.16 is generated by bedforms that possess along-crest migrating superimposed bedforms (Figure 46h in Rubin, 1987a). The parent bedforms in this model are migrating east; the superimposed bedforms on the stoss and lower flanks of the parent bedforms are moving north. Bedforms with superimposed bedforms migrating in another direction, and the resultant stratification, are common in aeolian environments (Rubin and Hunter, 1983; Sweet, 1992; Kocurek et al., 1999; Mountney and Thompson, 2002). The migration of the superimposed bedforms generates scour pits, due to the troughs of the two sets of bedforms intersecting and forming topographic depressions. The angle-of-climb is relatively steep for the smaller bedforms in this example, and is probably much steeper in this model than would be in in naturally occurring examples, but this steep angle-of-climb has been modelled intentionally to observe and study the effects on the preserved architecture of superimpositioning of bedforms. With regards to the migration vectors in this example, both scales of bedforms are migrating at the same rate, so the resultant migration vector bisects the two. In natural systems, the migration rate of the smaller bedforms would typically significantly exceed that of the slower moving parent bedforms. The vector mean of the foreset azimuths reflects neither the migration direction of the parent bedforms, nor that of the superimposed bedforms. The transport direction in this example is oriented 045° clockwise from the crestlines of the parent bedforms.

Facies packages defined here are long and thin, with wind-ripple strata at the edges encapsulating packages of grainflow strata in the centre of the preserved sets. Interaction of the two scales of bedforms causes a net sand migration that is oblique to the trend of both in the modelled co-ordinate system. This results in generation of superimposition surfaces that define genetic units that are elongated in the orientation of the sediment transport direction, in this case towards the northeast.

3.9.2 – Geometry of stratigraphic architecture

Figure 3.17a depicts the stratigraphic architecture generated by the bedforms in Sedimentological Model 4 in a section parallel to the trend of the main (parent) bedforms. As discussed in Section 3.9.1, the interaction of the two scales of bedforms here generates superimposition surfaces that produce facies packages elongated in the direction of net sediment transport. The stratal packages generated by this model are oriented northeast, which is oblique to the transport direction of the parent bedforms as well as the transport direction of the smaller superimposed bedforms. Both scales of bedforms allow for a high proportion of net reservoir facies to be preserved, here both grainflow and grainflow-dominated facies. This has favourable implications for the overall quality of the reservoir being modelled in this example. Figure 3.17b depicts the stratigraphic architecture generated in a section perpendicular to the trend of the main bedforms, and shows a very similar distribution of facies to those in Figure 3.17a. Although the horizontal section shown in Figure 3.17c comprises a relatively large proportion of grainflow and grainflow-dominated facies packages, these are again encapsulated within elongate distributions of typically wind-ripple dominated facies. Although this has better reservoir quality than the wind-rippled facies, it still has significantly less-favourable reservoir potential than the grainflow facies (see Section 3.4). However, the wind-rippled facies is not the dominant facies type preserved in this model. The horizontal section illustrated here once again underestimates the degree to which the grainflow and grainflow-dominated facies are connected, as these stratal packages are inclined at the angle-of-climb, and therefore project out of this horizontal surface at a slight angle. This issue is further discussed and rectified in Section 3.9.3 below.

3.9.3 – Geometry and orientation of net reservoir units

Figure 3.18 describes the geometry and orientation of the net reservoir units (grainflow and grainflow-dominated stratal packages) which are predicted by Sedimentological Model 4. The horizontal section (Figure 3.18a) underplays the likely degree of connectivity between the grainflow units, which is rectified in part by Figure 3.18b by illustrating the likely maximum grainflow development in a section inclined at the angle-of-climb for a level directly beneath a set bounding surface such that it captures the maximum amount of grainflow deposition. Directly beneath this surface, the maximum degree of connectivity of the grainflow units is depicted in plan-view (Figure 3.18c), and these grainflow units are simplified to geometric shapes in Figure 3.18d as a characterisation of the overall geometry in a manner suitable for forward reservoir modelling. The packages of facies are arranged in a similar manner to those seen in Sedimentological Model 3 (Figure 3.14d), but in this case the ellipses which contain the grainflow, grainflow-dominated and wind-ripple-dominated facies bodies are smaller and more closely packed in the reservoir volume. Some of the packages of facies do not contain pure grainflow facies, which makes these areas less favourable in terms of overall reservoir quality.

3.9.4 – Outcrop examples

This bedform morphology creates scalloped-cross bedding which is not related to variations in height as in Sedimentological Model 2 (Figure 3.9), but is instead attributed to migration of the superimposed bedforms. Examples of this structure have been described from the Triassic Helsby Sandstone Formation in the Cheshire Basin (Mountney and Thompson, 2002).

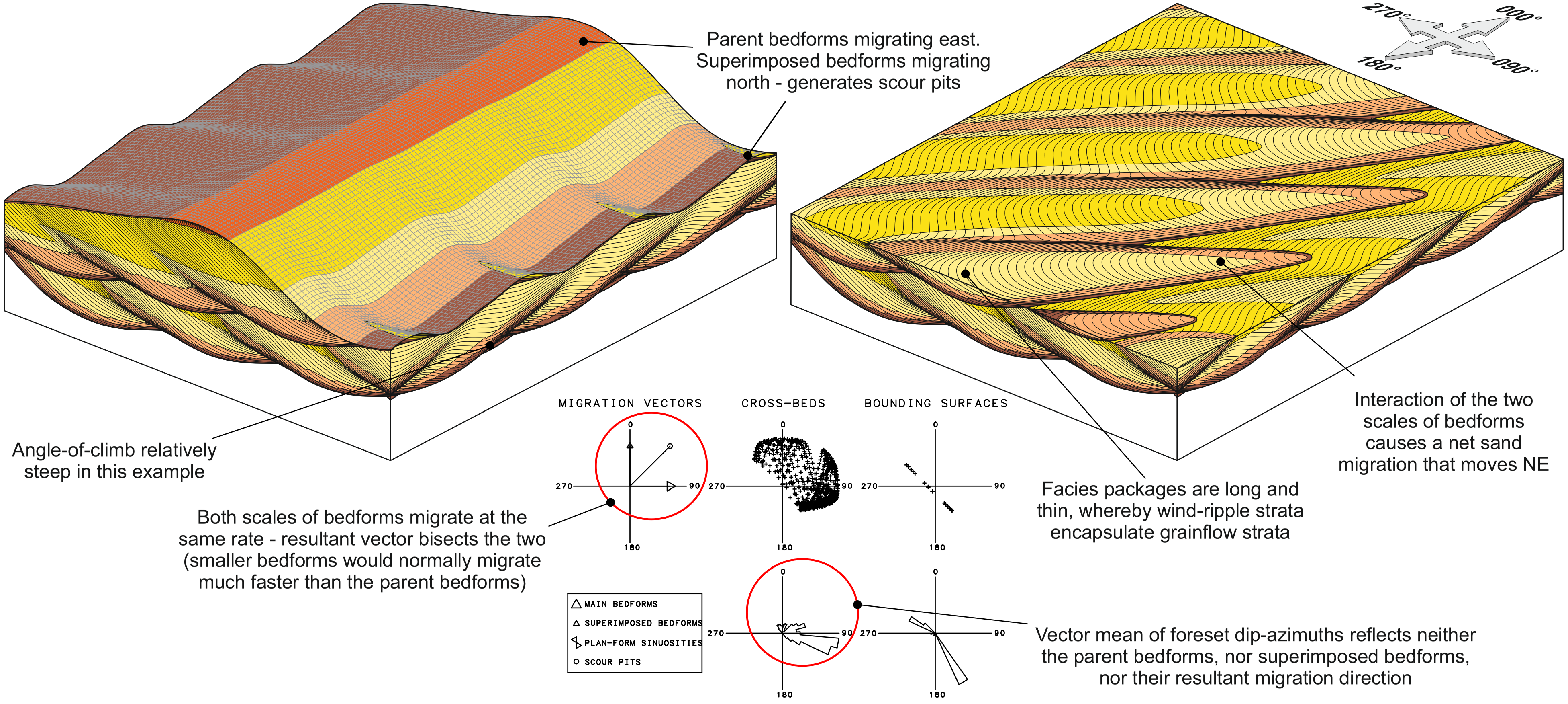

Parent bedforms migrating east. Superimposed bedforms migrating north - generates scour pits

Angle-of-climb relatively steep in this example

Both scales of bedforms migrate at the same rate - resultant vector bisects the two (smaller bedforms would normally migrate much faster than the parent bedforms)

Interaction of the two scales of bedforms causes a net sand migration that moves NE

Facies packages are long and thin, whereby wind-ripple strata encapsulate grainflow strata

Vector mean of foreset dip-azimuths reflects neither the parent bedforms, nor superimposed bedforms, nor their resultant migration direction

Figure 3.16. Sedimentological Model 4 (see Figure 3.3 for the input parameters used to generate this model). This model is generated by oblique bedforms with along-crest migrating superimposed bedforms. No scale implied.

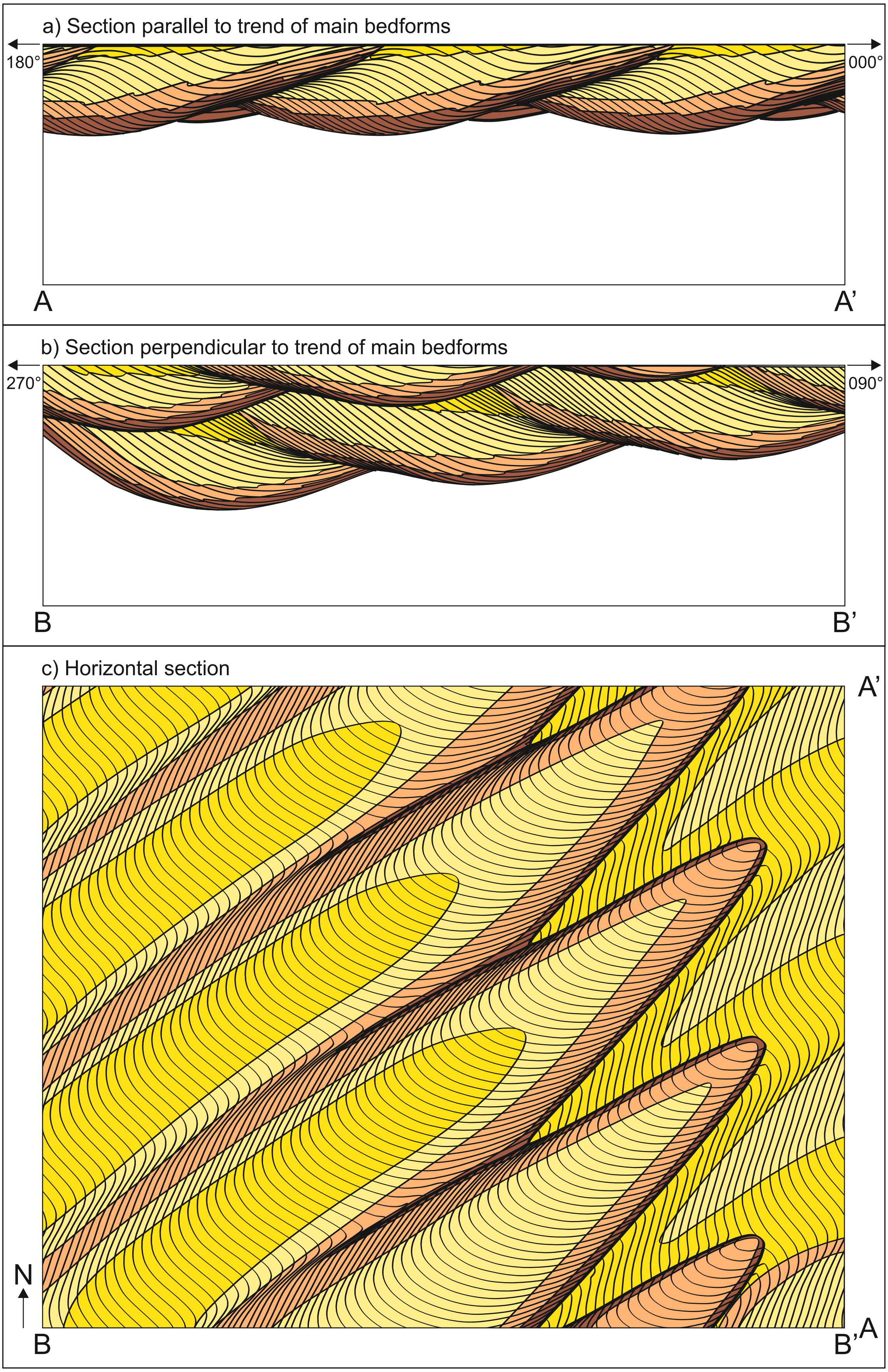

Figure 3.17. Stratigraphic architecture produced by Sedimentological Model 4. Estimated geometry of grainflow strata; note that the view in the horizontal section (c) under-plays the degree to which grainflow tongues are interconnected because the flat upper surface of these sand bodies will be inclined at the angle-of-climb and are therefore projecting out of the horizontal section at a slight angle.

a) Horizontal section

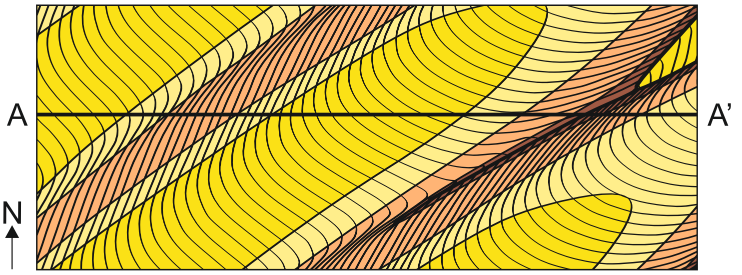

b) Vertical section

c) Section inclined at the level of maximum grainflow connectivity, plan view.

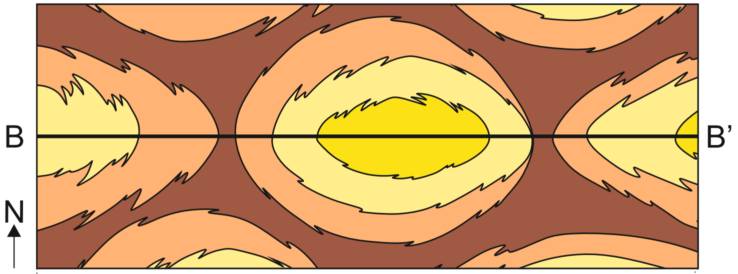

d) Simplified geometry, section inclined at the level of maximum grainflow connectivity, plan view

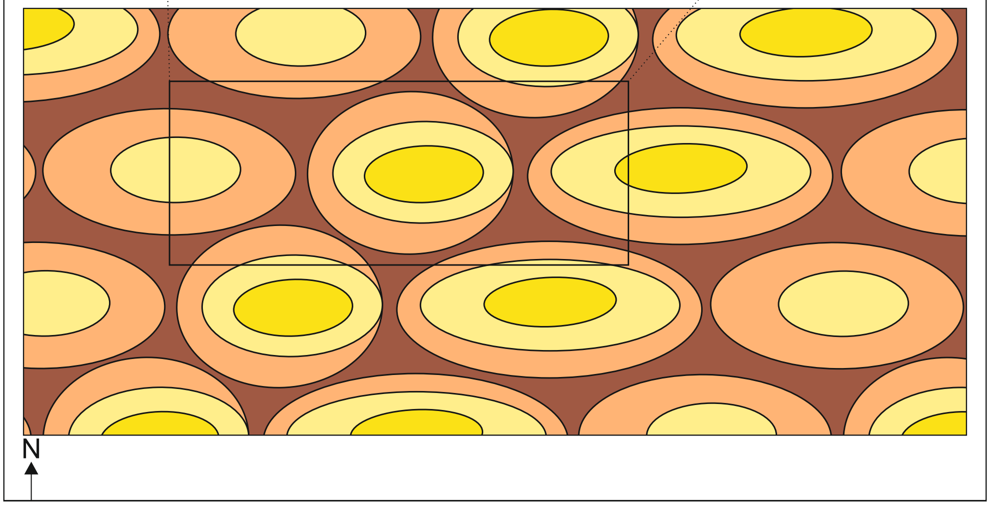

Figure 3.18. Geometry and orientation of net reservoir units predicted by Sedimentological Model 4: a) geometry seen in horizontal section under-plays the likely degree of connectivity of the grainflow units; b) vertical cross section illustrating maximum grainflow development in zone parallel to climbing upper bounding surface; c) plan view geometry seen in a section taken immediately beneath a surface at the level of likely maximum degree of connectivity of the grainflow units; d) resulting facies geometry simplified to geometric shapes for reservoir modelling purposes.

3.10 – Sedimentological Model 5: Three-dimensional, invariable, perfectly linear bedforms

See Figure 3.3 for detailed input parameters used in the Rubin modelling software package to generate this model.

3.10.1 – Facies distributions on bedforms

The depositional model depicted in Figure 3.19 was produced by perfectly linear (non-migrating) parent bedforms with along-crest-migrating sinuosities (Figure 55 in Rubin, 1987a). In this perfectly linear example, foreset dip-azimuths form a distinctly bimodal distribution. However, this near-perfect bimodality may not be expressed in naturally occurring examples, which in almost all cases will incorporate a minor component of transverse motion. As such, truly linear bedforms in nature are unlikely, because over time the crestlines will creep in a transverse direction, albeit at a slow rate (Rubin and Hunter, 1985; Bristow et al., 2000).

The preserved facies packages are elongated in the direction of bedform crests. The proportion of grainflow-dominated strata preserved is dependent on how far down the lee slope grainflow avalanches travelled; the model presented here envisages grainflow units extending to the lower parts of the dune lee slope, thereby preserving significant volumes of grainflow strata; these types of bedforms are common in the central portions of the Namib Desert (Lancaster, 1982). Many linear bedforms have low-angle-inclined lower dune flanks (plinths) which would preferentially preserve wind-ripple-dominated strata; such successions may lack significant grainflow packages. An example of this is the large linear bedforms preserved in the Auk Formation of the Central North Sea – these types of bedforms are explored further in Chapters 4 and 5.

In the vertical section of this model which is perpendicular to the bedform trend, the structures produced resemble zig-zag structures formed by reversing bedforms, or by those which have reversing lee-side spurs as in Sedimentological Model 6 (Figure 3.22) (Rubin, 1987a). However the bedforms in this example are non-migratory, so the zig-zag pattern depicted here has originated in response to the style of migration of the sinuosities.

3.10.2 – Geometry of stratigraphic architecture

Figure 3.20a portrays the stratigraphic geometry of the facies packages preserved for Sedimentological Model 5 in a section parallel to the trend of the main bedforms. The sets preserved by this model are thinner than those depicted for the perpendicular section in Sedimentological Model 3 (Figure 3.13b), because the wavelength of the bedforms in this model is smaller than the wavelength of the bedforms in Sedimentological Model 3.

Bedforms which have the same angle-of-climb but smaller dune wavelengths will preserve thinner sets (Romain and Mountney, 2014). Both of these models contain similar proportions of grainflow and grainflow-dominated strata to wind-ripple and wind-ripple-dominated strata. In the section perpendicular to the trend of the main bedforms (Figure 3.20b), the bounding surfaces cross-cut each other and are surrounded by packages of relatively low porosity and permeability wind-ripple strata. The geometry of the facies packages depicted here is a function of the sinuosities of the bedforms in this model. The grainflow and grainflow-dominated stratal packages are interconnected vertically, despite being encapsulated by non-net reservoir along-section.

In the horizontal section displayed in Figure 3.20c, grainflow facies are dominant. The facies types here are elongate, and are regularly cut-off by wind-ripple and wind-ripple-dominated facies, which would compartmentalise the reservoir volume being modelled here. In other areas, grainflow-dominated units are elongate in the direction of the bedform crests, and continue indefinitely. This is unlikely in natural examples, as these perfectly linear bedforms often have a transverse component of bedform migration, but here it is a function of the modelling process. The connectivity of the grainflow units depicted here is underestimated, as they are projecting out of this horizontal surface at a slight angle. This connectivity issue is further discussed in Section 3.10.3.

3.10.3 – Geometry and orientation of net reservoir units

In Figure 3.21, the geometry and orientation of units considered to be likely net reservoir bodies is shown in a series of models which rectify the issue of the underrepresented connectivity of the grainflow packages discussed in Section 3.10.2. In Figure 3.21a, the horizontal section underplays the likely connectivity of the grainflow-dominated units, as in Figure 3.20c. The most extensive development of units composed of grainflow and grainflow-dominated facies is through the section marked B-B’ in Figure 3.21b. The horizontal section (Figure 3.21c) is taken directly beneath this surface, which allows the likely maximum degree of connectivity of the grainflow-dominated units to be portrayed. The resulting facies geometry is then simplified to geometric shapes for reservoir modelling purposes (Figure 3.21d). Here, the grainflow-dominated units are arranged in individual packages, each of which is encapsulated by wind-ripple-dominated strata of moderate reservoir quality. The grainflow-dominated stratal packages are inclined NW-SE and NE-SW; this is the depositional result of the along-crest migration of the sinuosities. Grainflow and grainflow-dominated facies are most commonly preserved over wind-ripple-dominated facies in each of the packages, which have a smaller aerial extent than those predicted for Sedimentological Models 2, 3 and 4.

3.10.4 – Outcrop examples

Linear aeolian dunes with sinuous plan forms have been studied by Tsoar (1982; 1983). He did not detect lateral migration of the dunes as the sinuosities migrated along-crest. Examples of this type are rare, as to produce these types of bedforms the two converging winds, both of which are oblique to the bedform crestlines, must be balanced such that lateral migration of the bedforms is halted. If the winds are great enough to transport large volumes of sediment relative to the size of the bedforms, then the bedforms will reverse asymmetry, as shown in Sedimentological Model 8 (Figure 3.28). In most cases, linear dunes undertake a minor component of lateral migration, thereby depositing cross-strata that have unimodal cross-bed dip directions and therefore resembling the deposits of transverse dunes (Rubin and Hunter, 1985; Bristow et al., 2000). This means that very few ‘true’ linear dunes have been identified in ancient outcrop successions. Notable exceptions to this are: (i) the Permian Yellow Sands of County Durham - due to the rapid Zechstein transgression, this linear dune succession has been preserved in a case which would have otherwise had a very low preservation potential (Steele, 1983); and (ii) the aeolian deposits of the Jurassic (Oxfordian) Norphlet Sandstone at Mobile Bay in the subsurface of the Gulf of Mexico, which show linear dune morphologies preserved within the subsurface (Figure 1.2). A rapid, low-energy marine transgression during the Oxfordian, represented by the Smackover Formation (Mancini et al., 1985; Story, 1998; Ajdukiewicz et al., 2010) facilitated this rare preservation of linear dunes in the stratigraphy.

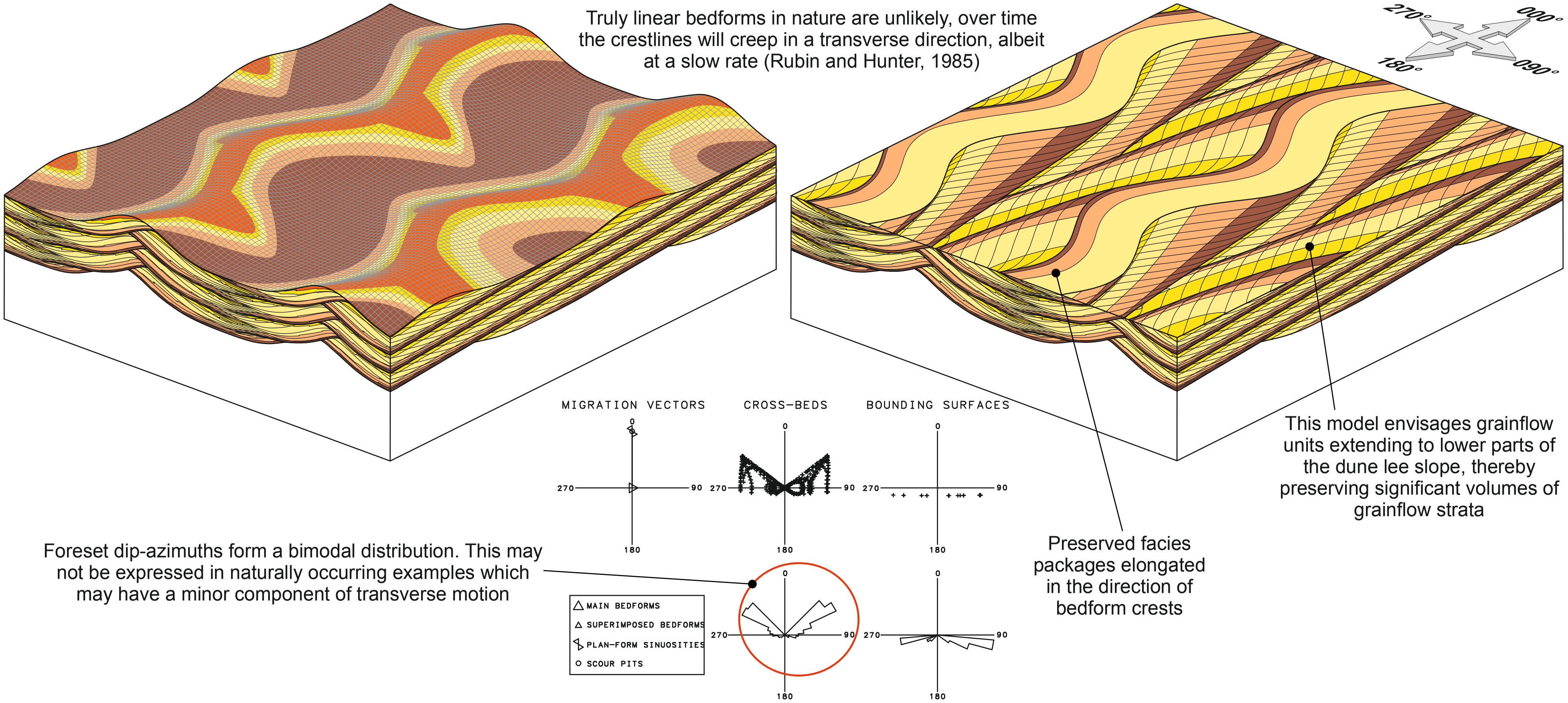

Truly linear bedforms in nature are unlikely, over time the crestlines will creep in a transverse direction, albeit at a slow rate (Rubin and Hunter, 1985)

Foreset dip-azimuths form a bimodal distribution. This may not be expressed in naturally occurring examples which may have a minor component of transverse motion

Preserved facies packages elongated in the direction of bedform crests

This model envisages grainflow units extending to lower parts of the dune lee slope, thereby preserving significant volumes of grainflow strata

Figure 3.19. Sedimentological Model 5 (see Figure 3.3 for the input parameters used to generate this model). This model is generated by perfectly linear (non-migrating) bedforms with along-crest-migrating sinuosities. No scale implied.

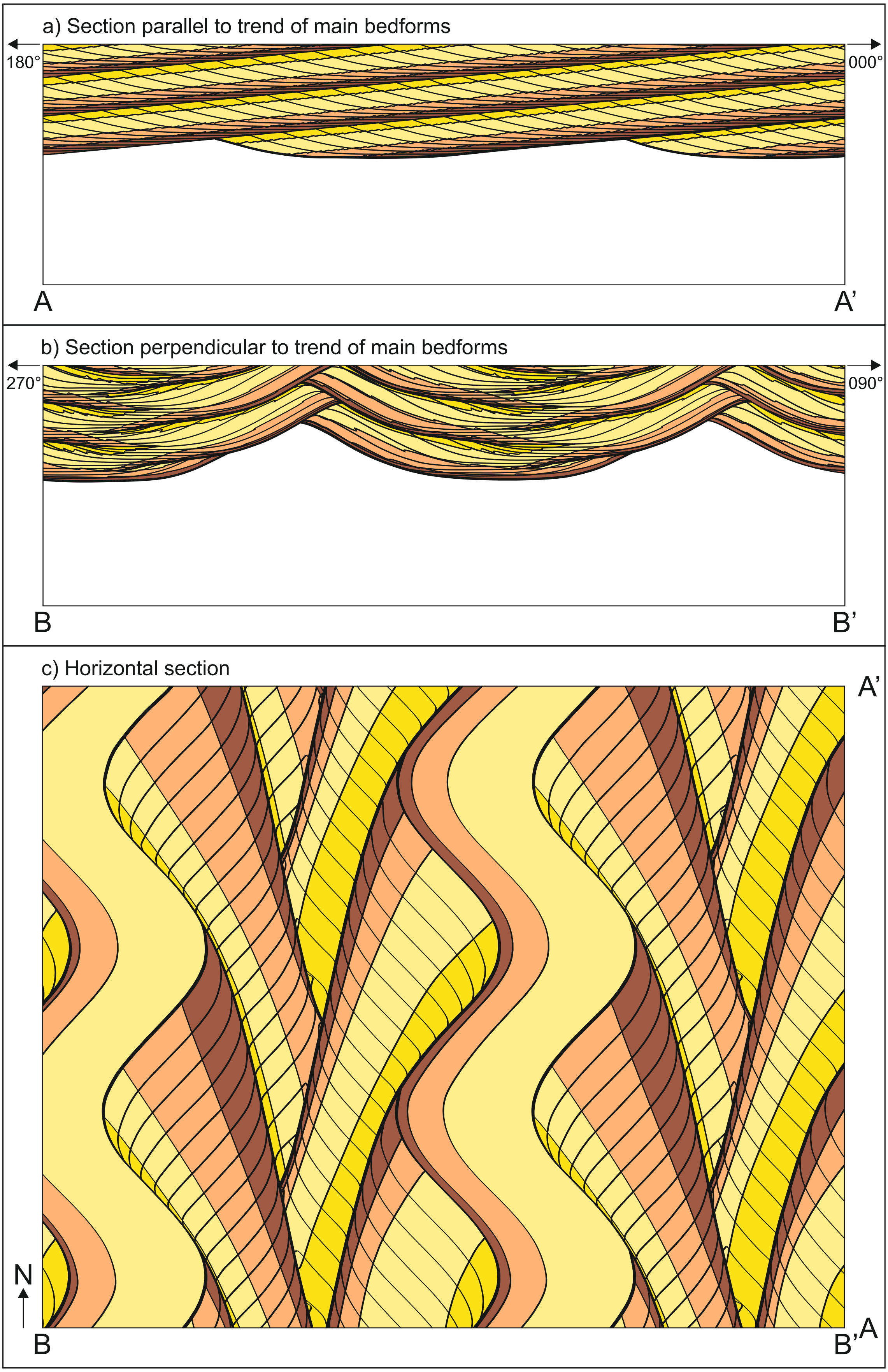

Figure 3.20. Stratigraphic architecture produced by Sedimentological Model 5. Estimated geometry of grainflow strata; note that the view in the horizontal section (c) under-plays the degree to which grainflow tongues are interconnected because the flat upper surface of these sand bodies will be inclined at the angle-of-climb and are therefore projecting out of the horizontal section at a slight angle.

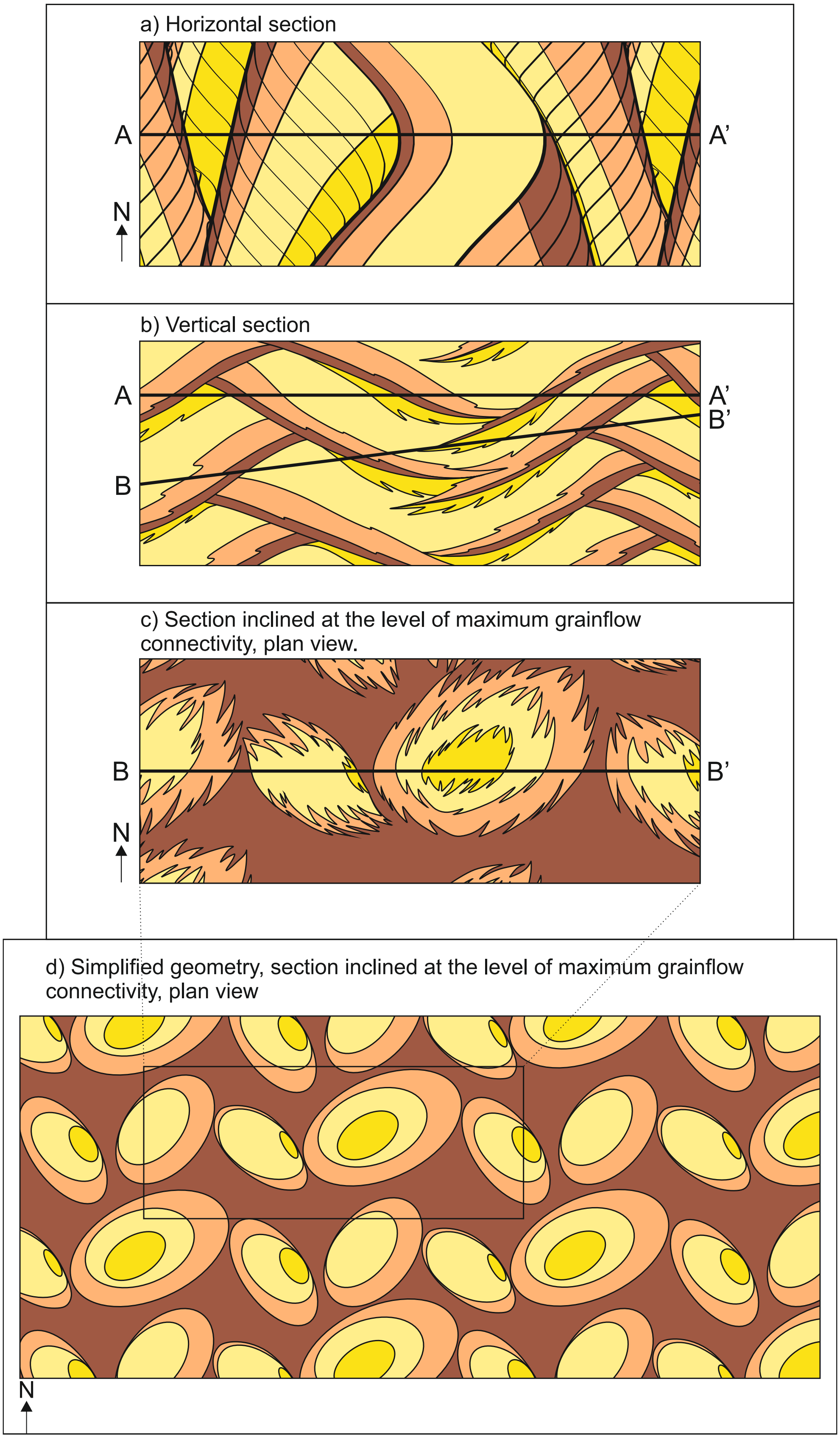

Figure 3.21. Geometry and orientation of net reservoir units predicted by Sedimentological Model 5: a) geometry seen in horizontal section under-plays the likely degree of connectivity of the grainflow units; b) vertical cross section illustrating maximum grainflow development in zone parallel to climbing upper bounding surface, and pinch-out of grainflow units in the middle part of the climbing cosets; c) plan view geometry seen in a section taken immediately beneath a surface at the level of likely maximum degree of connectivity of the grainflow units; d) resulting facies geometry simplified to geometric shapes for reservoir modelling purposes.

3.11 – Sedimentological Model 6: Three-dimensional, variable, perfectly transverse bedforms

See Figure 3.3 for detailed input parameters used in the Rubin modelling software package to generate this model.

3.11.1 – Facies distributions on bedforms

The deposition depicted in Figure 3.22 was formed by migrating bedforms with spurs that reverse asymmetry and migration direction, but which have no net along-crest displacement (Figure 59 in Rubin, 1987a). The parent bedforms in this example are migrating in an easterly direction. The superimposed bedforms on the stoss slope of the parent bedforms repeatedly reverse direction, with this scenario being quite common in nature. The migration of superimposed bedforms in this example gives rise to complex patterns of foreset dip-azimuths, as seen in Figure 3.22. The proportion of grainflow-dominated strata preserved is dependent on how far down the lee slope grainflow avalanches travelled, and also the angle-of-climb of the bedforms (Romain and Mountney, 2014).

3.11.2 – Geometry of stratigraphic architecture

Figure 3.23a depicts the facies architecture generated by Sedimentological Model 6 in a section parallel to the trend of the main bedforms. The bedding depicted here contains zig-zag structures, with grainflow and grainflow-dominated facies concentrated in the central upper portions, and the bounding surfaces defined by elongated packages of wind-ripple and wind-ripple-dominated strata. These zig-zag structures were previously thought to form only on the crests of lee-side spurs (Rubin and Hunter, 1983), but this model demonstrates that similar structures can form at the bottoms of scour pits (Rubin, 1987a). In the section perpendicular to the trend of the main bedforms (Figure 3.23b), the stratigraphic architecture generated is similar to that generated for Sedimentological Model 1 (Figure 3.7b) and is scalloped, however this model preserves much thicker sets by comparison, and therefore larger volumes of effective net reservoir facies (in this case, grainflow and grainflow-dominated stratal packages). Even in the horizontal section depicted in Figure 3.23c, where large volumes of net reservoir facies are displayed, their connectivity is underestimated as a function of the angle at which the bedforms are climbing, and therefore these grainflow packages are projecting on the horizontal section at a slight angle.

3.11.3 – Geometry and orientation of net reservoir units

The geometry and orientation of the net reservoir units depicted in Sedimentological Model 6 are shown in Figure 3.24. As previously described, the geometry shown in Figure 3.23c underplays the degree of connectivity of the net reservoir facies. This is rectified in the following figures: Figure 3.24b depicts a vertical cross-section which illustrates the maximum likely grainflow development in a zone parallel to the angle-of-climb. The plan-view geometry of this depiction, for which the expected grainflow geometries are maximised, is shown in Figure 3.24c, and also in a simplified form in Figure 3.24d where the net reservoir facies are summarised as geometric bodies for reservoir modelling purposes. The predicted facies geometry for Sedimentological Model 6 seen in Figure 3.24d is similar to that predicted by Sedimentological Model 3 (Figure 3.15). A large proportion of the modelled area is predicted to preserve grainflow strata, which would be highly unlikely in natural systems. This shows that bedforms which have distinctly different morphologies can generate preserved facies relationships that are potentially very difficult to distinguish from one another

3.11.4 – Outcrop examples

This bedform model generates a type of zig-zag structure, which resembles herringbone cross-bedding. However, true herringbone cross-bedding is commonly believed to be generated by transverse bedforms that frequently reverse in migration direction (Rubin, 1987a). Other processes that are likely to produce similar structures are zig-zagging of spurs and scour pits (such as this example, and that of Sedimentological Model 7), and the vertical stacking of trough cross-beds from bedforms with out-of-phase scour pits, such as Sedimentological Model 3. Figure 3.31e depicts an outcrop of Navajo Sandstone from a roadside section near Canyonlands National Park, SE Utah, and it is evident that the bedforms from Sedimentological Models 3 and 6 preserve structures that are commonly found together. Another example of the zig-zag structures formed by the bedforms in Sedimentological Model 6 is shown in Figure 3.31f, from an outcrop of Navajo Sandstone near Moab, SE Utah.

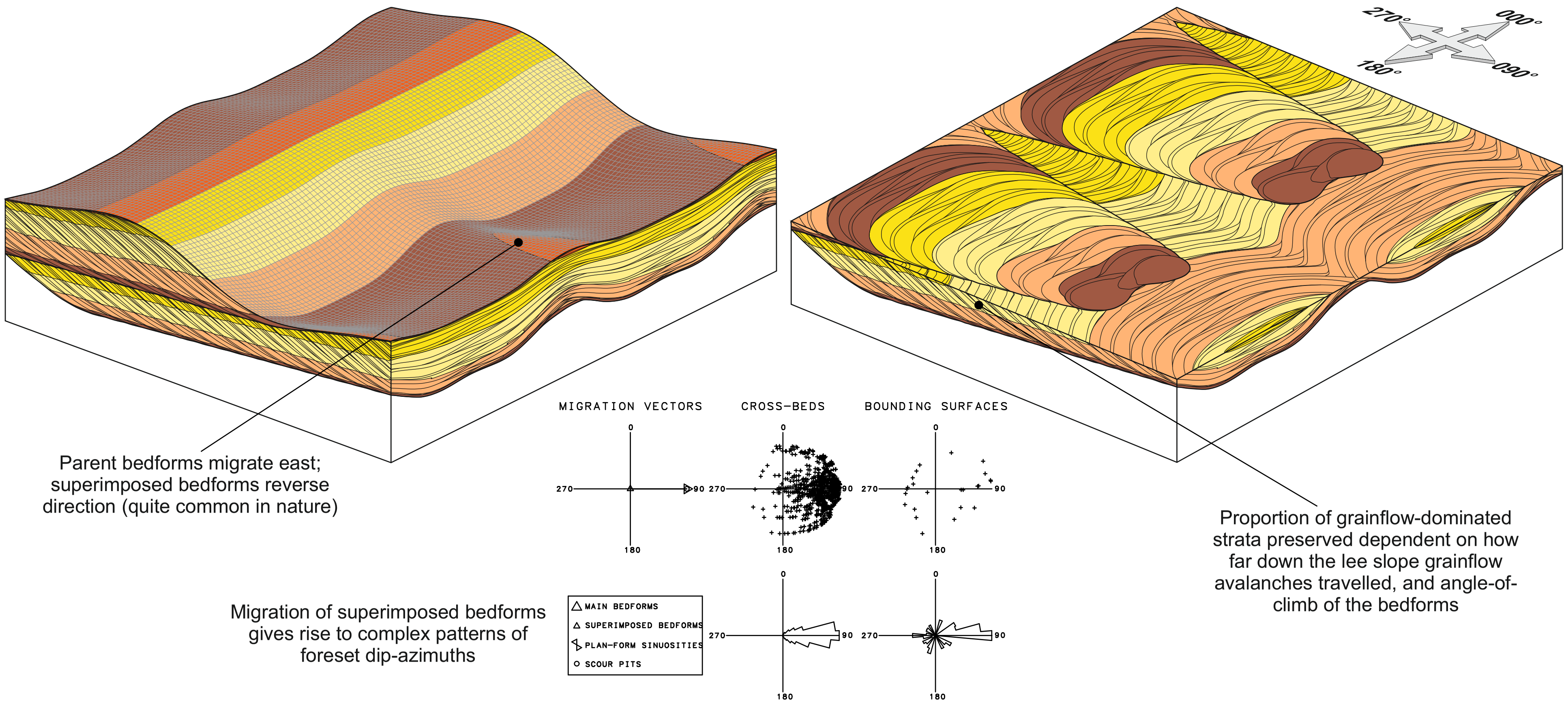

Parent bedforms migrate east; superimposed bedforms reverse direction (quite common in nature)

Proportion of grainflow-dominated strata preserved dependent on how far down the lee slope grainflow avalanches travelled, and angle-of-climb of the bedforms

Migration of superimposed bedforms gives rise to complex patterns of foreset dip-azimuths

Figure 3.22. Sedimentological Model 6 (see Figure 3.3 for the input parameters used to generate this model). This model is generated by migrating bedforms with spurs that reverse asymmetry and migration, but which have no net along-crest displacement. No scale implied.

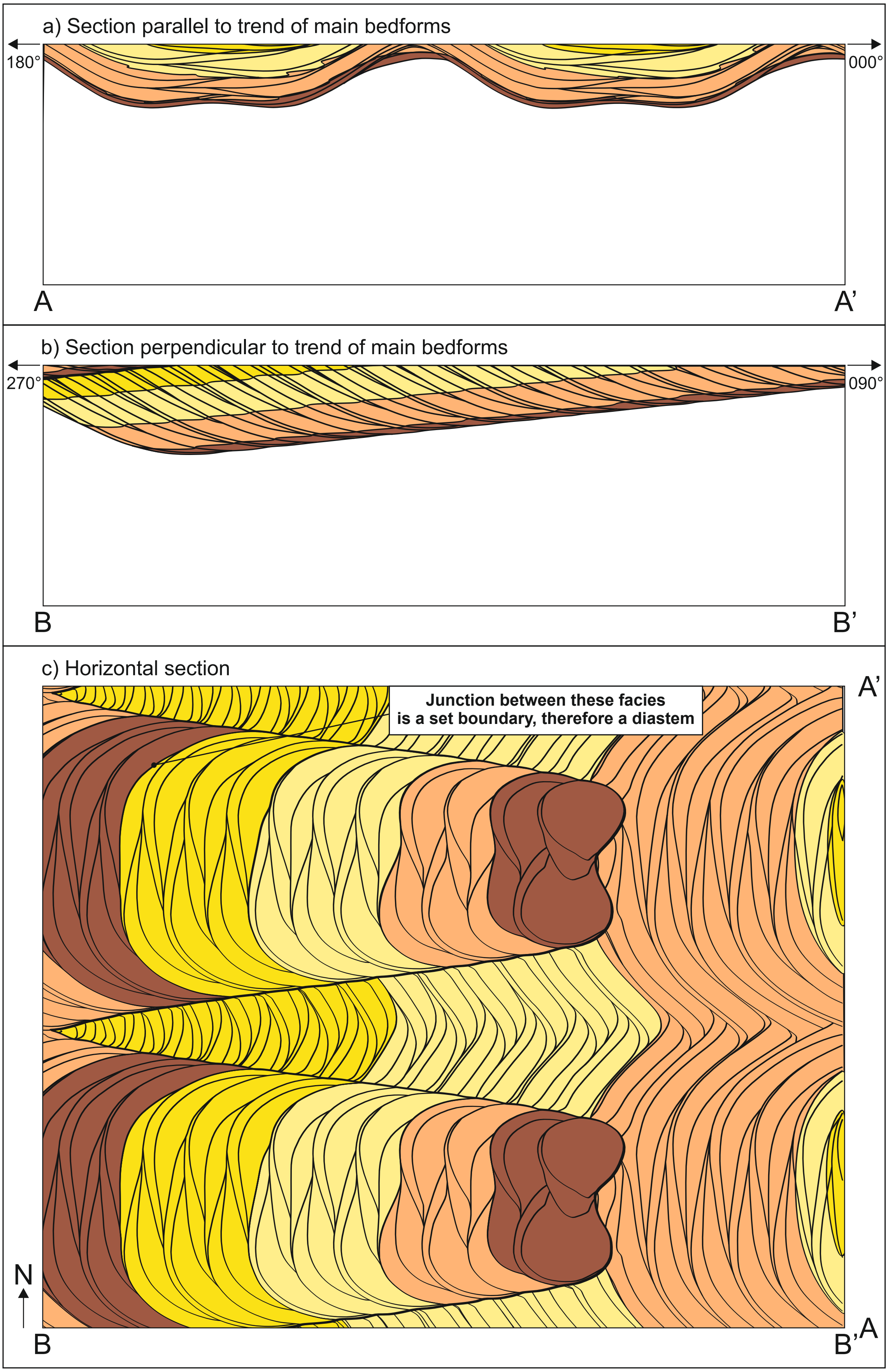

Figure 3.23. Stratigraphic architecture produced by Sedimentological Model 6. Estimated geometry of grainflow strata; note that the view in the horizontal section (c) under-plays the degree to which grainflow tongues are interconnected because the flat upper surface of these sand bodies will be inclined at the angle-of-climb and are therefore projecting out of the horizontal section at a slight angle.

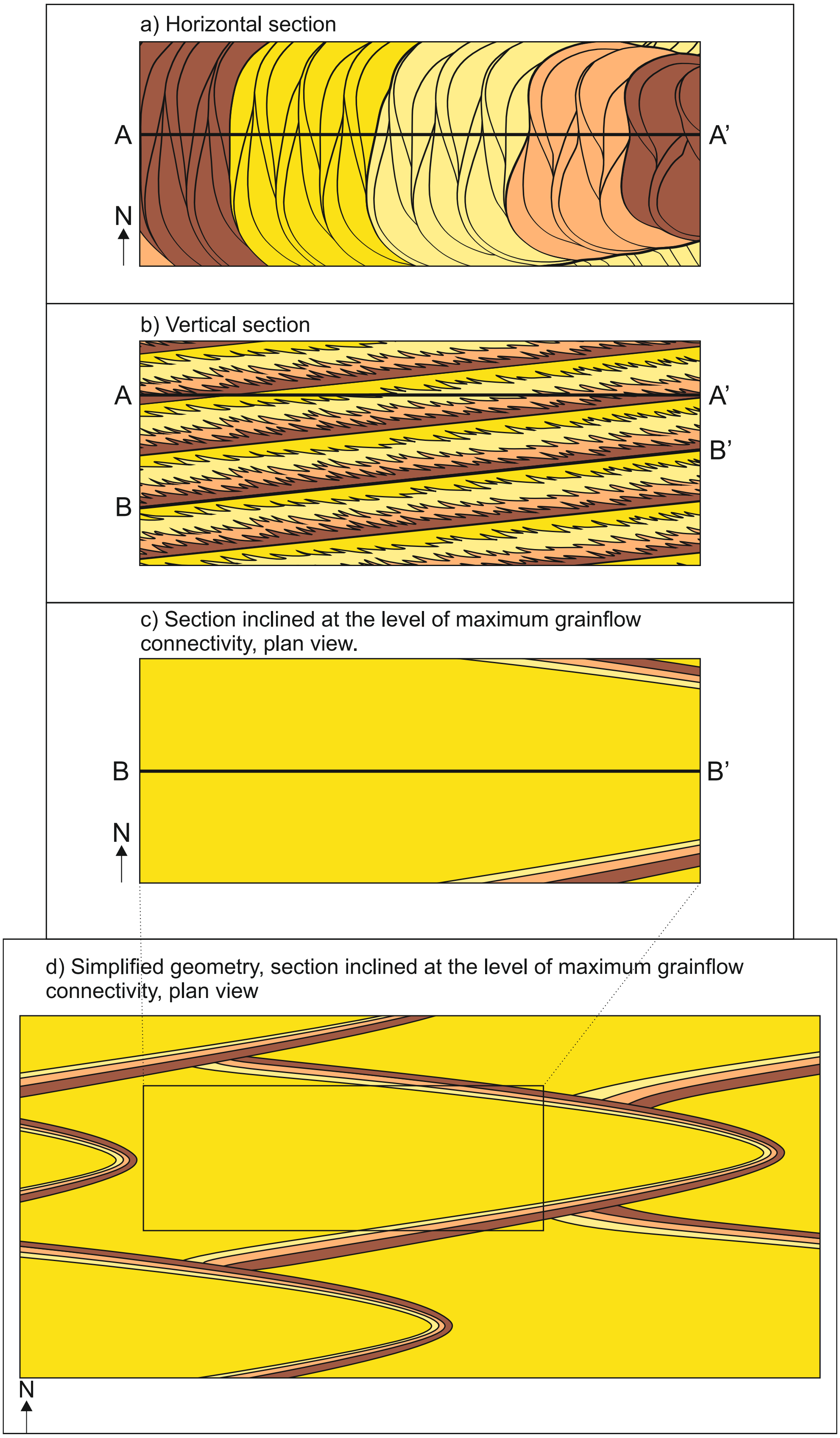

a) Horizontal section

b) Vertical section

c) Section inclined at the level of maximum grainflow connectivity, plan view.

d) Simplified geometry, section inclined at the level of maximum grainflow connectivity, plan view

Figure 3.24. Geometry and orientation of net reservoir units predicted by Sedimentological Model 6: a) geometry seen in horizontal section under-plays the likely degree of connectivity of the grainflow units; b) vertical cross section illustrating maximum grainflow development in zone parallel to climbing upper bounding surface, and pinch-out of grainflow units in the middle part of the climbing cosets; c) plan view geometry seen in a section taken immediately beneath a surface at the level of likely maximum degree of connectivity of the grainflow units; d) resulting facies geometry simplified to geometric shapes for reservoir modelling purposes.

3.12 – Sedimentological Model 7: Three-dimensional, variable, oblique bedforms

See Figure 3.3 for detailed input parameters used in the Rubin modelling software package to generate this model.

3.12.1 – Facies distributions on bedforms

This model (Figure 3.25) was formed by migrating bedforms with spurs that reverse asymmetry and migration direction, and which have net along-crest migration (Figure 71 in Rubin, 1987a). The main bedform is oblique to transport, and the lee-side scour pits and spurs migrate along-crest in addition to reversing back and forth (Rubin 1987a). This is an oblique-bedform analogue of Sedimentological Model 6 (Figure 3.22), and differs from it in that the spurs have a net along-crest migration. The complexity of the facies belts is due to the reversing (oscillating) behaviour of the superimposed bedforms in this example. Long and thin (elongate) grainflow-dominated units are entirely encapsulated within wind-ripple strata, which would have direct implications on fluid flow estimates in hydrocarbon reservoir successions. For a reservoir scenario, depending on the drill location, significantly different facies packages would be encountered, often within very short distances of one another. In some areas, the vast majority of facies encountered whilst drilling would be non-net reservoir, such as wind-ripple and wind-ripple-dominated strata, yet moving a short distance laterally exposes large amounts of preserved grainflow and grainflow-dominated strata.

3.12.2 – Geometry of stratigraphic architecture

The stratigraphic architecture generated by this model is complex due to the addition of oscillating superimposed bedforms. In the section parallel to the trend of the main bedforms (Figure 3.26a), thick accumulations of wind-ripple and wind-ripple-dominated facies at the base of the oscillating bedforms entirely encapsulate the swathes of net reservoir facies. In some areas, large portions of pure grainflow facies are present, but each package of net reservoir is surrounded by wind-ripple strata, making permeability across the reservoir volume a potential issue. Similar patterns are observed in the section perpendicular to the trend of the main bedforms (Figure 3.26b), where various sizes and geometries of net reservoir stratal packages are displayed, but are recurrently surrounded by wind-ripple strata.

In the horizontal section (Figure 3.26c) the confinement of the net reservoir facies is especially apparent. However in this section, the connectivity of the grainflow units is underplayed, as these stratal packages are inclined at the angle-of-climb of the bedforms, and therefore projecting out of this surface at a slight angle. This is further discussed and rectified in Section 3.12.3.

3.12.3 – Geometry and orientation of net reservoir units

As previously discussed, the horizontal sections depicted in Figure 3.26c and Figure 3.27a underplay the degree of connectivity of the grainflow tongues, because the flat upper surface of these sand bodies is inclined at the angle-of-climb, and are therefore projecting out of the horizontal sections shown at a slight angle. Figure 3.27b shows a vertical cross-section to illustrate the maximum grainflow development in a zone which captures the likely maximum grainflow and grainflow-dominated facies development, which is shown in plan-view in Figure 3.27c. When these facies packages are simplified to geometric shapes in Figure 3.27d, it is apparent that Sedimentological Model 7 produces a reservoir volume whereby net reservoir units are separated from one another, and encased within large portions of non-net reservoir wind-ripple and wind-ripple-dominated facies. The individual packages of facies are smaller than those predicted in previous models, and they are all inclined slightly towards NNW – SSE, with the grainflow and grainflow-dominated facies concentrated on the right-hand edge of the facies bodies. These are encapsulated by wind-ripple and wind-ripple-dominated strata, which have detrimental implications for hydrocarbon fluid flow between the net reservoir packages in this model.

3.12.4 – Outcrop examples

This model is an oblique version of Sedimentological Model 6, in which the bedforms are migrating in a direction transverse to transport. In this example the along-crest migration of the superimposed bedforms prevents the formation of the vertical zig-zagging structures seen in Figure 3.31e and 3.31f.

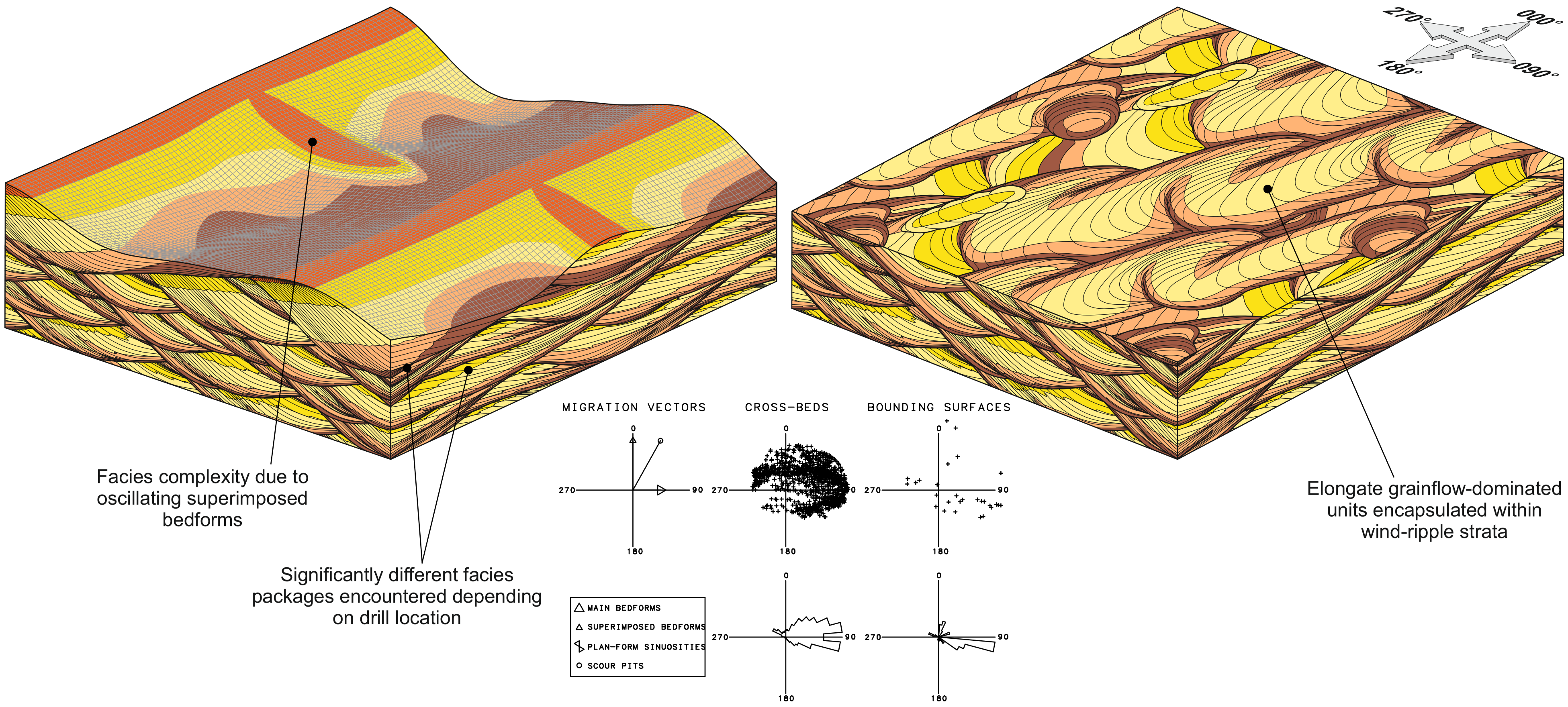

Figure 3.25. Sedimentological Model 7 (see Figure 3.3 for the input parameters used to generate this model). This model is generated by migrating bedforms that possess along-crest migrating spurs that reverse asymmetry and migration direction. No scale implied.

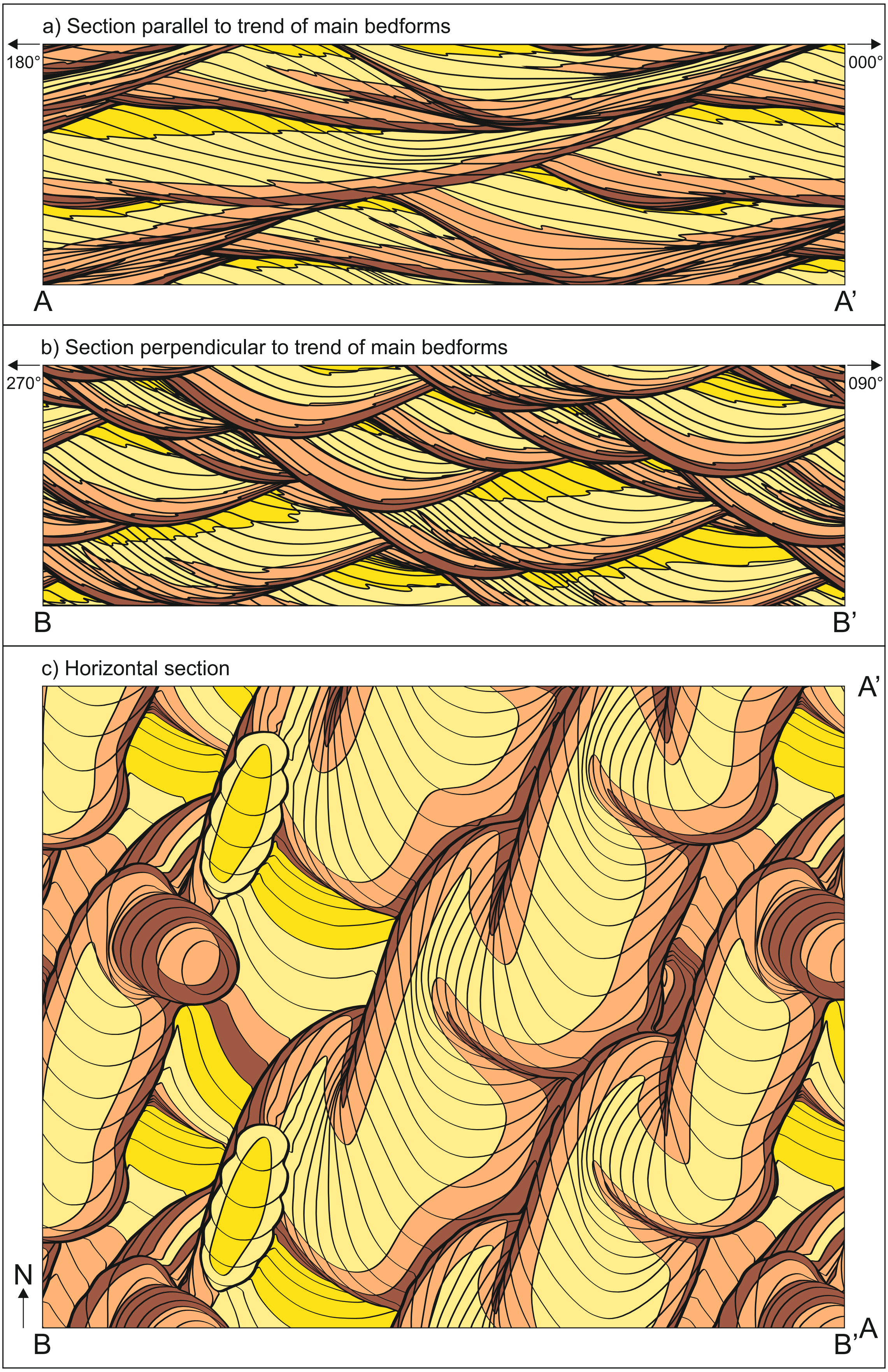

a) Section parallel to trend of main bedforms

b) Section perpendicular to trend of main bedforms

c) Horizontal section

Figure 3.26. Stratigraphic architecture produced by Sedimentological Model 7. Estimated geometry of grainflow strata; note that the view in the horizontal section (c) under-plays the degree to which grainflow tongues are interconnected because the flat upper surface of these sand bodies will be inclined at the angle-of-climb and are therefore projecting out of the horizontal section at a slight angle.

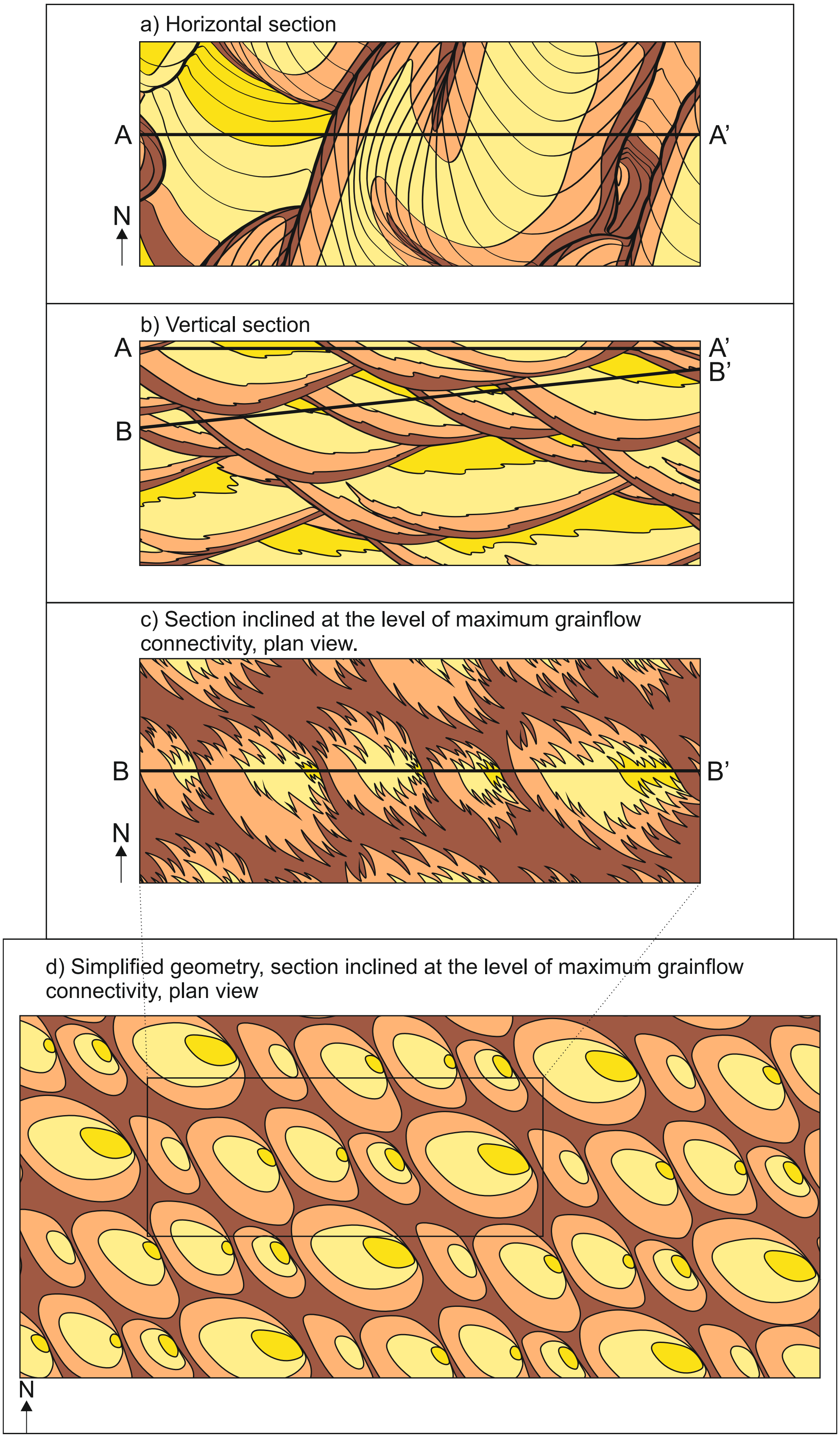
a) Horizontal section

b) Vertical section

c) Section inclined at the level of maximum grainflow connectivity, plan view.

d) Simplified geometry, section inclined at the level of maximum grainflow connectivity, plan view

Figure 3.27. Geometry and orientation of net reservoir units predicted by Sedimentological Model 7: a) geometry seen in horizontal section under-plays the likely degree of connectivity of the grainflow units; b) vertical cross section illustrating maximum grainflow development in zone parallel to climbing upper bounding surface; c) plan view geometry seen in a section taken immediately beneath a surface at the level of likely maximum degree of connectivity of the grainflow units; d) resulting facies geometry simplified to geometric shapes for reservoir modelling purposes.

3.13 – Sedimentological Model 8: Three-dimensional, variable, perfectly linear bedforms

See Figure 3.3 for detailed input parameters used in the Rubin modelling software package to generate this model.

3.13.1 – Facies distributions on bedforms

The model shown in Figure 3.28 was produced by reversing, non-migrating (perfectly linear) bedforms with along-crest migrating sinuosities (Figure 77 in Rubin, 1987a). In addition to parent bedforms that have sinuous crestlines with sinuosities migrating along-crest, the position of the parent bedforms is reversing from side-to-side in this model. These two factors give rise to numerous thin trough-like sets bounded by reactivation surfaces that are preferentially filled with wind-rippled strata. Dominance of wind-ripple over grainflow strata in this example contrasts with the model shown in Sedimentological Model 5 (Figure 3.19) due to the oscillating bedform motion in this case which generates multiple thin sets bounded by reactivation surfaces. This example would yield a relatively poor reservoir potential with a highly complex log signature, which would vary substantially over short distances and be dependent on drill locations.

3.13.2 – Geometry of stratigraphic architecture

Figure 3.29a depicts the stratigraphic architecture of the bedforms generated by Sedimentological Model 8 in a section parallel to the trend of the main bedforms. There are numerous thin sets preserved, which are dominated by non-net reservoir, in this case wind-ripple and wind-ripple-dominated strata. Similarly, in the section perpendicular to the trend of the main bedforms (Figure 3.29b), the grainflow and grainflow-dominated stratal packages are confined within the reactivated sets, and surrounded by wind-ripple and wind-ripple-dominated strata which have less favourable reservoir properties. The horizontal section shown in Figure 3.29c further demonstrates this pattern, whereby a significant proportion of the reservoir volume is dominated by wind-ripple and wind-ripple-dominated facies. However, as previously described, this horizontal view significantly underplays the degree to which the grainflow units are connected, which will be discussed further in Section 3.13.3.

3.13.3 – Geometry and orientation of net reservoir units

Figure 3.30 describes the geometry and orientation of the net reservoir units (grainflow and grainflow-dominated stratal packages) which are predicted by Sedimentological Model 8. The horizontal section (Figure 3.30a) underplays the likely degree of connectivity between the linear dune grainflow-dominated units, which is rectified in part by Figure 3.30b by illustrating the likely maximum grainflow development in a section inclined as such to capture the most likely maximum grainflow deposition predicted by Sedimentological Model

8. Directly beneath this surface, the maximum degree of connectivity of the grainflow units is depicted in plan-view (Figure 3.30c), and these grainflow units are simplified to geometric shapes in Figure 3.30d as a characterisation of the overall geometry in a manner suitable for forward reservoir modelling. For Sedimentological Model 8, the facies geometries predicted are the most complex of all the previous models. The facies bodies have the smallest aerial extent, and have varying shapes and sizes dependant on which part of the reservoir volume has been cut. This would make prediction of net reservoir elements difficult to constrain.

3.13.4 – Modern examples

The type of structure seen here is produced by reversing linear bedforms with migrating crestline sinuosities, previously described by Tsoar (1982; 1983) for linear dunes from the Sinai Desert.

3.14 – Conclusions

The application of numerical modelling techniques to simulate bedform behaviour and resultant preserved stratigraphic architecture has enabled estimates to be made of the likely geometry and degree of interconnectivity of net reservoir facies within three-dimensional space, by the novel addition of predicted facies distributions into previously developed models. The models are intentionally dimensionless to enable them to be retrospectively scaled to the features being modelled.

Modest changes in bedform morphology (and therefore the geometry of accumulated elements) can exert a marked control on preserved facies geometries, and therefore on the distribution of bodies considered to form effective net reservoir. However, this is not always the case. In some situations, bedforms which are constructed under the influence of varied wind directions, and bedforms which have distinctly different morphologies can generate preserved facies relationships that are potentially very difficult to distinguish from one another. Care must therefore be taken when interpreting these deposits in the subsurface, or conversely applying these forward models to subsurface examples where original depositional bedform types are known.

A new methodology and workflow for aeolian reservoir characterisation has been developed here, and it forms an important bridging step that spans the gap between sedimentology and reservoir modelling, therefore filling an important niche that has long been recognised but which has seldom been considered in detail. This is a particularly novel aspect of this study.

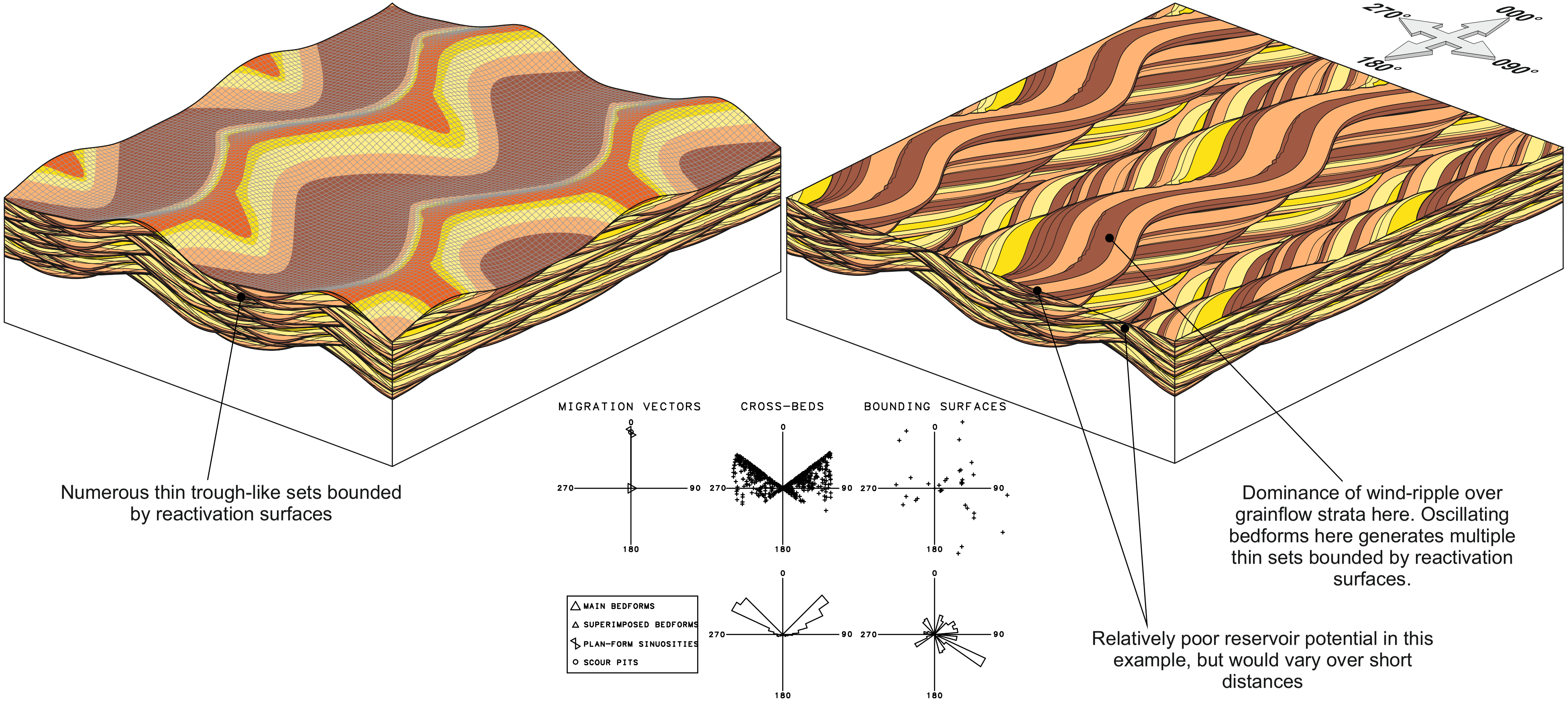

Numerous thin trough-like sets bounded by reactivation surfaces

Dominance of wind-ripple over grainflow strata here. Oscillating bedforms here generates multiple thin sets bounded by reactivation surfaces.

Relatively poor reservoir potential in this example, but would vary over short distances

Figure 3.28. Sedimentological Model 8 (see Figure 3.3 for the input parameters used to generate this model). This model is generated by reversing, non-migrating, perfectly linear bedforms with sinuosities that migrate along-crest. No scale implied.

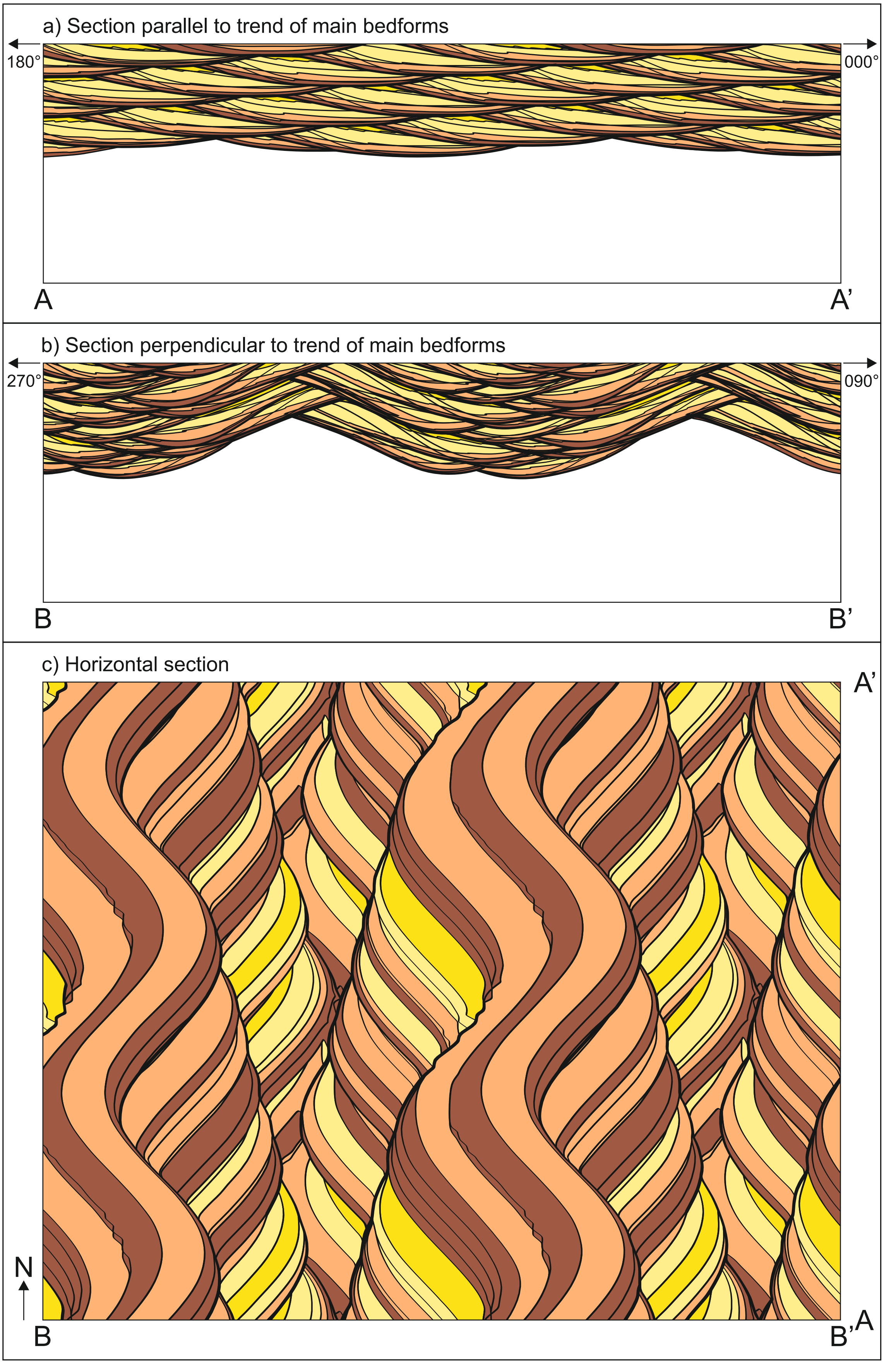

Figure 3.29. Stratigraphic architecture produced by Sedimentological Model 8. Estimated geometry of grainflow strata; note that the view in the horizontal section (c) under-plays the degree to which grainflow tongues are interconnected because the flat upper surface of these sand bodies will be inclined at the angle-of-climb and are therefore projecting out of the horizontal section at a slight angle.

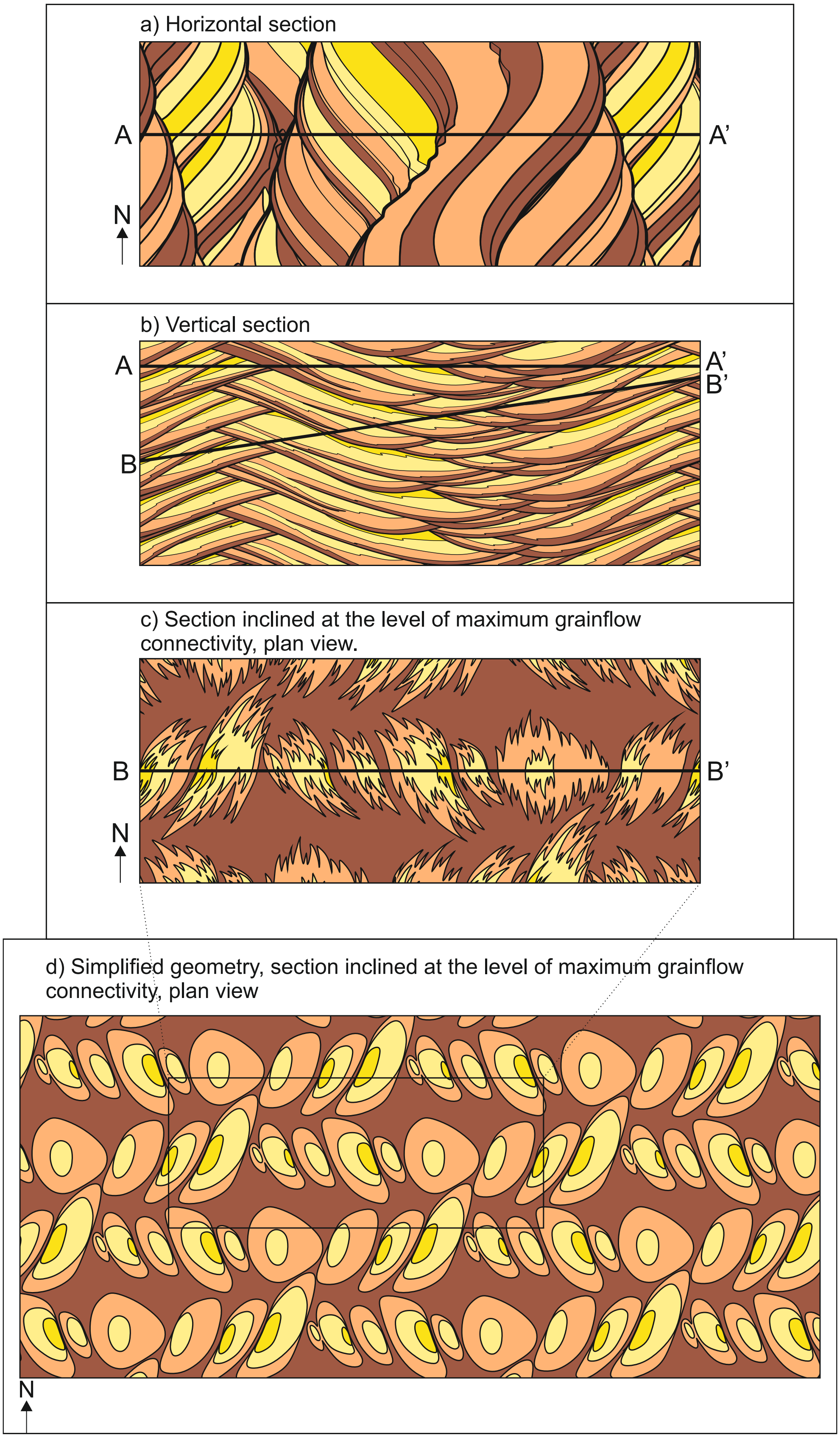

Figure 3.30. Geometry and orientation of net reservoir units predicted by Sedimentological Model 8: a) geometry seen in horizontal section under-plays the likely degree of connectivity of the grainflow units; b) vertical cross section illustrating maximum grainflow development in zone parallel to climbing upper bounding surface; c) plan view geometry seen in a section taken immediately beneath a surface at the level of likely maximum degree of connectivity of the grainflow units; d) resulting facies geometry simplified to geometric shapes for reservoir modelling purposes.

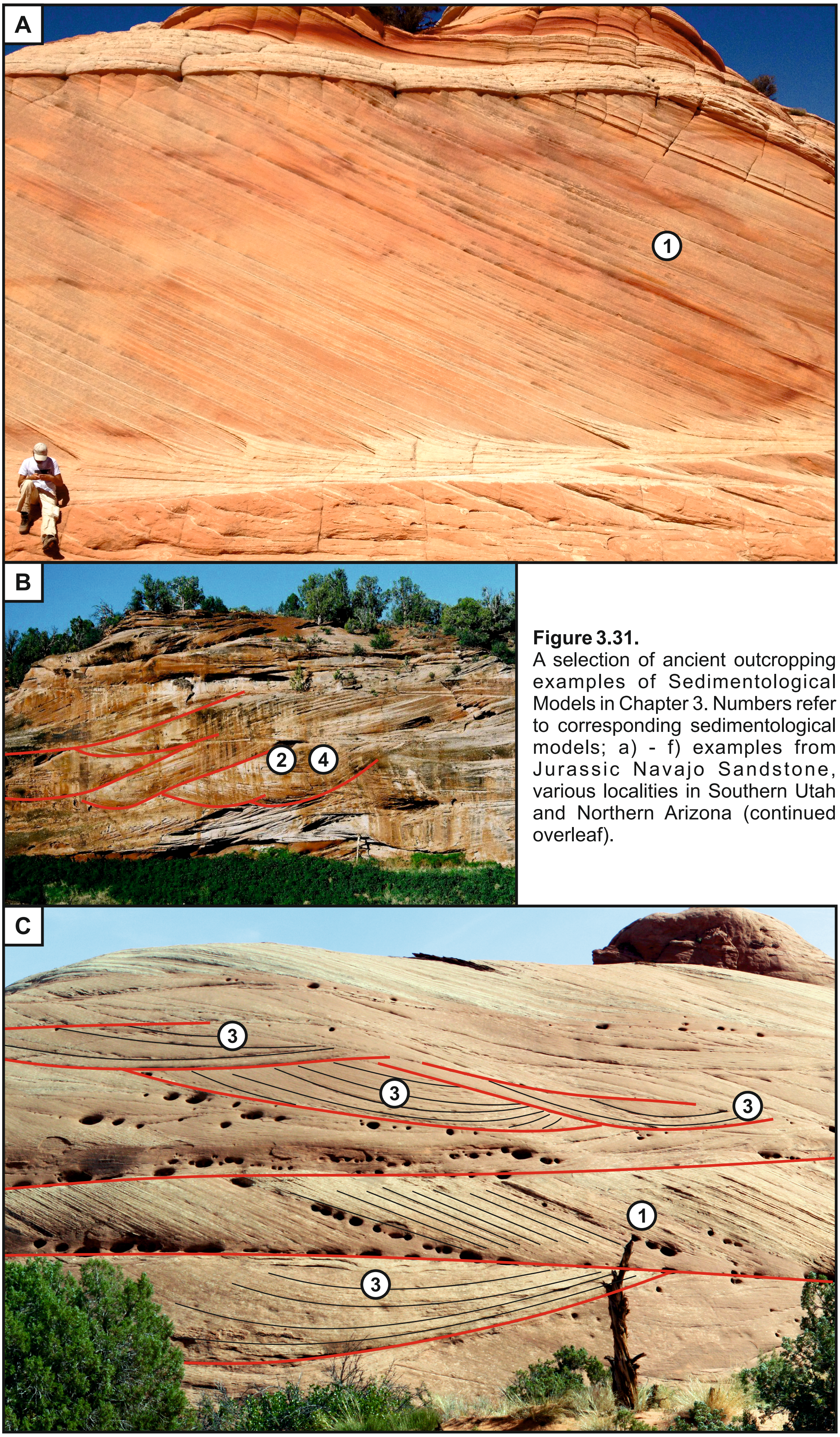

Figure 3.31.
A selection of ancient outcropping examples of Sedimentological Models in Chapter 3. Numbers refer to corresponding sedimentological models; a) - f) examples from Jurassic Navajo Sandstone, various localities in Southern Utah and Northern Arizona (continued overleaf).

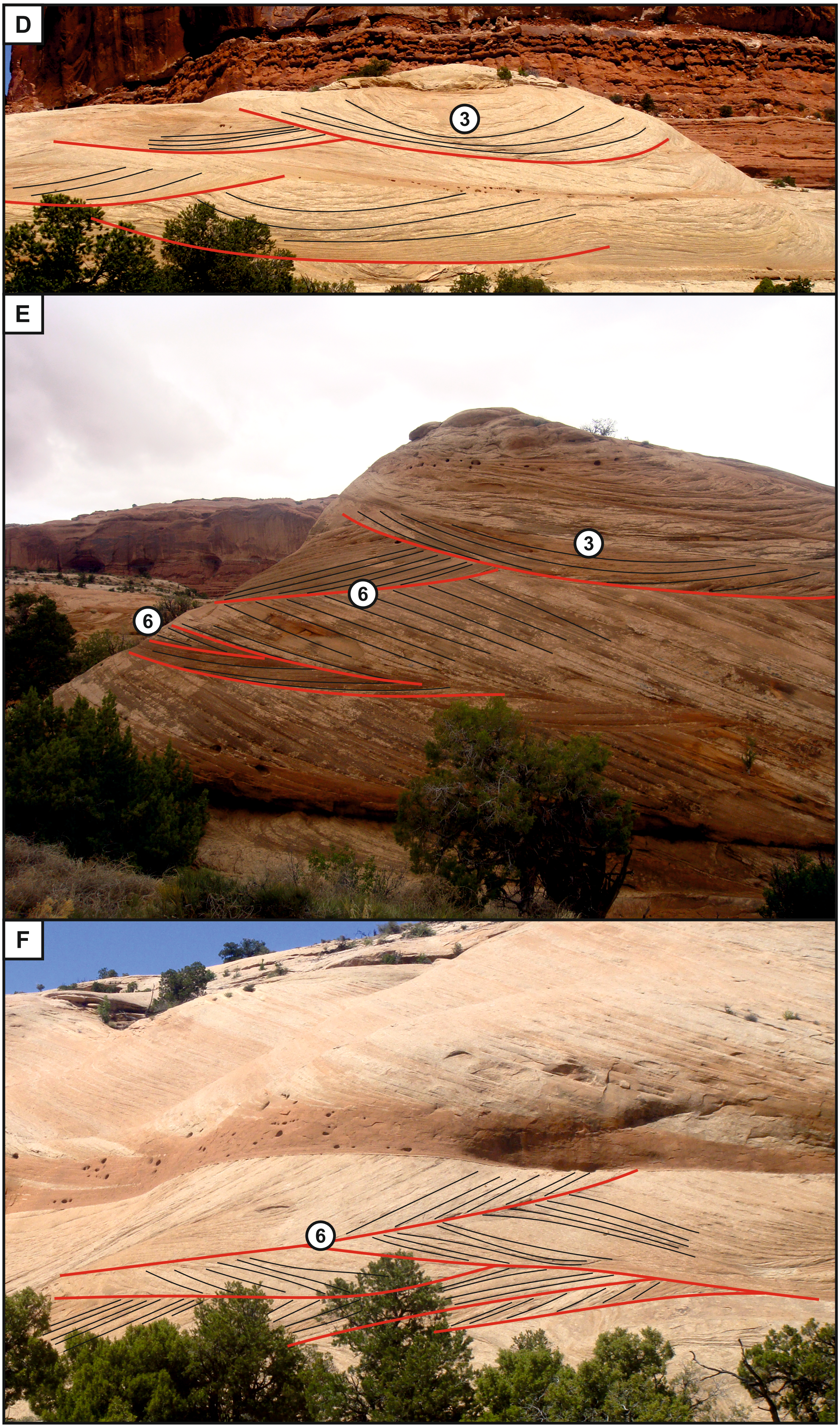
D
3
E
3
6
6
F
6

Chapter 4 – Reconstruction of linear dunes from ancient aeolian successions using subsurface data: a case study from the Permian Auk Formation, Central North Sea, UK

4.1 – Introduction

An integrated well log and core interpretation case study is presented here to demonstrate how observations from a subsurface dataset can be used to reconstruct dune type, morphology and temporal migratory behaviour of large bedforms within an aeolian dune and interdune succession known only from the subsurface. The method employed outlines objective criteria for interpreting changes in the style, rate and direction of aeolian bedform migration through recognition of stratigraphic evidence for temporal changes in bedform migration style, lee-slope steepness and asymmetry in subsurface data, and by comparison to analogous outcropping successions and aspects of modern bedforms in presently active dune fields.

Determination of original bedform type and style of migratory behaviour from ancient aeolian successions known only from subsurface intervals is problematic because such successions exhibit lithological heterogeneity at a number of scales in response to both the varied arrangement of lithofacies arising from complex autogenic bedform behaviour (e.g. Heward, 1991), and potentially also from allogenic controls on stratigraphic accumulation and preservation (e.g. Howell and Mountney, 1997). As such, the deposits of such accumulations may be highly variable over short lateral distances and elucidating the three-dimensional architecture of the deposits and then interpreting the significance of these deposits in terms of original formative processes is not straightforward.

Aeolian dune successions of the Permian Rotliegend Group of the southern and central North Sea and surrounding area have most commonly been interpreted as the accumulated deposits of transverse bedforms (e.g. Glennie et al., 1978; 1998a; Heward, 1991), including barchanoid forms. However, linear aeolian bedforms have also been reconstructed from some parts of this succession (e.g. Steele, 1983). Although spatial variations in bedform type across large aeolian dune fields are widely documented, such that transverse and linear forms are known to commonly co-exist (e.g. Namib Desert; Lancaster, 1983), there remain few documented examples of such variability from ancient preserved aeolian successions.

Despite linear bedforms accounting for >50% of dunes present in modern active dune fields, such bedforms are only rarely interpreted in the ancient record (Rubin and Hunter, 1985; Rodriguez-Lopez et al., 2014). As such, there are very few published descriptions relating to the internal facies and bounding-surface distributions of ancient linear dune successions. As a result, qualitative and quantitative data relating to the stratigraphy of successions generated by the accumulation of such bedforms – which might serve as valuable analogues for the Auk Formation – are few. The modest number of accounts that have been published are from successions that are either not especially close in terms of their analogy, or are not sufficiently well exposed to yield useful dimensional data.

Figure 4.1 depicts a schematic representation of a ‘simple’ (*sensu* McKee, 1979a) linear dune that has undertaken migration and aggradation under conditions of moderate climb. The angle-of-climb is in a direction perpendicular to the trend of the crestline, because the linear bedform creeps sideways over time (Section 1.3.3.2). Vertical successions located at various positions along an accumulated stratigraphic section depict typical vertical lithofacies profiles. This schematic illustration demonstrates the likely presence of a marked lateral variability in facies arrangements that are typically encountered over relatively short distances within aeolian dune deposits accumulated by the same migrating bedform. Individual vertical profiles within the same dune set (or coset) can be composed solely of wind-ripple and wind-ripple-dominated facies, whereas only a relatively short distance away, the same stratigraphic section might be represented by a suite of different aeolian dune facies types, including grainflow and grainflow-dominated units (Figure 4.1). This complexity in facies arrangements is dependent on a number of autogenic factors including, for example, how far down the lee-slope of the migrating bedform grainflow avalanches extended before terminating. Given this intrinsic complexity in facies arrangements, great care must be taken when interpreting individual one-dimensional cores taken from subsurface aeolian successions; this is especially important for aeolian reservoir intervals where the ability to reliably correlate between neighbouring wells – even those spaced only a few hundred metres apart, such as deviated sidetracks – is severely hindered by the absence of beds or bounding surfaces that can demonstrably be shown to serve as reliable markers for correlation purposes (Mountney, 2006a). In many cases, the inability to even establish the presence of features regarded to be reliable indicators of palaeo-horizontal in subsurface aeolian successions is highly problematic (Kocurek, 1988; 1991).

Despite these problems, reconstruction of aeolian dune type from subsurface data remains important because many aeolian successions are known wholly or principally from the subsurface, yet understanding these systems is important for improving palaeoenvironmental understanding. Examples include: (i) the Pennsylvanian-Permian Weber Sandstone of the Rangely Field, Colorado, USA (Fryberger, 1979b; Bowker and Jackson, 1989); (ii) the Permian Leman Sandstone of the UK Southern North Sea (Glennie et al., 1978; Weber, 1987); (iii) the Permian Auk Formation of the UK Central North Sea (Heward, 1991); (iv) parts of the Triassic Ormskirk Sandstone of the UK East Irish Sea Basin (Meadows, 2006); (v) the Jurassic Norphlet Sandstone of the Gulf of Mexico (Mancini

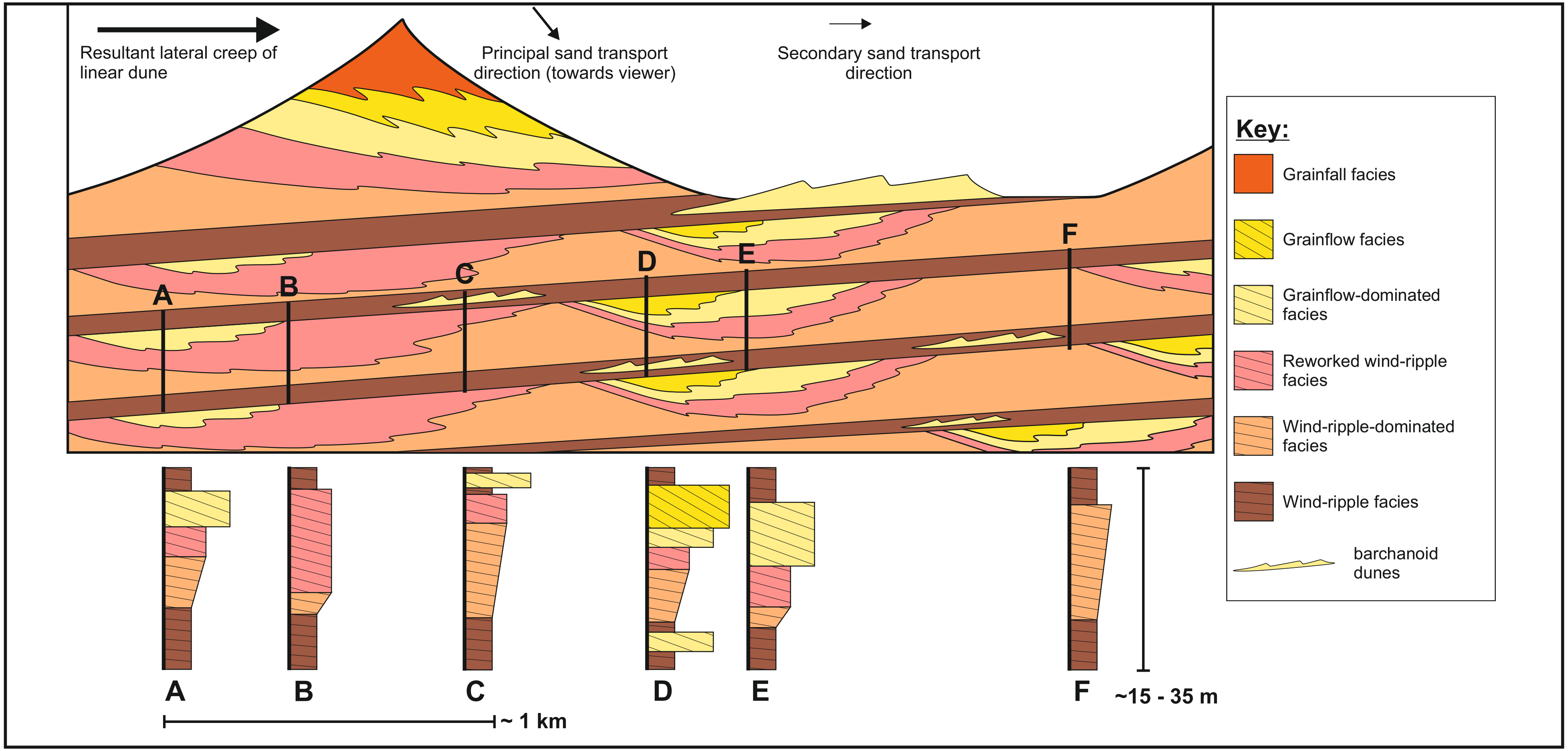

Figure 4.1. Schematic vertical successions deposited by a single episode of migration and aggradation of a 'simple' linear dune under conditions of moderate climb. Schematic lines on facies show dip-angle relationships. Note: a) the marked lateral variability over comparatively short distances of vertical successions deposited by the same migrating bedform; b) the persistence of the cleaning and steepening-upward cycle as seen in the typical vertical section (sections A, B and C); c) the uncertainty introduced in the recognition of this cyclicity where barchanoid dunes are present in interdune corridors (e.g. sections C and D); and d) the entire cycle deposited by a single dune migration episode may be represented by non-reworked wind-rippled facies (section F). Figure based largely on the work of Nigel Mountney (pers. comm.), with contributions from Bernard Besly.

et al., 1985); and (vi) the Cretaceous Kudu Sandstone, offshore Namibia (Wickens and McLachlan, 1990). From an applied perspective, these successions form important reservoirs for hydrocarbons and understanding dune type is a fundamental step in predicting lithofacies distribution and therefore determining lithological heterogeneity and the arrangement of packages of favourable reservoir quality.

The aim of this study is to demonstrate how a detailed palaeoenvironmental reconstruction of an aeolian system can be made from an ancient preserved succession known only from a subsurface dataset. Specific objectives of this study are as follows: (i) to identify a range of aeolian lithofacies types present in core data from the subsurface Auk Formation; (ii) to establish criteria for determining the type, morphology and migratory behaviour of the aeolian bedforms that gave rise to the Auk succession through analysis of preserved stratigraphic architecture and palaeocurrent data; and (iii) to demonstrate a methodology for reconstructing the depositional environment of an ancient aeolian succession based on key observations from subsurface datasets coupled with comparison to modern analogous aeolian dune systems. This research is novel and significant because deposits of the Auk Formation studied here are considered to represent the preserved remnants of large linear aeolian bedforms; this study therefore documents an example of an important aeolian dune system type that is rarely recognised in ancient successions. Results from this chapter form the basis of an interpretation with which to undertake numerical modelling of reconstructed aeolian architectural complexity in Chapter 5.

4.2 – Geological Setting

The Permian Auk Formation of the Rotliegend Group is present in the subsurface around the southern edge of the North Permian Basin in the UK sector of the Central North Sea (Figure 4.2). The succession accumulated in a subsiding basinal area in response to transtentional collapse following the Variscan Orogeny (Glennie, 1998a; Glennie et al., 2003). The Auk Formation underwent initial accumulation in the Early Permian (Figure 4.3): Capitanian to Wuchiapingian (Glennie et al., 2003). Thin grey claystone beds within the upper part of the formation have yielded spores of Late Permian age (Heward, 1991). The overlying Zechstein Group accumulated during the Late Tatarian (Taylor, 2009).

The aeolian system of the Auk Formation was constructed from wind-blown detritus that was derived from both the Caledonian Uplands which lay to the northwest (Glennie et al., 2003) and from the Variscan uplift of the Mid-North Sea High to the south (Bifani et al., 1987), based on analysis of regional palaeowind patterns from preserved palaeocurrent data including foreset dip-azimuths in cross-bedded sets and sediment provenance studies. Sediment transport pathways were complex and likely reflect both regional palaeodrainage and palaeowind patterns.

4.2.1 – Stratigraphy and reservoir layering

Previous stratigraphic studies of the Rotliegend Group in the Central North Sea region have yielded a five-fold layering scheme, numbered from stratigraphic top to bottom as Unit 1 to Unit 5 (Heward, 1991). Unit 1 is a distinct stratigraphic layer which comprises massive and slumped sandstones, interpreted to be the products of reworking and slumping of the large aeolian dunes in a wet climatic phase directly preceding the Zechstein transgression (Glennie and Buller, 1983). Unit 2 – Unit 4 are interpreted as aeolian dune sands, and are considered as effective net reservoir in varying proportions, with Units 2 and 3 present as significant layers of reservoir-quality sand above the oil-water contact (OWC); Unit 2 forms a lower net:gross reservoir interval than Unit 3. Unit 5 comprises a basal conglomerate layer that is rarely penetrated by wells. The interval studied here is Unit 2 from the upper part of the succession of the Auk Formation.

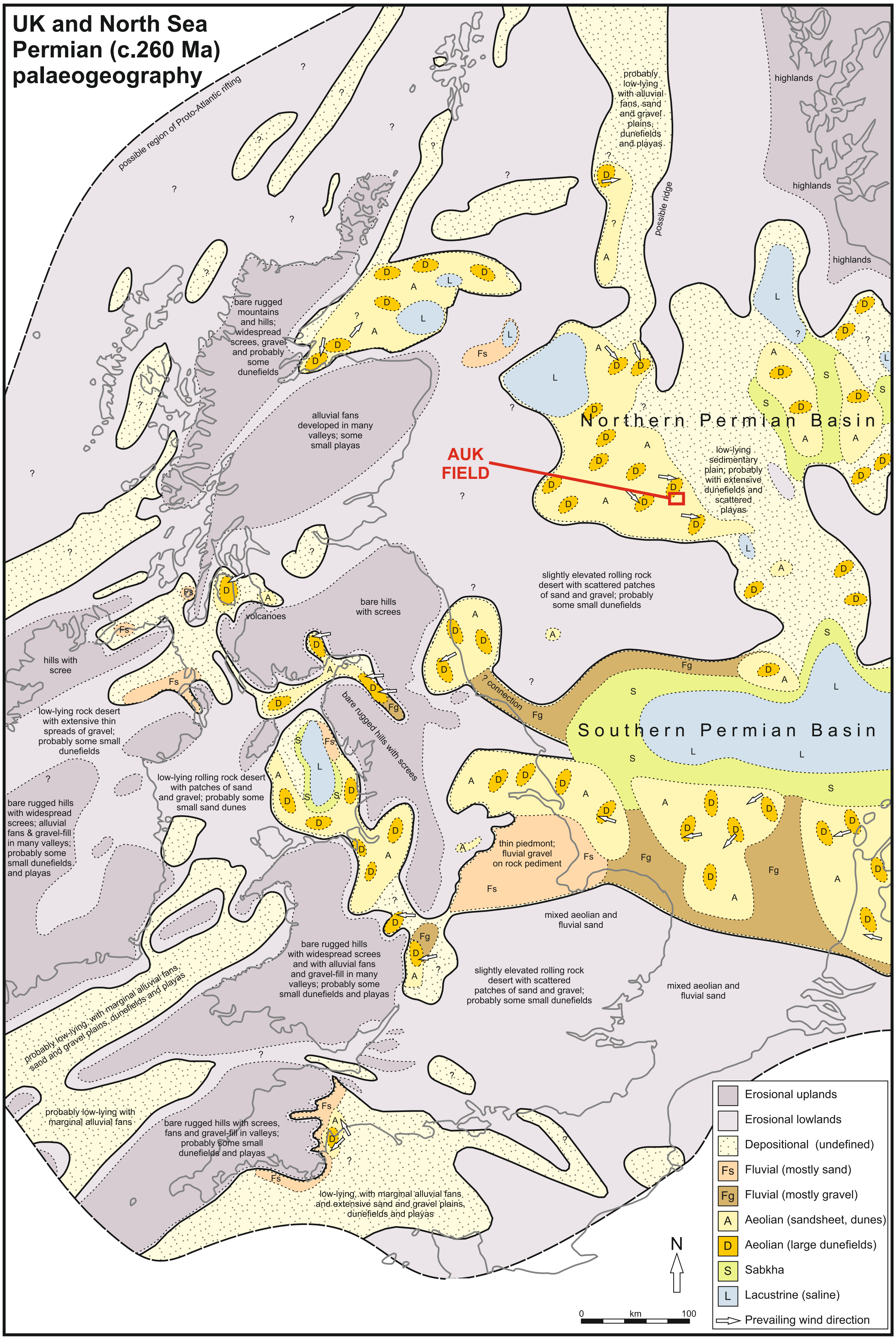

Figure 4.2. Permian (c. 260 Ma) palaeogeography of the United Kingdom and North Sea region. Position of Auk Field highlighted. Modified after Smith and Taylor (1992).

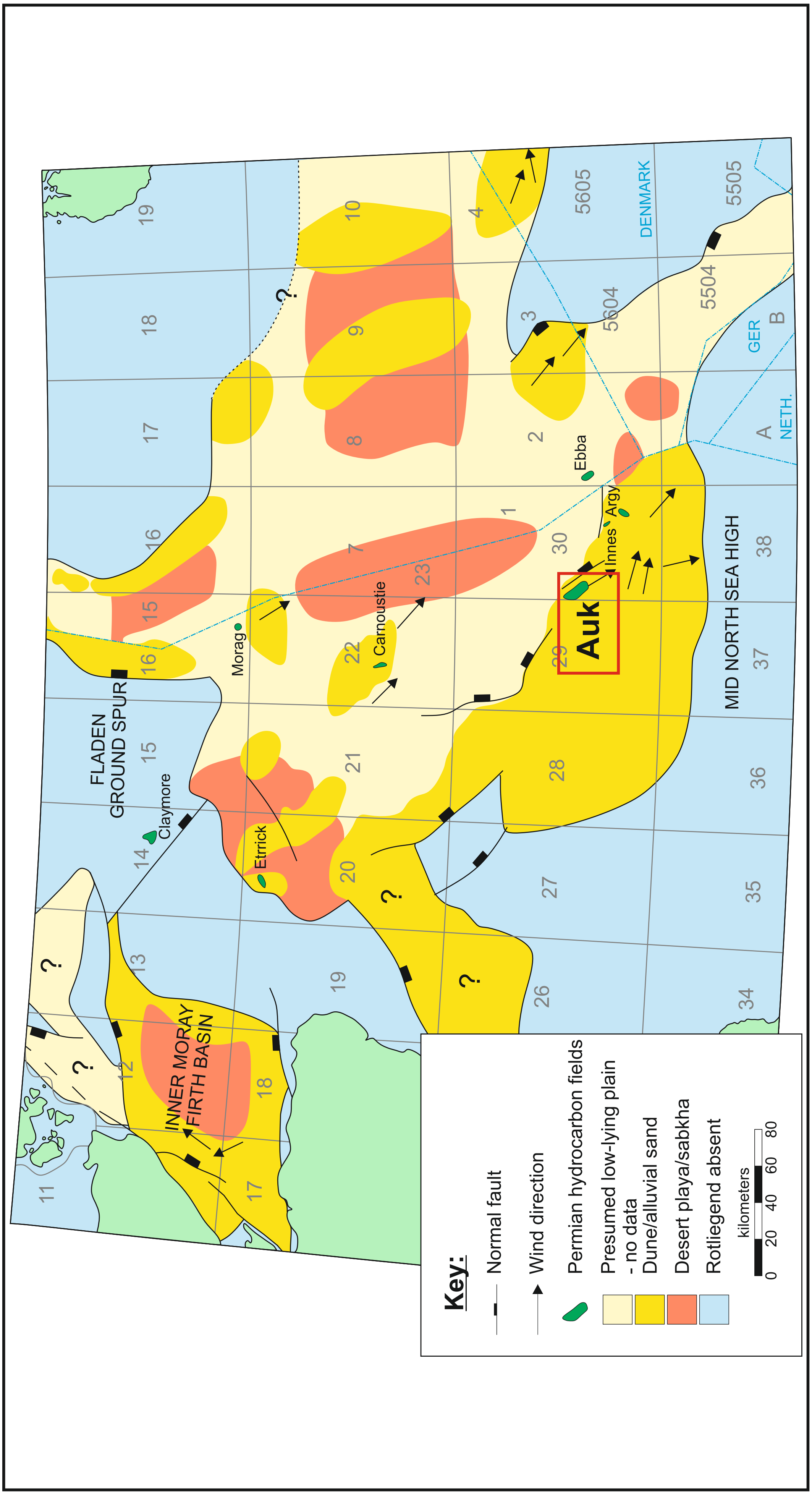

Figure 4.3. Regional setting of deposition, Rotliegend of Auk Field (from Glennie et al., 2003)

4.3 – Data and Methods

Core and well log data from 14 wells from Unit 2 of the Auk Formation, totalling 1139.83 m in length, were previously logged by Bernard Besly, with contributions from Nigel Mountney, as part of an earlier project and made available for the further detailed process and palaeoenvironmental interpretations presented in this study. Only summary logs are presented here, as the original logs are held in an internal confidential report by the field operator (Talisman Energy UK Ltd). However, the majority of the cores are on open release and are free to view (http://www.bgs.ac.uk). Core logs record lamination and bedding style, apparent depositional dips and textural properties of the sediments, and this information has been used to assign the deposits to 6 lithofacies. A review of all previously published sedimentological studies of the Auk Formation was also undertaken to supplement the primary dataset. Interpretations of the subsurface data were made on the basis of comparison with observed textural characteristics and patterns of aggradation of the sediments and depositional environments of recent aeolian sediments. Foreset dip-azimuths from dipmeter data and from oriented core were analysed to determine original aeolian bedform migration direction and to relate this to regional palaeowind directions.

The following parameters were available from the 14 studied wells (Figure 4.4):

Top and base depths of facies units. Depths were recorded of tops and bases of all facies units, sample gaps, rubble zones and core gaps. Depths were recorded to the nearest 15.0 mm.

Nature of basal contact of units. For all facies boundaries, information relating to the following aspects of the form of the basal contact of the unit were available: (i) angle of contact surface (relative to true horizontal in deviated wells); (ii) relationship of overlying laminae to bounding surface (concordant, downlapping, onlapping); (iii) relationship of underlying laminae to bounding surface (concordant, sub-parallel truncation, angular truncation). These attributes collectively allowed recognition of different types of aeolian bounding surface (Figure 4.5).

Facies. A total of 6 facies types were recognised: non-reworked wind-ripple, reworked wind-ripple, grainflow, grainfall, massive sands and conglomerates, of which 4 are considered in detail and described herein.

Bedding style. A description of the nature of the lamination (e.g. mm-bedded, mm-bedded with subordinate cm-bedding), comprising both lamina thickness, grain size, and an indication of the generalised nature of the sorting as expressed by the degree and nature of bimodality of grain size. The following four classes of sorting were recorded (Figure 4.6): (i) bimodal; (ii) bimodal within framework and between laminae; (iii) bimodal between laminae with unimodal framework; and (iv) unimodal.

Apparent dip angle, corrected for well deviation. Dip angles of laminae were systematically recorded. A template cut to the angle of well deviation was used to obtain corrected apparent dips in cores cut in deviated wells, where the combination of well path azimuth and orientation of the slabbed core surface allowed this.

Colour. The dominant colours in the studied interval of the Auk Formation (red and drab) were recorded. In many sections, these were too finely interlaminated to record on a bed-by-bed basis, and were instead recorded in 4 classes: (i) all red; (ii) red with subordinate drab; (iii) drab with subordinate red; (iv) all drab.

Oil stain. The presence of oil in the studied interval of the Auk Formation is marked by black staining and by the occurrence of bleached laminae. The latter records the passage of reducing fluids and is not in all cases associated with live oil. In some older cores, the recognition of weak oil staining is ambiguous, owing to the loss of oil by evaporation. A fourfold scale of oil staining was recorded: 0 – no stain; 1 – weak stain; 2 – moderate stain; 3 – strong stain. In addition, black impregnations of bitumen and/or residual oil were recorded as a stain of ‘R’. Type of oil staining is closely related to porosity and permeability, which are themselves controlled by primary lithofacies type; thus oil staining is an important indicator of primary sedimentological features.

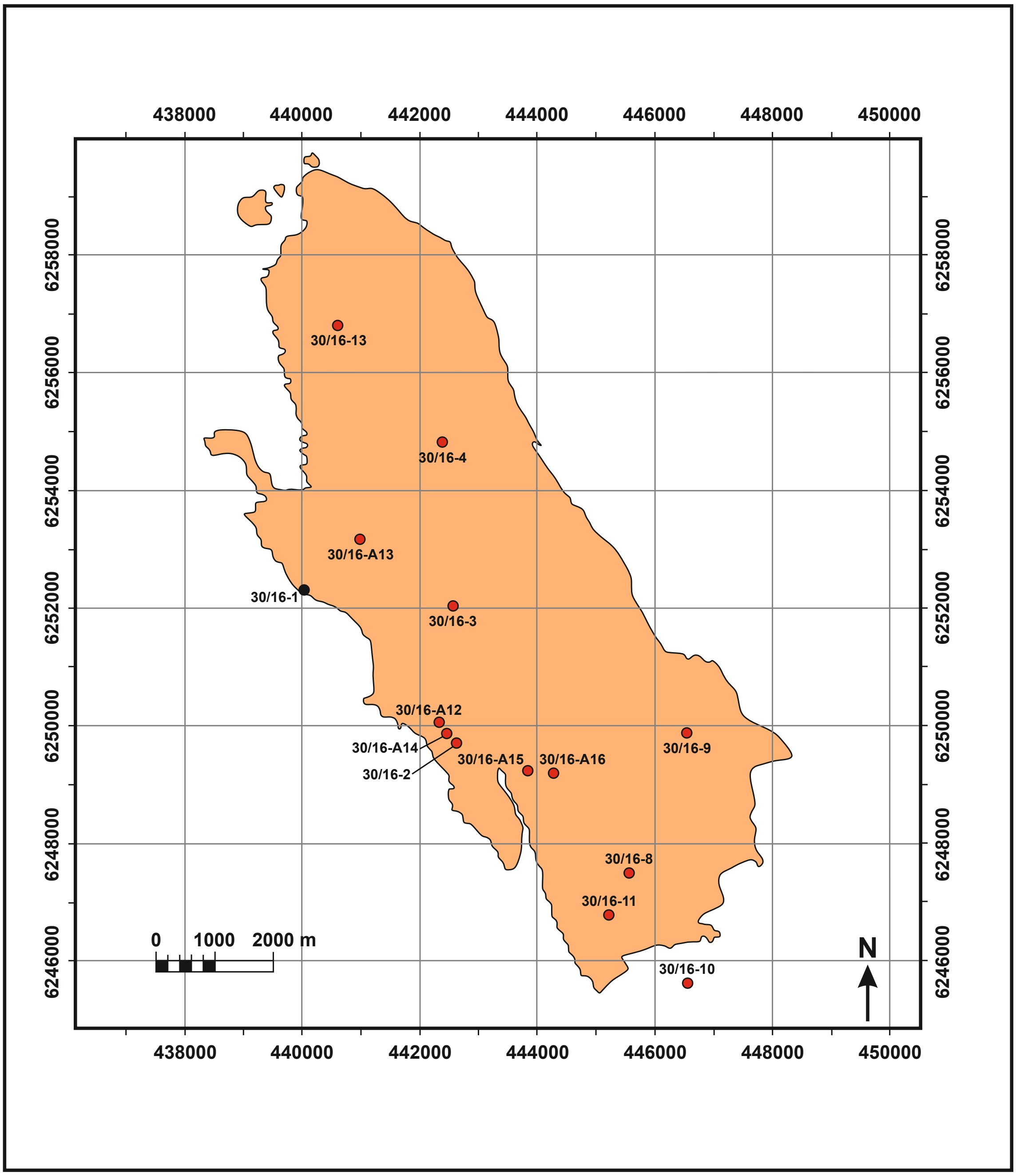

Figure 4.4. Auk Field, Block 30/16, UK Central North Sea: well location map with position of wells used in this study. Well symbols mark well positions at Top Rotliegend. Red well symbols indicate cored wells. Modified from Trewin et al. (2003).

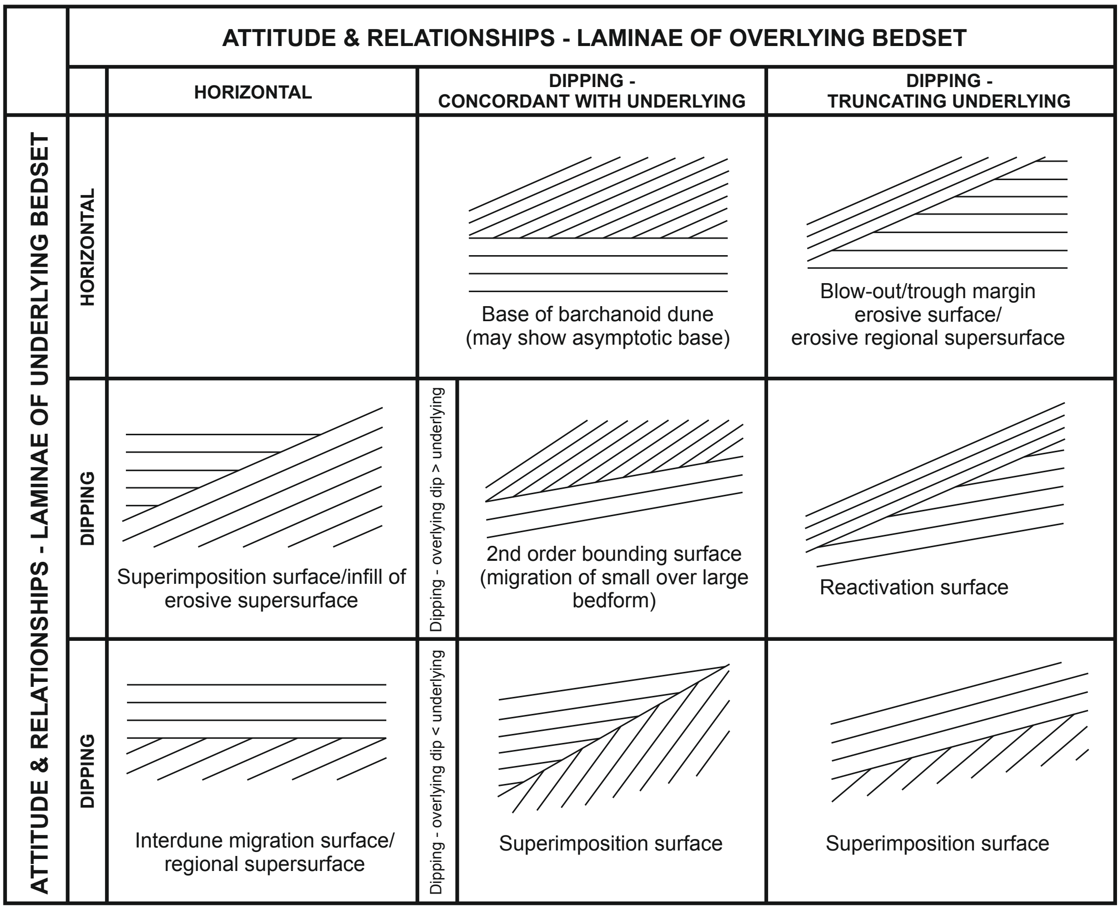

Figure 4.5. (above) Nature of bounding surfaces in the Auk Formation, with key to descriptive nomenclature for stratal relationships and typical occurrences of surface types. Note that many of the surface types may relate to either local or larger-scale stratal relationships, not differentiated in core. Figure reproduced from an original figure by Bernard Besly, with contributions from Nigel Mountney.

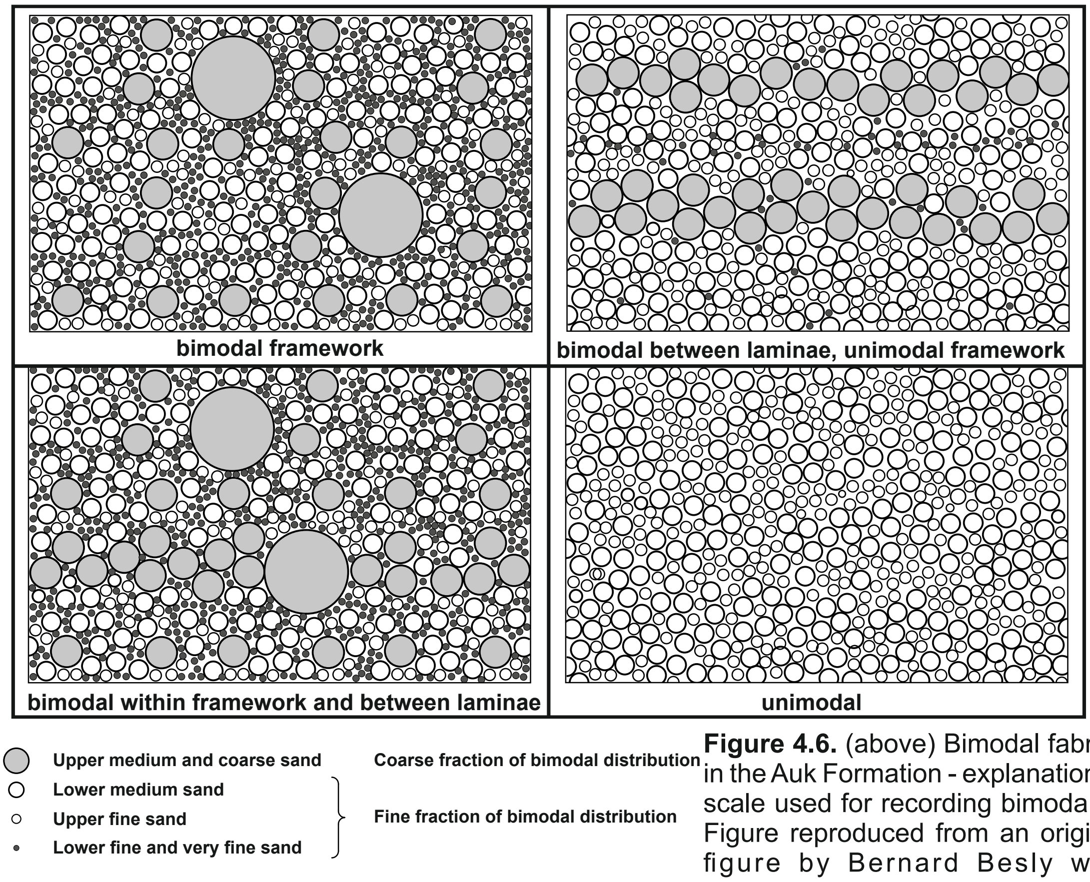

Figure 4.6. (above) Bimodal fabrics in the Auk Formation - explanation of scale used for recording bimodality. Figure reproduced from an original figure by Bernard Besly with contributions from Nigel Mountney.

4.4 – Sedimentology of the Auk Formation

The most detailed previously published study of the sedimentology and stratigraphy of the Auk Formation was conducted by Heward (1991) who proposed a four-fold facies scheme. This scheme has been adopted and extended in this study for which 6 types are recognised (Figure 4.7). The lithofacies composition of the aeolian dune and interdune sets are as follows: (i) predominantly fine-grained (rarely medium-grained) wind-ripple laminated sandstones, which typically exhibit bimodal sorting; (ii) fine to medium reworked wind-rippled sandstones, which exhibit a coarse skew; (iii) fine to medium sandstones of dune slipface (grainflow) origin, with generally the highest porosities; (iv) fine sandstones of grainfall origin; (v) fine to coarse sandstones that are predominantly massive (i.e. structureless), which occur at the top of the Rotliegend Group (named Weissliegend - Glennie and Buller, 1983); (vi) water-lain conglomerates, which occur locally at the base of the succession in the Argyll Field (Heward et al., 2003). Although present in some of the Auk cores, facies types (v) and (vi) are not present in the sections studied in detail here and are not considered further in this study.

4.4.1 – Wind-rippled facies

Description. Wind-rippled facies of the Auk Formation are composed of mm-scale laminated sandstone, with the grain size generally ranging from very fine to medium or coarse sand. This facies is characterised by strong bimodality, with a bimodal framework and segregation into laminae of contrasting grain size. Wind-rippled sandstone facies locally contain abundant pinstripe laminae (*sensu* Fryberger and Schenk, 1981), and commonly contain discrete lenses of coarser-grained sand. In almost all cases this facies is red in colour. The reconstructed (i.e. original) depositional dip of wind-rippled facies in the Auk Formation ranges from 0° to 26°.

Interpretation. Wind-ripple deposits are formed by migration of grains by creep and saltation, with a mixture of very fine sand and silt or clay material by fallout from suspension. Transport processes are well documented in recent aeolian systems (e.g. Kocurek, 1991; Mountney, 2006a) and have been simulated in experimental wind tunnels (Fryberger and Schenk, 1981). The pinstripe lamination represents interlaminations of very fine sandstone formed by grainfall, and the lenses of coarser-grained sand represent segregation of coarser grains on wind ripple crests.

4.4.2 – Reworked wind-rippled facies

Description. Reworked wind-rippled facies of the Auk Formation are characterised by mm-scale laminated sandstone as with the previously described wind-rippled facies, but additionally contain discrete laminae of better-sorted sand and that are either bimodal only between laminae, or are unimodal. The improved sorting and organisation of such laminae indicate reworking of the primary wind-rippled sands. Depositional dips range from 0° to

26°, but are usually greater than 7°. In places where reworked wind-rippled strata occur above the OWC, the reworked laminae may be bleached to a drab colour or may be oil-stained.

Interpretation. Reworked wind-rippled facies are the product of post-depositional winnowing of wind-rippled facies (Fryberger et al., 1992). Although the transport processes involved are the same as for wind-ripple generation – creep and saltation – slower deposition and/or exposure to stronger winds tends to result in the loss of the finer fractions by winnowing and transport in suspension. This facies usually comprises a significant proportion of sand grains greater than 0.5 mm diameter (medium sand) that are mainly transported by creep processes (Lancaster, 1995); aeolian transport of grains of this size tends to be restricted to interdunes and to the plinths and lower (less steeply-inclined) flanks of dunes. As such, this facies is preferentially excluded from the higher parts of topographically elevated bedforms. This reworked wind-rippled facies is not widely recognised in ancient aeolian dune deposits but the significance of the distinction between reworked and non-reworked wind-rippled facies is implicit from the descriptions of textural parameters and depositional processes in studies of modern dune systems (e.g. the Namib Desert, Lancaster, 1981).

4.4.3 – Grainflow facies

Description. Grainflow facies of the Auk Formation comprise cm-scale laminated fine- to medium-grained sandstone, with individual sediment packages usually having a massive appearance and looser grain packing structure than associated wind-rippled facies. The depositional dips of grainflow facies are usually greater than 20°. In places where grainflow facies occur above the OWC, they are almost always bleached to a drab colour or oil-stained.

Interpretation. Packages of grainflow facies are deposited by avalanching of sand grains down steeply-dipping dune slipfaces (Hunter, 1977a; Kocurek, 1991; 1996). Grainflow processes are associated with sets composed internally of laminations that indicate primary depositional dips of more than 17°, and typically up to 26° in buried and compacted sandstone. This reflects deposition from avalanches that were triggered by failure of slopes. On modern dunes, the critical angle of repose is between 32-34° for loose, dry sand (Allen, 1970; Carrigy, 1970): preserved inclinations are reduced as a result of post-depositional compaction. Grainflow-covered dune lee slopes inclined at the theoretical angle of repose for loose sand are common in modern dunes (e.g. Namib Sand Sea, Lancaster, 1981). In the case of large linear aeolian bedforms, slipfaces on which grainflows occur tend to be preferentially located on the middle and upper parts of the lee slopes (e.g. Sneh and Weissbrod, 1983) because such dune types tend to have large low-angle-inclined plinths at their bases where wind-ripple strata preferentially accumulate (McKee and Tibbitts, 1964). By contrast, other types of large dunes (e.g. transverse and

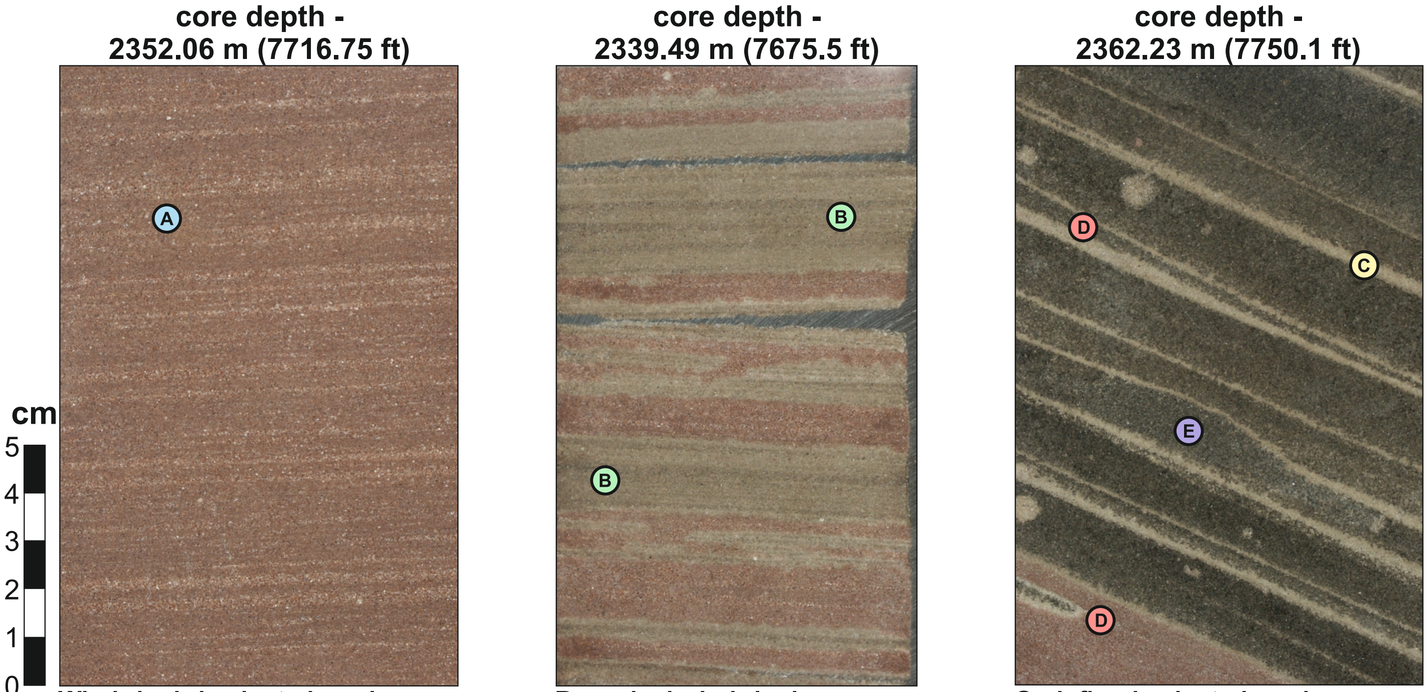

Wind-ripple laminated sand

mm-scale laminated sand, poorly to moderately sorted bimodal framework, with sporadic lenticular laminae of coarser grains (wind-ripple crests - Ⓐ); almost invariably red.

Reworked wind-ripple laminated sand

Wind-rippled sand in which a varying proportion of reworked laminae have smaller grain size range and better sorting (Ⓑ). Reworked laminae comprise mm-scale laminated sand, moderately to well sorted, generally unimodal framework (locally unimodal), bimodal between laminae.

Grainflow laminated sand

cm-scale laminated sand, with subordinate mm-scale lamination; well sorted upper fine to lower medium sand, unimodal framework, with local laminae of very fine grains (grainfall laminae Ⓒ); generally bleached and oil-stained above OWC.
Grainflow laminae locally pinch out marking toe of grainflow (Ⓓ), or swell and/or show soft sediment deformation (Ⓔ).

Figure 4.7. Characteristic features of facies in the Auk Formation reservoir from core 30/16-2. Contains British Geological Survey materials © NERC 2014.

barchanoid forms) tend to have slipfaces that extend directly to the base of the lee slope, and therefore to the bottom of the preserved set. In such dune types, grainflow facies will tend to be present close to the base of preserved sets (Kocurek and Dott, 1981).

4.4.4 – Grainfall facies

Description. Grainfall facies in the Auk Formation consist of mm-scale laminae of very-fine grained sandstone, occurring as pinstripe laminae in two distinct settings: (i) as laminae interbedded with wind-ripple laminated sand, in which case the facies is usually dark red in colour; and (ii) as laminae separating successive grainflow deposits, in which case the facies is usually bleached but not oil-stained, if occurring above the OWC.

Interpretation. Grainfall facies are formed when very-fine and fine sand is entrained into suspension, and later deposited on bedform slipface, plinth and interdune areas (Hunter, 1977a). These facies are seldom found associated with reworked wind-rippled facies due to the winnowing associated with the development of this facies. Rather, they are more commonly present draping grainflow facies, in which case thin grainfall laminae highlight boundaries between successive grainflow avalanche deposits (cf. Hunter, 1977a). Additionally, where accumulations of grainfall facies are recorded in interdune areas, such deposits record sustained fallout from suspension due to airflow deceleration downwind from the zone of turbulence associated with flow separation in the lee of large aeolian bedforms (Anderson, 1988; McDonald and Anderson, 1995). Such accumulations of grainfall facies tend to occur interbedded with wind-rippled sand deposits (cf. Hunter, 1981).

4.4.5 – Composite facies types

Facies descriptions used in this study are not based solely on discrete and individual facies types; additionally they incorporate combinations of two or more basic facies types in varying proportions: *grainflow-dominated* units are composed of >50% grainflow facies but additionally incorporate a secondary component of reworked wind-rippled strata; *wind-ripple-dominated* units are composed of >50% wind-rippled facies but additionally incorporate a minor component of reworked wind-rippled strata.

4.5 – Depositional Environment

Data are presented in this study which can be interpreted as evidence to demonstrate that the bedforms that accumulated to preserve the studied portion of the Auk Formation were large linear forms subject to a secondary component of lateral migration. The reasoning behind this interpretation is presented in the following sections by incrementally building a set of evidence-based observations that consider the following aspects of bedset geometry and bedform morphology: (i) the nature of accumulation surface (section 4.5.1); (ii) the reconstructed aeolian bedform type and morphology representrd by the preserved assemblage of bedsets (section 4.5.2); (iii) the presence of compound bedforms in the succession (section 4.5.3); (iv) the aeolian bedform scale and nature of the dune flanks (section 4.5.4); and (v) the migratory behaviour of the bedforms responsible for generating the bed-sets preserved in Auk (section 4.5.5), including detailed morphology and style of behaviour of the bedforms (section 4.5.6), the nature of the interdune flats (section 4.5.6.1), and the presence of coeval barchanoid dune fields (section 4.5.6.2). Each of the following sections adds progressively to the overall reconstruction of the palaeoenvironment, and will consider both the data and the reasoning behind its interpretation in detail.

The main evidence which supports an interpretation of linear dunes/draa in the Auk Formation is as follows:

(i) The presence of thick, low-angle-inclined dune plinths is typical of large linear bedforms in modern sand seas. In this study, the thick preserved sets (approximately 12 m) are characterised by low- to moderate-angle-inclined packages of strata which are largely composed of wind-ripple strata, a common arrangement in large linear draa of modern sand seas, such as the Namib desert (Lancaster, 1982) and the Rub Al'Khali in Saudi Arabia (Glennie, 1998b; Al-Masrahy and Mountney, 2013) (section 4.5.2);

(ii) The predominance of wind-ripple strata of various types preserved in the succession, and conversely the paucity of grainflow strata, is atypical of the majority of ancient aeolian outcrops that are themselves interpreted to represent transverse bedforms (section 4.5.2);

(iii) Preserved foreset azimuths exhibit a bimodal distribution, but with a large spread, which is indicative of linear dune development (*sensu* Parteli et al., 2009). Dipmeter data are not normally sufficient for the recognition of bedform type, but in this study the dipmeter data were used in conjunction with textural data, aeolian facies type, bounding surface types and larger genetic relationships in order to determine aeolian bedform type;

(iv) Bounding surfaces are easily recognisable in core, but the interpretation of the environmental significance of such data is problematic, because there are usually a large number of surface types which dip in a variety of angles and in a wide variety of orientations. In the studied interval of the Auk Formation, the recognition of thick cosets with internal sets defined by bounding surfaces whose attitudes are most obviously interpreted as a product of along crest-migration of crestline sinuosities to form scour troughs; in modern settings such behaviour is most common in linear bedforms.

4.5.1 – Nature of accumulation surface

Observation. In the studied succession, the facies types recognised are wind-ripple, reworked wind-ripple, grainflow and grainfall. Wind-ripple strata occur predominantly within flat- or near-flat-lying packages of strata between thicker cross-stratified sets and cosets (Figure 4.8 – Well 30/16-2, core runs 6 and 7).

Interpretation. The studied part of the Auk Formation represents the preserved remnant of a dry aeolian system (*sensu* Kocurek and Havholm, 1993). The facies types recognised collectively demonstrate accumulation without the presence of significant surface moisture and indicate aeolian sedimentation on a dry substrate. Wind-ripple strata inclined at low angles occur predominantly within interdune elements and indicate that, even in the lowest topographic depressions of the main palaeo-dune-field system of the studied interval, the substrate remained dry, such that there is no significant evidence for contact with a palaeo-water table or its capillary fringe (cf. Mountney, 2006a). However, examples of wet (ponded) interdune deposits of restricted thickness and lateral extent are known from other parts of the Auk Formation (Heward, 1991), as well as deposits of potentially fluvial origin in the lower part of the succession. The Weissliegend facies of the uppermost part of the succession (Unit 1 – Section 4.2.1) also preserves considerable evidence for marine reworking of aeolian sand, most likely in response to the Zechstein transgression of the palaeo-dune field (Glennie and Buller, 1983), but such features are not present in the part of the succession studied here.

4.5.2 – Aeolian bedform type and morphology

Observation. Facies in the Auk Formation are dominated by wind-ripple and reworked wind-ripple strata (85%), whereas grainflow and grainfall strata are considerably less common (15%) (Figure 4.8). The characteristic vertical arrangement of facies most common in the Auk Formation takes the form of thick sets (approximately 12 m), each characterised internally by low- to moderate-angle-inclined, wind-ripple-dominated stratal packages at their base. Packages of wind-ripple strata within sets gradually steepen up-section and become more abundant 2-5 m above the basal set bounding surface. In the uppermost 20-40% of many sets, wind-ripple dominated packages of strata steepen further (18-20°) before merging with packages of grainflow-dominated avalanche strata near the top of the sets (Figure 4.9). Grainflow deposits in the Auk Formation rarely reach the base of preserved dune sets and in most cases are confined to the uppermost half of sets.

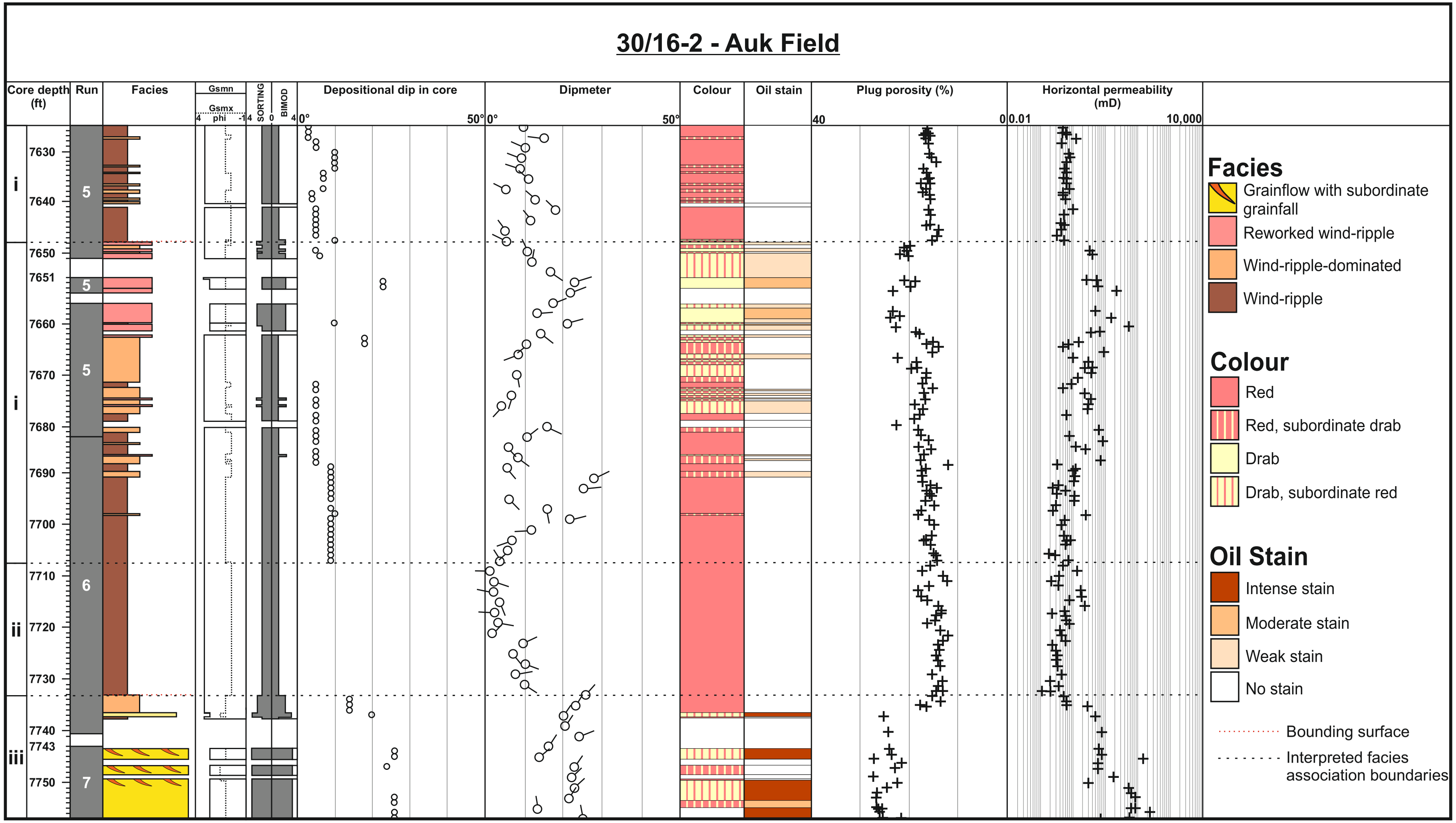

Figure 4.8. Well 30/16-2, core runs 5, 6 and 7. Facies bar width proportional to perceived reservoir quality. Interpreted facies associations: i) simple linear dune or draa aggradation unit; ii) interdune or long-lived sandsheet (planar depositional sites dominated by sediment by-pass lacking significant dune development), iii) stacked slipface-dominated transverse dunes. Original logging undertaken by Bernard Besly with contributions from Nigel Mountney; interpretation and significance of trends undertaken by Hollie Romain.

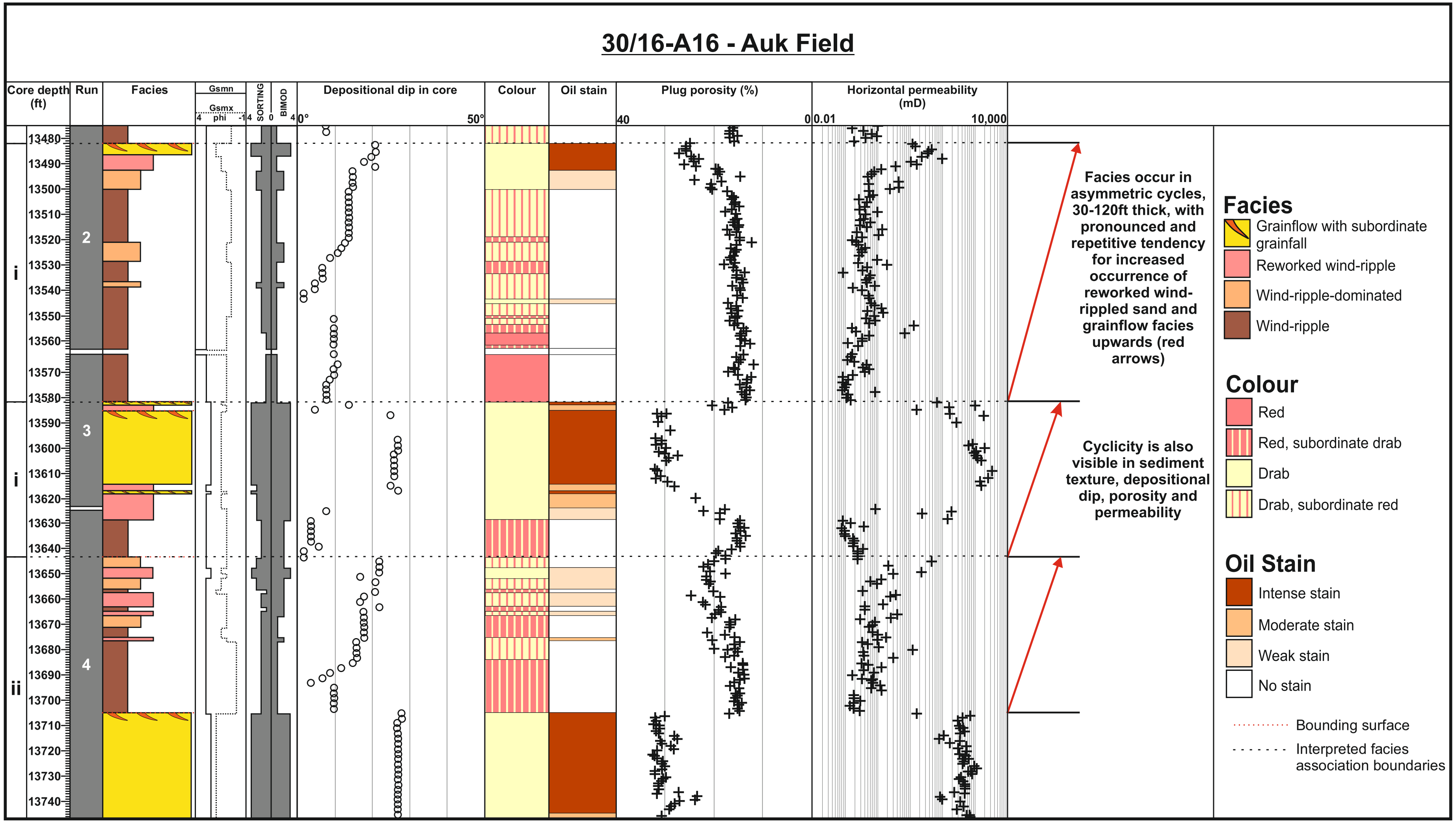

Figure 4.9. Typical vertical succession, showing aggradation of simple linear dune units, Auk Formation, Central North Sea: Well 30/16-A16, core runs 2, 3 and 4. Red dotted lines show positions of bounding surfaces; black dotted lines separate interpreted facies association boundaries: i) simple linear dune/draa aggradation unit; ii) compound linear dune/draa aggradation unit (see Figure 4.11). Original logging undertaken by Bernard Besly with contributions from Nigel Mountney; interpretation and significance of trends undertaken by Hollie Romain.

Commonly, numerous erosional bounding surfaces inclined at 5-10° are present and these define smaller scale sets that themselves occur within 10 to 20 m-thick cosets bounded by near horizontal truncation surfaces. The strata contained within the smaller scale sets dip in a variety of orientations (Figure 4.9). Bounding surfaces that delineate sets of this type typically become more steeply inclined upwards within a single coset, though sets composed internally of shallowing-upwards cross strata are also not uncommon (Figure 4.10).

Interpretation. The vertical arrangement of recorded facies - notably the occurrence of thick packages of wind-ripple and wind-ripple-dominated strata of various types, even in fairly steeply dipping deposits that have clearly been formed in a fairly elevated position on a major bedform (e.g. wind-ripple dominated sections with inclinations of 10° to 20°, well 30/16-13 – cores 3 to 4, 8488-8539 ft DD). Additionally, the upward-steepening within the sets combined with the angle of inclination of the set bounding surfaces are typical features of deposition on large linear bedforms (e.g. Tsoar, 1982; Bristow et al., 2000), especially on the lower and middle flanks of such forms (Lancaster, 1981; Livingstone, 1987; 1989a; McKee, 1982; McKee and Tibbitts, 1964; Sneh and Weissbrod, 1983). By contrast, the majority of transverse bedform types (including barchans, straight-crested transverse ridges and barchanoid dune ridges) observed in modern dune fields tend to be characterised by a single, downwind-facing slipface element, which in most cases is characterised by active avalanching down to a level within the bottom-most few metres of major cross-bedded sets (Hunter, 1985) and representing the accretion of sediment on a dune lee-slope that migrated consistently in a favoured direction (thereby giving rise to a tightly clustered range of foreset dip-azimuths). This is in contrast to the dominant pattern observed in the Auk Formation.

The occurrence of upward-steepening sets of cross-strata is consistent with the oblique migration of scour hollows or pits in the form of re-entrants on the advancing lee-side of linear draa (cf. Rubin, 1987a; 1987b). Upward-steepening sets of cross-strata between sets of shallowing-upwards cross strata imply oblique migration of spurs or lateral ridges in the form of dome-shaped forms on the advancing lee-side of linear draa (Rubin 1987a; 1987b). These two styles of stratal architectures together indicate the presence of a lee-side sinuosity on the bedforms recorded by the Auk Formation. Most linear dunes of the type envisaged for the Auk Formation possess sinuosities that migrate along the bedform crest in a downwind direction (Tsoar, 1983). The numerous erosive bounding surfaces described above are most likely to have been generated by the migration of such sinuosities (Rubin, 1987b).

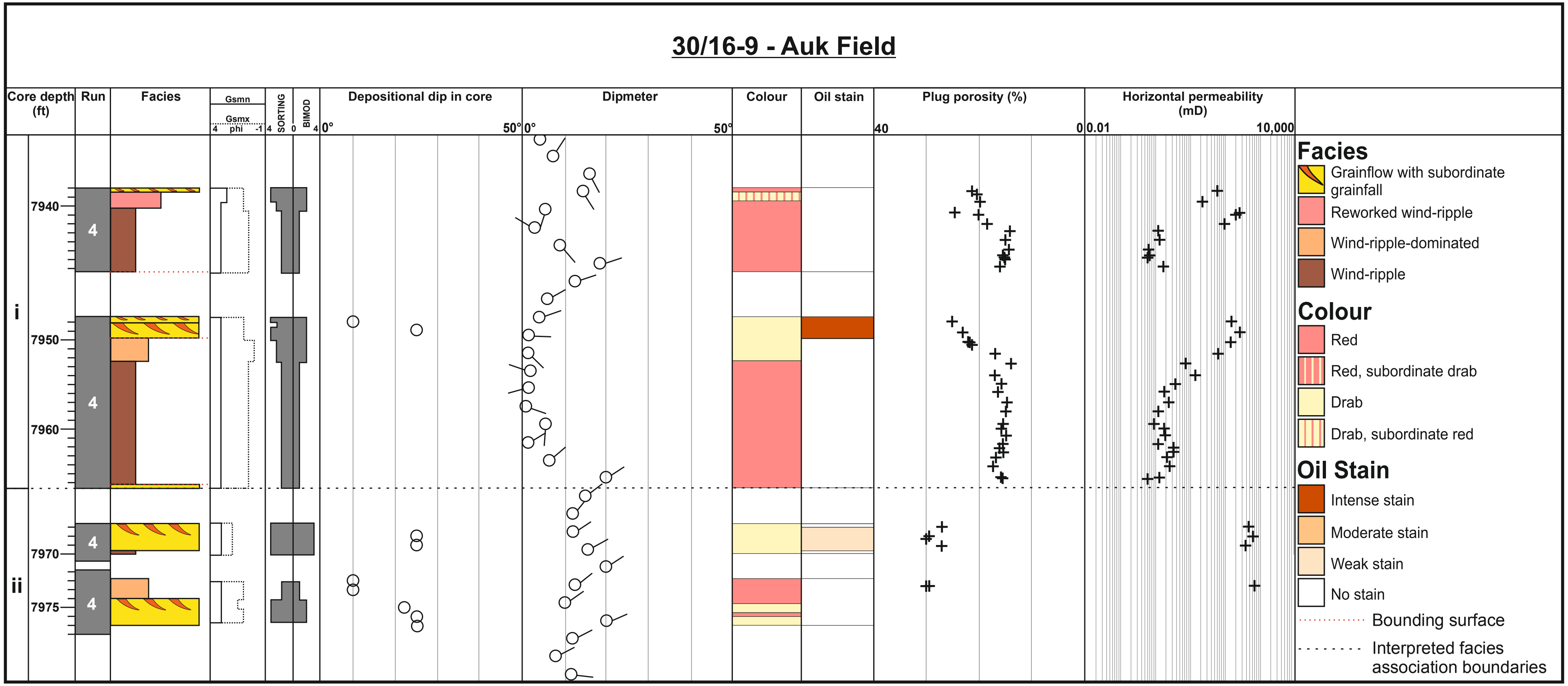

Figure 4.10. Well 30/16-9, core run 4. Red dotted lines show positions of bounding surfaces; black dotted lines separate interpreted facies association boundaries: i) interdune with isolated barchanoid dunes; ii) simple linear dune/draa aggradation unit. Original logging undertaken by Bernard Besly with contributions from Nigel Mountney; interpretation and significance of trends undertaken by Hollie Romain.

Bedform climbing – whereby successive migrating bedforms slowly migrate over and scour into one another to leave behind only the bottom-most parts of their predecessors as they do so – is the most common mechanism responsible for enabling the accumulation of thick sets of aeolian strata in the rock record (e.g. Kocurek, 1991), and is herein considered the most likely mechanism responsible for accumulation of the Auk succession. However, there are several alternative mechanisms for the accumulation and preservation of sets of aeolian strata of the type observed in the Auk Formation, including the infilling of localised accommodation space present between existing bedforms (e.g. Langford et al., 2008; Luzón et al., 2012), accumulation around relic aeolian topography (Fryberger, 1986), and exceptional bedform preservation following rapid inundation by water or other fluids (e.g. Glennie and Buller, 1983; Mountney et al., 1999; Benan and Kocurek, 2000). However the 'bedform climbing' mechanism remains the most convincing explanation for the origin of the majority of ancient preserved aeolian dune successions (Mountney, 2012) and is the most plausible explanation for the observed set architecture in the Auk Formation, given that the formation comprises multiple vertically stacked cosets of strata. Each of these is likely to represent the migration, accumulation and subsequent partial truncation of a single draa-scale bedform.

The process of bedform climb only commences once the bedforms have grown to such a size that the intervening interdune flats have been reduced to small, isolated topographic depressions (Wilson, 1971; 1972; 1973; Kocurek, 1996; Mountney, 2012). This, together with the presence of only limited occurrences of flat-lying wind-ripple interdune strata between thick cosets of cross strata, suggests the presence of only isolated interdune depressions, rather than wide, open interdune corridors in most of the Auk aeolian system.

Based on the points considered above, the bedforms represented by the deposits of the Auk Formation are interpreted to have been of a linear type due to the recorded facies arrangements outlined above, which is typical of deposition on large linear bedforms. The crest-lines are interpreted to be aligned within 30° to the resultant sand drift direction, based on the classification of Hunter et al. (1983) whereby dunes are classified as linear if their crestlines are aligned within 15° either side of perfectly parallel to the vector mean of the sand-transport direction (see Figure 2 in Hunter et al., 1983). The bedforms are also envisaged to possess along-crest migrating sinuosities, due to the occurrence of upward-steepening sets of cross-strata between upwards-shallowing sets of cross-strata (see Figure 4.9 for a typical vertical succession of the Auk Formation, showing aggradation of simple linear dune units).

4.5.3 – Compound bedforms

Observation. A small but significant proportion of what are interpreted to be linear dune flank facies (approximately 15%) show a vertical succession that diverges from the ‘simple’ vertical cycle depicted in Figure 4.9; a representative example of these is shown in Figure 4.11. Although a cyclicity similar to that seen in the ‘simple’ linear dune model (Figure 4.9) is present (upward-steepening dips, upward increase in amounts of reworking and occurrence of slipface facies), the pattern is subtly different. The basal unit in Figure 4.11, which defines a 10 m-thick coset, demonstrates the arrangement of dominantly non-reworked wind-rippled sands with an upward increase in dip, passing directly into a slipface complex developed low on the dune flank. Above this, a number of minor sets composed internally of cross beds with upward-steepening dip are present, but there is no reversion to typical interdune or dune-plinth sediments, and flat-lying depositional dips are rare.

Interpretation. Thicker units, dominated by dune flank facies, are interpreted as compound linear draa deposits, formed by the amalgamation of a number of linear dune ridges. A possible modern example from the Central Namib Desert is illustrated in Figure 4.12. Such amalgamation typically occurs in one of two settings:

Overriding of closely spaced linear bedforms. Bedforms may migrate at different speeds, resulting in one form catching another and overriding it (‘1’ in Figure 4.12). Overtaking dunes can generate bifurcations in the form of closely spaced ridges whose flanks interfinger and override one another (‘2’ in Figure 4.12).

Transverse ridges and star dunes. In situations where the wind direction is slightly more variable, bifurcations may evolve into transverse ridges that extend across the interdune area (‘3’ in Figure 4.12). The junctions of these transverse ridges with the main linear ridges may evolve into stable star dunes with three or four arms and complex patterns of reworked wind-ripple and slipface facies development (‘4’ , ‘5’ and ‘6’ in Figure 4.12). These forms allow for juxtaposition of middle/upper dune flank and slipface elements in complex geometric arrangements.

4.5.4 – Aeolian bedform scale and nature of dune flanks

Observation. The distribution of facies observed in core is typically characterised by 10 to 30 m-thick cosets of strata that are each made up of a series of nested sets, together with their delineating bounding surfaces (Figure 4.9). The facies types within these cosets commonly occur in a predictable order, such that apparently horizontal or near-horizontal, 2 to 10 m-thick packages of wind-ripple strata are overlain by low angle-inclined, 2 to 10 m-thick packages of partly reworked wind-ripple strata (Figure 4.8). Foresets within these facies types typically dip at low angles that rarely exceed 8-14°. The combined thickness of these two elements makes up the majority (up to 65%) of the preserved cosets.

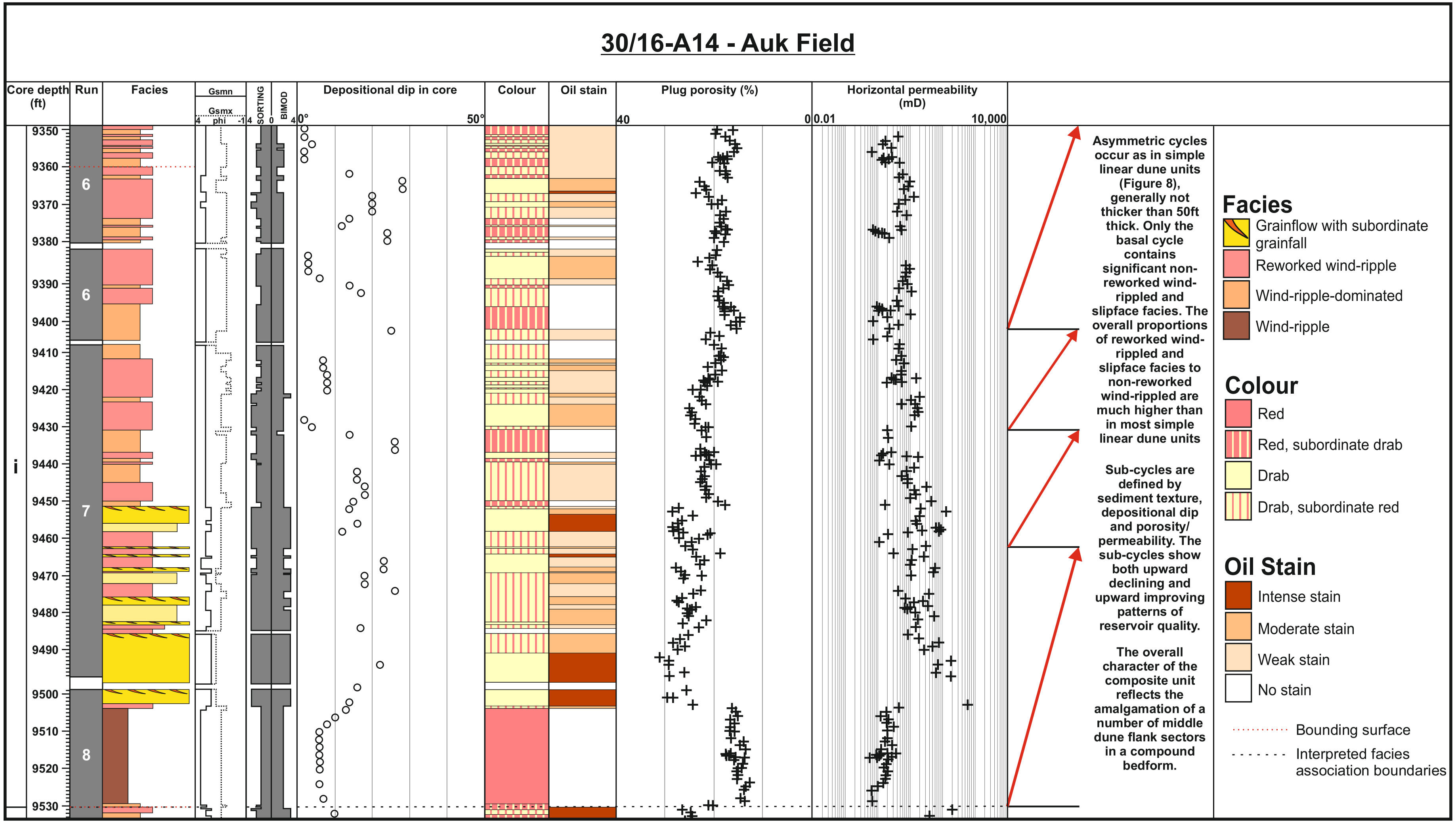

Figure 4.11. Typical vertical succession, showing aggradation of compound linear draa units, Auk Formation, Central North Sea: Well 30/16-A14, core runs 6, 7 and 8. Red dotted lines show positions of bounding surfaces; black dotted lines separate interpreted facies association boundaries: i) compound linear dune/draa aggradation unit. Original logging undertaken by Bernard Besly with contributions from Nigel Mountney; interpretation and significance of trends undertaken by Hollie Romain.

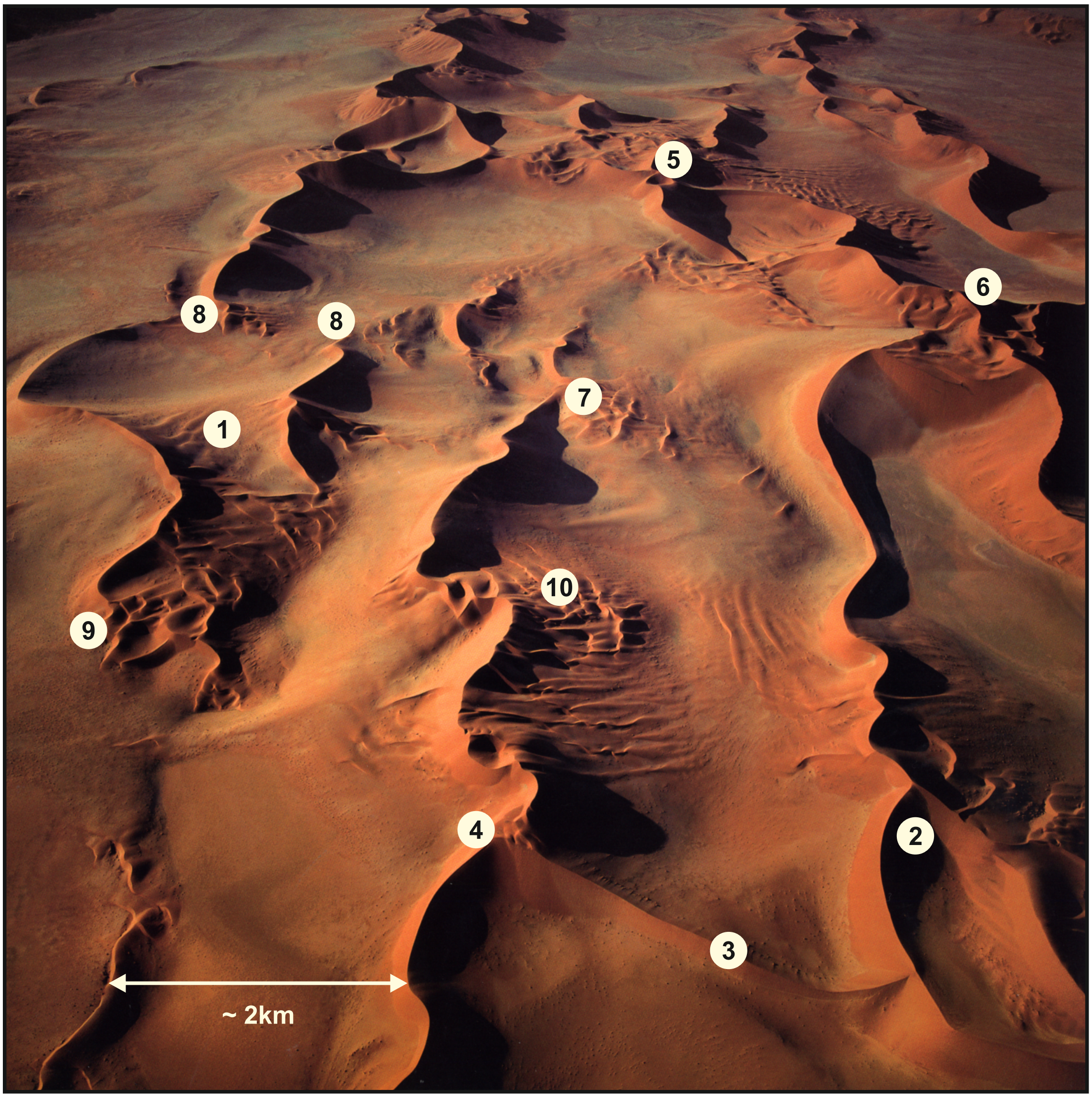

Figure 4.12. Features contributing to the formation of composite linear draa and barchanoid dune fields, Central Namib Desert, an analogue for Auk Model 6 (Chapter 5 - Figure 5.19). Sinuous-crested star and linear draa, many with opposing slipfaces developed on their upper slopes and with broad, moderate angle-inclined, wind-ripple-dominated flanks. Slipface elements generally occupy only the uppermost halves of the bedforms. Bedforms up to 180 m high. 1) Close-spaced linear dunes: right-hand ridge overriding (?) left-hand ridge; 2) Linear ridges diverging creating closely spaced ridges, one of which may override the other; 3) Ridge extending across interdune area; 4) Subordinate star elements; 5) Composite draa form created by amalgamation of linear ridges and barchanoid dune fields; 6) Large, mature star dune; 7) Barchanoid dunes migrating within interdune corridor; 8) Barchanoid dune fields associated with terminations and offsets of linear dune ridges; 9) Termination of linear ridge, with associated localised barchanoid dune field; 10) Barchanoid dunes migrating through nick points in linear dunes. Image reproduced with permission courtesy of Bernhard Edmaier.

Interpretation. Preserved 10 to 30 m-thick cosets were likely generated by large bedforms (see Romain and Mountney, 2014 for an explanation of the methodology developed for the reconstruction of original bedform height and wavelength from measurements of preserved set thickness in core or outcrop). The 2 to 10 m-thick packages of wind-ripple strata at the base of these cosets are representative of interdune-flat elements (cf. Kocurek and Nielson, 1986). For example in Figure 4.8, the section at core depth 2357 to 2349 m (7733 to 7707.5 ft) represents an interdune flat and the overlying packages of partly reworked wind-ripple strata at core depth 2332 to 2335 m (7650 to 7662 ft) are indicative of lowermost dune plinth elements (cf. Lancaster, 1981).

The facies types and distributions described above indicate that the bedforms possessed very thick, low angle-inclined toeset and plinth regions. Comparisons with modern linear dunes where this arrangement of facies has been observed (e.g. Sneh and Weissbrod, 1983; Lancaster, 1988a) suggests that the original Auk bedforms were likely to have been between 150 and 250 m high. This is based on comparisons of rates of upward-steepening of dune foresets from large modern linear bedforms, such as those in the Rub’ Al-Khali desert in Saudi Arabia (Al-Masrahy and Mountney, 2013) and the Namib Desert (Bristow et al., 2000). Data from these studies record gradual upward-steepening in the lowermost plinth areas of the bedforms, and dune heights for the Auk Formation have been reconstructed based on measured relationships documented in these published accounts. Modern linear bedforms that are 150 to 250 m high are common in the central parts of many modern dry aeolian systems, including the Central Namib Sand Sea (Breed et al., 1979). The lateral inter-bedform spacing of adjacent bedforms of this size (from crest to crest) typically varies from 1500 to 2500 m (Lancaster, 1988a; Al-Masrahy and Mountney, 2013), and this is considered to be a reasonable estimate for the Auk bedforms.

Based on the above discussion, the linear bedforms represented by the Auk succession were likely to have been large, draa-scale bedforms (Wilson, 1971; 1972), potentially with wavelengths of 1500 to 2500 m and with heights of 150 to 250 m. These ‘mega-bedforms’ tend to occur as fields of dunes only in the world’s largest ergs, where aeolian sediment supply and transport rates are high (Wilson, 1973; Mountney, 2006a). Modern linear draa that attain heights of 150 to 250 m typically have plan-form wavelengths and amplitudes of along-crest sinuosities of 500 to 1500 m and 250 to 500 m, respectively (c.f. Tsoar, 1982; Al-Masrahy and Mountney, 2013; Namib Desert – Figure 4.12), and such empirical relationships provide a method with which to estimate the form of along-crest sinuosities present on the bedforms represented by the Auk Formation.

4.5.5 – Bedform migratory behaviour

Observation. The arrangement of facies within the Auk succession and their delineation by bounding surfaces records the preservation of 15 to 30 m-thick cosets of cross strata, many with multiple internal bounding surfaces. Facies within these cosets are typically arranged into a predictable succession that indicates the preservation of the interdune flat, basal-most dune plinth and lower dune flank, with only rare occurrences where the middle and upper dune flank is preserved (Figure 4.9).

Interpretation. Preserved lithofacies successions in the Auk Formation record a stacked series of sets that likely originated via the coeval migration and accumulation of bedforms via a bedform climb mechanism. As adjacent bedforms migrated over one another at low angles, they preferentially preserved solely their lowermost parts (cf. Mountney, 2006a) and, for large linear bedforms with low-angle inclined flanks, such deposits are dominated by wind-ripple strata.

There are now many published studies that recognise that it is usual for linear aeolian dunes to undertake a minor component of transverse motion in addition to their primary along-crest component of motion (e.g. Hesp et al., 1989; Rubin, 1990). In particular, the work of Bristow et al. (2000) demonstrates unequivocally that linear dunes slowly creep laterally (relative to the primary sand migration direction) over long episodes. Rubin and Hunter (1985) and Rubin (1987a) demonstrated that it is this component of transverse motion that plays an important part in controlling the preserved architectural style of the accumulation.

The large linear bedforms responsible for generating the Auk Formation underwent accumulation that was most likely coincident with bedform migration. The primary component of sediment transport over these large linear draa was via the along-crest migration of the plan-view sinuosities (see discussion above). In addition, a secondary component of transverse bedform migration translated these bedforms sideways, but most likely at a much slower rate. The result of these two components of migration provides an approximate indication of the resultant drift direction (*sensu* Fryberger, 1979a). Results from 2 zones in the studied portion of the Auk Formation, with zones defined as groups of linear dune growth cycles determined by bounding surfaces in the wells, formed by dune migration are shown in Figure 4.13. The dip-azimuths in Dune Cycle Zone 20-25 are between 050° and 120°, with the resultant drift direction between NE and ESE (Figure 4.13a). The dominant dip-azimuths for Dune Cycle Zone 40-50 are towards ENE and SSW (Figure 4.13b).

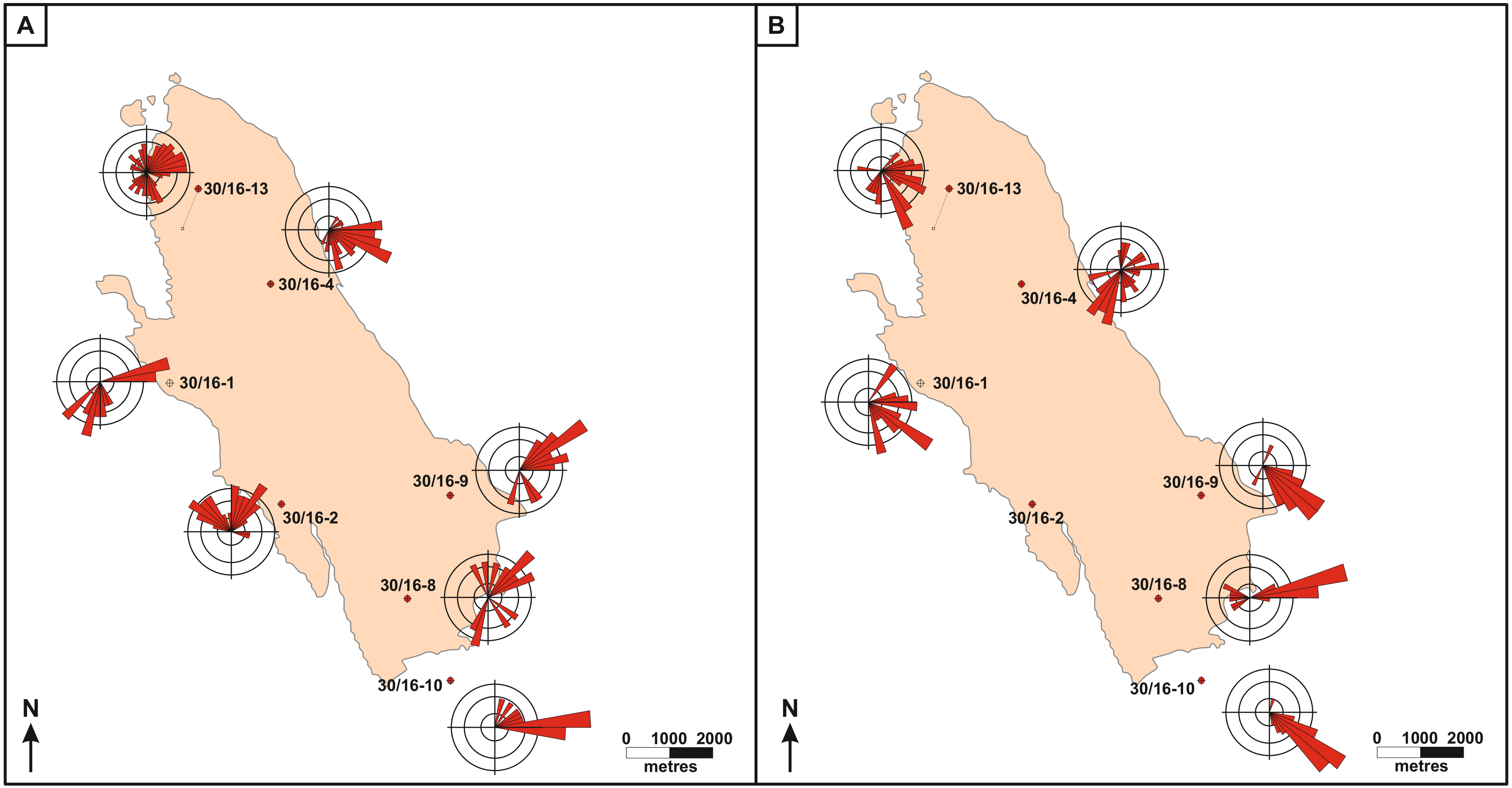

Figure 4.13. Grouped dipmeter dip-azimuth data for well penetrations in the Auk Formation. Red well symbol indicate cored wells: a) Dune Cycle Zone 20-25 – dip-azimuths dominantly between 050° and 120°, dominant wind direction WSW – ENE; b) Dune Cycle Zone 40-50 – dominant dip-azimuths between dips to ENE and SSW, wind direction between NW – SE and NE – SW. Original foreset dip-azimuth data obtained by Bernard Besly with contributions from Nigel Mountney; interpretation and significance of trends undertaken by Hollie Romain.

4.5.6 – Detailed morphology and style of behaviour of the bedforms responsible for generating the bed-sets preserved in Auk

Although the gross morphology and temporal behaviour of the bedforms recorded in the Auk Formation has been outlined above, there exist several examples of facies distributions in the Auk cores that cannot be readily explained by a relatively simple morphology and migration style (Figure 4.14): more complex arrangements of bedforms need to be invoked to account for such stratigraphic expressions. It is likely that a range of both simple and more complex bedform arrangements were variously responsible for the evolution of the Auk succession and that these types are likely to have developed and operated coevally and in close proximity to one another within the developing dune field.

4.5.6.1 – Morphology of interdune flats

Observation. Although the original morphology of interdune flats cannot be measured directly from the primary data recovered from the Auk Formation, general comparisons can be made between the interpretations of bedform type made above and the morphological relationships observed in analogous modern dune field systems. One of the closest modern analogues envisaged for the Auk Formation is the part of the Rub’ Al-Khali studied by Al-Masrahy and Mountney (2013). Based on comparisons between dunes and interdunes in this modern system, interdune flat areas between neighbouring linear draa represented by accumulations of the Auk Formation would have been best developed where two re-entrants in neighbouring bedforms were aligned adjacent to each other. Heights inferred for the Auk bedforms were 150 to 250 m (Section 4.5.4), as reconstructed from empirical relationships noted from modern dunes in the Rub’ Al-Khali and the Namib Desert. Given the variability in the foreset dip-azimuths and from the presence of inclined erosional bounding surfaces that represent scour surfaces in the Auk cosets, it is envisaged that the bedforms responsible for generating the preserved architecture must have had sinuous crestlines. It therefore follows that the interdunes must have varied in width and may have formed isolated elliptical flat areas between the major dunes.

Interpretation. For bedforms of the height envisaged for the Auk Formation, interdune flats may have been 500 to 1000 m wide, based on empirical relationships demonstrated in Al-Masrahy and Mountney (2013) for data from the Rub’ Al-Khali. By contrast, where two spurs (protruding ridges) present in adjacent bedforms were aligned with one another, interdune flats would have potentially been eliminated completely. In such circumstances, open elongate interdune corridors would have been replaced by elliptical-shaped enclosed interdune flats approximately 750 to 1500 m in length, in a direction parallel to the crests of the adjacent linear draa. The surface of interdune areas developed between the major linear bedforms was likely to have been covered largely by sheets of wind-rippled sand.

4.5.6.2 – Superimposed barchanoid dune fields

Observation. (i) In some parts of the Auk succession, stacked 1 to 5 m-thick sets of grainflow facies are preserved (Figure 4.10) and associated with thicker intervals of wind-ripple strata and reworked wind-ripple strata; (ii) in other rarer cases, thin sets of grainflow cross strata are found *within* larger cosets interpreted to be the deposits of large linear bedforms. In these cases, the cross strata of grainflow origin are not necessarily associated with reworked wind-ripple facies (Figure 4.15).

Interpretation. (i) The stacked sets of grainflow facies described above are interpreted to be representative of accumulation via the migration and climb of relatively small and simple barchanoid dunes. The thicker intervals of wind-ripple and reworked wind-ripple strata represent deposits of the bottom-most parts of large linear dunes. This implies that fields of small barchanoid dunes occupied some of the interdune depressions between neighbouring linear bedforms. Barchanoid dune fields lying between larger linear bedforms are common in modern dry aeolian systems, including many parts of the Central Namib Sand Sea (McKee, 1982; Figure 4.12); (ii) the presence of thin sets of grainflow cross strata within larger cosets implies that such grainflow-dominated units are the product of superimposed dunes developed on the lower or middle flanks of the larger bedforms, and that the bounding surfaces which delineate these units are therefore superimposition surfaces (*sensu* Kocurek, 1991). Parts of the aeolian system were therefore likely characterised by superimposed dunes (possibly transverse, barchanoid in form) which migrated obliquely over the middle flanks of the large, non-slipfaced linear bedforms in response to along-slope directed secondary winds which may have been deflected by the larger bedforms (cf. Mountney et al., 1999).

Figure 4.14. Auk Formation, Central North Sea: Well 30/16-2, core run 7 - 7756.5 ft - 7763 ft. 1-5 metre sets of simple grainflow facies, representative of accumulation of small barchanoid dunes, occurring between intervals of wind-ripple strata. Contains British Geological Survey materials © NERC 2014.

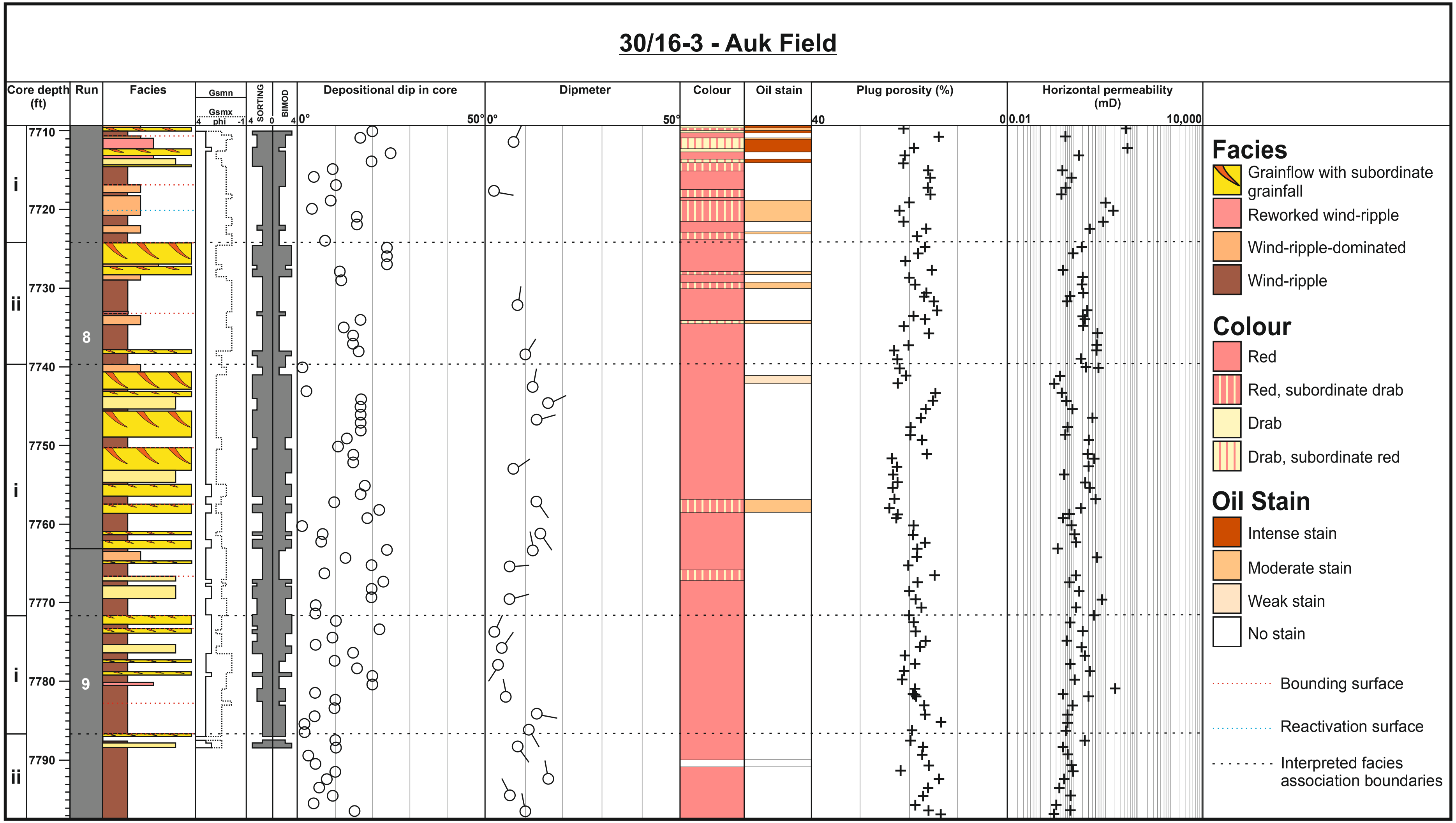

Figure 4.15. Auk Formation, Central North Sea: Well 30/16-3, core runs 8 and 9. Red dotted lines show positions of bounding surfaces; blue dotted lines mark positions of reactivation surfaces; black dotted lines separate interpreted facies association boundaries: i) simple linear dune/draa aggradation unit with superimposed dunes; ii) simple linear dune/draa aggradation unit. Original logging undertaken by Bernard Besly with contributions from Nigel Mountney; interpretation and significance of trends undertaken by Hollie Romain.

4.5.7 – The nature of the palaeowind responsible for generating the bedforms preserved in Auk (variability, seasonality, resultant direction)

Observation. The broad but unimodal spread of foreset azimuths present in the Auk succession (Figure 6 in Heward, 1991; Figure 4.13) is consistent with the oblique migration of large linear dunes and their preservation through bedform climbing (Rubin and Hunter, 1985; Rubin, 1987a) – see discussion above and Bristow et al. (2000) for further discussion.

Interpretation. The azimuth of maximum foreset dip records the approximate direction of resultant sand drift, but not the trend of the bedform crest-lines (DeCelles et al., 1983; Rubin and Hunter, 1983). Most large linear dunes develop in response to the convergence of two oblique wind directions, with alternations of wind direction typically occurring on a seasonal basis (e.g. Lancaster, 1983; McKee, 1982). The trend of the bedform crest-line will not usually be parallel to either of these wind directions and neither will the mean azimuth of the preserved foresets (Rubin and Hunter, 1987) because both wind directions are operating coevally over the entire depositional episode.

The moderate to relatively broad range of foreset azimuths present in the Auk succession could be explained by a number of factors: (i) the bedforms shifted their migration trajectory over time; (ii) several contemporaneous bedforms had slightly different orientations; (iii) the bedforms had significantly curved crestlines, parts of which faced in the direction of the resultant drift direction. The presence of migrating scour pits in the form of concave-shaped re-entrants seen in plan-view would generate a series of erosional bounding surfaces aligned approximately in the direction of the resultant drift direction (Rubin and Carter, 2006; Rubin and Hunter, 1983). In the case of the Auk Formation, it is likely that the range of foreset azimuths seen in the dataset originated from a combination of the scenarios listed above and likely in response to linear dunes that undertook a component of transverse motion (cf. Bristow et al., 2000).

4.6 – Conclusions

The studied interval of the Auk Formation represents the accumulated deposits of a series of linear aeolian dunes and draa that were present within a large dry aeolian dune-field system. The following conclusions relating to the reconstruction of original bedform type, size and style of migratory behaviour have been reached through a detailed core and well log analysis coupled with comparison to analogous outcropping successions and modern dune systems: (i) the facies types noted from core data in the Auk Formation (wind-ripple, reworked wind-ripple, grainflow and grainfall) represent aeolian sedimentation on a predominantly dry substrate; (ii) the predominance of wind-ripple and reworked wind-ripple strata in the succession, even in steeply-dipping deposits that have clearly been formed in an elevated position on a major bedform (e.g. wind-ripple-dominated sections with inclinations of 10° to 20°) indicates deposition typical of large linear bedforms, with the lower and middle flanks of these being preserved; (iii) the upward-steepening of cross strata indicates a lee-side sinuosity on the Auk bedforms; (iv) 15% of the linear dune flank facies do not show an upward reversion to deposits interpreted to be interdune or dune plinth sediments within a preserved coset, which implies that there are instances of compound linear draa within the Auk succession; (v) the occurrence of thick packages of wind-ripple and wind-ripple-dominated strata which contribute to up to 65% of the preserved cosets in the Auk Formation demonstrates that the bedforms had very thick low-angle-inclined plinths, and based on empirical relationships estimated to have been between 150-250 m high with wavelengths of 1500-2500 m and originated via a bedform climbing mechanism that resulted in preferential preservation of only their lowermost parts; (vi) the occurrence of 1-5 m-thick stacked sets of grainflow strata in some cores records the presence of small barchanoid dunes, either occupying interdune depressions where the grainflow units are associated with thick wind-ripple and reworked wind-ripple strata, or superimposed on the lower or middle flanks of linear draa where the grainflow units are found within larger cosets that are themselves interpreted to be deposits of these linear draa; (vii) the Auk Formation exhibits a broad but unimodal spread of foreset azimuths which is most likely in response to the linear dunes in Auk undertaking a minor component of transverse motion.

There are very few published accounts of ancient linear dune successions, yet linear dunes represent over fifty percent of the dune types present in modern dune fields (Rubin and Hunter, 1985; Rodríguez-López et al., 2014). Given that linear aeolian dune systems can potentially accumulate via bedform climbing or other mechanisms, such system types must be significantly under recognised in the ancient rock record. This study therefore represents a valuable case study for a rarely recognised but important type of aeolian dune system.

Chapter 5 – Modelling three-dimensional lithofacies distributions in subsurface aeolian successions: Permian Auk Formation, Central North Sea, UK

5.1 – Introduction

For aeolian systems that are known only from the subsurface, the data available for their reconstruction is limited chiefly to one-dimensional core data and well logs. In order to adequately model the geological complexities and inherent lithological heterogeneity present in such successions, quantitative estimates of the geometry of architectural elements and their internal facies compositions need to be made. Thus, a technique is required for the reconstruction of three-dimensional aeolian architecture from one-dimensional core data that typically provide information on only the following attributes, as discussed in Section 2.2: (i) preserved set thickness, which for bedsets that originated via bedform climbing is a function of both original bedform wavelength and the angle at which the bedforms climbed over one another as accumulation proceeded (Mountney and Howell, 2000); (ii) the thickness of grainflow units arising from individual sandflow avalanches, primarily a function of the length of the lee slope of the original bedform down which avalanching grains of sand cascaded to generate the deposit (Kocurek and Dott, 1981; Howell and Mountney, 2001); (iii) the shape of dune toesets and their style of interaction with deposits of underlying interdune elements, an indicator of the style of advance of the original bedform over a neighbouring interdune area (e.g. Pulvertaft, 1985; Mountney and Thompson, 2002); (iv) the rate of upward-steepening of foresets within a set, an indicator of the profile of the lower flanks of the original bedform (Rubin, 1987a); (v) the distribution of primary lithofacies (grainflow, wind-ripple and grainfall) within sets, a function of processes that operated on the lee slope of the original bedform (Hunter 1977a; 1977b; Kocurek and Dott, 1981); and (vi) the distribution of the occurrence of reactivation surfaces within cosets, an indicator of the periodicity with which the original bedforms undertook changes in lee-slope steepness, asymmetry, or migration direction (Rubin, 1987a; Fryberger, 1993).

A recent method has been proposed to reconstruct aeolian dune architecture from one-dimensional core data (Romain and Mountney, 2014; Chapter 2), and this forms the basis for palaeoenvironmental reconstruction of aeolian system type from one-dimensional core data. This approach to the palaeoenvironmental reconstruction of aeolian dune and interdune successions has recently been applied to a subsurface succession - the Permian Auk Formation (Chapter 4); thus, a reconstruction of aeolian dune type, size and style of migratory behaviour of the Auk Formation has been undertaken, and is summarised briefly in Section 5.4. To characterise the expected three-dimensional sedimentary architecture and lithofacies distribution, this study builds on the palaeoenvironmental reconstruction of the aeolian system represented by the Auk Formation (Chapter 4) by applying the modelling concepts introduced in Chapter 3 to this subsurface aeolian succession.

From an applied standpoint, difficulties arise when attempting to estimate volumetric sand content and regional porosity-permeability distributions for aeolian reservoirs, where the geometries of the various dune, interdune and extradune elements present within the overall three-dimensional rock volume are poorly constrained in the subsurface (Nagtegaal, 1979; Heward, 1991). The aim of this study is to introduce a forward modelling approach that sets out a methodology by which predictions can be made regarding the three-dimensional distribution of lithofacies in ancient aeolian dune successions. The approach is based on analysis of sedimentological features that are observable in core, including aeolian lithofacies and their arrangement into predictable packages that occur nested within sets of cosets of strata delimited by a variety of types of bounding surface and sets. From this, scenarios that depict the spatial arrangement of aeolian bedforms of differing morphological types and their migratory behaviour over time have been modelled (cf. Rubin, 1987a; Rubin and Carter, 2006). This approach enables reconstruction of the expected three-dimensional spatial arrangement of sets and cosets of strata that are themselves characterised internally by various arrangements of packages of primary lithofacies.

This method has been applied for the palaeogeographic and palaeomorphological reconstruction of accumulated aeolian deposits of the Permian Auk Formation (Rotliegend Group), Central North Sea to demonstrate the applicability of the modelling technique to a preserved aeolian succession known only from the subsurface and for which only one-dimensional data are available. Six model reconstructions depicting three-dimensional facies and architectural-element distributions have been proposed based on a range of interpretations of subsurface data available from core and well logs of the Auk Field reservoir that was formally operated by Shell, and which is currently operated by Talisman Energy (Prosser and Maskall, 1993; Follows, 1997; Trewin et al., 2003).

The six architectural models developed in this study represent interpretations of data available from different parts of the preserved succession: the first presents the simplest palaeoenvironmental reconstruction considered plausible for the given data set; each successive model incorporates additional detail based on complexities observed in the primary dataset coupled with the integration of data derived from a broader understanding of how aeolian dune systems are arranged and migrate over time to accumulate a stratigraphic record. The analysis has involved a re-interpretation of open-release well log and core and image-log and dipmeter data from the subsurface, combined with comparisons to potential modern and ancient outcrop analogue systems (Chapter 4).

There is a growing need to model the stratigraphic heterogeneity of aeolian reservoir successions in greater detail if recovery of reserves remaining in existing fields is to be maximised (Rodríguez-López et al., 2014). This is especially true in oil reservoirs like Auk, where the increased viscosity of the hydrocarbons means that fluid flow is especially sensitive to the arrangement of lithofacies packages. Recent discoveries of large oil reserves hosted in aeolian reservoirs such as the Jurassic Norphlet Sandstone of the Gulf of Mexico (Mancini et al., 1985) demonstrate the need to better understand stratigraphic heterogeneity in these types of successions.

5.2 – Geological setting

The Permian Auk Formation of the Rotliegend Group is present in the subsurface around the southern edge of the North Permian Basin in the UK sector of the Central North Sea (Smith and Taylor, 1992). The Rotliegend Group, of which the Auk Formation is commonly, yet informally, called the ‘Upper Rotliegend’ (Glennie, 2002), is a continental red-bed succession known from the subsurface, which underwent initial accumulation in the Early Permian (Glennie et al., 2003). The best-known and most intensely studied part of the Auk Formation is the Auk Field, an oil reservoir that produces primarily from aeolian sandstones but which additionally has historically produced from overlying evaporite layers of the Zechstein Group (Buchanan and Hoogteyling, 1979). In the Auk Field, the Rotliegend Group is up to 275 m thick (Trewin et al., 2003) and is capped at its top by a succession of non-reddened dune sandstones named the Weissliegend that show evidence for aqueous reworking (Glennie and Buller, 1983).

5.3 – Data and methods

Primary subsurface data (14 cores and well logs totalling 1139.83 m in length) from the Auk Formation were logged as part of a previous study by Bernard Besly, with contributions from Nigel Mountney, to record the detailed sedimentology of the succession (as previously discussed in Chapter 4). The interpretations presented in Chapter 4 have been the focus of a detailed study for the reconstruction of the Auk dune type (Chapter 4). The reconstructions developed in Chapter 4 are used as the basis for constraining the six forward stratigraphic models outlined here.

Geocellular models depicting preserved bed-set architectures and reconstructed bedform morphologies for the Auk Formation have been generated using the open-source 'Bedforms' software (Rubin, 1987a; Rubin and Carter, 2006). The software predicts the three-dimensional pattern of cross-bedding and erosional bounding surfaces that are generated by the migration and climb of a series of bedforms under a specified set of conditions. The style of migration, accumulation and preservation of dunes and interdunes within aeolian systems has been simulated by tracking the migration of bedforms over a series of time steps and by applying a set of rules to determine how older strata are truncated by younger strata. As discussed in Chapter 3, most common types of aeolian bedforms can be simulated and the effects of changes in bedform morphology (steepness, asymmetry, style of along-crest variability), migration speed, migration direction and rate of accumulation have been assessed.

The resultant architecture from a series of model runs is compared to the sedimentary style observed in the primary data set (e.g. preserved set and coset thickness, bounding surface arrangements, range of foreset dip-azimuths). Input parameters are then adjusted and the model re-run until an appropriate match to the primary data is achieved. The iterative best-fit procedure adopted is a limitation, as it could lead to multiple possible final configurations where there are non-unique solutions, as is common in nature. Once the architectural framework of the succession has been modelled, specific aeolian facies are mapped onto the preserved set architectures, based on distributions observed in core data and augmented by quantitative assessments of common styles of facies distributions known from a variety of ancient analogous outcrop successions and modern dune systems. The geometry, scale and degree of inter-connectivity of the various architectural elements and the facies that they contain can then be assessed and used to characterise subsurface three-dimensional sedimentary architecture.

Spatial and temporal units within the models produced by the software are dimensionless (see Section 3.3), which enables the modelled output to be retrospectively scaled according to dimensional data present in the primary dataset (see Section 5.12). For the purposes of modelling, a modelling co-ordinate system is used for tracking the orientation and alignment of geobodies: due north (000 degrees) is the direction of transverse aeolian bedform migration (i.e. normal to the trend of the crestline of the major aeolian bedforms being modelled) and 090 degrees is taken as the along-crest component of motion in a direction clockwise from the arbitrary north. Angular directions in the model are expressed in degrees (0-360). Model outputs have been retrospectively re-oriented by matching to directional data present in the primary subsurface dataset (e.g. dip-azimuth data derived from core; Section 5.12). Orientations used in the modelling process described here refer to the modelling co-ordinate system unless otherwise stated.

The architectural frameworks that arise as a direct output of the modelling have been populated with specific facies through reference to observations made from cores and well logs of the Auk Field (Chapter 4), and with open-release core data obtainable via the British Geological Survey (http://www.bgs.ac.uk). Primary aeolian lithofacies types have been determined through observation of cores: non-reworked wind-ripple, reworked wind-ripple, grainflow and grainfall facies are all readily identifiable from core (Figure 4.7). A summary of the observed facies types with their interpreted reservoir properties, and a key to the associated colours used in the forward modelling process is shown in Figure 5.1.

Facies descriptions used in this study are not based solely on discrete and individual facies types; additionally they incorporate combinations of two or more basic facies types in varying proportions: *grainflow-dominated* units are composed of >50% grainflow facies but additionally incorporate a secondary component of reworked wind-rippled strata; *wind-ripple-dominated* units are composed of >50% wind-rippled facies but additionally incorporate a minor component of reworked wind-rippled strata.

From an applied standpoint, in hydrocarbon plays it is preferential to target areas with a high proportion of grainflow and grainflow-dominated stratal packages composed of well-sorted, loosely-packed sandstone with permeabilities that are typically two to three (or more) orders of magnitude greater than packages of predominantly grainfall and wind-ripple strata that dominate in other aeolian elements (Chandler et al., 1989; Prosser and Maskall, 1993; Howell and Mountney, 2001; Romain and Mountney, 2014). Thus, the distribution of primary lithofacies serves as an indicator of general reservoir quality (Figure 5.1): prediction of the three-dimensional distribution of grainflow and grainflow-dominated packages of strata serves as the basis for developing aeolian reservoir models, whereby such facies packages typically represent effective net reservoir (Weber, 1987; Howell and Mountney, 2001).

Key	Facies	Observations from Auk Formation	Reservoir properties
🟫	**Wind-ripple facies**	mm-laminated sandstone; grain size ranging from very fine to medium or coarse sand; characterised by strong bimodality (bimodal framework and segregation into laminae of contrasting grain size); locally contains abundant pinstripe laminae of very fine sandstone formed by grainfall; often contains discrete lenses of coarser-grained sand representing segregation of coarser grains on wind ripple crests; in almost all cases red pigmented; depositional dip ranges from 0° to 26°.	Average porosities of 13% (range 9-18%) and average permeabilities of 0.24mD (range 0.055-2mD) for samples measured in interdune sections (Follows, 1997). However, Prosser and Maskall (1993) document wind-rippled sandstone deposits from elsewhere in the Auk Formation characterised by permeabilities that are considerably higher: average of 70mD and a range of 11-192mD.
🟧	**Wind-ripple-dominated facies**	Composed of >50% wind-rippled facies as above, but additionally incorporate a minor component of reworked wind-rippled strata (see below)	
🟥	**Reworked wind-ripple facies**	mm-laminated sandstone as above, but containing discrete reworked laminae of better sorted sand that either has bimodality only between laminae or is unimodal; dips range from 0° to 26°, but are usually greater than 7°; where occurring above the OWC the reworked laminae may be bleached to a drab colour, and may be oil-stained.	Samples measured in dune-apron settings from the Auk Formation have average porosities of 14% (range 12-18%) and average permeabilities of 0.65mD (range 0.6-6mD) (Follows, 1997). The degree of disparity in directional permeability is highly variable in wind-ripple deposits because of the range of textural characteristics they can possess (Lindquist, 1988).
🟨	**Grainflow facies**	cm-laminated fine to medium grained sandstone, usually having a massive appearance and looser grain packing structure than associated wind-rippled facies; depositional dips are usually greater than 20°; where occurring above the OWC this facies is almost always bleached to a drab colour and oilstained.	Average porosity of 20%, with a range from 14-27% (Follows, 1997). The average permeability for grainflow deposits is 50mD, ranging between 0.3-370mD (Follows, 1997). However, Prosser and Maskall (1993) have recorded permeability values for grainflow facies present elsewhere in the Auk Formation that are significantly higher, with an average of 403mD, ranging from 13-960mD.
🟨	**Grainflow-dominated facies**	Composed of >50% grainflow facies as above, but additionally incorporate a secondary component of reworked wind-rippled strata	
🟧	**Grainfall facies**	mm-scale laminae of very fine grained sandstone, occurring as pinstripe laminae in two distinct settings: a) as laminae interbedded with wind-ripple laminated sand, in which case the facies is usually dark red in colour; and b) as laminae separating successive grainflow deposits, in which case the facies is usually bleached but not oil-stained, if occurring above the OWC.	Grainfall facies have low recorded porosity and permeability values (Prosser and Maskall, 1993). Grainfall facies have been grouped with wind-ripple facies in porosity versus permeability plots for the Auk Formation by Prosser and Maskall (1993), and are considered unfavourable.

Figure 5.1. Facies descriptions and reservoir properties for the Auk Formation succession.

5.4 – Morphology and temporal behaviour of the Auk bedforms

Reconstruction of the type, morphology and temporal behaviour of the Auk bedforms used to construct the models in this study has been achieved by a re-interpretation of well log and core data for the Auk Field. A detailed reconstruction of the palaeoenvironment represented by the deposits of the Auk Formation is discussed in detail in Chapter 4, therefore only a summary is presented here. The six models presented in this study represent interpretations of the data available from different parts of the preserved succession.

For the interval studied, the Auk Formation represents the preserved remnant of an exclusively dry aeolian system (*sensu* Kocurek and Havholm, 1993), which was not subject to contact with the palaeo-water table or its capillary fringe (cf. Mountney, 2006a). The facies types recognised in the studied core intervals are dominated by grainfall, grainflow, wind-ripple and reworked wind-ripple strata (Figure 4.7) and such types are exclusively produced by aeolian sedimentation on a dry substrate. The predominance of preserved wind-ripple strata of various types (85% in the cores studied for the Auk Formation – Chapter 4 – Figure 4.8) is common in linear bedforms (e.g. Tsoar, 1982; Bristow et al., 2000), especially from the lower and middle flanks of such linear bedforms (Lancaster, 1981; Livingstone, 1987; 1989a; McKee, 1982; McKee and Tibbitts, 1964; Sneh and Weissbrod, 1983). In the Auk Formation, repetitive ‘cycles’ are observed in which flat-lying wind-rippled strata pass gradually upwards into strata that show a progressive upward increase in depositional dip, with an upward increase in the proportion of reworked wind-rippled facies (Figure 4.9). Grainflow-generated avalanche strata are generally only developed in the upper, most steeply dipping parts of such ‘cycles’. Although there is no explicit published description of such a cycle from an ancient outcropping aeolian deposit, this pattern exactly replicates the pattern of facies and dip development on modern linear dunes, which tend to be characterised by large, low to moderate angle-inclined, wind-ripple-dominated lower flanks that gradually steepen in an upslope direction before merging with grainflow-dominated avalanche strata on the middle and upper parts of the bedform slope.

The interpretation of linear bedforms outlined here, and in Chapter 4, is contrary to that of Heward (1991) who envisaged deposition by transverse compound draa with intermittent slipface development, due to the limited spread of slipface orientations per stratigraphic interval. However, there are now many published studies that recognise that it is usual for linear aeolian dunes to undertake a minor component of transverse motion in addition to their primary along-crest component of motion (e.g. Hesp et al., 1989; Rubin, 1990; Bristow et al., 2000). Rubin and Hunter (1985) and Rubin (1987a) demonstrated that it is this component of transverse motion that plays an important part in controlling the preserved architectural style of the accumulation, and that ancient linear dunes can preserve successions which are almost identical to those preserved by transverse bedforms.

A characteristic trait of deposits of the Auk Formation is the occurrence of upward-steepening sets of cross-strata between upwards-shallowing sets of cross-strata (Figure 4.10). These features demonstrate that the large linear bedforms that gave rise to the Auk Formation possessed along-crest migrating sinuosities (Chapter 4). This simple bedform morphology is considered in Auk Model 1 (Section 5.6).

In some parts of the studied section, there exist several examples of facies distributions which cannot be explained by the simple morphology and migration style discussed above. For example, in places stacked 1-5 m-thick sets of grainflow facies are preserved *within* larger cosets interpreted to be the deposits of large linear bedforms (Figure 4.15) and in successions associated with thicker intervals of wind-ripple strata and reworked wind-ripple strata. The stacked sets of grainflow facies are interpreted to be representative of the accumulation of relatively small and simple barchanoid dunes, with the wind-ripple facies representing the deposits of the bottom-most part of the linear draa (Chapter 4). Such smaller barchanoid dune fields likely occupied interdune depressions between neighbouring major linear draa (megadunes), and some smaller dunes likely developed in locations superimposed on the lower or middle flanks of the parent bedforms (Chapter 4). Barchanoid dune fields lying between larger linear bedforms are common in dry aeolian systems, including many parts of the Central Namib Sand Sea (McKee, 1982; Figure 4.12). This complex bedform morphology is considered in Auk Model 6 (Section 5.11).

5.5 – Modelling aeolian stratigraphic complexity in the Auk Formation

Six forward stratigraphic models with which to account for the geometry and stratigraphic architecture of units composed of commonly occurring assemblages of lithofacies have been developed in this study. They characterise the predicted three-dimensional distribution of architectural units within the Auk Formation and therefore reconstruct the likely palaeoenvironment of deposition and three-dimensional preserved set architecture to a level of detail that has not hitherto been attempted. Reconstruction of the expected geometry, scale and orientation of sedimentary architectural elements enables the identification of lithological heterogeneity within the succession and prediction of the connectivity of net reservoir units (Figure 5.2). Measurements used for input into the modelling process (see Rubin and Carter, 2006) were derived from both direct observation of core and well log data, supplemented by observation of modern analogous dune fields as explained above (Figure 5.3).

6 models are presented in this study which account for the variability of the Auk Formation succession, as discussed in Chapter 4. Auk Models 1 – 5 (Figures 5.4 – 5.18) present results for the migration and accumulation of simple linear dunes with intervening dry interdunes that are considered likely to account for much of the stratigraphy preserved in the Auk Formation. Auk Model 6 (Figures 5.19 – 5.21) presents results for the migration and accumulation of complex linear draa that support superimposed barchanoid dunes on their lower flanks and within intervening interdraa depressions (see Section 4.5.6.2 and Figure 4.15). All models provide quantitative estimates of likely three-dimensional sand-body geometries. The equivocal nature of the data means that, in most cases, a range of probable dimensions is proposed. The models serve as the basis for a palaeoenvironmental reconstruction, but from an applied perspective they provide hard data that constrain static and dynamic reservoir models.

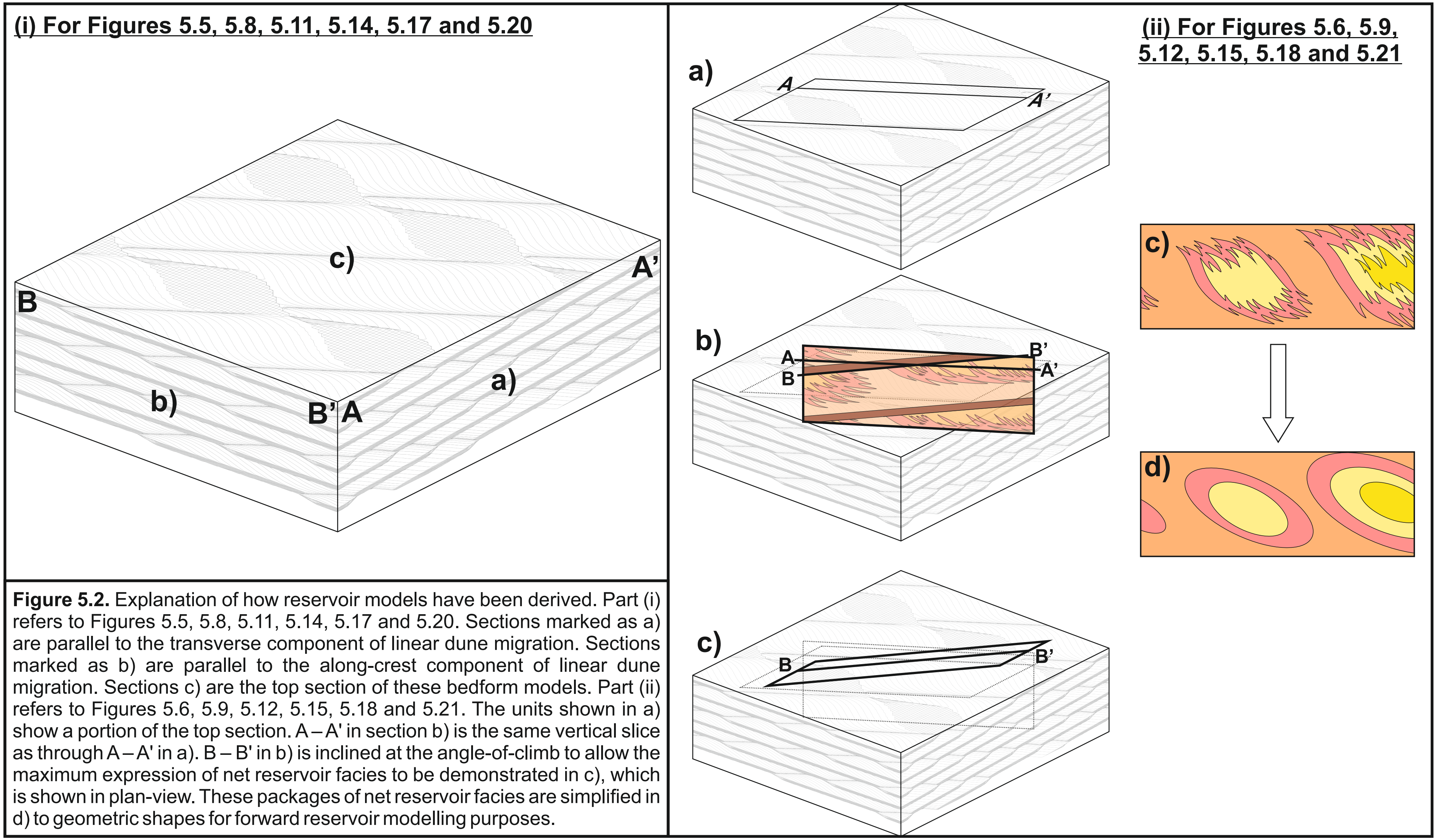

(i) For Figures 5.5, 5.8, 5.11, 5.14, 5.17 and 5.20

(ii) For Figures 5.6, 5.9, 5.12, 5.15, 5.18 and 5.21

Figure 5.2. Explanation of how reservoir models have been derived. Part (i) refers to Figures 5.5, 5.8, 5.11, 5.14, 5.17 and 5.20. Sections marked as a) are parallel to the transverse component of linear dune migration. Sections marked as b) are parallel to the along-crest component of linear dune migration. Sections c) are the top section of these bedform models. Part (ii) refers to Figures 5.6, 5.9, 5.12, 5.15, 5.18 and 5.21. The units shown in a) show a portion of the top section. A – A' in section b) is the same vertical slice as through A – A' in a). B – B' in b) is inclined at the angle-of-climb to allow the maximum expression of net reservoir facies to be demonstrated in c), which is shown in plan-view. These packages of net reservoir facies are simplified in d) to geometric shapes for forward reservoir modelling purposes.

Model # Input variable	Auk 1	Auk 2	Auk 3	Auk 4	Auk 5	Auk 6
Wavelength of bedforms in first set	100.0	100.0	100.0	100.0	100.0	75.0
Bedform phase (°)	90.0	90.0	90.0	90.0	90.0	180.0
Mean asymmetry	0.0	0.0	0.0	0.0	0.0	0.0
Amplitude of asymmetry cycle	0.0	0.0	0.0	0.0	0.0	0.0
Period of asymmetry cycle	1.0	1.0	1.0	1.0	1.0	0.0
Phase of asymmetry cycle	0.0	0.0	0.0	0.0	0.0	0.0
Mean bedform steepness	1.0	1.0	1.0	1.0	1.0	1.0
Amplitude of steepness cycle	0.0	0.0	0.0	0.0	0.0	0.0
Period of steepness cycle	1.0	1.0	1.0	1.0	1.0	1.0
Phase of steepness cycle	0.0	0.0	0.0	0.0	0.0	0.0
Wavelength of first set of plan-form sinuosities	50.0	50.0	50.0	50.0	50.0	50.0
Amplitude of first set of sinuosities	5.0	5.0	5.0	5.0	5.0	5.0
Phase of first set of sinuosities	0.0	0.0	0.0	0.0	0.0	90.0
Migration speed of first set of sinuosities	2.0	4.0	4.0	4.0	4.0	4.0
Wavelength of second set of plan-form sinuosities	0.0	0.0	0.0	0.0	0.0	0.0
Amplitude of second set of sinuosities	2.0	2.0	2.0	0.0	0.0	0.0
Phase of second set of sinuosities	270.0	270.0	270.0	0.0	0.0	0.0
Migration speed of second set of sinuosities	1.0	1.0	1.0	4.0	4.0	0.0
Migration direction of bedform	0.0	0.0	0.0	0.0	0.0	0.0
Mean migration speed of bedform	1.0	1.0	1.0	1.0	1.0	1.0
Amplitude of speed cycle	0.0	0.0	0.0	3.0	0.0	0.0
Period of speed cycle	1.0	1.0	1.0	10.0	0.0	0.0
Phase of speed cycle	0.0	0.0	0.0	0.0	0.0	0.0

Figure 5.3. Input variables to the Rubin software package (Rubin, 1987a) for Auk Models 1 – 6. Parameters have been split into those which relate to the first, second or third set of bedforms that have been modelled, or those parameters which relate to the entire depositional situation that is being modelled. Length: all length dimensions are defined relative to the lengths of the sides of the block, which are 100 units long. Phase: all phases are given in degrees and describe the situation at t=zero. Symmetry: dimensionless. Time: arbitrary units that describe all parameters of time (periods of cyclicity, migration speeds, and deposition rate). Direction: in degrees, oriented as indicated in the computer images (from Rubin and Carter, 2006).

This page - input variables describing the first set of bedforms.

Model # Input variable	Auk 1	Auk 2	Auk 3	Auk 4	Auk 5	Auk 6
Wavelength of bedforms in second set	100.0	100.0	100.0	100.0	100.0	10.0
Bedform phase (°)	270.0	270.0	270.0	270.0	270.0	0.0
Mean asymmetry	0.0	0.0	0.0	0.0	0.0	1.0
Amplitude of asymmetry cycle	0.0	0.0	0.0	0.0	0.0	0.0
Period of asymmetry cycle	1.0	1.0	1.0	1.0	1.0	1.0
Phase of asymmetry cycle	0.0	0.0	0.0	0.0	0.0	0.0
Mean bedform steepness	1.0	1.0	1.0	1.0	1.0	1.0
Amplitude of steepness cycle	0.0	0.0	0.0	0.0	0.0	0.0
Period of steepness cycle	1.0	1.0	1.0	1.0	1.0	1.0
Phase of steepness cycle	0.0	0.0	0.0	0.0	0.0	0.0
Wavelength of first set of plan-form sinuosities	50.0	50.0	50.0	50.0	50.0	40.0
Amplitude of first set of sinuosities	5.0	5.0	5.0	5.0	5.0	4.0
Phase of first set of sinuosities	180.0	180.0	180.0	180.0	180.0	0.0
Migration speed of first set of sinuosities	2.0	4.0	4.0	4.0	4.0	0.0
Wavelength of second set of plan-form sinuosities	0.0	0.0	0.0	0.0	0.0	0.0
Amplitude of second set of sinuosities	2.0	2.0	2.0	0.0	0.0	0.0
Phase of second set of sinuosities	270.0	270.0	270.0	180.0	180.0	0.0
Migration speed of second set of sinuosities	1.0	1.0	1.0	4.0	4.0	0.0
Migration direction of bedform	0.0	0.0	0.0	0.0	0.0	45.0
Mean migration speed of bedform	1.0	1.0	1.0	1.0	1.0	4.0
Amplitude of speed cycle	0.0	0.0	0.0	3.0	0.0	0.0
Period of speed cycle	1.0	1.0	1.0	10.0	0.0	1.0
Phase of speed cycle	0.0	0.0	0.0	0.0	0.0	0.0

This page - Input variables to describe the second set of bedforms.
All terms analogous to the corresponding terms for the first set of bedforms on the previous tables

Model # Input variable	Auk 1	Auk 2	Auk 3	Auk 4	Auk 5	Auk 6
Wavelength of bedforms in third set	0.0	0.0	0.0	0.0	0.0	0.0
Bedform phase (°)	0.0	0.0	0.0	0.0	0.0	0.0
Mean asymmetry	0.0	0.0	0.0	0.0	0.0	0.0
Amplitude of asymmetry cycle	0.0	0.0	0.0	0.0	0.0	0.0
Period of asymmetry cycle	1.0	1.0	1.0	1.0	1.0	1.0
Phase of asymmetry cycle	0.0	0.0	0.0	0.0	0.0	0.0
Mean bedform steepness	0.0	0.0	0.0	0.0	0.0	0.0
Amplitude of steepness cycle	0.0	0.0	0.0	0.0	0.0	0.0
Period of steepness cycle	1.0	1.0	1.0	1.0	1.0	1.0
Phase of steepness cycle	0.0	0.0	0.0	0.0	0.0	0.0
Wavelength of first set of plan-form sinuosities	0.0	0.0	0.0	0.0	0.0	0.0
Amplitude of first set of sinuosities	0.0	0.0	0.0	0.0	0.0	0.0
Phase of first set of sinuosities	0.0	0.0	0.0	0.0	0.0	0.0
Migration speed of first set of sinuosities	0.0	0.0	0.0	0.0	0.0	0.0
Wavelength of second set of plan-form sinuosities	0.0	0.0	0.0	0.0	0.0	0.0
Amplitude of second set of sinuosities	0.0	0.0	0.0	0.0	0.0	0.0
Phase of second set of sinuosities	0.0	0.0	0.0	0.0	0.0	0.0
Migration speed of second set of sinuosities	0.0	0.0	0.0	0.0	0.0	0.0
Migration direction of bedform	0.0	0.0	0.0	0.0	0.0	0.0
Mean migration speed of bedform	0.0	0.0	0.0	0.0	0.0	0.0
Amplitude of speed cycle	0.0	0.0	0.0	0.0	0.0	0.0
Period of speed cycle	1.0	1.0	1.0	1.0	1.0	0.0
Phase of speed cycle	0.0	0.0	0.0	0.0	0.0	0.0

This page - Input variables to describe the third set of bedforms.
All terms analogous to the corresponding terms for the first and second set of bedforms on the previous tables

Model # / Input variable	Auk 1	Auk 2	Auk 3	Auk 4	Auk 5	Auk 6
Type of superpositioning	3	3	3	3	3	2
Rotation option	0	0	0	0	0	0
Elevation of interdune flats	0.1	0.1	0.1	0.1	0.1	-1.0
Rate of deposition	0.1	0.1	0.2	0.1	0.1	0.1
Amplitude of cycle in rate of deposition	0.0	0.0	0.0	0.0	0.1	0.0
Period of cycle in rate of deposition	1.0	1.0	1.0	1.0	100	1.0
Phase of cycle in rate of deposition	0.0	0.0	0.0	0.0	0.0	0.0
Time from t=0 to beginning of depositional episode	300	300	300	300	300	100
Interval between drawing of crossbeds	1	1	1	1	1	1
Time from t=0 to end of depositional episode	1	1	1	1	1	100
Precision or speed?	1	1	1	1	1	1
Elevation of horizontal surface	1.0	1.0	1.0	1.0	1.0	1.0

This page - Input variables that apply to the entire depositional situation which is being modelled. All terms analogous to the corresponding terms for the bedforms on the previous tables.

5.6 – Auk Formation Sedimentological Model 1

Auk Model 1 depicts a simulation of the migration and accumulation of a train of simple linear bedforms, whereby the primary component of migration occurs in a direction parallel to the bedform crestline, and a secondary component of transverse migration occurs at half the major rate (Figure 5.4). This type of migration is considered to be present in almost all linear bedforms that develop and persist over long time periods (see Bristow et al., 2000) and is the main reason why the accumulations of such linear bedforms preferentially preserve foresets that tend to have relatively unimodal distributions (Rubin and Hunter, 1985). Rather than being purely linear with respect to net sediment transport direction, bedforms of this type are better classed as oblique (*sensu* Hunter et al., 1983). In this example, crestline sinuosities migrate towards 090° (arbitrary orientation value as explained in Section 5.3), whereas the transverse component of bedform migration is towards 000°. The presence of crestline sinuosity has been modelled based on observations of the form of large linear bedforms present in the Rub' Al-Khali, Saudi Arabia (Al-Masrahy and Mountney, 2013), and the Namib Sand Sea (Bristow, et al., 2000), which are considered analogous to the bedforms represented by the Auk Formation. Input parameters used to generate this model are summarised in Figure 5.3.

5.6.1 – Facies distribution on bedforms

The windward slopes of the dune bedforms in Figure 5.4 are dominated by a thin veneer of wind-ripple strata, but these deposits have a very low long-term preservation potential. The restricted interdune flats in this example are also dominated by wind-ripple strata. The lower plinths of the bedforms are dominated by reworked wind-ripple and wind-ripple-dominated facies, whereas the middle dune flank is characterised by purely reworked wind-ripple facies with an absence of wind-ripple-dominated facies. The original depositional facies that accumulated in the dune brink region was likely dominated by grainfall strata, but such deposits have a relatively low preservation potential, since they are unlikely to accumulate as part of a succession arising from the climb of migratory bedforms over one another. Thick packages of grainflow and grainfall facies accumulate preferentially on the upper dune slope but again, these have a low preservation potential. The lateral extent of these grainflow-dominated facies is limited by bounding surfaces generated by the migration of scour-pits.

In plan-view, the bedform deposits generated by Auk Model 1 are characterised by localised and spatially discontinuous preservation of packages of grainflow-dominated strata that are rather thin, and which are entirely encased by the reworked wind-ripple strata. More laterally extensive, continuous and thicker accumulations of reworked wind-ripple reflect the preferential preservation of the lower-most bedform plinths, as discussed in Section 4.5.4, as they climb over one another at low angles; the presence of low-angle-inclined dune plinths dominated by reworked wind-ripple strata is a common feature of many linear and oblique bedforms (Sneh and Weissbrod, 1983). Consequently, significant thicknesses of the preserved succession in the model are composed entirely of wind-ripple and reworked wind-ripple facies, which may feasibly act as non-net reservoir in oil-bearing intervals (Figure 1.19). The interdune migration bounding surfaces truncate the climbing dune sets, and are themselves usually overlain by dry interdune units of wind-ripple facies, which again may act as non-net reservoir.

Preservation of only the lowermost parts of packages of grainflow facies is a characteristic feature of Auk Model 1 (Figure 5.4). At the time of their development, such facies would have extended over substantial parts of the upper (non-preserved) lee-side bedform slope. The restricted lateral extent of the grainflow-dominated units reflects the control exerted by the plan-view sinuosity in determining where active lee-side slipfaces developed (Figure 1.5).

5.6.2 – Geometry and dimensions of stratigraphic architectural units

Figure 5.5 depicts the internal stratigraphic architecture related to Auk Model 1. The example shown in Figure 5.5a depicts the geometry and dimensions of packages (elements) of grainflow and grainflow-dominated strata in a section parallel to the transverse component of linear dune migration. For this section, packages of grainflow-dominated strata are approximately 475 m in length, measured parallel to the transverse component of linear dune migration, and internally incorporate around 125 m of amalgamated grainflow strata. The example shown in Figure 5.5b depicts facies geometries from a section parallel to the along-crest component of linear dune migration shown in Auk Model 1. For this section, packages of grainflow-dominated strata are approximately 1200 m in length, measured parallel to the along-crest component of linear dune migration, and internally incorporate approximately 125 m of amalgamated grainflow strata. In the horizontal section (Figure 5.5c); the individual grainflow-dominated packages are approximately 400 m in length. However, the section depicted in this orientation significantly underplays the degree to which individual grainflow tongues are interconnected because the flat upper surface of these sand bodies will be inclined at the angle-of-climb, and are therefore projecting out of the horizontal section at a slight angle. This issue is considered in detail in Section 5.6.3.

5.6.3 – Geometry, scale and orientation of net reservoir units

Figure 5.6 depicts the geometry, scale and orientation of net reservoir units in Auk Model 1. As described in Section 5.6.2, the geometry of the sand bodies seen in the horizontal section of Auk Model 1 (Figure 5.6a) underplays the likely degree of connectivity of the grainflow-dominated units (packages of strata) arising from the accumulation of the linear bedforms via a climbing mechanism. This is illustrated in Figure 5.6b, whereby the vertical cross-section illustrates maximum grainflow development in a zone parallel to the climbing upper bounding surface of the preserved coset. In Figure 5.6c, the plan-view geometry is

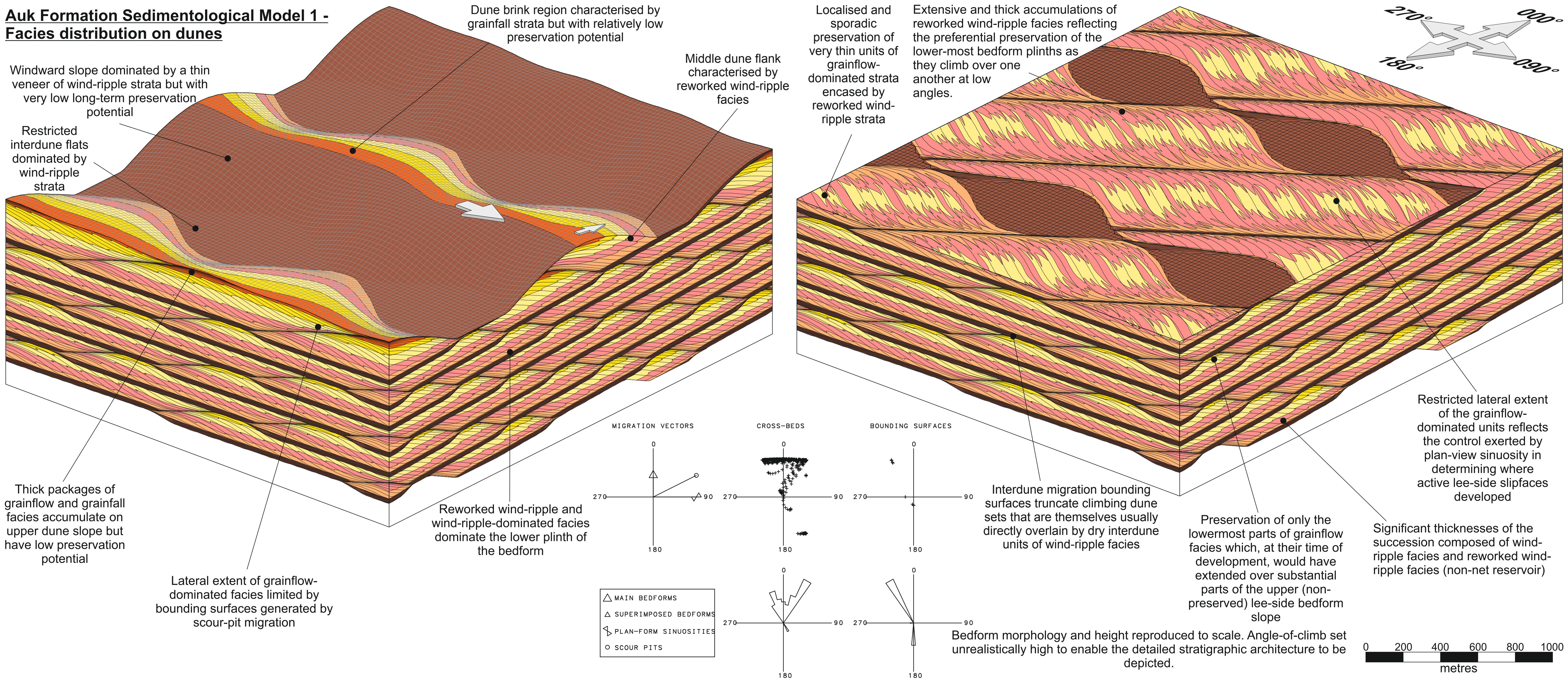

Bedform morphology and height reproduced to scale. Angle-of-climb set unrealistically high to enable the detailed stratigraphic architecture to be depicted.

Figure 5.4. Auk Formation Sedimentological Model 1 (see Figure 5.3 for the input parameters used to generate this model). Simulation of the migration and accumulation of a simple linear bedform whereby the primary component of migration occurs in a direction parallel to the bedform crestline but in which there is additionally a secondary component of transverse migration at half the major rate. Crestline sinuosities migrate towards 090°, while the transverse component of bedform migration is towards 000°. The presence of crestline sinuosity has been modelled based on observation of the form of many large linear bedforms in modern sand seas.

a) Section parallel to transverse component of linear dune migration

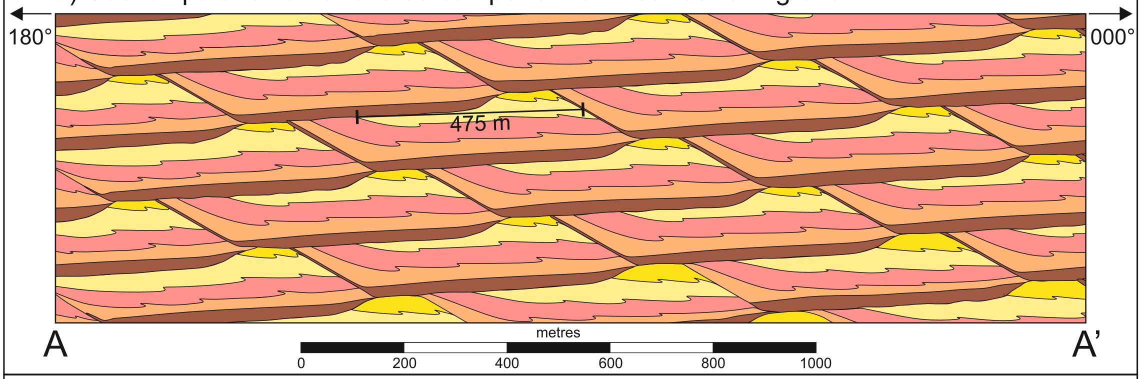

b) Section parallel to along-crest component of linear dune migration

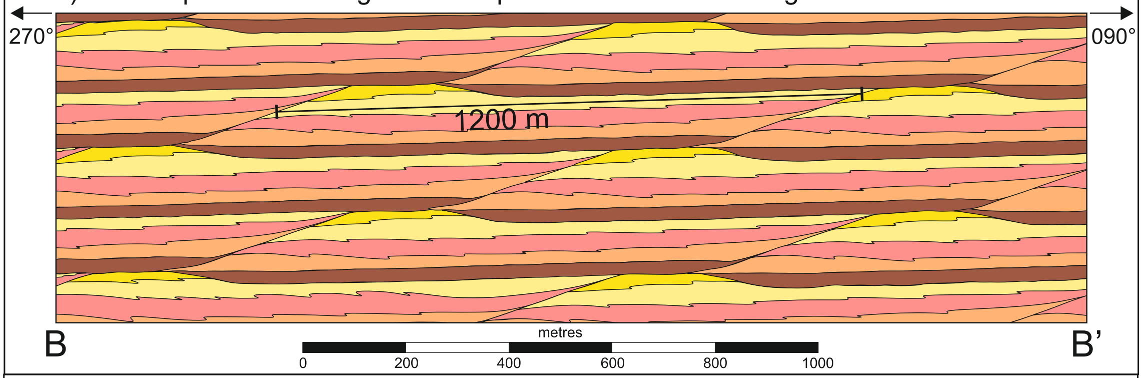

c) Horizontal section

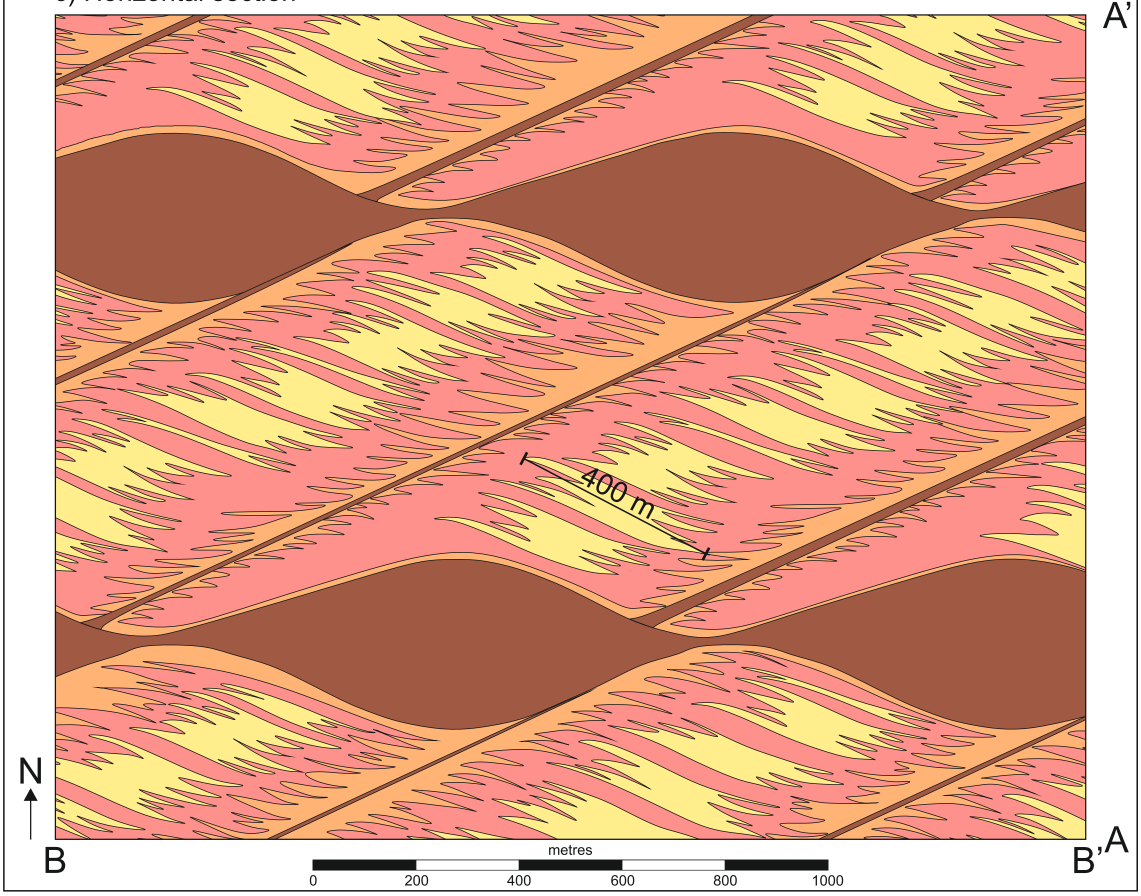

Figure 5.5. Stratigraphic architecture produced by Auk Model 1. Estimated geometry and dimensions of grainflow strata; note that the view in the horizontal section c) under-plays the degree to which grainflow tongues are interconnected because the flat upper surface of these sand bodies will be inclined at the angle-of-climb and are therefore projecting out of the horizontal section at a slight angle.

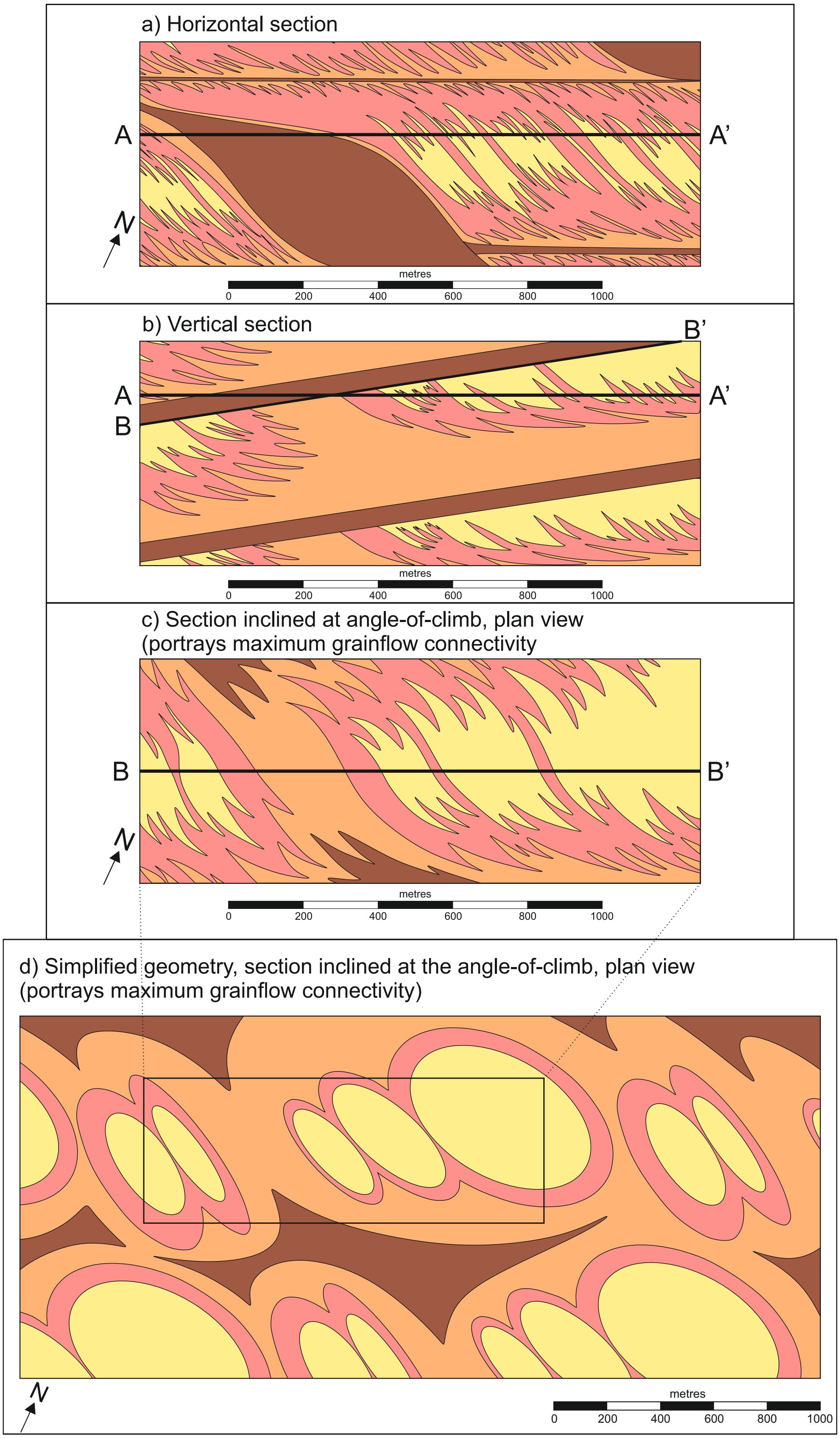

a) Horizontal section

b) Vertical section

c) Section inclined at angle-of-climb, plan view (portrays maximum grainflow connectivity

d) Simplified geometry, section inclined at the angle-of-climb, plan view (portrays maximum grainflow connectivity)

Figure 5.6. Geometry, scale and orientation of net reservoir units predicted by Auk Model 1: a) geometry seen in horizontal section under-plays the likely degree of connectivity of the linear dune grainflow units; b) vertical cross section illustrating maximum grainflow development in zone parallel to climbing upper bounding surface, and pinch-out of grainflow units in the middle part of the climbing cosets; c) plan view geometry seen in a section taken immediately beneath an interdune migration bounding surface and inclined at the angle-of-climb, portraying the likely maximum degree of connectivity of the grainflow units; d) resulting facies geometry simplified to geometric shapes for reservoir modelling purposes.

seen in a section taken directly beneath an interdune bounding surface that caps a preserved dune coset and this is inclined at the angle-of-climb, thereby portraying the likely maximum degree of connectivity of the grainflow units. This geometry is simplified to geometric shapes in Figure 5.6d for the purpose of summarising the overall gross-scale geometry and orientation of the facies packages and their relationship to surrounding packages. This simplified summary configuration is useful for reservoir modelling purposes as it distils a complex sedimentological body down to a simple geometric body that can be described in terms simple mathematical expressions describing shape, orientation and density of occurrence. The grainflow units depicted here are elongated WNW-ESE (arbitrary orientations based on the orientation of the original bedform relative to an arbitrary north value). The grainflow units in each case are not connected; instead they are encapsulated within a ring of reworked wind-ripple strata, which would typically possess primary porosity and permeability characteristics that might be expected to yield moderate reservoir quality (Follows, 1997; Figure 5.1), as opposed to the grainflow units which are likely to possess more desirable reservoir properties (Follows, 1997; Figure 5.1). These packages of grainflow and reworked wind-ripple strata are in turn encased by a background of wind-ripple-dominated and pure wind-ripple strata, which would be characterised by relatively poor reservoir properties. The individual grainflow-dominated units in this example have areas which range between 33 x 10^3 m^2 and 2.65 x 10^5 m^2

5.7 – Auk Formation Sedimentological Model 2

Auk Model 2 (Figure 5.7) differs from that of Model 1 (Figure 5.4) only in that the large linear bedforms in Auk Model 2 had an along-crest component of migration that was double that of Auk Model 1. The set architecture in Auk Model 2 therefore reflects a stratigraphy generated by bedforms that were closer to being perfectly linear than their counterparts in Auk Model 1. This has significant implications for the predicted distribution of net reservoir facies, most notably in terms of the likely width, lateral extent and orientation of packages of grainflow facies. Specifically, the width of the cosets in which these facies are preserved is narrower than the equivalent features in Auk Model 1, and the orientation of these features is 10 - 15° closer to parallel to the orientation of the crestlines of the original bedforms. Input parameters used to generate this model are summarised in Figure 5.3.

5.7.1 – Facies distributions on bedforms

The results from Auk Model 2 demonstrate the occurrence of units of wind-ripple strata deposited within migratory interdune flats that advanced alongside the migratory bedforms (Figure 5.7). Migration coupled with accumulation of these forms preserves elongate slivers of relatively low-permeability facies in the sections close to parallel net sand transport. Thick and laterally extensive units of reworked wind-rippled facies are also present, and these represent deposition on the dune plinth and the lower flank of the bedform.

Elliptical-shaped dry interdune elements form elongate lenses of wind-ripple strata inclined at the angle-of-climb. These are surrounded by bounding surfaces that arose as the result of oblique migration of lee-side sinuosities on the larger linear bedforms. Cosets adjacent to these bounding surfaces are composed of reworked wind-ripple and rare grainflow strata, and are of narrower lateral extent than those predicted by Auk Model 1. The overstepping geometry of packages of wind-ripple strata is representative of dry interdune units.

5.7.2 – Geometry and dimensions of stratigraphic architectural units

Figure 5.8 depicts the geometry and stratigraphic architecture of grainflow-dominated units from Auk Model 2. The example shown in Figure 5.8a demonstrates the facies distribution of the model in a section parallel to the transverse component of linear dune migration. For Auk Model 2, the grainflow-dominated units have apparent lengths of around 200 m in this orientation, with no packages of exclusively grainflow strata preserved. In the section parallel to the along-crest component of linear dune migration (Figure 5.8b), the grainflow-dominated units are approximately 600 m in length. There are no exclusively grainflow strata preserved in this example because the uppermost parts of the aeolian dune slipfaces are not preserved. In the horizontal section (Figure 5.8c), grainflow-dominated units are approximately 175 m in length, and oriented NW-SE. However, this horizontal section underplays the degree to which the grainflow tongues are interconnected, because the flat upper surface of these sand bodies will be inclined at the angle-of-climb of the system, and

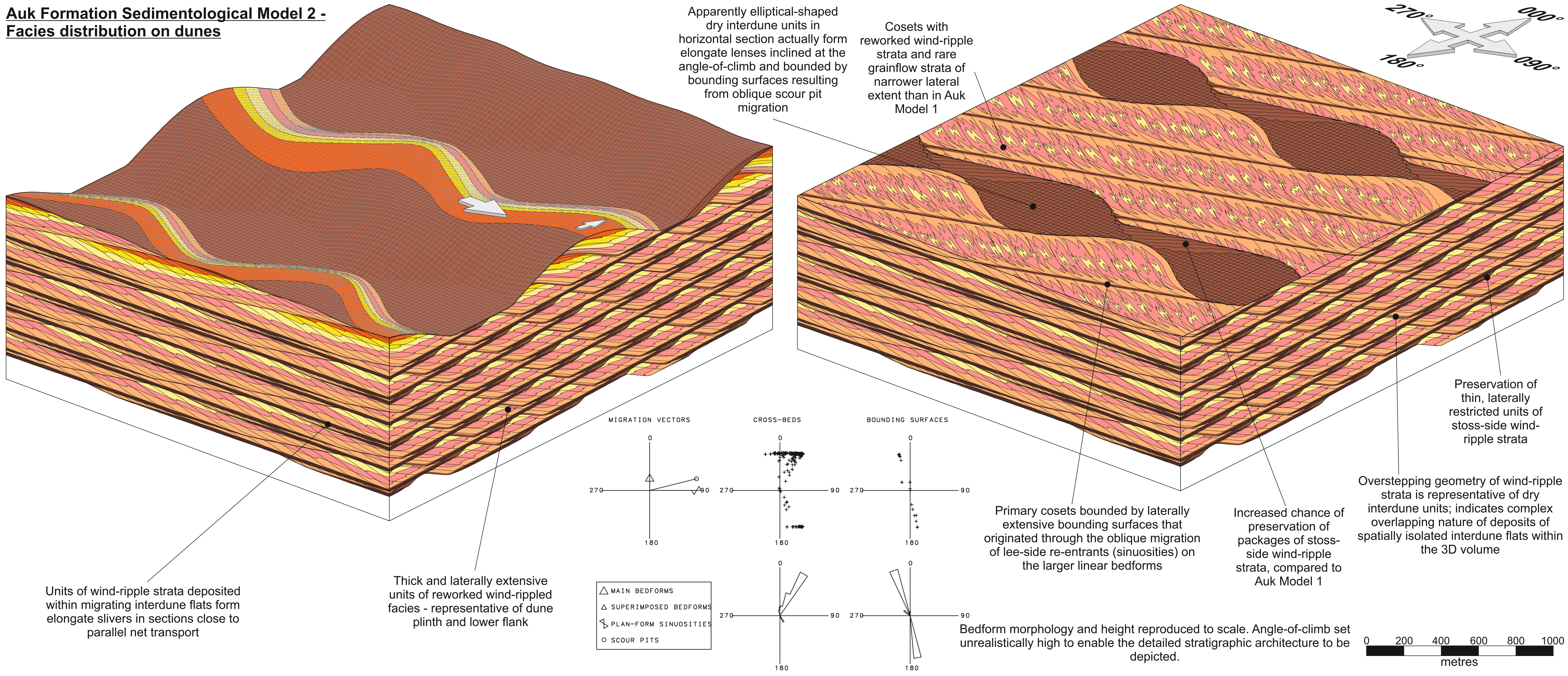

Auk Formation Sedimentological Model 2 - Facies distribution on dunes

Apparently elliptical-shaped dry interdune units in horizontal section actually form elongate lenses inclined at the angle-of-climb and bounded by bounding surfaces resulting from oblique scour pit migration

Cosets with reworked wind-ripple strata and rare grainflow strata of narrower lateral extent than in Auk Model 1

Preservation of thin, laterally restricted units of stoss-side wind-ripple strata

Overstepping geometry of wind-ripple strata is representative of dry interdune units; indicates complex overlapping nature of deposits of spatially isolated interdune flats within the 3D volume

Primary cosets bounded by laterally extensive bounding surfaces that originated through the oblique migration of lee-side re-entrants (sinuosities) on the larger linear bedforms

Increased chance of preservation of packages of stoss-side wind-ripple strata, compared to Auk Model 1

Units of wind-ripple strata deposited within migrating interdune flats form elongate slivers in sections close to parallel net transport

Thick and laterally extensive units of reworked wind-rippled facies - representative of dune plinth and lower flank

Bedform morphology and height reproduced to scale. Angle-of-climb set unrealistically high to enable the detailed stratigraphic architecture to be depicted.

Figure 5.7. Auk Formation Sedimentological Model 2 (see Figure 5.3 for the input parameters used to generate this model).The only difference between this model and Auk Model 1 (Figure 5.4) is that the large linear bedforms in this example had an along-crest component of migration that was double that of Model 1. The set architecture in this model therefore reflects a stratigraphy generated by bedforms that were closer to being perfectly linear than their counterparts in Model 1. This has significant implications for the predicted distribution of net reservoir facies, most notably in terms of the likely width, lateral extent and orientation of the linear grainflow facies.

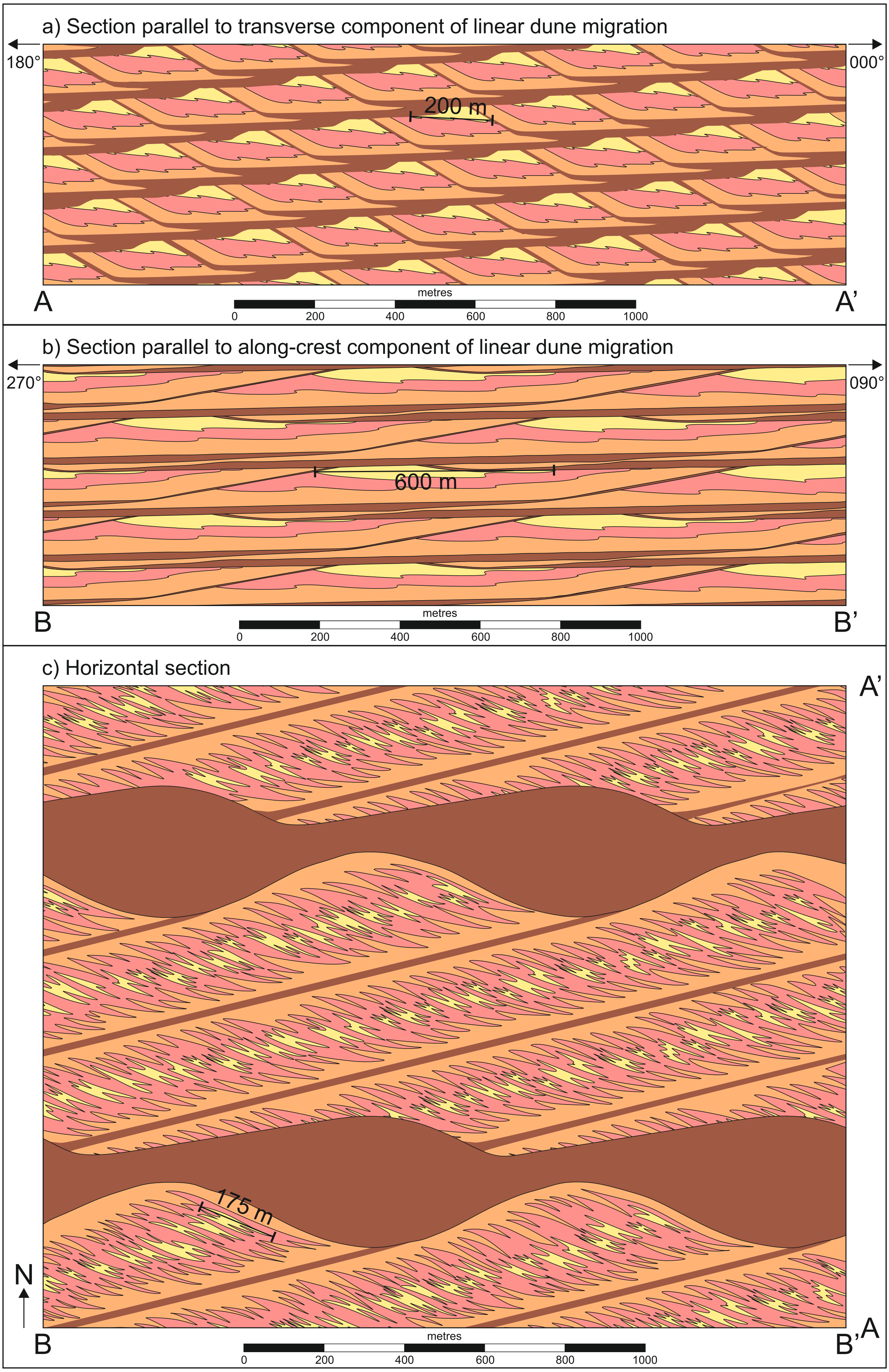
a) Section parallel to transverse component of linear dune migration

b) Section parallel to along-crest component of linear dune migration

c) Horizontal section

Figure 5.8. Stratigraphic architecture produced by Auk Model 2. Estimated geometry and dimensions of grainflow strata; note that the view in the horizontal section c) under-plays the degree to which grainflow tongues are interconnected because the flat upper surface of these sand bodies will be inclined at the angle-of-climb and are therefore projecting out of the horizontal section at a slight angle.

are therefore projecting out of the horizontal section at a slight angle (this is considered in greater detail below).

5.7.3 – Geometry, scale and orientation of net reservoir units

Figure 5.9 describes the likely geometry, scale and orientation of net reservoir units predicted by Auk Model 2. In Figure 5.9b, the vertical cross-section illustrates maximum grainflow development in a zone parallel to the climbing (i.e. slightly inclined) upper bounding surface of a major dune element. In Figure 5.9c, the near-plan-view geometry is depicted for a section taken directly beneath an interdune migration bounding surface and inclined at the angle-of-climb, thereby portraying the likely maximum degree of connectivity of the grainflow units, with this geometry simplified to basic geometric shapes in Figure 5.9d. The grainflow units here are elongated in a range from W-E to NNW-SSE (expressed in arbitrary orientations for modelling purposes). The grainflow units in each case are not connected; instead they are encapsulated within a zone of reworked wind-ripple strata, which itself would yield moderate reservoir quality, as opposed to the grainflow units which themselves would be expected to yield excellent reservoir quality. These packages of grainflow and reworked wind-ripple strata are entirely surrounded by a background of wind-ripple-dominated strata, which is in turn punctuated by poor reservoir quality wind-ripple strata. The individual grainflow-dominated units in this example range from 0.2×10^3 m^2 to 3.3×10^4 m^2.

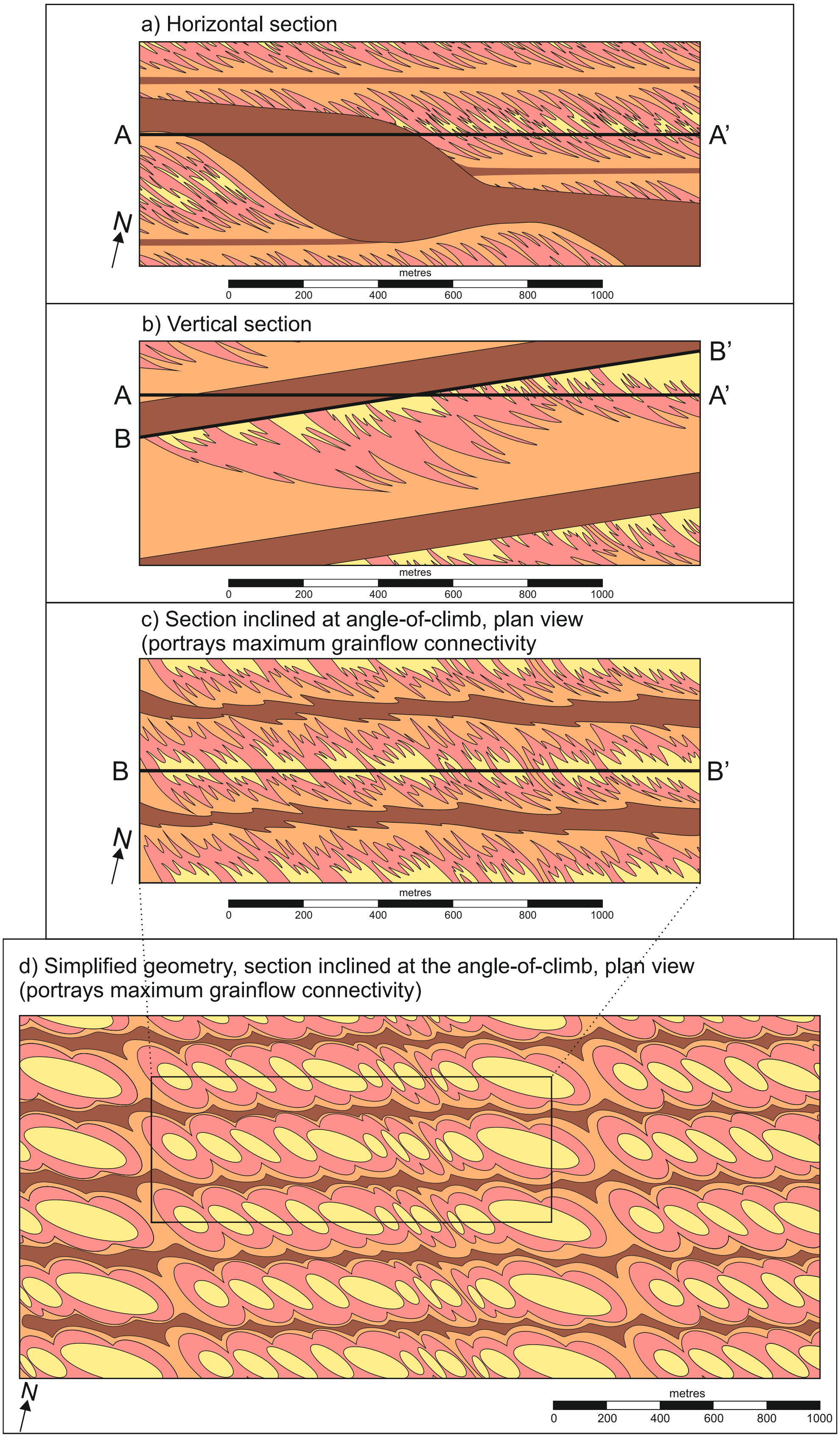

Figure 5.9. Geometry, scale and orientation of net reservoir units predicted by Auk Model 2: a) geometry seen in horizontal section under-plays the likely degree of connectivity of the linear dune grainflow units; b) vertical cross section illustrating maximum grainflow development in zone parallel to climbing upper bounding surface, and pinch-out of grainflow units in the middle part of the climbing cosets; c) plan view geometry seen in a section taken immediately beneath an interdune migration bounding surface and inclined at the angle-of-climb, portraying the likely maximum degree of connectivity of the grainflow units; d) resulting facies geometry simplified to geometric shapes for reservoir modelling purposes.

5.8 – Auk Formation Sedimentological Model 3

Auk Model 3 (Figure 5.10) differs from Auk Model 2 (Figure 5.7) in that the rate of accumulation at the depositional surface in Auk Model 3 is double that of Auk Model 2. The set architecture in Auk Model 3 therefore reflects a stratigraphy generated by bedforms that climbed at a higher angle than their counterparts in Auk Model 2. This has significant implications for the predicted distribution of net reservoir facies, most notably because higher climb angles enable more of the middle and upper parts of the bedform lee-slope to be preserved, including volumetrically larger and laterally more continuous packages of grainflow avalanche strata. Angles-of-climb in dry aeolian systems, similar to that in which the Auk Formation was deposited, are controlled by the rate of subsidence, the rate of bedform migration and the availability of any pre-existing unfilled accommodation space (Mountney, 2006a). Typically, migrating aeolian dunes climb at angles of a few tenths of a degree, though in exceptional circumstances angles of up to 5° have been recorded from outcrop studies (e.g. Mountney and Howell, 2000). Input parameters used to generate this model are summarised in Figure 5.3.

5.8.1 – Facies distributions on bedforms

The cosets representing the migration of successive linear dunes in the Auk Formation have an average thickness of 20 m. If these bedforms had a lateral spacing of 2000 m (as suggested by the preserved facies distribution and comparison with modern analogues – see Chapter 4 and Figure 4.12), then the angle-of-climb would be approximately 0.5°, which lies within a well-documented range based on observations from ancient outcrop studies (e.g. Mountney, 2006a; Romain and Mountney, 2014). The bounding surfaces preserved in Auk Model 3 (Figure 5.10) are inclined at steeper angles than those depicted in Auk Model 2 (Figure 5.7). This is due to the input parameter relating to the rate of accumulation used in the model being double that of the example in Auk Model 2. This increased rate of accumulation allows for preservation of thicker sets of strata through a steeper angle-of-climb. The vertical distribution of facies within the preserved cosets of strata reflects the increased preservation of facies which originally accumulated on the middle and upper parts of the linear dune lee-slope; more grainflow and grainflow-dominated packages of strata, which tend to have higher porosities and permeabilities than their wind-ripple-dominated counterparts. There is also an increase in lateral extent and degree of connectivity of middle-dune-flank deposits, which are dominated by packages of reworked wind-ripple and grainflow-dominated facies, and which would be expected to yield moderate and good reservoir quality, respectively. In Figure 5.10, although the geometry of the foresets and bounding surfaces depicted in the horizontal section are nearly identical to those in Auk Model 2, the distribution of facies within this framework is slightly different. In this example, there is increased preservation of more extensive and better connected units composed of grainflow facies. However, there are similarities between this example and

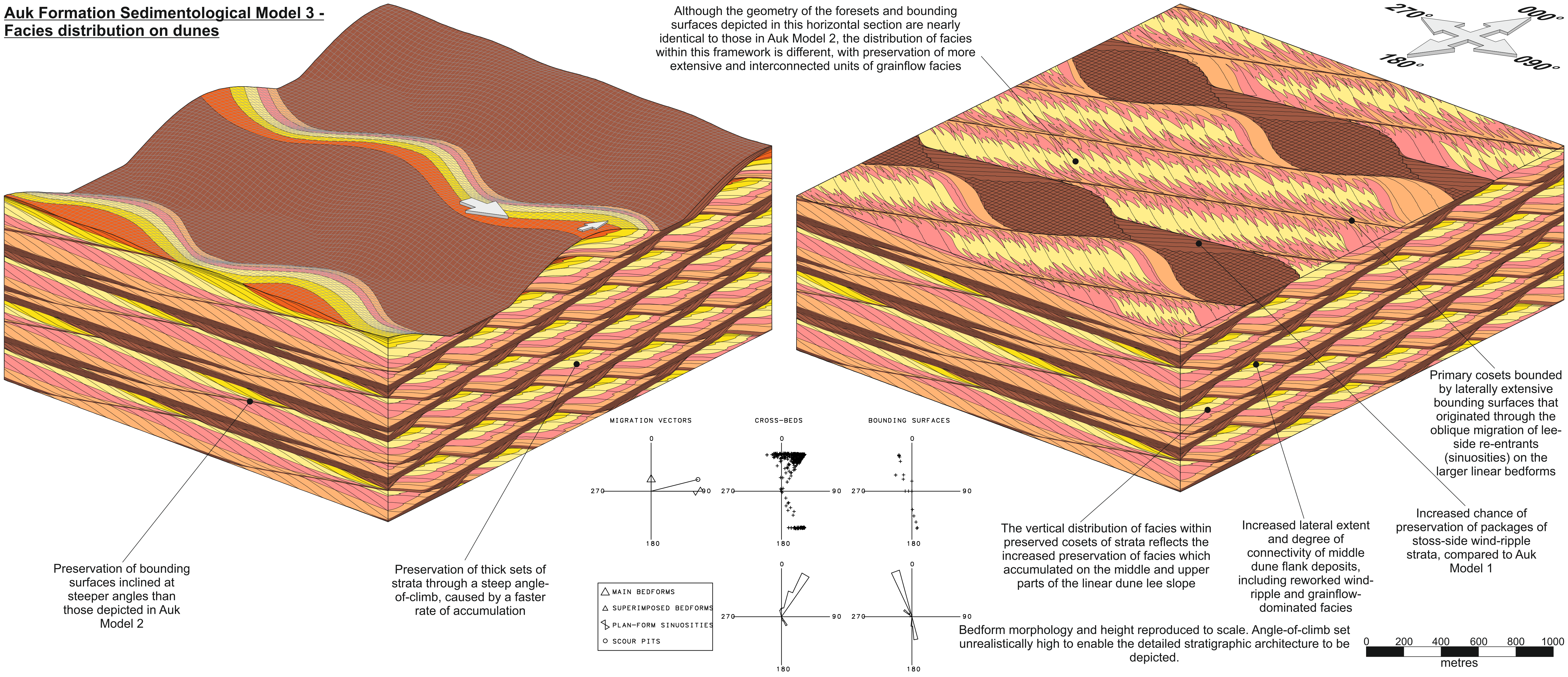

Figure 5.10. Auk Formation Sedimentological Model 3 (see Figure 5.3 for the input parameters used to generate this model). The only difference between this model and that of Auk Model 2 (Figure 5.7) is that the rate of accumulation at the depositional surface in this example is double that of Model 2. The set architecture in this model therefore reflects a stratigraphy generated by bedforms that climbed at a higher angle than their counterparts in Auk Model 2. This has significant implications for the predicted distribution of net reservoir facies, most notably because higher climb angles enable more of the middle and upper parts of the bedform lee slope to be preserved, including more continuous grainflow avalanche deposits.

that of Auk Model 2. For example, the primary cosets are again delineated by laterally extensive bounding surfaces, which originated through the oblique migration of lee-side sinuosities on the larger linear bedforms. Additionally, there is increased preservation potential of packages of stoss-side wind-ripple strata than compared to Auk Model 1.

5.8.2 – Geometry and dimensions of stratigraphic architectural units

Figure 5.11 depicts the stratigraphic architecture produced by Auk Model 3. Similarly to Auk Model 1, the pure grainflow units are preserved in the parallel sections as well as the grainflow-dominated units, thus increasing reservoir quality in this example. In the section parallel to the transverse component of linear dune migration (Figure 5.11a), the grainflow and grainflow-dominated strata packages are approximately 325 m in length when measured parallel to the transverse component of linear dune migration. In Figure 5.11b, which demonstrates the stratigraphic architecture of Auk Model 3 in a section parallel to the along-crest component of linear dune migration, the grainflow and grainflow-dominated units are approximately 1000 m in length when measured in this orientation. This is less than the lengths measured for grainflow units in Auk Model 1 (Figure 5.5b), but nearly double the length of those depicted in Auk Model 2 (Figure 5.8b). Again, in the horizontal section (Figure 5.11c), the degree to which the grainflow units are interconnected is underplayed, as the flat upper surface of these sand bodies is inclined at the angle-of-climb, and therefore project out of the horizontal section at an angle. The grainflow-dominated units seen in plan-view measure at approximately 1875 m in length and 325 m in width. In Auk Model 3, these grainflow packages are elongate and connected. This configuration exerts a favourable influence on expected reservoir quality of this example, as hydrocarbons would flow with ease through the grainflow units.

5.8.3 – Geometry, scale and orientation of net reservoir units

Figure 5.12 describes the geometry, scale and orientation of the net reservoir units which are predicted by Auk Model 3. The horizontal section (Figure 5.12a) underplays the likely degree of connectivity between the linear dune grainflow-dominated units, which is rectified in part by Figure 5.12b by illustrating the likely maximum grainflow development in a section inclined parallel to the upper climbing bounding surface. Directly beneath this interdune migration bounding surface and inclined at the angle-of-climb, the maximum degree of connectivity of the grainflow units is depicted in plan-view (Figure 5.12c), and these grainflow units are simplified to basic geometric shapes in Figure 5.12d as a characterisation of the overall geometry in a manner suitable for forward reservoir modelling. For Auk Model 3, the grainflow-dominated strata are arranged as 1.53 x 10^5 m^2 and 2.23 x 10^5 m^2 in plan-view. Each grainflow-dominated package is entirely encompassed by reworked-wind-ripple strata, which has moderate reservoir quality.

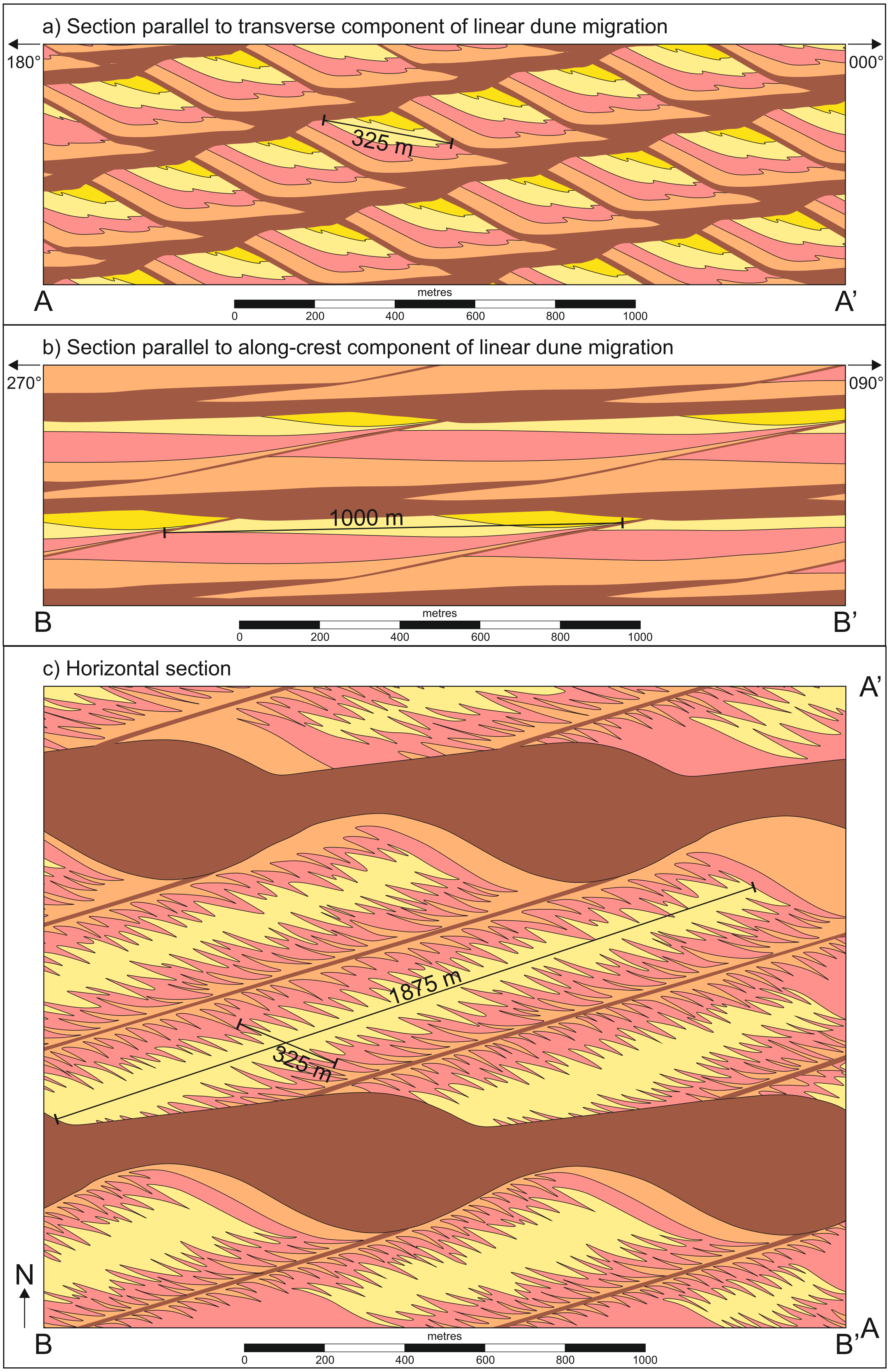

Figure 5.11. Stratigraphic architecture produced by Auk Model 3. Estimated geometry and dimensions of grainflow strata; note that the view in the horizontal section c) under-plays the degree to which grainflow tongues are interconnected because the flat upper surface of these sand bodies will be inclined at the angle-of-climb and are therefore projecting out of the horizontal section at a slight angle.

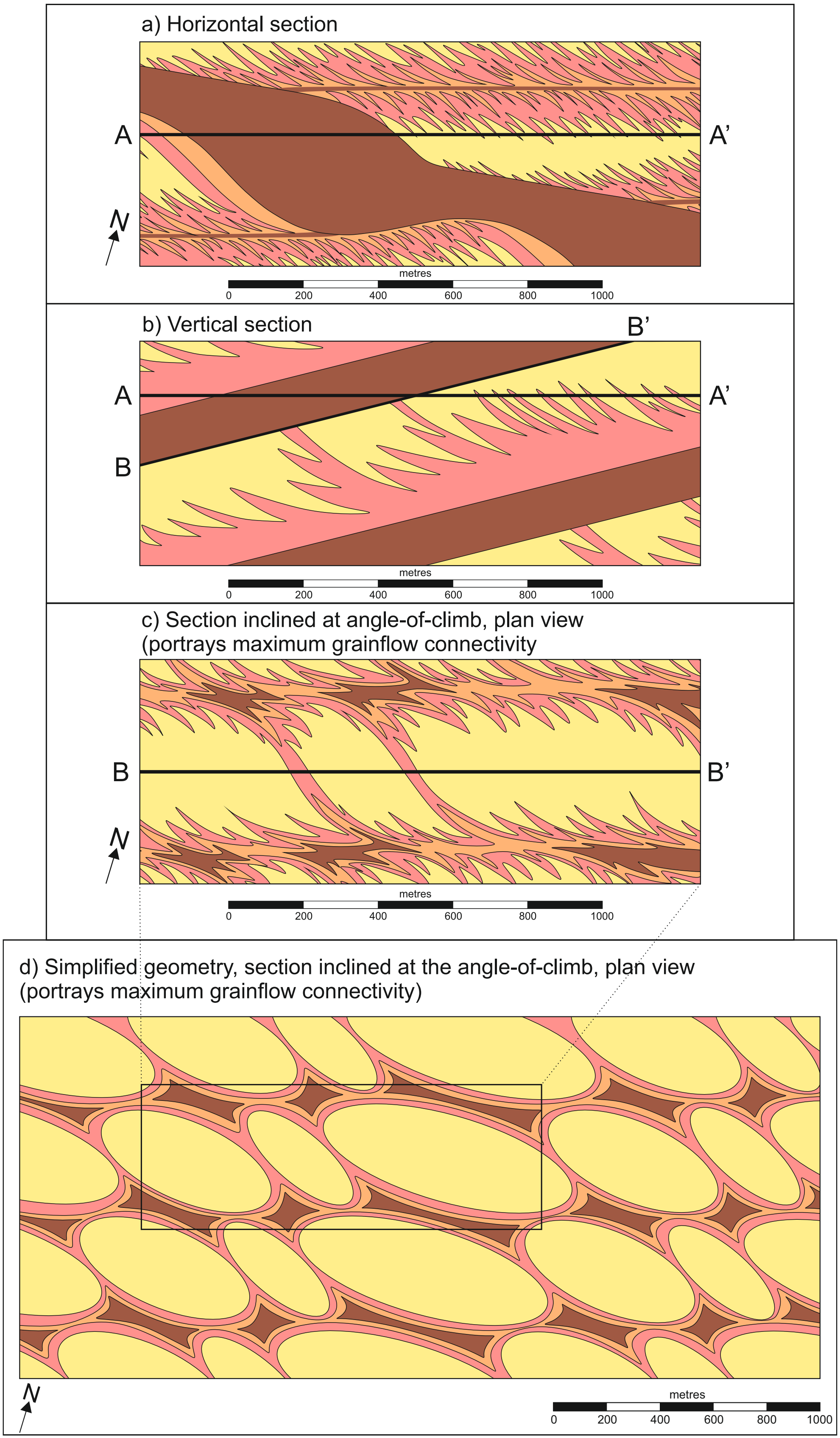

Figure 5.12. Geometry, scale and orientation of net reservoir units predicted by Auk Model 3: a) geometry seen in horizontal section under-plays the likely degree of connectivity of the linear dune grainflow units; b) vertical cross section illustrating maximum grainflow development in zone parallel to climbing upper bounding surface, and pinch-out of grainflow units in the middle part of the climbing cosets; c) plan view geometry seen in a section taken immediately beneath an interdune migration bounding surface and inclined at the angle-of-climb, portraying the likely maximum degree of connectivity of the grainflow units; d) resulting facies geometry simplified to geometric shapes for reservoir modelling purposes.

5.9 – Auk Formation Sedimentological Model 4

Auk Model 4 (Figure 5.13) differs from Auk Model 2 (Figure 5.7) in that the large linear bedforms in Auk Model 4 experienced changes in the rate of secondary transverse migration, along with brief, periodic reversals in migration direction. The set architecture in this model therefore reflects a stratigraphy generated by bedforms that vary in their temporal migratory behaviour, unlike their counterparts in Auk Model 2. This has significant implications for the predicted distribution of net reservoir facies, most notably in terms of the likely lateral extent and continuity of packages of grainflow facies. Periodic changes of speed and reversals of direction of bedform migration are common in linear dunes because such bedforms typically develop in response to two converging wind directions, and these are likely to vary in both magnitude and direction over time; e.g. the Namib Sand Sea – Bristow et al. (2000). Input parameters used to generate this model are summarised in Figure 5.3.

5.9.1 – Facies distributions on bedforms

In the vertical sections of Figure 5.13, the presence of both convex-up and concave-up surfaces reflects the preservation of both dome-shaped spurs and scoop-shaped re-entrants (scour pits). Preferential preservation of the foresets, which dip towards orientations of 030° - 040° (in terms of the arbitrary co-ordinate system used for the modelling exercise), and which reflect the resultant sand transport direction is also seen. Periodic minor reversals of the secondary, transverse component of bedform migration results in the generation of reactivation surfaces, which are bounded by relatively low-permeability wind-ripple-dominated strata. This arrangement of facies is commonly seen in the Auk Formation (see Figure 5b in Heward, 1991).

Major bounding surfaces seen in the horizontal section, generated by the migration of lee-side scour pits (sinuous re-entrants), carve large scallop-shaped erosional surfaces that delineate cosets of linear dune strata. Changes in the foreset azimuth between adjoining cosets are generated by periodic reversal in the transverse component of linear dune migration. In plan-view, these cosets define horn-shaped bodies that are of limited extent in the direction of foreset dip.

Changes in the spacing of the foresets in this model reflect the cyclic nature of the variation in speed of the transverse component of migration of the linear bedforms, but such changes would not be apparent in core and neither would they necessarily be so regular in natural systems.

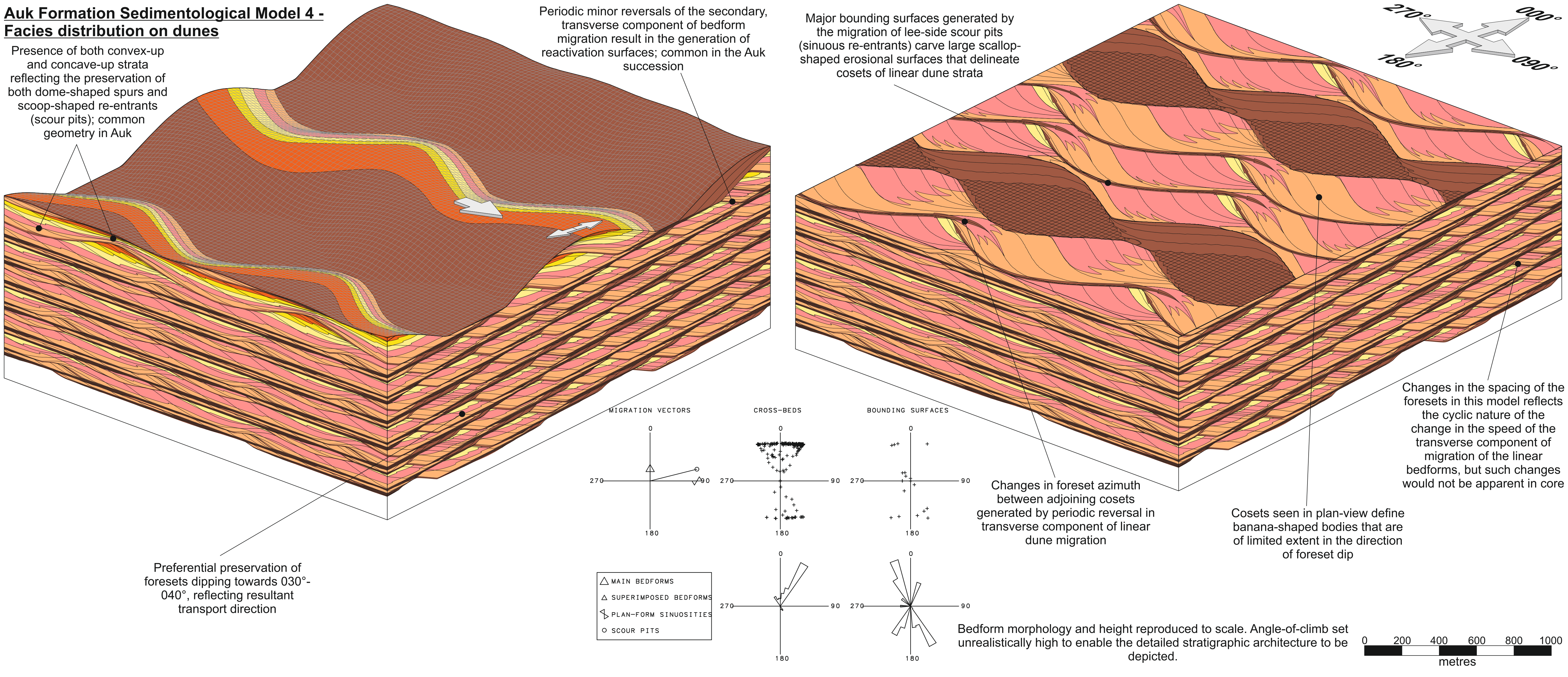

Auk Formation Sedimentological Model 4 - Facies distribution on dunes

Presence of both convex-up and concave-up strata reflecting the preservation of both dome-shaped spurs and scoop-shaped re-entrants (scour pits); common geometry in Auk

Periodic minor reversals of the secondary, transverse component of bedform migration result in the generation of reactivation surfaces; common in the Auk succession

Major bounding surfaces generated by the migration of lee-side scour pits (sinuous re-entrants) carve large scallop-shaped erosional surfaces that delineate cosets of linear dune strata

Preferential preservation of foresets dipping towards 030°-040°, reflecting resultant transport direction

Changes in foreset azimuth between adjoining cosets generated by periodic reversal in transverse component of linear dune migration

Cosets seen in plan-view define banana-shaped bodies that are of limited extent in the direction of foreset dip

Changes in the spacing of the foresets in this model reflects the cyclic nature of the change in the speed of the transverse component of migration of the linear bedforms, but such changes would not be apparent in core

Bedform morphology and height reproduced to scale. Angle-of-climb set unrealistically high to enable the detailed stratigraphic architecture to be depicted.

Figure 5.13. Auk Formation Sedimentological Model 4 (see Figure 5.3 for the input parameters used to generate this model). The only difference between this model and Auk Model 2 (Figure 5.7) is that the large linear bedforms in this example experienced changes in the rate of secondary transverse migration, along with brief, periodic reversals in migration direction. The set architecture in this model therefore reflects a stratigraphy generated by bedforms that vary their temporal migratory behaviour, unlike their counterparts in Auk Model 2. This has significant implications for the predicted distribution of net reservoir facies, most notably in terms of the likely lateral extent and continuity of the grainflow facies.

5.9.2 – Geometry and dimensions of stratigraphic architectural units

The periodic changes in speed and reversals of the direction of bedform migration in Auk Model 4 have significant implications for the size and distribution of units composed of net reservoir facies (in this case, grainflow-dominated strata). In the section parallel to the transverse component of linear dune migration (Figure 5.14a), the pure grainflow units are not preserved, whereas the grainflow-dominated units range in length at 75 m, 100 m and 175 m when measured parallel to the transverse component of linear dune migration. The grainflow-dominated units preserved in the section parallel to the along-crest component of linear dune migration are more uniform in length, at approximately 600 m when measured in this orientation (Figure 5.14b). In the horizontal section (Figure 5.14c), wind-ripple, wind-ripple-dominated and reworked wind-ripple facies dominate, with the grainflow-dominated facies a mere 200 m in length, significantly less than those depicted in Auk Models 1, 2 and 3. This marked decrease in net reservoir facies distribution would have a detrimental effect on reservoir quality, most notably in the ability for hydrocarbons to punctuate the less permeable wind-ripple-dominated facies. However, this horizontal section in Figure 5.14c underplays the degree to which the grainflow-dominated units are interconnected, because the flat upper surface of these sand bodies will be inclined at the angle-of-climb and are therefore projecting out of the horizontal section at a slight angle.

5.9.3 – Geometry, scale and orientation of net reservoir units

In Figure 5.15, the geometry, scale and orientation of units considered to be likely net reservoir bodies is shown in a series of models which attempt to rectify the inclination issue discussed in Section 5.9.2. In Figure 5.15a, the horizontal section underplays the likely connectivity of the grainflow-dominated units, as in Figure 5.14c. The most extensive development of units composed of grainflow-dominated facies is in a zone parallel to the climbing upper bounding surface (Figure 5.15b). The horizontal section (Figure 5.15c) is taken directly beneath an interdune migration bounding surface and inclined at the angle-of-climb, which allows the likely maximum degree of the grainflow-dominated units to be portrayed. The resulting facies geometry is then simplified to basic geometric shapes for reservoir modelling purposes (Figure 5.15d). Here, the grainflow-dominated units are arranged in individual packages, each of which is encapsulated by reworked wind-ripple strata of moderate reservoir quality. The grainflow-dominated stratal packages are inclined NW-SE (arbitrary orientation) and have values which range between 9×10^3 m^2 and 2.6×10^4 m^2.

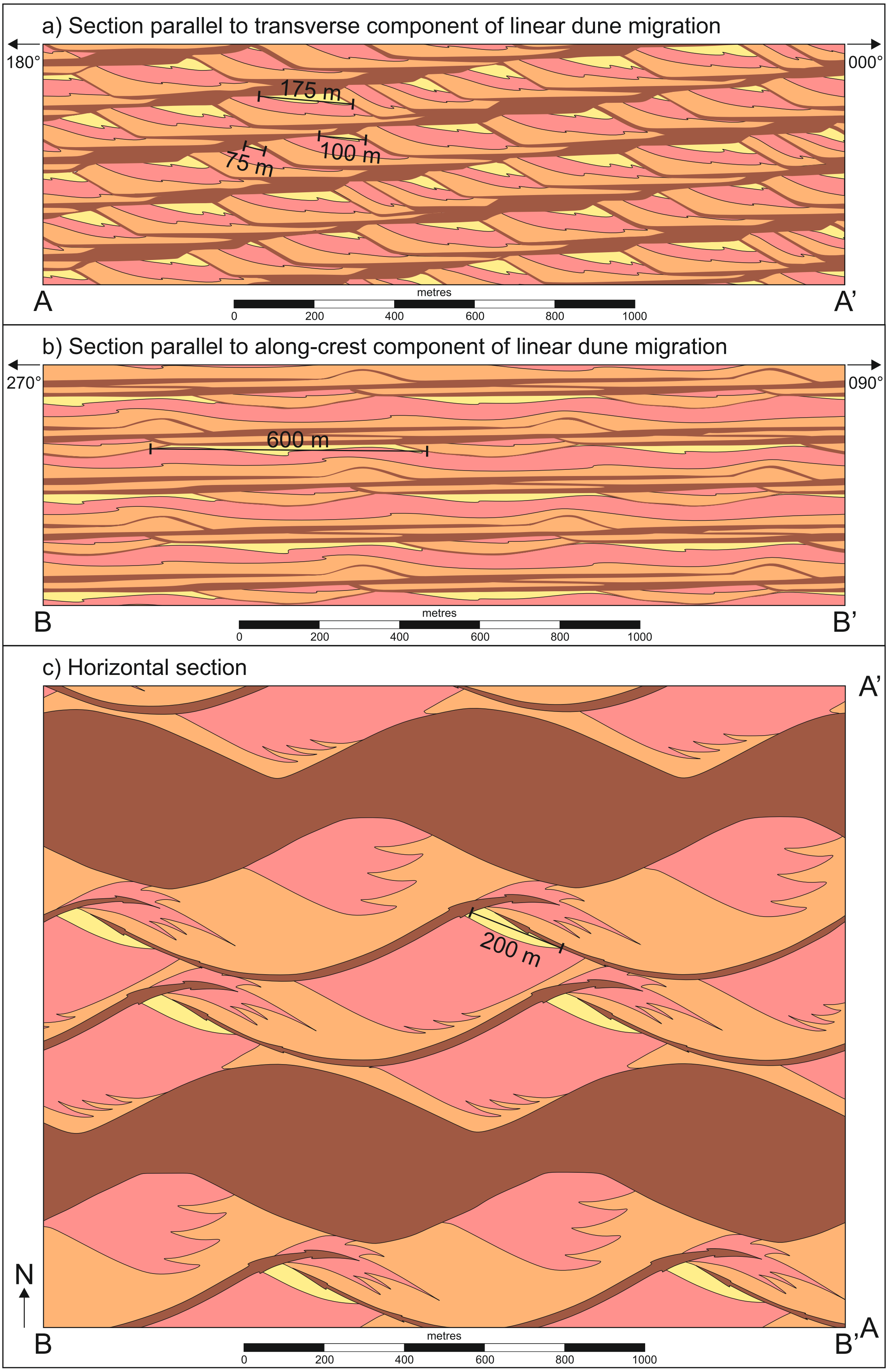

Figure 5.14. Stratigraphic architecture produced by Auk Model 4. Estimated geometry and dimensions of grainflow strata; note that the view in the horizontal section c) under-plays the degree to which grainflow tongues are interconnected because the flat upper surface of these sand bodies will be inclined at the angle-of-climb and are therefore projecting out of the horizontal section at a slight angle.

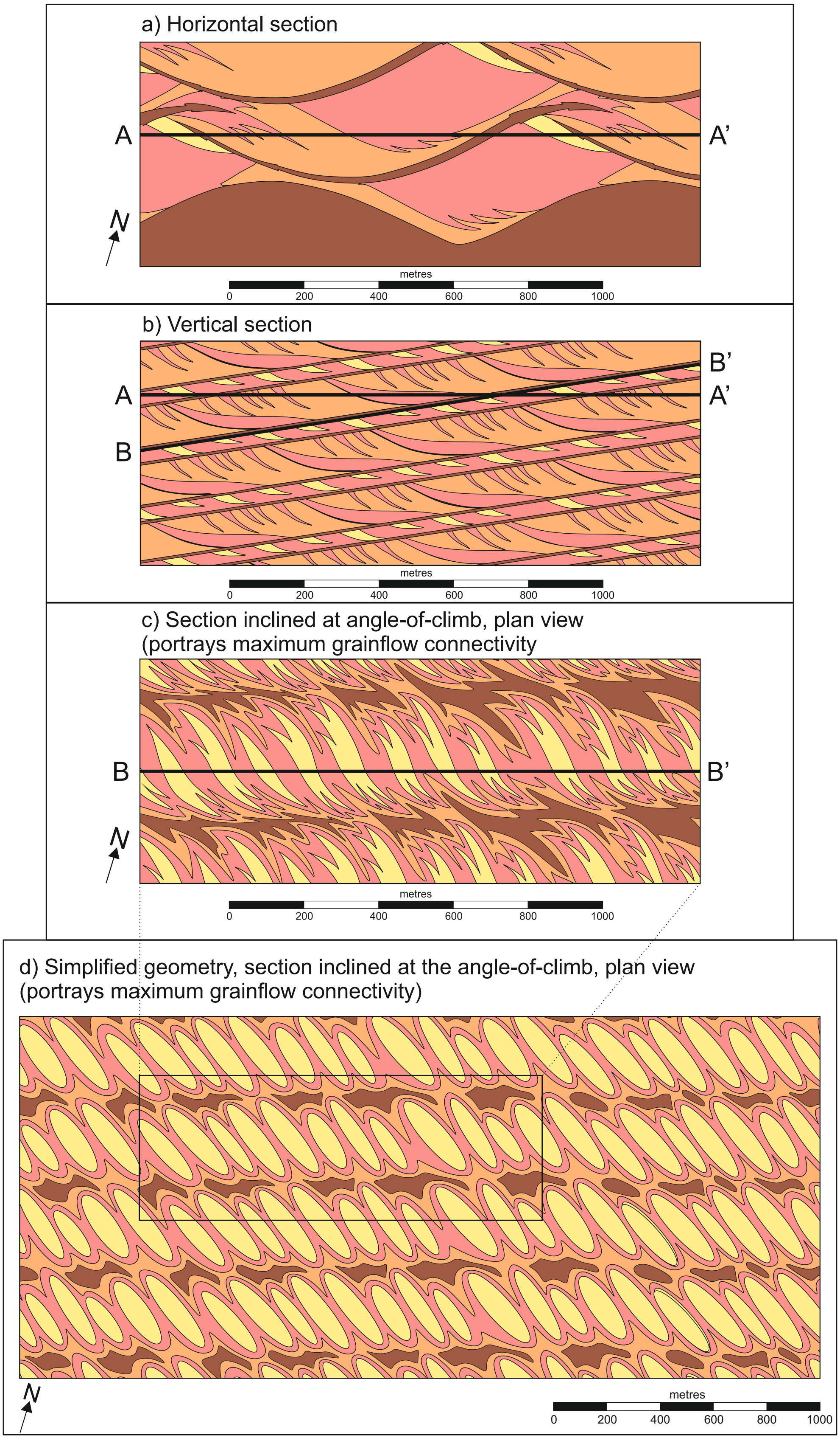

Figure 5.15. Geometry, scale and orientation of net reservoir units predicted by Auk Model 4: a) geometry seen in horizontal section under-plays the likely degree of connectivity of the linear dune grainflow units; b) vertical cross section illustrating maximum grainflow development in zone parallel to climbing upper bounding surface, and pinch-out of grainflow units in the middle part of the climbing cosets; c) plan view geometry seen in a section taken immediately beneath an interdune migration bounding surface and inclined at the angle-of-climb, portraying the likely maximum degree of connectivity of the grainflow units; d) resulting facies geometry simplified to geometric shapes for reservoir modelling purposes.

5.10 – Auk Formation Sedimentological Model 5

Auk Model 5 (Figure 5.16) generates bedforms with identical morphologies and with identical styles of migration to those in Auk Model 2 (Figure 5.7), however in Auk Model 5 the rate of accumulation varies temporally about a mean rate of 0.1 with an amplitude of 0.1, over a period of 100 (dimensionless time steps for modelling purposes – see Rubin (1987a) and Rubin and Carter (2006) for an explanation of the modelling terminology and algorithms). The input variables used for the modelling software are dimensionless, but spatial and temporal scales have subsequently been added to the models here. The scale is determined by the thickness of the preserved sets and cosets in Auk (Chapter 4) and also by the height, wavelength and spacing of dunes and interdunes considered to be representative analogues from modern systems. Input parameters used to generate this model are summarised in Figure 5.3.

5.10.1 – Facies distributions on bedforms

Systems that accumulate bedform deposits at temporally variable rates are common in nature (c.f. Mountney, 2012); this results in the preservation of cosets of aeolian dune strata that vary in thickness, and in doing so, control the extent to which net reservoir units (composed of facies which originated higher on bedform slopes) are preserved. Net reservoir facies (grainflow and grainflow-dominated) are more likely to be accumulated during episodes when the angle-of-climb attained its maximum value because this enables the middle and upper flanks of the migrating bedforms to be preserved. By contrast, they tend not be accumulated during episodes when the angle-of-climb is low and, under such circumstances, the preserved accumulation will be dominated by reworked wind-ripple, wind-ripple-dominated and wind-ripple facies which are representative of the interdune and lowermost linear dune plinth elements. Thus, the preserved distribution of net reservoir facies is controlled not only by the mean angle-of-climb, but also the amplitude and periodicity of its variation (Mountney, 2006a; 2012). A well-documented example of an essentially dry aeolian erg system that underwent a periodically changing angle-of-climb is the erg centre of the Permian Cedar Mesa Sandstone of SE Utah (Mountney, 2006b). Measurements demonstrating this variability are shown in Romain and Mountney (2014) and Chapter 2.

5.10.2 – Geometry and dimensions of stratigraphic architectural units

The variation in accumulation rate for Auk Model 5 has considerable implications for the distribution of units composed of net reservoir facies (Figure 5.17). In the section parallel to the transverse component of linear dune migration, it is evident that during periods of elevated angles-of-climb, facies developed on the upper flanks of the migrating aeolian bedforms, namely packages of grainfall and pure grainflow strata are accumulated and

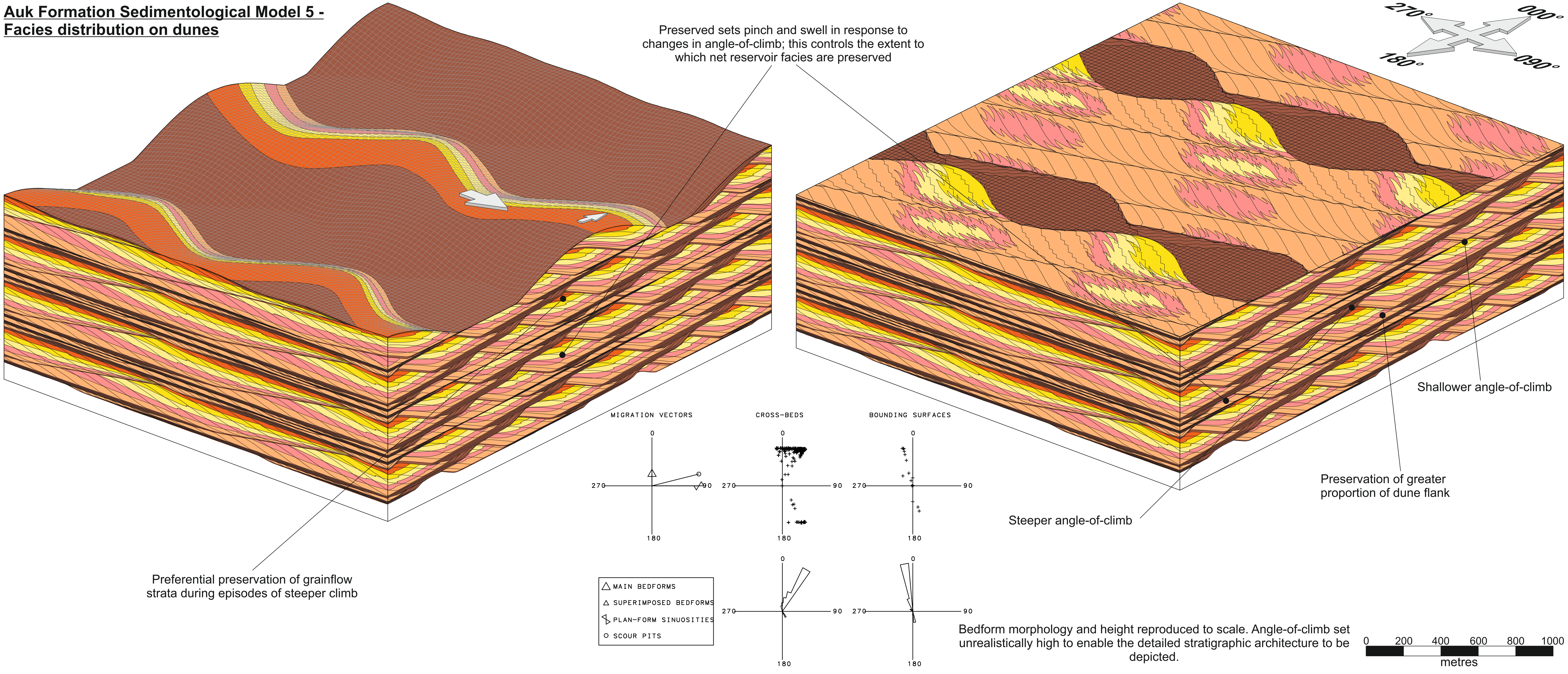

Preserved sets pinch and swell in response to changes in angle-of-climb; this controls the extent to which net reservoir facies are preserved

Preferential preservation of grainflow strata during episodes of steeper climb

Shallower angle-of-climb

Preservation of greater proportion of dune flank

Steeper angle-of-climb

Bedform morphology and height reproduced to scale. Angle-of-climb set unrealistically high to enable the detailed stratigraphic architecture to be depicted.

Figure 5.16. Auk Formation Sedimentological Model 5 (see Figure 5.3 for the input parameters used to generate this model). This model generates bedforms with identical morphologies and with identical styles of migration to those in Auk Model 2 (Figure 5.7) but here the rate of accumulation varies temporally about a mean rate of 0.1 with an amplitude of 0.1, over a period of 100 (dimensionless time steps for modelling purposes). This results in the preservation of cosets of aeolian dune strata that vary in thickness and, in doing so, control the extent to which net reservoir units, composed of facies which originated on the higher parts of bedform slopes, are preserved.

preserved. When the angle-of-climb is lower, these facies are no longer accumulated: in some cases sets are composed solely of wind-ripple-dominated facies encapsulated by pure wind-ripple strata – both of which would be expected to possess significantly less favourable reservoir quality than their grainflow-dominated counterparts. In Figure 5.17a, net reservoir facies range in length depending on the angle-of-climb, as discussed above, measured in this model as 100 m, 225 m, 325 m, 375 m and 300 m in length, measured parallel to the transverse component of linear dune migration. In Figure 5.17b, which depicts the geometry and stratigraphic architecture of net reservoir units in a section parallel to the along-crest component of linear dune migration, the grainflow-dominated, grainflow and grainfall components are approximately 1350 m in length when measured in this orientation, which is a similar geometry to the net reservoir facies depicted in Auk Model 1. However, in this example a greater proportion of the facies associated with the upper part of the dune flank are preserved compared to equivalent sections in Auk Model 1. In the horizontal section (Figure 5.17c) the variation in accumulation rate for this model is also apparent. Net reservoir facies are only documented in two places in the reservoir volume; a grainflow-dominated package measuring at 400 m in length, which is surrounded by a unit of reworked wind-ripple strata, and a combination of pure grainflow and grainflow-dominated strata which is again encapsulated by reworked wind-ripple facies and directly adjacent to a relatively impermeable barrier of pure wind-ripple strata, measuring around 550 m in length. The view in this horizontal section (Figure 5.17c) underplays the connectivity of the net reservoir units. This is because the flat upper surface of these grainflow units is inclined at the angle-of-climb, and therefore projects out of the section at a slight angle.

5.10.3 – Geometry, scale and orientation of net reservoir units

The geometry, scale and orientation of the net reservoir units depicted in Auk Model 5 are shown in Figure 5.18. As Figure 5.18a underplays the degree of connectivity of the net reservoir facies, Figure 5.18b depicts a vertical cross-section which illustrates the maximum likely grainflow development in a zone parallel to the angle-of-climb. The plan-view geometry of this depiction, for which the expected grainflow geometries are maximised, is shown in Figure 5.18c, and also in a simplified form in Figure 5.18d where the net reservoir facies are summarized as simplified geometric bodies for reservoir modelling purposes. Here, the grainflow-dominated stratal packages are inclined WNW-ESE in the arbitrary co-ordinate system used for the modelling exercise. The first has an approximate area of 1.98 x 10^5 m^2, with pure grainflow strata (5.5 x 10^4 m^2) surrounded by grainflow-dominated strata, and in turn encased in reworked wind-ripple strata. The second has only a grainflow-dominated component of net reservoir facies, again encapsulated by reworked wind-ripple strata. This unit measures 1.02 x 10^5 m^2. These net reservoir packages punctuate through a background of wind-ripple-dominated and pure wind-ripple facies, which acts as non-net reservoir.

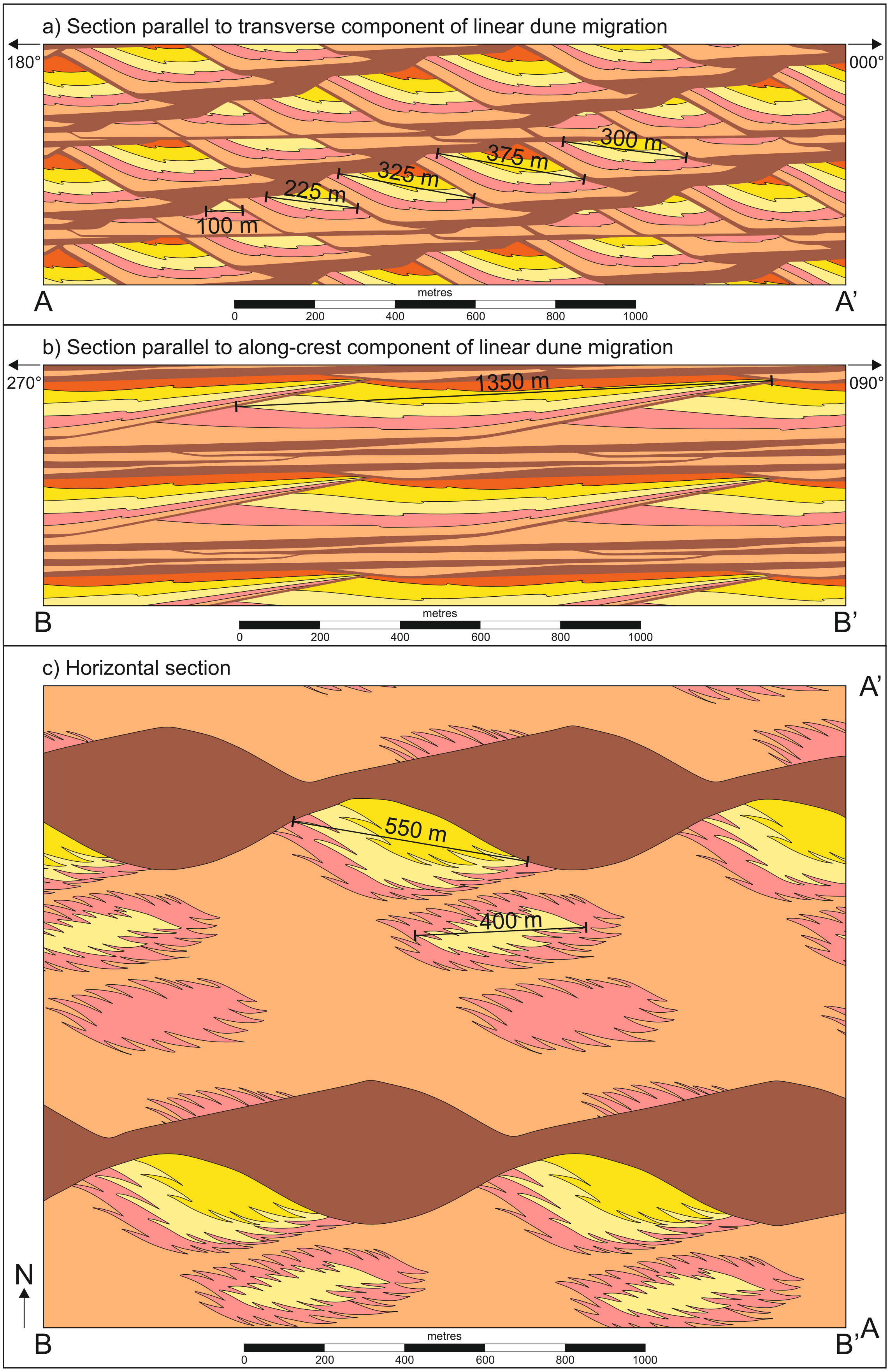

Figure 5.17. Stratigraphic architecture produced by Auk Model 5. Estimated geometry and dimensions of grainflow strata; note that the view in the horizontal section c) under-plays the degree to which grainflow tongues are interconnected because the flat upper surface of these sand bodies will be inclined at the angle-of-climb and are therefore projecting out of the horizontal section at a slight angle.

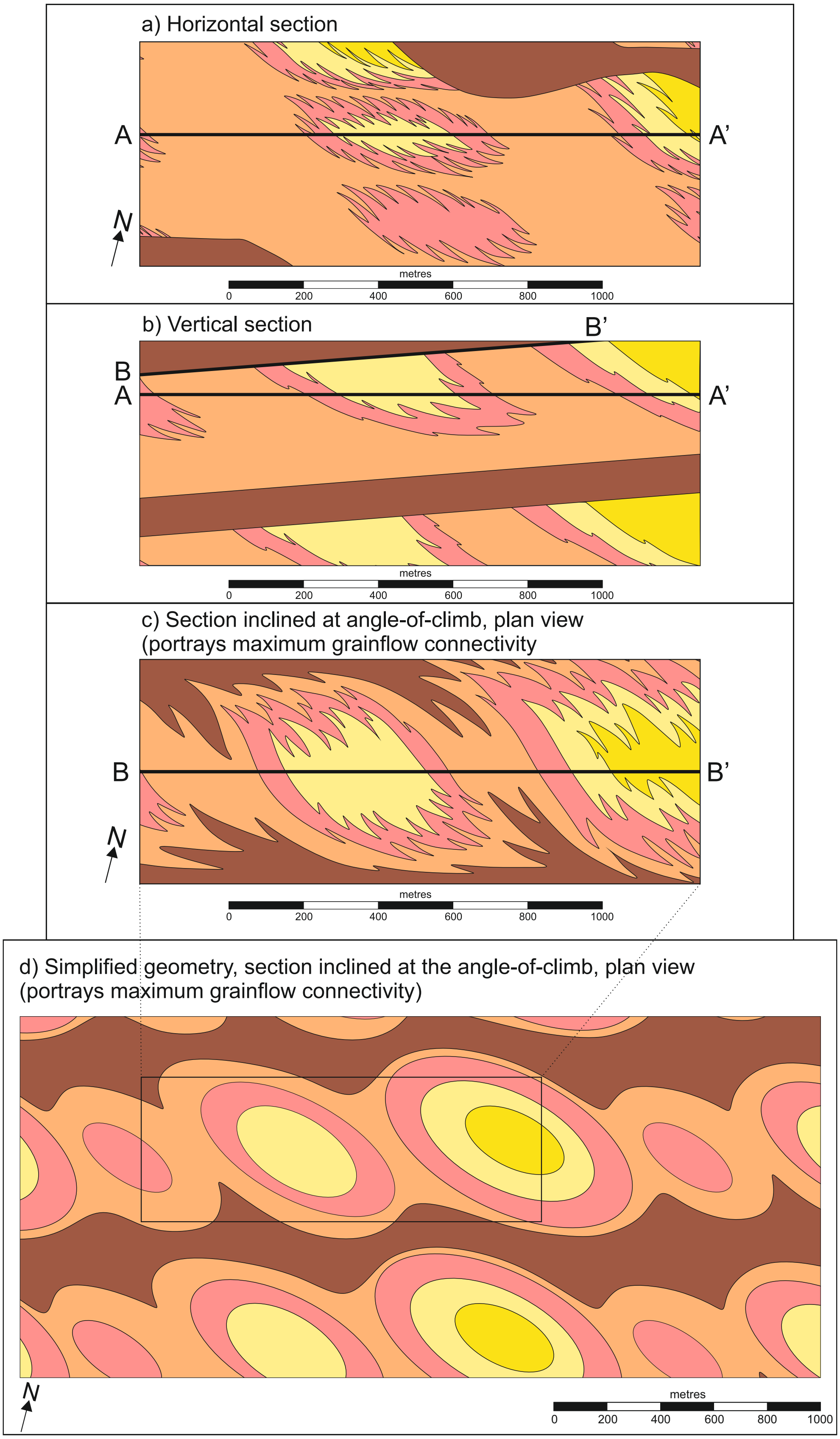

a) Horizontal section

b) Vertical section

c) Section inclined at angle-of-climb, plan view (portrays maximum grainflow connectivity

d) Simplified geometry, section inclined at the angle-of-climb, plan view (portrays maximum grainflow connectivity)

Figure 5.18. Geometry, scale and orientation of net reservoir units predicted by Auk Model 5: a) geometry seen in horizontal section under-plays the likely degree of connectivity of the linear dune grainflow units; b) vertical cross section illustrating maximum grainflow development in zone parallel to climbing upper bounding surface, and pinch-out of grainflow units in the middle part of the climbing cosets; c) plan view geometry seen in a section taken immediately beneath an interdune migration bounding surface and inclined at the angle-of-climb, portraying the likely maximum degree of connectivity of the grainflow units; d) resulting facies geometry simplified to geometric shapes for reservoir modelling purposes.

5.11 – Auk Formation Sedimentological Model 6

Auk Model 6 (Figure 5.19) introduces additional complexity to the relatively simple models 1-5 discussed previously. It simulates the migration of large linear bedforms with morphologies and styles of migration similar to those in Auk Model 2 (Figure 5.7), but replaces the elliptical interdune flats of that model with fields of obliquely migrating smaller barchanoid dunes within the lower-lying parts of the interdraa of the parent bedforms (see Chapter 4 for justification and Figures 4.12 and 4.15). Input parameters used to generate this model are summarised in Figure 5.3.

5.11.1 – Facies distribution on bedforms

In Auk Model 6, the large flat areas developed between the bedforms are referred to as interdraa areas (as opposed to interdune areas) because the large parent bedforms and their intervening depressions support superimposed bedforms at a smaller scale (see Wilson, 1971; 1972). These smaller superimposed bedforms are barchanoid forms, interpreted as such due to the presence in core of thinner sets of cross-strata dominated by more steeply-inclined cross-strata that are characterised by grainflow deposits, and with foreset azimuths that vary such that they demonstrate sinuous-crested (three-dimensional) bedforms that are typical of smaller barchanoid dunes. Where such sets occur stacked on top of each other, they most likely record the migration of trains of such dunes and therefore suggest the presence of a barchanoid dune field. In the Auk core where these smaller sets are present, they typically occur nested at the base of much thicker cosets that represent the larger linear draa. Thus the barchanoid dune sets may represent dunes that were present between larger migrating linear draa. Such relationships are seen in modern settings in areas such as the Namib Desert (Figure 4.12). A possible alternative interpretation is that the large linear draa deposits are genetically unrelated to the smaller barchanoid dune deposits and the two styles developed in response to different sand sediment budgets: the inference here being that the different types of deposits were therefore separated by supersurfaces (*sensu* Kocurek, 1988) and subsequently represent different aeolian sequences. However in the case of the Auk Formation dune forms, it is more likely that these were coeval barchanoid dune forms, as there is no difference in sediment grain size, petrography, provenance, or diagenesis between different dune types. There is also no evidence for any common supersurface features (e.g. polygonal cracks, coarse grain deflation lags, and rhizoliths - Mountney, 2006b; 2012). It is for these reasons that the interpretation of coeval barchanoid dune forms is the one considered below.

Migration of bedforms within these barchanoid dune fields that are present between the larger linear bedforms preserves units of stacked sets of small- and medium-scale cross stratification characterised by grainflow deposits. These are likely to be characterised by grainflow deposits, as barchanoid dunes commonly have small slipfaces that fully extend down their lee-slopes, and smaller dune-scale bedforms tend to climb at steeper angles

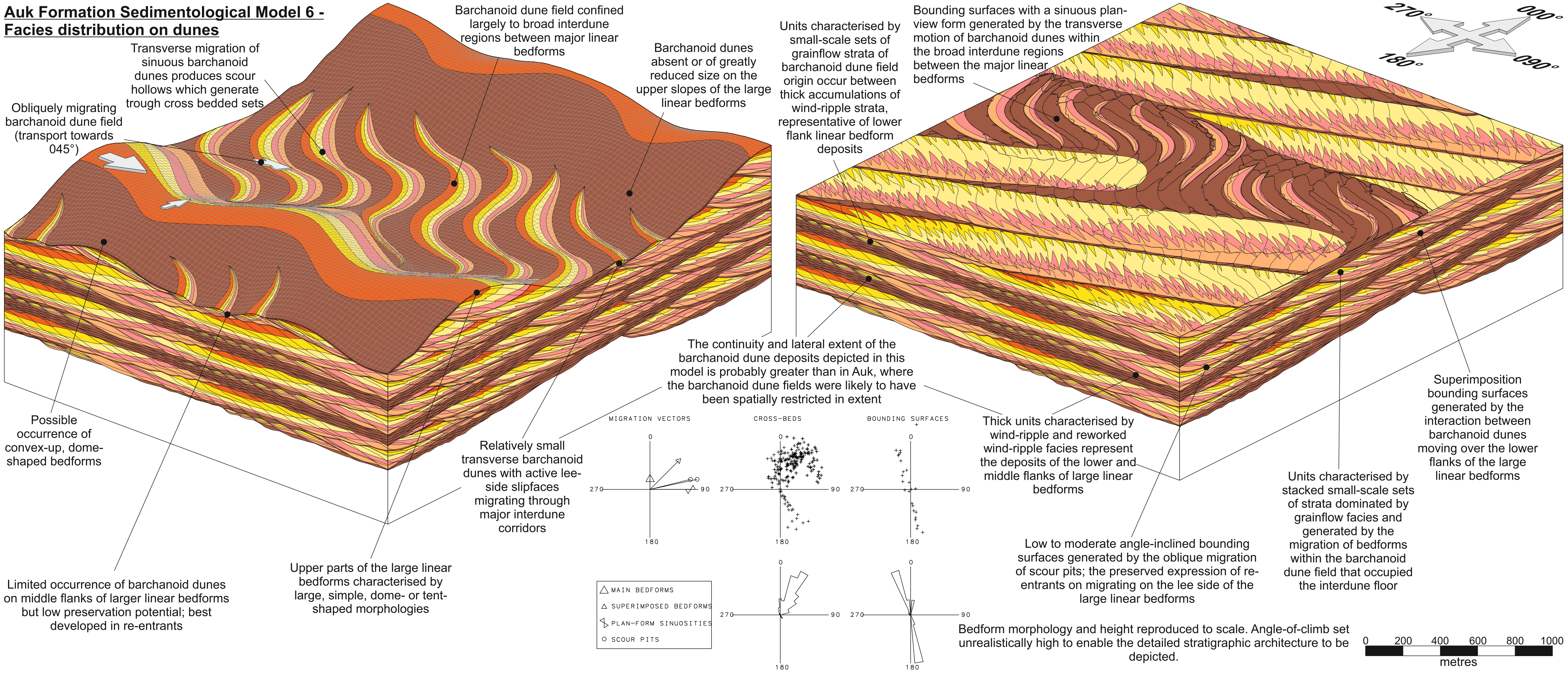

Figure 5.19. Auk Formation Sedimentological Model 6 (see Figure 5.3 for the input parameters used to generate this model). This model simulates the migration of large linear bedforms with morphologies and styles of migration similar to those in Auk Model 2 (Figure 5.7) but replaces the elliptical interdune flats of that model with fields of obliquely migrating smaller barchanoid dunes within the lower-lying parts of the of the interdraa of the parent bedforms. Migration of these barchanoid dune fields between the larger linear bedforms preserves units of stacked sets of small- and medium-scale cross stratification characterised by grainflow deposits. These are overlain by wind-ripple-dominated units of the larger linear bedforms.

(Romain and Mountney, 2014; Chapter 2). These grainflow deposits are overlain by wind-ripple-dominated units of the large linear bedforms (Figure 4.15).

In Figure 5.19, the obliquely migrating barchanoid dune field is migrating towards 045° (arbitrary orientation based on foreset dip-azimuth data relationships in core) and is largely confined to the broad interdraa regions between the major linear bedforms. The barchanoid dunes are absent, or of greatly reduced size, on the upper slopes of the large linear bedforms and are relatively small with active lee-side slipfaces. There is limited occurrence on the middle flanks of the large linear bedforms, but these have low preservation potential, they are best developed in the re-entrants. The transverse migration of barchanoid dunes with sinuous crestlines produces scour hollows that generate trough cross-bedded sets. The upper parts of the large linear bedforms are characterised by large, simple, dome- or tent-shaped morphologies.

In plan-view, bounding surfaces with a sinuous form are generated by the transverse motion of the barchanoid dunes within the broad interdraa regions between the major linear bedforms. In the vertical cross-sections of Figure 5.19, units characterised by small-scale sets of grainflow strata of barchanoid dune origin occur between thick accumulations of wind-ripple strata, representative of lower flank linear bedform deposits. The thick units characterised by wind-ripple and reworked wind-ripple facies represent the deposits of the lower and middle flanks of the same linear bedforms. Low-to-moderate-angle-inclined bounding surfaces are generated here by the oblique migration of scour pits, which are the preserved expression of re-entrants migrating on the lee-side of the large linear bedforms. The superimposition bounding surfaces (Kocurek, 1996) are generated by the interaction between barchanoid dunes moving over the lower flanks of the large linear bedforms.

5.11.2 – Geometry and dimensions of stratigraphic architectural units

The stratigraphic architecture depicted in Auk Model 6 is the most complex of all the models generated here for the Auk Formation. The addition of a barchanoid dune field migrating across the interdraa corridor of the main linear dune accumulation adds a considerable complexity to the distribution and size of the net reservoir units (Figure 5.20). In the section parallel to the transverse component of linear dune migration (Figure 5.20a), the net reservoir facies, in this case packages of grainflow and grainflow-dominated strata, vary in length between the preserved sets. They range from 175 to 450 m in length in this orientation, with the majority being approximately 300 m in length and incorporating a thin veneer of grainfall strata at their top. In the section parallel to the along-crest component of linear dune migration (Figure 5.20b), the lengths of elements composed of net reservoir facies also varies depending on which bedform type is encountered. Elements of net reservoir facies associated with the barchanoid-dune-field deposits are 100 to 175 m in length when measured parallel to the along-crest component of linear dune migration, whereas the units composed of net reservoir facies that are associated with the large linear bedforms are approximately 1200 m in length when measured in this orientation. Both types of package depict a mixture of grainflow and grainflow-dominated strata; whereas the packages associated with the large linear bedforms additionally encompass a minor component of preserved grainfall strata found as laminae separating successive grainflow deposits in core (Chapter 4).

The horizontal section (Figure 5.20c) underplays the connectivity of the grainflow units, and therefore shows the barchanoid dune field preserving only reworked wind-ripple and wind-ripple-dominated facies, with no grainflow or grainflow-dominated units. The net reservoir facies that are preserved in association with the large linear bedforms are elongate and continuous, with the preservation of the upper parts of the dune flank decreasing moving towards the pure wind-ripple strata in the interdraa corridors.

5.11.3 – Geometry, scale and orientation of net reservoir units

The horizontal sections depicted in Figure 5.20c and 5.21a underplay the degree of connectivity of the grainflow tongues. Rather than being horizontal, the planar upper surface of these sand bodies is inclined at the angle-of-climb of the system, and these bodies therefore project out of the horizontal section shown at a slight angle. Figure 5.21b shows a vertical cross-section to illustrate the maximum grainflow development in a zone parallel to the upper climbing bounding surface, which is shown in plan-view in Figure 5.21c. When these facies packages are simplified to basic geometric shapes (Figure 5.21d), it is apparent that Auk Model 6 produces a reservoir volume whereby net reservoir units are disconnected and arranged in a repetitive fashion, with a unit of reworked wind-ripple and wind-ripple-dominated strata between each of the net reservoir packages. The individual grainflow-dominated units have an approximate area of 5.2×10^4 m^2 in plan-view, and the pure grainflow units are 2.5×10^4 m^2. These packages are encapsulated by reworked wind-ripple and wind-ripple-dominated strata, which have detrimental implications for hydrocarbon fluid flow between the net reservoir packages in this part of the reservoir.

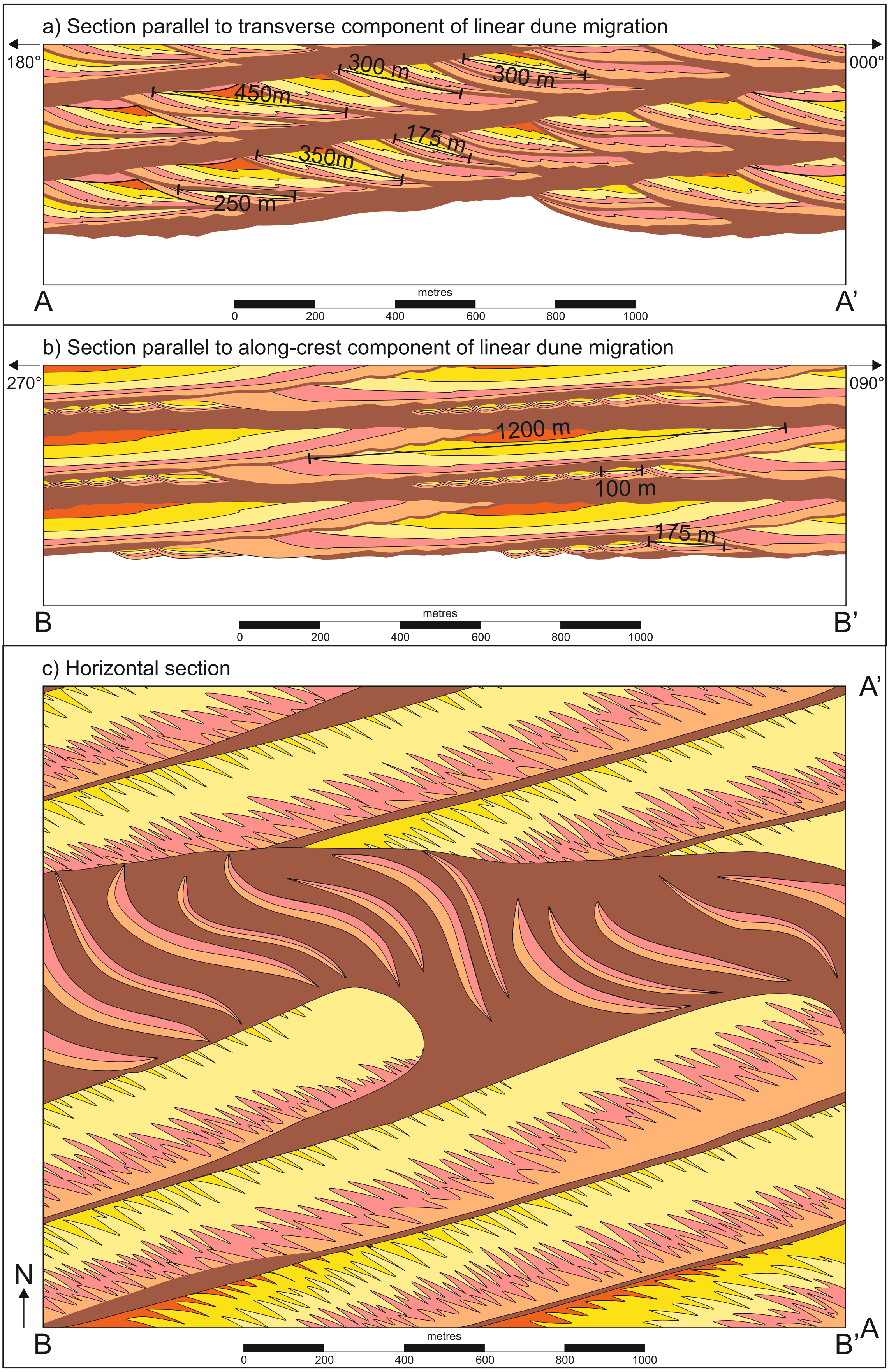

Figure 5.20. Stratigraphic architecture produced by Auk Model 6. Estimated geometry and dimensions of grainflow strata; note that the view in the horizontal section (c) under-plays the degree to which grainflow tongues are interconnected because the flat upper surface of these sand bodies will be inclined at the angle-of-climb and are therefore projecting out of the horizontal section at a slight angle.

a) Horizontal section

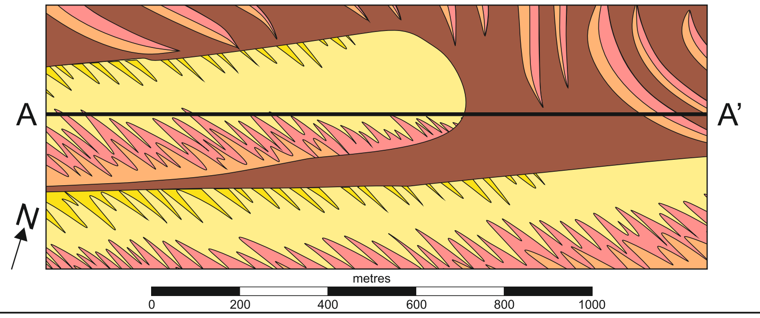

b) Vertical section

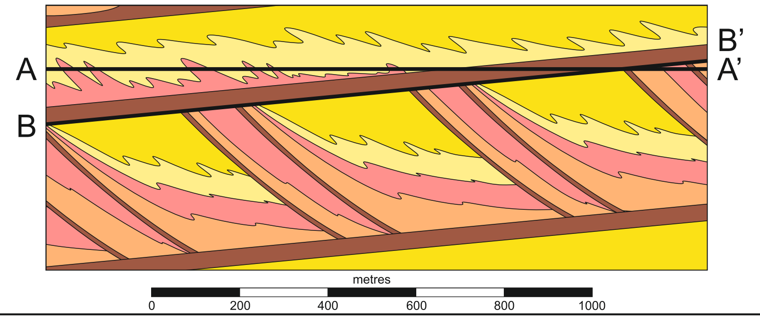

c) Section inclined at angle-of-climb, plan view
(portrays maximum grainflow connectivity

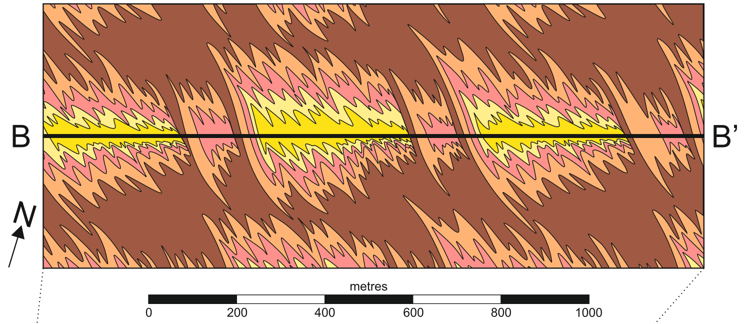

d) Simplified geometry, section inclined at the angle-of-climb, plan view
(portrays maximum grainflow connectivity)

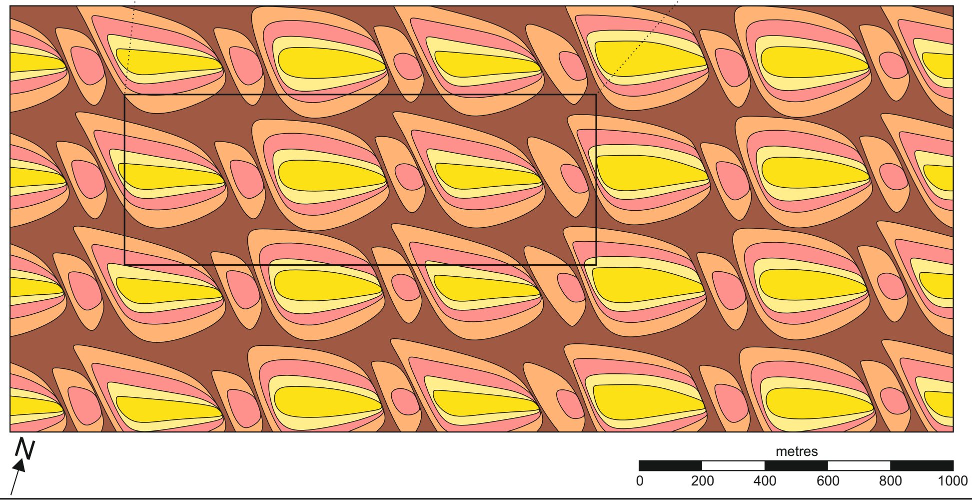

Figure 5.21. Geometry, scale and orientation of net reservoir units predicted by Auk Model 6: a) geometry seen in horizontal section under-plays the likely degree of connectivity of the linear dune grainflow units; b) vertical cross section illustrating maximum grainflow development in zone parallel to climbing upper bounding surface, and pinch-out of grainflow units in the middle part of the climbing cosets; c) plan view geometry seen in a section taken immediately beneath an interdune migration bounding surface and inclined at the angle-of-climb, portraying the likely maximum degree of connectivity of the grainflow units; d) resulting facies geometry simplified to geometric shapes for reservoir modelling purposes.

5.12 – Re-orientation of directional data in the Auk Formation

As discussed above, spatial and temporal units within the models produced by the software are dimensionless, which enables the modelled output to be retrospectively scaled according to dimensional data present in the primary dataset. Foreset dip-azimuths were analysed in an attempt to determine the prevailing palaeowind direction(s) and identify any preferred elongation of reservoir bodies.

Model outputs have been retrospectively re-oriented by matching to directional data present in the primary subsurface dataset (e.g. dip-azimuth data derived from core) (Figure 5.22). Orientations used in the modelling process described previously refer to the modelling co-ordinate system unless otherwise stated, but by using the dip-azimuth data derived from core, these can be re-oriented to give an insight into the original palaeowind direction and reservoir body orientation in the subsurface.

5.12.1 – Orientation and aspect ratios of bodies

The reservoir bodies modelled by the semi-quantitative forward modelling take the form of oblate ellipsoids, possibly approaching circular disc-shaped forms when appropriately projected onto a surface parallel to the climb angle of the dune system (Figure 5.22a). The elongation direction of the ellipsoid is sub-parallel to the trace of the lee-side re-entrant section of the sinuous linear dune crestline (Figure 5.22b). The semi-quantitative models include an analysis of cross bed dip-azimuths (Figures 5.4, 5.7, 5.10, 5.13, 5.16 and 5.19). These show an obvious relationship with the orientation of the slipface packages and the elongation of the resulting reservoir body ellipsoids (Figure 5.22b). The elongation of the ellipsoids is sub-parallel to the direction of elongation of the major linear dune, rotated by 15° - 20°. Given the general lack of dipmeter data in the field, an attempt has been made from such data as are available to establish overall palaeowind directions for the Auk Field, for use as a guide to reservoir body orientation.

5.12.2 – Palaeowind directions and reservoir body orientation

All dipmeter and image dip-azimuth data, initially collected by Bernard Besly with contributions from Nigel Mountney, have been grouped by linear dune growth cycles, determined by bounding surfaces in the wells which are formed by dune migration, to obtain averaged palaeowind directions using the approach illustrated in Figure 5.22c. Thirty linear dune cycles were interpreted, and grouped into Dune Cycle Zones 20-25, 25-30, 30-35, 35-40 and 40-50. The results from 2 Dune Cycles Zones, Dune Cycle Zone 20-25 and Dune Cycle Zone 40-50 are illustrated in Figure 5.23.

Interpretation of the azimuth roses relies on the notional wind directions generated by the numerical forward modelling (Figures 5.4, 5.7, 5.10, 5.13, 5.16 and 5.19). In most cases, it is possible to derive fairly consistent wind directions assuming that not all the dunes had

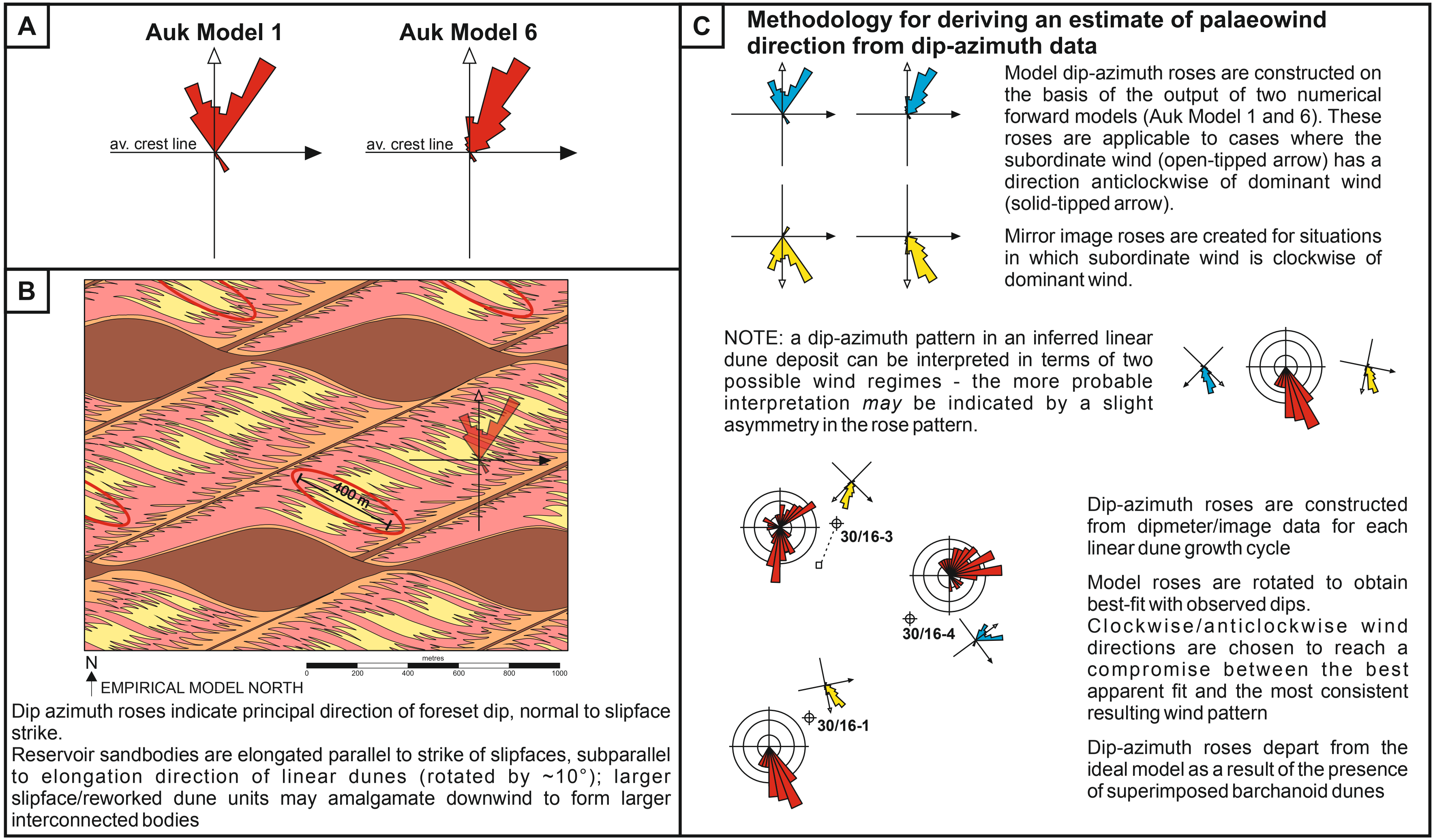

Dip azimuth roses indicate principal direction of foreset dip, normal to slipface strike.

Reservoir sandbodies are elongated parallel to strike of slipfaces, subparallel to elongation direction of linear dunes (rotated by ~10°); larger slipface/reworked dune units may amalgamate downwind to form larger interconnected bodies

Methodology for deriving an estimate of palaeowind direction from dip-azimuth data

Model dip-azimuth roses are constructed on the basis of the output of two numerical forward models (Auk Model 1 and 6). These roses are applicable to cases where the subordinate wind (open-tipped arrow) has a direction anticlockwise of dominant wind (solid-tipped arrow).

Mirror image roses are created for situations in which subordinate wind is clockwise of dominant wind.

NOTE: a dip-azimuth pattern in an inferred linear dune deposit can be interpreted in terms of two possible wind regimes - the more probable interpretation *may* be indicated by a slight asymmetry in the rose pattern.

Dip-azimuth roses are constructed from dipmeter/image data for each linear dune growth cycle

Model roses are rotated to obtain best-fit with observed dips. Clockwise/anticlockwise wind directions are chosen to reach a compromise between the best apparent fit and the most consistent resulting wind pattern

Dip-azimuth roses depart from the ideal model as a result of the presence of superimposed barchanoid dunes

Figure 5.22. Illustration of relationships between linear dune facies architecture, dip-azimuth data and reservoir body orientation: a) palaeocurrent roses derived from numerical forward modelling; b) plan view cross-section through Auk Model 1 showing relationship of dip-azimuths to net reservoir body orientation; c) methodology for deriving palaeowind directions from dipmeter and image log dip- azimuth data.

the same sense of flank accretion. If fairly consistent dominant winds are assumed, flank accretion reflects subordinate winds that showed varied directions, giving rise to accretion in both clockwise and anticlockwise directions relative to the main axis of dune elongation. The complexity of desert wind systems, particularly secondary circulation systems, does not make this an impossible suggestion. Alternatively, these results may indicate the presence of more star-like dune forms than have hitherto been suggested, having complex flank accretion patterns. If simple linear dunes are invoked with accretion on both flanks, the dominant wind directions are from the NW–N, with a subsidiary wind direction from the SW, particularly in Dune Cycle Zone 20-25 (Figure 5.23a).

Both of these palaeo-wind directions suggest dominant patterns of linear dune elongation lying between NW-SE and N-S, with directions possibly swinging round more to more NE-SW in Dune Cycle Zone 20-25 (Figure 5.23a) and Dune Cycle Zone 40-50 (Figure 5.23b), and subordinate bodies trending more or less W-E in some cycles. Having established generalised dune axis elongation directions and the sense of accretion of the dune foresets, the long axis elongation of the reservoir bodies can be inferred from the relationship illustrated in Figure 5.22b; the ellipsoids having a rotation of approximately 10° relative to dune long axis.

5.13 – Conclusions

Results from forward stratigraphic modelling exercises demonstrate that a range of interpretations regarding the likely internal facies architecture of the Permian Auk Formation of the Central North Sea are plausible. Stratigraphic modelling results predict expected three-dimensional geometries and facies distributions, and therefore the subsurface architecture of the succession. Results are constrained by comparison of the modelled stratigraphy to observations of key features identified in the core and wireline log data.

The application of numerical modelling techniques to simulate bedform behaviour and resultant preserved stratigraphic architecture has led to the development of six depositional models, enabling estimation of the likely geometry, scale and degree of interconnectivity of net reservoir facies within three-dimensional space. The models presented here illustrate how subtle variations in controlling parameters can have significant effects on the distribution of net reservoir facies. This approach to the documentation of the range of likely sand-body dimensions is important for constraining inputs used in aeolian reservoir modelling workflows. The technique is especially valuable in reservoir successions for which core data do not necessarily provide direct insight regarding sand-body geometry, orientation and style of interconnectivity. The method developed here is both novel and innovative and can potentially be applied to other preserved aeolian successions from both outcrop and subsurface deposits.

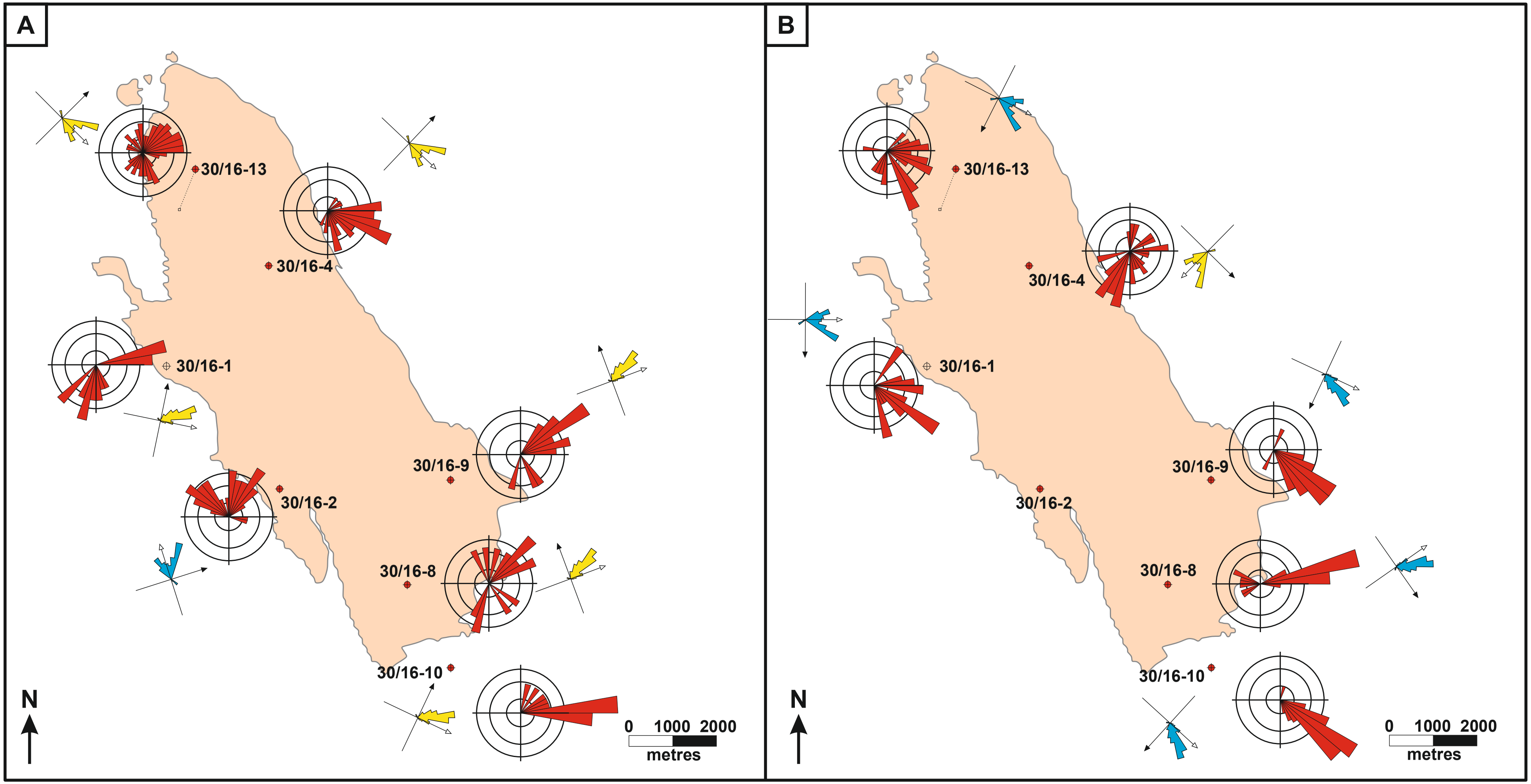

Figure 5.23. Grouped dipmeter dip-azimuth data for well penetrations in the Auk Field, with conceptual palaeowind regime. See Figure 5.22c for methodology used for deriving palaeowind directions from dip-azimuth data. Red well symbol indicate cored wells: a) Dune Cycle Zone 20-25 – dip-azimuths dominantly between 050° and 120°, dominant wind direction WSW – ENE; b) Dune Cycle Zone 40-50 – dominant dip-azimuths between dips to ENE and SSW, wind direction between NW – SE and NE – SW. Original foreset dip-azimuth data obtained by Bernard Besly with contributions from Nigel Mountney; interpretation and significance of trends undertaken by Hollie Romain.

Chapter 6 – Synthesis and Key Advances

6.1 – Relating preserved aeolian bed-set architecture to original bedform morphology and behaviour

A key research issue that has been the focus of several recent studies of aeolian successions is how ancient preserved sets of aeolian strata can be related to the morphology and migratory behaviour of the original bedforms, and to the conditions that enabled accumulation and preservation. Are there any key observations that can be made in outcropping aeolian successions or cored intervals from the subsurface to enable the informed reconstruction of original aeolian dune type and morphology, and the style in which the bedforms undertook migration and accumulation? This synthesis chapter is focused on the integration of the interpretations presented previously in Chapters 2-5, in a view to better understand the wider applied implications of the specific research ideas developed earlier in the thesis.

6.1.1 – Empirical relationships

Chapter 2 introduced an outcrop-based study that successfully identified key empirical relationships between measurements of small-scale aeolian architecture from a number of outcrop studies in SE Utah. Such empirical relationships can be used to derive a number of details of aeolian architecture in the subsurface not directly observable in core data. By using these empirical relationships, a relatively small number of observable parameters – chiefly preserved set thickness, the thickness of grainflow units, the shape of dune toesets and their style of interaction with deposits of underlying interdune elements, the rate of upward-steepening of foresets within a set, the distribution of the occurrence of reactivation surfaces within cosets, and the distribution of primary lithofacies (grainflow, wind-ripple, and grainfall) within sets – can be collectively used to reconstruct likely larger-scale sedimentary architecture and therefore regional reservoir-scale stratigraphic heterogeneity (Figure 6.1).

There are several ways in which extrapolating three-dimensional architectures of aeolian stratigraphy can be used to make wider interpretations on the nature of a subsurface reservoir interval. Specifically, the identification of relationships between grainflow thickness, length and width is important because it allows the three-dimensional reconstruction of the expected geometry of grainflow sediment packages, considered net reservoir based on porosity and permeability measurements from existing aeolian fields (Figure 1.18; Figure 1.19), solely from a measurement of their thicknesses preserved in core. This is important for modelling lamina- and bed-scale heterogeneity, directional permeability and a more informed calculation of expected net reservoir quantities in aeolian reservoirs (Weber, 1982; 1986; 1987; Chandler et al., 1989; Krystinik, 1990).

Preserved set thickness in cored intervals can also yield information on the subsequent quality of the reservoir interval. By preserving thicker sets, it would be expected that a larger proportion of facies which originated from higher up the dune lee slope would be preserved, such as grainflow and grainflow-dominated facies considered net reservoir, meaning that the overall quality of the reservoir interval would be more favourable than reservoirs that are comprised of thinner preserved sets. However, despite preserved set thickness being only partly dependent on original dune wavelength (it is also dependant on the angle-of-climb of the bedforms), for the studied successions in Chapter 2 a clear positive relationship exists between preserved set thickness and dune wavelength (Figure 2.7b; Figure 6.1a). It is reasonable to expect that these larger bedforms would have lower angle-inclined dune plinths, geometries which are a characteristic of many large modern bedforms, and in preserved successions such as the bedforms which migrated and accumulated to preserve the Auk Formation (Chapter 4; Section 4.5.4). In these cases, grainflow avalanches rarely reach the base of set, and terminate relatively high on the lee slopes of the actively migrating bedforms. Consequently, relatively thick preserved sets can potentially comprise predominantly, or even exclusively, wind-rippled facies of various types, considered non-net reservoir in this study. Preserving thicker sets in aeolian reservoir successions therefore does not directly imply a higher quality reservoir interval.

6.1.1.1 – Key advances

A suite of empirical relationships have been developed which enable parameters measured directly from one-dimensional core to be related to larger-scale aeolian architectural elements observable in outcrop successions. This underpins a simple method for reconstructing three-dimensional aeolian geometries in the subsurface from one-dimensional subsurface datasets alone, such as the three-dimensional reconstruction of the expected geometry of net reservoir grainflow sediment packages. This study has revealed relationships between measurements of small- and larger-scale aspects of sedimentary architecture, and these relationships form the basis for the development of a predictive tool that can be applied to subsurface datasets for the prediction of regional reservoir stratigraphic heterogeneity, and overall net reservoir quantities in subsurface intervals. This is discussed further in Section 6.2.

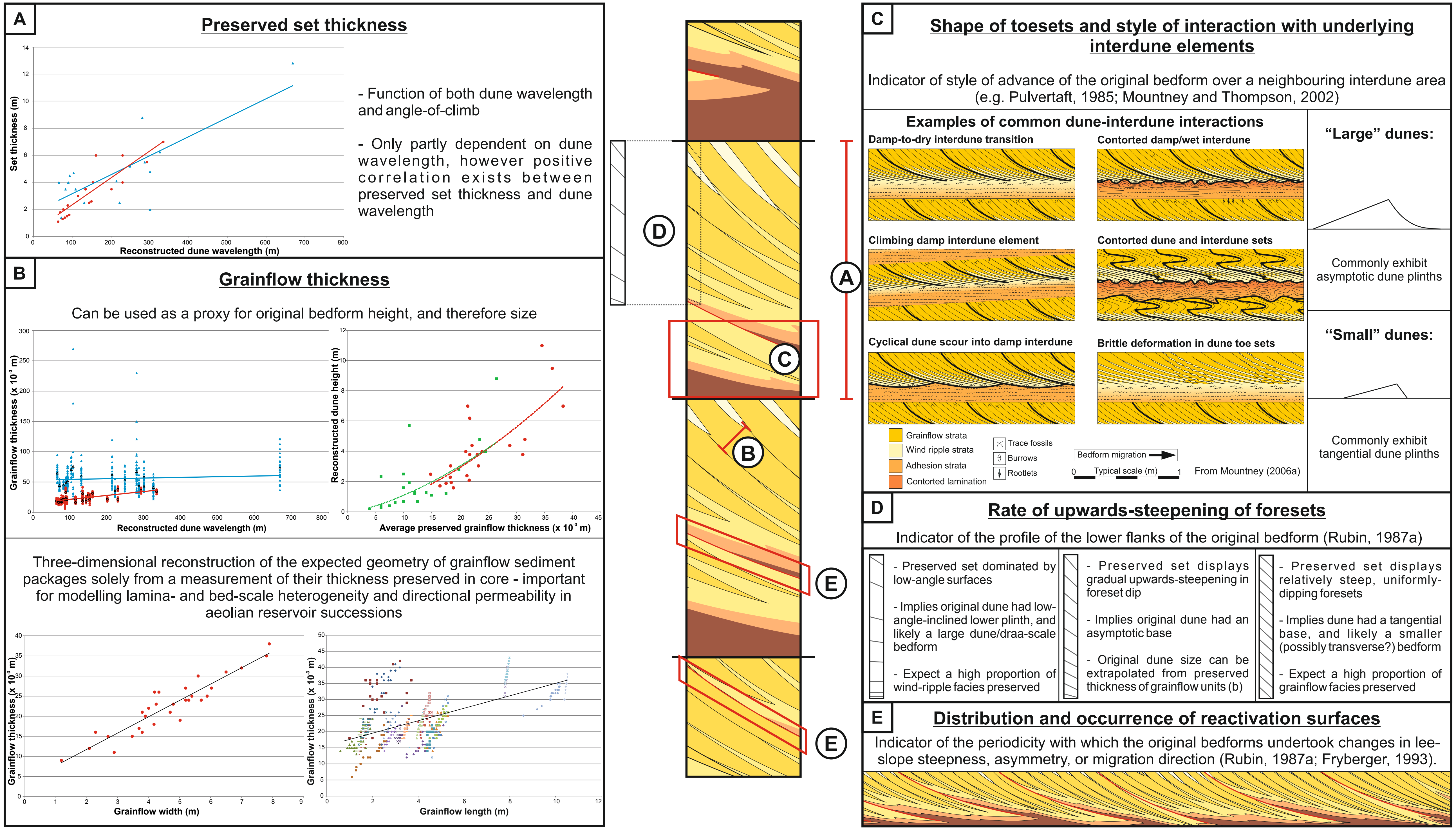

- Function of both dune wavelength and angle-of-climb

- Only partly dependent on dune wavelength, however positive correlation exists between preserved set thickness and dune wavelength

Can be used as a proxy for original bedform height, and therefore size

Three-dimensional reconstruction of the expected geometry of grainflow sediment packages solely from a measurement of their thickness preserved in core - important for modelling lamina- and bed-scale heterogeneity and directional permeability in aeolian reservoir successions

Indicator of style of advance of the original bedform over a neighbouring interdune area (e.g. Pulvertaft, 1985; Mountney and Thompson, 2002)

Commonly exhibit asymptotic dune plinths

Commonly exhibit tangential dune plinths

From Mountney (2006a)

Indicator of the profile of the lower flanks of the original bedform (Rubin, 1987a)

- Preserved set dominated by low-angle surfaces

- Implies original dune had low-angle-inclined lower plinth, and likely a large dune/draa-scale bedform

- Expect a high proportion of wind-ripple facies preserved

- Preserved set displays gradual upwards-steepening in foreset dip

- Implies original dune had an asymptotic base

- Original dune size can be extrapolated from preserved thickness of grainflow units (b)

- Preserved set displays relatively steep, uniformly-dipping foresets

- Implies dune had a tangential base, and likely a smaller (possibly transverse?) bedform

- Expect a high proportion of grainflow facies preserved

Indicator of the periodicity with which the original bedforms undertook changes in lee-slope steepness, asymmetry, or migration direction (Rubin, 1987a; Fryberger, 1993).

Figure 6.1. Methods for reconstructing likely three-dimensional aeolian dune architecture from one-dimensional core data. The small number of observable parameters from aeolian cored intervals can all be used to reconstruct likely larger-scale sedimentary architecture and therefore regional reservoir stratigraphic heterogeneity. Common observable parameters from core; a) preserved set thickness; b) grainflow thickness; c) shape of dune toesets and style of interaction with underlying interdune elements; d) rate of upwards-steepening of foresets within a set; and e) distribution and occurrence of reactivation surfaces within cosets. The distributions of primary aeolian lithofacies within preserved sets, and subsequent implications on original bedform architecture, will be considered separately in Section 6.1.3. Graphical data presented for preserved set thickness and grainflow thickness from Romain and Mountney (2014).

6.1.2 – Theoretical cores from bedform models

Given that a large proportion of data relating to the subsurface expression of aeolian bedforms is one-dimensional in nature, and that the vast majority of this one-dimensional data are well logs and cored intervals, it is pertinent to examine in detail the information that can be extracted from these cored intervals and investigate any key parameters which can be used in the determination of original aeolian bedform type and style of migratory behaviour. Both original bedform type and style of migratory behaviour can have significant implications on the overall quality of aeolian reservoir intervals, and this is explored further in Section 6.2.

One of the most readily identifiable features that can be directly measured in cored intervals is the foreset dip-azimuth distributions for cross-bedded strata representative of accumulated aeolian bedforms. Transverse bedforms represent the accretion of sediment on a dune lee-slope that migrated consistently in a favoured direction (McKee, 1979a), suggesting that such bedforms would generate a tightly-clustered range of foreset dip-azimuths. McKee (1979b, p. 194) states that “the amount of spread and distribution of cross-strata dip directions are perhaps the most satisfactory features for differentiating types of dunes in ancient rocks”, implying that original dune type can be directly related to the dip-azimuth plot for the succession.

However, because linear dunes have now been unequivocally demonstrated to undertake lateral creep in a transverse motion relative to their crestline orientation (Rubin and Hunter, 1985; Bristow et al., 2000), such bedforms are now known to be capable of accumulating foresets whose dip-azimuth plots are considerably narrower in their range than previously envisaged. Techniques used previously (e.g. identifying linear dunes by a wide spread in foreset dip-azimuth data) are unreliable (Rubin and Hunter, 1985), as the minor component of transverse motion envisaged for the majority of linear bedforms can preserve foreset dip-azimuths that are almost identical to those preserved by transverse bedforms (Figure 1.3). Linear bedforms could also have azimuths that are in orientations oblique to the dominant wind direction (Scherer, 2000). Furthermore, the spread of dip-azimuth data generated by the accumulation of dune lee-slope deposits via migration are dependent on a number of other features, such as crestline sinuosity and shape and behaviour of any superimposed dunes; dip-azimuths are therefore unlikely to represent a straightforward indicator of wind variability (Rubin and Hunter, 1985), rather they simply indicate the resultant sand drift direction of the moving bedform.

6.1.2.1 – Aims and objectives: theoretical cores

The synthesis presented in this chapter is based upon a further interrogation of a selection of bedform models previously presented in Chapters 3 and 5. The aim of this study, whereby pseudo-cores and subsequent foreset dip-azimuth plots have been generated from the original bedform models, was to demonstrate that bedforms of different architectures can yield almost identical foreset dip-azimuths in core data, and conversely that bedforms of an identical type can yield very different foreset dip-azimuths, often over very short distances, depending on how they are intersected and sampled (see Figure 4.1 for a theoretical example from the Auk Formation). Although foreset dip-azimuth distributions alone are not necessarily a diagnostic feature of aeolian bedform type, subtle trends do exist, and this is explored further in Section 6.1.2.7.

6.1.2.2 – Methodology: theoretical cores

The bedform models chosen from Chapter 3 are those of perfectly transverse bedforms, generating trough-cross bedding in the section parallel to the trend of the bedform (Figure 6.2a – Sedimentological Model 3, Section 3.8); and perfectly linear bedforms with along-crest migrating sinuosities (Figure 6.3a – Sedimentological Model 5, Section 3.10). Given the current understanding that linear dunes almost always invoke a minor component of lateral movement, allowing them to generate foreset dip-azimuth plots that are almost impossible to distinguish from transverse bedforms, the Auk Formation Sedimentological Model 2 from Chapter 5 has been interrogated in the same manner as above to demonstrate how these bedforms can generate foreset dip-azimuth distributions which are largely the same as those produced for transverse bedforms. This model depicts linear bedforms with a minor component of transverse motion (Figure 6.4a – Auk Sedimentological Model 2, Section 5.7). A further bedform model of the Auk Formation from Chapter 5 (Figure 6.5a – Auk Formation Sedimentological Model 6, Section 5.11), depicting linear bedforms with the same morphology and style of migratory behaviour as Auk Model 2, but with the addition of a barchanoid dune field migrating through the interdune corridors, was also interrogated in the aforementioned manner to investigate how the additional complexity of this model affects the resultant foreset dip-azimuth plots.

For each bedform model, transects were taken in sections perpendicular and parallel to the trend of the main bedforms, and in two opposing sections oriented obliquely to the migration direction of the main bedforms to investigate the effect, if any, of minor variations in bedform migration direction on the resultant preserved stratigraphy and to allow for a more informed interrogation of the data in a more realistic scenario, as cores and outcrop data are highly unlikely to fall in perfectly parallel or perpendicular transects. The theoretical foreset dip-azimuths were generated from a series of pseudo-cores (56 cores in total) from the perpendicular, parallel and oblique transects, displaying the expected preserved facies arrangements and subsequent foreset dip-azimuth data. The foreset dip-azimuth plots discussed here were generated solely from the accumulated sets that were truncated by successive dunes, and foreset dip-azimuth data from "modern" (i.e. actively migrating) parts of dunes were not included. The pseudo-cores have been used to generate not only the foreset dip-azimuths discussed in this section, but also used to calculate net reservoir distributions for the bedform models (see Section 6.2.1). A discussion of the predicted reservoir quality from each of these models is outlined in Section 6.2.

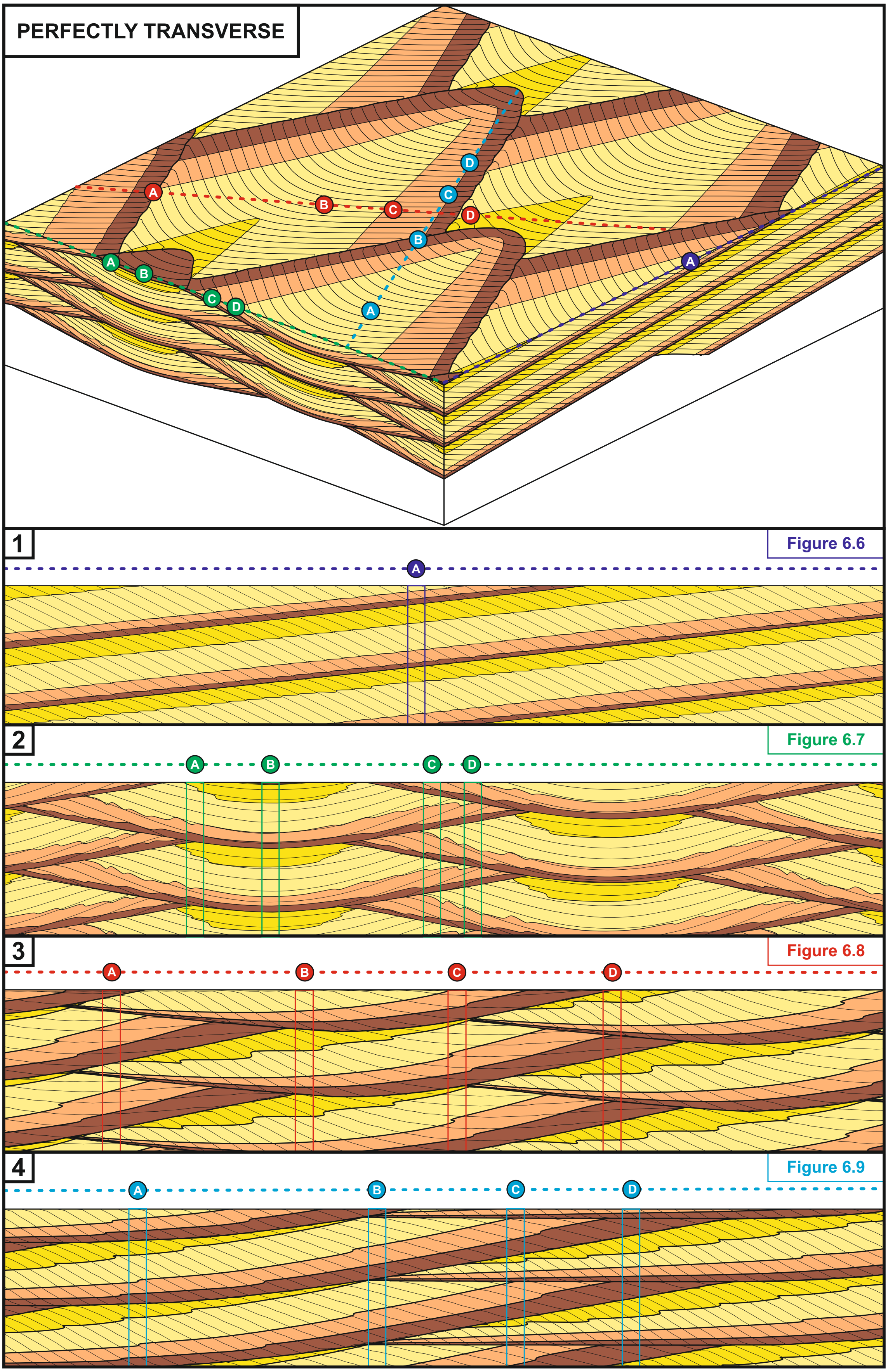

Figure 6.2a. Perfectly transverse bedform model from Chapter 3 showing positions of cross-sections used to generate pseudo-cores: 1) section perpendicular to trend of main bedforms; 2) section parallel to trend of main bedforms; 3) and 4) sections oblique to trend of main bedforms.

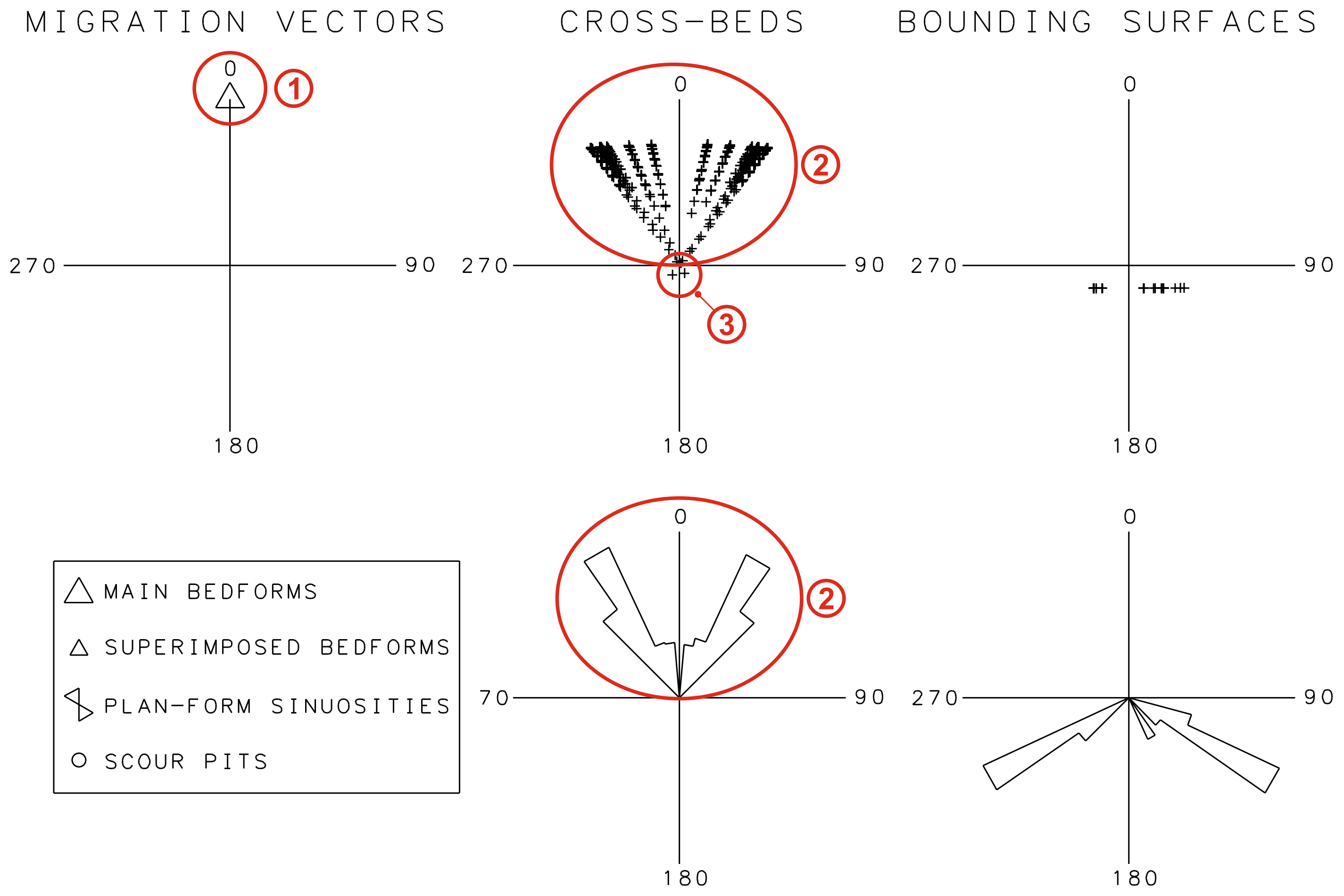

Figure 6.2b. Bedform migration and stratal azimuth plot for the perfectly transverse bedform model, generated by the modelling software developed by David Rubin (Rubin, 1987a): 1) primary component of migration towards 000°; 2) overall foreset dip-azimuth distribution is bimodal; 3) minor switch in foreset dip-azimuth direction likely reflects the rare preservation of stoss-side wind-ripple strata.

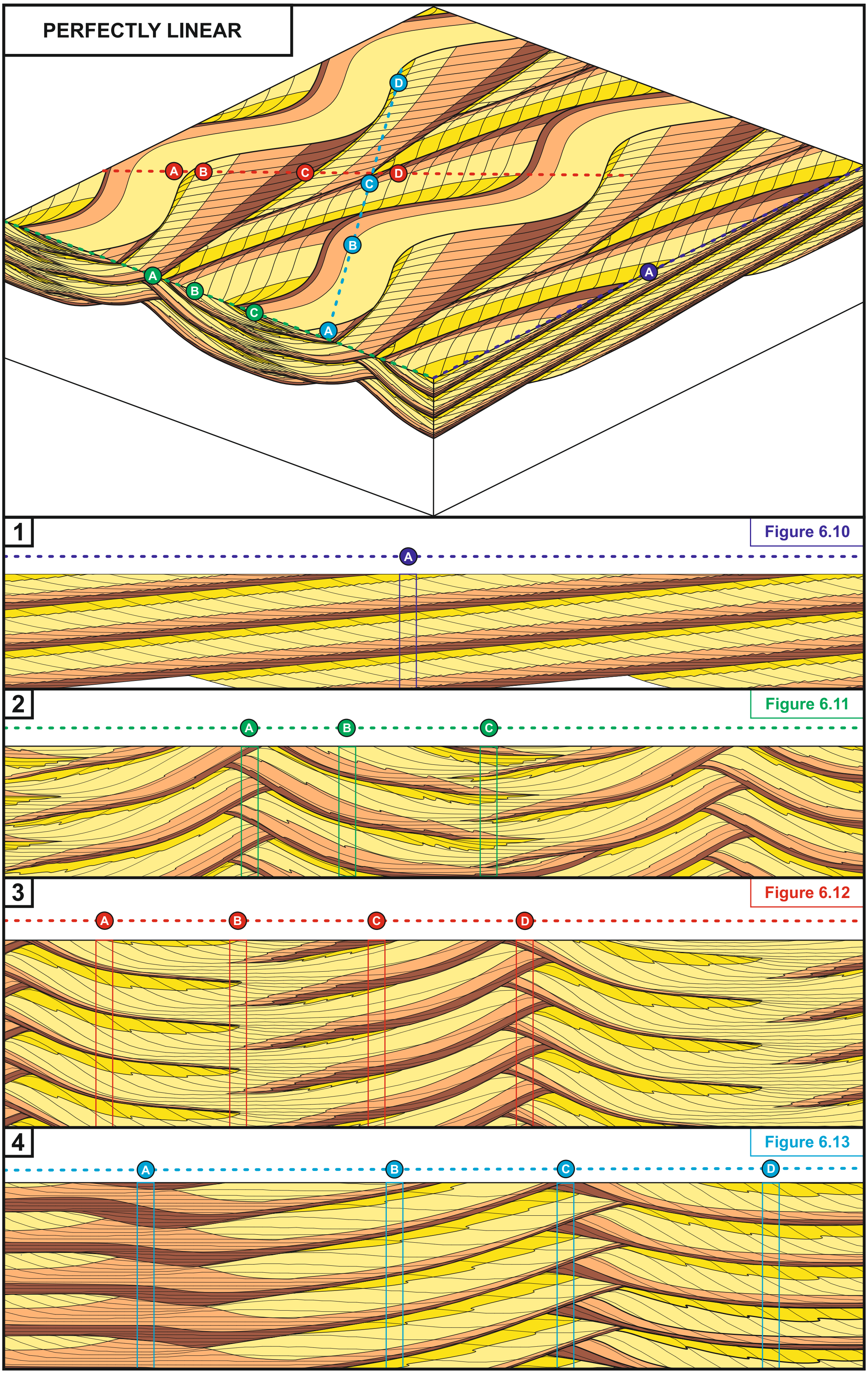

Figure 6.3a. Perfectly linear bedform model from Chapter 3 showing positions of transects used to generate pseudo-cores: 1) section parallel to trend of main bedforms; 2) section perpendicular to trend of main bedforms; 3) and 4) sections oblique to trend of main bedforms.

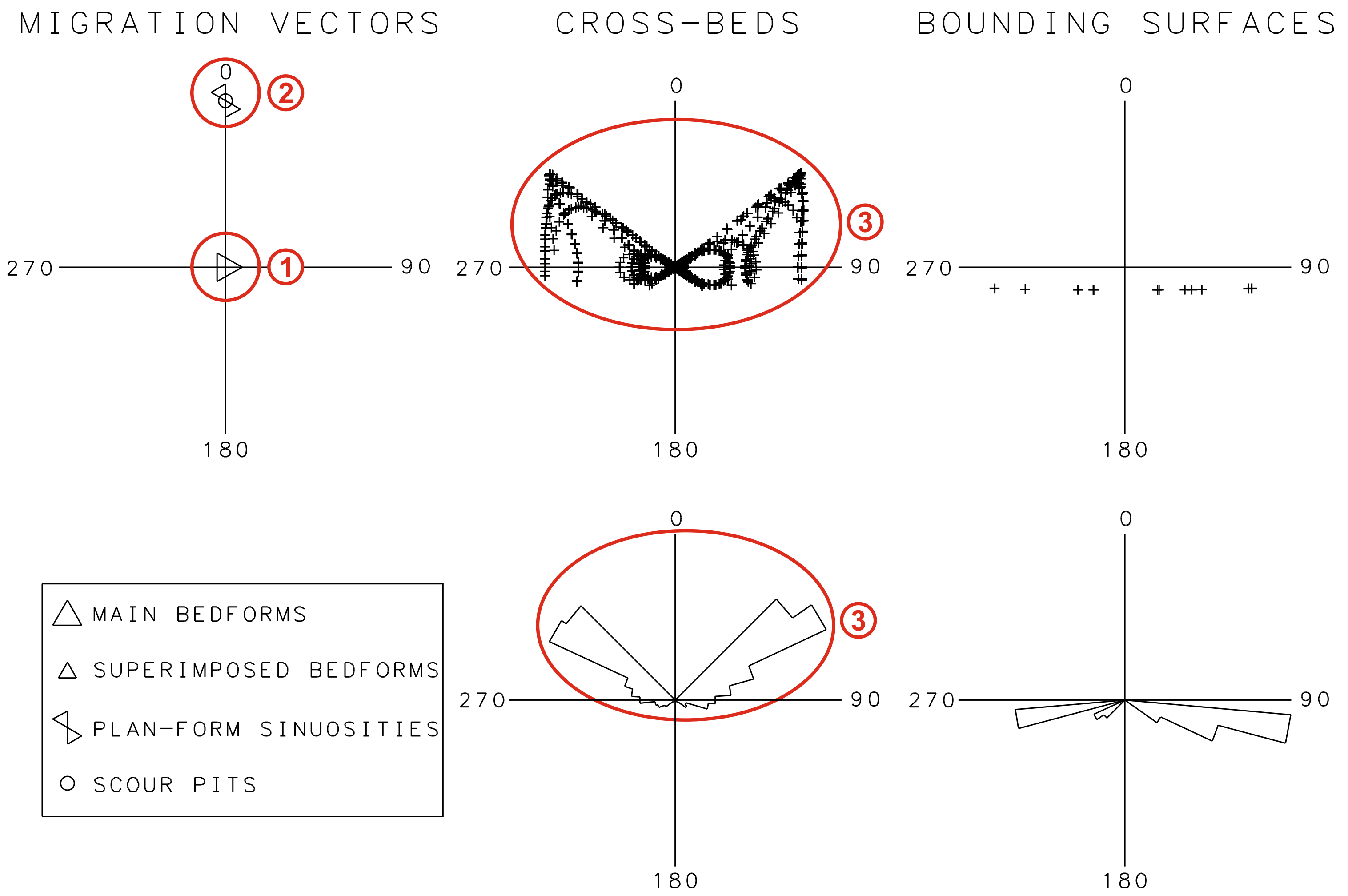

Figure 6.3b. Bedform migration and stratal azimuth plot for the perfectly linear bedform model, generated by the modelling software developed by David Rubin (Rubin, 1987a): 1) Primary bedforms do not show net-migration; 2) the sinuosities migrate along-crest towards 000°; 3) overall foreset dip-azimuth distribution is bimodal - this may not be expressed in naturally occurring examples which may have a minor component of transverse motion.

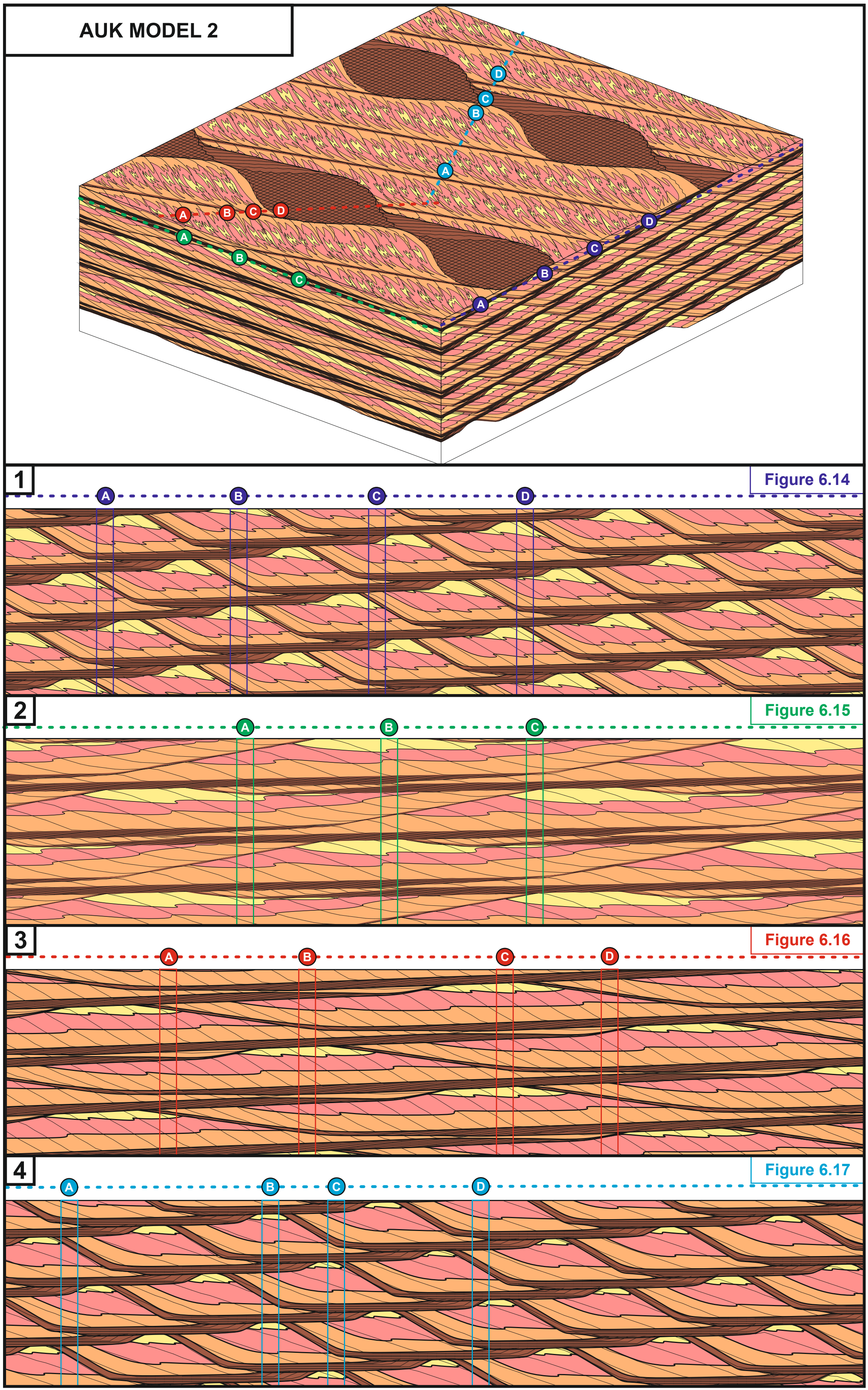

Figure 6.4a. Auk Model 2 from Chapter 5 depicting linear bedforms with a minor component of transverse motion, with positions of cross-sections used to generate pseudo-cores: 1) section parallel to transverse component of linear dune migration; 2) section parallel to along-crest component of linear dune migration; 3) and 4) oblique sections.

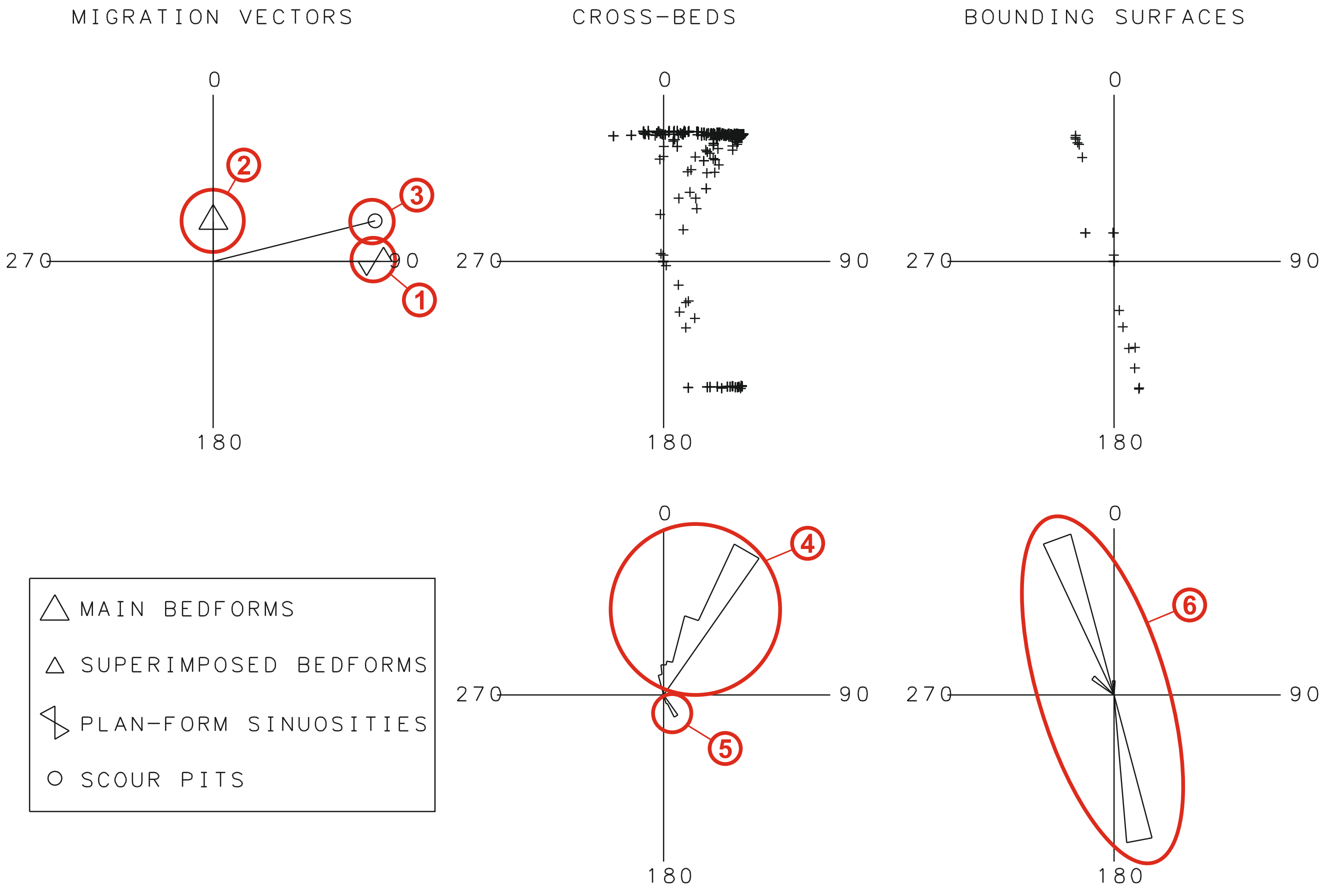

Figure 6.4b. Bedform migration and stratal azimuth plot for Auk Model 2, generated by the modelling software developed by David Rubin (Rubin, 1987a): 1) primary component of migration via the along-crest movement of the plan-form sinuosities towards 090°; 2) secondary component of migration via lateral movement of the main bedforms at a slower rate towards 000° (ratio of primary to secondary components of migration = 4:1); 3) resultant path of the scour pits determined by their net oblique translation towards 075°; 4) the majority of foreset dip-azimuths clustered between 030° - 040°; 5) minor cluster of southerly-dipping foresets reflects the rare preservation of stoss-side wind-ripple deposits; 6) bounding surfaces generated by the oblique migration of scour pits are inclined relatively steeply down towards 170° and 350°. Note - The modelling process has employed an arbitrary co-ordinate system whereby due north (000°) is always taken as the direction of transverse bedform migration. The data has been reoriented to match the Auk dataset in Chapter 5, but this is unnecessary for the purposes of this part of the research, therefore the arbitrary migration directions are used.

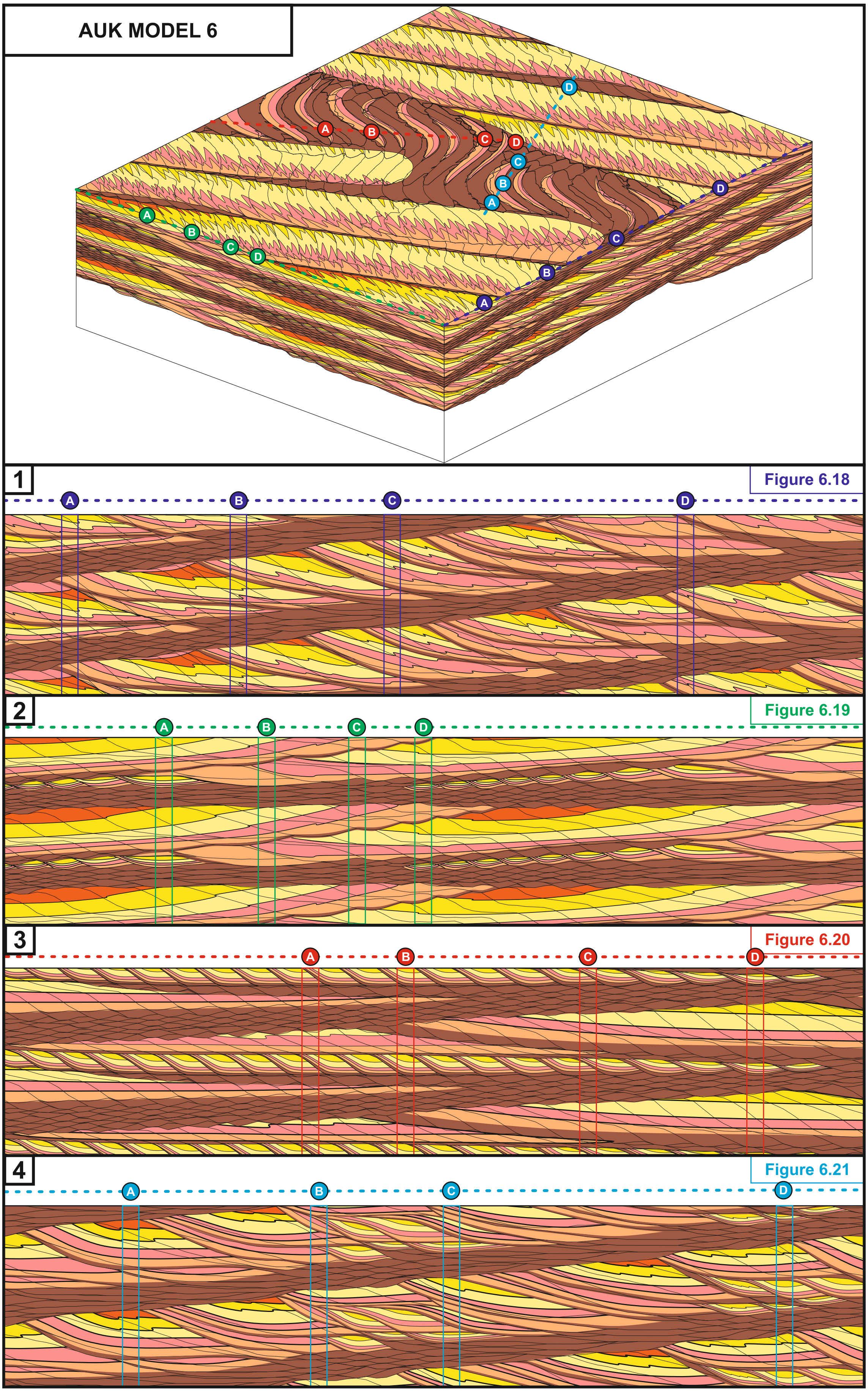

Figure 6.5a. Auk Model 6 from Chapter 5 depicting linear bedforms with a minor component of transverse motion and obliquely migrating barchanoid dunes, with positions of cross-sections used to generate pseudo-cores: 1 - section parallel to transverse component of linear dune migration; 2 - section parallel to along-crest component of linear dune migration; 3 and 4 - oblique sections.

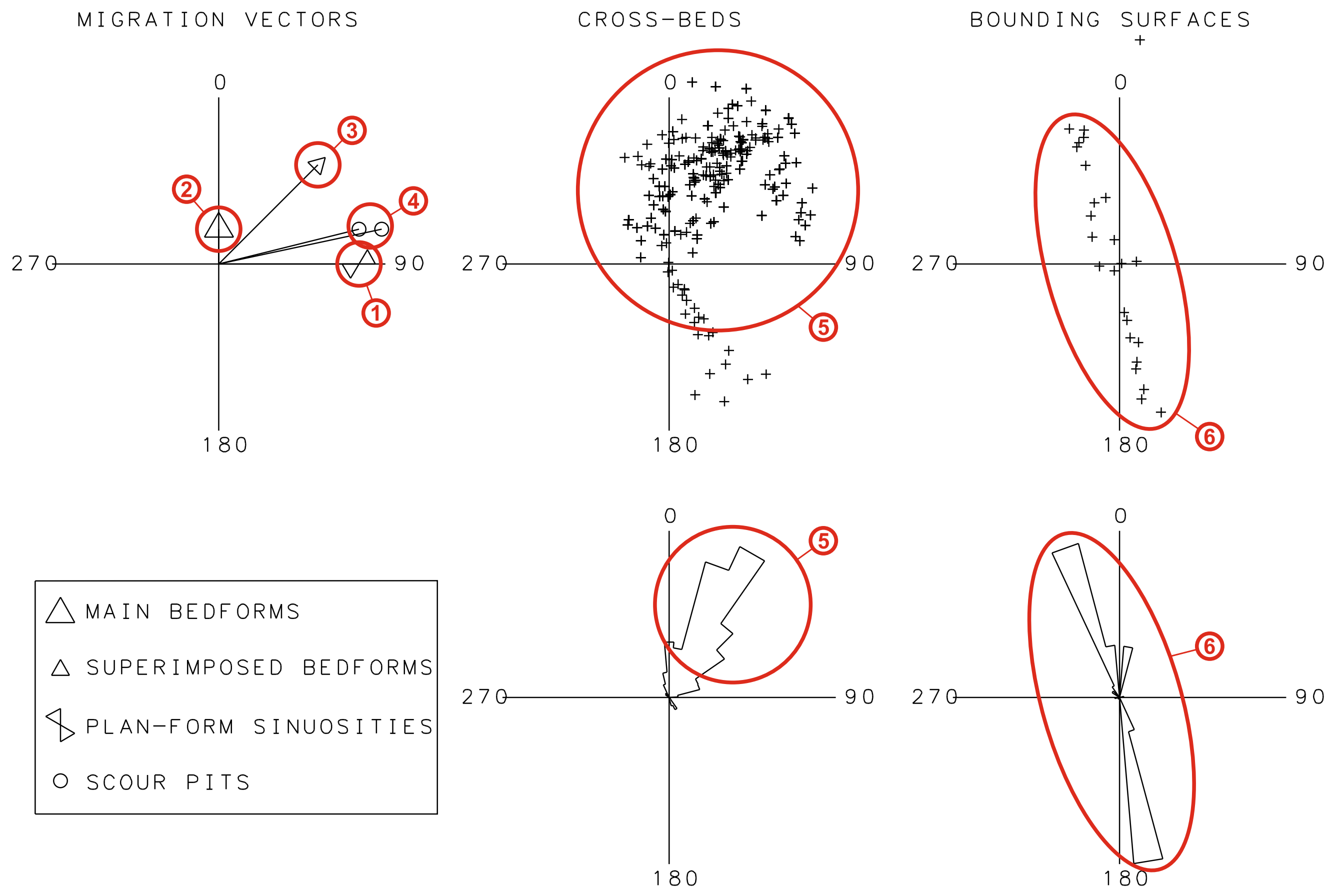

Figure 6.5b. Bedform migration and stratal azimuth plot for Auk Model 6, generated by the modelling software developed by David Rubin (Rubin, 1987a): 1) primary component of migration via along-crest movement of plan-form sinuosities towards 090°; 2) secondary component of migration via lateral movement of the main bedforms at a slower rate towards 000°; 3) migration of dunes in barchanoid dune field towards 045° (bedforms confined to low-lying interdune areas); 4) migration of scour pits generated by both re-entrants of large linear bedforms and by barchanoid dunes (060°- 070°); 5) preserved foresets exhibit variable dip and azimuths show a broad unimodal distribution with a mean towards 035°; 6) preserved bounding surfaces exhibit variable dip and azimuths show a bimodal distribution. Note - The modelling process has employed an arbitrary co-ordinate system whereby due north (000°) is always taken as the direction of transverse bedform migration. The data has been reoriented to match the Auk dataset in Chapter 5, but this is unnecessary for the purposes of this part of the research, therefore the arbitrary migration directions are used.

6.1.2.3 – Perfectly transverse bedforms; Model 3 (Section 3.8)

This bedform model (Figure 3.12) depicts perfectly transverse bedforms with sinuous, out-of-phase crestlines (see Figure 3.3 for the input variables used in the Rubin modelling software (Rubin, 1987a) to generate this model). Pseudo-cores have been generated in a section perpendicular to the trend of the main bedforms (Figure 6.6), in a section parallel to the trend of the main bedforms (Figure 6.7), and two sections taken obliquely to the trend of the main bedforms (Figures 6.8 and 6.9). The position of these transects within the overall bedform model, and the position of the pseudo-cores, is depicted in Figure 6.2a.

A number of cores generated for this model display foreset dip-azimuths which shallow-upwards towards the top of each preserved set (Figure 6.6 – core A; Figure 6.7 – cores A, B and C; Figure 6.8 – cores B and D; Figure 6.9 – cores A-D). Ideally, they would show steeping-upward dips throughout the preserved set; however the angle-of-climb has been over-steepened in the generation of this model, and therefore the foresets show a slight sigmoidal shape at their tops. The angle-of-climb depicted in this model is steeper than that which would be encountered for most migratory dune-scale bedforms in nature to allow better recognition of the sets – set thickness is partly a function of the angle-of-climb, whereby steeper angles allow for the preservation of thicker sets (e.g. Mountney and Howell, 2000).

Where cores are generated close to the centre of the troughs, they depict the maximum preserved set thickness of the succession (highlighted in light blue on the foreset dip-azimuth plots: Figure 6.7 – cores A and B; Figure 6.8 – cores B and C; Figure 6.9 – core A). These examples show uniformly-distributed bounding surfaces; this can be used as a diagnostic feature in these theoretical models to determine whether the true maximum preserved set thickness has been achieved. However, in nature it is highly unlikely that each successive bedform in a train would be identical in size, shape and migratory behaviour to the previous bedform (all factors which ultimately influence the resulting preserved set thickness), so it is unlikely that each successive set would be identical in thickness. In more natural scenarios, it is highly unlikely that cores would be drilled through the exact centres of troughs multiple stacked troughed sets. Periodically, they intersect the junction of two troughs, or contiguously to such junctions (Figure 6.7 – cores C and D; Figure 6.8 – cores A and D; Figure 6.9 – cores B, C and D); these cores generate set thicknesses which are much thinner than true maximum. Although in all these cases the set thicknesses preserved are not the true maximum set thickness, some preserve sets of equal thickness (Figure 6.7 – core C), and others show a variety of preserved set thicknesses within the same cored section (Figure 6.7 – core D; Figure 6.8 – cores A and D; Figure 6.9 – cores B, C and D). This disparity in preserved set thickness generated from the same bedform model means that the empirical relationships derived from the measurement of preserved set thicknesses in Chapter 2 can show inconsistency, as values of set thicknesses determined from two-dimensional outcrops or from one-dimensional core

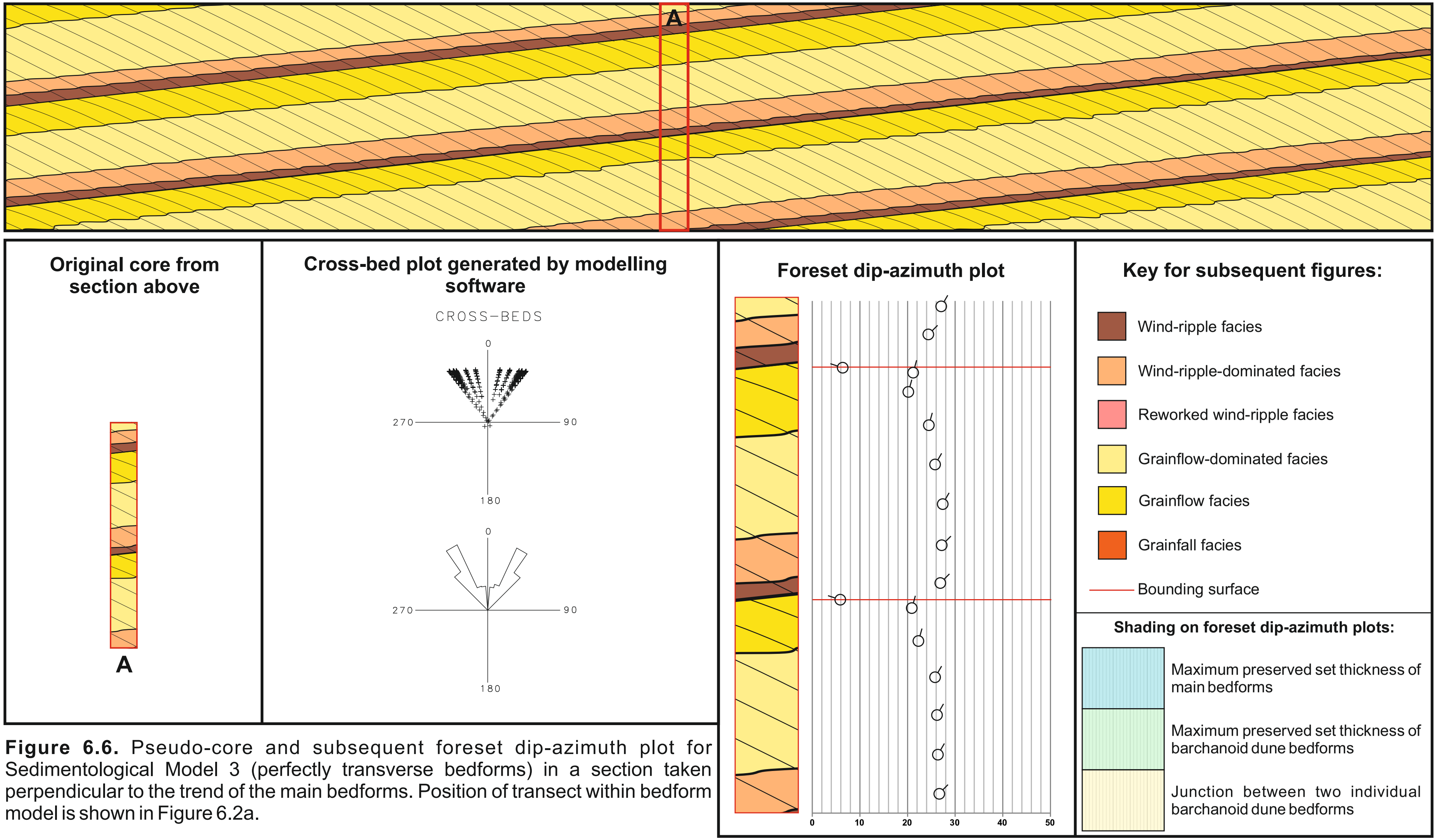

Figure 6.6. Pseudo-core and subsequent foreset dip-azimuth plot for Sedimentological Model 3 (perfectly transverse bedforms) in a section taken perpendicular to the trend of the main bedforms. Position of transect within bedform model is shown in Figure 6.2a.

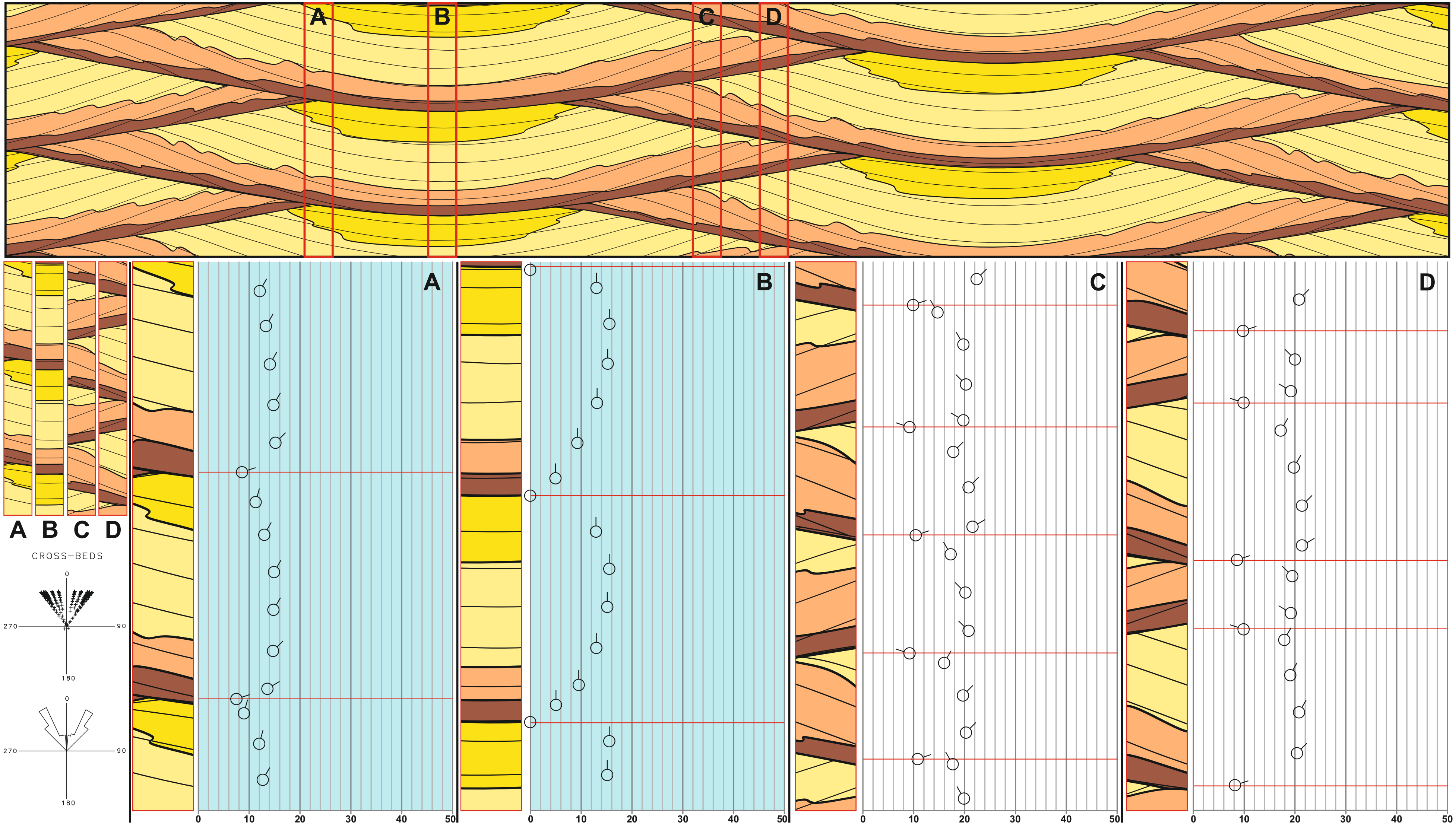

Figure 6.7. Pseudo-cores and subsequent foreset dip-azimuth plots for Sedimentological Model 3 (perfectly transverse bedforms) in a section taken parallel to the trend of the main bedforms. Position of transect within bedform model is shown in Figure 6.2a.

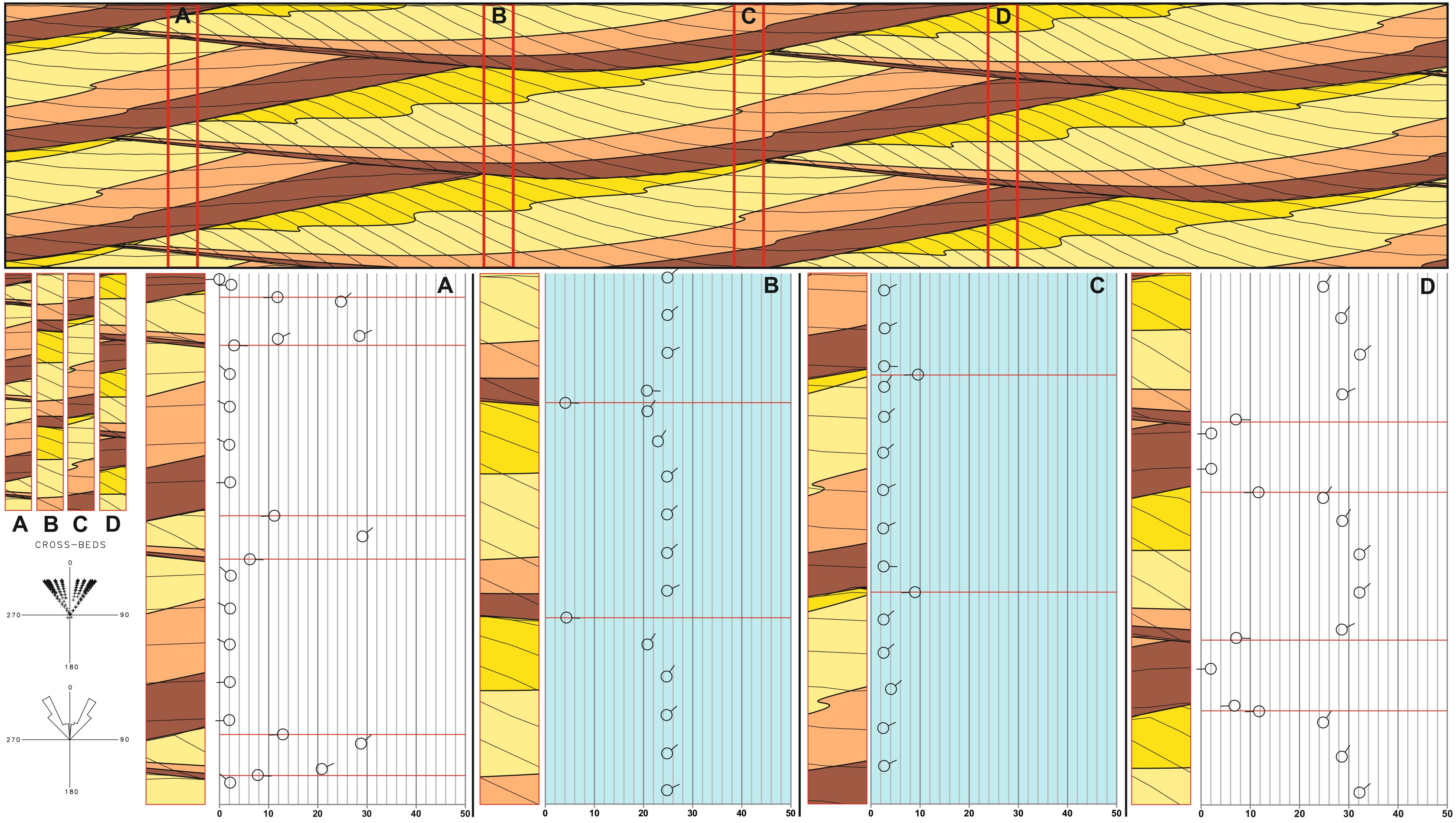

Figure 6.8. Pseudo-cores and subsequent foreset dip-azimuth plots for Sedimentological Model 3 (perfectly transverse bedforms) in a section taken oblique to the trend of the main bedforms. Position of transect within bedform model is shown in Figure 6.2a.

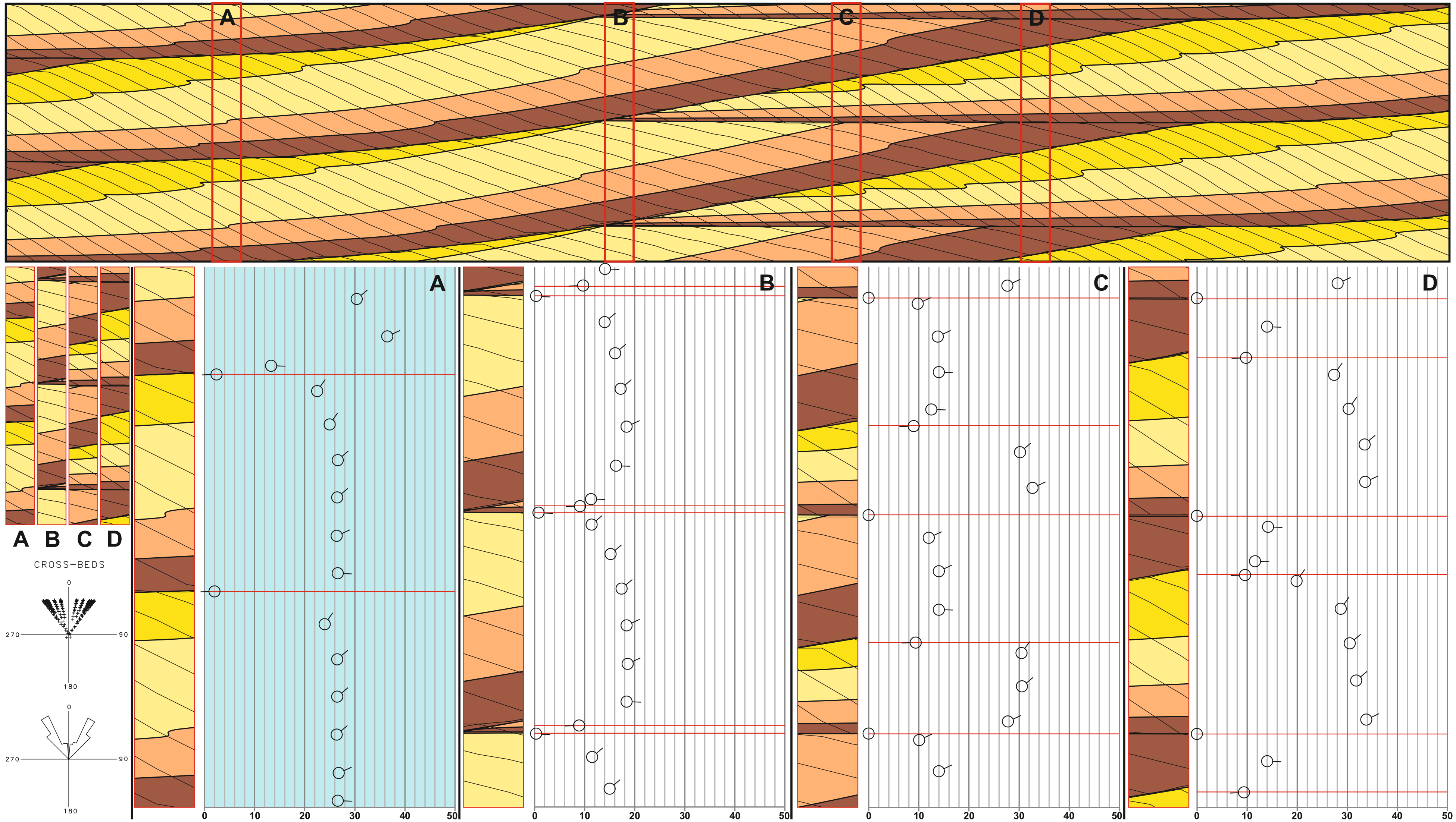

Figure 6.9. Pseudo-cores and subsequent foreset dip-azimuth plots for Sedimentological Model 3 (perfectly transverse bedforms) in a section taken oblique to the trend of the main bedforms. Position of transect within bedform model is shown in Figure 6.2a.

do not necessarily represent the maximum thickness of a set, since they might be clipping the edges of troughs that are significantly thicker in their central parts (Figure 2.10b). This conceptual shortcoming, initially explored in Chapter 2, has been supported in the generation of pseudo-cores and subsequent foreset dip-azimuths for this model. The result of this inconsistency is likely a major cause of the scatter observed in the empirical relationship between grainflow thickness and preserved set thickness (Figure 2.9; Figure 2.10).

Transverse bedforms have been previously noted to yield a tight cluster of foreset dip-azimuths due to the migration of these bedforms in a single, favoured direction, in this case towards an arbitrary direction of 000° (Figure 6.2b); this is the case especially for near-two-dimensional transverse bedforms, but also for three-dimensional transverse bedforms with gently sinuous crestlines. However, the modelled output for the overall foreset dip-azimuth distribution is bimodal for this example (Figure 6.2b). Although this is true for the modelled output of the entire bedform model, there are very few instances which display this bimodal distribution in the individually cored sections (Figure 6.7 – cores C and D; Figure 6.8 – cores A and D). To generate this bimodality in a single cored section, the core must intersect the exact junction of two troughs, or very near to such junctions, which enables penetration through the edges of two preserved sets with internal foresets that dip in markedly different directions. However, this is as unlikely as punctuating the exact centres of troughs (as described above, giving rise to maximum preserved set thickness). Given a random sampling policy, it is substantially more likely that cores will be drilled somewhere between the centre and edges of these troughs in transverse bedforms. It is for this reason that three-dimensional transverse bedforms do not necessarily display a bimodal foreset dip-azimuth distribution, and can generate unimodal foreset dip-azimuth distributions in single cores, as displayed in Figure 6.6; Figure 6.7 – cores A and B; Figure 6.8 – cores B and C; and Figure 6.9 – cores A, B, C and D. In the case of Figure 6.8 – core C, and all cores from Figure 6.9, the foreset dip-azimuths are largely unimodal; the only difference in overall azimuth is at the basal-most section, which likely reflects the rare preservation of stoss-side wind-ripple strata (Figure 6.2b).

In cases where unimodal distributions are displayed (Figure 6.6; Figure 6.7 – cores A and B; Figure 6.8 – cores B and C; and Figure 6.9 – cores A, B, C and D), it is partly a function of the modelling process, whereby the pseudo-cores only intersect 2 or 3 preserved sets. If these cores were sufficient in length to capture successive vertical sets representing the different sides of curved troughs that overall have their axes aligned in the same direction, then the datasets from the individual cores would exhibit a more obvious spread in the foreset dip-azimuth distribution, as displayed in the foreset dip-azimuth plots generated by the modelling software for the entire bedform model (Figure 6.2b). However, some cored intervals may not be extensive in length and therefore relying on a core of sufficient length for the determination of original bedform type solely from foreset dip-azimuth plots is an unreliable method. In all cases, the distribution of the foreset dip-azimuths is governed by the shape of the troughs in plan-view, which itself is controlled by the wavelength and the amplitude of the plan-view along-crest sinuosity. If there is a gentle rate of curvature, whereby the bedforms exhibit wide open trough shapes in plan-view, then a broad spread of foreset dip-azimuths would be generated over a wide range, as is the case modelled here (Figure 6.2b). Conversely, if the troughs depict a ‘diamond-shape’ in plan-view with a tight trough apex, then the distribution of foreset dip-azimuths would demonstrate more obvious bimodality; the range of the foreset dip-azimuth distribution is directly dictated by the amount of curvature in the trough.

6.1.2.4 – Perfectly linear bedforms; Model 5 (Section 3.10)

This bedform model (Figure 3.19) depicts perfectly linear bedforms, meaning that they are non-migratory (see Figure 3.3 for the input variables used in the Rubin modelling software (Rubin, 1987a) to generate this model), but which additionally possess along-crest migrating sinuosities. Pseudo-cores have been generated in a section parallel to the trend of the main bedforms (Figure 6.10), in a section perpendicular to the trend of the main bedforms (Figure 6.11), and two sections taken obliquely to the trend of the main bedforms (Figures 6.12 and 6.13). Positions of these transects within the overall bedform model, and their subsequent pseudo-cores, is depicted in Figure 6.3a.

A common assumption (that is often misapplied) is that linear dune sets should be characterised by a bimodal foreset dip-azimuth distribution, as shown in the modelled foreset dip-azimuth distribution for the entire bedform model in this example (Figure 6.3b). Although this may be true for the morphology of modern dunes with their opposing slipfaces (Tsoar, 1982), and for the perfectly linear bedforms modelled here which do not migrate, it is not the case for the preserved sets arising from linear bedforms which undertake a component of transverse motion (Rubin and Hunter, 1985); this style of migration is explored further in Sections 6.1.2.5 and 6.1.2.6 for the Auk Formation bedforms. Additionally, the development of superimposed dunes on large linear bedforms results in the preservation of stacked trough cross-stratified sets, which are often misinterpreted as the product of migrating transverse bedforms (Bristow et al., 2000).

In the section taken perfectly parallel to the trend of the linear bedforms (Figure 6.10), all the log responses across this section would be identical as this is a very simplistic expression of the stratigraphy. The foresets preserved are almost identical to those for perfectly transverse bedforms taken in a section perpendicular the trend of the transverse bedforms (Figure 6.6). In this example, the true maximum set thickness is preserved (highlighted in light blue on the foreset dip-azimuth plot). True maximum set thickness is also preserved in the section taken perfectly perpendicular to the trend of the linear bedforms (Figure 6.11 – core B). The two oblique sections show a similar pattern, and maximum set thickness is preserved in Figure 6.12 – cores A and C which punctuate the stratigraphy from opposing sides of the same bedform, and in Figure 6.13 – core D.

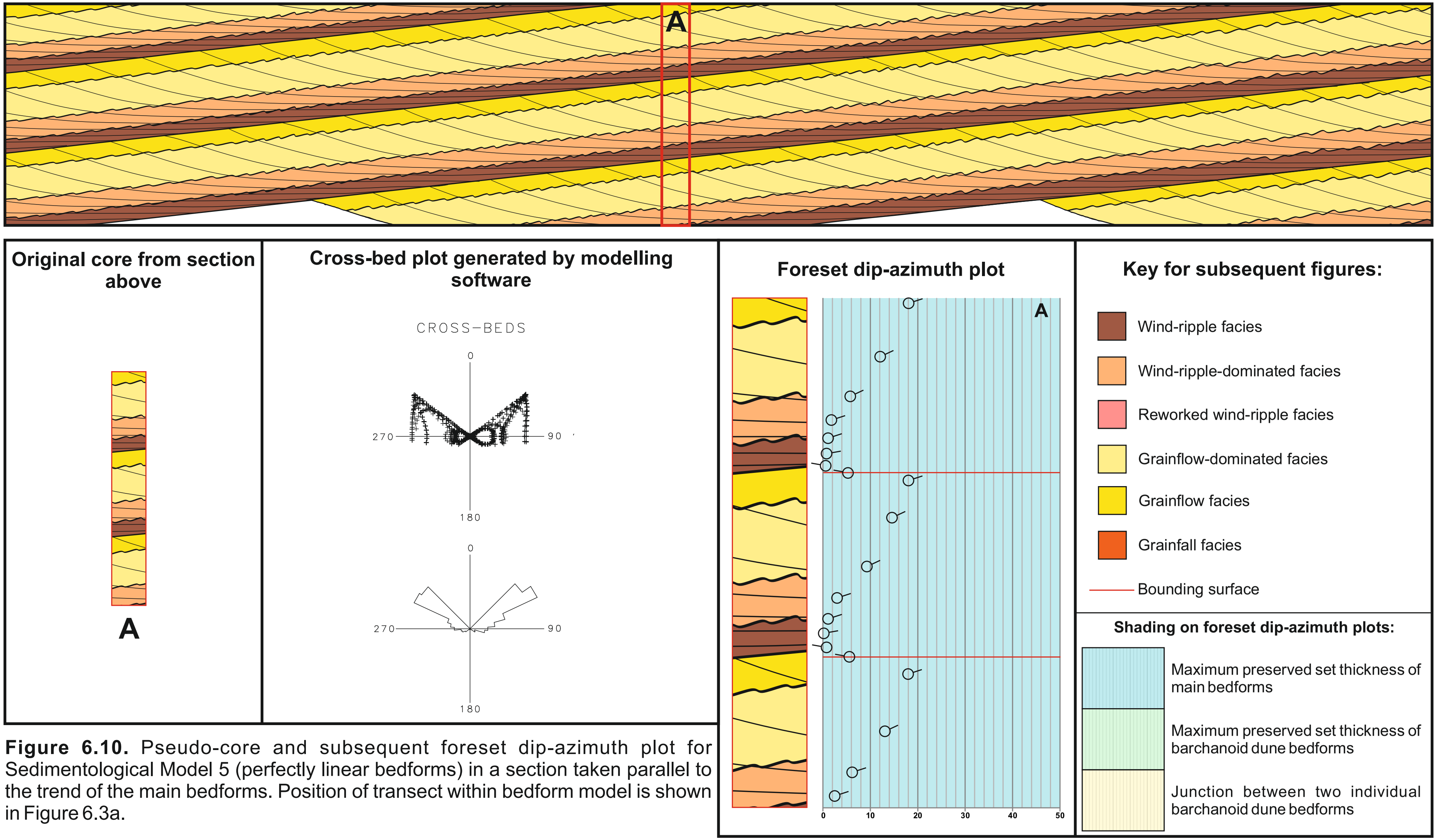

Figure 6.10. Pseudo-core and subsequent foreset dip-azimuth plot for Sedimentological Model 5 (perfectly linear bedforms) in a section taken parallel to the trend of the main bedforms. Position of transect within bedform model is shown in Figure 6.3a.

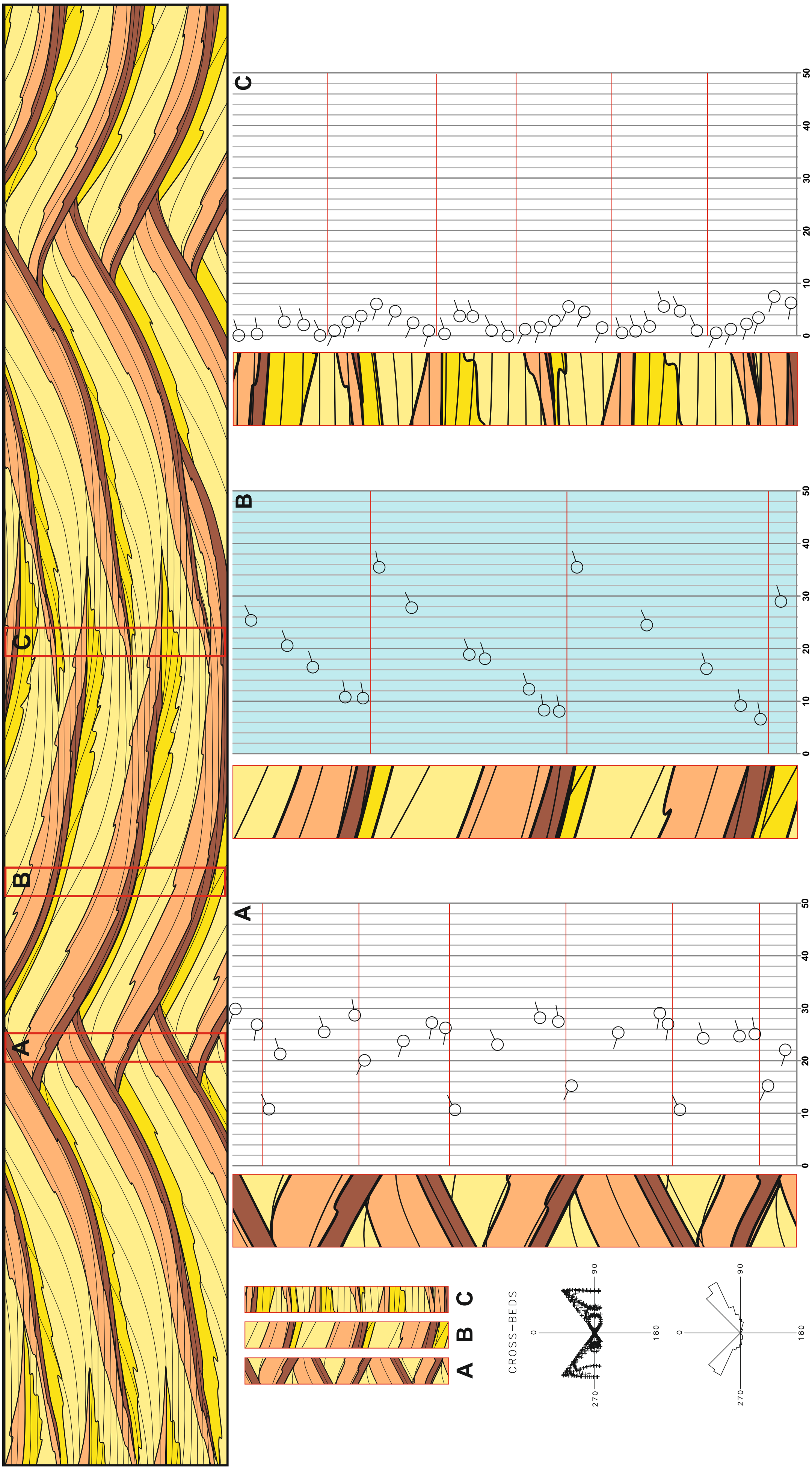

Figure 6.11. Pseudo-cores and subsequent foreset dip-azimuth plots for Sedimentological Model 5 (perfectly linear bedforms) in a section taken perpendicular to the trend of the main bedforms. Position of transect within bedform model is shown in Figure 6.3a.

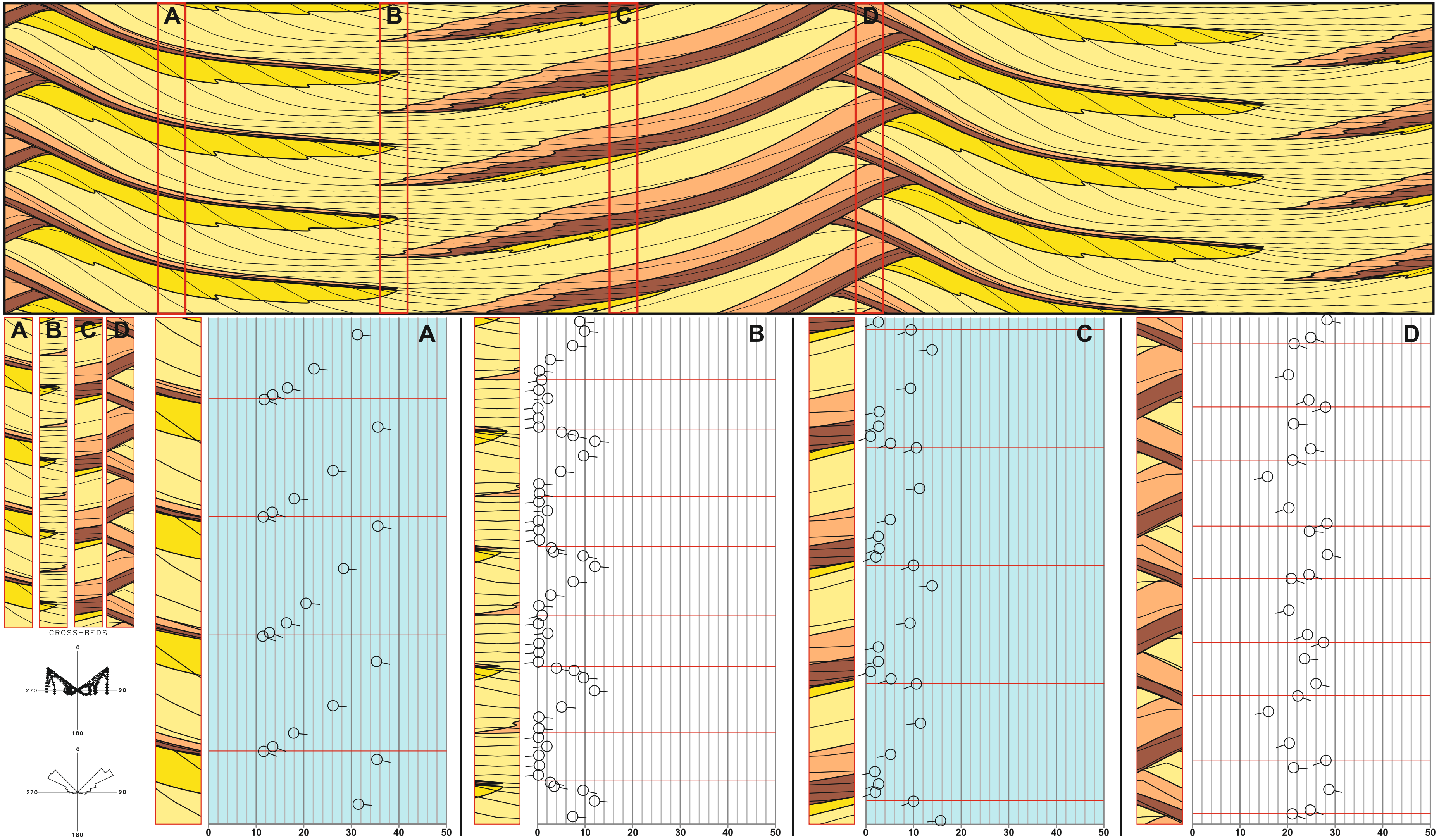

Figure 6.12. Pseudo-cores and subsequent foreset dip-azimuth plots for Sedimentological Model 5 (perfectly linear bedforms) in a section taken oblique to the trend of the main bedforms. Position of transect within bedform model is shown in Figure 6.3a.

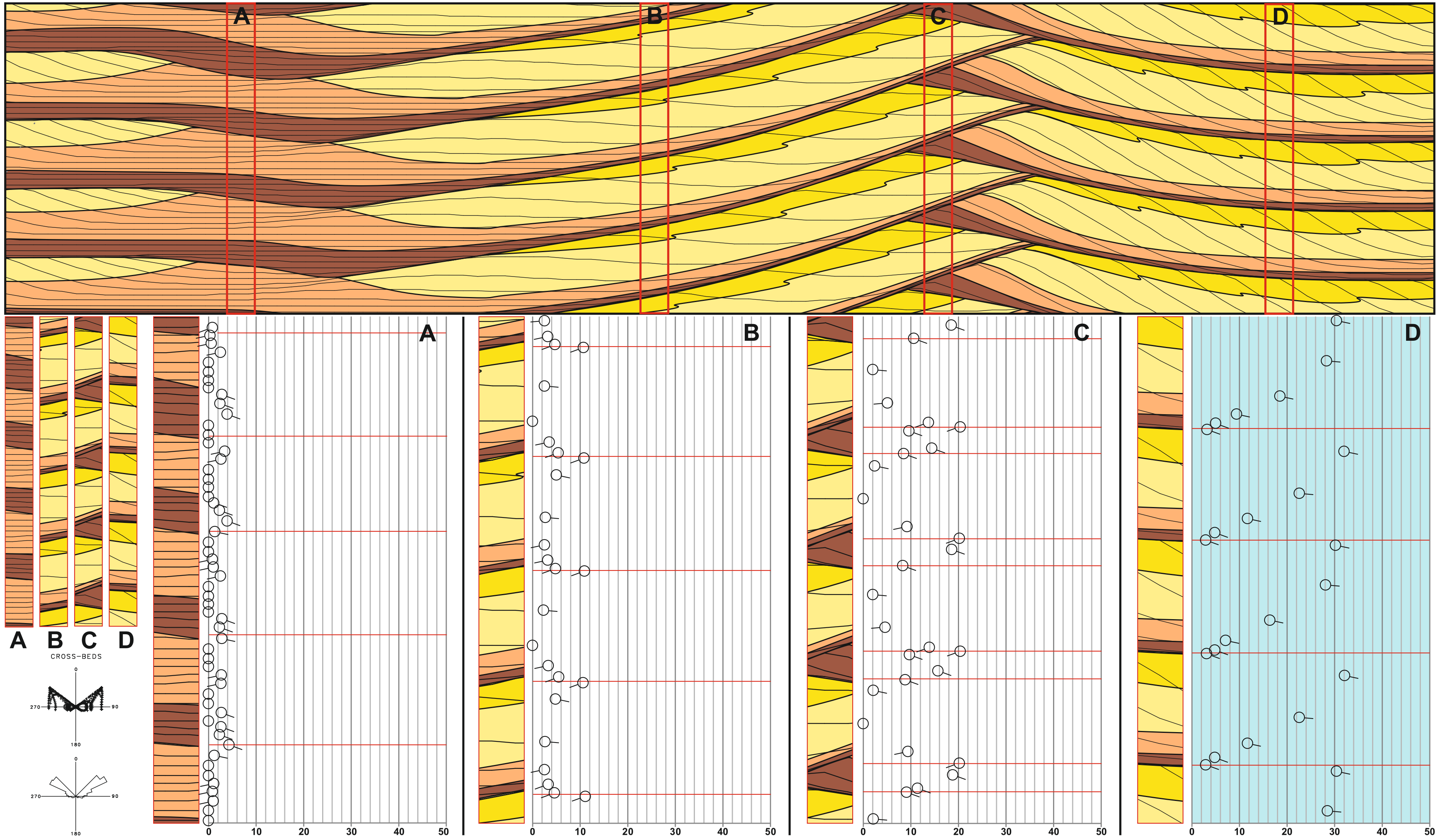

Figure 6.13. Pseudo-cores and subsequent foreset dip-azimuth plots for Sedimentological Model 5 (perfectly linear bedforms) in a section taken oblique to the trend of the main bedforms. Position of transect within bedform model is shown in Figure 6.3a.

The preserved set thickness from Figure 6.12 – cores B and D are almost identical, where one core is at very edge of two bedforms (core D) and the other from the direct centre (core B). The only difference between these two core expressions is the foreset dip-azimuths, and preserved facies arrangements. Cores A and B from Figure 6.13 also preserve sets which are very close to maximum thickness, and both these cores preserve sets of similar thicknesses.

Although core C from Figure 6.11 punctuates the centre of two adjacent linear crestlines, true maximum preserved set thickness is not achieved here, as in the examples for transverse bedforms. True maximum preserved set thickness is only displayed in Figure 6.11 – core B, which also displays the unimodal foreset dip-azimuths which are now known to characterise a large proportion of linear dune accumulations. Other examples which display unimodal foreset dip-azimuths are Figure 6.10, which displays foreset dip-azimuths that should be entirely unimodal, but the bounding surfaces dip in the opposite direction as the angle-of-climb has been exaggerated in the generation of the bedform models, Figure 6.12 – cores A and C, and Figure 6.13 – core D.

Although a unimodal dip-azimuth distribution is expected for linear bedforms as described above, other cores from this bedform model display bimodal foreset dip-azimuths (Figure 6.11 – cores A and C; Figure 6.12 – cores B and D; Figure 6.13 – cores A, B and C). In Figure 6.12 – core B and Figure 6.13 – core A, a bimodal distribution exists, however, the foresets are dipping at very shallow angles which may not be readily determined in natural datasets. Core D in Figure 6.12 shows a switch in foreset dip-azimuth between successive preserved sets, as this core clips the edges of two bedforms which dip in opposing directions. Cores B and C from Figure 6.13 both display a bimodal distribution of foreset azimuths *within* the same preserved set.

This bedform model confirms that foreset dip-azimuths distributions from single cored intervals of linear bedforms can show a wide range of expressions and are therefore not necessarily a diagnostic feature, even in this perfectly theoretical model.

6.1.2.5 – Auk Sedimentological Model 2 (Section 5.7)

This bedform model (Figure 5.7) has been generated on the basis of a major component of linear dune migration and a minor component of transverse bedform migration, at a ratio of 4:1 respectively (see Figure 5.3 for the input variables used to generate this model). Pseudo-cores have been generated in a section parallel to the transverse component of linear dune migration (Figure 6.14), in a section parallel to the along-crest component of linear dune migration (Figure 6.15), and two oblique sections (Figures 6.16 and 6.17). Positions of these transects within the overall bedform model, and their subsequent pseudo-cores, is depicted in Figure 6.4a.

None of the pseudo-cores generated for Auk Model 2 display true maximum preserved set thickness in every successive coset throughout the entire cored section. The lateral migration of the linear bedforms means that in a single core which punctuates the stratigraphy vertically, each successive set will preserve a different section of the bedform.

In some instances, sets will be at the maximum preserved thickness intercalculated with thinner preserved sets. The cosets which preserve maximum set thickness are highlighted in light blue on the following sections: Figure 6.14 – core B in the section taken parallel to the transverse component of linear dune migration; Figure 6.15 – cores B and C in the section taken parallel to the along-crest component of linear dune migration; Figure 6.16 – cores B and C, and Figure 6.17 – cores B and C, for the sections taken obliquely through the bedform model.

All the pseudo-cores generated for Auk Model 2 in Figures 6.14 – 6.17 display the unimodal foreset dip-azimuth distributions which are now envisaged for the majority of linear bedforms undertaking a minor component of transverse bedform motion. The ratio of primary to transverse bedform motion in this model is 4:1, meaning that these bedforms are almost purely linear in migratory style; this demonstrates that only a small amount of transverse motion is required to produce a unimodal foreset dip-azimuth distribution. In each case, it is only the dip-azimuths for the basal-most wind-rippled facies and the bounding surfaces which diverge from this trend (reflecting the rare preservation of stoss-side wind-ripple deposits) but in most cases the dip value is negligible and would be incredibly difficult to discern in cored datasets from naturally occurring aeolian reservoir successions.

As discussed previously in Section 6.1.2.3, the width of the troughs is dictated by the wavelength and the amplitude of the plan-view along-crest sinuosity, and the range of foreset dip-azimuths is directly dictated by the amount of curvature in the trough; a gentle rate of curvature produces a broad spread of foreset dip-azimuths over a wide range and troughs with a tight apex generate more obvious bimodality in the foreset dip-azimuth distributions. If the troughs depict a ‘diamond-shape’, with a tight trough apex, then the foreset dip-azimuths would demonstrate more obvious bimodality. The overall mean foreset dip-azimuth is a function of the primary and secondary transport vectors and their respective vector magnitudes (Figure 6.4b) which determines the nature of the oblique trend of the preserved sets.

For Auk Model 2, the primary component of migration is via along-crest movement of plan-form sinuosities towards 090° and the secondary component of migration is via the lateral movement of the main bedforms at a slower rate, towards 000° (Figure 6.4b); the ratio of migration rates for this bedform model is 4:1 respectively. The resultant path of the scour pits is determined by their net oblique translation, in this case towards 075°. The majority of foreset dip-azimuths are clustered between 030° and 040° with a minor cluster of southerly-dipping foresets reflecting the rare preservation of stoss-side wind ripple deposits, and the bounding surfaces generated by the oblique migration of scour pits are inclined relatively steeply down towards 170° and 350°.

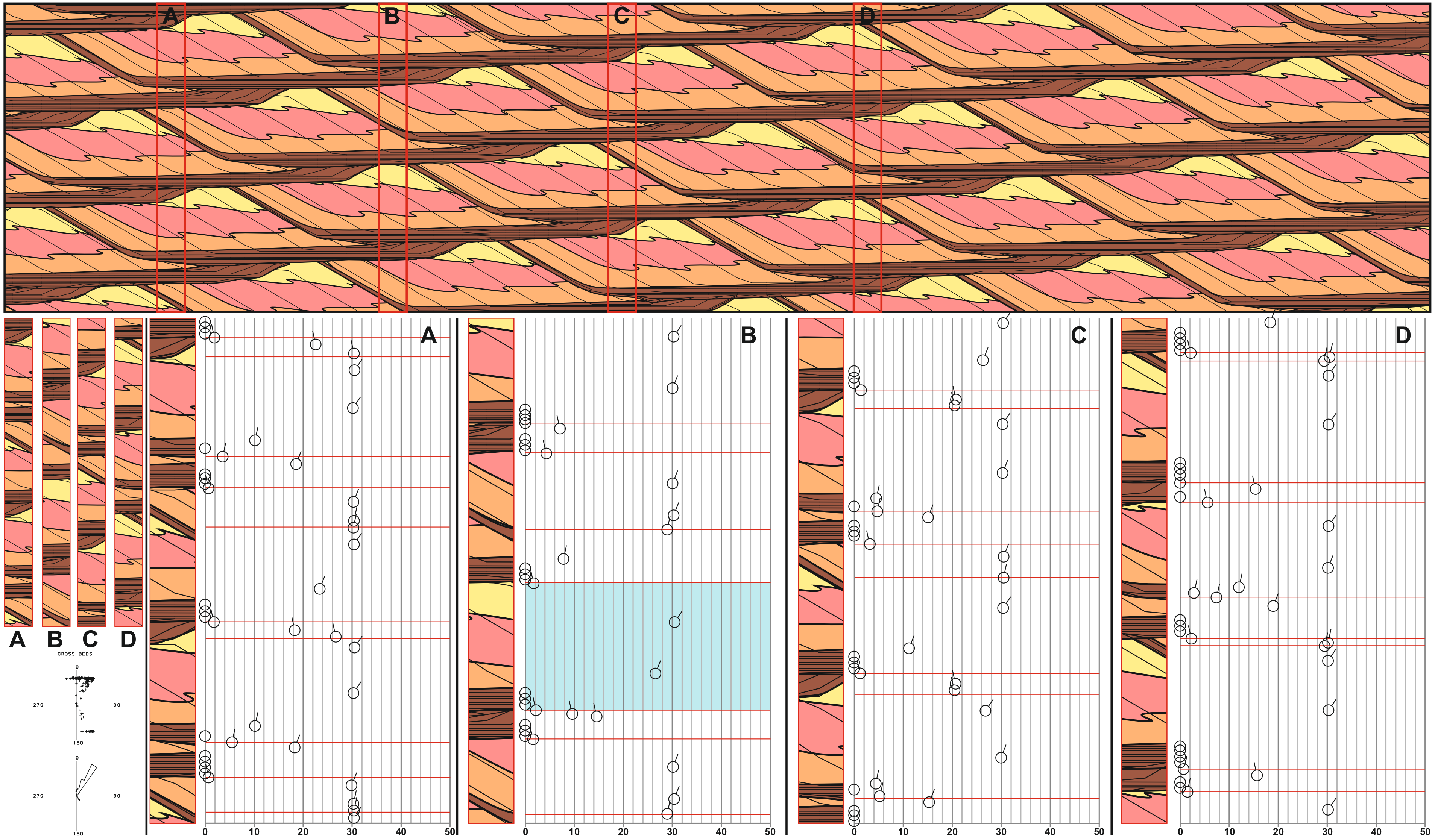

Figure 6.14. Pseudo-cores and subsequent foreset dip-azimuth plots for Auk Model 2 in a section taken parallel to the transverse component of linear dune migration. Position of transect within bedform model is shown in Figure 6.4a.

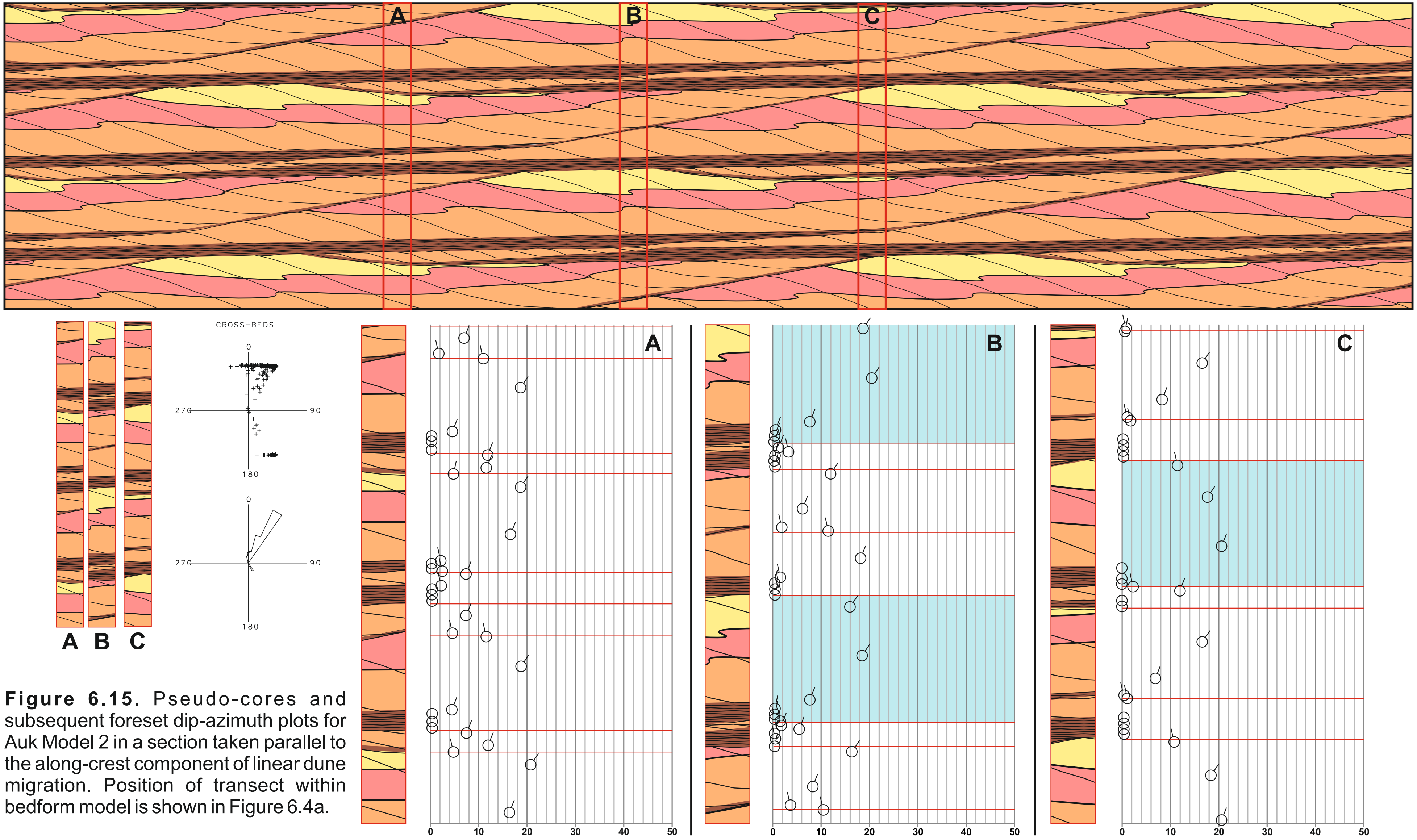

Figure 6.15. Pseudo-cores and subsequent foreset dip-azimuth plots for Auk Model 2 in a section taken parallel to the along-crest component of linear dune migration. Position of transect within bedform model is shown in Figure 6.4a.

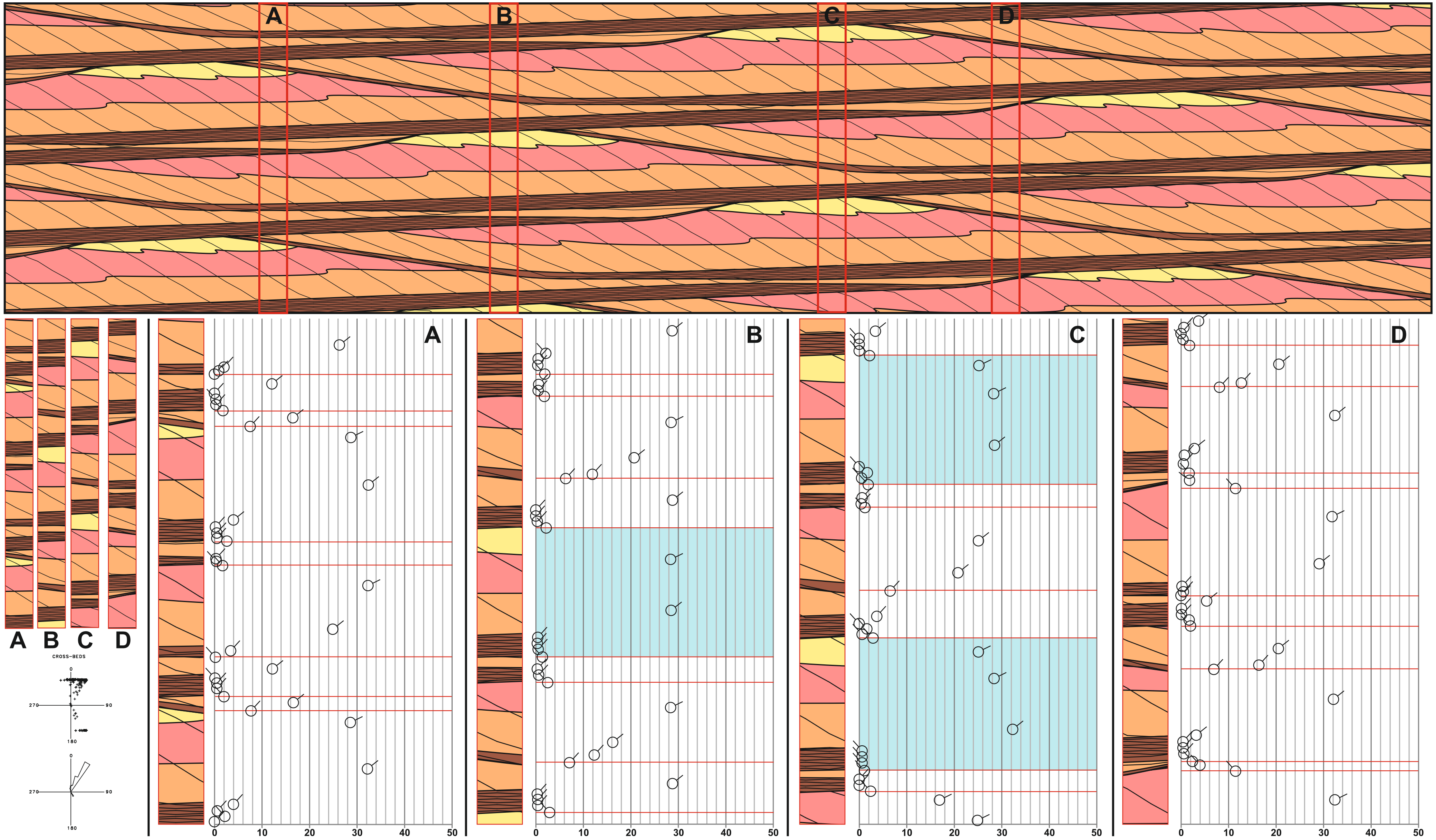

Figure 6.16. Pseudo-cores and subsequent foreset dip-azimuth plots for Auk Model 2 in a section taken oblique to linear dune migration. Position of transect within bedform model is shown in Figure 6.4a.

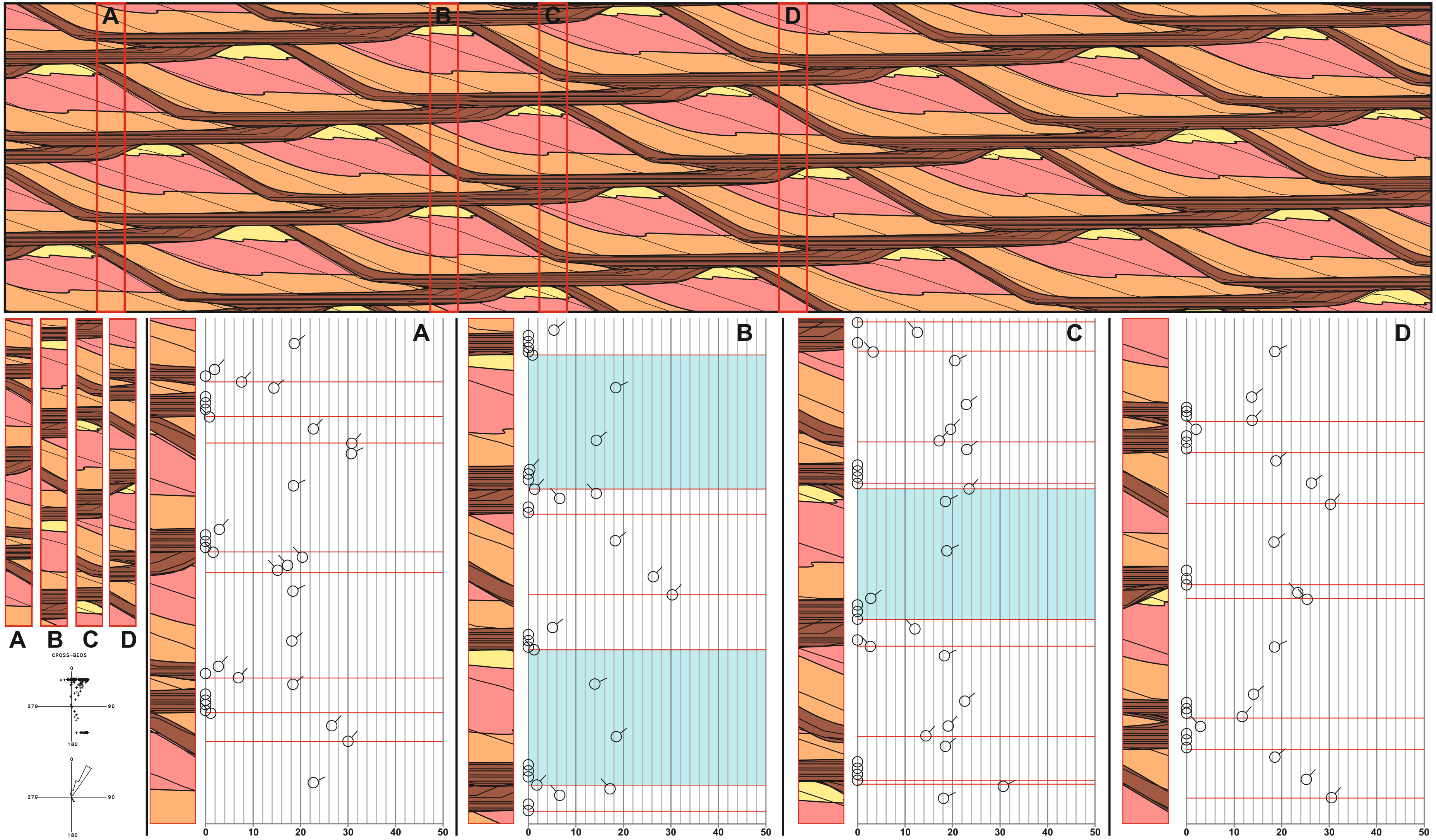

Figure 6.17. Pseudo-cores and subsequent foreset dip-azimuth plots for Auk Model 2 in a section taken oblique to linear dune migration. Position of transect within bedform model is shown in Figure 6.4a.

6.1.2.6 – Auk Sedimentological Model 6 (Section 5.11)

Auk Model 6 from Chapter 5 (Figure 5.19) was also interrogated in the same manner as above to investigate how the addition of a barchanoid dune field migrating through the interdune corridors of the main linear bedforms affects the resultant foreset dip-azimuth plots (see Figure 5.3 for the input variables used to generate this model). Pseudo-cores have been generated in a section parallel to the transverse component of linear dune migration (Figure 6.18), in a section parallel to the along-crest component of linear dune migration (Figure 6.19), and two oblique sections (Figures 6.20 and 6.21). Positions of these transects within the overall bedform model, and their subsequent pseudo-cores, is depicted in Figure 6.5a. In places where the maximum set thickness of the linear draa has been preserved, the section has been highlighted in light blue (Figure 6.18 – core A; Figure 6.19 – core A; Figure 6.21 – core A). In the areas where the maximum set thickness of the barchanoid dunes has been preserved, the section has been highlighted in light green (Figure 6.19 – cores A and D; Figure 6.20 – cores B and D; Figure 6.21 – cores C and D); where the core has intersected the junction between two separate barchanoid dunes, the cosets have been highlighted in light yellow (Figure 6.20 – cores A and C). The addition of a coeval barchanoid dune field in this model contributes an additional complexity to the foreset dip-azimuth distributions. Although a large proportion of the pseudo-cores exhibit the expect unimodal distributions (Figure 6.18 – all cores) as was the case for Auk Model 2, the barchanoid dunes in this model are migrating in a different direction to the larger linear bedforms. The foreset dip-azimuths show a predominantly unimodal distribution, and in some cases a switch in foreset dip-azimuth is seen in the very thick deposits of wind-rippled facies at the base of the linear draa (all cores from both oblique sections – Figures 6.20 and 6.21), partly due to the way in which the bedforms have been modelled with an over-steepened angle-of-climb to preserve thicker sets and also reflecting the rare preservation of stoss-side wind-ripple deposits. As discussed previously (Sections 6.1.2.3 and 6.1.2.5), the morphology of the troughs is dictated by the wavelength and the amplitude of the plan-view along-crest sinuosity, and the range of foreset dip-azimuths is directly dictated by the amount of curvature in the trough. For Auk Model 6 (Section 5.11), the primary component of migration is via along-crest movement of plan-form sinuosities towards 090° and the secondary component of migration is via the lateral movement of the main bedforms at a slower rate, towards 000° (Figure 6.5b). The bedforms in the barchanoid dune field migrate towards 045°, and these bedforms are confined to low-lying interdune areas. The resultant path of the scour pits is determined by their net oblique translation generated by both the re-entrants of the large linear bedforms and also the barchanoid dunes, in this case between 060° and 070°. The preserved foresets exhibit a variable dip and the azimuths show a broad unimodal distribution, with a mean towards 035°. The preserved bounding surfaces also show a variable dip, but unlike the preserved foresets they show a bimodal distribution.

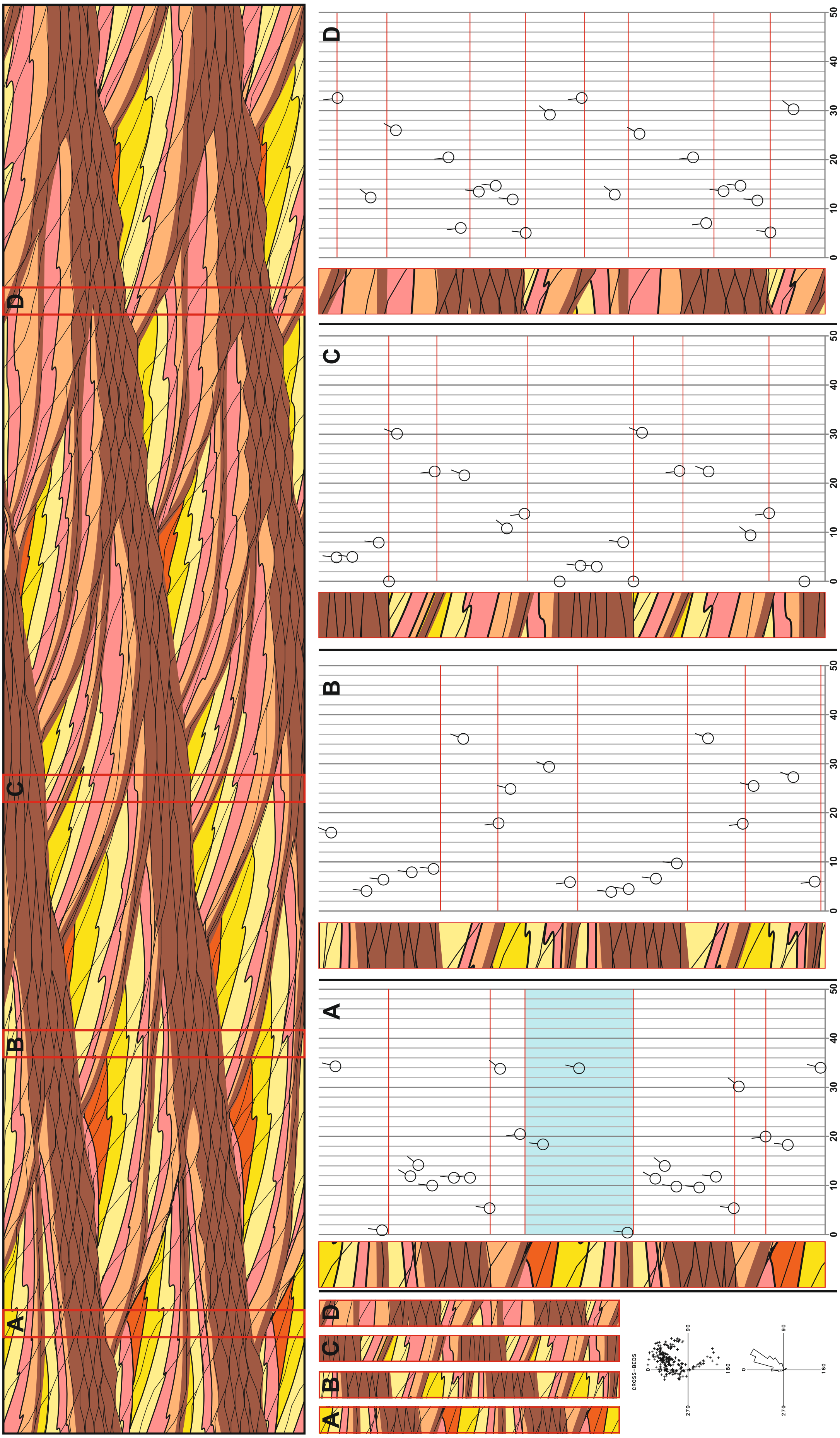

Figure 6.18. Pseudo-cores and subsequent foreset dip-azimuth plots for Auk Model 6 in a section taken parallel to the transverse component of linear dune migration. Position of transect within bedform model is shown in Figure 6.5a.

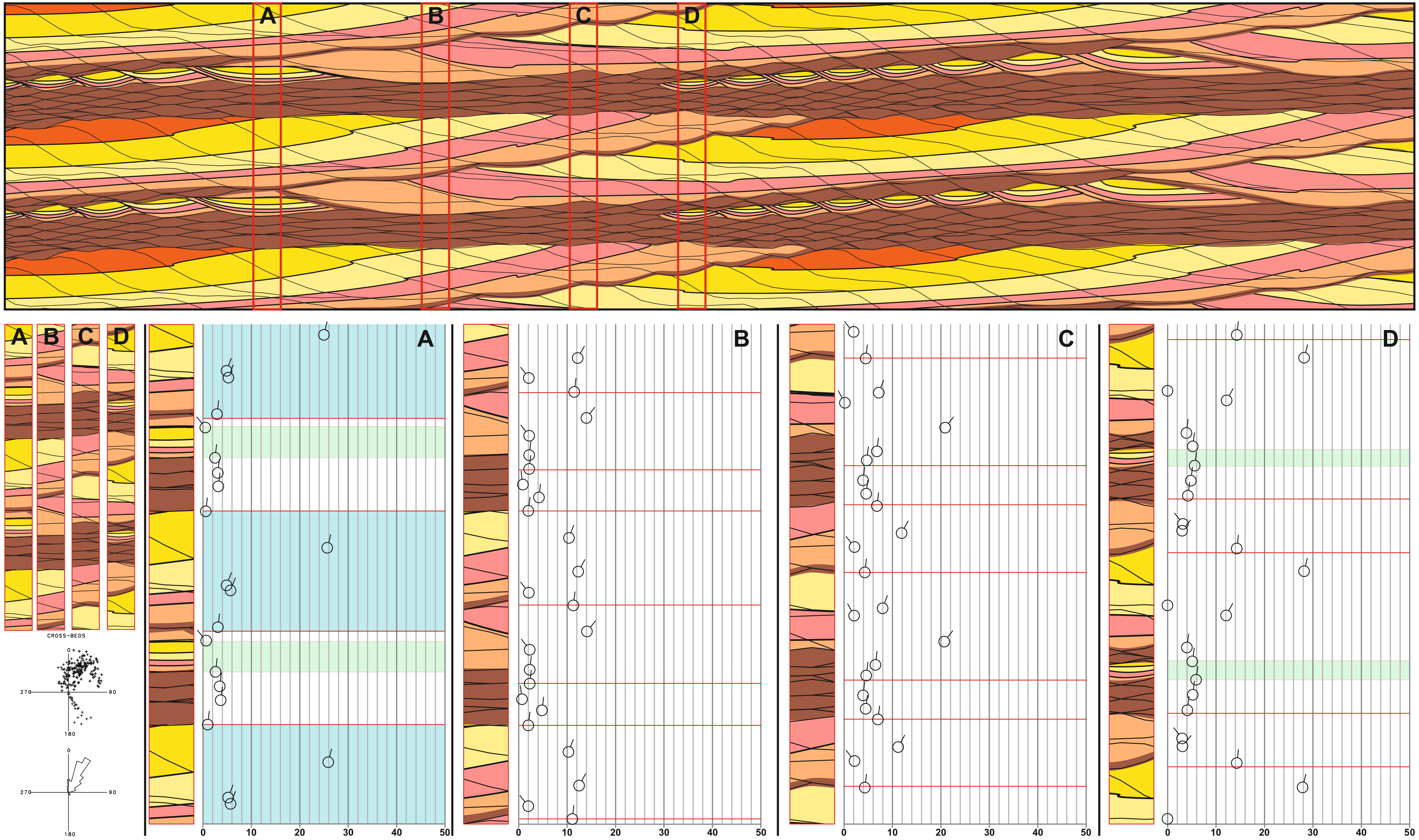

Figure 6.19. Pseudo-cores and subsequent foreset dip-azimuth plots for Auk Model 6 in a section taken parallel to the along-crest component of linear dune migration. Position of transect within bedform model is shown in Figure 6.5a.

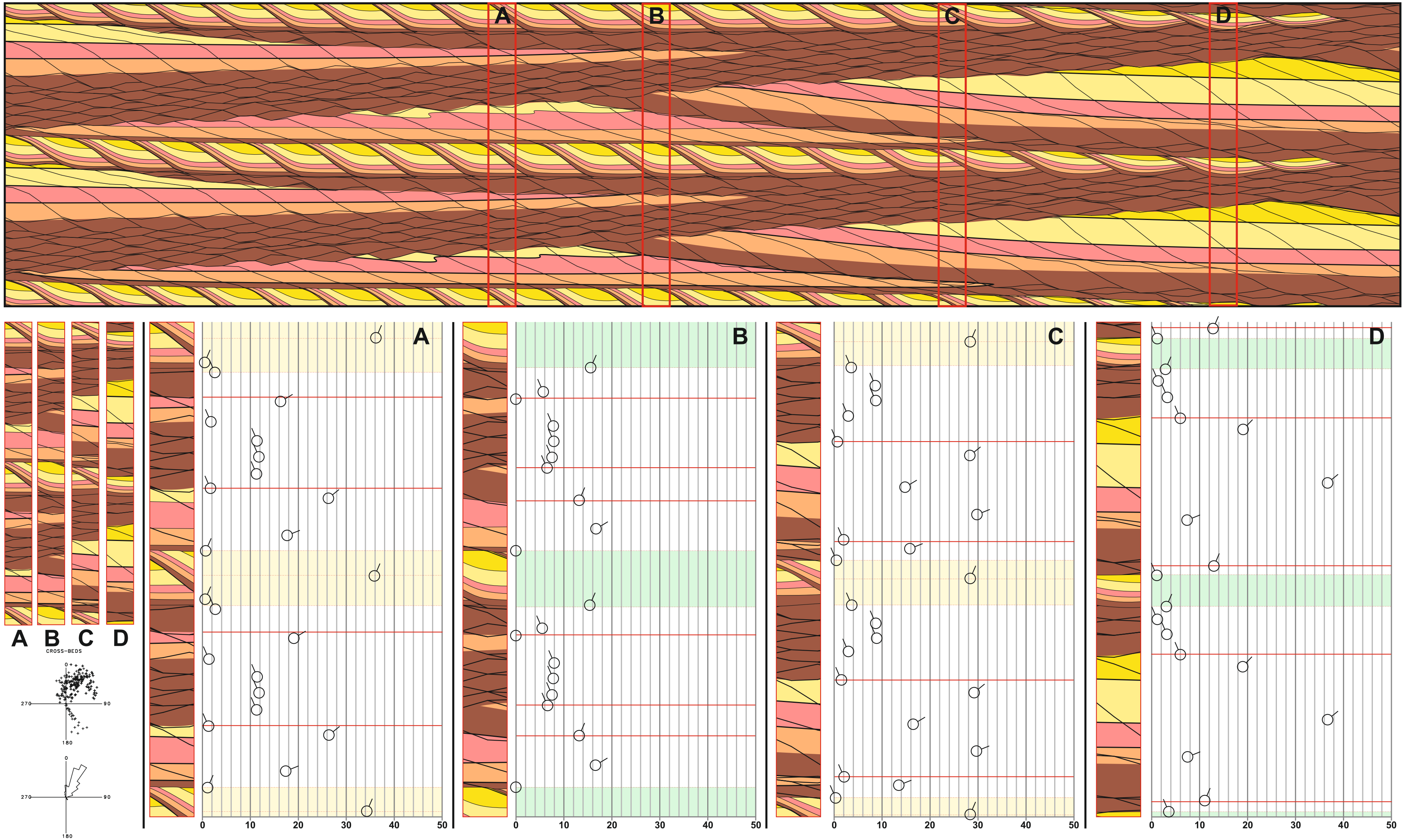

Figure 6.20. Pseudo-cores and subsequent foreset dip-azimuth plots for Auk Model 6 in a section taken oblique to linear dune migration. Position of transect within bedform model is shown in Figure 6.5a.

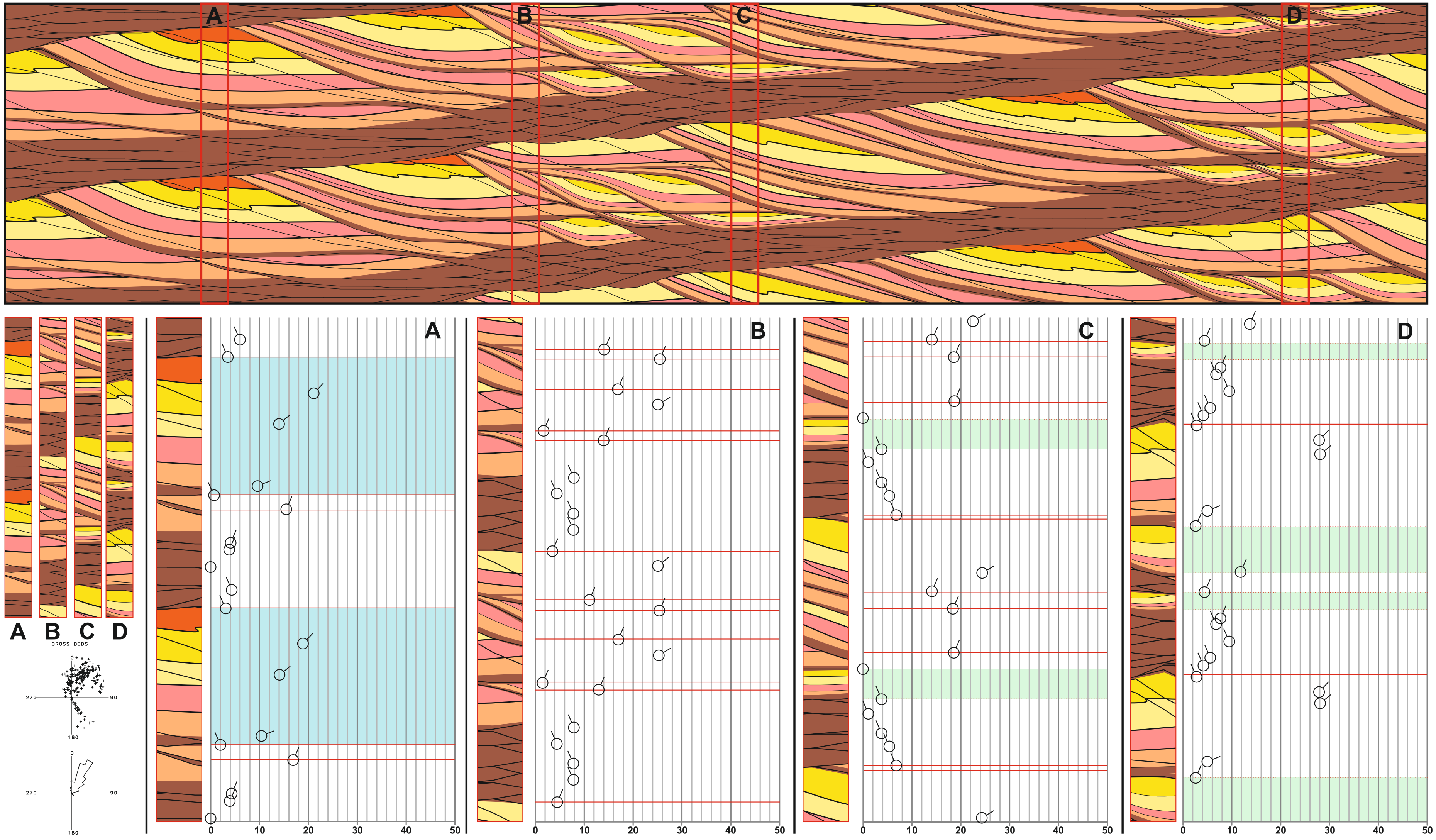

Figure 6.21. Pseudo-cores and subsequent foreset dip-azimuth plots for Auk Model 6 in a section taken oblique to linear dune migration. Position of transect within bedform model is shown in Figure 6.5a.

6.1.2.7 – Key advances

Reconstructing the type of bedforms responsible for generating the Auk Formation in Chapter 4 was possible because there was supplementary data available, and a suitable set of analogues from which to derive informed interpretations. As seen above, very different bedform morphologies can generate near-identical dipmeter log responses. It is almost impossible to differentiate between the dipmeter responses generated for perfectly transverse bedforms in Figure 6.7 – core C, and the cored section for perfectly linear bedforms in Figure 6.11 – core A. Conversely, in other cases, very different log responses can be generated from the same bedform model, usually over very short distances. This pattern is seen over almost all of the sections generated for the bedform models.

Although the observations outlined above are clear in a large proportion of the pseudo-cores, subtle trends do exist which may be useful in making a distinction between bedform types. For perfectly transverse bedforms, the cores show a gradual upwards-increase in the dip-azimuth range through an individual preserved set (e.g. Figure 6.6; Figure 6.7 – cores A and D; Figure 6.8 – all cores and Figure 6.9 – all cores), displaying an azimuth at the very top of the preserved sets which is approximate to the primary component of bedform migration, in this case towards 000° (e.g. Figure 6.6; Figure 6.7 – cores A, C and D; Figure 6.8 – cores A, B and D; Figure 6.9 – cores A and D). The cores generated from the perfectly linear bedform model tend to show a smaller range in foreset dip-azimuths (Figures 6.10 – 6.13); this is largely a function of the wavelength of the crestline sinuosity, whereby a tight trough apex (in plan view) generates more obvious bimodality in the distribution of foreset dip-azimuths. Model 5 for perfectly transverse bedforms was generated with an arbitrary value of 75 for the wavelength of crestline sinuosity, compared with an arbitrary value of 50 for the perfectly linear bedform model (Figure 3.3); the gentler rate of curvature is displayed in the increased range of foreset dip-azimuths in the model for perfectly transverse bedforms. For the cores generated from perfectly transverse bedforms, 70% show a unimodal distribution (9 cores) and 30% display a bimodal distribution (4 cores), where each preserved set displays azimuths in one direction or the other. Conversely, for the cores generated from perfectly linear bedforms, 42% display a unimodal distribution (5 cores) and 58% display a bimodal distribution (7 cores). Importantly, there are examples in the preserved sets from this perfectly linear model that show two opposing azimuths within the same preserved set (Figure 6.13 – cores B and C). This is the only bedform model from this study which displays this style; it is reasonable to interpret this as a diagnostic feature of foreset dip-azimuth distributions in bedforms of this type.

The foreset dip-azimuths for Auk Model 2 are tightly clustered around 030°-040° (Figure 6.4b); an arbitrary input value of 50 was used for the wavelength of crestline sinuosity (Figure 5.3), identical to the perfectly linear bedforms discussed above (Figure 3.3). For this reason, both of these models display a small range in the distribution of foreset dip-azimuths. Auk Model 6 was also generated with an arbitrary input value of 50 for the wavelength of crestline sinuosity (Figure 5.3); however this model displays a substantially greater range in the distribution of foreset dip-azimuths (Figure 6.5b). The reason for this increased range is therefore not attributable to a gentler rate of crestline curvature; rather it is the addition of the superimposed bedforms migrating obliquely to the parent bedforms. This increased range in the distribution of foreset dip-azimuths is feasibly a diagnostic feature of superimposed bedforms, the presence of which has favourable implications for overall net reservoir volumes (see Section 6.2.1.6).

6.1.3 – Facies distributions on aeolian bedforms

Different types of bedforms yield distinct arrangements of facies on their lee- and stoss-slopes, and therefore record a predictable set of characteristics within preserved sets. A suite of graphical models which depict the predicted arrangements of aeolian facies on dune lee- and stoss-slopes of bedforms with markedly different morphologies and migration styles have been developed (Figure 6.22) to capture this inherent variability.

6.1.3.1 – Methodology: facies distributions

For each of the theoretical bedform models introduced in Chapter 3 (Sedimentological Models 1-8; Sections 3.6 – 3.13), and for two bedform models of the Auk Formation from Chapter 5 (Auk Model 2 – Section 5.7; Auk Model 6 – Section 5.11), expected aeolian lithofacies have been mapped onto the modelled outputs using CorelDraw, based on a series of rules to determine the positions on the modelled dunes where the different facies packages accumulate (Figure 6.22). The implemented rules are outlined in Section 3.4.3.

6.1.3.2 – Transverse bedforms

The majority of transverse bedform types (including barchans, straight-crested transverse ridges and barchanoid dune ridges) observed in modern dune fields tend to be characterised by a single, downwind-facing slipface element, which in most cases is characterised by active avalanching down to a level within the bottom-most few metres of major cross-bedded sets (Hunter, 1985); a higher percentage of slipface facies, notably grainflow and grainflow-dominated facies, are expected to be preserved. Although this is a general trend that has been observed, exceptions abound. In the Namib Desert, over 250 m-high star forms have slipfaces which extend to the bases of the bedforms (Figure 1.12), and therefore using the criteria considered previously to reconstruct dune height or dune morphology would be problematic.

Four models depicting various migration styles of transverse bedforms and their associated facies distributions have been developed: Sedimentological Model 1 (Figure 6.22a); Sedimentological Model 2 (Figure 6.22b); Sedimentological Model 3 (Figure 6.22c); and Sedimentological Model 6 (Figure 6.22f). Model 1 (Figure 6.22a) depicts very simple two-dimensional transverse bedforms with a relatively low-angle-inclined dune plinth, meaning the grainflow avalanches have been modelled terminating at a higher position on the dune slope compared with bedforms which possess steeper dune plinths, as in Model 3 (Figure 6.22c). For bedforms that undertake a periodic fluctuation in height (Model 2 – Figure 6.22b), the result is regularly repeating reactivation surfaces at which wind-ripple strata is preferentially deposited, commonly seen in ancient outcropping successions of this type (Herries, 1993). The final model for transverse bedforms is similar to that of Model 1 (Figure 6.22a) in the section taken perpendicular to the trend of the main bedforms, but in this case the model preserves thicker sets by comparison, and therefore larger volumes of effective net reservoir facies are preserved (Model 6 - Figure 6.22f). The variable nature of the bedforms in Model 6, plus the addition of superimposed bedforms which are migrating in a different direction to the parent bedforms, gives rise to a complex distribution of facies, where grainflow avalanches are separated by repeated reactivations associated with wind-ripple strata. This complex geometry means that grainflow units are regularly punctuated by wind-ripple facies considered non-net reservoir, which has detrimental implications for fluid flow across the reservoir volume in bedforms of this nature.

6.1.3.3 – Linear bedforms

Although recognition of linear dunes is not an easy task, sedimentological and architectural features have been proposed as useful tools for their recognition in the sedimentary record (see Scherer, 2000 and Rodríguez-López, et al. 2008). Linear bedforms tend to show an upward-increase in the occurrence of slipface facies, a style of deposition which is typically observed on large linear bedforms (e.g. Tsoar, 1982; Bristow et al., 2000).

Two models depicting various migration styles of perfectly linear bedforms and their associated facies distributions have been developed: Sedimentological Model 5 (Figure 6.22e); and Sedimentological Model 8 (Figure 6.22h). Although both of these bedform models have along-crest migrating sinuosities, the position of the parent bedforms modelled in Model 8 (Figure 6.22h) reverses from side-to-side. It is the combination of the along-crest migrating sinuosities and the oscillating parent bedform motion that gives rise to the numerous reactivation surfaces in Model 8, with the grainflow packages confined within these reactivated sets.

With all aeolian facies distributions, the preservation potential of grainflow-dominated units is dependent on three primary factors: (i) the distance down the lee-slope that the original grainflow facies extended; (ii) the wavelength of the original bedforms; and (iii) the angle at which the bedforms climbed over one another to generate the accumulated sets. The first parameter is governed by the shape of the dune lee slope: where a thick, low-angle-inclined plinth is present, grainflows tend to terminate higher up the dune slope. The latter two parameters (wavelength and angle-of-climb of the original bedforms) jointly determine the level at which dunes are truncated to preserve sets of cross strata of a given thickness. For the perfectly linear bedforms in Figure 6.22e, the grainflows extend to the lower parts of the dune lee slope which is common in bedforms in the central portion of the Namib Desert

(Lancaster, 1982). Conversely, the linear bedforms in Figure 6.22h are reversing from side-to-side and therefore preserve a higher proportion of wind-ripple facies at the reactivation surfaces, which adversely impacts the resultant reservoir quality.

6.1.3.4 – Oblique bedforms

The bedforms modelled in Sedimentological Model 4 are oblique forms, and possess along-crest migrating superimposed bedforms (Figure 6.22d). The interaction of these two scales of bedforms allows for a higher proportion of grainflow and grainflow-dominated facies to be preserved, which has positive implications for reservoir volumes dominated by bedforms of this style. The parent bedforms in Sedimentological Model 7 (Figure 6.22g) are oblique to transport, and the lee-side scour pits and spurs migrate along-crest in addition to reversing back and forth (Rubin 1987a). This is an oblique-bedform analogue of Sedimentological Model 6 (Figure 6.22f), and differs from it in that the spurs have a net along-crest migration. The complexity of the facies distributions is due to the oscillating behaviour of the superimposed bedforms in this example. Although there are still large portions of grainflow and grainflow-dominated facies present, these are recurrently encapsulated with wind-ripple facies. This makes permeability across this reservoir volume potentially problematic as the net reservoir facies are isolated; this is discussed further in Section 6.2.3.

6.1.3.5 – Auk Formation bedforms

A detailed core and well-log analysis which incorporated additional information from analogous outcropping successions and modern dunes in Chapter 4 allowed the reconstruction of original bedform type, size, and style of migratory behaviour for the Auk Formation, a succession known only from subsurface. This research is a valuable case study of preserved linear draa, which have been previously under recognised in literature. The bedforms which migrated and accumulated to give rise to the Auk Formation represent ancient linear draa in a large, dry aeolian system based on key observations made in the available core data (Chapter 4). The observations which gave rise to this interpretation were largely due to the vertical arrangement of recorded facies, notably the occurrence of thick packages of wind-ripple and wind-ripple-dominated strata of various types, even in fairly steeply-dipping deposits that have clearly been deposited in a fairly elevated position on a major bedform (e.g. wind-ripple-dominated sections with inclinations of 10° to 20°).

Facies distributions for two models predicted for different parts of the Auk Formation succession are displayed in Figure 6.22i (Auk Model 2) and Figure 6.22j (Auk Model 6). In contrast to Sedimentological Model 5 (Figure 6.22e), the linear bedforms which migrated and accumulated to preserve the Auk Formation succession are envisaged to have had low-angle-inclined lower dune flanks which preferentially preserved wind-ripple strata (Chapter 4 – Section 4.5.4), thereby lacking significant amounts of grainflow strata associated with the linear bedforms. By contrast, the addition of a barchanoid dune field migrating through the interdune corridors of the main linear bedforms in Auk Model 6 (Figure 6.22j) means that a higher proportion of grainflow facies is preserved in this model. Barchanoid dunes commonly have small slipfaces where grainflow avalanches fully extend down their lee slopes, and therefore these grainflow facies associated with the barchanoid dunes are more likely to be preserved in a succession of bedforms which arose via a bedform climbing mechanism.

6.1.3.6 – Key advances

It is evident from this analysis that aeolian facies are not arranged in the same way on the lee and stoss slopes of all types of bedforms; although this has been noted previously (e.g. Karpeta, 1990; Mountney, 2006a), a unifying model has yet to be developed to account for facies distributions on aeolian bedforms of various types. Previous assumptions on facies arrangements in bedforms of different morphologies, such as transverse bedform types being characterised by active avalanching down to a level within the bottom-most few metres of major cross-bedded sets, are not universally applicable. It is evident that there are no set rules which govern facies distributions, as some 250 m-high star dunes in the Namib Desert have slipfaces which extend to the base of the slope. It is more applicable to interpret the expected facies distributions for bedforms of different morphologies on the bedform architectures generated by this forward modelling process, and the interactions of bedforms with one another.

These examples are, in the most part theoretical, and the distributions of aeolian facies types will still vary in natural examples from those shown here based on other allogenic factors, such as the effect of wind strength on grainflow and grainfall activity; for example, production of grainfall is reduced at lower speeds and increased at higher speeds (Eastwood et al., 2012). Nevertheless, a number of factors clearly influence the resulting facies distributions. The type of aeolian facies preserved in cored intervals can be used to deduce key information on the morphology of the original bedforms, and the style in which they migrated to accumulate a preserved succession.

If a greater proportion of wind-rippled facies is preserved in the set, it is reasonable to infer one or more of the following: (i) the original bedforms possessed low-angle-inclined asymptotic lower plinths, commonly seen in larger dunes (Figure 6.1), whereby the grainflow avalanches rarely reached the base of slope (Model 1 – Figure 6.22a; Model 8 – Figure 6.22h; Auk Model 2 – Figure 6.22i); (ii) the preserved sets are relatively thin, as a function of original dune wavelength and angle-of-climb whereby lower angles-of-climb preserve thinner sets (Romain and Mountney, 2014) which is commonly seen in larger dunes, and therefore most of the upper parts of the dune slipface where grainflows occur have been cut-off by the successive advancing bedform in the train (Model 8 – Figure 6.22h); or (iii) that the bedforms were oscillating or regularly fluctuating in height, generating numerous thin sets bounded by reactivation surfaces that preferentially deposit wind-ripple strata (Model 2 – Figure 6.22b; Model 6 – Figure 6.22f; Model 7 – Figure 6.22g; Model 8 – Figure 6.22h).

If a greater proportion of facies associated with deposition on a bedform lee slope at an angle-of-repose (e.g. grainflow facies) is encountered, it is reasonable to infer one or more of the following: (i) that the original bedforms possessed a dune plinth that failed to develop to any great height, commonly seen in smaller dunes (Figure 6.1), such that the angle-of-repose lee slope extended down very close to the dune base (Model 3 – Figure 6.22c; Model 5 – Figure 6.22e; Model 6 – Figure 6.22f); (ii) the preserved sets are relatively thick, as a function of original dune wavelength and angle-of-climb whereby higher angles-of-climb preserve thicker sets (Romain and Mountney, 2014), commonly seen in smaller dunes, and the thicker preserved sets therefore capture a higher proportion of facies associated with the upper slipface (Model 6 – Figure 6.22f); or (iii) the presence of superimposed bedforms, which preserves a higher proportion of slipface facies due to the interaction of two scales of bedforms, and increases the probability of grainflow facies being preserved (Model 4 – Figure 6.22d; Model 7 – Figure 6.22g; Auk Model 6 – Figure 6.22j).

However, there are complications which arise from the addition of superimposed bedforms; although it is likely that a higher proportion of grainflow facies are preserved, the interaction of two scales of bedforms create multiple superimposition surfaces which preferentially preserve wind-ripple facies (Model 7 – Figure 6.22g). Similarly, Model 6 (Figure 6.22f) preserves a large proportion of grainflow facies by virtue of the relatively thick sets, but the reversing nature of the superimposed bedforms generates multiple reactivation surfaces which preferentially preserve wind-ripple facies. In Auk Model 6 (Figure 6.22j) the modelled bedforms possessed low-angle-inclined plinths as well as numerous superimposition surfaces, both factors which are conducive to increased preservation of wind-ripple facies, but in this case the presence of superimposed barchanoid dunes overrides the influence that the other factors have on the resulting stratigraphy, and this model preserves a high proportion of net reservoir facies (see Section 6.2.1.6).

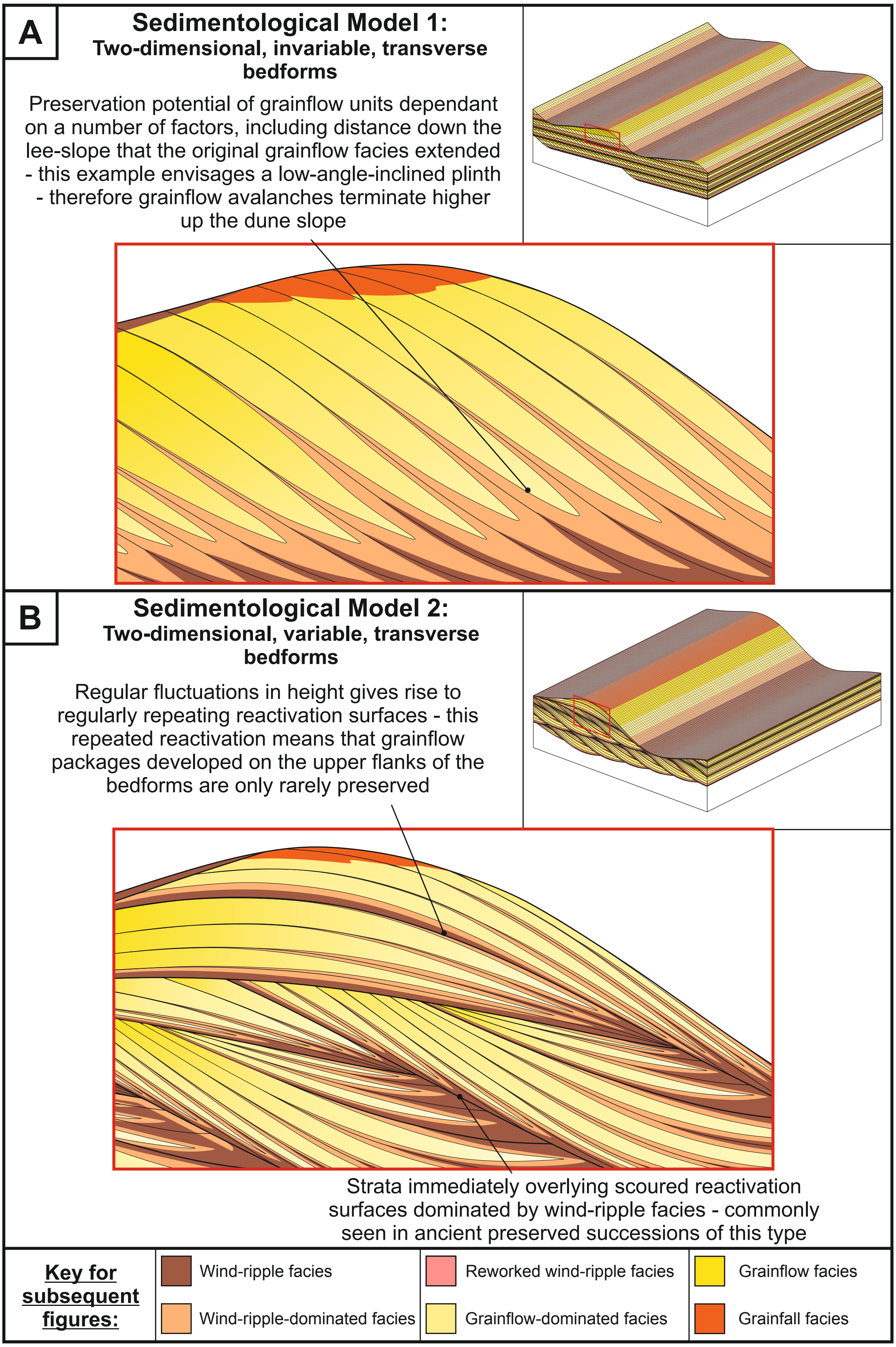

Figure 6.22. Expected facies distributions for a number of bedform types with distinct morphologies and styles of migratory behaviour: a) two-dimensional, invariable, transverse bedforms; b) two-dimensional, variable, transverse bedforms; c) three-dimensional, invariable, perfectly transverse bedforms; d) three-dimensional, invariable, oblique bedforms; e) three-dimensional, invariable, perfectly linear bedforms; f) three-dimensional, variable, perfectly transverse bedforms; g) three-dimensional, variable, oblique bedforms; h) three-dimensional, variable, perfectly linear bedforms; i) linear bedforms with a minor component of transverse motion; and j) linear bedforms with a minor component of transverse motion, and superimposed barchanoid dunes.

C

Sedimentological Model 3:
Three-dimensional, invariable, perfectly transverse bedforms

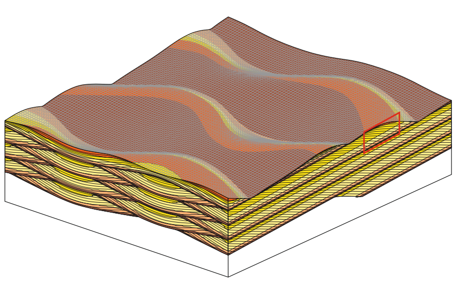

In contrast to Sedimentological Model 1 (A) - this example envisages a steeper dune plinth, and therefore the grainflow facies extend further down the dune lee slope than their counterparts in (A). This has positive implications for overall reservoir quality

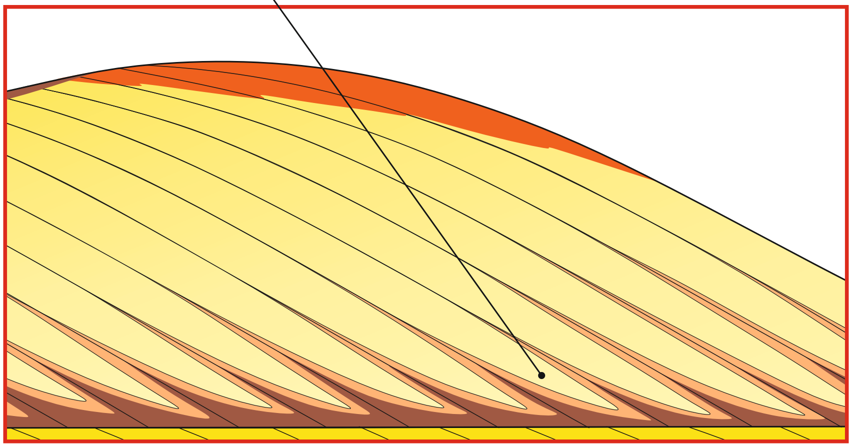

D

Sedimentological Model 4:
Three-dimensional, invariable, oblique bedforms with along-crest migrating superimposed bedforms

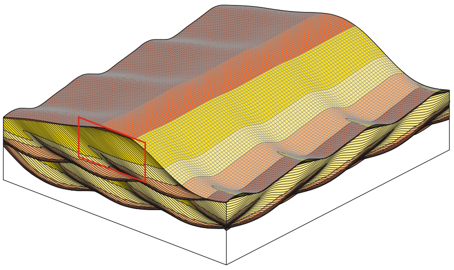

Two scales of bedforms allow for a higher proportion of net reservoir facies to be preserved, both grainflow and grainflow-dominated facies, with favourable implications for reservoir quality

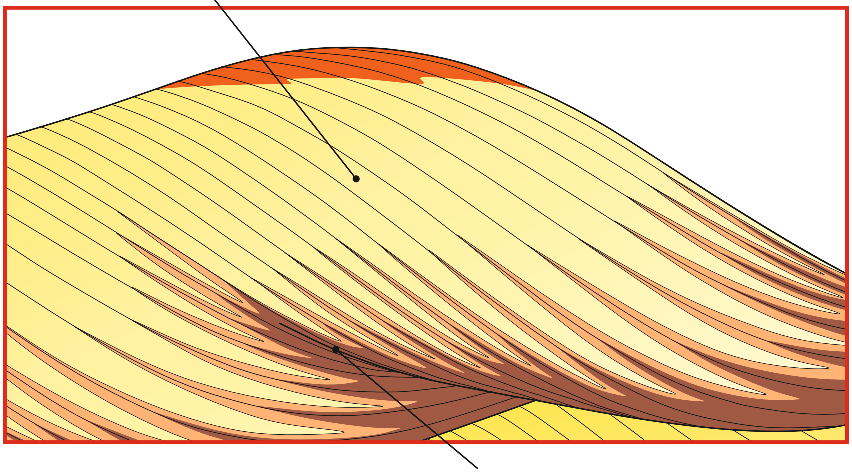

Interaction of two scales of bedforms generates superimposition surfaces

E

Sedimentological Model 5:

Three-dimensional, invariable, perfectly linear bedforms

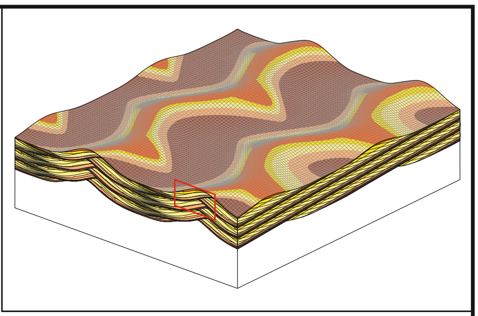

This model envisages grainflow units extending to the lower parts of the dune lee slope, thereby preserving significant volumes of grainflow strata; these types of bedforms are common in the central portions of the Namib Desert (Lancaster, 1982).

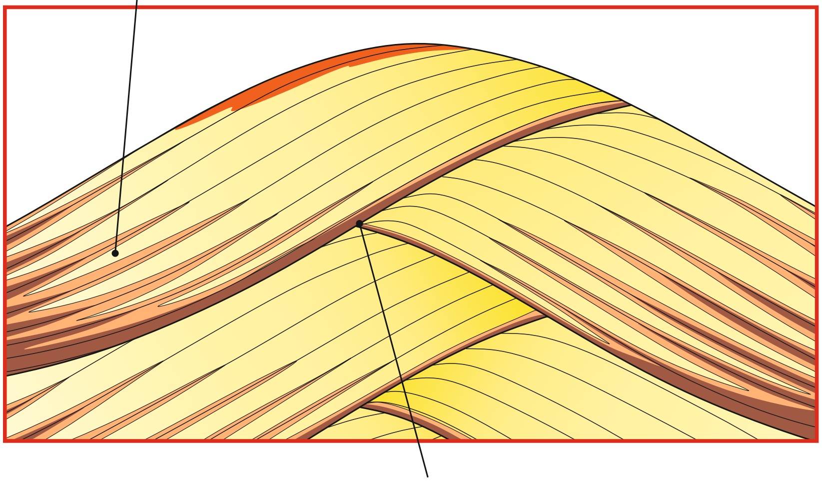

Bounding surfaces cross-cut each other and are lined with relatively low porosity and permeability wind-ripple strata

F

Sedimentological Model 6:

Three-dimensional, variable, perfectly transverse bedforms

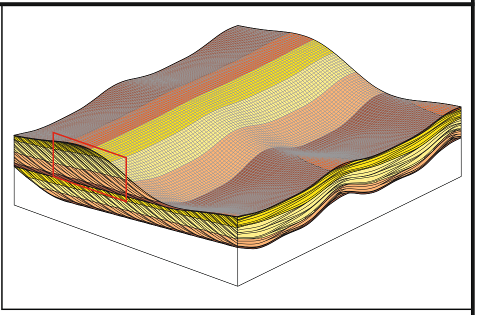

Stratigraphic architecture generated here is similar to that for Sedimentological Model 1 (A) - however this model preserves much thicker sets by comparison, and therefore larger volumes of effective net reservoir facies

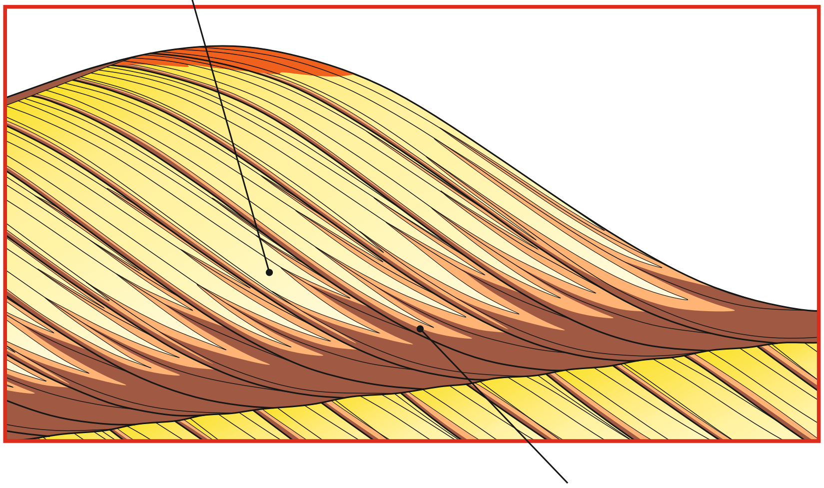

Numerous bounding surfaces characterised by wind-ripple and wind-ripple-dominated facies

G

Sedimentological Model 7:

Three-dimensional, variable, oblique bedforms

Oblique-bedform analogue of Sedimentological Model 6 (F) - here the spurs have a net along-crest migration

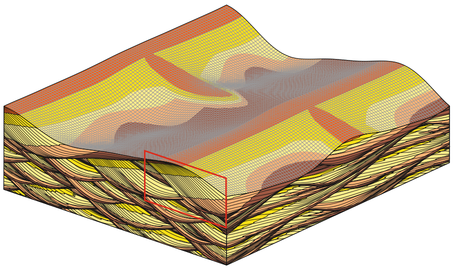

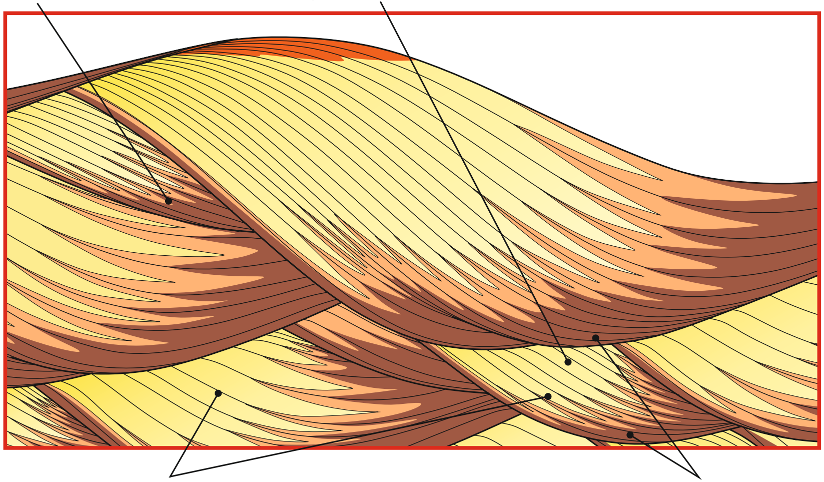

Complex facies distributions due to reversing (oscillating) behaviour of the superimposed bedforms

Large portions of grainflow facies are present but each is surrounded by wind-ripple facies - permeability across the reservoir volume a potential issue

Various sizes and geometries of net reservoir stratal packages are displayed - recurrently surrounded by wind-ripple facies

Thick accumulations of wind-ripple and wind-ripple-dominated facies at the base of the oscillating bedforms entirely encapsulate the net reservoir facies

H

Sedimentological Model 8:

Three-dimensional, variable, perfectly linear bedforms with along-crest migrating sinuosities

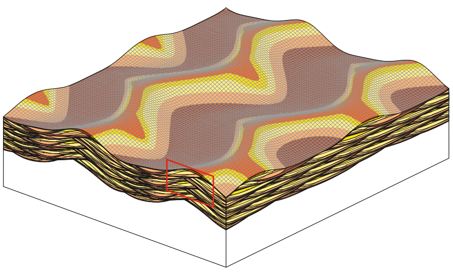

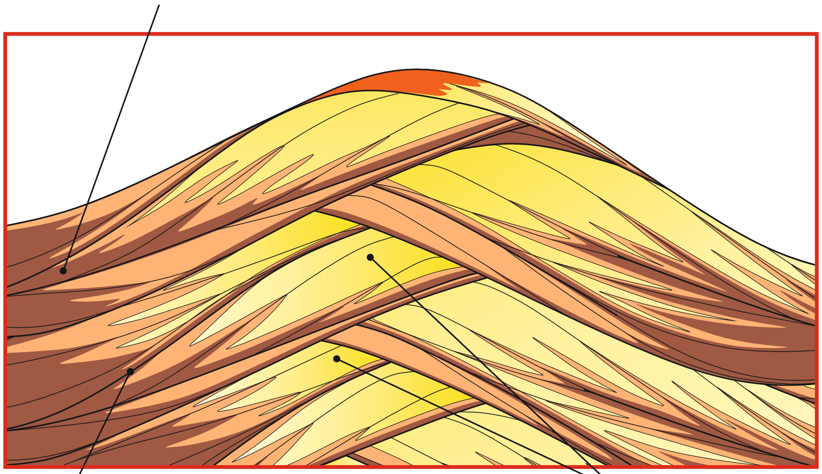

Dominance of wind-ripple over grainflow facies in this model contrasts with Sedimentological Model 5 (E) due to the oscillating bedform motion here - generates multiple thin sets bounded by reactivation surfaces

Numerous thin trough-like sets bounded by reactivation surfaces preferentially lined with wind-rippled strata

Grainflow and grainflow-dominated facies packages confined within the reactivated sets - a significant proportion of the reservoir volume is dominated by non-net reservoir

I

Auk Model 2:

Linear bedforms with minor component of transverse motion

In contrast to Sedimentological Model 5 (E), the linear draa in the Auk Formation had low-angle-inclined lower dune flanks which preferentially preserved wind-ripple-dominated strata (Chapter 4), thereby lacking significant amounts of preserved grainflow packages associated with the linear draa in cored sections

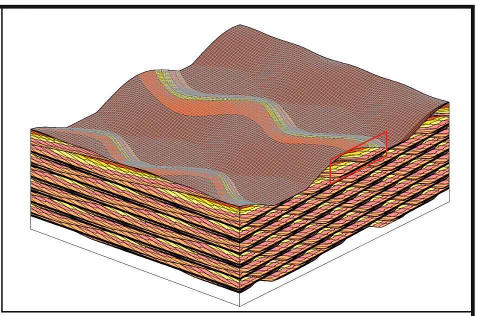

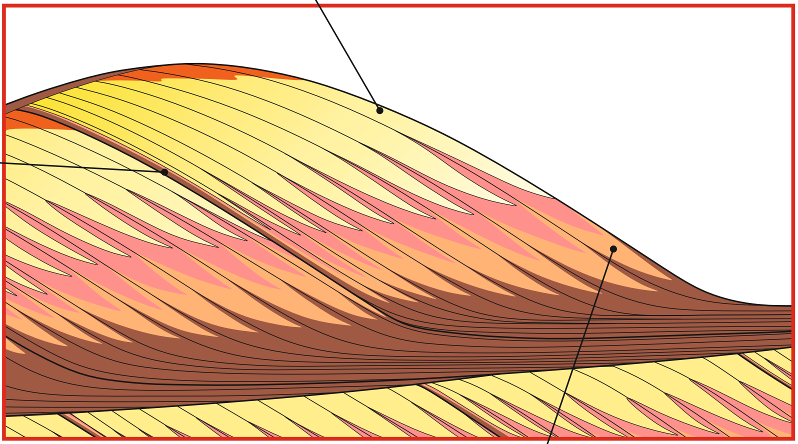

Bounding surfaces preferentially lined with wind-ripple strata

Basal plinth region dominated by wind-rippled facies of various types

J

Auk Model 6:

Linear bedforms with minor component of transverse motion and superimposed barchanoid dunes

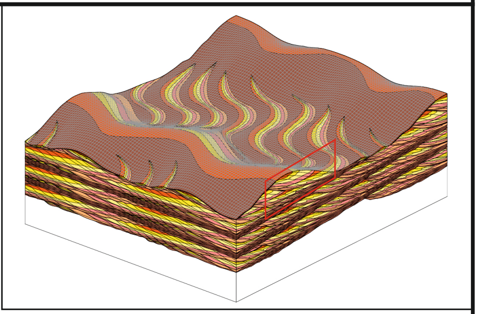

Facies associated with larger linear draa - grainflow facies restricted to upper slipface

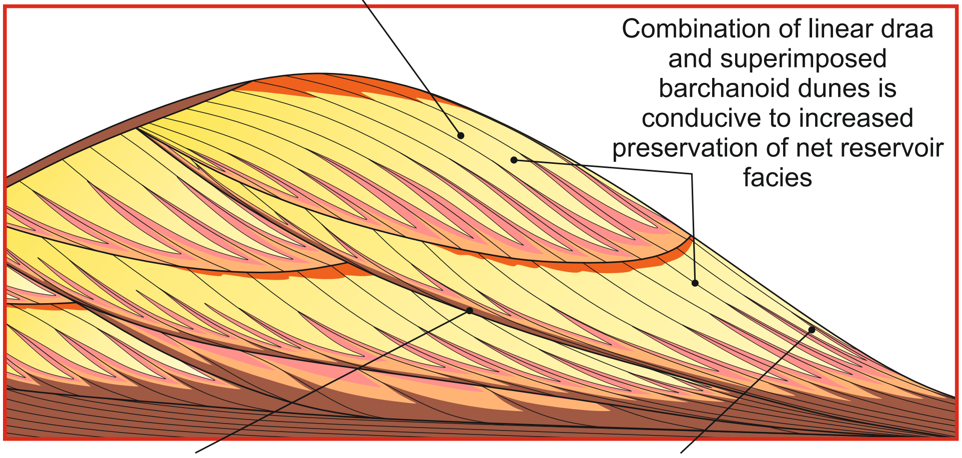

Combination of linear draa and superimposed barchanoid dunes is conducive to increased preservation of net reservoir facies

Numerous sumperimposition surfaces arise as a result of the interaction of two scales of bedforms - preferentially lined with wind-rippled facies

Facies associated with smaller barchanoid dunes - grainflow facies extend to base of plinth. Barchanoid dunes commonly have small slipfaces where grainflows fully extend down their lee-slopes

6.2 – The effect of original bedform morphology and migratory behaviour on overall reservoir quality

6.2.1 – Net reservoir calculations

To investigate the effect that original bedform morphology and migratory behaviour has on the resultant reservoir quality, the percentage of each facies types in the pseudo-cores from Figures 6.6 to 6.21 has been calculated. Results from these calculations are depicted in a series of charts (Sedimentological Model 3; perfectly transverse bedforms – Figure 6.23; Sedimentological Model 5; perfectly linear bedforms – Figure 6.24; Auk Model 2 – Figure 6.25; Auk Model 6 – Figure 6.26). This exercise enabled an overall estimate to be made of the likely preserved facies and resultant reservoir quality expected for specific aeolian bedform types.

Within the remit of this study, net reservoir is defined as grainflow and grainflow-dominated facies, based on porosity and permeability plots from existing aeolian oil reservoirs (Figure 1.18 and Figure 1.19). Wind-ripple, wind-ripple-dominated, reworked wind-ripple and grainfall facies are all considered non-net reservoir; these facies would likely make effective net reservoir in many gas plays, but typically do not in oil reservoirs There are other scales of observation which could be included, such as the occurrence of thin wind-ripple laminations between successive avalanching grainflow deposits. For the purposes of this study, the calculations have been made based on the most common expected facies type, as the architectural-element-scale of observation used in this research is the most pertinent scale of observation adopted in reservoir modelling software.

6.2.1.2 – Methodology: net reservoir calculations

The pseudo-cores generated in Section 6.1.2 were used to calculate the net reservoir values for the bedform models (Sedimentological Model 3; perfectly transverse bedforms – Figure 6.23; Sedimentological Model 5; perfectly linear bedforms – Figure 6.24; Auk Model 2 – Figure 6.25; Auk Model 6 – Figure 6.26). Net reservoir quantities were calculated for the following: (i) each individual pseudo-core; (ii) each individual perpendicular, parallel and oblique sections, by calculating the average value for the individual pseudo-cores associated with the section being considered; (ii) the total average of the perfectly perpendicular and perfectly parallel sections for the bedform model being considered; (iv) the total average of the two obliquely oriented sections for the bedform model being considered; and (v) the overall average net to gross value for the entire bedform model.

The values (percentages) of net to gross stated in the subsequent sections include only preserved sets; the effects of sediment compaction have not been quantifiable within the remit of this study. The bedform models have been generated with an artificially steep angle-of-climb so the bedform architecture can be clearly seen, as the steeper angle-of-climb preserves thicker sets (Romain and Mountney, 2014) and therefore a higher proportion of facies generated on the upper parts of bedform slopes (considered net reservoir in this study); the over-steepened angle-of-climb will have a minor impact on results. However, the angle-of-climb has been over-steepened in all of the models used for this study; therefore they can be directly related to one another.

6.2.1.2 – Perfectly transverse bedforms

The net reservoir calculations for perfectly transverse bedforms are displayed in Figure 6.23. In the sections taken perfectly parallel and perpendicular to the trend of the main bedforms, cores which punctuate the centres of troughs have the highest preserved reservoir quality (net reservoir 76% and 81%), whereas cores from the intersection of two bedforms have markedly less grainflow and grainflow-dominated facies because the strata directly above the bounding surfaces are preferentially associated with non-net reservoir facies comprising wind-ripple strata of various types; net reservoir values for the cores which intersect the two bedforms are 26% and 36%. The combined averages of these ‘normal’ sections of the volume comprise 62% net reservoir facies. A higher percentage of non-net reservoir facies is intersected in the oblique sections of this model, therefore perceived reservoir quality is poorer than the sections aligned perfectly perpendicular and parallel to trend of the main bedforms. The average net reservoir value for the combined oblique sections is reduced to 48% from 62% in the ‘normal’ sections.

The calculated net to gross values for individual cores across the 4 sections of the bedform model show a wide variety of values. The lowest preserved volume of net reservoir facies is from the oblique section in Figure 6.9 – core C (21% net reservoir). The highest preserved volume of net reservoir facies is from the section perfectly parallel to the trend of the main bedforms in Figure 6.7 core B (82% net reservoir). The two oblique sections have the poorest reservoir quality overall, with a higher proportion of wind-rippled facies preserved in these sections. This is displayed where all the cores from the oblique sections are averaged. The oblique sections have 48% net reservoir, whereas the normal sections have 62% net reservoir. Overall, there is a high proportion of net to gross preserved in these perfectly transverse bedforms (overall bedform model – 55% net reservoir).

6.2.1.3 – Perfectly linear bedforms with along-crest migrating sinuosities

The net reservoir calculations for perfectly linear bedforms are displayed in Figure 6.24. In the section parallel to the trend of the linear bedform, the core has a higher proportion of net reservoir preserved (63% net reservoir). Net reservoir decreases to 51% in the section perpendicular to the trend of the main bedforms. Figure 6.11 – core A punctuates the intersection of two bedforms, thereby preserving the highest proportion of non-net reservoir as the bounding surfaces are lined with wind-rippled facies.

The cores from the oblique section in Figure 6.12 have a higher net to gross than those in Figure 6.13. In Figure 6.12 – core B, the net reservoir facies make up 94% of the core. However at a short distance away, core D has only 24% net reservoir facies, as it punctuates the interval between two successive bedforms and therefore intersects the bounding surfaces which are commonly associated with wind-ripple facies. In Figure 6.13 – core A, there is zero net reservoir preserved as this core punctuates a long-lived interdune flat. The bedforms in this model do not migrate, so this interdune flat is present throughout the upward expression of the stratigraphy – however this would be unlikely in nature, as over time the bedforms would likely show net migration, meaning these interdunes would be overlain by grainflow facies of the successive bedform.

As with the perfectly transverse bedforms described previously, each individual cored interval from this bedform model show vast differences in perceived reservoir quality. The highest quality reservoir is from the oblique section (Figure 6.12), where core B preserves 94% net reservoir facies. The poorest reservoir quality is from the alternative oblique section (Figure 6.13) where core A preserves zero net reservoir facies.

When the cores from the individual sections are combined, Figures 6.10 and 6.12 preserve the best reservoir, with 63% and 64% net reservoir respectively. The other two sections (Figures 6.11 and 6.13) have a lower preserved reservoir quality, with the 51% and 52% preserved net reservoir. Overall, the bedform model for non-migrating linear bedforms preserves a reservoir volume of excellent quality, with 57% net reservoir preserved over the entire volume; slightly better than the reservoir interval predicted for perfectly transverse bedforms (55% net reservoir).

6.2.1.4 – Theoretical bedform models versus Auk bedform models

The bedforms which migrated and accumulated to preserve the Auk Formation succession are envisaged to have been draa-scale bedforms (between 150-250 m high with wavelengths of 1500-2500 m – Chapter 4, Section 4.5.4), and for this reason the facies distributions on the bedforms have been modelled such that the majority of the facies preserved are those deposited on the lower flanks and plinths of these bedforms. The bedforms are perceived to have originated via a bedform climbing mechanism that resulted in preferential preservation of only their lowermost parts; therefore the following bedform models for the Auk Formation have a considerable decrease in net reservoir facies compared with the theoretical bedform models described above. For this reason, the reservoir quality of the bedform models for Auk will be considered separately to the theoretical bedform models.

6.2.1.5 – Linear bedforms with minor component of transverse motion

As explained above, the bedform models envisaged for the Auk Formation preserve a high proportion of non-net reservoir facies, which conforms to the facies distributions observed in core data from the reservoir interval described in Chapter 4 (e.g. well 30/16-2 – Figure 4.8). The net reservoir calculations for Auk Model 2 are displayed in Figure 6.25. Contrary to the theoretical models described for perfectly transverse and perfectly linear bedforms in Sections 6.2.1.2 and 6.2.1.3, the cores for various transects through Auk Model 2 are largely similar. There are two instances which show zero net reservoir, both of which are in the oblique sections (Figure 6.16 – core D and Figure 6.17 – core A).

The two sections taken parallel to the along-crest and transverse component of linear dune migration have the best predicted reservoir quality (combined values – 10% net reservoir). Of these, the section taken parallel to the along-crest component of linear dune migration (Figure 6.15) preserves the highest percentage of net reservoir (12%). The oblique sections in Figures 6.16 and 6.17 preserve the least net reservoir, with 6% and 4% net reservoir respectively. The combined values for both the oblique sections have 5% preserved net reservoir facies. Overall, Auk Model 2 preserves a reservoir volume of poor quality, with 8% net reservoir facies. The configuration modelled here alone would make Auk an improbable hydrocarbon prospect: most producing aeolian reservoirs are deemed to have effective net reservoir volumes of >25%, any less than this and the body cannot establish sufficient connectivity to be viable (King, 1990). Therefore, parts of the reservoir must be characterised by alternative, more favourable facies architectures; these are explained in Section 6.2.1.6.

6.2.1.6 – Linear bedforms with minor component of transverse motion and superimposed barchanoid dunes

The net reservoir calculations for Auk Model 6 are displayed in Figure 6.26. The addition of a barchanoid dune field migrating through the interdraa corridors of the main linear bedforms in this model modifies the preserved stratigraphy considerably. Whilst thick interdune areas dominated by wind-rippled facies of various types are still pervasive (Figure 6.22j), the addition of the smaller barchanoid dunes preserve a higher proportion of facies deposited on the upper parts of these smaller bedforms, notably a marked increase in the preservation of grainflow and grainflow-dominated facies which are considered net reservoir in this study. This increases the perceived reservoir quality overall compared with the stratigraphic expression envisaged for Auk Model 2.

Each individual core constructed for Auk Model 6 show the same prominent lateral disparity as was evident in the theoretical models described for perfectly transverse and perfectly linear bedforms in Sections 6.2.1.2 and 6.2.1.3. The net reservoir calculations for the section taken parallel to the transverse component of linear dune migration vary between 6% and 35% (Figure 6.18). Although the net reservoir calculations for the section taken parallel to the along-crest component of linear dune migration are noticeably higher (Figure 6.19), there is still a distinct difference between the measurements, with net reservoir facies varying between 19% (core B) and 49% (core A). These two cores are only a short distance from one another (~200 m when scaled to the Auk Formation), and demonstrate the complexity that can arise from the addition of the superimposed bedforms. The increased net reservoir calculation of 49% from core A is directly related to the existence of these smaller bedforms in the reservoir volume, as this core precisely intersects the barchanoid dune field. The cores constructed for the oblique sections of Auk Model 6 show largely the same results as those for the sections parallel to the transverse and along-crest components of linear dune migration. In both of these oblique sections, core D has the best perceived reservoir quality, as both these cores punctuate the junction between the interdune and large linear draa, capturing both the grainflow facies of the smaller barchanoid dune field and the grainflow facies from the larger linear draa in a single cored section (Figure 6.20 – core D and Figure 6.21 – core D). Overall, the reservoir volume predicted for Auk Model 6 is good, with 25% net reservoir facies. This increase in reservoir quality is directly related to the barchanoid dune field migrating through the interdune corridors of the linear draa.

6.2.1.7 – Key advances

Individual cores taken across a reservoir volume show significant differences in net reservoir facies calculations. This means that care must be taken when using only a small number of data points (e.g. core or well logs) to predict net reservoir in the subsurface. However, when comparing the entire bedform model calculations for perfectly transverse bedforms (Figure 6.23) and perfectly linear bedforms (Figure 6.24), the difference in overall quality of the two reservoir volumes is modest (transverse bedforms – 55% net reservoir facies; linear bedforms – 57% net reservoir facies). There are factors which will affect these calculations, such as the distance down the lee-slope that grainflow avalanches terminate (whereby bedforms with higher angled plinths are expected to preserve a higher proportion of grainflow strata), and the angle-of-climb of the bedforms (whereby increased angles-of-climb preserve thicker sets that would likely include a higher proportion of facies from the upper parts of bedforms, such as grainflow facies).

The bedform models for the Auk Formation depict markedly reduced proportions of net reservoir facies bodies compared to the theoretical models described above, and are therefore considered separately in Section 6.2.1.5 and Section 6.2.1.6. It is apparent from the models for the Auk Formation that the addition of superimposed bedforms in Auk Model 6 (Figure 6.26) significantly increases the predicted reservoir quality of the succession, with 25% net reservoir preserved compared with 8% net reservoir facies preserved in Auk Model 2 (Figure 6.25). Auk Model 6 will likely preserve grainflow facies (net reservoir) from the linear bedforms in addition to the grainflow facies from the smaller barchanoid dunes, where the grainflow avalanches often reach the base of the dune lee-slope; this significantly increases the preserved net reservoir quantities in reservoir successions of this type. The presence of small barchanoid dunes between major linear draa and their superimposition on the lower draa flanks is the most likely explanation for the ability of the Auk Formation to act as a viable reservoir; the large linear draa alone would not be directly conducive to a viable reservoir volume.

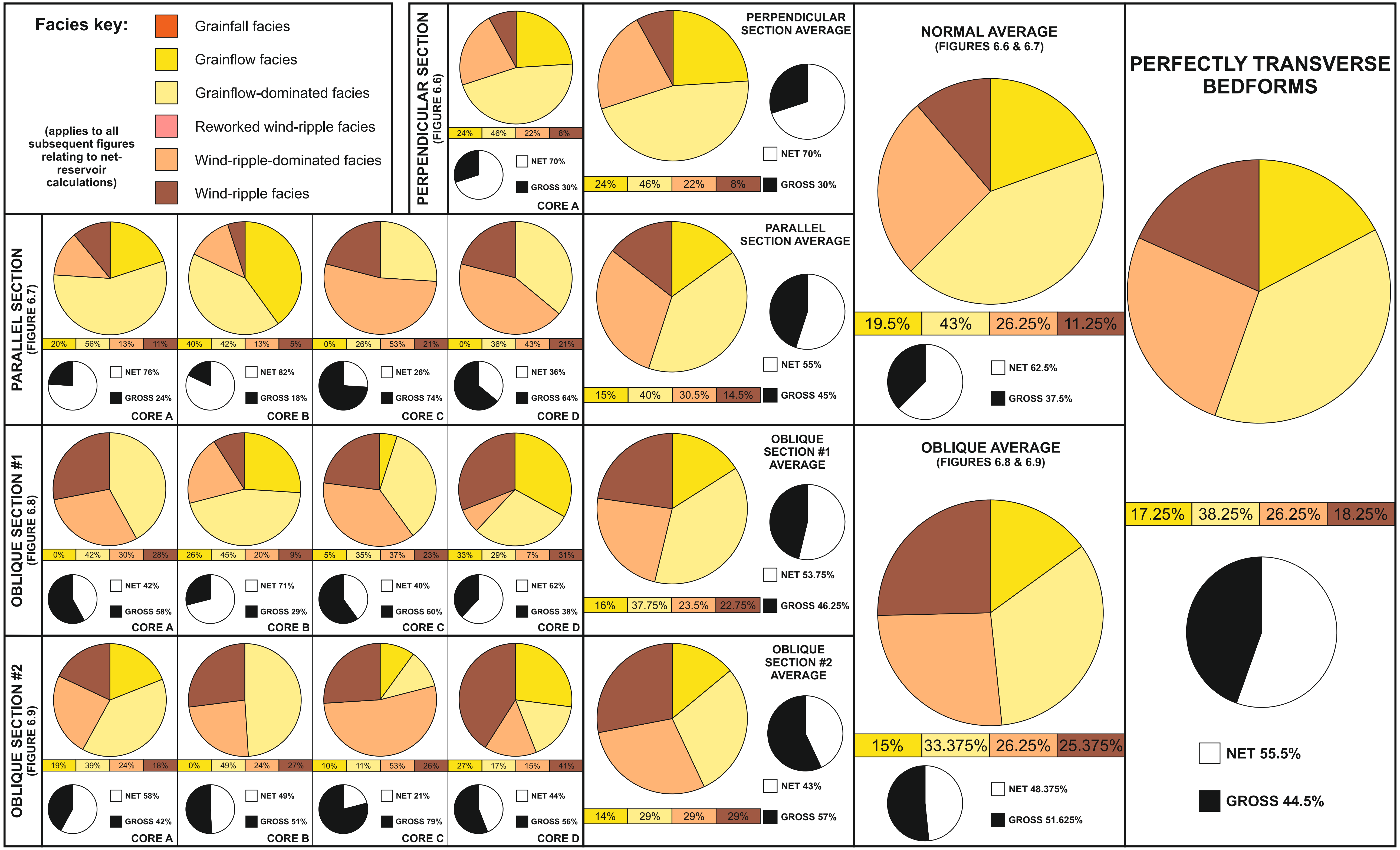

Figure 6.23. Net reservoir calculations for Sedimentological Model 3, depicting perfectly transverse bedforms with sinuous, out-of-phase crestlines. Positions of the cored sections and corresponding pseudo-cores within the overall bedform model are shown in Figure 6.2a. The facies distributions from each individual pseudo-core from Model 3 are displayed, as are averages of each section and the overall reservoir quality of Model 3.

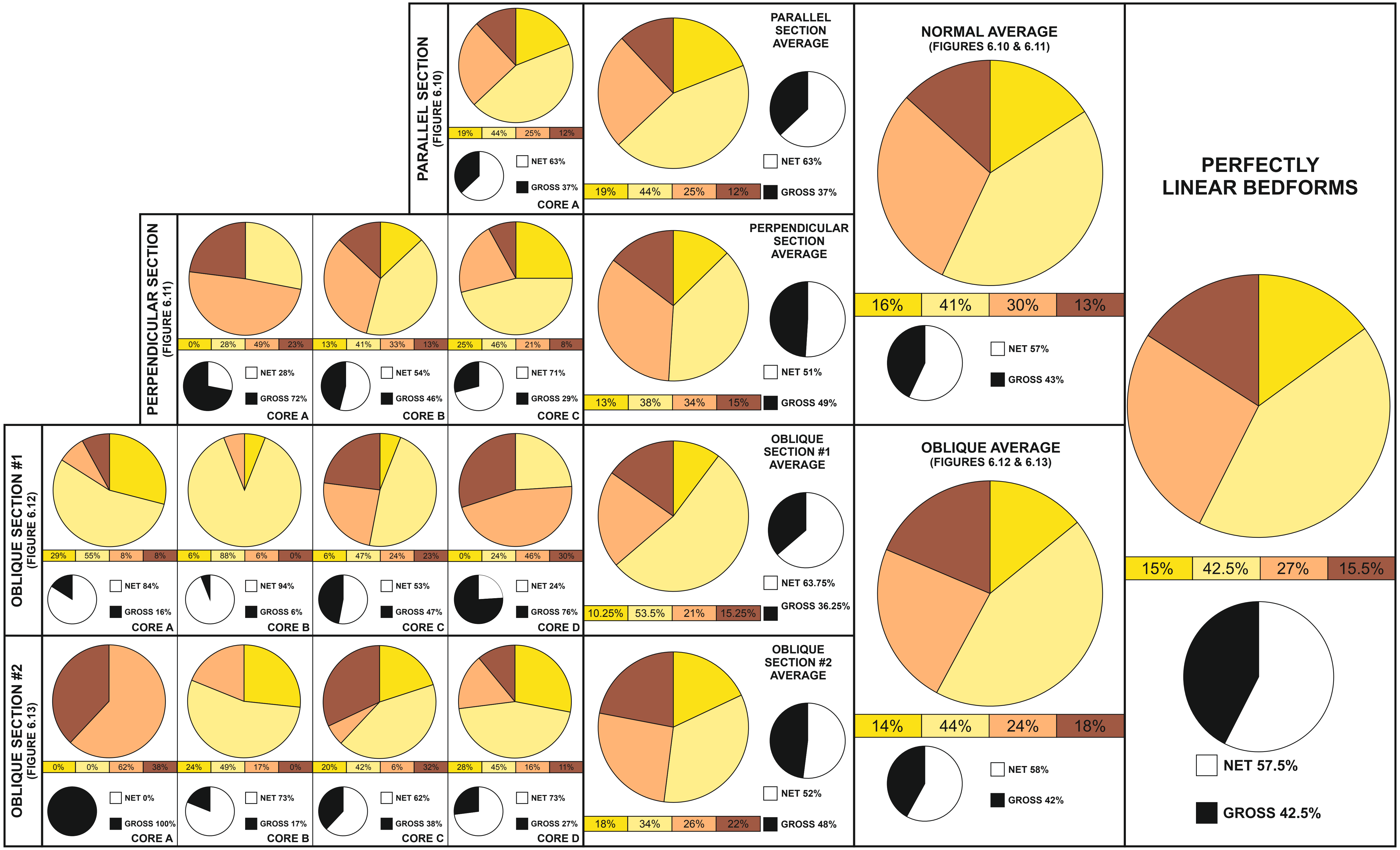

Figure 6.24. Net reservoir calculations for Sedimentological Model 5, depicting perfectly linear bedforms with along-crest migrating sinuosities. Positions of the cored sections and corresponding pseudo-cores within the overall bedform model are shown in Figure 6.3a. The facies distributions from each individual pseudo-core from Model 5 are displayed, as are averages of each section and the overall reservoir quality of Model 5.

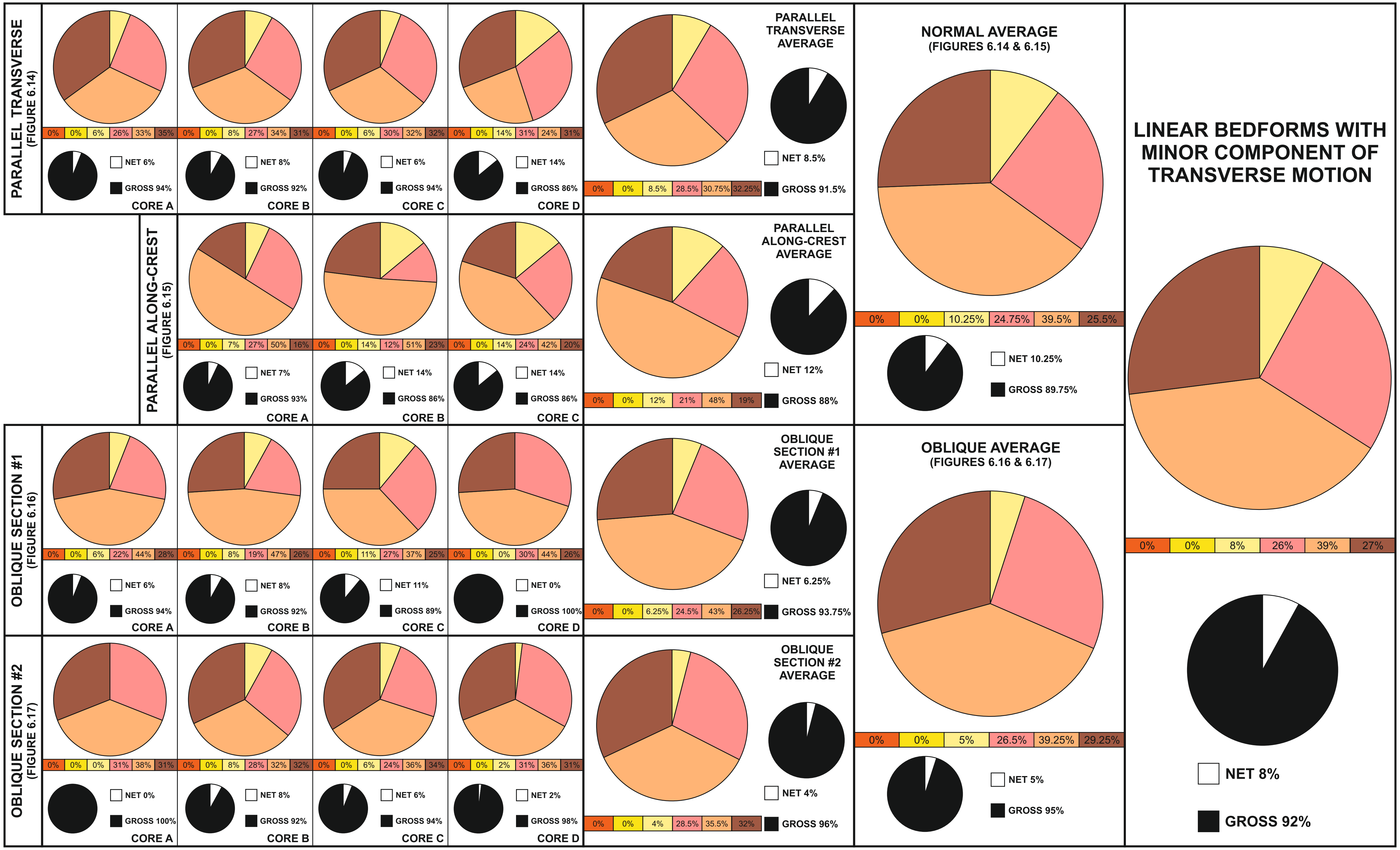

Figure 6.25. Net reservoir calculations for Auk Model 2, depicting bedforms with a major component of linear dune migration and a minor component of transverse bedform migration, at a ratio of 4:1 respectively. Positions of the cored sections and corresponding pseudo-cores within the overall bedform model are shown in Figure 6.4a. The facies distributions from each individual pseudo-core from Auk Model 2 are displayed, as are averages of each section and the overall reservoir quality of Auk Model 2.

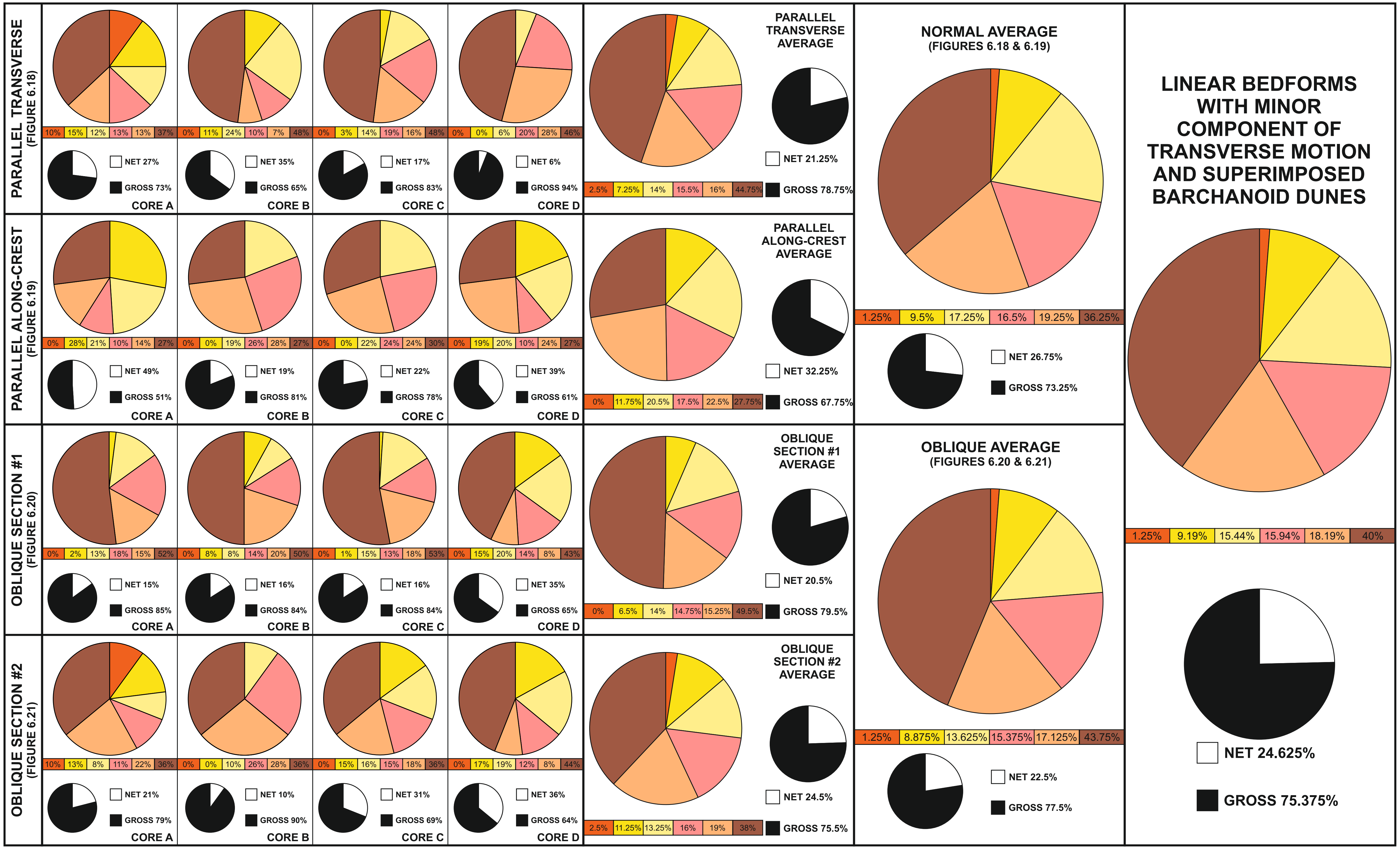

Figure 6.26. Net reservoir calculations for Auk Model 6, depicting bedforms with a major component of linear dune migration and a minor component of transverse bedform migration at a ratio of 4:1 respectively, and a small barchanoid dune field migrating through the interdune corridor of the main linear bedforms. Positions of the cored sections and corresponding pseudo-cores within the overall bedform model are shown in Figure 6.5a. The facies distributions from each individual pseudo-core from Auk Model 6 are displayed, as are averages of each section and the overall reservoir quality of Auk Model 6.

6.2.2 – Connectivity of net reservoir units

Within the discipline of reservoir analysis, connectivity of effective net reservoir units is typically considered at several scales: (i) *reservoir-to-well connectivity,* which relates to the connection of the wells to the net reservoir units on a large-scale within the overall reservoir body; and (ii) *geobody connectivity*, which is related to the connectivity between the individual net reservoir units in the subsurface (Larue and Hovadik, 2006), and is the scale of observation used in this study. The aim of this analysis is to directly compare the resultant connectivity and distribution of net reservoir geobodies for bedforms with markedly different morphologies and styles of migratory behaviour, and to investigate the effect, if any, that original bedform type and migratory behaviour has on the resultant net reservoir geobody connectivity within the reservoir volume.

6.2.2.1 – Methodology: connectivity of net reservoir

The likely geometry and degree of interconnectivity of net reservoir facies in three-dimensional space was determined for a range of bedform morphologies and styles of migratory behaviour in Chapter 3, and the results of this process demonstrate how facies distributions for different bedform types can enhance or restrict overall reservoir quality (see Section 6.1.3). A similar approach was adopted in Chapter 5 for the Auk Formation, an aeolian reservoir known only from the subsurface; by adopting this method it was possible to reconstruct the three-dimensional spatial arrangement of sets, and their internal facies arrangements. However, the modelling process used for this study only models the net reservoir units on a flat plane, and therefore the three-dimensional connectivity of the net reservoir units has not be quantified; this is discussed further in Chapter 7.

Bedform models from Chapter 3 for perfectly transverse bedforms (Figure 3.12) and perfectly linear bedforms (Figure 3.19) were processed for forward reservoir purposes, the results of which are displayed here (Figure 6.27a; Figure 6.27b; Figure 6.27c). Two models of the Auk Formation (Auk Model 2 – Figure 5.7; Auk Model 6 – Figure 5.19) were also interrogated in the same way to generate the predicted geometry and orientation of the net reservoir units for these models (Figure 6.27d; Figure 6.27e). The method used for this forward modelling is described in Section 3.3 (Figure 3.1) and Section 5.5 (Figure 5.2). Figures depicting information comparable those presented in Figure 3.1 and Figure 5.2, but for various alternative modelled scenarios, form the basis for the novel technique developed as part of this research for constraining geobody shapes in reservoir models.

6.2.2.2 – Perfectly transverse bedforms

Chapter 3, Section 3.8.3 described the geometry and orientation of the net reservoir units generated from this model of perfectly transverse bedforms. As described previously, the degree of connectivity of the grainflow and grainflow-dominated units is underestimated in the horizontal sections of Sedimentological Model 3 (Figures 3.13c and 3.14a). In Figure 3.14b, a vertical cross-section is presented in which the maximum grainflow development is shown for a level that captures the likely maximum grainflow development. Figure 6.27a illustrates this geometry in plan-view, and this section is taken directly beneath a surface which shows the maximum net-reservoir development of the trough-cross bedded sets.

In a plan-view section taken directly beneath a surface showing the maximum net reservoir development of the trough-cross bedded sets (Figure 6.27a), each package of grainflow, grainflow-dominated and wind-ripple-dominated facies is isolated within the reservoir volume, with each net reservoir geobody disconnected from the adjacent geobodies. This raises issues relating to the ability of hydrocarbon fluids to pass freely throughout the reservoir volume. If this method was adapted by taking a section at 90° to that of Figure 6.27a, then Figure 6.27b would portray the reservoir volume from a section parallel to the crestline of the bedforms. This would yield a reservoir volume which is largely composed of grainflow strata (Figure 6.27b). However, this geometry would be unlikely in natural systems, as at some point the bedforms would naturally terminate and not continue indefinitely, generating a reservoir volume which is much more like the former than the latter. Importantly, the distinct disparity in these two predicted net reservoir outputs for perfectly transverse bedforms (Figure 6.27a and Figure 6.27b) indicates that significantly different *apparent* reservoir geometries can be demonstrated depending on how the reservoir volume is sliced through.

6.2.2.3 – Perfectly linear bedforms with along-crest migrating sinuosities

Chapter 3, Section 3.10.3 described the geometry and orientation of the net reservoir units arising from this model, which depicts perfectly linear (non-migrating) parent bedforms with along-crest-migrating sinuosities. As discussed in Chapter 3, the geometry, scale and orientation of units considered to be likely net reservoir bodies is shown in a series of models which rectify the issue of the underrepresented connectivity of the grainflow packages discussed in Section 3.10.2. In Figure 3.21a, the horizontal section underplays the likely connectivity of the grainflow-dominated units. The most extensive development of units composed of grainflow and grainflow-dominated facies is through the section marked B-B’ in Figure 3.21b. The horizontal section displayed here (Figure 6.27c) is taken directly beneath this surface, which allows the likely maximum degree of connectivity of the grainflow-dominated units to be portrayed.

In a section taken to reflect the likely maximum degree of connectivity of the net reservoir units, these net reservoir units (grainflow-dominated facies) are arranged in individual packages, each of which is encapsulated by wind-ripple-dominated strata of moderate reservoir quality (Figure 6.27c). The grainflow-dominated stratal packages are inclined at an angle which reflects the along-crest migration of the sinuosities. Grainflow and grainflow-dominated facies are most commonly preserved over wind-ripple-dominated facies in each of the packages, which have a smaller aerial extent than those predicted for Model 3 (Figure 6.27a).

6.2.2.4 – Linear bedforms with minor component of transverse motion

Chapter 5, Section 5.7.3 described the geometry and orientation of the net reservoir units generated from a model of the Auk Formation bedforms (Auk Model 2), which have a major component of linear dune migration and a minor component of transverse bedform migration, at a ratio of 4:1 respectively. This type of migration is considered to be present in almost all linear bedforms that develop and persist over long time periods (see Bristow et al., 2000). As discussed previously, the likely geometry, scale and orientation of net reservoir units predicted by Auk Model 2 are underestimated in the horizontal sections (Figure 5.8c; Figure 5.9a).

A near-plan-view section was taken directly beneath an interdune migration bounding surface and inclined at the angle-of-climb, thereby portraying the likely maximum degree of connectivity of the grainflow units and therefore the maximum likely net reservoir architecture (Figure 6.27d). The grainflow units in each case are not connected; instead they are encapsulated within a zone of reworked wind-ripple strata, which itself would yield moderate reservoir properties, as opposed to the grainflow units which themselves would be expected to yield excellent reservoir properties (Figure 6.27d). These packages of grainflow and reworked wind-ripple strata are entirely surrounded by a background of wind-ripple-dominated strata, which is punctuated by wind-ripple strata of reduced reservoir quality.

6.2.2.5 – Linear bedforms with minor component of transverse motion and superimposed barchanoid dunes

Chapter 5, Section 5.11.3 described the geometry and orientation of the net reservoir units generated from the most complex model envisaged for the migration and accumulation of the Auk bedforms (Auk Model 6). It simulates the migration of large linear bedforms with morphologies and styles of migration similar to those in Auk Model 2 (as above), but replaces the elliptical interdune flats of that model with fields of obliquely-migrating smaller barchanoid dunes within the lower-lying parts of the interdraa of the parent bedforms. Such coeval relationships between different bedform types are seen in modern settings, such as the Namib Desert (McKee, 1982) (Figure 4.12). As described previously, the horizontal sections through the bedform model depicted in Figure 5.20c and 5.21a underplay the degree of connectivity of the grainflow tongues. Rather than being horizontal, the planar upper surface of these sand bodies is inclined at the angle-of-climb of the system, and these bodies therefore project out of the horizontal section shown at a slight angle.

Figure 6.27e shows a vertical cross-section which illustrates the maximum grainflow development, taken directly beneath an interdune migration bounding surface and inclined at the angle-of-climb, thereby portraying the likely maximum degree of connectivity of the grainflow units and therefore the maximum likely net reservoir architecture. It is apparent that Auk Model 6 produces a reservoir volume whereby net reservoir units are disconnected and arranged in a repetitive fashion, with a unit of reworked wind-ripple and wind-ripple-dominated strata between each of the net reservoir packages (Figure 6.27e). These packages are encapsulated by reworked wind-ripple and wind-ripple-dominated strata, which have detrimental implications for hydrocarbon fluid flow between the net reservoir packages in this part of the reservoir.

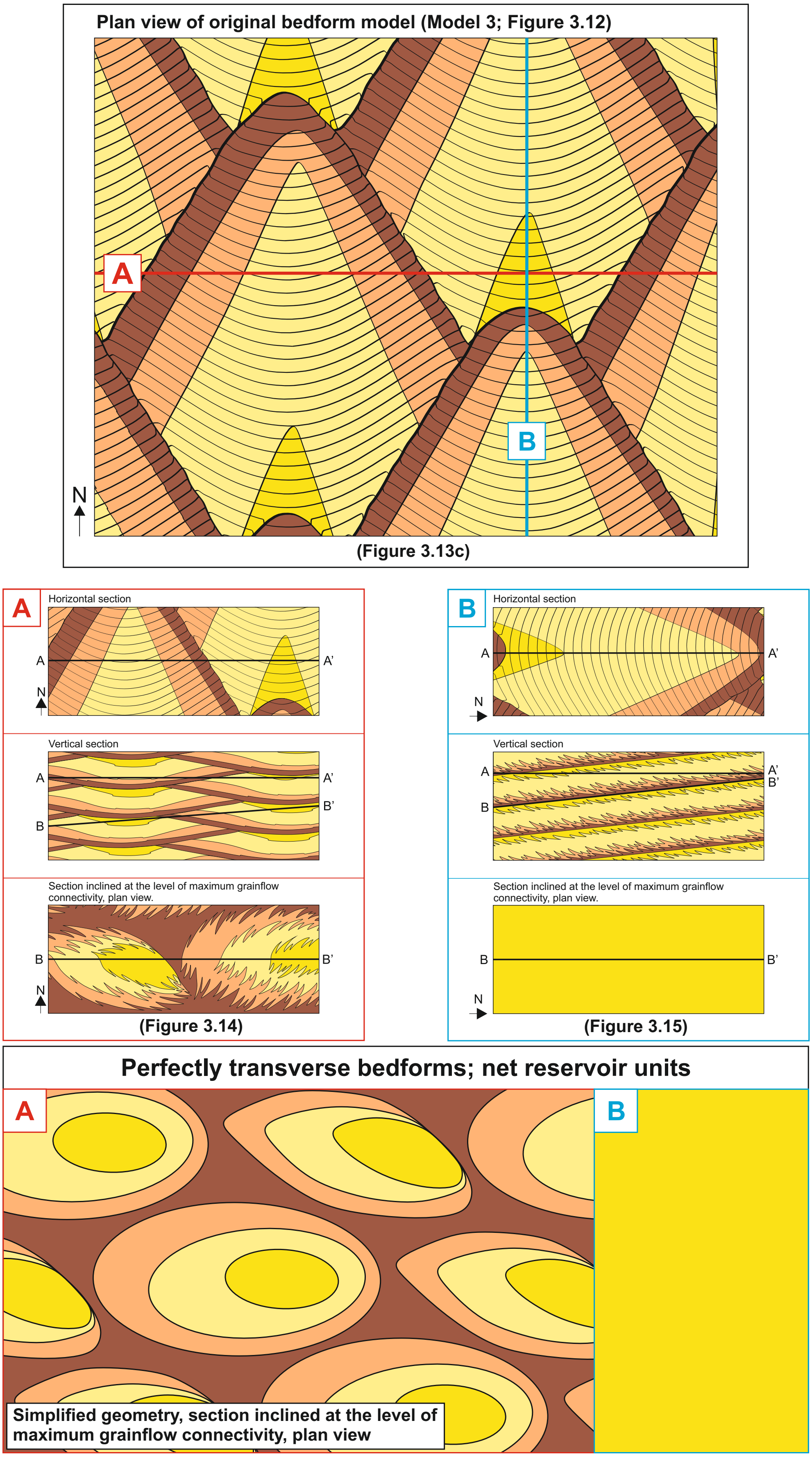

Figure 6.27. Geometry of net reservoir units predicted by a selection of bedform models from Chapters 3 and 5; a) and b) perfectly transverse bedforms; c) perfectly linear bedforms with along-crest migrating sinuosities; d) linear dunes with a minor component of transverse motion; e) linear dunes as in d), but with the addition of a small barchanoid dune field migrating through the interdune corridors. In all cases the net reservoir facies are encapsulated within a background of non-net reservoir facies.

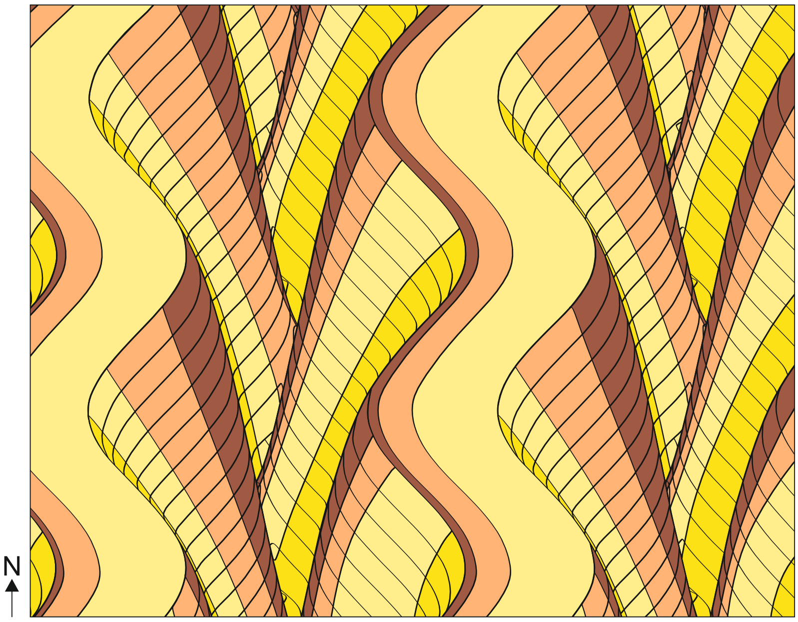
Plan view of original bedform model (Model 5; Figure 3.19)

(Figure 3.20c)

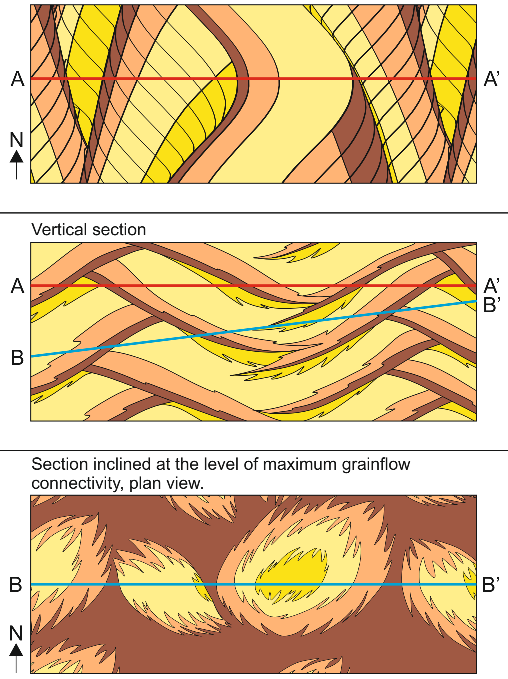

(Figure 3.21)

Perfectly linear bedforms; net reservoir units

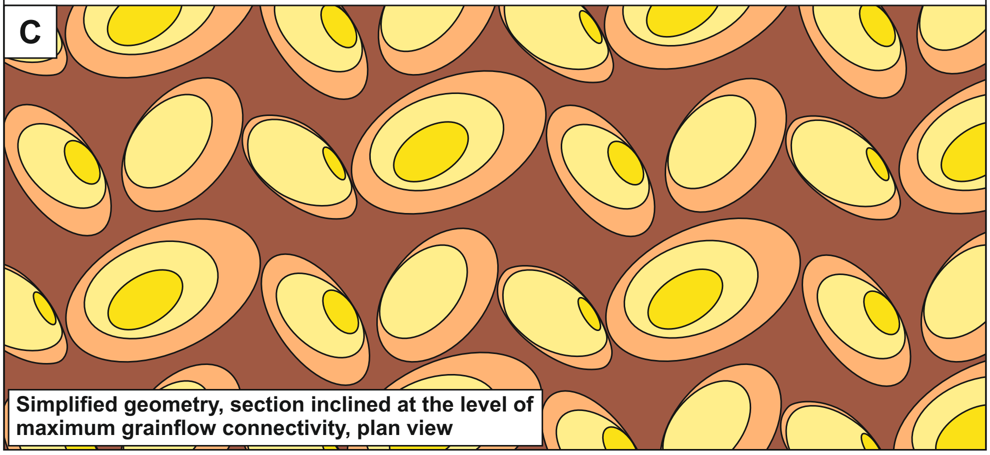

Simplified geometry, section inclined at the level of maximum grainflow connectivity, plan view

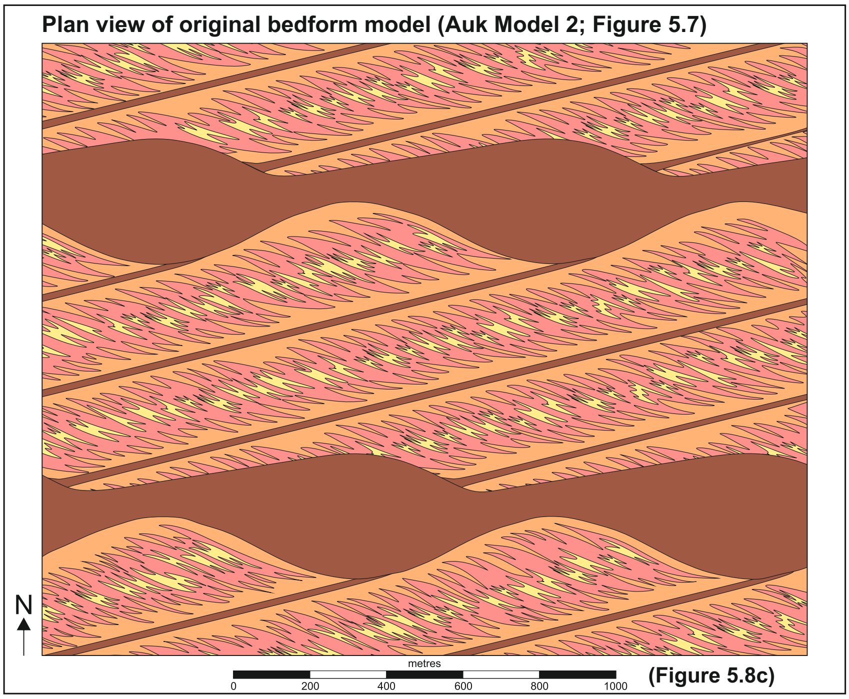

Plan view of original bedform model (Auk Model 2; Figure 5.7)

(Figure 5.8c)

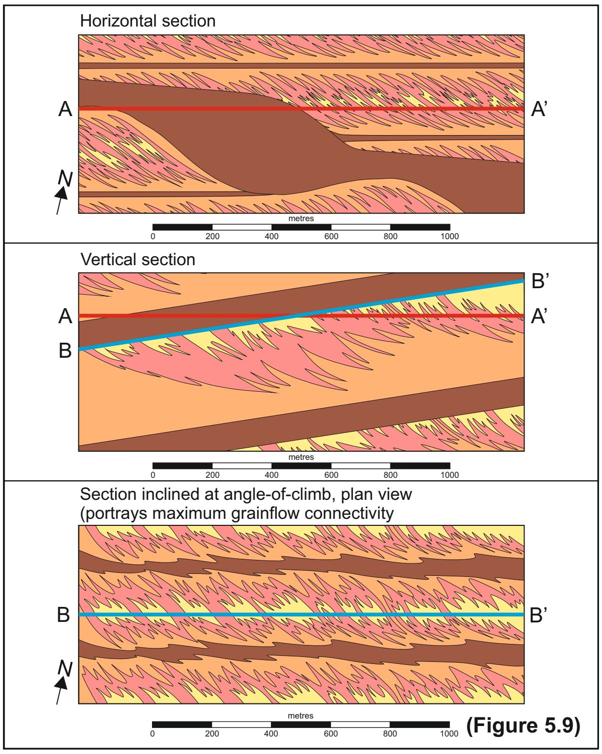

Horizontal section

Vertical section

Section inclined at angle-of-climb, plan view
(portrays maximum grainflow connectivity

(Figure 5.9)

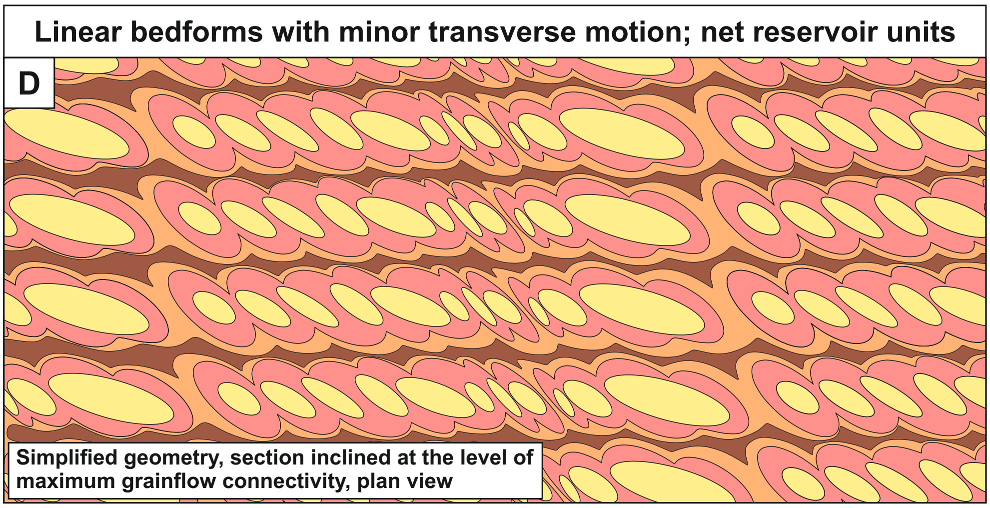

Linear bedforms with minor transverse motion; net reservoir units

Simplified geometry, section inclined at the level of maximum grainflow connectivity, plan view

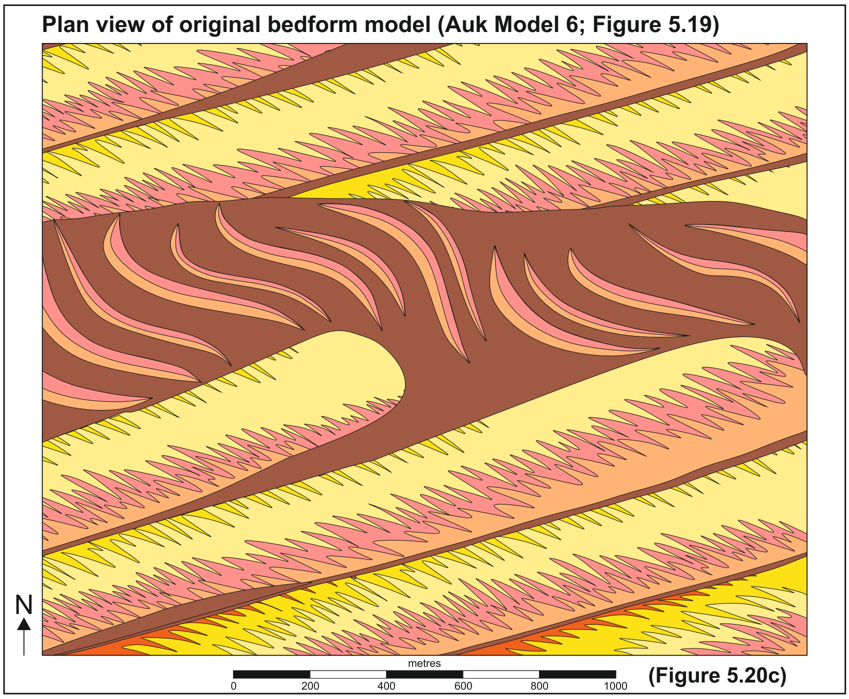

Plan view of original bedform model (Auk Model 6; Figure 5.19)

(Figure 5.20c)

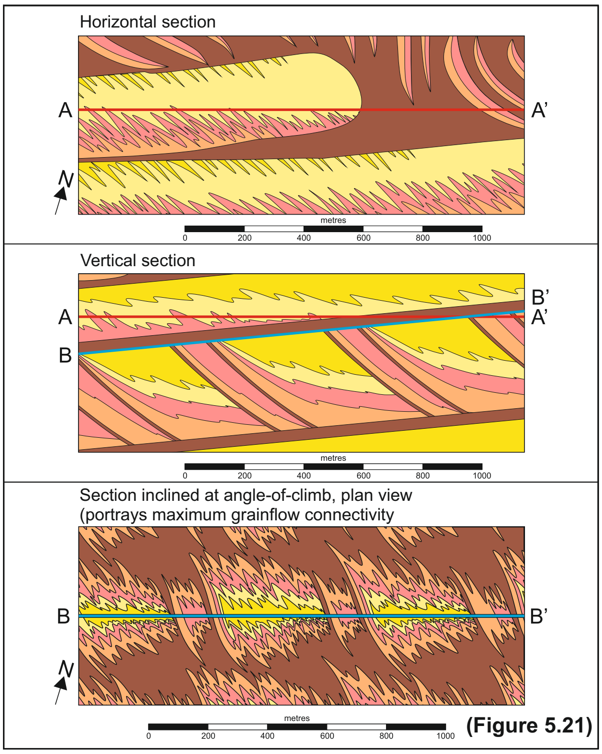

Horizontal section

Vertical section

Section inclined at angle-of-climb, plan view
(portrays maximum grainflow connectivity

(Figure 5.21)

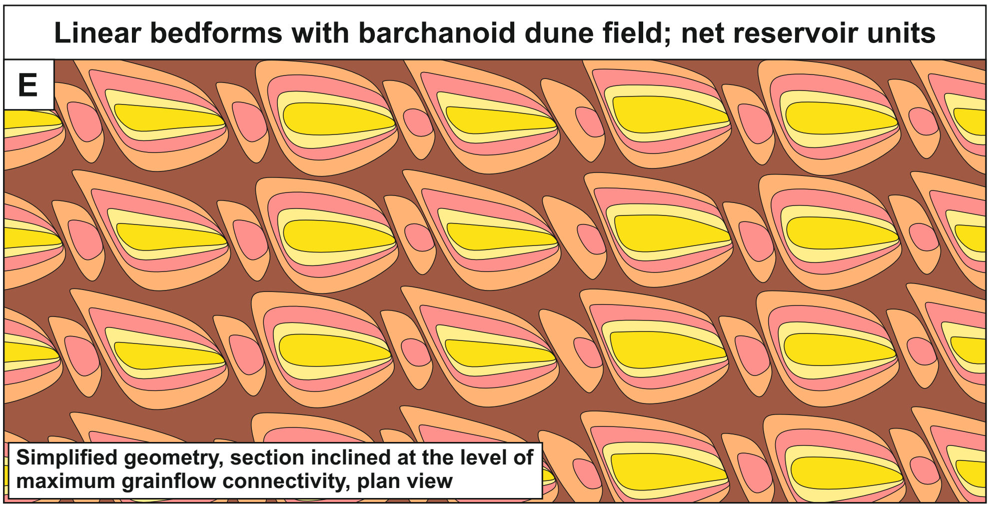

Linear bedforms with barchanoid dune field; net reservoir units

Simplified geometry, section inclined at the level of maximum grainflow connectivity, plan view

6.2.2.6 – Key advances

Bedforms which have distinctly different morphologies can generate preserved facies relationships that are potentially difficult to distinguish from one another, such as the reservoir architecture predicted for perfectly transverse bedforms (Figure 6.27a), and the reservoir architecture predicted for perfectly linear bedforms (Figure 6.27c). Grainflow and grainflow-dominated facies for perfectly linear bedforms (Figure 6.27c) have a smaller aerial extent than those predicted for perfectly transverse bedforms (Figure 6.27a); this is partly due to the increased value for the wavelength of the crestline sinuosity in the transverse bedform model, generating a gentler rate of curvature which is directly attributable to the greater aerial extent of net reservoir facies. If the wavelength value for both bedform models were the same, then the connectivity of the reservoir intervals generated by perfectly transverse and perfectly linear bedforms would be almost impossible to distinguish.

Although the net reservoir calculation for Auk Model 6 (Figure 6.26) is significantly enhanced by the addition of the superimposed bedforms, compared to that of Auk Model 2 (Figure 6.25), the superimposition surfaces which arise from the interaction of two scales of bedforms have detrimental implications for the connectivity of net reservoir units in Auk Model 6 (Figure 6.27e), and the connectivity is less favourable than that predicted for Auk Model 2 (Figure 6.27d). The superimposition surfaces preferentially preserve wind-ripple strata (non-net reservoir in this study) where the lee slopes of the superimposed dunes do not extend down to the dune base.

All of the sections described above are taken at a zone which portrays the maximum likely net reservoir development. The sections depicted in this study are pertinent, as hydrocarbon fluids would rise due to buoyancy to the level of the surface directly beneath the baffle; this is the surface shown in this study and so the connectivity models depicted here are appropriate and typical. It is apparent from the forward modelling process that modest changes in bedform architecture can have a marked difference in net reservoir morphology and distribution, but importantly, bedforms with very different morphologies generate very similar net reservoir distributions and inherent connectivity issues, with grainflow packages commonly entirely encapsulated within non-net reservoir (wind-ripple facies of various types). Care must therefore be taken when interpreting these deposits in the subsurface, or conversely applying these forward models to subsurface examples where original depositional bedform types are known. The forward-modelling method developed in this research is a novel and valuable technique which can be applied to other reservoir successions where core data do not necessarily provide insight on sand-body geometry, orientation and style of interconnectivity. This approach to the documentation of the range of likely sand-body dimensions is important for constraining inputs used in aeolian reservoir modelling workflows.

6.2.3 – Directional permeability

The complex three-dimensional structure of preserved dune sets defines the spatial distribution of heterogeneity, and therefore their individual preferred permeability directions. This heterogeneity affects reservoir behaviour, the impact of which in terms of fluid flow behaviour commonly increases later in the life of a hydrocarbon field (Tatum and Francke, 2012). Based on the classification of Galloway and Hobday (1996), aeolian stratigraphic intervals can be subdivided on four heterogeneity scales: (i) *megascopic heterogeneity* is the relationship between permeable and relatively impermeable units at the oil field scale (Bongiolo and Scherer, 2010). Here, the main controlling parameters of reservoir compartmentalisation are the key stratigraphic surfaces resulting from the juxtaposition of aeolian dune architectural elements with non-aeolian architectural elements, such as fluvial, shallow-marine and lake deposits; (ii) *macroscopic heterogeneity* reflects vertical and lateral relationships between facies associations within the reservoir, such as the stacking patterns of cross-beds; (iii) *mesoscopic heterogeneity* refers to the lamination of different stratification types, whereby individual aeolian packages possess internal textural differences (Sweet et al., 1996); and (iv) *microscopic heterogeneity*, expressed at the scale of individual grains and pores. Whilst diagenesis has been noted to emphasise the inherent differences in porosity and permeability that result from depositional texture (i.e. facies type – see Heward, 1991), the consideration of microscopic heterogeneity is beyond the remit of this study.

Models for directional permeability in aeolian reservoir successions have been previously described by Weber (1982; 1987), Lindquist (1988 – Figure 6.28a; Figure 6.28b), Chandler et al. (1989 – Figure 6.28c), Krystinik (1990 – Figure 6.28d; Figure 6.28e) and Prosser and Maskall (1993 – Figure 6.28f). However, consideration must be made to the scale of observation in the aeolian reservoir volume. Previous stratigraphic models are typically constructed with a focus on the larger-scale features, which leads to an underestimation of heterogeneity, specifically at the bedform- and lamina- scales (Tatum and Francke, 2012). This research has investigated reservoir heterogeneity on both an architectural-element scale (macroscopic heterogeneity) and bed-scale (mesoscopic heterogeneity); a research question therefore arises as to whether a change in observation scale affects the preferred direction of permeability in the reservoir volume. An advance to the bed-scale level of permeability observation (mesoscopic heterogeneity) has already been achieved through measurement of the three-dimensional distribution of grainflow deposits from the Navajo Sandstone, outlined in Chapter 2, Section 2.5.1 (Figure 6.1). By measuring not only the grainflow thickness, but also the associated length and width of these deposits, an empirical relationship has been developed for the three-dimensional reconstruction of the expected geometry of grainflow sediment packages solely from a measurement of their thickness preserved in core. This is important for modelling bed-scale heterogeneity and directional permeability in aeolian reservoir successions.

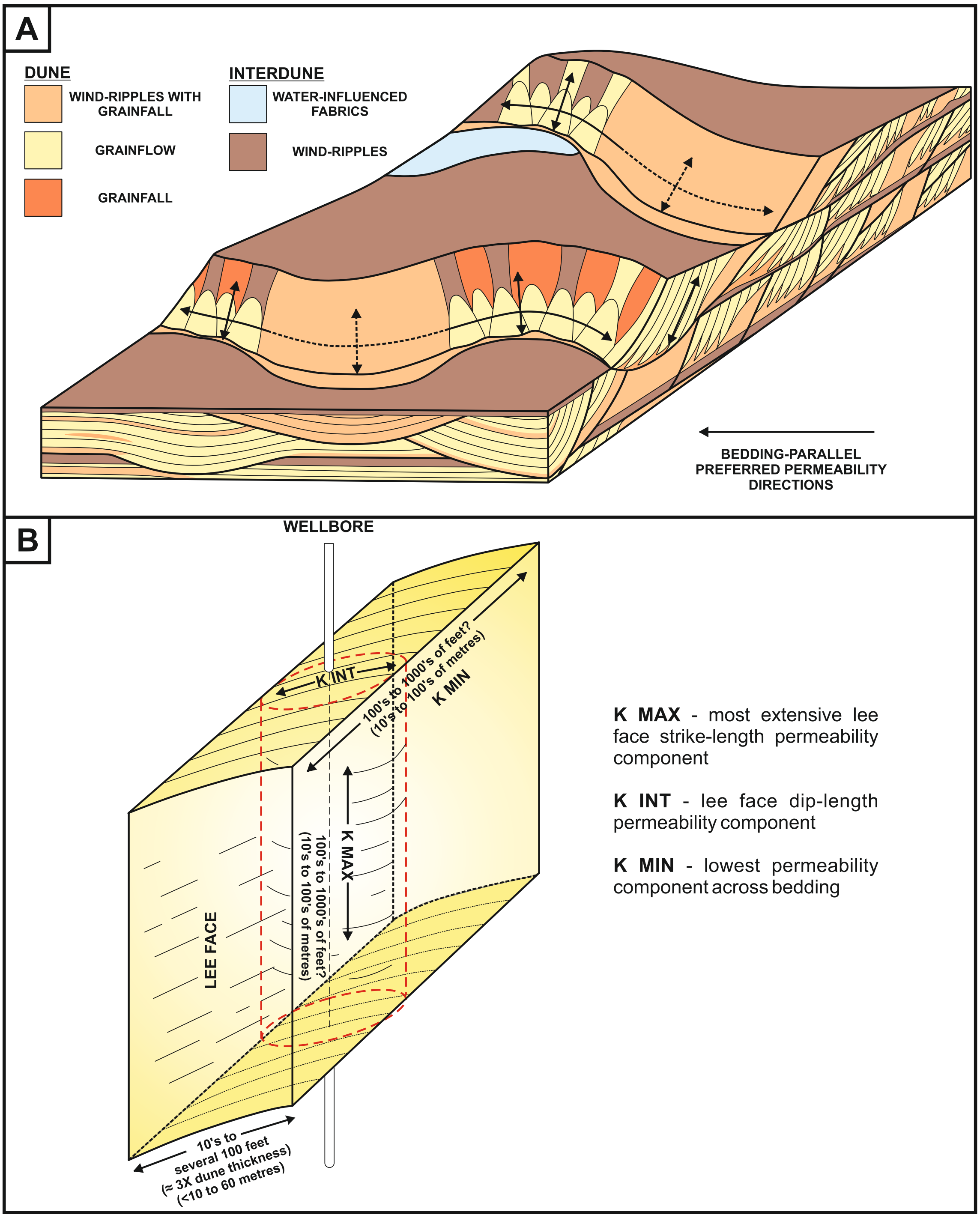

Figure 6.28. Examples of previously published studies on preferred permeability directions in aeolian reservoir successions: a) Hypothetical, downwind-climbing, sinuous-crested aeolian dune and interdune sequences. Note lateral and vertical variability in stratification type, preferred permeability components, and interdune barrier continuity (from Lindquist, 1988); b) Vertical structural orientation of a straight-crested dune. Lateral drainage around the hypothetical wellbore is controlled most by the permeability component associated with the lee face dip length (from Lindquist, 1988); c) Common styles of cross-strata in the Page Sandstone. Directional permeability indicated by arrows; more arrows denote higher potential flow (from Chandler et al., 1989); d) Directional-preferred permeability and layered behaviour in aeolian reservoirs. Maximum permeability (Kmax) is parallel to dune strike (perpendicular to wind transport direction); intermediate permeability (K90°) is parallel to the wind transport direction, across cross bed laminae; minimum permeability (Kv) is in the vertical direction, across interdune/sabkha layers (from Krystinik, 1990); e) Ideal orientation for slabbing to show maximum depositional dip and plugs oriented to best characterise directional permeability (from Krystinik, 1990); f) Summary diagram indicating possible optimum sampling strategies for cores of different orientation through aeolian deposits within the Auk reservoir (from Prosser and Maskall, 1993).

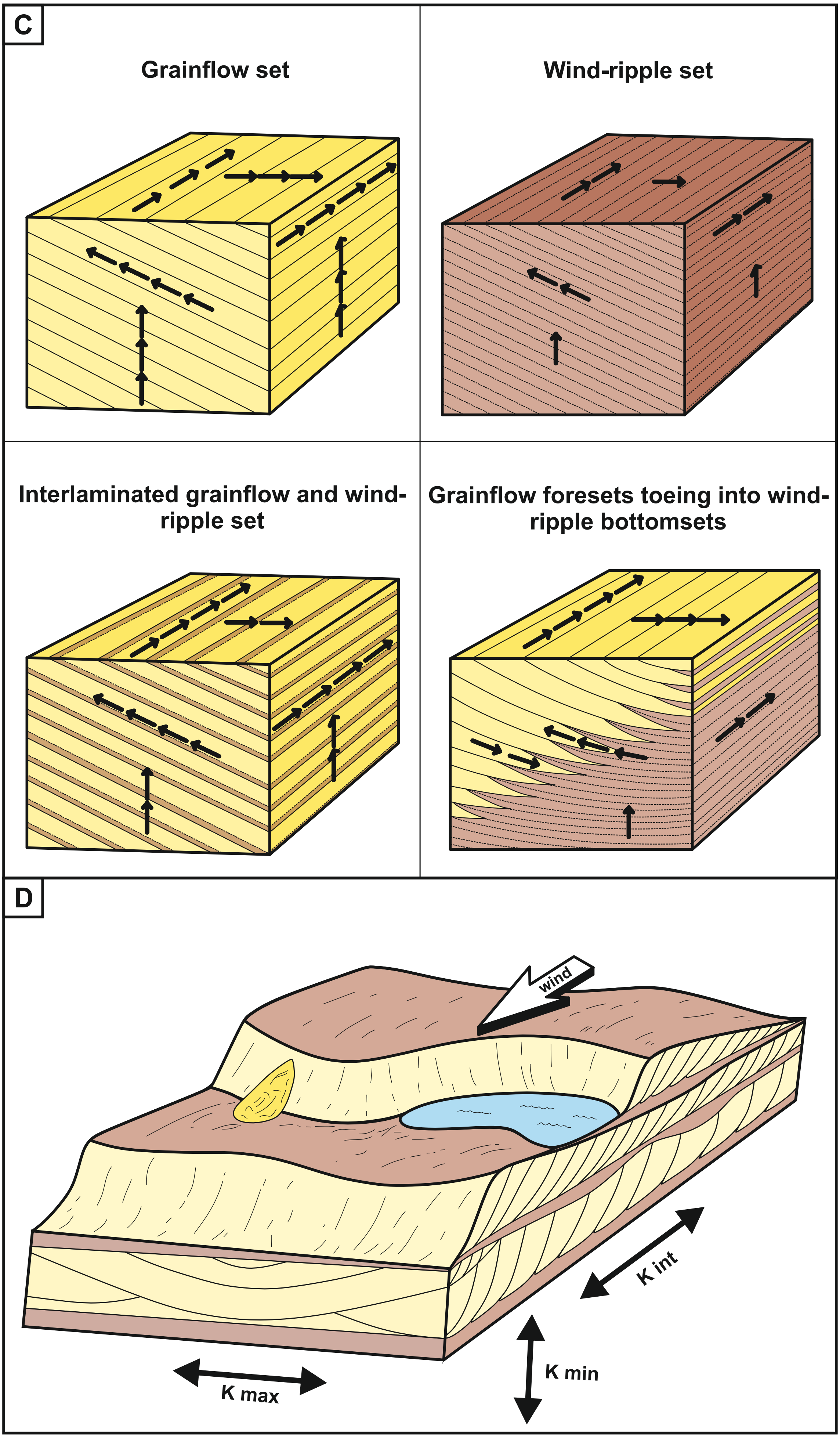
C
Grainflow set
Wind-ripple set
Interlaminated grainflow and wind-ripple set
Grainflow foresets toeing into wind-ripple bottomsets
D
wind
K int
K min
K max

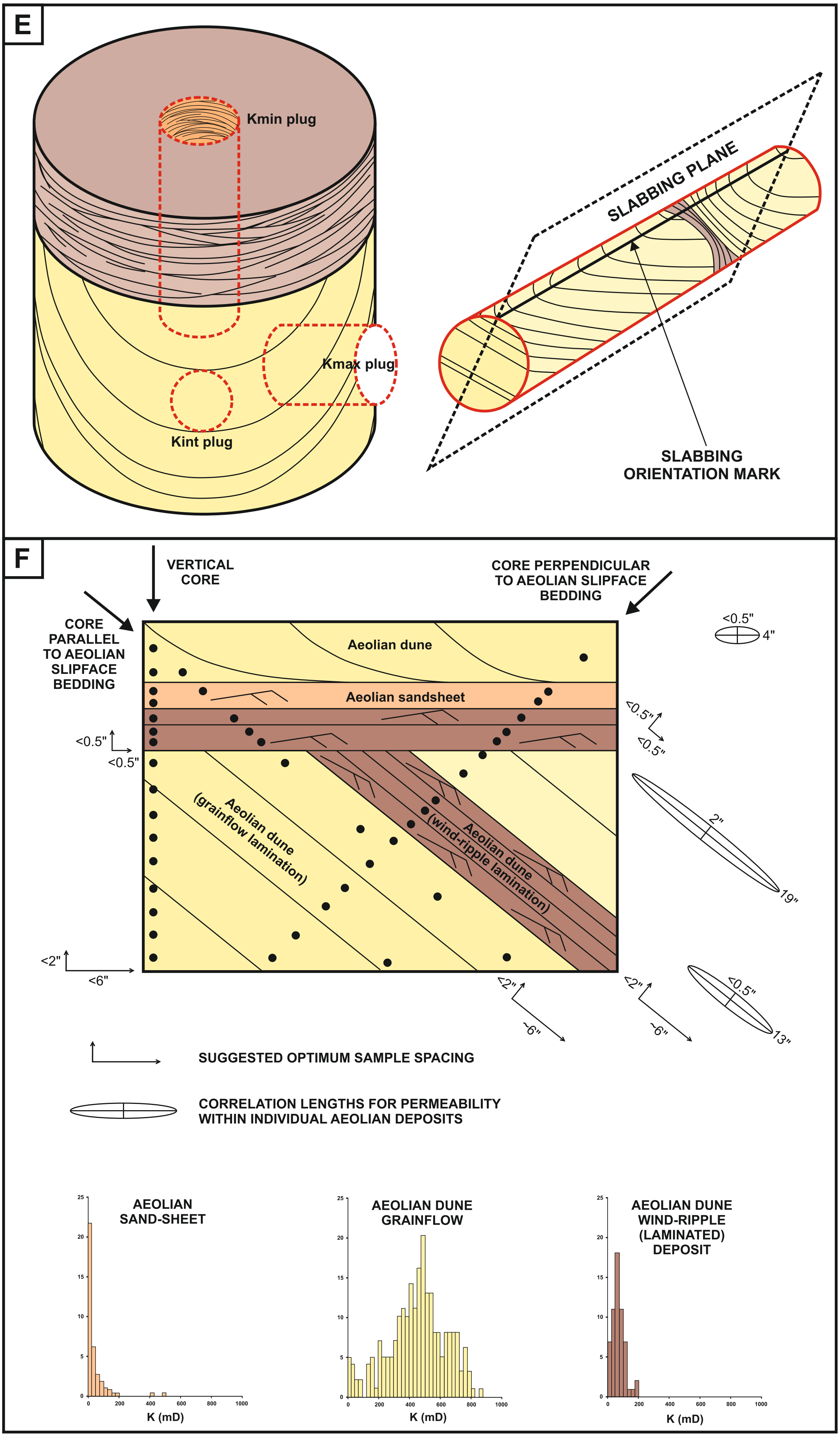
E
Kmin plug
Kmax plug
Kint plug
SLABBING PLANE
SLABBING ORIENTATION MARK
F
VERTICAL CORE
CORE PERPENDICULAR TO AEOLIAN SLIPFACE BEDDING
CORE PARALLEL TO AEOLIAN SLIPFACE BEDDING
Aeolian dune
Aeolian sandsheet
Aeolian dune (grainflow lamination)
Aeolian dune (wind-ripple lamination)
<0.5"
4"
<0.5"
<0.5"
<0.5"
<0.5"
2"
19"
<2"
<6"
<2"
~6"
<2"
~6"
<0.5"
13"
SUGGESTED OPTIMUM SAMPLE SPACING
CORRELATION LENGTHS FOR PERMEABILITY WITHIN INDIVIDUAL AEOLIAN DEPOSITS
AEOLIAN SAND-SHEET
AEOLIAN DUNE GRAINFLOW
AEOLIAN DUNE WIND-RIPPLE (LAMINATED) DEPOSIT
25
20
15
10
5
0
0
200
400
600
800
1000
K (mD)

6.2.3.1 – Methodology: directional permeability

For each of the theoretical bedform models introduced in Chapter 3 (Sedimentological Models 1-8; Sections 3.6 – 3.13), and for two bedform models of the Auk Formation from Chapter 5 (Auk Model 2 – Section 5.7; Auk Model 6 – Section 5.11), predicted preferred permeability directions have been mapped onto the modelled outputs using CorelDraw, at both an architectural-element-scale and a bed-scale, based on the facies distributions described in Section 6.1.3. The distribution of the lithofacies types on the individual bedform models directly governs the preferred permeability directions for each bedform type.

6.2.3.2 – Architectural-element-scale directional permeability

For all the models displayed in Figure 6.29, the maximum preferred permeability direction is along the crest of the bedform in the preserved set, capturing the maximum extent of the grainflow deposits. There are only two exceptions to this: (i) in the model for perfectly transverse bedforms (Figure 6.29c), where the maximum preferred permeability direction is upwards through the preserved troughs. The impact of this preferred permeability is dependent on the shape of the original trough set – if the original trough was elongated, the maximum preferred permeability would be angled upwards through the set; conversely if the trough was wider, the likelihood is that the greatest preserved extent of the grainflow deposits would be along the width of the trough, thereby changing the preferred permeability directions for this model; and (ii) in Auk Model 6 (Figure 6.29j), where the maximum preferred permeability would be through the deposits of the barchanoid dune field, rather than along the crests of the linear bedsets, as they preserve a higher proportion of their grainflow avalanches than the larger linear draa.

The intermediate direction of preferred permeability is aligned parallel with the angle-of climb of the bedsets, across the preserved units of avalanching grainflow deposits; the ability to reconstruct angle-of-climb from simple measurements in cored intervals, as demonstrated in Chapter 2 (Section 2.5.5), is therefore a key advantage when estimating preferred permeability directions in reservoir intervals at the architectural-element scale. In all cases, the minimum permeability direction is perpendicular to the preserved units of grainflow deposits, as this punctuates the highest proportion of facies associated with the interdunes and lower-plinths of the original bedforms, considered non-net reservoir in this study.

6.2.3.3 – Bed-scale directional permeability

Most of the previous studies on directional permeability have envisaged the maximum preferred directional permeability direction as parallel to the deposition of the individual grainflow deposits, as depicted in Figure 6.29c. Although this is true in most cases at a bed-scale level, this is highly dependent on the shape of the original bedform: in cases where the dune plinth has a lower angle; grainflow avalanches rarely reach the base of slope (as for Sedimentological Model 8 – Figure 6.29h and Auk Model 2 – Figure 6.29i), and these models therefore preserve grainflow deposits that are much shorter in length than those for bedforms which have steeper plinths.

The likely length of grainflow deposits can be estimated by measuring the thickness of grainflow deposits in cored sections, and then applying the empirical relationship for grainflow length developed in Chapter 2 (Figure 6.1b). In these cases where the dune plinth has a low angle, the maximum preferred permeability direction is across the preserved grainflow deposits along the lee-slope, which is typically deemed the intermediate preferred permeability direction. Grainflow development on the lee-slope of a bedform is also dependant on the preserved bed-set expression that reflects the sinuosity of the bedform crestline (Figure 6.29c). In cases of sedimentary architecture generated by the passage of bedforms that possessed relatively more sinuous crestlines, the grainflows have a much smaller plan-view extent, as opposed to crestlines with only minor sinuosity, where the grainflows will have a greater extent (Figure 6.29c).

The intermediate direction of preferred permeability at a bed-scale across the lee-slope of the bedset exploits the width of the individual grainflow avalanches. However as described previously, the width of the grainflow avalanches (as a function of crestline sinuosity) is a critical factor on the resultant permeability in this direction, as is the connectivity of the grainflow avalanches along-crest. The likely width of single grainflow deposits can be estimated by measuring the thickness of an individual preserved grainflow unit in cored sections, and then applying the empirical relationship for grainflow width developed in Chapter 2 (Figure 6.1b).

In some cases, superimposed bedforms or spurs can create a relative topographic high on the bedform, in which case the grainflows are diverted into the lower portions of the bedform slope (Figure 6.29d; Figure 6.29f; Figure 6.29g). This means that the grainflow avalanche deposits are not connected, with negative implications for the ability of fluids to flow freely along this direction of the reservoir volume. In all cases, the minimum permeability direction is perpendicular to the individual grainflow avalanches as the intercalculated wind-ripple deposits, commonly seen between grainflow events (Figure 1.17), would be intersected.

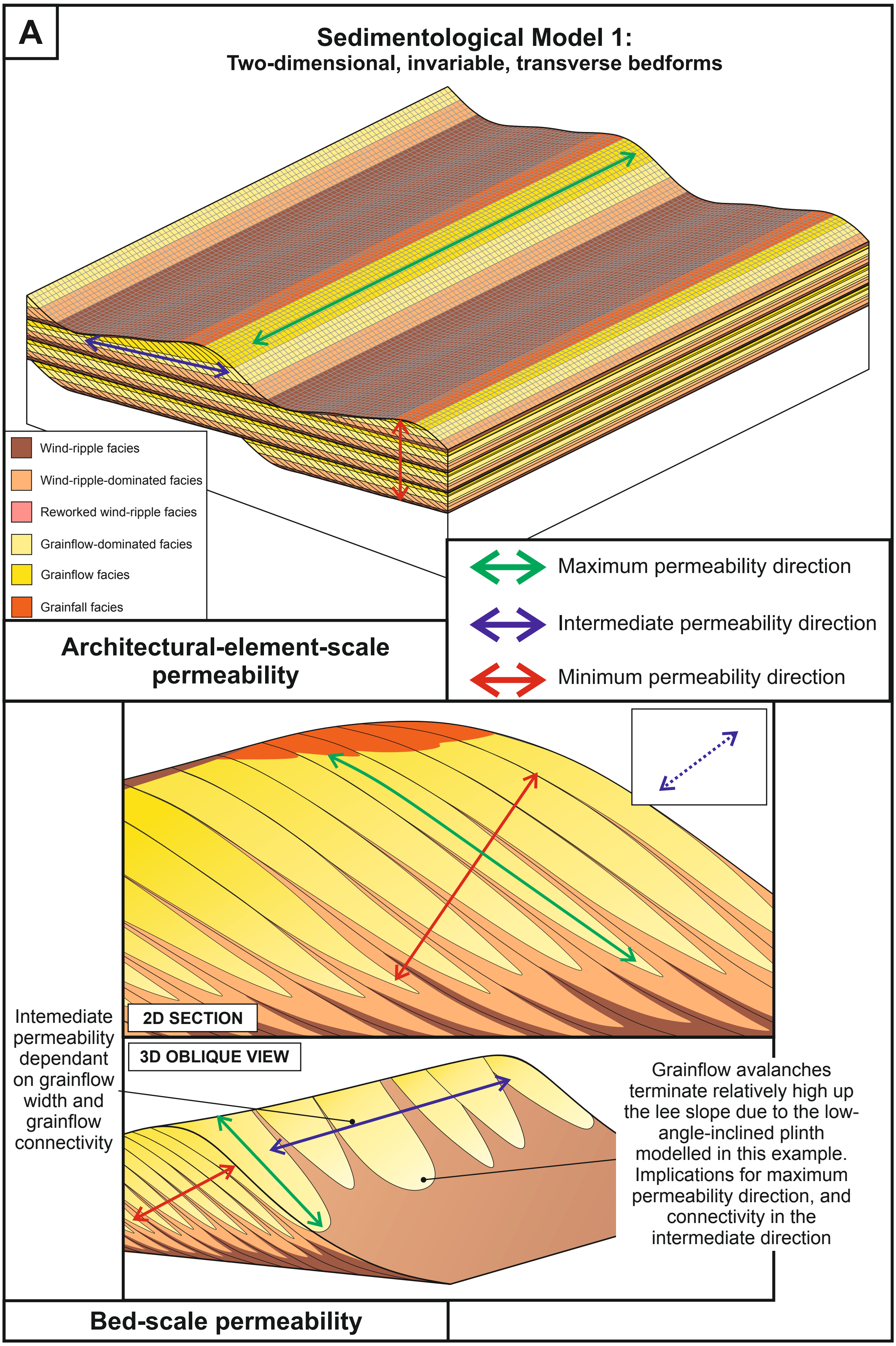

Figure 6.29. Preferred directional permeability for a number of aeolian bedform types with different morphologies and styles of migratory behaviour: a) two-dimensional, invariable, transverse bedforms; b) two-dimensional, variable, transverse bedforms; c) three-dimensional, invariable, perfectly transverse bedforms; d) three-dimensional, invariable, oblique bedforms; e) three-dimensional, invariable, perfectly linear bedforms; f) three-dimensional, variable, perfectly transverse bedforms; g) three-dimensional, variable, oblique bedforms; h) three-dimensional, variable, perfectly linear bedforms; i) linear bedforms with a minor component of transverse motion; j) linear bedforms with a minor component of transverse motion, and superimposed barchanoid dunes. No scale implied.

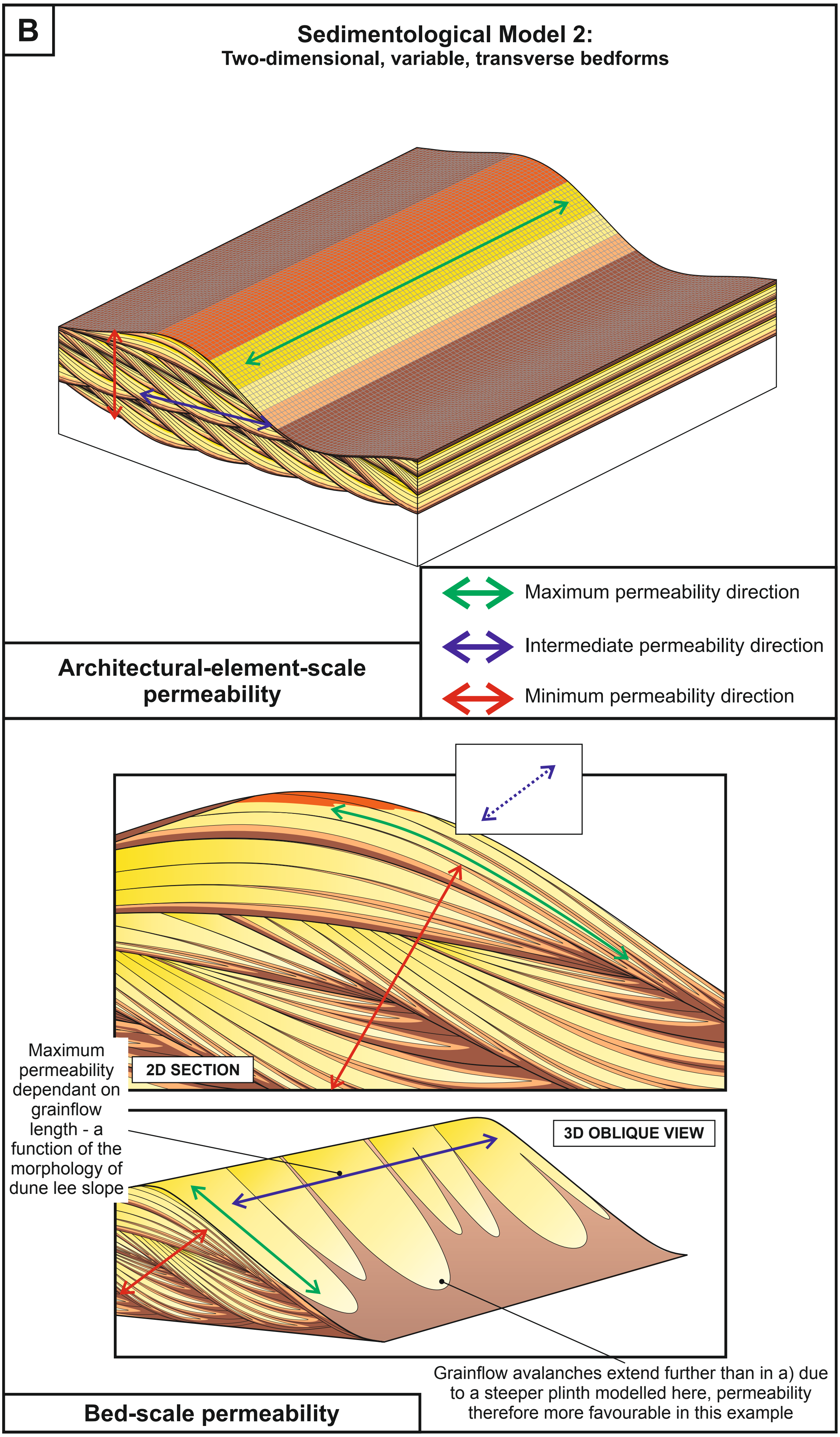

Sedimentological Model 2:
Two-dimensional, variable, transverse bedforms

Architectural-element-scale permeability

Bed-scale permeability

Maximum permeability dependant on grainflow length - a function of the morphology of dune lee slope

Grainflow avalanches extend further than in a) due to a steeper plinth modelled here, permeability therefore more favourable in this example

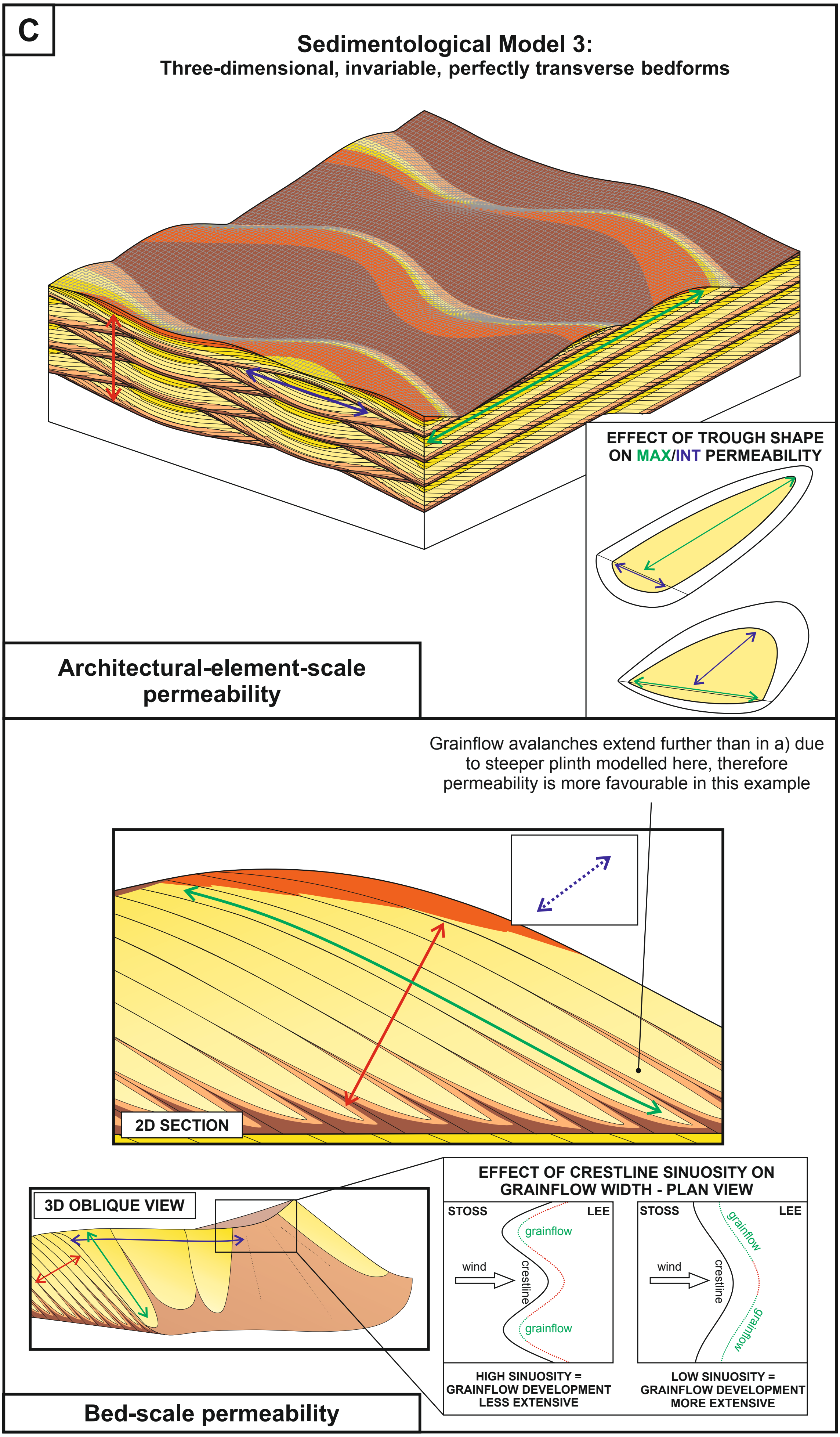

Sedimentological Model 3:
Three-dimensional, invariable, perfectly transverse bedforms

Grainflow avalanches extend further than in a) due to steeper plinth modelled here, therefore permeability is more favourable in this example

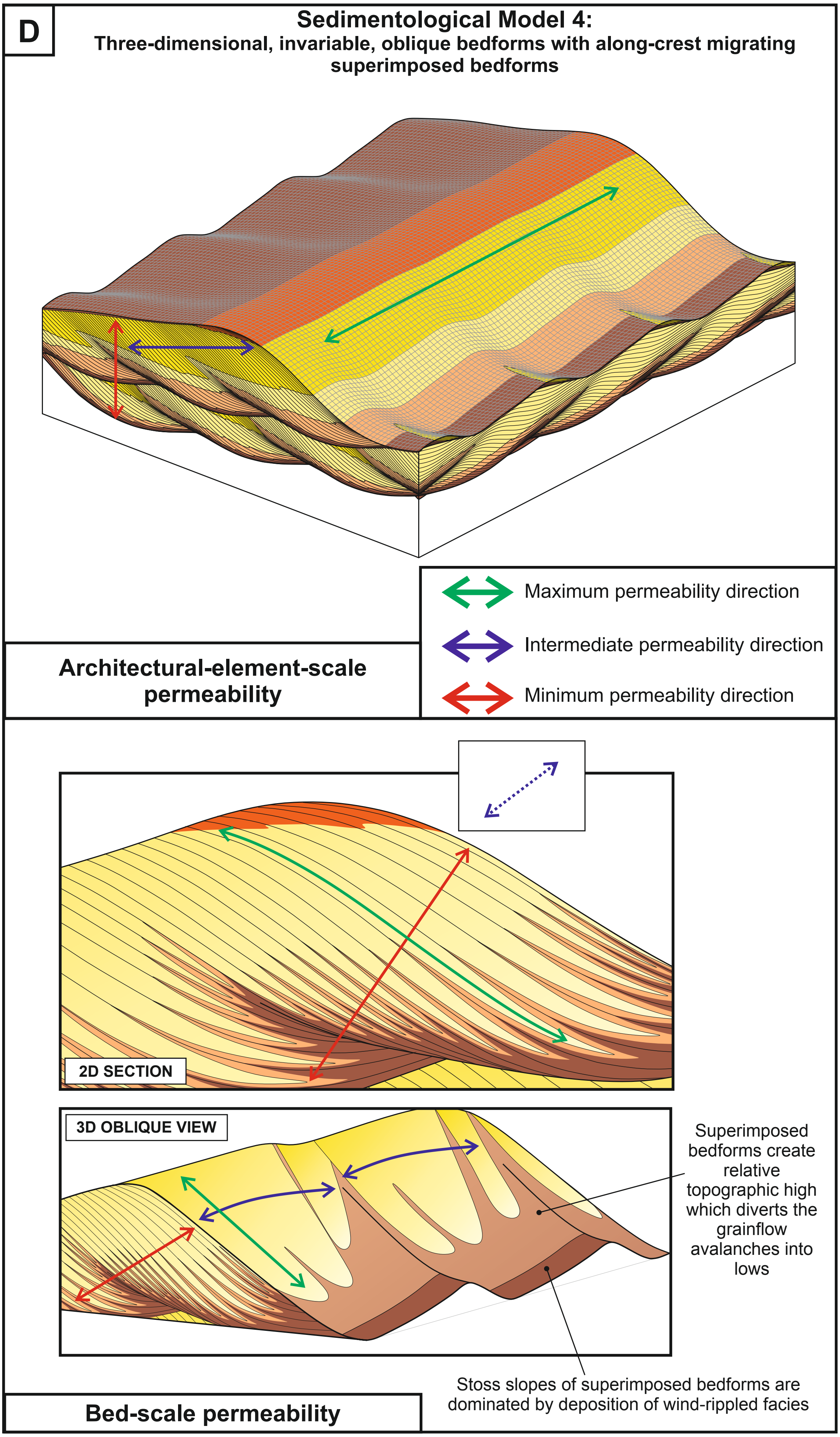
D
Sedimentological Model 4:
Three-dimensional, invariable, oblique bedforms with along-crest migrating superimposed bedforms
Maximum permeability direction
Intermediate permeability direction
Minimum permeability direction
Architectural-element-scale permeability
2D SECTION
3D OBLIQUE VIEW
Superimposed bedforms create relative topographic high which diverts the grainflow avalanches into lows
Stoss slopes of superimposed bedforms are dominated by deposition of wind-rippled facies
Bed-scale permeability

E

Sedimentological Model 5:

Three-dimensional, invariable, perfectly linear bedforms

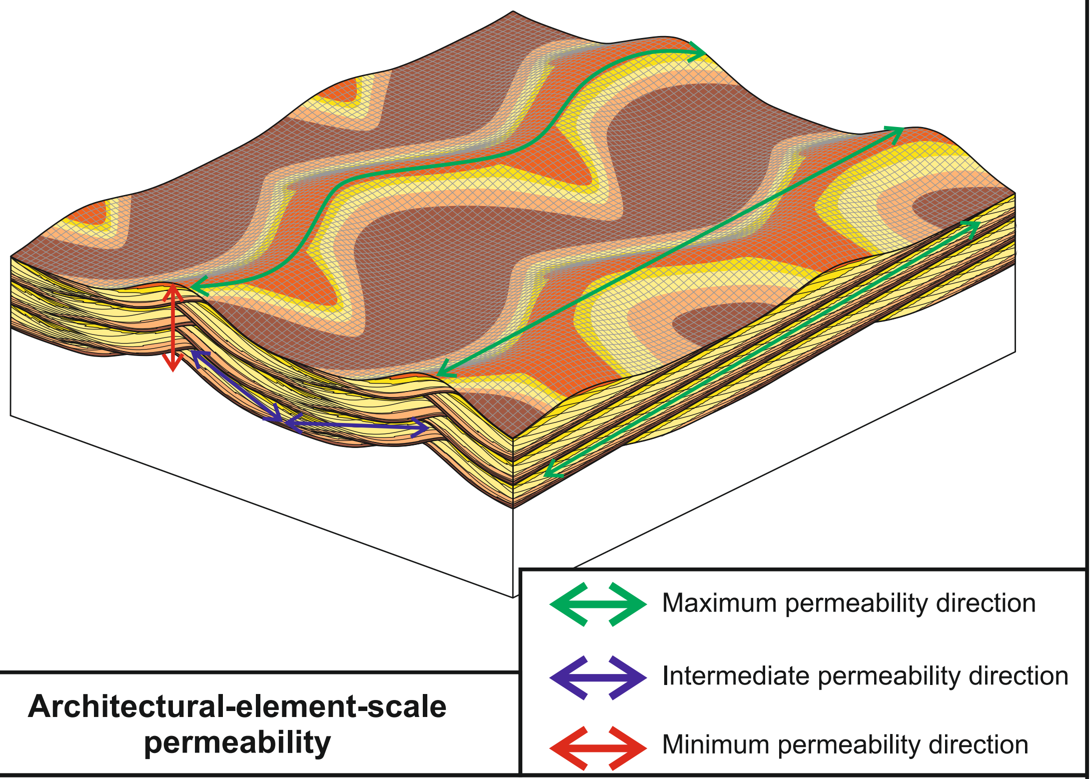

Architectural-element-scale permeability

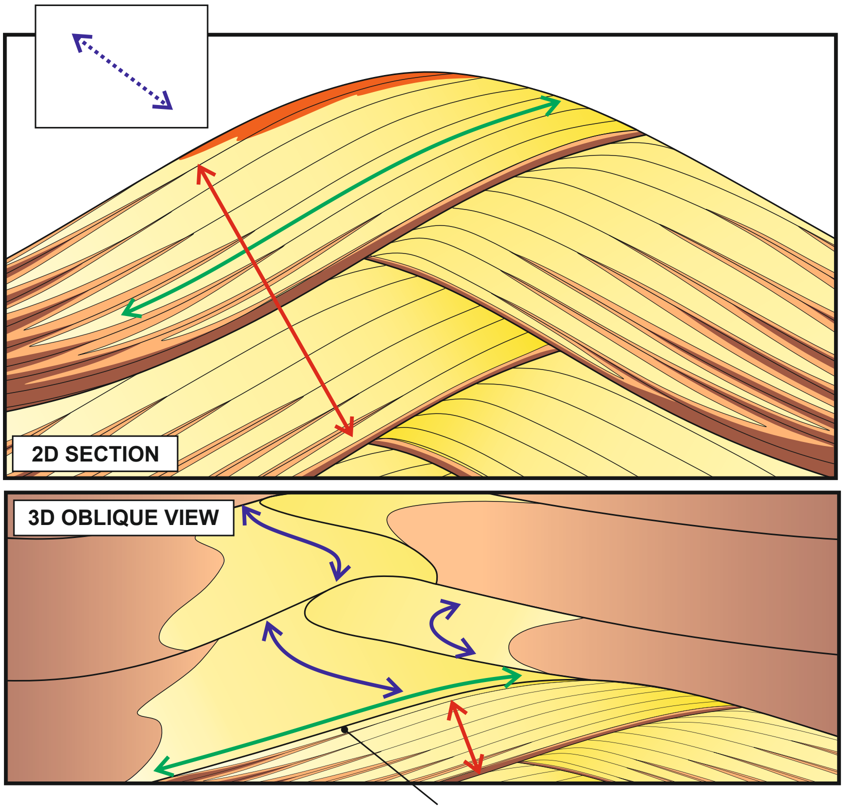

Grainflow avalanches extend further down the lee slope than in h) due to steeper dune plinth modelled here, permeability more favourable in this example

Bed-scale permeability

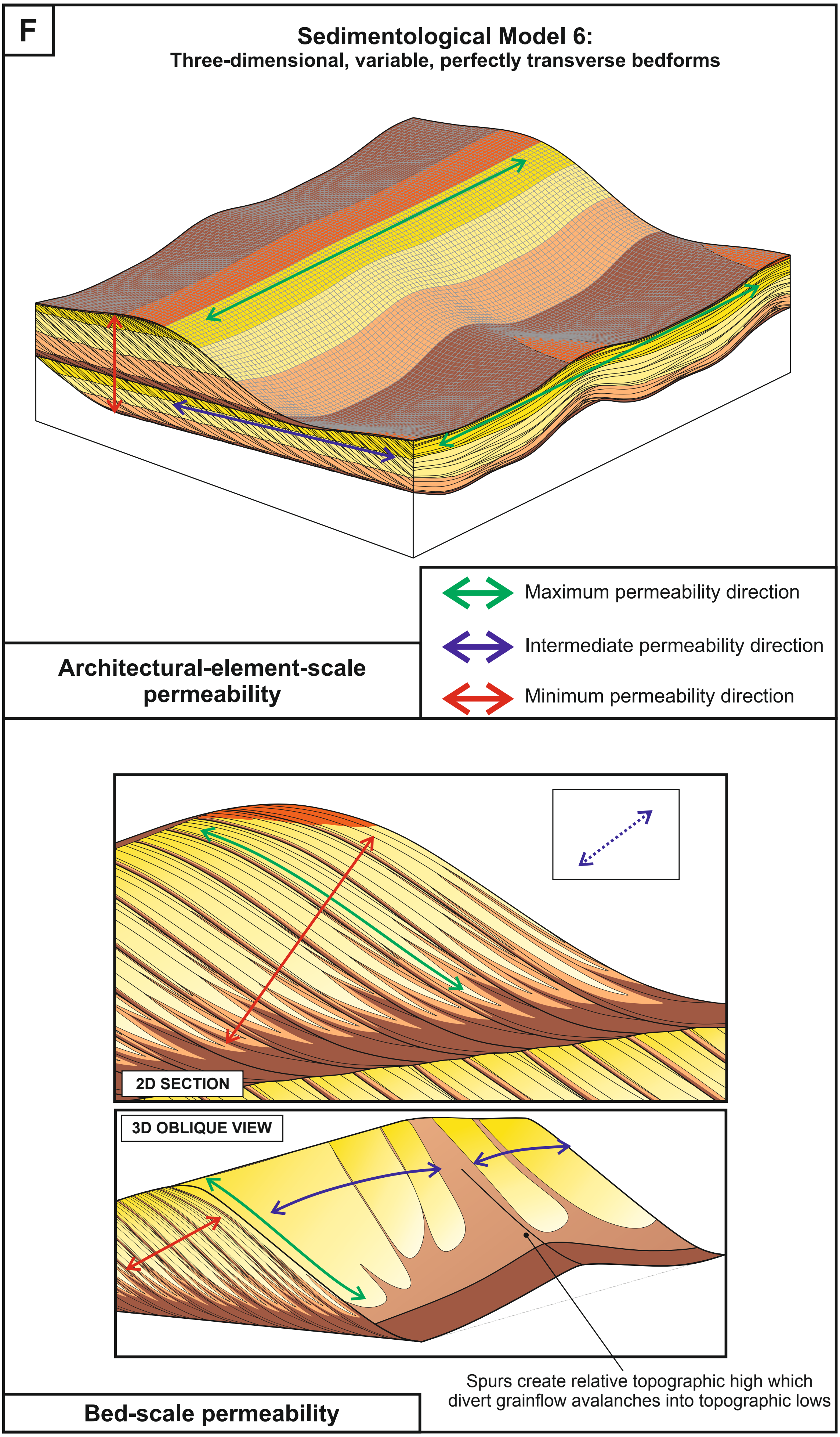
F
Sedimentological Model 6:
Three-dimensional, variable, perfectly transverse bedforms
Maximum permeability direction
Intermediate permeability direction
Minimum permeability direction
Architectural-element-scale permeability
2D SECTION
3D OBLIQUE VIEW
Spurs create relative topographic high which divert grainflow avalanches into topographic lows
Bed-scale permeability

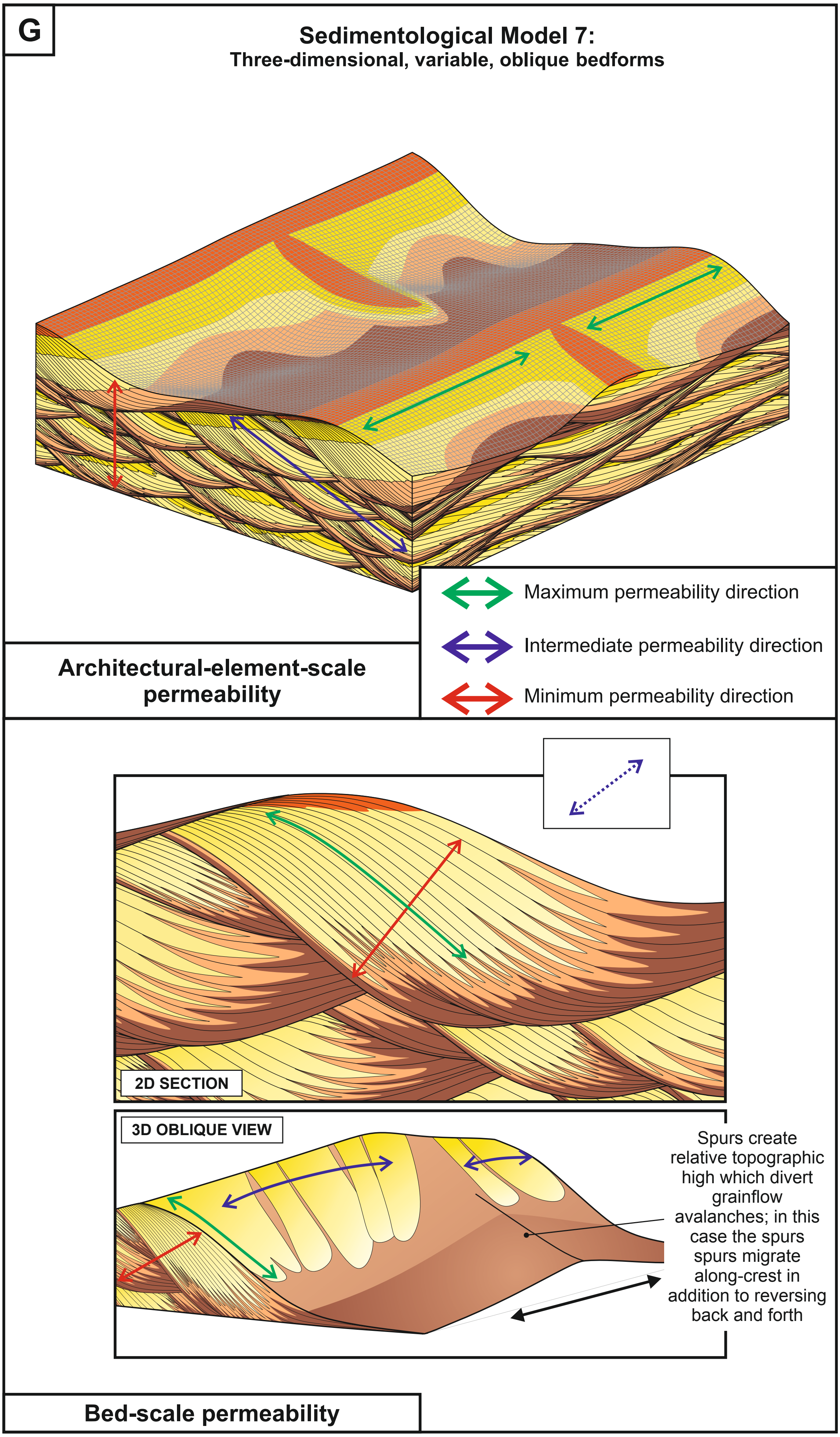

Spurs create relative topographic high which divert grainflow avalanches; in this case the spurs spurs migrate along-crest in addition to reversing back and forth

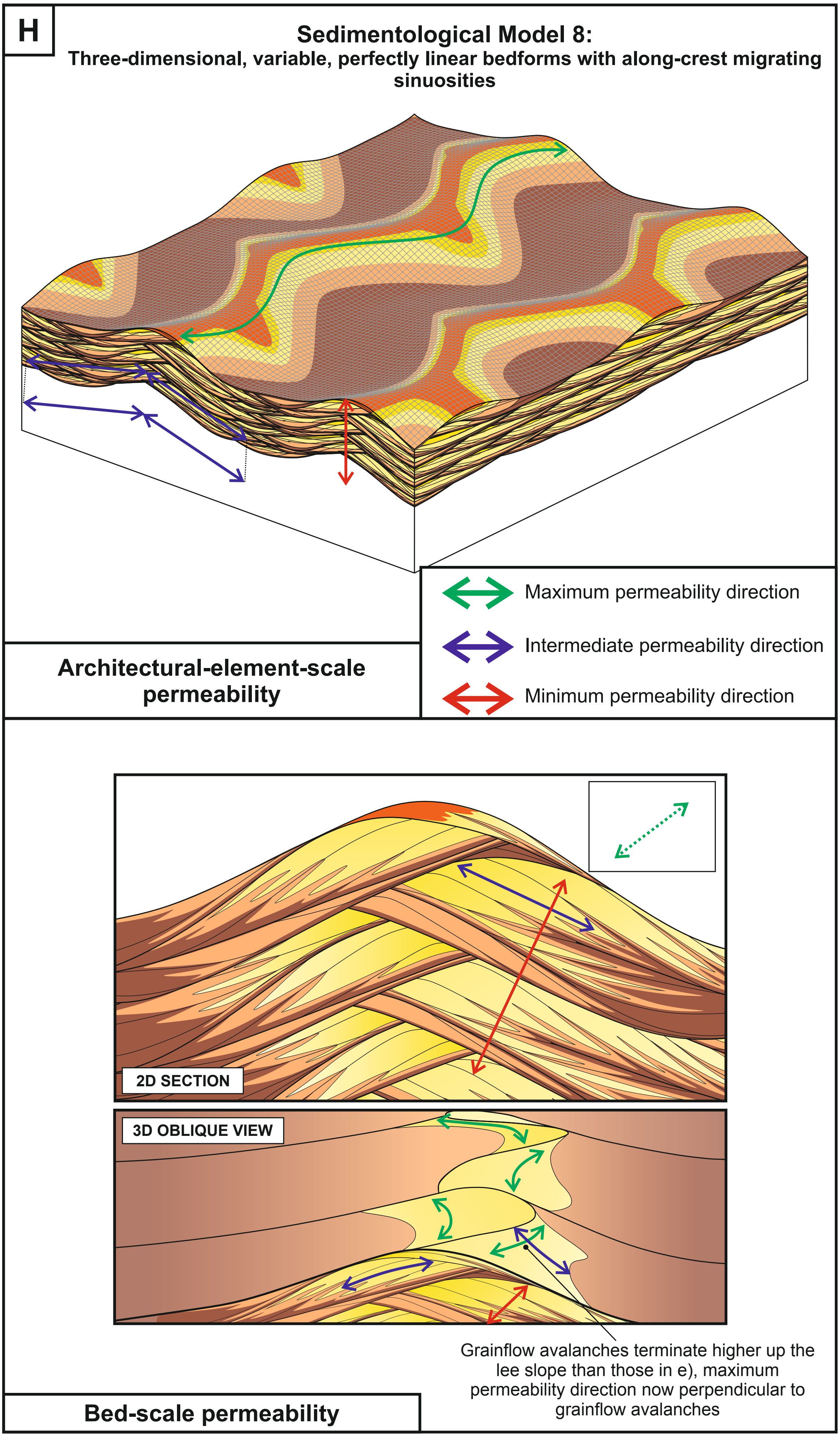

Sedimentological Model 8:
Three-dimensional, variable, perfectly linear bedforms with along-crest migrating sinuosities

Grainflow avalanches terminate higher up the lee slope than those in e), maximum permeability direction now perpendicular to grainflow avalanches

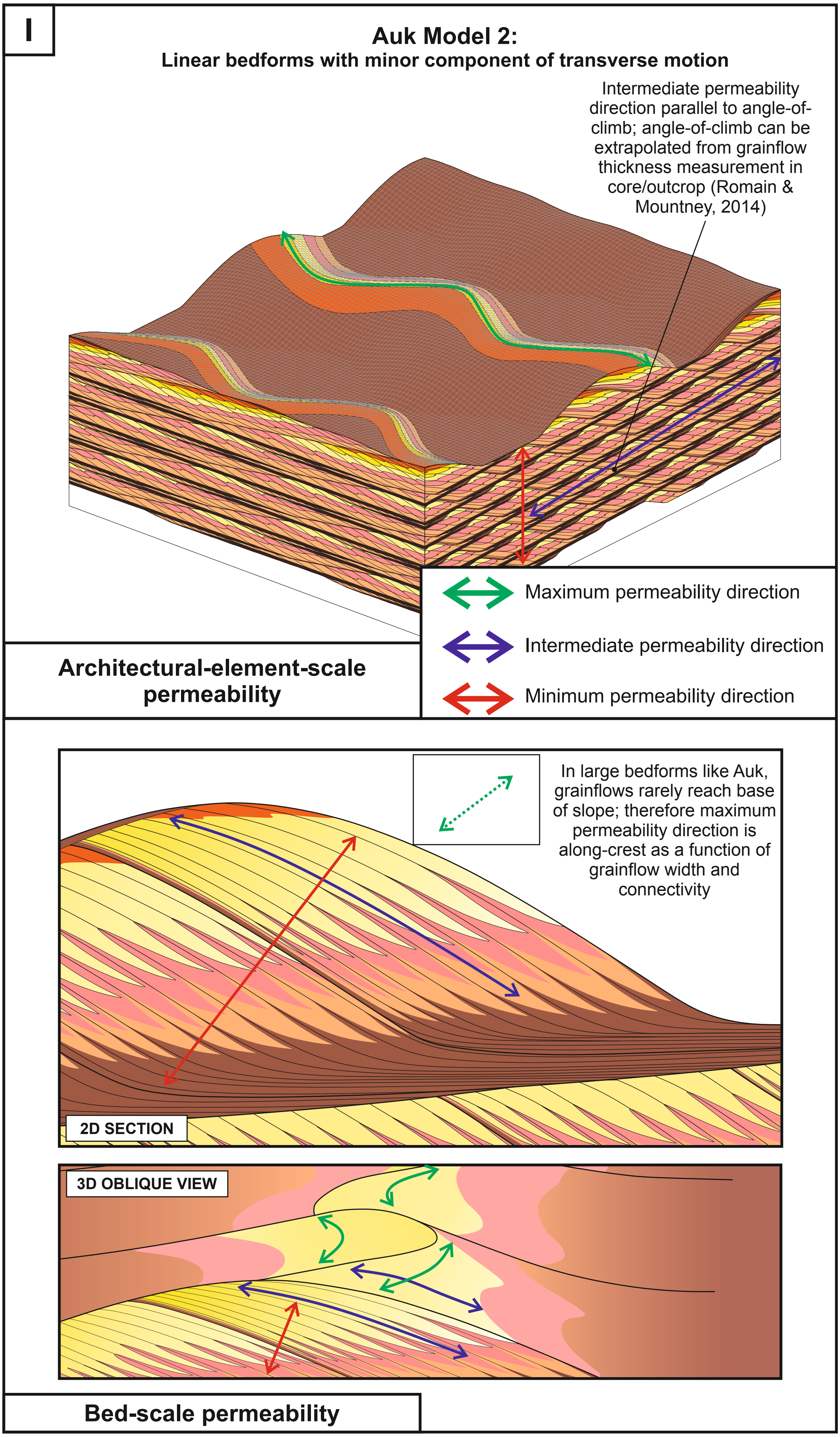

Auk Model 2:

Linear bedforms with minor component of transverse motion

Intermediate permeability direction parallel to angle-of-climb; angle-of-climb can be extrapolated from grainflow thickness measurement in core/outcrop (Romain & Mountney, 2014)

In large bedforms like Auk, grainflows rarely reach base of slope; therefore maximum permeability direction is along-crest as a function of grainflow width and connectivity

J

Auk Model 6:
Linear bedforms with minor component of transverse motion and superimposed barchanoid dunes

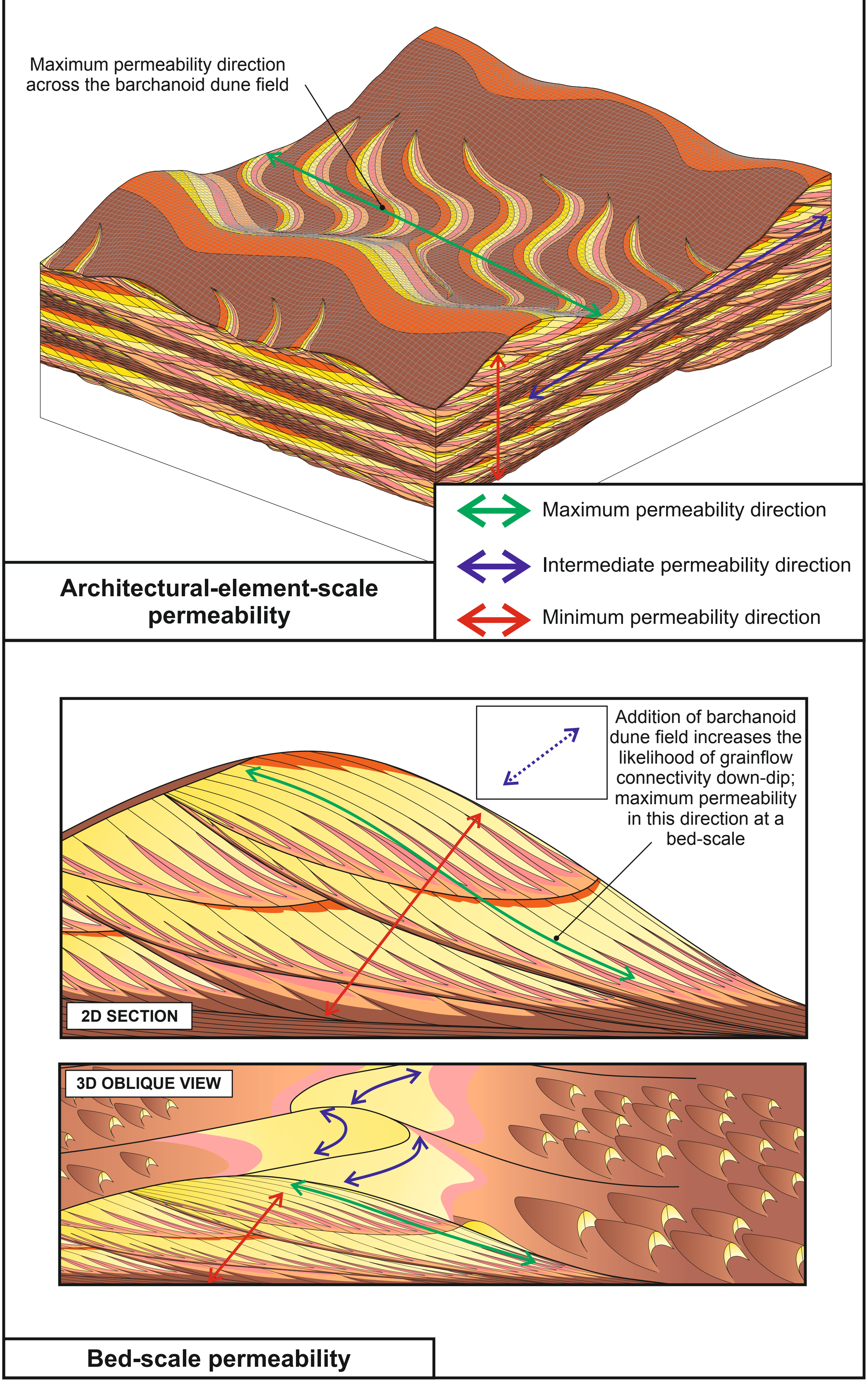

The bedforms which migrated and accumulated to give rise to the Auk Formation are envisaged to have been draa-scale linear bedforms, where the grainflows rarely reached the base of slope, therefore the maximum directional permeability of Auk Model 2 at a bed-scale is along the crest of the original bedforms as opposed to through the grainflow deposits. Therefore, information on original dune wavelength and bedform height can be advantageous when estimating preferred permeability directions, both of which can be derived from the empirical relationships developed in Chapter 2. For the case of Auk Model 6, the addition of the barchanoid dune field increases the likelihood that grainflow deposits from both scales of bedforms would be connected down dip, and so the maximum permeability direction for Auk Model 6 at a bed-scale is along the grainflow length, parallel to the dune lee slope. This connectivity could be compromised by the superimposition surfaces which arise due to the interaction of two scales of bedforms.

6.2.3.4 – Key advances

A suite of graphical models which depict the expected preferred permeability directions for bedforms with markedly different morphologies and migration styles has been developed (Figure 6.29). Preferred permeability directions at an architectural-element-scale are often not the same as the preferred permeability directions at a bed-scale within the same bedform model. Notably, there are a number of morphological features, such as superimposed bedforms and crestline sinuosity, which can have significant implications on the resultant preferred permeability directions of a given reservoir volume.

6.3 – Validation of sedimentological models with subsurface data

The six sedimentological models developed for the Auk Formation in Chapter 5 were based on a reinterpretation of the available core data from the Auk Field, described in Chapter 4. Data resulting from these models were then analysed further to yield expected foreset dip-azimuth distributions, facies proportions, and net to gross values from a selection of pseudo-cores that punctuated the modelled stratigraphy. These synthetic pseudo-cores were located at various positions along transects taken in sections perpendicular and parallel to the trend of the main bedforms, and in two opposing sections oriented obliquely to the migration direction of the main bedforms. Additionally, these bedform models yield palaeocurrent data – summary rose-diagram data plots have been generated which have been used to make direct comparison to the observed core data from the Auk Formation.

A number of observations can be made from the data generated as the output of the sedimentological models and these observations can be used to validate the use and input variables of the models by directly comparing them to the observed trends in the Auk Formation cores.

6.3.1 – Facies proportions

The facies proportions calculated for the Auk Formation in Section 6.1.3 match closely with the observed preserved facies distributions in the cores of the Auk Formation in Chapter 4.

Figure 6.17 core A from Auk Model 2 appears analogous with well 30/16-2 (Figure 4.8), where there is a thick section of wind-rippled strata at the base of the preserved set, moving upwards into wind-ripple-dominated strata and reworked wind-ripple strata, and with no grainflow facies preserved. Well 30/16-A16 (Figure 4.9) also bears close similarity with pseudo core A in Figure 6.14 and core D from Figure 6.15, where thicker and thinner grainflow units are preserved between each successive set.

The facies proportions generated from the pseudo-cores in Figure 6.20, which intersect the stacked barchanoid dunes interpreted in the studied portion of the Auk Formation succession, are directly comparable with well 30/16-9 (Figure 4.10). Similarly, all of the facies distributions depicted in the pseudo-cores generated for Auk Model 6 (Figures 6.18-6.21) are comparable with well 30/16-3 (Figure 4.15).

6.3.2 – Net to gross

In the cored data for the Auk Formation in Chapter 4, it was noted that the preserved succession preserved a net to gross of 15:85 (Section 4.5.2). The succession was dominated by wind-ripple and reworked wind-ripple facies (85%) whereas grainflow facies were much less common (15%).

In this study, the net reservoir calculations for the bedform models generated for the Auk Formation show a similar pattern; Auk Model 2 predicts a net to gross value of 8:92, and Auk Model 6 predicts a net to gross value of 25:75. Although these two outputs are different, when the two modelled outputs are combined and averaged, the overall modelled net to gross value for the Auk Formation is 16.5:83.5, almost identical to the observed cored dataset in Chapter 4.

6.3.3 – Palaeocurrent data

Comparison of the modelled output palaeocurrent roses in Chapter 5 with the actual palaeocurrent data from the Auk Formation reveals marked similarities. The data matches especially well in Figure 5.23a, wells 30/16-4, 30/16-9, 30/16-10 and in Figure 5.23b, wells 30/16-13, 30/16-9, 30/16-8 and 30/16-10.

Collectively, these observations indicate that the sedimentological models generated for the Auk Formation in Chapter 5 models are a reasonable and geologically suitable representation of the core data from the Auk Formation.

6.4 – Research advances

A number of key interpretations have been made as a result of this research which advance our ability to predict three-dimensional aeolian architecture in the subsurface, the geometry and connectivity of net reservoir units and preferred directional permeability in aeolian reservoir successions; the advances of this research are summarised below.

The ability to reconstruct the likely three-dimensional distribution of grainflow facies, considered net reservoir in this study, solely from a measurement of grainflow thickness in core allows for a more informed calculation of expected net reservoir quantities in subsurface reservoir intervals. With all aeolian facies distributions, the preservation potential of grainflow-dominated units is dependent on three primary factors: (i) the distance down the lee-slope that the original grainflow facies extended, which is governed by the shape of the dune lee slope: where a thick, low-angle-inclined plinth is present, grainflows tend to terminate higher up the dune slope – this is the case for bedforms that have accumulated via bedform migration and climb, which appears to be the case for the large majority of aeolian successions; (ii) the wavelength of the original bedforms; and (iii) the angle at which the bedforms climbed over one another to generate the accumulated sets; the latter two parameters (wavelength and angle-of-climb of the original bedforms) jointly determine the level at which dunes are truncated to preserve sets of cross strata of a given thickness (Figure 2.8).

By making observations on the distributions and quantities of specific aeolian facies preserved in cores, a suite of interpretations can be made regarding the expected original bedform morphology and the style in which the bedforms migrated to accumulate the preserved succession. By preserving thicker sets, a larger proportion of facies which originated from higher up the dune lee slope would be preserved, such as grainflow and grainflow-dominated facies considered net reservoir, meaning that the overall quality of the reservoir interval would be more favourable than reservoirs that are comprised of thinner sets. The preservation of thicker sets is directly attributable to a higher angle-of-climb, often a characteristic of smaller bedforms; although this implies that smaller bedforms preserve thicker sets (as a function of a steeper angle-of-climb), this is not typically the case given that larger bedforms tend to have long wavelengths – another major control on preserved set thickness (Romain and Mountney, 2014). These smaller bedforms typically possess a dune plinth that failed to develop to any great height, such that the angle-of-repose lee slope extended down very close to the dune base; a high proportion of grainflow facies is preserved in sets arising from the migration of these bedforms. Conversely, the preservation of thinner sets is associated with the migration of bedforms at a shallower angle-of-climb, often seen in larger dunes; these larger bedforms tend to have asymptotic bases with low-angle-inclined dune plinths whereby grainflow facies terminate higher up the dune lee slope, therefore preserving a large proportion of wind-ripple facies.

The presence of superimposed dune-scale bedforms on the flanks of, and in between, migrating draa-scale bedforms can increase the amount of grainflow facies preserved in reservoir successions; superimposed bedforms can arise with increasing dune height, width and sinuosity because sand transport rates are then sufficient to support migrating dunes on the dune slopes (Bristow et al., 2000), therefore an observed increase in preserved grainflow facies does not necessarily indicate that the original bedforms were small. Furthermore, although the presence of superimposed bedforms can markedly increase the preservation potential of grainflow facies implying a more favourable reservoir interval in successions of this type (e.g. Auk Model 6 – 25% net reservoir facies, compared with Auk Model 2 – 8% net reservoir facies), the connectivity of the net reservoir units is compromised by the numerous superimposition surfaces which arise as a result of the interaction between the two scales of bedforms, resulting in the net reservoir units being encapsulated by wind-rippled facies associated with the superimposition surfaces (Figure 6.27e), impacting on the ability for fluids to flow freely through the reservoir volume. The increased range in the distribution of foreset dip-azimuths in Auk Model 6 (Figure 6.5b) as compared with Auk Model 2 (Figure 6.4b) is feasibly a diagnostic indicator of the presence of superimposed bedforms.

There is little to distinguish between the resulting reservoir quality of perfectly linear and perfectly transverse bedforms. The difference in overall net reservoir calculations for perfectly transverse bedforms and perfectly linear bedforms is negligible (transverse bedforms – Figure 6.23, 55% net reservoir facies; linear bedforms – Figure 6.24, 57% net reservoir facies), as is the connectivity of the net reservoir units arising from the migration of these two types of bedforms (perfectly transverse – Figure 6.27a and Figure 6.27b; perfectly linear – Figure 6.27c). However, an important observation of this study is the distinct disparity in the two predicted net reservoir outputs for perfectly transverse bedforms (Figure 6.27a and Figure 6.27b), indicating that significantly different *apparent* reservoir geometries can be demonstrated depending on how the reservoir volume is intersected. There are also examples in the foreset dip-azimuth distributions from preserved sets of perfectly linear bedforms that show two opposing azimuths within the same preserved set (Figure 6.13 – cores B and C). This is the only bedform model from this study which displays this style; it is reasonable to interpret this as a diagnostic feature of foreset dip-azimuth distributions in perfectly linear bedforms.

Many of the previous studies on directional permeability in aeolian reservoirs have envisaged the maximum preferred permeability direction as parallel to the deposition of the grainflow deposits, as a function of the length of the preserved grainflow deposit. Whilst this is largely true at a bed-scale level of observation, at the architectural-element-scale the maximum preferred direction of permeability is no longer in this position (Figure 6.29). The architectural-element-scale of aeolian architecture investigated in this research is the most pertinent scale of observation used in reservoir modelling software.

Chapter 6 – Synthesis and Key Advances

Chapter 7 – Conclusions

This chapter summarises how the primary research objectives of this study have been addressed, and considers the way in which our understanding of the controls on aeolian bed-set architecture and subsequent reservoir heterogeneity has been advanced. Additionally, this chapter proposes future research opportunities that have arisen as an outcome of this study.

7.1 – Research objectives

This research demonstrates how the measurement of predictable sedimentological features present in aeolian successions can be used for the gross-scale reconstruction of three-dimensional aeolian bedform architecture through fulfilment of the objectives initially proposed in Chapter 1 (Section 1.2).

7.1.1 – To investigate predictable sedimentological features present in core and ancient outcropping successions that can be used to reliably reconstruct aspects of the original aeolian form, including bedform and interdune morphology, scale (height, wavelength, spacing) orientation, and style of migratory behaviour

A suite of empirical relationships were developed in Chapter 2, which enabled parameters measured directly from one-dimensional core to be related to larger-scale aeolian architectural elements observable in outcrop successions. Detailed characterisation of individual aeolian dune sets and relationships between neighbouring dune and interdune elements has been undertaken through outcrop studies of the Permian Cedar Mesa Sandstone and the Jurassic Navajo Sandstone in southern Utah.

The style of transition between lithofacies types seen vertically in preserved sets, and therefore measurable in analogous core intervals, enables predictions to be made regarding the relationship between preserved set thickness, individual grainflow thickness, original bedform dimensional properties (e.g. wavelength and height), the likely proportion of the original bedform that is preserved to form a set, the angle-of-climb of the system, and the likely along-crest variability of facies distributions in sets generated by the migration of sinuous-crested bedforms. This underpins a method for reconstructing three-dimensional aeolian geometries in the subsurface from one-dimensional subsurface datasets alone, forming the basis of a predictive tool that can be applied to subsurface datasets for the prediction of regional reservoir stratigraphic heterogeneity and overall net reservoir quantities in subsurface intervals (Figure 7.1a).

Key information relating to the morphology of the original bedforms and the style in which they migrated to accumulate a preserved succession can be obtained through detailed analysis of core and well-log data; the observations required as part of this methodology are summarised in Figure 7.1. The type and proportions of facies preserved in a given aeolian succession yield information on the mode of sedimentation, plus key information on the original bedforms (Figure 7.1b). If a greater proportion of facies associated with deposition on the lower portions of bedforms (e.g. wind-rippled facies) is encountered, it is reasonable to infer one or more of the following:

(i) The original bedforms possessed low-angle-inclined asymptotic lower plinths (commonly seen in larger dunes – Figure 6.1) whereby the grainflow avalanches rarely reached the base of slope (e.g. Figures 6.22a, 6.22h and 6.22i). In a studied succession of the Auk Formation, thick deposits of wind-ripple and reworked wind-ripple facies comprise up to 65% of the preserved coset (Section 4.5.4; Figure 4.8) indicating that the original bedforms had very thick low-angle-inclined plinths. By making comparisons to analogous dune fields, the Auk bedforms are envisaged to have been 150-250 m high with wavelengths of 1500-2500 m originating through a bedform climbing mechanism, preferentially preserving only the lowermost parts of the bedforms;

(ii) The preserved sets are relatively thin, as a function of original dune wavelength and angle-of-climb, whereby lower angles-of-climb preserve thinner sets (Figure 2.8), commonly seen in larger dunes. Therefore, most of the upper parts of the dune slipface where grainflows occur have been cut-off by the successive advancing bedform in the train (e.g. Figure 6.22h);

(iii) The bedforms were oscillating or episodically fluctuating in height, generating numerous thin sets bounded by reactivation surfaces that preferentially deposit wind-ripple strata (e.g. Figures 6.22b, 6.22f, 6.22g and 6.22h).

If a greater proportion of facies associated with deposition on the upper portions of bedforms (e.g. grainflow facies) is encountered, it is reasonable to infer one or more of the following:

(i) The original bedforms possessed a dune plinth that failed to develop to any great height, commonly seen in smaller dunes (Figure 6.1), such that the angle-of-repose lee slope extended down very close to the dune base (e.g. Figures 6.22c, 6.22e and 6.22f);

(ii) The preserved sets are relatively thick, as a function of original dune wavelength and angle-of-climb whereby higher angles-of-climb preserve thicker sets (Figure 2.8) commonly seen in smaller dunes: the thicker preserved sets therefore capture a higher proportion of facies associated with the upper slipface (e.g. Figure 6.22f);

(iii) The presence of superimposed bedforms, which preserve a higher proportion of slipface facies due to the interaction of two scales of bedforms, whereby the smaller coeval bedforms have steeper slipfaces conducive to grainflow avalanches extending further down their slipfaces; this increases the probability of grainflow facies being preserved (e.g. Figures 6.22d, 6.22g and 6.22j).

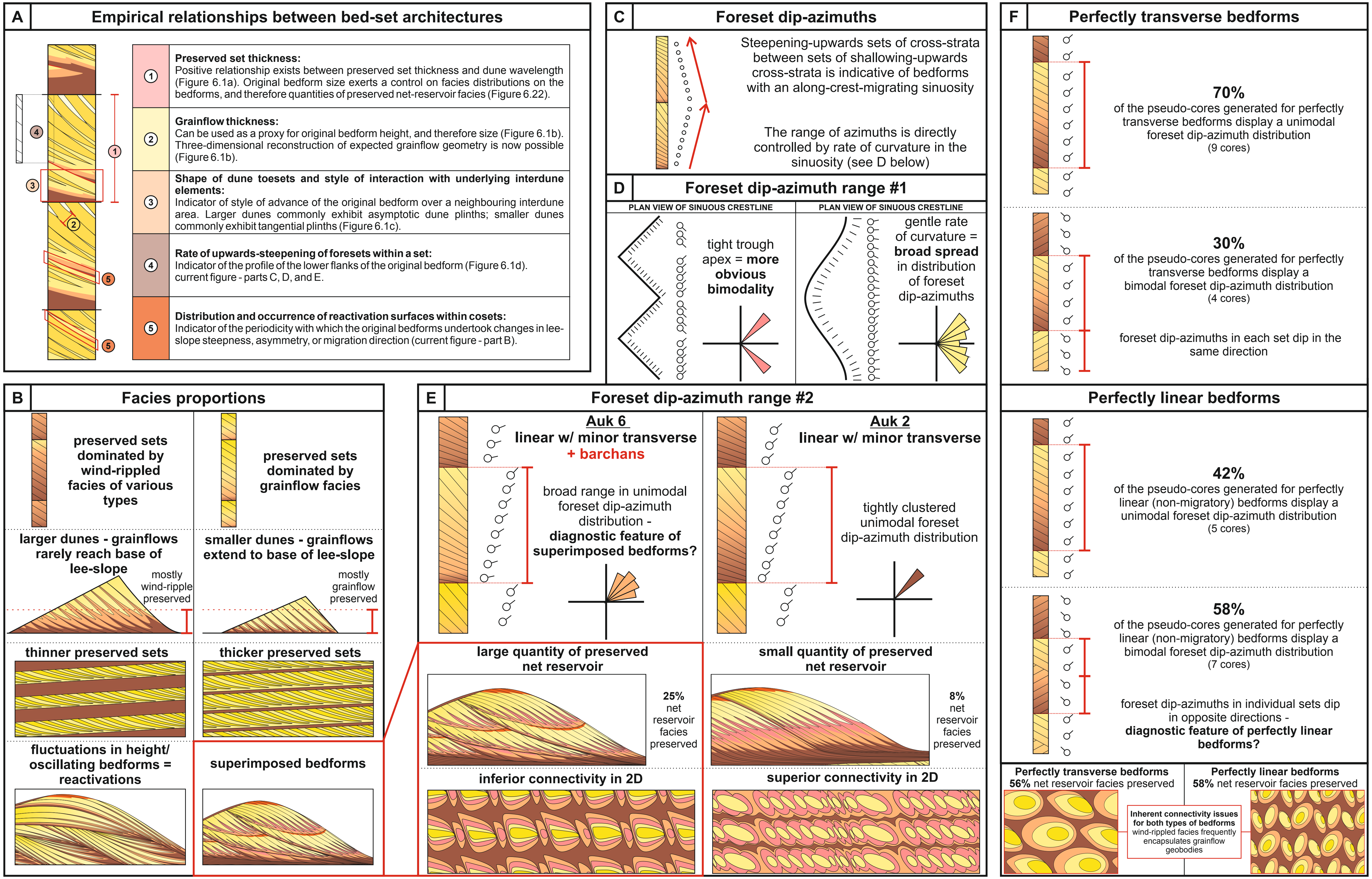

Preserved set thickness:
Positive relationship exists between preserved set thickness and dune wavelength (Figure 6.1a). Original bedform size exerts a control on facies distributions on the bedforms, and therefore quantities of preserved net-reservoir facies (Figure 6.22).

Grainflow thickness:
Can be used as a proxy for original bedform height, and therefore size (Figure 6.1b). Three-dimensional reconstruction of expected grainflow geometry is now possible (Figure 6.1b).

Shape of dune toesets and style of interaction with underlying interdune elements:
Indicator of style of advance of the original bedform over a neighbouring interdune area. Larger dunes commonly exhibit asymptotic dune plinths; smaller dunes commonly exhibit tangential plinths (Figure 6.1c).

Rate of upwards-steepening of foresets within a set:
Indicator of the profile of the lower flanks of the original bedform (Figure 6.1d). current figure - parts C, D, and E.

Distribution and occurrence of reactivation surfaces within cosets:
Indicator of the periodicity with which the original bedforms undertook changes in lee-slope steepness, asymmetry, or migration direction (current figure - part B).

Figure 7.1. Controls on aeolian bed-set architectures and implications for reservoir heterogeneity: a) Methods for reconstructing likely three-dimensional aeolian dune architecture from one-dimensional core data; b) Facies distributions as a proxy for information on original bedform morphology; c) Steepening-upwards sets of cross-strata between sets of shallowing-upwards cross-strata is indicative of bedforms with an along-crest-migrating sinuosity. The range of azimuths is directly controlled by rate of curvature in the sinuosity, whereby in d) a tight trough apex generates a more obvious bimodality in the distribution of foreset dip-azimuths, and a gentler rate of curvature generates a broader spread in the distribution of foreset dip-azimuths; e) The addition of superimposed bedforms in Auk Model 6 increases the range of foreset dip-azimuths - feasibly a diagnostic feature of superimposed bedforms. The presence of superimposed bedforms increases preserved net reservoir quantities, but reservoir connectivity is compromised; f) Where perfectly linear bedforms display a bimodal foreset dip-azimuth distribution, two opposing azimuths are evident within the same preserved set - interpreted here as a diagnostic feature of perfectly linear bedforms. The difference in overall net reservoir calculations between perfectly transverse and perfectly linear bedforms is modest, as is the connectivity of the net reservoir units arising from the migration of these two types of bedforms.

7.1.2 – To determine expected facies distributions and their resultant architectures for a variety of common aeolian bedform morphologies

A new methodology and workflow for aeolian reservoir modelling has been developed in Chapters 3 and 5 which forms an important bridging step between sedimentological and stratigraphical analysis, and reservoir modelling. Estimates were made of the likely geometry and degree of interconnectivity of net reservoir facies within three-dimensional space. This was achieved through the application of numerical modelling techniques to simulate bedform behaviour and resultant preserved stratigraphic architecture, and the population of the models with predicted facies distributions based on an understanding of the processes known to operate on modern dunes, and to facies distributions known from ancient outcrops. Interpretations regarding the gross-scale morphology and style of migratory behaviour of a variety of modern and ancient aeolian successions were used as input into modelling software that predicts the three-dimensional pattern of cross-bedding and erosive bounding surfaces generated by the migration and climb of a series of bedforms. The modelling software used (Rubin, 1987a) simulates the morphology of the bedforms and sets of rules are applied to determine how older strata are truncated by younger strata. A suite of different aeolian bedform types were simulated and the effects of changes in bedform steepness, asymmetry, migration speed, migration direction and rate of deposition were assessed. Once the architectural framework of the succession was modelled, specific aeolian facies were mapped onto the resultant stratigraphic framework. This second step was a semi-quantitative process based on an understanding of how aeolian facies types are distributed in similar modern dunes and in ancient aeolian successions exposed in outcrop (Figure 3.31). The results of these modelling exercises demonstrate that modest changes in bedform morphology can exert a marked control on preserved facies geometries, and therefore on the distribution of bodies considered to form effective net reservoir. Sedimentological Model 5 (Figure 3.21) and Sedimentological Model 8 (Figure 3.30) are both generated by three-dimensional, perfectly linear bedforms; the invariability of Model 5 generates net reservoir units of greater aerial extent than its counterpart in Model 8 where the individual foresets in the sets of variable cross-beds are not geometrically identical. Conversely, bedforms constructed under the influence of varied wind directions and bedforms which have distinctly different morphologies can generate preserved facies relationships that are potentially very difficult to distinguish from one another. The predicted net reservoir distributions for Sedimentological Model 5 – perfectly linear bedforms (Figure 3.21) and Sedimentological Model 7 – oblique bedforms (Figure 3.27) are very similar. The predicted net reservoir facies geometry for Sedimentological Model 6 (Figure 3.24d) is identical to that predicted by Models 1, 2 and 3 (Figures 3.8d, 3.11d and 3.15d respectively). Care must be taken when interpreting these deposits in the subsurface, or conversely applying these forward models to subsurface examples where original depositional bedform types are known; subsurface datasets can almost always be interpreted in multiple ways.

7.1.3 – To reconstruct the original bedform morphology and style of migratory behaviour of an aeolian reservoir interval known only from the subsurface, and to demonstrate how the geological complexities and lithological heterogeneities present in the interval can be modelled to provide insight into likely stratigraphic complexity that induces heterogeneity at a variety of scales

A series of well logs and cores penetrating the predominantly aeolian Auk Formation of the Permian Rotliegend Group, Central North Sea, UK, were evaluated in Chapter 4 to determine the morphology and style of migratory behaviour of the original dune bedforms and the overall depositional environment. This has been achieved by detailed facies analysis of subsurface datasets and by comparison of the observed sedimentary styles of accumulation to analogous modern aeolian dune fields.

Analysis of the architecture of preserved cross-bedded sets and cosets of the dune system represented by the Auk Formation (Section 4.5) demonstrates that the large linear bedforms accumulated on a dry substrate via migration and climb, and possessed large, low-angle-inclined lower plinths dominated by wind-ripple and reworked wind-ripple strata. The wind-ripple and reworked wind-ripple strata were preferentially preserved as successive bedforms migrated over one another at low angles; packages of grainflow-dominated strata representative of accumulation on the higher part of the bedform lee slope are less common and tend to be preserved mostly in the upper parts of thick cosets of strata. Trains of large linear bedforms were separated by elliptical, enclosed dry interdune areas. Although the primary direction of sand transport within the original bedforms was along the elongated crests of the bedforms, a secondary component of transverse motion enabled the preferential preservation of stratigraphic features arising from the along-crest migrating sinuosities present on the lee-side of the bedforms, in the form of a complex arrangement of bounding surfaces arranged within compound cosets. In places, the architecture records the preservation of small barchanoid dune deposits, either within interdune depressions or superimposed on the lower flanks of the large linear bedforms (Section 4.5.6.2). Few previous studies have documented linear dunes in ancient successions; these findings represent a valuable case example.

Six sedimentological models were developed in Chapter 5 to explain the likely mode of evolution and style of preservation of the Auk Formation. Specific aeolian facies were mapped onto the preserved set architectures based on the interpretation of both core and well log data from Chapter 4, and on comparison of the deposits with analogous modern dune systems and ancient outcrop successions. Stratigraphic complexity and variability is evident from the cored successions of the Auk Formation and this indicates that different parts of the formation arose in response to different configurations of aeolian bedforms that each undertook distinct styles of migratory behaviour. Thus, various arrangements of three-dimensional stratigraphic architecture are predicted and the six proposed palaeoenvironmental reconstructions account for this variability (Figures 5.4 – 5.21).

This research has advanced our ability to characterise aeolian reservoir intervals in a number of ways. By adopting the methodology of detailed core and well log analysis presented in Chapter 4 and applying it to additional aeolian reservoir systems, a more informed interpretation on original bedform morphology and style of migratory behaviour can be made. It is pertinent to make these interpretations, as both of these factors have significant implications for the resulting quality of the overall volume. However, from an applied perspective, the key research advance is the subsequent forward modelling technique developed herein, which reveals informed quantitative estimates of net reservoir distributions in subsurface aeolian reservoir successions. This forward modelling procedure is especially valuable in reservoir successions for which core data do not necessarily provide direct insight regarding net reservoir geometry, orientation and style of interconnectivity.

7.1.4 – To investigate any predictable responses in well log data (e.g. dipmeter data) for a variety of aeolian bedform types that could be used to determine original bedform morphology

By interrogating the bedform models in Chapter 6, it was apparent that markedly different bedform morphologies can generate almost identical dipmeter log responses, and conversely that various log responses can be generated from the same bedform model, usually over very short distances. This pattern is seen over the great majority of the sections generated for the bedform models (Figures 6.6 – 6.21). However, there are key observations that can aid the determination of bedform morphology.

Observing upwards-steepening sets of cross-strata between sets of shallowing-upwards cross strata in subsurface datasets is indicative of bedforms which possessed an along-crest-migrating sinuosity (Chapter 4 – Figure 7.1c). This sinuosity controls the shape of dune troughs in plan-view, which in turn governs the overall distribution of foreset dip-azimuth data. If there is a gentle rate of curvature, whereby the bedforms exhibit wide open trough shapes in plan-view, then a broad spread of foreset dip-azimuths would be generated over a wide range, as is the case modelled in Figure 6.2b. Conversely, if the troughs depict a ‘diamond-shape’ in plan-view with a tight trough apex, then the distribution of foreset dip-azimuths would demonstrate more obvious bimodality; the range of the foreset dip-azimuth distribution is directly dictated by the amount of curvature in the trough (Figure 7.1d).

The unimodal foreset dip-azimuth distribution noted for the Auk Formation in Chapter 4, together with sedimentological and stratigraphic trends, was indicative of linear dunes with a minor component of transverse motion; linear dune deposits can therefore be expressed as tightly clustered unimodal trends in foreset dip-azimuth data. Each cored section generated for the Auk Formation in Chapter 6 also displays this characteristic unimodal distribution as a result of the minor component of transverse motion. Subsequently, differentiating between the preserved deposits of linear and transverse dunes is often problematic. Auk Model 2 and Auk Model 6 were generated with identical values for the wavelength of crestline sinuosity, however Auk Model 6 displays a far greater range in the distribution of foreset dip-azimuths which is not attributable to a gentler rate of crestline curvature (as a function of the input value for crestline sinuosity); rather it is the addition of the superimposed bedforms migrating obliquely to the parent bedforms (Figure 7.1e). This increased range in the distribution of foreset dip-azimuths is feasibly a diagnostic feature of superimposed bedforms, the presence of which has favourable implications for overall net reservoir quantities but detrimental implications for net reservoir connectivity at a macroscopic scale of observation (Section 7.1.5).

In the theoretical bedform models, transverse bedforms frequently display unimodal foreset dip-azimuth distributions (70% - 9 cores), whereas linear bedforms typically display a bimodal distribution (58% - 7 cores). Importantly, there are examples in the preserved sets from the perfectly linear model that show two opposing azimuths within the same preserved set: this is the only bedform model from this study which displays this style and it is reasonable to interpret this as a diagnostic feature of foreset dip-azimuth distributions in bedforms of this type (Figure 7.1f).

7.1.5 – To investigate the effect that original bedform morphology and style of migratory behaviour has on the overall reservoir quality of the volume (facies distributions, net reservoir calculations and connectivity)

Individual cores taken across the reservoir volumes in Chapter 6 (Section 6.2.1) show significant differences in net reservoir facies calculations, but the difference in overall quality of the reservoir volumes for transverse and linear bedforms is modest (Figures 6.23 and 6.24). Grainflow and grainflow-dominated facies for perfectly linear bedforms (Figure 6.27c) have a smaller aerial extent than those predicted for perfectly transverse bedforms (Figure 6.27a); this is partly due to the increased value for the wavelength of the crestline sinuosity in the transverse bedform model, generating a gentler rate of curvature which is directly attributable to the greater aerial extent of net reservoir facies. If the wavelength value for both bedform models were the same, then the connectivity of the reservoir intervals generated by perfectly transverse and perfectly linear bedforms would be almost impossible to distinguish. The values for wavelength of the crestline sinuosity were different in each of these models to investigate the effect, if any, that a change in crestline sinuosity would have on the resultant net reservoir architecture. It is apparent from the forward modelling process that modest changes in bedform architecture can have a marked influence on net reservoir morphologies and distributions, but importantly bedforms with very different morphologies generate very similar net reservoir distributions and inherent connectivity issues, with grainflow packages commonly entirely encapsulated within non-net reservoir (wind-ripple facies of various types).

There are several factors which have a marked impact on the overall quality of the reservoir volume:

Wavelength of crestline sinuosity. Grainflow development on the lee-slope of a bedform is dependent on the wavelength of the crestline sinuosity (Figure 1.5; Figure 6.29c). In cases of sedimentary architecture generated by the passage of bedforms that possessed relatively more sinuous crestlines, the grainflows have a much smaller plan-view extent, as opposed to crestlines with only minor sinuosity, where the grainflows will have a greater extent: this has further implications for preferred permeability directions at a bed-scale of observation.

Reactivation and superimposition surfaces. Reactivation surfaces in aeolian successions arise from a variety of scenarios, such as in cases where bedforms oscillate or episodically fluctuate in height, generating numerous thin sets bounded by reactivation surfaces that preferentially deposit wind-ripple strata (e.g. Figures 6.22b, 6.22f, 6.22g and 6.22h). The addition of superimposed bedforms generates superimposition surfaces (originally called second-order surfaces, *sensu* Brookfield, 1977). Whilst the addition of superimposed bedforms in Auk Model 6 significantly increases the preserved net reservoir quantities in reservoir successions of this type (Figure 6.26), the superimposition surfaces which arise from the interaction of the two scales of bedforms have detrimental implications for the connectivity of net reservoir units (e.g. Figure 6.27e).

Grainflow geometry. The distance down the lee-slope that the original grainflow facies extended is governed by the shape of the dune lee slope: where a thick, low-angle-inclined plinth is present, grainflows tend to terminate higher up the dune slope. In cases where the grainflows extend to near the base of the plinth (Model 5 – Figure 3.21), the net reservoir facies have a greater aerial extent and a larger volume; in cases where the grainflows terminate higher up the dune slope (Model 8 – Figure 3.30), larger proportions of non-net reservoir encapsulate the net reservoir geobodies, which has detrimental implications for connectivity of the grainflow geobodies.

Temporal variability in accumulation rate. Bedforms which accumulate at variable rates preserve sets of aeolian dune strata that vary in thickness, which controls the extent to which net reservoir units are preserved. Net reservoir facies (grainflow and grainflow-dominated) are more likely to be accumulated during episodes when the angle-of-climb attained its maximum value because this enables the middle and upper flanks of the migrating bedforms to be preserved; volumetrically larger and laterally more continuous packages of grainflow facies are preserved during periods of increased angles-of-climb. Angles-of-climb in dry aeolian systems are controlled by the rate of subsidence, the rate of bedform migration and the availability of any pre-existing unfilled accommodation space

(Mountney, 2006a). Grainflow facies tend not be accumulated during episodes when the angle-of-climb is low and, under such circumstances, the preserved accumulation will be dominated by reworked wind-ripple, wind-ripple-dominated and wind-ripple facies. Thus, the preserved distribution of net reservoir facies is controlled not only by the mean angle-of-climb, but also the amplitude and periodicity of its variation (Mountney, 2006a; 2012).

Original bedform type. Although original bedform type exerts a partial control on the quantities of preserved net reservoir facies, the issues concerning reservoir connectivity are largely the same for all modelled scenarios in this research. In each modelled scenario, wind-rippled facies of poorer reservoir quality compartmentalise the net reservoir grainflow facies, with detrimental implications on fluid flow estimates in hydrocarbon reservoir successions.

7.2 – Shortcomings and limitations

There a several limitations of the techniques developed in this research. Care must be exercised in the application of the empirical relationships developed in Chapter 2. As with most statistical data derived from natural datasets, the spread of the data is, in many cases, considerable, chiefly as a result of the variability inherent in natural depositional systems such as those studied in this work. This results in data distributions that yield best-fit trends with low R^2 values that are statistically weak. However, despite these shortcomings, relationships between measurements of small- and larger-scale aspects of sedimentary architecture form the basis for the development of a predictive tool that can potentially be applied with care to subsurface datasets for elucidation of larger-scale sedimentary architecture and prediction of regional reservoir stratigraphic heterogeneity.

Additionally, there is typically insufficient subsurface data available to reliably identify the key measurements required for the detailed reconstruction of original aeolian bedform type and style of migratory behaviour, as was possible for the Auk Formation in Chapter 4. Auk is an old reservoir (first discovery in 1971) and has many wells (41 wells as of 2003 – Trewin et al., 2003) drilled over a relatively small area, therefore it was particularly suitable for this study. Even in cases such as the Auk Formation, where the data was sufficient for an informed interpretation of original aeolian form, a range of possible scenarios were still feasible given the available data. Each modelled scenario accounted for the inherent variability of naturally-occurring aeolian systems, but it would be challenging to select a single appropriate model for the reservoir interval given the datasets which are typically available.

7.3 – Future work

7.3.1 – Rubin modelling software

The modelling software package used to generate the bedform models in Chapters 3, 5 and 6 predicts the three-dimensional pattern of cross-bedding and erosive bounding surfaces that are generated by the migration and climb of a series of bedforms (Rubin, 1987a). This is achieved by simulating the morphology of the bedforms by approximating their shape as a series of sine waves. The style of migration of these bedforms is simulated by translating these sine waves over a series of time steps and by applying a set of rules to determine how older strata are truncated by younger strata.

In this research, the resultant facies distributions on the bedform models were manually added as a qualitative process based on an understanding of how aeolian facies types are distributed in similar modern dunes and in ancient aeolian successions exposed in outcrop. If the modelling software used in this study was augmented with a set of rules for the stochastic generation of expected facies distributions on bedforms with various morphologies and styles of migratory behaviour, then the data could be interrogated in a more efficient and systematic manner. The ability to slice the reservoir volume at any chosen interval would yield quantitative three-dimensional net reservoir distributions for a variety of aeolian bedform types. An additional benefit of this stochastic modelling technique would be the ability to run variations in combinations of parameters to generate a statistical comparison between key observations made in cored intervals as a way of ranking different models of aeolian reservoir intervals.

The forward modelling technique developed in Chapters 3 and 5 can potentially be applied to other aeolian successions, including systems that are outcropping, and for which the predictive power of the method developed in this research could be presented more clearly. The predictive results that arise as an output of the modelling software could therefore be directly tested, by comparing the modelled results to the equivalent outcropping stratigraphy.

7.3.2 – Empirical relationships

The empirical relationships identified in Chapter 2 were developed from measurement of outcropping successions of the Permian Cedar Mesa Sandstone and the Jurassic Navajo Sandstone. The relationships outlined in this study would benefit from additional datasets from a variety of aeolian outcropping successions, such as the Entrada Sandstone which is interpreted as a wet aeolian system (Crabaugh and Kocurek, 1993), and to include successions that are not on the Colorado Plateau to remove bias. This would provide a more robust and varied dataset with which to further develop the empirical relationships established in Chapter 2.

With additional data, the empirical relationships that have been developed could be tested for a range of dry, wet and stabilizing aeolian system types, to investigate how the observed relationships vary in different aeolian systems, and how they relate to external controls as well as intrinsic behaviour. The technique developed in Chapter 2 could also be applied to a variety of subsurface reservoir successions to demonstrate the validity of the technique in a wide range of aeolian system types. The qualitative and empirical quantitative relationships developed in Chapter 6 could be developed further and related to wider issues of reservoir heterogeneity, whereby fluid-flow and pressure communication data (i.e. dynamic reservoir data) could be used to demonstrate the validity of the models.

References

Ajdukiewicz, J.M., Nicholson, P.H. and Esch, W.L. (2010) Prediction of deep reservoir quality using early diagenetic process models in the Jurassic Norphlet Formation, Gulf of Mexico. *American Association of Petroleum Geologists Bulletin,* **94**, 1189-1227.

Allen, J.R.L. (1970) The avalanching of granular solids on dune and similar slopes. *Journal of Geology*, **78**, 326–351.

Al-Masrahy, M.A. and Mountney, N.P. (2013) Remote sensing of spatial variability in aeolian dune and interdune morphology in the Rub' Al-Khali, Saudi Arabia. *Aeolian Research*, **11**, 155-170.

Anderson, R.S. (1988) The pattern of grainfall deposition in the lee of aeolian dunes. *Sedimentology*, **35**, 175–188.

Bagnold, R.A. (1941) The Physics of Blown Sand and Desert Dunes. Methuen & Co. Ltd., London, 265 pp.

Bell, C.M. (1991) The relationships between sedimentary structures, transport directions and dune types in Mesozoic aeolian sandstones, Atacama Region, Chile. *Sedimentology*, **38**, 289-300.

Benan, C.A.A. and Kocurek, G. (2000) Catastrophic flooding of an aeolian dune field: Jurassic Entrada and Todilito Formations, Ghost Ranch, New Mexico, USA. *Sedimentology*, **47**, 1069-1080.

Bifani, R., George, G.T. and Lever, A. (1987) Geological and reservoir characteristics of the Rotliegend sandstone in the Argyll field. In: *Petroleum Geology of North West Europe.* (Eds. J. Brooks, and K.W. Glennie). Graham & Trotman, London, 509–522.

Blakey, R.C. and Ranney, W. (2008) Ancient Landscapes of the Colorado Plateau. Grand Canyon Association, 176 pp.

Bloomfield, J.P., Moreau, M.F. and Newell, A.J. (2006) Characterization of permeability distributions in six lithofacies from the Helsby and Wilmslow sandstone formations of the Cheshire Basin, UK. In: *Fluid flow and solute movement in sandstones: the onshore UK Permo-Triassic red bed sequence* (Eds. B.D. Barker and J.H. Tellam). Geological Society Special Publication, **263**, 83-101.

Boersma, J.R. and Terwindt, J.H.J. (1981) Neap–spring tide sequences of intertidal shoal deposits in a mesotidal estuary. *Sedimentology*, **28**, 151–170.

Bongiolo, D.E. and Scherer, C.M.S. (2010) Facies architecture and heterogeneity of the fluvial-aeolian reservoirs of the Sergi formation (Upper Jurassic), Recôncavo Basin, NE Brazil. *Marine and Petroleum Geology*, **27**, 1885-1897.

Bowker, K.A. and Jackson, W.D. (1989) The Weber Sandstone at Rangely Field, Colorado. In: *Petrogenesis and petrophysics of selected sandstone reservoirs of the Rocky Mountain region* (Ed. E.B. Coalson). *Rocky Mountain Association of Geologists Annual Guide Book*, 65-80.

Breed, C.S., Fryberger, S.G., Andrews, S., McCauley, C.K., Lennartz, F., Gebel, D. and Horstman, K. (1979) Regional studies of sand seas using Landsat (ERTS) imagery. In: *A study of global sand seas* (Ed. E.D. McKee). *U.S. Geological Survey Professional Paper*, **1052**, 305-397.

Bristow, C. and Mountney, N.P. (2013) Aeolian stratigraphy. In: *Treatise on Geomorphology* (Eds. J. Shroder, N. Lancaster, D.J. Sherman, A.C.W. Baas). Academic Press, San Diego, CA. *Aeolian Geomorphology*, **11**, 246–268.

Bristow, C.S., Bailey, S.D. and Lancaster, N. (2000) The sedimentary structure of linear sand dunes. *Nature*, **406**, 56-59.

Bristow, C.S., Duller, G.A.T. and Lancaster, N. (2007) Age and dynamics of linear dunes in the Namib Desert. *Geology,* **35,** 555-558.

Brookfield, M.E. (1977) The origin of bounding surfaces in ancient aeolian sandstones. *Sedimentology*, **24**, 303-332.

Buchanan, R. and Hoogteyling, L. (1979) Auk Field Development: A Case History Illustrating the Need for a Flexible Plan. *Journal of Petroleum Technology*, **31**, 1305–1312.

Carrigy, M.A. (1970) Experiments on the angles of repose of granular materials. *Sedimentology*, **14**, 147–158.

Chan, M.A. and Kocurek, G. (1988) Complexities in eolian and marine interactions - processes and eustatic controls on erg development. *Sedimentary Geology*, **56**, 283-300.

Chandler, M.A., Kocurek, G., Goggin, D.J. and Lake, L.W. (1989) Effects of stratigraphic heterogeneity on permeability in eolian sandstone sequence, Page Sandstone, northern Arizona. *American Association of Petroleum Geologists Bulletin,* **73**, 658-668.

Clemmensen, L.B. and Abrahamsen, K. (1983) Aeolian stratification and facies association in desert sediments, Arran basin (Permian), Scotland. *Sedimentology*, **30**, 311–339.

Cox, D.L., Lindquist, S.J., Bargas, C.L., Havholm, K.G. and Srivastava, R.M. (1994) Integrated modeling for optimum management of a giant gas condensate reservoir, Jurassic eolian Nugget Sandstone, Anschutz Ranch East Field, Utah Overthrust (U.S.A.). In: *Stochastic modeling and geostatistics: principles, methods and case studies* (Eds. J.M. Yarus and R.L. Chambers). *American Association of Petroleum Geologists Computer Applications in Geology*, **3**, 287-321.

Crabaugh, M. and Kocurek G. (1993) Entrada Sandstone: an example of a wet aeolian system. In: *The Dynamics and Environmental Context of Aeolian Sedimentary Systems* (Ed. K. Pye) *Geological Society of London Special Publication* **72**, 103-126.

DeCelles, P.G., Langford, R.P. and Schwartz, R.K. (1983) Two new methods of palaeocurrent determination from trough cross-stratification. *Journal of Sedimentary Petrology*, **53**, 629-642.

Eastwood, E.N., Kocurek, G., Mohrig, D. and Swanson, T. (2012) Methodology for reconstructing wind direction, wind speed, and duration of wind events from aeolian cross-strata. *Journal of Geophysical Research – Earth Surface*, **117**, F03035.

Ellis, D. (1993) The Rough gas field: distribution of Permian aeolian and non-aeolian reservoir facies and their impact on field development. In: *Characterization of fluvial and aeolian reservoirs* (Eds. C.P. North and D.J. Prosser). *Geological Society of London Special Publication* **73**, 265-277.

Ellwood, J.M., Evans, P.D. and Wilson, I.G. (1975) Small scale aeolian bedforms. *Journal of Sedimentary Petrology*, **45**, 554-561.

Fischer, C., Gaupp, R., Dimke, M. and Sill, O. (2007) A 3D high resolution model of bounding surfaces in aeolian-fluvial deposits: An outcrop analogue study from the Permian Rotliegend, Northern Germany. *Journal of Petroleum Geology*, **30**, 257-274.

Follows, E. (1997) Integration of inclined pilot hole core with horizontal image logs to appraise an aeolian reservoir, Auk Field, Central North Sea. *Petroleum Geoscience*, **3**, 43-55.

Fryberger, S.G. (1979a) Dune forms and wind regime. In: *A study of global sand seas* (Ed. E.D. McKee). *U.S. Geological Survey Professional Paper*, **1052**, 137-169.

Fryberger, S.G. (1979b) Eolian-fluviatile (continental) origin of ancient stratigraphic trap for petroleum in Weber Formation, Rangely field, Colorado. *Mountain Geologist*, **16**, 1-36.

Fryberger, S.G. (1986) Stratigraphic traps for petroleum in wind-laid rocks. *American Association of Petroleum Geologists Bulletin*, **70**, 1765-1776.

Fryberger, S.G. (1993) A review of aeolian bounding surfaces, with examples from the Permian Minnelusa Formation, USA. In: *Characterization of fluvial and aeolian reservoirs* (Eds. C.P. North and D.J. Prosser). *Geological Society of London Special Publication* **73**, p. 167-197.

Fryberger, S.G. and Schenk, C. (1981) Wind sedimentation tunnel experiments on the origins of aeolian strata. *Sedimentology*, **28**, 805-822.

Fryberger, S.G. and Schenk, C. (1988) Pin stripe lamination: A distinctive feature of modern and ancient eolian sediments. *Sedimentary Geology*, **55**, 1-15.

Fryberger, S.G., Hesp, P. and Hastings, K. (1992) Aeolian granule ripple deposits, Namibia. *Sedimentology*, **39**, 319 – 331.

Galloway, W.E. and Hobday, D.K. (1996) Eolian Systems. In: *Terrigenous clastic depositional systems (Second Edition)* (Eds. W.E. Galloway and D.K. Hobday) Heidelberg, Springer-Verlag, 250-269.

Garden, R., Mentiply, M., Cook, R. and Sylvester, I. (2005) Modelling fine scale heterogeneity for optimal history matching from aeolian gas reservoirs, Neptune Field, UKCS. In: *Petroleum Geology of Northwest Europe: Proceedings of the Conference* (Eds. A.G. Doré and B.A. Vining). *Geological Society of London*, **6**, 695-706.

George, G.T. and Berry, J.K. (1993) A new lithostratigraphy and depositional model for the Upper Rotliegend of the UK sector of the southern North Sea. In: *Characterization of fluvial and aeolian reservoirs* (Eds. C.P. North and D.J. Prosser). *Geological Society of London Special Publication*, **73**, 291-319.

Glennie, K.W. (1972) The Permian Rotliegendes of northwest Europe interpreted in light of modern desert sedimentation studies. *American Association of Petroleum Geologists Bulletin*, **56**, 1048-1071.

Glennie, K.W. (1998a) Lower Permian, Rotliegend. In: *Petroleum Geology of the North Sea: basic concepts and recent advance. (4th edition)* (Eds. K.W. Glennie). Blackwell Science, Oxford, 137-173.

Glennie, K.W. (1998b) The desert of southeast Arabia: A product of Quaternary climatic change. In: *Quaternary Deserts and Climate Change* (Eds. A.S. Alsharhan, K.W. Glennie, G.L. Whittle and C.G.St. Kendall). A.A. Balkema, Rotterdam, 279-291.

Glennie, K.W. (2002) Permian and Triassic. In: *The geology of Scotland (4th edition)* (Ed. N.H. Trewin). Geological Society of London, 301–321.

Glennie, K.W. and Buller, A.T. (1983) The Permian Weissliegend of NW Europe: the partial deformation of aeolian dune sands caused by the Zechstein transgression. *Sedimentary Geology*, **35**, 43-81.

Glennie, K.W. and Provan, M.G. (1990) Lower Permian Rotliegend reservoir of the southern North Sea gas province. In: *Classic petroleum provinces* (Ed. J. Brooks). *Geological Society of London Special Publication*, **50**, 399-416.

Glennie, K.W., Boegner, P.L.E. and Nagtegaal, P.J.C. (1978) Depositional environment and diagenesis of Permian Rotliegendes Sandstone in Leman Bank and Sole Pit areas of the U.K. Southern North Sea. *Journal of the Geological Society, London*, **135**, 25–34.

Glennie, K.W., Higham, J. and Stemmerik, L. (2003) Permian. In: *The Millenium Atlas: petroleum geology of the central and northern North Sea.* (Eds. D. Evans, C. Graham, A. Armour, and P. Bathhurst). Geological Society London, 91-103.

Herries, R.D. (1993) Contrasting styles of fluvio-aeolian interaction at a downwind erg margin: Jurassic Kayenta-Navajo transition, northern Arizona, USA. In: *Characterization of fluvial and aeolian reservoirs* (Eds. C.P. North and D.J. Prosser). *Geological Society of London Special Publication,* **73**, 199-218.

Hesp, P., Hyse, R., Hesp, V. and Zhengyu, Q. (1989) Longitudinal dunes can move sideways. *Earth Surface Processes and Landforms*, **14**, 447-451.

Heward, A.P. (1991) Inside Auk – the anatomy of an eolian oil reservoir. In: *The three-dimensional architecture of terrigenous clastic sediments and its implications for hydrocarbon discovery and recovery* (Eds. A.D. Miall and N. Tyler). *Society of Economic Paleontologists and Mineralogists Concepts in Sedimentology and Paleontology*, **3**, 44-56.

Heward, A.P., Schofield, P. and Gluyas, J.G. (2003) The Rotliegend reservoir in Block 30/24, UK Central North Sea: including the Argyll (renamed Ardmore) and Innes fields. *Petroleum Geoscience*, **9**, 295-307.

Howell, J. and Mountney, N.P. (1997) Climatic cyclicity and accommodation space in arid to semi-arid depositional systems: an example from the Rotliegend Group of the UK southern North Sea. In: *Petroleum Geology of the Southern North Sea: future potential* (Eds. K. Ziegler, P. Turner and S. Daines). *Geological Society of London Special Publication,* **123**, 63-86.

Howell, J. and Mountney, N.P. (2001) Aeolian grain flow architecture: hard data for reservoir models and implications for red bed sequence stratigraphy. *Petroleum Geoscience*, **7**, 51-56.

Hunter, R.E. (1977a) Basic types of stratification in small eolian dunes. *Sedimentology*, **24**, 361-387.

Hunter, R.E. (1977b) Terminology of cross-stratified sedimentary layers and climbing-ripple structures. *Journal of Sedimentary Petrology*, **47**, 697-706.

Hunter, R.E. (1981) Stratification styles in eolian sandstones: some Pennsylvanian to Jurassic examples from the Western Interior USA. In: *Recent and Ancient Non-Marine Depositional Environments: Models for Exploration* (Eds. F.G. Etheridge and R. M. Flores). *Society of Economic Paleontologists and Mineralogists Special Publication*, **31**, 315-329.

Hunter, R.E. (1985) A kinematic model for the structure of lee-side deposits. *Sedimentology*, **32**, 409-422.

Hunter, R.E., Richmond, B.M. and Alpha, T.R. (1983) Storm-controlled oblique dunes of the Oregon coast. *Geological Society of America Bulletin*, **94**, 1450-1465

Inman, D.L., Ewing, G.C. and Corliss, B. (1966) Coastal sand dunes of Guerrero Negro, Baja California. *Geological Society of America Bulletin*, **77**, 787-802.

Jordan, O.D. and Mountney, N.P. (2010) Styles of interaction between aeolian, fluvial and shallow marine environments in the Pennsylvanian to Permian lower Cutler beds, south-east Utah, USA. *Sedimentology*, **57**, 1357-1385.

Jordan, O.D. and Mountney, N.P. (2012) Sequence stratigraphic evolution and cyclicity of an ancient coastal desert system: the Pennsylvanian-Permian lower Cutler beds, Paradox Basin, Utah, USA. *Journal of Sedimentary Research*, **82**, 755-780.

Karpeta, W.P. (1990) The morphology of Permian palaeodunes – a reinterpretation of the Bridgnorth Sandstone around Bridgnorth, England in the light of modern dune studies. *Sedimentary Geology*, **69**, 59-75.

King, P.R. (1990) The connectivity and conductivity of overlapping sand bodies. In: *North Sea oil and gas reservoirs II* (Eds. A.T. Buller, E. Berg, O. Hjelmeland, J. Kleppe, O. Torsaeter, and J.O. Aasen). London, United Kingdom, Graham and Trotman, 353-361.

Kocurek, G. (1981) Significance of interdune deposits and bounding surfaces in aeolian dune sands. *Sedimentology*, **28**, 753-780.

Kocurek, G. (1988) First-order and super bounding surfaces in eolian sequences – Bounding surfaces revisited. *Sedimentary Geology*, **56**, 193-206.

Kocurek, G. (1991) Interpretation of ancient eolian sand dunes. *Annual Reviews of Earth & Planetary Sciences*, **19**, 43-75.

Kocurek, G. (1996) Desert aeolian systems. In: *Sedimentary environments: Processes, facies and stratigraphy* (Ed. H.G. Reading). Oxford, Blackwell Science, 125-153

Kocurek, G. (1999) The aeolian rock record (Yes, Virginia, it exists, but it really is rather special to create one). In: *Aeolian Environments, Sediments and Landforms* (Eds. A. Goudie and I. Livingstone). John Wiley, London, 239-259.

Kocurek, G. and Dott, R.H. (1981) Distinctions and uses of stratification types in the interpretation of eolian sand. *Journal of Sedimentary Petrology*, **51**, 579-595.

Kocurek, G. and Havholm, K.G. (1993) Eolian sequence stratigraphy – A conceptual framework. In: *Siliciclastic Sequence Stratigraphy* (Eds. P. Weimer and H. Posamentier). *American Association of Petroleum Geologists Memoir*, **58**, 393-409.

Kocurek, G. and Nielson, J. (1986) Conditions favourable for the formation of warm-climate aeolian sand sheets. *Sedimentology*, **33**, 795-816.

Kocurek, G., Lancaster, N., Carr, M. and Andfrank, A. (1999) Tertiary Tsondab Sandstone Formation: preliminary bedform reconstruction and comparison to modern Namib Sand Sea dunes. *Journal of African Earth Sciences*, **29**, 629-642.

Kocurek, G., Robinson, N.I. and Sharp, J.M., J$_R$. (2001) The response of the water table in coastal aeolian systems to changes in sea level. *Sedimentary Geology*, **139**, 1-13.

Krystinik, L.F. (1990) Development Geology in Eolian Reservoirs. In: *Modern and Ancient Eolian Deposits: Petroleum Exploration and Production* (Eds. S.G. Fryberger, L.F. Krystinik and C.J. Schenk). *Rocky Mountain Section Society of Economic Paleontologists and Mineralogists*, 135-146.

Lancaster, N. (1981) Grain size characteristics of Namib Desert linear dunes. *Sedimentology*, **28**, 115-122.

Lancaster, N. (1982) Linear dunes. *Progress in Physical Geography*, **6**, 475-504.

Lancaster, N. (1983) Controls of dune morphology in the Namib Desert. In: *Eolian Sediments and Processes* (Eds. M.E. Brookfield and T.S. Ahlbrandt). *Developments in Sedimentology*, **38**, 407-427.

Lancaster, N. (1988a) Controls of eolian dune size and spacing. *Geology*, **16**, 972-975.

Lancaster, N. (1988b) The development of large aeolian bedforms. *Sedimentary Geology*, **55**, 69-89.

Lancaster, N. (1995) Geomorphology of desert dunes. Routledge, London & New York, 290 pp.

Langford, R.P. and Chan, M.A. (1993) Downwind changes within an ancient dune sea, Permian Cedar Mesa Sandstone, southeast Utah. In: *Aeolian sediments: ancient and modern* (Eds. K. Pye and N. Lancaster). *International Association of Sedimentologists Special Publication*, **16**, 109-126.

Langford, R.P., Pearson, K.M., Duncan, K.D., Tatum, D., Adams, L. and Depret, P. (2008) Eolian topography as a control on deposition, with lessons from modern dune seas:

Permian Cedar Mesa Sandstone, SE Utah. *Journal of Sedimentary Research*, **78**, 410-422.

Larue, D.K. and Hovadik, J. (2006) Connectivity of channelized reservoirs: a modelling approach. *Petroleum Geoscience,* **12**, 291-308.

Lewis, H. and Couples, G.D. (1993) Production evidence for geological heterogeneities in the Anschutz Ranch East Field, western USA. In: *Characterization of fluvial and aeolian reservoirs* (Eds. C. P. North and D. J. Prosser). *Geological Society of London Special Publication*, **73**, 321-338.

Lewis, J.J.M. and Rosvoll, K.J. (1991) The improved prediction of permeability variation in selected Rotligendes aeolian reservoirs from the southern North Sea. *American Association of Petroleum Geologists Bulletin*, **75**, 620-621.

Lindquist, S.J. (1988) Practical characterization of eolian reservoirs for development: Nugget Sandstone, Utah-Wyoming Thrust Belt. *Sedimentary Geology*, **56**, 315-339.

Livingstone, I. (1987) Grain-size variation on a ‘complex’ linear dune in the Namib desert. In: *Desert Sediment: Ancient and Modern* (Eds. L. Frostick and I. Reid). *Geological Society Special Publication*, **35**, 281-291.

Livingstone, I. (1989a) Temporal trends in grain-size measures on a linear sand dune. *Sedimentology*, **36**, 1017-1022.

Livingstone, I. (1989b) Monitoring surface change on a Namib linear dune. *Earth Surface Processes and Landforms*, **14**, 317-332.

Loope, D.B. (1985) Episodic deposition and preservation of eolian sands: A late Paleozoic example from southeastern Utah. *Geology*, **13**, 73-76.

Luthi, S.M. and Banavar, J.R. (1988) Application of borehole images to three-dimensional geometric modeling of eolian sandstone reservoirs, Permian Rotliegende, North Sea. *American Association of Petroleum Geologists Bulletin*, **72**, 1074-1089.

Luzón, A., Rodríguez-López, J.P., Pérez, A., Soriano, M.A., Gil, H. and Pocoví, A. (2012) Karst subsidence as a control on the accumulation and preservation of aeolian deposits: a Pleistocene example from a proglacial outwash setting, Ebro Basin, Spain. *Sedimentology*, **59**, 2199-2225.

McDonald, R.R. and Anderson, R.S. (1995) Experimental verification of aeolian saltation and lee side deposition models. *Sedimentology*, **42**, 39-55.

McKee, E.D. (1979a) Introduction to a study of global sand seas. In: *A study of global sand seas* (Ed. E.D. McKee). *Geological Survey Professional Paper*, **1052**, 1-19.

McKee, E.D. (1979b) Ancient sandstones considered to be eolian. In: *A study of global sand seas* (Ed. E.D. McKee). *Geological Survey Professional Paper*, **1052**, 187-238.

McKee, E.D. (1982) Sedimentary Structures in Dunes of the Namib Desert, South West Africa. *Geological Society of America Special Paper*, **188**, 64 pp.

McKee, E.D. and Tibbitts, G.C. (1964) Primary structures of a seif dune and associated deposits in Libya. *Journal of Sedimentary Petrology*, **34**, 5-17.

Mancini, E.A., Mink, R.M., Bearden, B.L. and Wilkerson, R.P. (1985) Norphlet Formation (Upper Jurassic) of southwestern and offshore Alabama: environments of deposition and petroleum geology. *American Association of Petroleum Geologists Bulletin*, **69**, 881-898.

Meadows, N.S. (2006) The correlation and sequence architecture of the Ormskirk Sandstone Formation in the Triassic Sherwood Sandstone Group of the East Irish Sea Basin, NW England. *Geological Journal*, **41**, 93-122.

Mou, D.C. and Brenner, R.L. (1982) Control of reservoir properties of Tensleep Sandstone by depositional and diagenetic facies: Lost Soldier Field, Wyoming. *Journal of Sedimentary Petrology*, **52**, 367-381.

Mountney, N.P. (2006a) Eolian Facies Models. In: *Facies Models Revisited* (Eds. H. Posamentier and R.G. Walker). *Society of Economic Paleontologists and Mineralogists Memoir*, **84**, 19-83.

Mountney, N.P. (2006b) Periodic accumulation and destruction of aeolian erg sequences in the Permian Cedar Mesa Sandstone, White Canyon, southern Utah, USA. *Sedimentology*, **53**, 789-798.

Mountney, N.P. (2012) A stratigraphic model to account for complexity in aeolian dune and interdune successions. *Sedimentology*, **59**, 964-989.

Mountney, N.P. and Howell, J. (2000) Aeolian architecture, bedform climbing and preservation space in the Cretaceous Etjo Formation, NW Namibia. *Sedimentology*, **47**, 825-849.

Mountney, N.P. and Jagger, A. (2004) Stratigraphic evolution of an erg margin aeolian system: The Permian Cedar Mesa Sandstone, SE Utah, USA. *Sedimentology*, **51**, 713-743.

Mountney, N.P. and Russell, A.J. (2009) Aeolian dune field development in a water table-controlled system: Skeiđarársandur, southern Iceland. *Sedimentology*, **56**, 2107-2131.

Mountney, N.P. and Thompson, D.B. (2002) Stratigraphic evolution and preservation of aeolian dune and damp/wet interdune strata: an example from the Triassic Helsby Sandstone Formation, Cheshire Basin, UK. *Sedimentology*, **49**, 805-833.

Mountney, N.P., Howell, J.A., Flint, S. and Jerram, D.A. (1999) Relating eolian bounding-surface geometries to the bed forms that generated them: Etjo Formation, Cretaceous, Namibia. *Geology*, **27**, 159-162.

Nagtegaal, P.J.C. (1979) Relationship of facies and reservoir quality in Rotliegendes desert sandstones, southern North Sea region. *Journal of Petroleum Geology*, **2**, 145-158.

Nielson, J. and Kocurek, G. (1987) Surface processes, deposits, and development of star dunes: Dumont dune field, California. *Geological Society of America Bulletin,* **99**, 177-186.

North, C.P. and Boering, M. (1999) Spectral gamma-ray logging for facies discrimination in mixed fluvial-eolian successions: a cautionary tale. *American Association of Petroleum Geologists Bulletin*, **83**, 155-169.

North, C.P. and Prosser, D.J. (1993) Characterization of fluvial and aeolian reservoirs: problems and approaches. In: *Characterization of fluvial and aeolian reservoirs* (Eds. C.P. North and D.J. Prosser). *Geological Society of London Special Publication*, **73**, 1-6.

Nurmi, R.D. (1985) Eolian sandstone reservoirs; bedding facies and production geology modeling. *Society of Petroleum Engineers, SPE Paper* **#14172**.

Parteli, E.J.R., Durán, O., Tsoar, H., Schwämmle, V. and Herrmann, H.J. (2009) Dune formation under bimodal winds. *Proceedings of the National Academy of Sciences of the United States of America*, **106**, 22085–22089.

Porter, M.L. (1986) Sedimentary record of erg migration. *Geology,* **14**, 497-500.

Prosser, D.J. and Maskall, R. (1993) Permeability variation within aeolian sandstone: a case study using core cut sub-parallel to slipface bedding, Auk Field, Central North Sea, UK. In: *Characterization of fluvial and aeolian reservoirs* (Eds. C.P. North and D.J. Prosser). *Geological Society of London Special Publication*, **73**, 377-397.

Pryor, W.A. (1973) Permeability-porosity patterns and variations in some Holocene sand bodies. *American Association of Petroleum Geologists Bulletin*, **57**, 162-189.

Pulvertaft, T.C.R. (1985) Aeolian dune and wet interdune sedimentation in the Middle Proterozoic Dala-Sandstone, Sweden. *Sedimentary Geology*, **44**, 93-111.

Rodríguez-López, J.P., Clemmensen, L., Lancaster, N., Mountney, N.P. and Veiga, G. (2014) Archean to Recent aeolian sand systems and their preserved successions: current understanding and future prospects. *Sedimentology,* **61**, 1487-1534.

Rodríguez-López, J.P., Meléndez, N., de Boer, P.L. and Soria, A.R. (2008) Aeolian sand sea development along the mid-Cretaceous western Tethyan margin (Spain): erg sedimentology and palaeoclimate implications. *Sedimentology*, **55**, 1253-1292.

Romain, H.G. and Mountney, N.P. (2014) Reconstruction of three-dimensional eolian dune architecture from one-dimensional core data through adoption of analog data from outcrop. *American Association of Petroleum Geologists Bulletin*, **98**, 1-22.

Rubin, D.M. (1987a) Cross-bedding, Bedforms, and Paleocurrents. *Concepts in Sedimentology and Paleontology*, **1**, Society of Economic Paleontologists and Mineralogists, Tulsa, 187 pp.

Rubin, D.M. (1987b) Formation of scalloped cross-bedding without unsteady flows. *Journal of Sedimentary Petrology*, **57**, 39-45.

Rubin, D.M. (1990) Lateral migration of linear dunes in the Strzelecki Desert, Australia. *Earth Surface Processes and Landforms*, **15**, 1-14.

Rubin, D.M. and Carter, C.L. (2006) Cross-Bedding, Bedforms, and Paleocurrents. *Society of Economic Paleontologists and Mineralogists Concepts in Sedimentology and Paleontology (2nd edition)*, **1**, 195 pp.

Rubin, D.M. and Hunter, R.E. (1982) Bedform climbing in theory and nature. *Sedimentology*, **29**, 121-138.

Rubin, D.M. and Hunter, R.E. (1983) Reconstructing bedform assemblages from compound crossbedding. In: *Eolian Sediments and Processes* (Eds. M.E. Brookfield and T.S. Ahlbrandt). *Developments in Sedimentology*, **38**, 407-427.

Rubin, D.M. and Hunter, R.E. (1985) Why deposits of longitudinal dunes are rarely recognized in the geologic record. *Sedimentology*, **32**, 147-157.

Rubin, D.M. and Hunter, R.E. (1987) Bedform alignment in directionally varying flows. *Science*, **237**, 276-278.

Schenk, C.J. (1990) Core Examples of Eolian Sandstone. In: *Modern and Ancient Eolian Deposits: Petroleum Exploration and Production* (Eds. S.G. Fryberger, L.F. Krystinik and C.J. Schenk). *Rocky Mountain Section Society of Economic Paleontologists and Mineralogists*, 171-189.

Scherer, C.M.S. (2000) Eolian dunes of the Botucatu Formation (Cretaceous) in southernmost Brazil: morphology and origin. *Sedimentary Geology*, **137**, 63-84.

Smith, D.B. and Taylor, J.C.M. (1992) Permian. In: *Atlas of Palaeogeography and Lithofacies* (Eds. J.C.W. Cope, J.K. Ingham and P.F. Rawson). *Geological Society of London Memoir*, **13**, 87-96.

Sneh, A. and Weissbrod, T. (1983) Size-frequency distribution of longitudinal dune rippled flank sands compared to that of slipface sands of various dune types. *Sedimentology*, **30**, 717-725.

Spalletti, L.A., Limarino, C.O. and Colombo, F. (2010) Internal anatomy of an erg sequence from the aeolian-fluvial system of the De La Cuesta Formation (Paganzo Basin, northwestern Argentina). *Geologica Acta*, **8**, 431-447.

Stanesco, J.A. and Campbell, J.C. (1989) Eolian and non-eolian facies of the Lower Permian Cedar Mesa Sandstone Member of the Cutler Formation, Southeastern Utah. *U.S. Geological Survey Bulletin*, **1808-F**, F1-F13.

Stanistreet, I. G. and Stollhofen, H. (2002) Hoanib River flood deposits of Namib Desert interdunes as analogues for thin permeability barrier mudstone layers in aeolianite reservoirs. *Sedimentology*, **49**, 719-736.

Steele, R.P. (1981) Aeolian sands and sandstones. Unpublished PhD thesis, University of Durham, UK. Two volumes.

Steele, R.P. (1982) A case study of an aeolian sandstone: the Permian yellow sands of N.E. England. *11th International Congress on Sedimentology, Abstracts of Papers*, p. 170

Steele, R.P. (1983) Longitudinal draa in the Permian Yellow Sands of north-east England. In: *Eolian Sediments and Processes* (Eds. M.E. Brookfield and T.S. Ahlbrandt). *Developments in Sedimentology*, **38**, 543-550.

Story, C. (1998) Norphlet geology and 3-D geophysics: Fairway Field, Mobile Bay, Alabama. *The Leading Edge*, **17**, 243-248.

Strömbäck, A., Howell, J.A. and Veiga, G.D. (2005) The transgression of an erg - sedimentation and reworking/soft-sediment deformation of aeolian facies: the Cretaceous Troncoso Member, Neuquen Basin, Argentina. *Geological Society of London Special Publication*, **252**, 163-183.

Sweet, M.L. (1992) Lee-face airflow, surface processes, and stratification types: Their significance for refining the use of eolian cross-strata as paleocurrent indicators. *Geological Society of America Bulletin*, **104**, 1528-1538.

Sweet, M.L., Blewden, C.J., Carter, A.M. and Mills, C.A. (1996) Modeling heterogeneity in a low-permeability gas reservoir using geostatistical techniques, Hyde Field, Southern North Sea. *American Association of Petroleum Geologists Bulletin*, **80**, 1709-1735.

Taggart, S., Hampson, G.J. and Jackson, M.D. (2010) High-resolution stratigraphic architecture and lithological heterogeneity within marginal aeolian reservoir analogues. *Sedimentology*, **57**, 1246-1279.

Tanner, W.F. (1965) Upper Jurassic paleogeography of the Four Corners region. *Journal of Sedimentary Petrology,* **35**, 564-574.

Tatum, D.I. and Francke, J. (2012) Constructing hydrocarbon reservoir analogues of aeolian systems using ground penetrating radar. *Journal of Applied Geophysics,* **81**, 21-28.

Taylor, J.C.M. (2009) Chapter 6 – Upper Permian - Zechstein In: *Petroleum Geology of the North Sea: basic concepts and recent advance* (Ed. K.W. Glennie). Blackwell, Oxford, 174-211.

Terwindt, J.H.J. (1981) Origin and sequences of sedimentary structures in inshore mesotidal deposits of the North Sea. In: *Holocene Marine Sedimentation in the North Sea Basin* (Eds. S.-D. Nio, R.T.E. Shüttenhelm, Tj.C.E. Van Weering). *International Association of Sedimentologists Special Publication*, **5**, Blackwell Scientific Publications, Oxford, 4-26.

Trewin, N.H., Fryberger, S.G. and Kreutz, H. (2003) The Auk Field, Block 30/16, UK North Sea. *Geological Society of London Memoirs*, **20**, 483-496.

Tsoar, H. (1978) The dynamics of longitudinal dunes. *Final Technical report A-ERO 76-g-072: US Army European Research Office*, London.

Tsoar, H. (1982) Internal structure and surface geometry of longitudinal (seif) dunes. *Journal of Sedimentary Petrology*, **52**, 823-831.

Tsoar, H. (1983) Dynamic processes acting on a longitudinal (seif) sand dune. *Sedimentology*, **30**, 567-578.

Wakefield, O.J.W. and Mountney, N.P. (2013) Stratigraphic architecture of back-filled incised-valley systems: Pennsylvanian-Permian lower Cutler beds, Utah, USA. *Sedimentary Geology*, **298**, 1-16.

Weber, K.J. (1982) Influence of common sedimentary structures on fluid flow in reservoir models. *Journal of Petroleum Technology*, **34**, 665-672.

Weber, K.J. (1986) How heterogeneity affects oil recovery. In: *Reservoir Characterization* (Eds. L.W. Lake and H.B.J. Carroll). Orlando, FL, Academy Press, 487–544.

Weber, K.J. (1987) Computation of initial well productivities in aeolian sandstone on the basis of a geological model, Leman Gas Field, U.K. In: *Reservoir Sedimentology* (Eds. R.W. Tillman and K.J. Weber). *Society of Economic Paleontologists and Mineralogists Special Publication*, **40**, 333-354.

Wickens, H. de V. and McLachlan, I.R. (1990) The stratigraphy and sedimentology of the reservoir interval of the Kudu 9A-2 and 9A-3 boreholes. *Communications of the Geological Survey of Namibia*, **6**, 9-22.

Wilson, I.G. (1971) Desert sandflow basins and a model for the development of ergs. *Geographical Journal*, **137**, 180-199.

Wilson, I.G. (1972) Aeolian bedforms - their development and origins. *Sedimentology*, **19**, 173-210.

Wilson, I.G. (1973) Ergs. *Sedimentary Geology*, **10**, 77-106.

Yaalon, D.H. and Laronne, J. (1971) Internal structures in eolianites and paleowinds, Mediterranean coast, Israel. *Journal of Sedimentary Petrology*, **41**, 1059-1064.